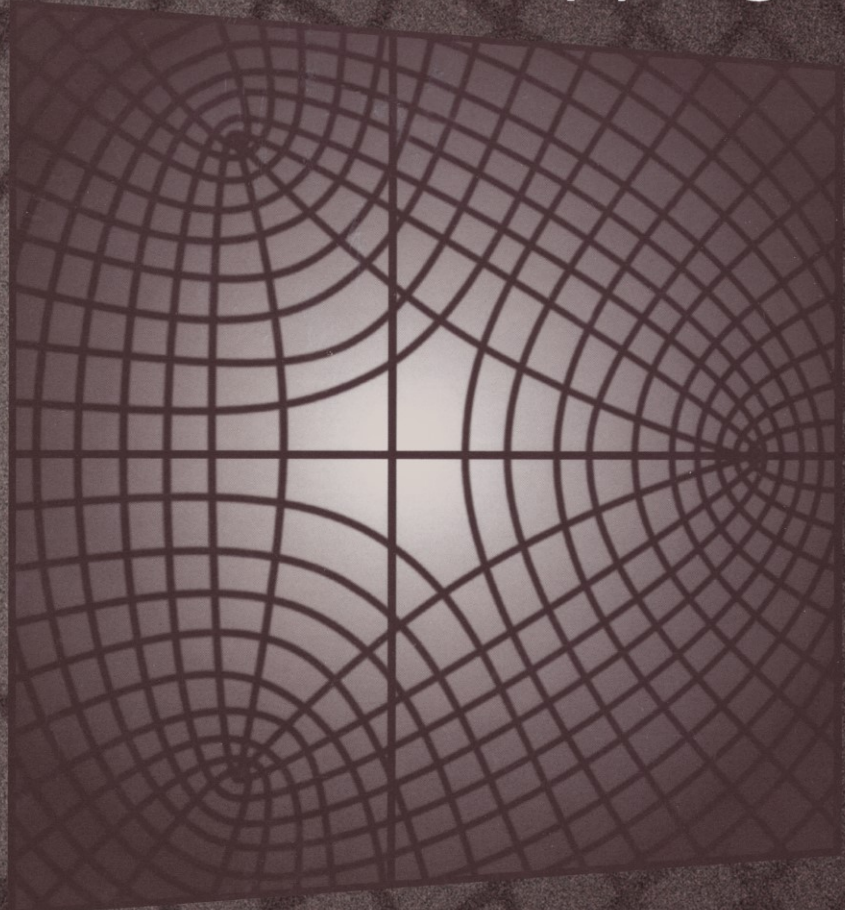


# Computational Conformal Mapping



Prem K. Kythe

ERRATA: Kythe: Computational Conformal Mapping

Page 16, line 6: ‘An open’ should read ‘The open’.

Page 26, Eq (1.2.11) should read:  $f(z_0) = -\frac{1}{i\pi} \int_{\Gamma} \frac{f(\zeta)}{\zeta - z_0} d\zeta + 2 f(\infty)$

Page 43, line 3:  $G = \{n\theta_0 + 2m\pi < \arg\{w\} < n\theta_1 + 2m\pi\}$  should read  $G = \{n\theta_0 + 2m\pi < \arg\{w\} < n\theta_1 + 2m\pi\}$

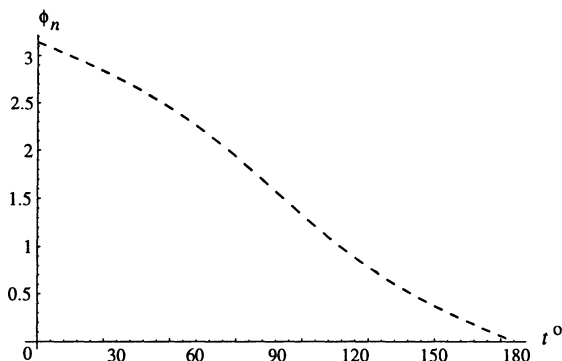
Page 55, lines 18 and 21:  $(x + 11)$  should read  $(x + 1)$

Page 94, The first two lines of Theorem 4.1.2 should read: The function  $f_0(z)$  is orthogonal to every function  $g \in L^2(D)$  with  $g(a) = 0$ , i.e,

Page 148, Eq (6.2.1) and page 149, line 1, should read:  $\mathcal{G}(z, z_0) = \frac{1}{2\pi} \log \frac{1}{r} + g(z, z_0)$ ,  $r = |z - z_0|$ , where  $g(z, z_0)$  is harmonic everywhere in  $D$ .

Page 161, Eq (6.5.8) and the following line should read:  $\mathcal{N}(z, z_0) = \log \frac{z - z_0}{z - z^*} + n(z, z_0)$ , where  $n(z, z_0)$  is a regular analytic function on  $D$ .

Page 190: Fig 7.4.2 is



Pages 199–200:  $L^l$  should read  $L^2($ .



FILIO • PRIMO  
HVNC • LIBELLVM  
D • D • D

# **Computational Conformal Mapping**

Prem K. Kythe

Springer Science+Business Media, LLC

Prem K. Kythe  
University of New Orleans  
Department of Mathematics  
New Orleans, LA 70148

Library of Congress Cataloging-in-Publication Data

Kythe, Prem K.

Computational Conformal Mapping/Prem K. Kythe.  
p. cm.

ISBN 978-1-4612-7376-9 ISBN 978-1-4612-2002-2 (eBook)

DOI 10.1007/978-1-4612-2002-2

1. Conformal Mapping -- Data Processing. I. Title

QA360.K97 1998  
516.3'6--dc21

98-4748  
CIP

Printed on acid-free paper

© 1998 Springer Science+Business Media New York



Originally published by Birkhäuser Boston in 1998

Softcover reprint of the hardcover 1st edition 1998

Copyright is not claimed for works of U.S. Government employees.

All rights reserved. No part of this publication may be reproduced, stored in a retrieval system, or transmitted, in any form or by any means, electronic, mechanical, photocopying, recording, or otherwise, without prior permission of the copyright owner.

Authorization to photocopy items for internal or personal use of specific clients is granted by Birkhäuser Boston provided that the appropriate fee is paid directly to Copyright Clearance Center (CCC), 222 Rosewood Drive, Danvers, MA 01923, USA (Telephone: (978) 750-8400), stating the ISBN, the title of the book, and the first and last page numbers of each article copied. The copyright owner's consent does not include copying for general distribution, promotion, new works, or resale. In these cases, specific written permission must first be obtained from the publisher.

ISBN 978-1-4612-7376-9

9 8 7 6 5 4 3 2 1

---

## Contents

---

Preface, ix

**Chapter 0. Introduction, 1**

- 0.1. Historical Background, 1
- 0.2. Modern Developments, 8

**Chapter 1. Basic Concepts, 15**

- 1.1. Notation and Definitions, 15
- 1.2. Some Basic Theorems, 23
- 1.3. Harmonic Functions, 27
- 1.4. Conformal Mapping, 30
- 1.5. Problems, 38

**Chapter 2. Conformal Mappings, 41**

- 2.1. Polynomials, 41
- 2.2. Bilinear Transformations, 45
- 2.3. Schwarz–Christoffel Transformations, 51
- 2.4. Catalog of Conformal Maps, 64
- 2.5. Problems, 65

**Chapter 3. Schwarz–Christoffel Integrals, 68**

- 3.1. Parameter Problem, 68
- 3.2. Newton’s Method, 72
- 3.3. Numerical Computations, 76
- 3.4. Kirchhoff Flow Problem, 83
- 3.5. Problems, 89

**Chapter 4. Polynomial Approximations, 92**

- 4.1. Minimum Area Problem, 92
  - 4.1.1. Bergman Kernel, 94
- 4.2. Numerical Methods for Problem I, 95
  - 4.2.1. Ritz Method, 95
  - 4.2.2. Bergman Kernel Method, 101
- 4.3. Minimum Boundary Problem, 103
- 4.4. Ritz Method for Problem II, 105
- 4.5. Orthogonal Polynomials, 109
  - 4.5.1. Polynomials Orthogonal to the Boundary, 109
  - 4.5.2. Polynomials Orthogonal to a Region, 116
- 4.6. Problems, 118

**Chapter 5. Nearly Circular Regions, 120**

- 5.1. Small Parameter Expansions, 120
- 5.2. Method of Infinite Systems, 125
- 5.3. Three Special Cases, 132
- 5.4. Exterior Regions, 140
- 5.5. Problems, 145

**Chapter 6. Green's Functions, 147**

- 6.1. Mean–Value Theorem, 147
- 6.2. Dirichlet Problem, 148
- 6.3. Numerical Computation, 152
- 6.4. Schwarz Formula, 158
- 6.5. Neumann Problem, 159
- 6.6. Series Representations, 162
- 6.7. Problems, 165

**Chapter 7. Integral Equation Methods, 168**

- 7.1. Neumann Kernel, 168
- 7.2. Interior Regions, 171
  - 7.2.1. Lichtenstein's Integral Equation, 171
  - 7.2.2. Gershgorin's Integral Equation, 172
  - 7.2.3. Carrier's Integral Equation, 173
- 7.3. Exterior Regions, 174
  - 7.3.1. Banin's Integral Equation, 176
  - 7.3.2. Warschawski–Stiefel's Integral Equation, 177
  - 7.3.3. Interior and Exterior Maps, 177
- 7.4. Iterative Method, 178
- 7.5. Degenerate Kernel, 192
- 7.6. Szegő Kernel, 198
- 7.7. Problems, 204

**Chapter 8. Theodorsen's Integral Equation, 207**

- 8.1. Classical Iterative Method, 207
- 8.2. Convergence, 209
- 8.3. Proofs, 211
- 8.4. Integral Representation, 222
- 8.5. Starlike Regions, 224
- 8.6. Exterior Regions, 226
- 8.7. Trigonometric Interpolation, 228
- 8.8. Wegmann's Method, 229
- 8.9. Newton's Method, 234
- 8.10. Problems, 236

**Chapter 9. Symm's Integral Equation, 237**

- 9.1. Symm's Integral Equation, 237
  - 9.1.1. Interior Regions, 237
  - 9.1.2. Exterior Regions, 239
- 9.2. Orthonormal Polynomial Method, 240
- 9.3. Modified ONP Method, 247
- 9.4. Lagrange Interpolation, 251
- 9.5. Spline Approximations, 258
- 9.6. Problems, 265

**Chapter 10. Airfoils, 269**

- 10.1. Joukowski Function, 269
- 10.2. Generalized Joukowski Mappings, 274
  - 10.2.1. Glauert's Modification, 275
  - 10.2.2. Symmetric Joukowski Airfoil, 276
- 10.3. Nearly Circular Approximations, 277
- 10.4. James's Method, 279
  - 10.4.1. Single-Element Airfoils, 280
  - 10.4.2. von Karman-Trefftz transformations, 283
  - 10.4.3. Two-Element Airfoils, 288
  - 10.4.4. Multi-Element Airfoils, 291
- 10.5. Problems, 292

**Chapter 11. Doubly Connected Regions, 295**

- 11.1. Conformal Modulus, 295
  - 11.1.1. Conformal Invariants, 296
  - 11.1.2. Area Theorem, 298
- 11.2. Source Density, 305
- 11.3. Dipole Distribution, 308
- 11.4. Problems, 317

**Chapter 12. Singularities, 320**

- 12.1. Arbenz's Integral Equation, 320
- 12.2. Boundary Corner, 325
- 12.3. Singularity Behavior, 328
- 12.4. Pole–Type Singularities, 330
- 12.5. Exterior Regions, 339
- 12.6. Doubly Connected Regions, 345
- 12.7. Problems, 351

**Chapter 13. Multiply Connected Regions, 358**

- 13.1. Existence and Uniqueness, 359
- 13.2. Dirichlet Problem, 364
- 13.3. Mikhlin's Integral Equation, 367
- 13.4. Mayo's Method, 370
- 13.5. Fast Poisson Solver, 373
- 13.6. Problems, 377

**Chapter 14. Grid Generation, 379**

- 14.1. Computational Region, 379
- 14.2. Inlet Configurations, 384
- 14.3. Cascade Configurations, 390
- 14.4. Problems, 399

**Appendix A. Cauchy P. V. Integrals, 401**

- A.1. Numerical Evaluation, 401

**Appendix B. Green's Identities, 407****Appendix C. Riemann–Hilbert Problem, 410**

- C.1. Homogeneous Hilbert Problem, 410
- C.2. Nonhomogeneous Hilbert Problem, 415
- C.3. Riemann–Hilbert Problem, 417

**Appendix D. Successive Approximations, 425**

- D.1. Tables, 425

**Appendix E. Catalog of Conformal Mappings, 428****Bibliography, 431****Notation, 449****Index, 453**

---

## Preface

---

This book evolved out of a graduate course given at the University of New Orleans in 1997. The class consisted of students from applied mathematics and engineering. They had the background of at least a first course in complex analysis with emphasis on conformal mapping and Schwarz–Christoffel transformation, a first course in numerical analysis, and good to excellent working knowledge of Mathematica\* with additional knowledge of some programming languages. Since the class had no background in Integral Equations, the chapters involving integral equation formulations were not covered in detail, except for Symm’s integral equation which appealed to a subset of students who had some training in boundary element methods. Mathematica was mostly used for computations. In fact, it simplified numerical integration and other operations very significantly, which would have otherwise involved programming in Fortran, C, or other language of choice, if classical numerical methods were attempted.

---

## Overview

Exact solutions of boundary value problems for simple regions, such as circles, squares or annuli, can be determined with relative ease even where the boundary conditions are rather complicated. Green’s functions for such simple regions are known. However, for regions with complex structure the solution of a boundary value problem often becomes more difficult, even for a simple problem such as the Dirichlet problem. One approach to solving these difficult problems is to conformally transform a given multiply connected region onto

---

\*Mathematica is a registered trade mark of Wolfram Research, Inc.

simpler canonical regions. This will, however, result in change not only in the region and the associated boundary conditions but also in the governing differential equation. As compared to the simply connected regions, conformal mapping of multiply connected regions suffers from severe limitations, one of which is the fact that equal connectivity of regions is not a sufficient condition to effect a reciprocally connected map of one region onto another. There are though a few methods that carry out such mappings where most of the computational details are done numerically.

The main purpose of this book is to provide a self-contained and systematic introduction to the theory and computation of conformal mappings of simply or multiply connected regions onto the unit disk or canonical regions. It provides a comprehensive and systematic coverage of the basic theory and related numerical analysis with applications to different areas in mathematical physics and engineering. The material is presented at a level that can readily be followed by graduate students and researchers. The prerequisites, besides the theory of conformal mapping, include knowledge of basic methods of numerical analysis, the theory of Fredholm and Stieltjes integral equations, and a programming language. Depending on the background of students, this book may cover two semesters of graduate course work, the first involving classical developments (chapters 1 through 6, 10, and 14), and the second involving the integral equation formulations and the study of singularities (chapters 7 through 9 and 11 through 13).

---

## Salient Features

Besides an exposition on the history of the subject, there are 14 chapters in the book the first two provide a review of the theory of conformal mapping and Schwartz–Christoffel transformations to map a polygon onto the upper half-plane. The computation of improper Schwartz–Christoffel integrals and the related parameter problem is one of the important classical topics which is studied in detail in Chapter 3. An old problem, known as the Kirchhoff flow problem that started in 1868, is presented with its very recent complete solution. Chapter 4 deals with the methods of polynomial approximations, first, with the minimum area problem with detailed accounts and algorithms for the Ritz and Bergman kernel methods, and secondly, with the minimum boundary problem with the related Ritz method and the Szegö kernel and its applications. Polynomials orthogonal to the boundary and those orthogonal to the region are investigated. Nearly circular regions are studied in Chapter 5 through the method of infinite systems and successive approximations, where

special cases are treated separately, and computational algorithms with examples are presented. Techniques of numerical evaluation of Green's functions for various kinds of regions are studied in Chapter 6, with special topics like the Dirichlet and Neumann problems, Schwarz formula, and associated series representation.

Various integral equation formulations of the conformal mapping problem have been discussed in Chapters 7, 8, 9, 11, and 13. These equations are mostly Fredholm equations of the first or second kind and provide boundary correspondence functions and their computation by iterative methods. Chapter 7 starts with the Neumann kernel and presents Lichtenstein's, Gershgorin's, Carrier's, Banin's, and Warschawski-Siefel's integral equations. An algorithm for the iterative method is provided with detailed explanations. The chapter discusses the case of a degenerate kernel and ends with the Szegő kernel and the related method for solving the conformal mapping problem. Chapter 8 deals with the classical Theodorsen's integral equation, discusses convergence of the iterative method, provides proofs for the convergence theorem due to Warschawski, and investigates the cases of starlike and exterior regions. A trigonometric interpolation method is outlined and the modern iterative and Newton's methods are presented. Chapter 9 deals with Symm's integral equations for the interior and exterior regions, based on a single-layer potential. The orthonormal polynomial method, Lagrange interpolation, and spline approximation method are discussed. Doubly connected regions are studied in Chapter 11, and the related integral equation based on the dipole distribution is presented with an algorithm for numerical computation. Chapter 13 deals with multiply connected regions. Based on the dipole distribution, Mikhlin's integral equation that determines the density function and related boundary correspondence is solved by a fast Poisson solver. This method is very efficient and solves problems for both simply and multiply connected regions.

A detailed account of airfoils is presented in Chapter 10. Various methods, like James's method for single-element airfoils, von Karman-Trefftz transformation and Garrick's method of conjugated functions for two-element airfoils are explained with related algorithms and examples. Chapter 12 presents an important aspect of the conformal mapping problem, related to the location and behavior of corner singularities on the boundary and pole-type singularities of the mapping functions near the boundary in simply and doubly connected regions. Their effect on the polynomial methods is analyzed and, by considering various cases, certain methods are presented to augment the bases in the polynomial methods studied in Chapter 4 and 9. The last chapter provides useful insight into the application of conformal mapping in adaptive grid generation. Effective programming aspects are discussed and cases examined to exhibit the importance of this application.

Although it is not possible to include every written word on the subject, the topics included in this book are carefully selected and meticulously presented, thereby making it a book very useful to graduate students and researchers in mathematics, physics, and engineering. The scope of the book can be judged from the table of contents. The bibliography at the end of the book is extensive and contains references, some not cited in the text, to computer programs and other articles useful in theoretical and computational development. The book ends with a notation and a subject index.

---

## Intended Readers

The book is intended to contribute to an effective study program at the graduate level and to serve as a reference book for scientists, engineers, and mathematicians in industry. A partial list of readers of this book includes persons interested in the study of acoustics, plane elasticity, electromagnetic theory, fluid flows, inlet configurations, transonic flow problems, cascade of blades in airfoil and wing designs, heat transfer, ion optics, solidification, solid propellant rocket motors, plates, and vibrations. In most cases, the results are developed throughout the book from the basics at a level consistent with the mathematical background of the intended readers. In a few instances the results are stated and the original references are cited. Each chapter ends with exercises in the form of problems, some of which are more challenging and a few are at the research level. Possible references are provided where solutions to these problems may be found. Each chapter ends with a list of references used in presenting the related subject matter. The intended readers fall into one of several categories. First, they are students ready for a graduate course in this subject. For them the book can be used as a textbook or a reference book. The second category is that of graduate students engaged in research. For them the book should become a constant companion, because it is filled with a vast amount of information on methodology and an almost complete bibliography on the subject. The third category consists of scientists and researchers in various areas of applied mathematics, engineering and physics. For them the book is a vital source of information in classical as well as modern trends in research in the subject itself as well as in numerical methods for Fredholm integral equations of the first and the second kind. Research scientists, engineers, and mathematicians will appreciate this comprehensive and up-to-date account of all methods available on the subject. Some of the techniques are very efficient, and, although not explicit in the title of this work,

numerical treatment of Fredholm integral equations is dealt with in depth in this book.

---

## Computational Aspects

It has been my experience that Mathematica and a programming language, like Fortran or C++, are sufficient to carry out any and all computational aspects of the methods presented in the book. Many programs that may be needed to complete computations are available in the public domain. Most of them deal with numerical solution of Fredholm integral equations. Only a few need be developed. The algorithms provided in the book are detailed enough to generate computer programs with ease. Besides the algorithms, there are 74 cases studies presented in the book, supplemented by 96 suggested problems with hints for finding solutions.

---

## Acknowledgements

The help provided by some of my colleagues and students is gratefully acknowledged. Thanks are also due to the editors at Birkhauser – Boston who offered valuable suggestions for editorial improvements. I am very grateful to my wife, Mrs. B. D. ‘Kiran’ Kulshrestha, for continuous support and inspiration over the years, including the period for preparing this book.

New Orleans, Louisiana  
March, 1998

“Die Ausführung dieser Theorie, welche, wie bemerkt, einfache durch Grössenoperationen bedingte Abhängigkeitsgesetze ins Licht zur setzen bestimmt ist, unterlassen wir indess jetzt, da wir die Betrachtung des Ausdrucken einer Function gegenwärtig ausschliessen.

Aus demselben Grunde befassen wir uns hier auch nicht damit, die Brauchbarkeit unserer Sätze als Grundlagen einer allgemeinen Theorie dieser Abhängigkeitsgesetze darzuthun, wozu der Beweis erfordert wird, dass der hier zu Grunde gelegte Begriff einer Function einer veränderlichen complexen Grösse mit dem einer durch Grössenoperationen ausdrückbaren Abhängigkeit völlig zusammenfällt.”

*Bernhard Riemann  
Inaugural Dissertation, Göttingen, 1851*

## The Author

---

Prem Kishore Kythe (formerly Kulshrestha), b. India, 29 January 1930. Naturalized U. S. citizen. *Educ.*: Ph. D. (Mathematics, Univalent Functions), Aligarh Muslim University, India, 1961. *Prof. Exp.*: Faculty member at Aligarh Muslim University 1958–60; at Indian Institute of Technology, Bombay, 1960–67; at University of New Orleans (UNO) 1967–; Professor of Mathematics at UNO since 1974. Invited speaker at the NATO Advanced Institute for Automatic Translation (from Russian) at Venice, Italy, July 1962. UNESCO Fellow in Linguistic Data Processing (Machine Translation) 1963. Consultant, Institute of Human Learning, University of California at Berkeley 1964. Guest participant in the Summer Linguistics Institute, University of Washington, Seattle, WA, June–August 1963. Participant in Summer School on Complex Function Theory, University of Cork, Ireland, 1971. Visitor at Mathematics Department, Imperial College, London, Fall 1973. Visiting Professor, Department of Computer Science, University of Illinois at Urbana-Champaign, Spring 1986. Reviewer for the Bulletin, Institute of Mathematics, Academia Sinica, for the JEMT ASME, for NSF, for Zentralblatt für Mathematik, and for Applied Mechanics Reviews. Over 15 books/monographs and some research papers translated from Russian into English. Over 40 research publications in the areas of univalent functions, boundary value problems in continuum mechanics, differential equations, Laplace transform, wave theory, and wave structure in rotating flows. Numerous citations in research articles, and graduate text/monographs. Listed in American Men and Women of Science. Author of three books: *An Introduction to Boundary Element Methods* (CRC Press, 1995), *Fundamental Solutions for Differential Operators and Applications* (Birkhäuser, 1996), and *Partial Differential Equations and Mathematica* (co-authors: P. Puri and M. R. Schäferkotter, CRC Press, 1997).

# Chapter 0

---

## Introduction

---

Current research in computational conformal mapping has taken two major directions. One direction involves the conformal mapping from a standard region, like the unit disk or the upper half-plane, onto the problem region, whereas in the other it is from the problem region onto a standard region. In the former case one solves a nonlinear integral equation involving the conjugate operator (e.g., Theodorsen's integral equation), by fast Fourier transform (FFT), polynomial approximation, iteration, or Newton's method. In the latter case the integral equation, derived from the Dirichlet problem, is linear or singular linear if it is derived from potential theory (e.g., Symm's integral equation). Depending on the nature of the problem region, these methods sometimes use the Schwarz–Christoffel transformations. The historical development of different methods for computational conformal mapping of simply and multiply connected regions is sketched below.

---

### 0.1. Historical Background

The oldest transformation, known as the stereographic projection of the sphere, was used by Claudius Ptolemy (ca. 150 A.D.) to represent the celestial sphere. In a totally different mapping of a sphere onto a plane, known as Mercator's projection, the spherical earth is cut along a meridian circle and conformally mapped onto a plane strip. Gerhardus Mercator which was the Latinized name of the Flemish geographer Gerhard Kremer published the first world map in 1569 using this technique, and ever since all sea maps are

constructed by the method. These two projections, however, do not produce similar maps of the same region of the earth, which shows that conformal mapping does not imply similarity of figures. Johann Lambert (1728–1777) was the first mathematician who made contributions to the mathematical projection of maps. These and other similar considerations enabled Lagrange (1779) to obtain all conformal representations of a portion of the earth’s surface onto a plane where all circles of longitudes and latitudes are represented by circular arcs. Gauss (1822) was the first to state and completely solve the general problem of determining all conformal mappings that transform a very small neighborhood of a point on an arbitrary analytic surface onto a plane area. However, Gauss’ work did open the harder problem of finding the way whereby a given finite portion of a surface can be mapped onto a portion of the plane. A breakthrough came in 1851 when Riemann gave the fundamental result, known as the Riemann mapping theorem, which has since been a turning point for all subsequent developments in the theory of conformal mapping. In the proof of this theorem he assumed that a variational problem, now known as the Dirichlet problem, possesses a solution. It was fifty years later that Hilbert (1901) proved the existence of the solution of the Dirichlet problem. In the mean-time the validity of Riemann’s result was established rigorously by Schwarz (1890) by using a number of theorems from the theory of logarithmic potential.

After the basic theoretical aspects of the theory of functions of a complex variable and conformal mapping were established by Cauchy, Riemann, Schwarz, Christoffel, Bieberbach, Carathéodory, Goursat, Koebe, and others in the nineteenth and early decades of the twentieth century, the first numerical research into developing a method for mapping a region bounded by finitely many Jordan curves  $\Gamma_i$  onto an  $n$ -sheeted Riemann surface where the curves  $\Gamma_i$  correspond to rectilinear slits was done by Burnside (1891). A minimizing principle was established by Bieberbach (1914), namely, that among all suitably normed conformal maps of a given simply connected region the one with the least area is the conformal map onto a circle. In particular, this principle evolved as a result of minimizing the integral  $\iint_D \|f'(z)\|^2 dx dy$ , where  $f$  is regular in  $D$  and normalized by  $f(0) = 0$ ,  $f'(0) = 1$ , and the area theorem. Bieberbach used the Ritz method to find an approximate solution in the form of a polynomial for the above integral and used it to construct the conformal map of a simply connected region onto a circle. An exposition of the Ritz method can be found in Kantorovich and Krylov (1936). The estimates obtained by this method were later improved by Höhndorf (1926) and Müller (1938) in the problem of a conformal map of a nearly circular region onto a circle. Other improvements on the Bieberbach method were produced by Landau (1926), Julia

(1926), and Kantorovich and Krylov (1936) who also developed a graphical method of conformal mapping due to Melent'ev (1937).

The first integral equation method was developed by Lichtenstein (1917) who solved the problem of conformally mapping a simply connected region bounded by a Jordan contour onto a circle by reducing it to the solution of an integral equation. Other attempts in this direction were made by Krylov and Bogolyubov (1929) who reduced the Dirichlet problem to an integral equation which is approximately solved by the Fredholm method with error estimates. Nyström (1930) gave a method for an approximate solution of integral equations, which is useful in conformal mapping. For conformal mappings of nearly circular regions the first numerical work was done by Fock (1929) who determined numerically the mapping function for a circular quadrilateral with angles  $\pi/2, \pi/2, \pi/2, 0$ . An important result, now known as Theodorsen's integral equation, was developed by Theodorsen (1931) and improved upon by Theodorsen and Garrick (1933) for conformally mapping nearly circular regions onto a circle. Another integral equation, known as Gershgorin's equation, was developed by Gershgorin (1933) as a result of conformally mapping a simply connected region bounded by a Jordan contour onto a circle, which is solved by the Nyström method. An exposition on Gershgorin's integral equation and its application to the mapping of a simply connected region onto a circle, of a doubly connected region onto an annulus, and of a multiply connected region, in general, onto slit planes is available in Kantorovich and Krylov (1936). Various applications of conformal mapping are available in the monograph by Kantorovich and Krylov (1936), where both harmonic and biharmonic functions are studied. The Dirichlet and Neumann problems in  $\mathbb{R}^2$  are solved by conformal mapping for different boundary conditions, and the general Hilbert problem is also investigated. Later Banin (1943) developed a method of approximately replacing Gershgorin's integral equation by a system of linear differential equations. Krylov (1938) also reduced the problem of conformally mapping an  $n$ -connected region bounded by  $n$  Jordan contours onto various canonical regions to the problem of solving a system of simultaneous integral equations.

Successive approximations in the integral equation method for simply and multiply connected regions were used by Kantorovich (1933, 1937). Following Theodorsen's integral equation method, Warschawski (1945) reduced the problem of conformal mapping of a simply connected region bounded by a Jordan contour onto the unit circle to that of solving a nonlinear integral equation which is then solved by the method of successive approximations where the precise estimates for the convergence are also provided. Goluzin (1934)

investigated the region exterior to the circles  $C_1, \dots, C_n$  and determined a harmonic function  $u(x, y)$  for this region such that it takes preassigned values on  $C_i$ ,  $i = 1, \dots, n$ , and  $u(\infty) < \infty$ . The problem is then reduced to that of solving a finite system of functional equations which are solved by successive approximations. He applied this method to solve the Neumann problem for the Laplace equation for such regions and determined the Green's function for such regions and the conformal maps that carry such regions onto slit planes. The Schwarz method is used to develop an integral equation which is solved by successive approximations in Nevanlinna (1939) and Epstein (1948).

Julia (1927) determined a sequence of polynomials which converges to a suitably normed mapping of a simply connected region. An application of orthogonal polynomials to conformal mapping of simply connected regions was first developed by Szegö (1921). He defines a set of polynomials  $P_0(z), P_1(z), \dots, P_n(z), \dots$  (subsequently known as the Szegö polynomials) for a closed Jordan contour  $\Gamma$  in the  $z$ -plane, satisfying the following two properties: (i)  $P_n(z)$  is a polynomial of degree  $n$ , i.e.,  $P_n(z) = a_n z^n + a_{n-1} z^{n-1} + \dots + a_1 z + a_0$ , such that  $a_n > 0$ , and (ii)  $\frac{1}{l} \int_{\gamma} P_m(z) \overline{P_n(z)} ds = \delta_{m,n}$ , where  $l$  is the length of  $\Gamma$ ,  $s$  its arc length, and  $\delta_{m,n}$  the Kronecker delta. Then the series  $K(a, z) = \sum_{n=0}^{\infty} \overline{P_n(a)} P_n(z)$  converges uniformly and absolutely in every closed subregion of the interior of  $\Gamma$ . A formula is then obtained which defines the mapping function of the interior of  $\Gamma$  onto the unit disk in terms of  $K(a, z)$ . Szegö also gave a mapping function for the exterior of  $\Gamma$  by the polynomials  $P_n(z)$ . Further developments in the Szegö polynomial method were produced by Smirnov (1928) and later by Kantorovich and Krylov (1936) who investigated the Szegö and Bochner–Bergman type polynomials and applied them to the minimizing problem. Some results about approximate mapping functions for a simply connected region by means of certain polynomials were given by Schaginyan (1944).

The problem of minimizing a functional was first solved by Hadamard (1908) which later became known as the Hadamard variational method. Löwner (1923) also developed an important variational method, whereas Julia (1926) provided another characterization of the mapping function by a minimum principle. The problem of reducing the mapping problem to that of minimizing of a functional was solved by Douglas (1931) who used the Riemann mapping theorem and the Osgood–Carathéodory theorem. Kufarev (1935–1937) investigated a minimal problem for a single-valued analytic function in an annulus

and discussed the mapping of the minimizing function. Later in 1947 he used the Löwner method to study a polygonal problem region which consists of the whole plane cut by a broken polygonal line with finitely many sides, one of which extends to infinity. The problem of mapping a doubly connected region onto an annulus was reduced to that of minimizing an area integral by Khajalia (1940), who also showed that if the region is accessible from without, then there exists a sequence of minimal rational functions that converges uniformly to the desired mapping function. The problem of mapping a simply connected region bounded by a Jordan contour is reduced by Shiffman (1939) to that of minimizing a functional, almost similar to that of Douglas. This problem deals with the Plateau problem, and the electrostatic characterization of the resulting functional provides an effective method for determining the conformal maps. The Hadamard formula and the variation of domain functions were used by Schiffer (1946) to derive a new variational method.

In 1931 Grötsch solved the problem of conformally mapping a multiply connected region onto some canonical regions based on the assumption that the solution of a similar problem for a simply connected region is known. Iterative methods were established by Goluzin (1939) who used to map a multiply connected region conformally onto some canonical regions, thereby reducing the problem to a sequence of conformal maps of simply connected regions. Heinhold (1947) investigated the problem of conformally mapping the simply connected region lying in the exterior of the unit circle onto the exterior of the unit circle.

Green's function method for an arbitrary region was established by Leja (1934, 1936) where the approximating functions were found closely related to Lagrange polynomials. A set of polynomials was also obtained which were used as mapping function for a region  $D$ , containing the point at infinity, onto the exterior of the unit circle. It was determined that the map is univalent if  $D$  is simply connected.

The Schwarz–Christoffel formula was used by Bergman in 1923–24 to map a half-plane onto a particular polygon where a method for determining the parameters in the formula from the lengths of the sides of the polygon is given. In 1925 he investigated the conformal map of a special polygon onto a rectangle and computed level curves and their orthogonal trajectories which were presented in tabular and graphical forms. Bergman also gave the first punch–card machine method in 1947 to solve the torsion problem where the orthogonal polynomials were applied to solve the Laplace equation numerically. The notion of the kernel functions was developed by Bergman in 1922 where

the existence of a complete orthonormal system with respect to a region is established and the kernel of the system is related to the conformal map of the region. Based on Bergman's kernel function and complete orthonormal sets of functions, Zarankiewicz (1934) found a method for effectively constructing the conformal map of a doubly connected region onto an annulus; in 1934 he published details of this method. Schiffer (1946) found an expression for Bergman's kernel function  $K(z, a)$  of a region in terms of Green's function for the region and gave formulas for the variation of  $K(z, a)$ . In 1948 he extended the concept of kernel functions and orthonormal sets of functions to a wider class of functions. Further study of the relationship between the kernel function and conformal mappings of regions was done by Bergman and Schiffer (1948-1951).

Hodgkinson and Poole (1924) used elliptic functions to map doubly connected regions of certain types onto the whole plane with two slits on the real axis. Using hyperelliptic integrals, a generalization of the solution by Hodgkinson and Poole was given by Vladimirska (1941) for the problem of conformal mapping of a doubly connected region bounded by rectangular segments or circular arcs, who also extended the solution to  $n$ -tuply connected regions ( $n > 2$ ). Hodgkinson (1930) also established the relationship between the theory of Lamé differential equations and the Schwarz theory of conformal mapping. An up-to-date survey of conformal mapping of multiply connected regions onto canonical domains was published by Keldyš (1939). Important formulas for various conformal maps of  $n$ -tuply connected regions in terms of the kernel function of the region were established by Nehari in 1949. These formulas served as tools for numerical computation of conformal maps since the kernel functions are constructed more easily than the mapping function. Gerabedian and Schiffer (1949) obtained many significant relations between various domain functions of an  $n$ -tuply connected region and solved some minimal problems.

The first systematic construction of conformal maps by the method of networks was done by Liebmann (1918). The Dirichlet problem in  $\mathbb{R}^2$  and  $\mathbb{R}^3$  was first solved by this method by Phillips and Wiener (1923). The boundary problems in  $\mathbb{R}^2$  with the Laplace equation were solved numerically by this method by Luysternik (1947).

Relaxation methods were first applied to the problems of conformal mapping by Gandy and Southwell (1940) and Southwell (1946). Several examples of technical interest were given, in which regions of arbitrary shape are mapped onto the interior and exterior of circles and onto rectangles.

The small parameters method developed by Kantorovich (1933) was later used by Rosenblatt and Turski (1936) for conformal mapping of a special type of region. Rosenblatt (1943) constructed the conformal maps of regions onto the unit disk by the Kantorovich method of small parameters and applied it to the dynamic problems of airfoils.

Special conformal mappings were studied by Rothe (1908) who constructed the mapping function for a circular quadrilateral with angles  $\pi/2, \pi/2, \pi/2, \rho\pi$  ( $\rho = 1/\sqrt{20}$ ). Hodgkinson's work (1924) on a similar problem has been mentioned above. Wirtinger (1927) derived an explicit formula for computing the conformal map of a triangle with circular arcs and arbitrary angles. The mapping of an ellipse onto a circle and of a region bounded by two symmetrically placed ellipses onto an annulus were investigated by Zmorovich (1935) who also gave an approximate solution in the latter problem. Catalogs of various types of explicit mappings are available in Koppenfels' papers (1937, 1939). Other authors on special conformal mappings during this period were Muratov (1937), Krylov (1937), Melent'ev (1937), and Goluzin (1937). Later Jeffreys and Jeffreys (1946) and Wittich (1947) produced special conformal maps. A very useful dictionary of conformal mappings, which is still a source work in this area, was produced by Kober (1945–1948).

The theory of homogeneous boundary problems for analytic functions was presented by Hilbert (1924) for a boundary that is a single Jordan contour. Then he transformed this problem into a Fredholm integral equation, for which Green's functions of the Neumann problem must be determined. Hilbert did not give a complete solution of this integral equation. A complete solution by means of Cauchy integrals for a particular case had already been given by Plemelj (1908). The solution for the general case, based on the Plemelj method, was later provided by Khvedelidze (1941). Picard (1927) had studied the homogeneous Hilbert problem earlier. The nonhomogeneous Hilbert problem which is solved to determine a sectionally analytic function  $\Phi(z)$  of finite degree at infinity such that  $\Phi^+(\zeta) = G(\zeta)\Phi^-(\zeta) + g(\zeta)$  on the boundary  $\Gamma$ , where  $G(\zeta)$  and  $g(\zeta)$  are defined on the boundary  $\Gamma$  and satisfy the Hölder condition there, was first considered by Carleman (1922). Later Privalov (1934) investigated it for the case when the boundary  $\Gamma$  is a rectilinear contour,  $G(\zeta)$  and  $g(\zeta)$  are Lebesgue-integrable,  $G(\zeta)$  is bounded, and the limiting value of the solution is taken along a nontangential path. He used Picard's method but did not find a complete solution. A complete solution was first given by Gakhov (1937) for the case when  $\Gamma$  is a single contour. Later Khvedelidze (1941) gave a complete solution of the nonhomogeneous Hilbert problem. Carleman's and Gakhov's methods are essentially alike. In 1851 Riemann considered a very general

boundary problem which is now known as the Riemann boundary problem. This problem was also studied and solved by Hilbert in 1904, and therefore it is also called the Riemann–Hilbert problem. It deals with determining an analytic function in a given region with boundary values involving a relation between its real and imaginary parts. Hilbert reduced this problem to a singular equation and then applied it to the solution of two Dirichlet problems. Later Noether (1921) used this solution to study the subject of singular integral equations.

One of the widely investigated practical aspects of conformal mapping was the development of the airfoil theory which started with the pioneering work by Joukowski (1890). He studied the flows around a variety of so-called Joukowski airfoils. The developments in this area are very pertinent for computational aerodynamic flows. Extensive research to develop computational methods for solving the direct and inverse problems of airfoil theory has been done by Theodorsen (1931), Glauert (1948), Andersen, Christiansen, Møller and Tornehave (1962), Timman (1951), James (1971), Ives (1976), and Halsey (1979, 1982). In single and multi-element airfoils, Theodorsen’s integral equation has been solved with the von Karman–Treffitz transformation and the FFT by Garrick’s method of conjugate functions (Garrick, 1949) by Ives (1976). James’s method (James, 1971) is another approach in the conformal mapping of single and multiple-element airfoils (Halsey 1979, 1982).

## 0.2. Modern Developments

During the last four decades several methods have evolved for numerical and computational evaluation of mapping functions. The results of some of these methods provide us with an explicit form of a function which approximately evaluates the mapping function for a certain source region. This is possible because of an important result which states that an analytic function defined on a simply connected and bounded region  $D \subset \mathbb{C}$  can always be uniformly approximated on every compact subset of  $D$  with any preassigned accuracy by means of a polynomial. In most applications the mapping function is continuous in  $\bar{D}$ , and it can be uniformly approximated in  $D$  by a polynomial.

One major approach in developing methods for numerical conformal mapping is based on the following interpretation of the Riemann mapping theorem: there exists a conformal mapping  $f : D \mapsto U$  with  $f(z_0) = 0$

and  $f'(z_0)$  nonzero real, where  $z_0 \in D$ , and this function has a power series expansion  $f(z) = c_1 (z - z_0) + \sum_{n=2}^{\infty} c_n (z - z_0)^n$ , with  $c_1$  nonzero real

and  $z_0 \in D$ , which converges uniformly in every closed disk with center  $z_0$  and contained in  $D$ . However, a polynomial which is a good approximation of  $f$  in  $D$  is not the same as a truncated power series. If a polynomial

$$p(z) = c'_1 (z - z_0) + \sum_{n=2}^N c'_n (z - z_0)^n$$

approximates  $f$  with accuracy  $\varepsilon > 0$ ,

then it is necessary that every term of  $p(z)$  must approximate the corresponding term of the power series with accuracy  $\varepsilon > 0$  on the set  $D \cap B(z_0, R)$ , where  $R = |z - z_0|$  is the radius of convergence of the power series. All this means is that a polynomial  $p$  which is a good approximation of the power series starts in the same way as the power series, but the relative error in the coefficients increases with increasing  $n$ .

Another direction for developing numerical methods for conformal mapping is based on computing a table of values for the mapping function  $f$  at several points of  $D$ . The mapping function  $f$  always maps the boundary of the source region  $D$  in a simple way onto the boundary of the unit disk  $U$ . Once the mapping of the boundary is known, the mapping of  $D$  itself is determined by the Cauchy formula with positive orientation of the boundary curve. Thus, it is sufficient to determine the mapping of the boundary of  $D$  onto the boundary of  $U$ , and once we obtain a parametric representation of the boundary of  $D$ , we determine only one real-valued function of a real variable  $t$ . But in this approach it so happens that this unknown real-valued function satisfies an integral equation. Hence, solving the problem of conformal mapping reduces to that of solving an integral equation.

The widely used current computational techniques are based on the integral equation methods where an integral equation is developed to relate the boundaries of the problem region and the standard region like the unit disk. Once the boundaries are discretized at  $n$  points, the integral equation reduces to an algebraic system of equations. The majority of ongoing research in computational conformal mapping is divided basically into two groups: one where the maps are constructed from a standard region such as the unit disk onto the problem region, and the other where the maps are constructed the other way around. In the first group the integral equation is nonlinear and involves the conjugation operator, which can be solved by FFT on a discrete mesh in  $O(n \log n)$  operations. This method evolves with the numerical solution of Theodorsen's integral equation, or a related equation, which is solved by us-

ing the fixed-point iteration method. The recent development of Newton's method is faster for sufficiently smooth boundaries and the choice of a good initial guess. The basic work in this group has been produced by Wegmann (1978, 1986), Hübner (1986), and Gutknecht (1986). The first quadratically convergent algorithm for Theodorsen's equation was presented by Wegmann (1978) based on the following two ideas: an induction scheme along tangents to the boundary of the problem region, and a computation scheme similar in formulation to the Riemann–Hilbert problem for the unit disk at each iteration. This method is efficient because the solution of the Riemann–Hilbert problem can be represented by Cauchy integrals. A generalization of this algorithm to the conformal mapping of an annulus onto a doubly connected region was published by Wegmann in 1986. This algorithm is also based on the Riemann–Hilbert problem and is so far the fastest known for this problem. Hübner (1979, 1986) studied Newton's method for the solution of Theodorsen's integral equation. His method is also based on the solution of the Riemann–Hilbert problem. He established the quadratic convergence of Newton's method and obtained a quadratically convergent conformal mapping. An extensive survey of almost all known methods for numerical conformal mapping of the unit disk onto a simply connected region is available in Gutknecht's work (1986). He has derived integral and integro–differential equations involving the conjugation operator for the boundary correspondence function. Then various iterative schemes for solving these equations are presented in this work. The general theory is described by specific methods, especially the successive conjugation methods of Theodorsen (1931), Timman (1951), Freiberg (1951), the projection method of Bergström (1958), Newton's method of Vertgeim (1958), Wegmann (1978), and Hübner (1979).

In the other group where the maps are constructed from the problem region onto the unit disk, the integral equations, mostly derived from the Dirichlet problem, are generally linear, and require  $O(n^2 \log n)$  operations. In cases where the geometry is simpler, they may require a smaller number of operations. The methods in this group are based on Symm's equation (1966) which is a singular integral equation of the first kind derived by using a single-layer potential as the basis of conformal mapping. Symm (1966, 1969) investigated an integral equation method, like the one he developed for the boundary integral equation method, for computing the conformal mapping of a simply connected region onto the unit disk. Berrut (1976, 1985, 1986) solved Symm's equation numerically by a Fourier method. This equation is a Fredholm integral equation of the second kind for the derivative of the boundary correspondence function for the conformal mapping of a Jordan region with a piecewise twice differentiable boundary onto the unit disk. Kerzman and Trummer (1986) presented a new

method to compute the Riemann mapping function numerically. The solution of the integral equation of the second kind is expressed in terms of the Szegö kernel and is based on an earlier work of Kerzman and Stein (1978) on the Cauchy kernel, Szegö kernel and Riemann mapping function, and of Kerzman and Trummer (1986) on a method for the numerical solution of the conformal mapping problem.

A variant of Symm's integral equation which is suitable for conformal mapping of both simply and multiply connected regions was presented by Reichel (1985). It uses a Fourier–Galerkin technique to produce an extremely fast iterative solution of  $\mathcal{O}(n^2 \log n)$  which is due to the singularity of the kernel so that the linear algebraic system becomes block diagonally dominant. Another fast method for solving Symm's equation for multiply connected regions was presented by Mayo (1986). This integral equation formulation is based on a similar formulation in Mikhlin (1957) and has the advantage of reducing the problems to integral equations of the second kind with unique solutions and boundary kernels. Because the solutions are periodic, the trapezoidal rule can be applied effectively. Once the integral equation is solved, a rapid method is available to determine the mapping function in the interior of the region. This method uses a fast Poisson solver for the Laplacian, thus avoiding the time-consuming computation of integrals at singular points near the boundary.

Other significant modern research includes work by Hoidn (1982) which deals with conformal mapping of simply connected regions where the singularity problem near and on the boundary is solved by reparametrization of the boundary curve. Then this method is applied to Symm's equations which are solved by using spline functions. The singularity problem has been solved by Levin, Papamichael and Sideridis (1978), Hough and Papamichael (1981, 1983), Papamichael and Kokkinos (1981, 1982), Papamichael and Warby (1984), and Papamichael, Warby and Hough (1983, 1986) by integral equation methods as well as expansion methods based on the Bergman kernel or on the Ritz approximation. No research is available in this area for multiply connected regions of higher connectivity. The Chebyshev approximation in conjunction with linear programming has been used by Hartman and Opfer (1986) for conformal mapping of simply connected regions onto the unit disk. A simple approximation formula has been derived by Zemach (1986) for the boundary mapping function which gives a remarkably good fit for mappings of regions with highly distorted boundaries. This method is based on reducing the nonlocal integral equation for the mapping function to a local equation depending on the nature of the distorted regions. The Schwarz–Christoffel formula has always been used in mappings of polygons and related regions,

but the treatment of the singularity problem in these cases has been only recently investigated by Barnard and Pearce (1986), Elcrat and Trefethen (1986), and Trefethen and Williams (1986). Boundary problems for analytic functions and integral equations with transformations have been discussed by Lu (1994), and a comprehensive theoretical account on conformal mapping and boundary problems can be found in Wen (1992).

The advantages of integral equation formulation in conformal mapping can be summarized as follows: All integral equations obtained in any conformal mapping problem (except Arbenz's integral equation, see §12.1) are Fredholm integral equations of the second kind with bounded kernel, except for Symm's integral equation which is of the first kind with a kernel that has a logarithmic singularity. The Fredholm integral equations of second kind are never ill-conditioned, and there are reliable error estimates available for them. However, the drawback with the equations of second kind is that the kernel has singularity at points in the neighborhood of the boundary (but not on the boundary itself unless it has a corner singularity) where computational difficulties often arise. This situation, on the other hand, does not occur with the equations of the first kind.

The best strategy for developing a computational method based on an integral equation formulation is to make sure that the solution is periodic and unique. This permits an effective use of the trapezoid rule which is highly accurate on smooth contours. Another feature to look for is that the mapping onto canonical regions (unit disk, annulus, or slit disks) produces systems of linear equations and avoids solving systems of nonlinear equations as in Fornberg's, Guteknecht's, or Wegman's methods.

Some classical applications of conformal mappings to steady state problems of mathematical physics and especially for the solution of the Laplace equation can be traced to the beginning of the twentieth century. A noteworthy contribution to the theory of elasticity is by Muskhelishvili (1963). Modern contributions can be found in areas of fluid flow, heat conduction, solidification, electromagnetics, ion optics, acoustics, vibrations, wave guides, and grid generation, to name a few; a detailed review and biography of the applications through 1972 is available in Laura (1975). The problem of flow and heat transfer in conduits of arbitrary shape in space vehicles was investigated by Sparrow and Haji-Sheikh (1966). This study was extended to noncircular conduits with uniform wall temperature by Casarella et al (1971). Unsteady heat conduction problems in bars of arbitrary cross section were investigated by Laura et al.(1964, 1965, 1968). Ives (1976) analyzed the incompressible flow between

two concentric circles and computed the streamlines by using Garrick's method of conjugate functions. The problem of solidification of steady-state and transient frozen layers in rectangular channels has been solved by Siegel, Goldstein and Savino (1970). In transient solidification the shape of a frozen region is determined by mapping it onto a potential plane and then computing the time-dependent conformal map between the potential and the physical plane. The thermoelastic problem of uniform heat flow distributed by an isolated hole of ovaloid form was investigated by Florence and Goodier (1960) and extended by Deresiewicz (1961) to holes which are mapped onto the unit circle and approximated by polynomials.

Wilson (1963) and Richardson (1965) used conformal mapping to determine the stresses in solid propellant rocket grains by solving an integral equation of the Fredholm type and a system of coupled integral equations. The method of computing the conformal mapping function and the related eigenvalue problem for plane regions with irregular boundaries was published by Laura (1968). The ion problem connected with the trajectory of a charged particle in a plane electric field and a normal magnetic field was solved by Naidu and Westphal (1966) by using the Schwarz-Christoffel transformation. Conformal mapping techniques of simply and doubly connected regions have been used, among others, by Kasin and Merkulov (1966), Laura (1967), and Laura et al. (1972).

Conformal mapping has been applied to acoustic waveguides of complicated cross section where the Galerkin method is applied to obtain a functional approximation for the solution of the boundary value problem. The grain of a solid propellant rocket motor with a starlike internal propagation is in the form of a circular cylinder bounded by a thin case. To solve any boundary value or eigenvalue problem, the grain cross section is conformally mapped onto a circle or an annulus. Studies on the shear vibrations of such rocket motors were done by Baltrukonis et al. (1965) and Laura and Shahady (1966). Conformal mapping techniques are used in a study on the Rayleigh-Taylor instability for ideal fluid by Menikoff and Zemach (1980, 1983). Grid generation for cascades of blades and inlet flows has been investigated by Inoue (1983, 1985). The Kirchhoff flow problem past a polygonal obstacle was solved by Trefethen (1986). Other contemporary applications can be found in the book on numerical conformal mapping edited by Trefethen (1986).

Computational conformal mapping in the present decade is still progressing steadily. Fast algorithms are being developed. Computational conformal mapping is being used in engineering problems that require grid generation and related domain simplification. Although the use of conformal mapping in reduc-

ing or eliminating singularities in solutions of integral and integro-differential equations is one important issue, the choice of an initial good guess in Newton's method is another. Much has developed since the evolution of computer technology around 1955, but this subject has not yet reached maturity.

REFERENCES USED: Andersen et al. (1962), Barnard and Pearce (1986), Berrut (1986), Carathéodory (1969), Elcrat and Trefethen (1986), Freiberg (1951), Gaier (1964, 1983), Goluzin (1969), Gutknecht (1986), Hartman and Opfer (1986), Hoidn (1986), Hübner (1979, 1986), Ives (1982), James (1971), Jawson (1963), Jawson and Symm (1977), Kantorovich and Krylov (1958), Kerzman and Stein (1978), Kerzman and Trummer (1986), Kober (1957), Laura (1975), Lawrentjew and Schabat (1967), Lu (1994), Mayo (1986), Mikhlin (1957), Nehari (1949, 1952), Papamichael et al. (1981, 1983, 1984, 1986), Riemann (1851), Seidel (1952), Symm (1966), Trefethen (1980), Trefethen and Williams (1986), Wegmann (1979, 1986), Wen (1992), Zemach (1986).

# Chapter 1

---

## Basic Concepts

---

Some basic concepts and results from complex analysis are presented. They include harmonic functions, Cauchy's theorem, Cauchy kernel, Riemann mapping theorem, analytic continuation, and the Schwarz reflection principle. Proofs for most of the results can be found in textbooks. References that were mostly used are cited at the end of the chapter.

---

### 1.1. Notation and Definitions

A complex-valued function  $f$  is said to belong to the class  $C^k(D)$  if it is continuous together with its  $k$ -th derivatives, in a domain  $D$ ,  $0 \leq k < \infty$ . In this case we shall often write that  $f$  is a  $C^k(D)$ -function, or that  $f$  is a  $C^k$ -function on  $D$ , and a  $C^0$ -function is written as a  $C$ -function. The function  $f$  in the class  $C^k(D)$ , for which all  $k$ -th derivatives admit continuous continuations in the closure  $\bar{D}$ , form the class of functions  $C^k(\bar{D})$ . The class  $C^\infty(D)$  consists of functions  $f$  which are infinitely differentiable on  $D$ , i.e., continuous partial derivative of all orders exist. These classes are linear sets. Thus, every linear combination  $\lambda f + \mu g$ , where  $\lambda$  and  $\mu$  are arbitrary complex numbers, also belongs to the respective class.

Let  $\mathbb{R}^n$  denote the Euclidean  $n$ -space, and  $\mathbb{R}^+$  the set of nonnegative real numbers. The complement of a set  $B$  with respect to a set  $A$  is denoted by  $A \setminus B$  (or  $\text{compl}(B)$  if the reference to set  $A$  is obvious), the product of the sets  $A$  and  $B$  by  $A \times B$ , and the closure of a set  $A$  by  $\bar{A}$ .

Let  $\mathbb{C}$  denote the complex plane. If  $a \in \mathbb{C}$  and  $r > 0$ , then

$$\begin{aligned} B(a, r) &= \{z \in \mathbb{C} : |z - a| < r\}, \\ \bar{B}(a, r) &= \{z \in \mathbb{C} : |z - a| \leq r\}, \\ \partial B(a, r) &= \{z \in \mathbb{C} : |z - a| = r\}, \end{aligned} \quad (1.1.1)$$

denotes, respectively, an open disk, a closed disk, and a circle, each of radius  $r$  and centered at  $a$ . An open unit disk  $B(0, 1)$  is sometimes denoted by  $U$ . A connected open set  $A \subseteq \mathbb{C}$  is called a region (or domain). The extended complex plane is denoted by  $\mathbb{C}_\infty$ . Then  $\partial_\infty D$  is the boundary of a set  $D$  in  $\mathbb{C}_\infty$ , i.e.,

$$\partial_\infty D = \begin{cases} \partial D & \text{if } D \text{ is bounded,} \\ \partial D \cup \{\infty\} & \text{if } D \text{ is unbounded.} \end{cases}$$

If  $D$  is a region in  $\mathbb{C}_\infty$ , then the following statements are equivalent: (a)  $D$  is simply connected, (b)  $\mathbb{C}_\infty \setminus D$  is connected, and (c)  $\partial_\infty D$  is connected. Regions that have more than one layer over the complex plane are called Riemann surfaces.

Let  $z = x + iy$  be a complex number. Then  $\bar{z} = x - iy$ ,  $x = \frac{z + \bar{z}}{2}$ , and  $y = \frac{z - \bar{z}}{2i}$ . Also

$$\partial f = \frac{\partial f}{\partial z} = \frac{1}{2} (f_x - i f_y), \quad \bar{\partial} f = \frac{\partial f}{\partial \bar{z}} = \frac{1}{2} (f_x + i f_y). \quad (1.1.2)$$

A function  $f : D \mapsto \mathbb{C}$  is analytic on  $D$  iff  $\bar{\partial} f = 0$ , which is equivalent to the Cauchy–Riemann equations for the function  $w = f(z) = u(x, y) + iv(x, y)$ :

$$u_x = v_y, \quad u_y = -v_x, \quad (1.1.3)$$

or, in polar form ( $z = re^{i\theta}$ ),

$$u_r = \frac{1}{r} v_\theta, \quad v_r = -\frac{1}{r} u_\theta. \quad (1.1.4)$$

Thus,

$$f'(z) = u_x + iv_x = v_y - iu_y. \quad (1.1.5)$$

The Cauchy–Riemann equations are necessary conditions for  $f(z)$  to be analytic on  $D$ . However, merely satisfying the Cauchy–Riemann equations alone is not sufficient to ensure the differentiability of  $f(z)$  at a point in  $D$ .

The following results are obvious:  $\partial(\log|z|) = \frac{1}{2z}$ ,  $\bar{\partial}(\log|z|) = \frac{1}{2\bar{z}}$ ,  $\overline{\partial f} = \bar{\partial}\bar{f}$ , and the Laplacian

$$\nabla^2 \equiv \frac{\partial^2}{\partial x^2} + \frac{\partial^2}{\partial y^2} = 4\bar{\partial}\partial = 4\partial\bar{\partial}. \quad (1.1.6)$$

The Cauchy–Riemann equations (1.1.3) for the function  $f(z) = u(x, y) + iv(x, y)$  satisfy the partial differential equations

$$\begin{aligned} u_x v_x + u_y v_y &= 0, \\ \nabla^2 u &= 0, \quad \nabla^2 v = 0. \end{aligned} \quad (1.1.7)$$

Using the gradient vector  $\nabla \equiv i\frac{\partial}{\partial x} + j\frac{\partial}{\partial y}$ , the first equation in (1.1.7) can be written as the inner (scalar) product:

$$\langle \nabla u, \nabla v \rangle = 0. \quad (1.1.8)$$

Then the Cauchy–Riemann equations yield  $|\nabla u| = |\nabla v| = |f'(z)|$ . Eq (1.1.8) also signifies the orthogonality condition for the families of level curves defined by  $u(x, y) = \text{const}$  and  $v(x, y) = \text{const}$ .

If  $w = u + iv$ , then

$$\Re\{z\} \cdot \Re\{w\} = \Re\left\{\frac{z^2 + |z|^2}{2z} w\right\}, \quad \Im\{z\} \cdot \Im\{w\} = \Im\left\{\frac{z^2 - |z|^2}{2iz} w\right\}. \quad (1.1.9)$$

Let  $E$  denote a closed bounded infinite set of points in the  $z$ –plane. For the points  $z_1, z_2, \dots, z_n \in E$  the Vandermonde determinant is defined by

$$V(z_1, z_2, \dots, z_n) = \prod_{\substack{i,j=1 \\ i \neq j}}^n (z_i - z_j), \quad n \geq 2. \quad (1.1.10)$$

Let us define the numbers

$$d_n = V_n^{2/n(n-1)}, \quad (1.1.11)$$

where  $d_{n+1} \leq d_n$ . Since  $d_n$  does not exceed the diameter\* of the set  $E$  for any  $n$ , it follows that the sequence  $\{d_n\}$  approaches a finite limit as  $n \rightarrow \infty$ .

---

\*The diameter of the set  $E$  is defined as  $\sup_E \{|z_i - z_j| : z_i, z_j \in E\}$ ,  $i, j = 1, 2, \dots, n$  ( $i \neq j$ ).

This limit is called the *transfinite diameter* of the set  $E$  and is denoted by  $\text{diam}(E)$ , i.e.,  $\text{diam}(E) = \lim_{n \rightarrow \infty} d_n$ . When the set  $E$  has finitely many points, we take  $\text{diam}(E) = 0$ .

A simple closed curve  $\Gamma$  in  $\mathbb{C}$  is a path  $\gamma : [a, b] \mapsto \mathbb{C}$  such that  $\gamma(t) = \gamma(s)$  iff  $t = s$  or  $|t - s| = b - a$ . In what follows, a simple closed curve shall be called a *Jordan contour*. The Jordan curve theorem states that if  $\Gamma$  is a simple contour, then  $\mathbb{C} \setminus \Gamma$  has two components, one called the interior of  $\Gamma$ , denoted by  $\text{Int}(\Gamma)$ , and the other called the exterior of  $\Gamma$ , denoted by  $\text{Ext}(\Gamma)$ , each of which has  $\Gamma$  as its boundary. Thus, if  $\Gamma$  is a Jordan contour, then  $\text{Int}(\Gamma)$  and  $\text{Ext}(\Gamma) \cup \{\infty\}$  are simply connected regions.

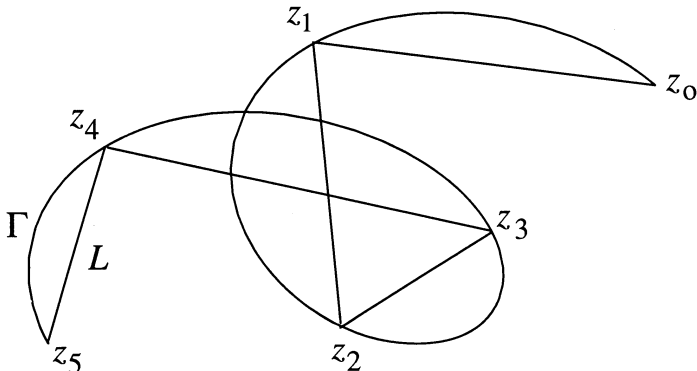


Fig. 1.1.1. Rectifiable curve.

Let a continuous curve  $\Gamma$ , defined by  $\gamma(t) = \alpha(t) + i\beta(t)$ , be divided into  $n$  arcs  $\sigma_k = z_{k-1} \widehat{z}_k$ ,  $k = 1, \dots, n$ , where  $z_k = \gamma(t_k)$  for  $k = 0, 1, \dots, n$ , such that the end point of each arc, except the last one, overlaps the initial point of the next arc. If we join each segment  $[z_{k-1}, z_k]$ ,  $k = 1, \dots, n$ , by straight line segments (see Fig. 1.1.1 where  $n = 5$ ), we obtain a polygonal line  $L$  inscribed in  $\Gamma$ . The segments of  $L$  are the chords joining the end points of the arcs  $\sigma_k$ , and

$$\text{length of } L = \sum_{k=1}^n |z_k - z_{k-1}|. \quad (1.1.12)$$

The curve  $\Gamma$  is said to be *rectifiable* if

$$\sup_{\mathcal{P}} \sum_{k=1}^n |z_k - z_{k-1}| = l < +\infty,$$

where the least upper bound is taken over all partitions  $\mathcal{P} = \{a = t_0, t_1, \dots, t_n = b\}$  of the interval  $[a, b]$ ,  $a \leq t \leq b$ . The nonnegative number  $l$  is called the length of the curve  $\Gamma$ . The curve is said to be *nonrectifiable* if the sums (1.1.10) become arbitrarily large for suitably chosen partitions.

A piecewise smooth curve  $\tilde{\Gamma}$ , defined by  $\tilde{\gamma} = [\tilde{a}, \tilde{b}] \mapsto \mathbb{C}$ , is called a *reparametrization* of a curve  $\Gamma$ , defined by  $\gamma = [a, b] \mapsto \mathbb{C}$  if there exists a function  $\alpha \in C^1$ ,  $\alpha : [a, b] \mapsto [\tilde{a}, \tilde{b}]$  with  $\alpha'(t) > 0$ ,  $\alpha(a) = \tilde{a}$  and  $\alpha(b) = \tilde{b}$ , such that  $\gamma(t) = \tilde{\gamma}(\alpha(t))$ ,  $t \in [a, b]$ . Then  $\int_{\Gamma} f = \int_{\tilde{\Gamma}} f$  for any  $C$ -function  $f$  defined on an open set containing the image of  $\gamma$  (which is equal to the image of  $\tilde{\gamma}$ ).

Let  $f$  be a  $C$ -function on an open set  $D \subset \mathbb{C}$ , and let  $\Gamma$  be a piecewise  $C^1$ -continuous curve in  $D$ . If  $|f(z)| \leq M$  for all points  $z \in \Gamma$ , i.e., for all  $z = \gamma(t)$  for  $t \in [a, b]$ , where  $M > 0$  is a constant, then

$$\left| \int_{\Gamma} f dz \right| \leq M l(\Gamma), \quad (1.1.13)$$

where

$$l(\Gamma) = \int_a^b |\gamma'(t)| dt = \int_a^b \sqrt{x'(t)^2 + y'(t)^2} dt \quad (1.1.14)$$

is the arc length of the path  $\Gamma$ . In general, by applying the triangle inequality,

$$\left| \int_{\Gamma} f dz \right| \leq \int_{\Gamma} |f| |dz| = \int_a^b |f(\gamma(t))| |\gamma'(t)| dt. \quad (1.1.15)$$

If  $\gamma : [a, b] \mapsto \mathbb{C}$  defines a piecewise smooth contour  $\Gamma$  and  $F$  is a function defined and analytic on a region containing  $\Gamma$ , then

$$\int_{\Gamma} F'(z) dz = F(\gamma(b)) - F(\gamma(a)). \quad (1.1.16)$$

If  $\gamma(a) = \gamma(b)$ , then

$$\int_{\Gamma} F'(z) dz = 0. \quad (1.1.17)$$

This results is known as the *fundamental theorem for line integrals (contour integration)* in the complex plane. Thus, if a function  $f$  is defined and analytic on a region  $D \subset \mathbb{C}$  and if  $f'(z) = 0$  for all points  $z \in D$ , then  $f$  is a constant

on  $D$ . If  $f$  is a  $C$ -function on a region  $D$ , then the following three statements are equivalent:

- (i) If  $\Gamma_1$  and  $\Gamma_2$  are two paths in  $D$  from a point  $z_1 \in D$  to a point  $z_2 \in D$ , then  $\int_{\Gamma_1} f(z) dz = \int_{\Gamma_2} f(z) dz$ , i.e., the integrals are path-independent.
- (ii) If  $\Gamma$  is a Jordan contour lying in  $D$ , then  $\int_{\Gamma} f(z) dz = 0$ , i.e., the integrals on a closed contour are zero.
- (iii) There exists a function  $F$  defined and analytic on  $D$  such that  $F'(z) = f(z)$  for all  $z \in D$ , i.e., there exists a global antiderivative of  $f$  on  $D$ .

A function  $\Phi(z)$ , analytic inside a region with boundary  $\Gamma = \cup_{k=1}^n \Gamma_k$ , is said to be *sectionally analytic* on  $\Gamma$  if  $\Phi(z)$  is continuous on each  $\Gamma_k$  from both left and right except at the end points where it satisfies the condition  $|\Phi(z)| \leq \frac{C}{|z - c|^{\alpha}}$ , where  $c$  is the corresponding end point of  $\Gamma_k$ , and  $C$  and  $\alpha$  are real constant with  $\alpha < 1$ .

**HÖLDER CONDITION.** Let  $f(t)$  be defined on a Jordan curve  $\Gamma$  (open or closed). If

$$|f(t_1) - f(t_2)| \leq A |t_1 - t_2|^{\alpha}, \quad 0 < \alpha \leq 1, \quad (1.1.18)$$

for arbitrary points  $t_1, t_2 \in \Gamma$  ( $t_1 \neq t_2$ ), where  $A > 0$  and  $\alpha$  are real constants, then  $f(t)$  is said to satisfy the *Hölder condition of order  $\alpha$* , or simply the condition  $H^\alpha$ , denoted by  $f(t) \in H^\alpha$ . The condition  $H^1$  is known as the *Lipschitz condition*. If  $f(t) \in C(\Gamma)$  and  $f(t) \in H^\alpha$ , then we say that  $f(t)$  is *Hölder-continuous* on  $\Gamma$ . If  $f \in C(\Gamma)$  and  $f \in H^1$ , then  $f(t)$  is said to be *Lipschitz-continuous*.

**FATOU'S LEMMA.** Let  $f_n : I \mapsto \mathbb{R}$  be nonnegative, extended real-valued, measurable functions defined in an interval  $I$  and such that the sequence  $\{f_n\}$  converges pointwise to the function  $f : I \mapsto \mathbb{R}$ . If  $\liminf_{n \rightarrow \infty} \int_{\Gamma} f_n < \infty$ , then  $f$  is integrable and

$$\int_I f \leq \liminf_{n \rightarrow \infty} \int_{\Gamma} f_n. \quad (1.1.19)$$

**METRIC SPACES.** Let  $S$  denote the set of all real-valued sequences. Then  $S$  is a vector space if addition and scalar multiplication of vectors  $s_i, t_i \in S$  for  $i = 1, 2, \dots$  are defined coordinatewise, i.e.,  $\{s_i\} + \{t_i\} = \{s_i + t_i\}$ , and

$\lambda \{s_i\} = \{\lambda s_i\}$  for a scalar  $\lambda$ . The *Fréchet metric* (distance)  $d(\{s_i\}, \{t_i\})$  is defined for  $\{s_i\}, \{t_i\} \in S$  by

$$d(\{s_i\}, \{t_i\}) = \sum_{i=1}^{\infty} \frac{|s_i - t_i|}{(1 + |s_i - t_i|)} 2^i. \quad (1.1.20)$$

The space  $\ell^p$ ,  $1 \leq p < \infty$ , is defined by  $\ell^p = \left\{ \{s_i\} : \sum_{i=1}^{\infty} |s_i|^p < \infty \right\}$ . Since the sum of any two elements in  $\ell^p$  is also in  $\ell^p$ , then  $\ell^p$  is a vector subspace of  $S$ . Define a norm  $\|\cdot\|_p$  on  $\ell^p$  by

$$\|\{s_i\}\|_p = \left( \sum_{i=1}^{\infty} |s_i|^p \right)^{1/p}. \quad (1.1.21)$$

Then it can be shown that  $\ell^p$  is closed under vector addition and  $\|\cdot\|_p$  satisfies the triangle inequality. Let  $\{s_i\}, \{t_i\} \in \ell^p$  be such that  $\sum |s_i|^p = 1$  and  $\sum |t_i|^q = 1$ , where  $p$  and  $q$  are called conjugate exponents such that  $p > 1$  and  $\frac{1}{p} + \frac{1}{q} = 1$ . Then

Hölder inequality:

$$\sum_{i=1}^{\infty} |s_i t_i| \leq \left( \sum_{i=1}^{\infty} |s_i|^p \right)^{1/p} \left( \sum_{i=1}^{\infty} |t_i|^q \right)^{1/q}. \quad (1.1.22)$$

Cauchy–Schwarz inequality:

$$\sum_{i=1}^{\infty} |s_i t_i| \leq \sqrt{\sum_{i=1}^{\infty} |s_i|^2} \sqrt{\sum_{i=1}^{\infty} |t_i|^2}. \quad (1.1.23)$$

Minkowsky's inequality:

$$\left( \sum_{i=1}^{\infty} |s_i + t_i|^p \right)^{1/p} \leq \left( \sum_{i=1}^{\infty} |s_i|^p \right)^{1/p} + \left( \sum_{i=1}^{\infty} |t_i|^p \right)^{1/p}, \quad p \geq 1. \quad (1.1.24)$$

Note that  $p = 1$  gives the triangle inequality.

Let  $L^2$  denotes the Hilbert space of all square–integrable analytic functions  $f$  in a simply connected region  $D$  with boundary  $\Gamma$ . A function  $f(z)$  regular in  $D$  is said to belong to the class  $L^2(D)$  (we say,  $f \in L^2(D)$ ) if the integral

$\iint_D |f(z)|^2 dS_z < +\infty$ , where  $dS_z = dx dy$  denotes an area element in  $D$ . The (surface)-norm  $\|f\|_{2,D}$  of  $f(z)$  is defined by

$$\|f\|_{2,D}^2 = \iint_D |f(z)|^2 dS_z.$$

If two functions  $f, g \in L^2(D)$ , then their inner product is defined by

$$\langle f, g \rangle = \iint_D f(z) \overline{g(z)} dS_z. \quad (1.1.25)$$

Let  $\Gamma$  be the rectifiable Jordan boundary of the region  $D$ , of length  $l$ , and let  $\Gamma_\rho$  denote the image of the circle  $|w| = \rho$  under the mapping  $z = g(w) = f^{-1}(w)$ ,  $0 < \rho < R$ . If  $f(z)$  is regular in  $D$ , then the integral

$$\int_{\Gamma_\rho} |f(z)|^2 ds_z = \rho \int_{\phi=0}^{2\pi} \left| f(g(w)) \sqrt{g'(w)} \right|^2 d\phi, \quad w = \rho e^{i\phi}, \quad (1.1.26)$$

where  $ds_z$  denotes a line element on  $\Gamma$ , is a monotone increasing function. We say that  $f \in L^2(\Gamma)$  if this integral remains bounded as  $\rho \rightarrow R$ , i.e.,

$$\lim_{\rho \rightarrow R} \int_{\Gamma_\rho} |f(z)|^2 ds_z = \int_{\Gamma} |f(z)|^2 ds_z = \|f\|_{2,\Gamma}^2,$$

where  $\|f\|_{2,\Gamma}^2$  is the (line)-norm of  $f$ . For any two functions  $f, g \in L^2(\Gamma)$ , we define their inner product as

$$\langle f, g \rangle = \int_{\Gamma} f(z) \overline{g(z)} ds_z. \quad (1.1.27)$$

If the disk  $B(z_0, r) \subset D$ , then

$$|f(z_0)|^2 = \begin{cases} \frac{1}{\pi r^2} \iint_D |f(z)|^2 dS_z, & \text{if } f \in L^2(D), \\ \frac{1}{2\pi r} \int_{\Gamma} |f(z)|^2 ds_z, & \text{if } f \in L^2(\Gamma). \end{cases} \quad (1.1.28)$$

Let a region have a piecewise continuous boundary  $\Gamma$ , and let  $f(z), g(z)$  be regular in  $D$ , and  $f'(z)$  and  $g'(z)$  continuous in  $\bar{D}$ . Then

$$\langle f, g' \rangle = \iint_D f(z) \overline{g'(z)} dS_z = \frac{1}{2i} \int_{\Gamma} f(z) \overline{g(z)} ds_z. \quad (1.1.29)$$

This is known as *Green's formula*. It is useful in converting a surface integral into a line integral. This formula also holds for multiply connected regions. The integral along  $\Gamma$  is taken in the positive sense, i.e., the region  $D$  remains to the left as one traverses the contour  $\Gamma$ . The following inequality is also useful: If  $f \in L^2(D)$ , then  $f \in L^2(\Gamma)$ , and

$$\iint_D |f(z)|^2 dS_z \leq \frac{l}{2} \int_{\Gamma} |f(z)|^2 ds_z. \quad (1.1.30)$$

We shall denote by  $L^\infty$  the Hilbert space of  $2\pi$ -periodic and bounded functions  $f$  with the norm

$$\|f\|_\infty = \max_{[0, 2\pi]} |f(x)|, \quad (1.1.31)$$

and by  $W$  the Sobolev space of  $2\pi$ -periodic and absolutely continuous functions  $f$ , with  $f' \in L^2[0, 2\pi]$ . Then  $\|f\| = \max (\|f\|_\infty, \|f'\|_2)$ , and  $(W, \|\cdot\|)$  is a Banach space. Thus, if  $f, g \in (W, \|\cdot\|)$ , then (i)  $\|f\| \geq 0$ ; (ii)  $\|f\| = 0$  implies that  $f = 0$ ; (iii)  $\|\alpha f\| = |\alpha| \|f\|$  for a scalar  $\alpha$ ; and  $\|f + g\| \leq \|f\| + \|g\|$  which is known as the triangle inequality.

---

## 1.2. Some Basic Theorems

Some basic theorems from the theory of functions of a complex variable are presented without proofs which can be found in standard textbooks on the subject.

**THEOREM 1.2.1 (CAUCHY'S THEOREM).** *Let  $f$  be analytic on a region  $D$ , and let  $\Gamma$  be a closed contour which is homotopic to a point in  $D$ . Then  $\int_{\Gamma} f = 0$ .*

Note that a set is said to be simply connected if every closed contour  $\Gamma \subset D$  is homotopic (as a closed curve) to a point in  $D$ , i.e., to some constant curve. Some local versions of Cauchy's theorem are as follows:

**THEOREM 1.2.2 (CAUCHY–GOURSAT THEOREM FOR A DISK).** *Let  $f : B \mapsto \mathbb{C}$  be analytic on a disk  $B = B(z_0, r) \subset D$ . Then*

- (i) *there exists a function  $F : B \mapsto \mathbb{C}$  which is analytic on  $B$  and is such that  $F'(z) = f(z)$  for all  $z \in B$  (i.e.,  $f$  has an antiderivative on  $B$ ); and*
- (ii) *If  $\Gamma$  is a closed contour in  $B$ , then  $\int_{\Gamma} f = 0$ .*

This theorem also holds if  $f$  is continuous on  $B$  and analytic on  $D \setminus \{z_1\}$  for some fixed  $z_1 \in D$ .

**THEOREM 1.2.3 (CAUCHY–GOURSAT THEOREM FOR A RECTANGLE).** *Let  $R$  denote a rectangle with sides parallel to the coordinate axes, and let  $f$  be a function defined and analytic on an open set  $D$  containing  $R$ . Then  $\int_{\Gamma} f = 0$ .*

Even if the function  $f$  is analytic on  $D$  except at some fixed point  $z_1 \in D$  which does not lie on the contour  $R$ , and if  $\lim_{z \rightarrow z_1} (z - z_1)f(z) = 0$ , then also  $\int_{\Gamma} f = 0$ . The two theorems 1.2.2 and 1.2.3 hold (a) if  $f$  is bounded on a deleted neighborhood of  $z_1$ , or (b) if  $f$  is continuous on  $D$ , or (c) if  $\lim_{z \rightarrow z_1} f(z)$  exists.

The index of a curve  $\Gamma$  with respect to a point  $z_0 \in \mathbb{C}$  is the integer  $n$  that expresses how many times  $\Gamma$  winds around  $z_0$ . This index is denoted by  $I(\Gamma, z_0)$  and is called the winding number of  $\Gamma$  with respect to  $z_0$ . Thus,

$$I(\Gamma, z_0) = \frac{1}{2i\pi} \int_{\Gamma} \frac{dz}{z - z_0}. \quad (1.2.1)$$

In fact,

$$I(\Gamma, z_0) = \begin{cases} \pm n & \text{if } z_0 \in \text{Int}(\Gamma), \\ 0 & \text{if } z_0 \in \text{Ext}(\Gamma). \end{cases}$$

**THEOREM 1.2.4 (CAUCHY'S INTEGRAL FORMULA).** *Let  $f$  be analytic on a region  $D$ , and let  $\Gamma$  be a simple closed contour in  $D$  that is homotopic to a point in  $D$ . Let  $z_0 \in D$  be a point not on  $\Gamma$ . Then*

$$f(z_0) \cdot I(\Gamma, z_0) = \frac{1}{2i\pi} \int_{\Gamma} \frac{f(\zeta)}{\zeta - z_0} d\zeta. \quad (1.2.2)$$

The integrand in (1.2.2) is known as the *Cauchy kernel* defined by

$$H(z, z_0) = \frac{1}{2i\pi} \frac{f(z)}{z - z_0}. \quad (1.2.3)$$

The formula (1.2.2) is a special case of integrals of the Cauchy type. If we set

$$F(z) = \frac{1}{2i\pi} \int_{\Gamma} \frac{g(\zeta)}{\zeta - z} d\zeta, \quad (1.2.4)$$

where  $\Gamma : [a, b] \mapsto \mathbb{C}$  is a simple contour and  $g$  a  $C$ -function defined on the image  $\Gamma([a, b])$ , then  $F$  is analytic on  $\mathbb{C} \setminus \Gamma([a, b])$  and is infinitely differentiable, such that its  $k$ -th derivative is given by

$$F^{(k)}(z) = \frac{k!}{2i\pi} \int_{\Gamma} \frac{g(\zeta)}{(\zeta - z)^{k+1}} d\zeta, \quad k = 1, 2, \dots. \quad (1.2.5)$$

Then Cauchy's integral formula for the derivatives is

$$f^{(k)}(z) \cdot I(\Gamma, z_0) = \frac{k!}{2i\pi} \int_{\Gamma} \frac{f(\zeta)}{(\zeta - z)^{k+1}} d\zeta, \quad k = 1, 2, \dots. \quad (1.2.6)$$

Let  $f$  be analytic on a region  $D$  and let  $\Gamma = \partial B(z_0, R)$  be a circle lying in  $D$ . If  $|f| \leq M$  for all  $z \in \Gamma$ , then for  $k = 0, 1, \dots$

$$|f^{(k)}(z_0)| \leq \frac{k!}{R^k} M. \quad (1.2.7)$$

This result is known as *Cauchy's inequality*. A corollary is the *Liouville theorem* which states that the only bounded entire functions are constants. A partial converse of Cauchy's theorem is known as *Morera's theorem* which states that if  $f$  is continuous on a region  $D$  and if  $\int_{\Gamma} f dz = 0$  for every closed contour  $\Gamma$  in  $D$ , then  $f$  is analytic on  $D$ , and  $f = F'$  for some analytic function  $F$  on  $D$ .

Two very useful corollaries of Cauchy's integral formula (1.2.2) are

- (i) The *maximum modulus theorem* which states that if  $f$  is a nonconstant analytic function on a region  $D$  with a simple boundary  $\Gamma$ , then  $|f|$  cannot have a local maximum anywhere in  $\text{Int}(\Gamma)$ .
- (ii) The *mean value property* of an analytic function  $f$  defined on the circle  $\partial B(z_0, r)$  states that

$$f(z_0) = \frac{1}{2\pi} \int_0^{2\pi} f(z_0 + re^{i\theta}) d\theta. \quad (1.2.8)$$

An application of the maximum modulus theorem is

**SCHWARZ LEMMA.** Let  $f$  be analytic on the open unit disk  $U$ , and suppose that  $|f(z)| \leq 1$  for all  $z \in U$  and  $f(0) = 0$ . Then  $|f(z)| \leq |z|$  for all  $z \in U$  and  $|f'(0)| \leq 1$ . If  $|f(z_0)| = |z_0|$  for some  $z_0 \in U$ ,  $z_0 \neq 0$ , then  $f(z) = cz$  for all  $z \in U$ , where  $c$  is some constant such that  $|c| = 1$ .

**BOUNDARY VALUES FOR CAUCHY'S INTEGRAL.** If the boundary  $\Gamma$  of a simply connected region  $D$  is rectifiable and if  $f(z)$  is regular in  $D$  and continuous on  $\bar{D}$ , then Cauchy's integral formula (1.2.2) holds for every  $z_0 \in D$ . For the boundary values we have the following result: Let the boundary  $\Gamma$  of  $D$  be smooth, and let  $f(z)$  be regular in  $D$  and continuous on  $\bar{D}$ . Then for a point  $z_0 \in \Gamma$  which is not a corner point

$$f(z_0) = \frac{1}{i\pi} \int_{\Gamma} \frac{f(\zeta)}{\zeta - z_0} d\zeta. \quad (1.2.9)$$

In the case when  $z_0 \in \Gamma$  is a corner point with inner angle  $\alpha\pi$ ,  $0 < \alpha < 2$ , the boundary value  $f(z_0)$  is given by

$$f(z_0) = \frac{1}{i\alpha\pi} \int_{\Gamma} \frac{f(\zeta)}{\zeta - z_0} d\zeta, \quad (1.2.10)$$

where the integral is taken as a Cauchy p.v. If  $D$  is the region exterior to the Jordan curve  $\Gamma$  which is traversed in the positive sense and if  $f(z)$  is regular at  $z = \infty$ , then the boundary value at a point  $z_0 \in \Gamma$  which is not a corner point is given by

$$f(z_0) = -\frac{1}{i\pi} \int_{\Gamma} \frac{f(\zeta)}{\zeta - z_0} + 2 f(\infty) d\zeta, \quad (1.2.11)$$

and at a corner point  $z_0 \in \Gamma$  with the inner angle  $\alpha$ ,  $0 < \alpha < 2$ , by

$$f(z_0) = \frac{1}{i(2-\alpha)\pi} \int_{\Gamma} \frac{f(\zeta)}{\zeta - z_0} d\zeta + 2 f(\infty). \quad (1.2.12)$$

The integrals in (1.2.9)–(1.2.12) are taken as Cauchy p.v.'s.

**PLEMELJ FORMULAS:** If  $\Gamma$  is a contour, then

$$\begin{aligned} F^+(\zeta_0) &= \frac{1}{2} f(\zeta_0) + \frac{1}{2i\pi} \int_{\Gamma} \frac{f(\zeta)}{\zeta - \zeta_0} d\zeta, \\ F^-(\zeta_0) &= -\frac{1}{2} f(\zeta_0) + \frac{1}{2i\pi} \int_{\Gamma} \frac{f(\zeta)}{\zeta - \zeta_0} d\zeta, \end{aligned} \quad (1.2.13)$$

where  $F^+(\zeta_0)$  and  $F^-(\zeta_0)$  are the limiting values from the right and left of  $\Gamma$ , respectively,  $f(\zeta)$  satisfies the Hölder condition on  $\Gamma$ , and  $\zeta_0$  does not coincide with those end points where  $f(\zeta_0) \neq 0$ . If  $\zeta_0$  coincides with an end point where  $f(\zeta_0) = 0$ , then  $F^+(\zeta_0) = F^-(\zeta_0) = f(\zeta_0)$ . A proof for these formulas can be found in Muskhelishvili (1946,1992).

Another set of useful formulas is as follows:

$$\sin \pi z = \pi z \prod_{n=1}^{\infty} \left(1 - \frac{z^2}{n^2}\right), \quad (1.2.14)$$

$$\pi \cot \pi z = \sum_{n=-\infty}^{\infty} \frac{1}{z-n} = \frac{1}{z} + \sum_{n=1}^{\infty} \left( \frac{1}{z-n} + \frac{1}{z+n} \right), \quad (1.2.15)$$

where the series converges in the Cauchy sense.

### 1.3. Harmonic functions

The functions whose Laplacian is zero are known as harmonic functions. Thus, a real-valued function  $u(x, y) \in C^2(D)$  is said to be *harmonic* in a region  $D$  if  $\nabla^2 u = 0$ . Some properties of harmonic functions in  $\mathbb{R}^2$  are as follows:

(i) The function

$$\frac{1}{r} = \frac{1}{\sqrt{(x-x_0)^2 + (y-y_0)^2}} \quad (1.3.1)$$

is harmonic in a region that does not contain the point  $(x_0, y_0)$ .

(ii) If  $u(x, y)$  is a harmonic function in a simply connected region  $D$ , then there exists a conjugate harmonic function  $v(x, y)$  in  $D$  such that  $u(x, y) + i v(x, y)$  is an analytic function of  $z = x + iy = (x, y)$  in  $D$ . In view of the Cauchy–Riemann equations (1.1.3),

$$v(x, y) - v(x_0, y_0) = \int_{x_0, y_0}^{x, y} (-u_y dx + u_x dy), \quad (1.3.2)$$

where  $(x_0, y_0) = z_0$  is a given point in  $D$ . This property is also true if  $D$  is multiply connected. However, in that case the conjugate function  $v(x, y)$  can

be multiple-valued, as we see by considering  $u(x, y) = \log r = \log \sqrt{x^2 + y^2}$  defined on a region  $D$  containing the origin which has been indented by a small circle centered at the origin. Then, in view of (1.3.2),

$$v(x, y) - v(x_0, y_0) = \tan^{-1} \frac{y}{x} \pm 2n\pi + \text{const}, \quad n = 1, 2, \dots,$$

which is multiple-valued.

(iii) Since derivatives of all orders of an analytic function exist and are themselves analytic, any harmonic function will have continuous partial derivatives of all orders, i.e., a harmonic function belongs to the class  $C^\infty(D)$ , and a partial derivative of any order is again harmonic.

(iv) A harmonic function must satisfy the mean-value theorem, where the mean value at a point is evaluated for the circumference or the area of the circle around that point. If  $u$  is harmonic on a region containing the closed disk  $\bar{B}(z_0, r)$ , where  $z_0 = x_0 + iy_0$ , then

$$u(x_0, y_0) = \frac{1}{2\pi} \int_0^{2\pi} u(z_0 + r e^{i\theta}) d\theta. \quad (1.3.3)$$

(v) In view of the maximum modulus theorem (§1.2), the maximum (and also the minimum) of a harmonic function  $u$  in a region  $D$  occurs only on the boundary of  $D$ . This result is known as

**THEOREM 1.3.1 (MAXIMUM PRINCIPLE).** *A nonconstant function which is harmonic inside a bounded region  $D$  with boundary  $\Gamma$  and continuous in the closed region  $\bar{D} = D \cup \Gamma$  attains its maximum and minimum values only on the boundary of the region.*

Thus,  $u$  has a maximum (or minimum) at  $z_0 \in D$ , i.e., if  $u(z) \leq u(z_0)$  (or  $u(z) \geq u(z_0)$ ) for  $z$  in a neighborhood  $B(z_0, \varepsilon)$  of  $z_0$ , then  $u = \text{const}$  in  $B(z_0, \varepsilon)$ .

(vi) The value of a harmonic function  $u$  at an interior point in terms of the boundary values  $u$  and  $\frac{\partial u}{\partial n}$  is given by Green's third identity (B.8).

(vii) If  $u$  and  $U$  are continuous in  $\bar{D}$  and harmonic in  $D$  such that  $u \leq U$  on  $\Gamma$ , then  $u \leq U$  also at all points inside  $D$ . In fact, the function  $U - u$  is continuous

and harmonic in  $D$ . Hence  $U - u \geq 0$  on  $\Gamma$ . Then, in view of the maximum principle (Theorem 1.3.1), we require that  $U - u \geq 0$  at all points inside  $D$ .

(viii) If  $u$  and  $U$  are continuous in  $\bar{D}$  and harmonic in  $D$  for which  $|u| \leq U$  on  $\Gamma$ , then  $|u| \leq U$  also at all points inside  $D$ . In fact, the three harmonic functions  $-U$ ,  $u$ , and  $U$  satisfy the relation  $-U \leq u \leq U$  on  $\Gamma$ . Then, by (vii),  $-U \leq u \leq U$  at all points inside  $D$ , or  $|u| \leq U$  inside  $D$ .

**HARNACK THEOREM:** Suppose that  $\{u_n(z)\}$  is a monotone increasing sequence of harmonic functions on a region  $D$ , which is convergent at a point  $z_0 \in D$ . Then  $\{u_n(z)\}$  is uniformly convergent on closed sets in  $D$ .

Let  $z_0 \neq \infty$  be any point inside  $D$ , and let  $K$  denote the closed disk  $\bar{B}(z_0, R)$  such that  $K \subset D$ . Then, if  $r = |z - z_0| \leq R$ , the Harnack inequality

$$u_n(z_0) \frac{R - r}{R + r} \leq u_n(z) \leq u_n(z_0) \frac{R + r}{R - r} \quad (1.3.4)$$

holds for any annulus  $0 < r < R$  with center at  $z_0$ , provided that  $u_n(z)$  are harmonic and nonnegative on the disk  $B(z_0, R)$ .

**IDENTITY THEOREM:** If  $f(z)$  is analytic on a region  $D$ ,  $z_0 \in D$ , and  $\{z_k\}_1^\infty$  is a sequence of distinct points in  $D$  such that  $z_k \rightarrow z_0$ , and  $f(z_k) = 0$  for  $k = 1, 2, \dots$ , then  $f(z) \equiv 0$  on  $D$ . This theorem is useful in establishing certain identities, including the concept of analytic continuation.

**CAPACITY:** Let  $D^*$  denote the complement of the region  $D$  that includes the point  $z = \infty$ . Then the region  $D^*$  can be covered by regions  $D^{*(n)}$  with boundaries  $\Gamma^{*(n)}$ ,  $n = 1, 2, \dots$ . The Green's function  $\mathcal{G}_n(z, \infty)$  of the regions  $D^{*(n)}$  is a harmonic function in  $D^{*(n)}$  except at the point  $z = \infty$  which assumes the value zero on  $\Gamma^{*(n)}$  and in a neighborhood of  $\infty$  behaves such that  $\lim_{z \rightarrow \infty} [\mathcal{G}_n(z, \infty) - \log |z|] = \gamma_n$  exists (and is finite). The quantity  $\gamma_n$  is called *Robin's constant* for the regions  $D^{*(n)}$ . Hence, in a neighborhood of  $z = \infty$

$$\mathcal{G}_n(z, \infty) = \log |z| + u_n(z) + \gamma_n, \quad (1.3.5)$$

where  $u_n(z)$  is a harmonic function in  $D^{*(n)}$ , including the point  $z = \infty$ , and  $u_n(z) \rightarrow 0$  as  $z \rightarrow \infty$ . Since  $\overline{D^{*(n)}} \subset D^{*(n+1)}$ , the function  $\mathcal{G}_{n+1}(z, \infty) - \mathcal{G}_n(z, \infty)$  is harmonic in  $D^{*(n)}$ , including the point  $\infty$ . In view of the maximum principle (Theorem 1.3.1), the last statement is true everywhere in the region  $D^{*(n)}$ , i.e., for all  $z \in D^{*(n)}$

$$\mathcal{G}_{n+1}(z, \infty) \geq \mathcal{G}_n(z, \infty), \quad \gamma_{n+1} \geq \gamma_n. \quad (1.3.6)$$

In view of the Harnack theorem, the sequence of functions  $\{u_n + \gamma_n\}$ , where  $u_n(\infty) = 0$ , either converges to  $\infty$  in  $D^*$  or converges to a harmonic function  $u(z) + \gamma$  such that  $u(\infty) = 0$ . In the latter case, the quantity  $\gamma$  is called Robin's constant for the region  $D^*$ , the quantity  $C = e^{-\gamma}$  is called the capacity of the region  $D^*$  (denoted by  $\text{cap}(D^*)$ ), and the function  $\mathcal{G}(z, \infty)$  is called Green's function for the region  $D^*$ , which assumes nonnegative values everywhere in  $D^*$ , but these values need not be zero. For example, at isolated boundary points of  $D^*$  the value of  $\mathcal{G}(z, \infty)$  is positive. In the case when  $u_n(z) + \gamma_n \rightarrow \infty$  for  $z \in D^*$ , we have  $\gamma_n \rightarrow \infty$  because  $u_n(\infty) = 0$ . In this case the capacity of the region  $D$  is taken as zero. The following results are useful:

**THEOREM 1.3.2.** *For the region  $D^*$ , containing the point at infinity, to have a Green's function  $\mathcal{G}(z, \infty)$ , it is necessary and sufficient that the capacity of its boundary  $\Gamma$  be positive.*

**THEOREM 1.3.3.** *The capacity of an arbitrary closed and bounded region  $D$  is equal to its transfinite diameter, i.e.,  $\text{cap}(D) = \text{diam}(D)$ .*

## 1.4. Conformal Mapping

If we place a sphere such that the complex plane is tangent to it and the origin coincides with the south pole, then we can transfer all points of  $\mathbb{C}$  to the sphere by projection from the north pole. This is called a *stereographic projection* which is a one-to-one map of  $\mathbb{C}$  onto the sphere, such that its image is the whole sphere except the north pole which then corresponds to the point at infinity  $z = \infty$ .

A mapping  $f$  of a region  $D$  onto a region  $G$  is called *analytic* iff it is differentiable. The mapping  $f$  is called *conformal* if it is bijective and analytic. The *conformal mapping theorem* states that if a mapping  $f : D \mapsto G$  is analytic and  $f'(z_0) \neq 0$  for each  $z \in D$ , then  $f$  is conformal. Thus,  $f$  rotates tangent vectors to curves through  $z_0$  by a definite angle  $\theta$  and magnifies (or contracts) them by a factor  $r$ . The mapping  $f$  is *conformal* if it is analytic with a nonzero derivative. Two important properties are the following:

- (i) If  $f : D \mapsto G$  is conformal and bijective (i.e., one-to-one and onto), then  $f^{-1} : G \mapsto D$  is also conformal and bijective.

(ii) If  $f : D \mapsto G$  and  $g : G \mapsto E$  are conformal, then the composition  $f \circ g : D \mapsto E$  is conformal and bijective.

Property (i) is useful in solving boundary value problems (e.g., the Dirichlet problem) for a region  $D$ . The method involves finding a map  $f : D \mapsto G$  such that  $G$  is a simpler region on which the problem can be first solved, and then the result for the original problem is provided by  $f^{-1}$ . Since the Dirichlet problem involves harmonic functions (see §1.3), the following result on the composition of a harmonic function with a conformal map is useful: If  $u$  is harmonic on a region  $G$  and if  $f : D \mapsto G$  is conformal, then  $u \circ f$  is harmonic on  $D$ . In fact, let  $z \in D$  and  $w = f(z) \in G$ . Then there is an analytic function  $g$  on the open disk  $B(w, \rho) \subset G$  such that  $u = \Re\{g\}$ . Thus,  $u \circ f = \Re\{g \circ f\}$ , which is harmonic since  $g \circ f$  is analytic. A mapping in which both the magnitude and the sense of the angles between the curves and their images are preserved is said to be a conformal mapping of the first kind, but if the sense of the angles is reversed, then it is called a conformal mapping of the second kind.

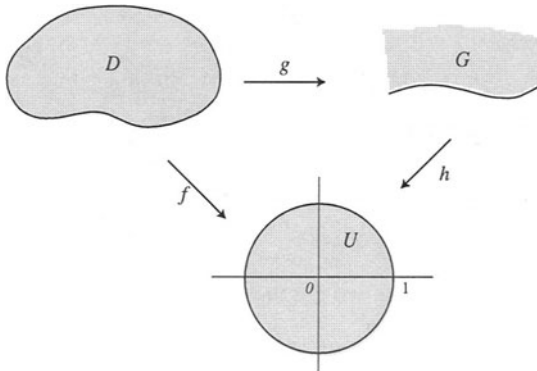


Fig. 1.4.1.

**THEOREM 1.4.1 (RIEMANN MAPPING THEOREM).** *Let  $D \subset \mathbb{C}$  be a simply connected region. Then there exists a bijective conformal map  $f : D \mapsto U$ , where  $U$  is the open unit disk. Moreover, the map  $f$  is unique provided that  $f(z_0) = 0$  and  $f'(z_0) > 0$  for  $z_0 \in D$ .*

This theorem implies that if  $D$  and  $G$ , both contained in  $\mathbb{C}$ , are any two simply connected regions, then there exists a bijective conformal map  $g : D \mapsto G$ . If  $f : D \mapsto U$  and  $h : G \mapsto U$ , then  $g = h^{-1} \circ f$  is bijective conformal (Fig. 1.4.1). Thus, the two regions  $D$  and  $G$  are said to be *conformal* if there exists a bijective conformal map between them.

A bijective conformal map is also called a *univalent* map. A function  $w = f(z)$  defining a univalent mapping is called a univalent function. Its inverse image is also a univalent function defined on the image region. In the study of univalent mappings the first question asked is whether a given region can be mapped univalently onto another region. In the case of simply connected regions it is necessary that the two regions have the same connectivity. Once this condition is met, we can inquire about the possibility of univalent conformal mapping of various regions onto a given simply connected region. To determine how a simply connected region is mapped onto a simply connected region, we must know their mappings onto a standard region, such as the unit disk. This enables us to obtain the required mapping first by mapping the given region onto the unit disk and then mapping the unit disk onto the other region. Now the question arises whether an arbitrary simply connected region can be mapped onto the unit disk. It turns out that this is always possible except for two cases, namely, when the region is the entire plane and when it has a single boundary point. Note that the requirement that the boundary orientation be preserved even in the mapping of regions with non-Jordan boundaries is important. Consider, for example, the map  $w = \sin z$  which is analytic on the strip  $-\pi/4 < x \leq 3\pi/4$  and maps bijectively the two boundaries of this strip onto the two boundaries of the hyperbola  $u^2 - v^2 = 1/2$ , which make the boundary of a simply connected region (curved strip). But the boundary of this curved strip is not traversed in the positive sense. Other simple examples of functions that are not univalent in the lower or the upper half-plane are  $w = z^2$ , and  $w = \sinh z$ , although they are analytic in  $\mathbb{C}$  and map bijectively the real axis  $\Im\{z\} = 0$  onto the real axis  $\Im\{w\} = 0$ . Thus, the function  $w = f(z)$ , analytic on the half-plane  $\Im\{z\} > 0$  and continuous on the closed region  $\Im\{z\} \geq 0$ , grows as  $|z| \rightarrow \infty$  at most as fast as  $Cz^2$ , i.e., the ratio  $\frac{f(z)}{z^2}$  is bounded for  $0 \leq \arg\{z\} \leq \pi$  and a sufficiently large  $|z|$ .

The Riemann mapping theorem also implies that there exists a unique function  $w = F(z)$  that is regular in  $D$ , that is normalized at a finite point  $z_0 \in D$  by the conditions  $F(z_0) = 0$  and  $F'(z_0) = 1$ , and that maps the region  $D$  univalently onto the disk  $|w| < 1$ . In fact, the function  $F(z) = \frac{f(z)}{f(z_0)}$  is such a function, where  $f(z)$ , with  $f(z_0) = 0$  and  $f'(z_0) > 0$ , is the function mentioned in the Riemann mapping theorem, and the radius of the disk onto which the function  $w = F(z)$  maps the region  $D$  is  $R = \frac{1}{f'(z_0)}$ . If there exists another function  $w = F_1(z)$ , with  $F_1(z_0) = 0$  and  $F'_1(z_0) = 1$ , that maps  $D$  onto a disk  $|w| < R_1$ , then, by the Riemann mapping theorem, we could

have  $\frac{F_1(z)}{R} = f(z)$ , and hence,  $\frac{1}{R_1} = f'(z_0)$ , i.e.,  $F_1(z) = \frac{f(z)}{f'(z_0)} = F(z)$ , which proves the uniqueness of the mapping function  $w = F(z)$ . The quantity  $R = \frac{1}{f'(z_0)}$  is called the *conformal radius* of the region  $D$  at the point  $z_0 \in D$ .

Since  $D^* = \text{Ext}(\Gamma)$  is simply connected, Green's function  $\mathcal{G}(z, \infty)$  for  $D^*$  coincides with  $\log |f(z)|$ , where the function  $w = f(z)$  maps  $D^*$  univalently onto  $|w| > 1$  such that  $f(\infty) = \infty$ . Then, Robin's constant  $\gamma$  for the region  $D^*$  is equal to  $\log |f'(\infty)|$ , and  $\text{cap}(D^*) = \frac{1}{|f'(\infty)|} = R$ , where  $R$  is the conformal radius of the region  $D^*$  (with respect to  $\infty$ ), i.e., the number  $R$  is such that the region  $D^*$  is mapped univalently onto  $|w| > R$  by a normalized function  $w = F(z)$  with  $F(\infty) = \infty$  and  $F'(\infty) = 1$ . Thus, in view of Theorems 1.3.2 and 1.3.3, we have the following theorem.

**THEOREM 1.4.2.** *The capacity, and hence the transfinite diameter of a bounded simply connected region  $D$ , is equal to the conformal radius of the region  $D^*$  which is the complement of the region  $D$  in  $\mathbb{C}_\infty$  and contains the point at infinity.*

**CHAIN PROPERTY:** Let  $D_0, \dots, D_n$  be regions in  $\mathbb{C}$ , and let  $f_k : D_{k-1} \mapsto D_k$  denote conformal mappings for  $k = 1, \dots, n$ . Then the mapping  $g = f_n \circ \dots \circ f_1$ , defined by

$$g(z) = f_n(f_{n-1}(\dots f_2(f_1(z))\dots)) \quad (1.4.1)$$

is a conformal mapping of  $D_0$  onto  $D_n$ . The mapping  $g$  is said to be composed of a *chain* of mappings  $f_1, \dots, f_n$  and is represented by the scheme

$$D_0 \xrightarrow{f_1} D_1 \xrightarrow{f_2} D_2 \xrightarrow{f_3} \dots \xrightarrow{f_{n-1}} D_{n-1} \xrightarrow{f_n} D_n. \quad (1.4.2)$$

Thus, the set of regions on  $\mathbb{C}$  can be divided into *mapping classes* such that two regions can be mapped conformally onto each other iff they belong to the same mapping class. Fig. 1.4.2 represents an example of this chain property.

The practical applications of conformal mappings are related to the problem of constructing a function which maps a given region onto a given region. Often we find an explicit expression for the mapping function and determine it by

applying the chain property.

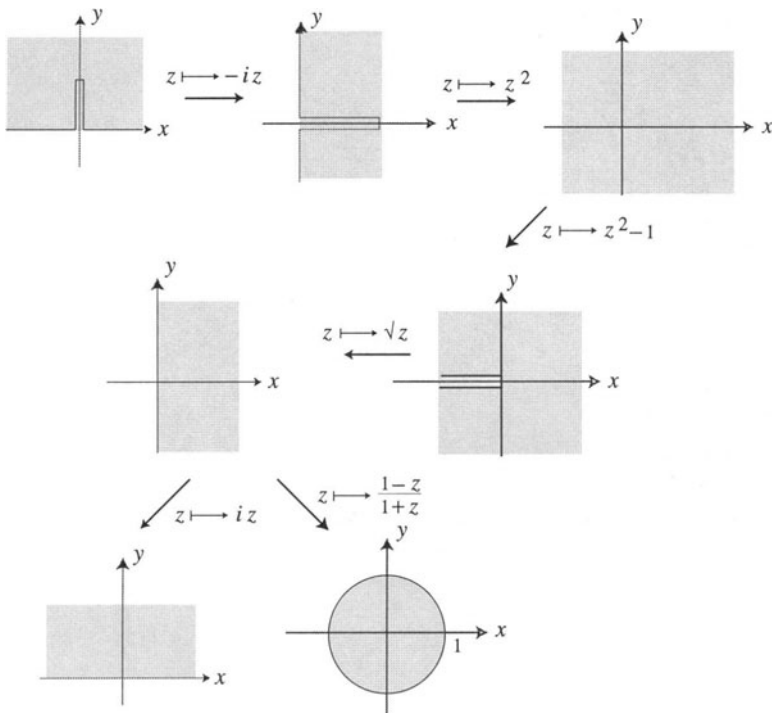


Fig. 1.4.2. Chain property of conformal mappings.

**ANALYTIC CONTINUATION:** If  $A$  and  $B$  are two regions that overlap, i.e.,  $A \cap B \neq \emptyset$ , and if  $f$  is analytic on  $A$ ,  $g$  is analytic on  $B$ , and  $f(z) \equiv g(z)$  on  $A \cap B$ , then  $g$  is called the analytic continuation of  $f$  from  $A$  into  $B$ . This analytic continuation is unique. In fact, suppose that  $g_1$  and  $g_2$  are analytic continuations of  $f$  from  $A$  into  $B$ . Then  $g_1(z) \equiv g_2(z)$  on  $A \cap B$ , and thus, by identity theorem (§1.3),  $g_1 = g_2$  throughout  $B$ . Thus, in practice we shall determine a single function  $F(z)$  that is analytic on  $A \cup B$  and is given by  $F(z) = f(z)$  on  $A$ , and  $F(z) = g(z)$  on  $B$ . For example, let  $f(z) = \int_0^\infty e^{-zt} dt$ . Notice that  $f(z)$  is analytic on  $\Re\{z\} > 0$  because after evaluating the improper integral we find that  $f(z) = 1/z$  is analytic on  $\Re\{z\} > 0$ . So we take  $g(z) = 1/z$ . Since  $g(z)$  is analytic on  $\mathbb{C} \setminus \{0\}$ ,  $g(z)$  becomes the analytic continuation of  $f(z)$  from the right half-plane into the whole plane indented at the origin.

Similarly, the Laplace transform of  $\cos at$  is analytic for  $\Re\{z\} > 0$ ; but the function  $\frac{z}{z^2 + a^2}$  is its analytic continuation from the right half-plane into the whole plane indented at the points  $\pm ia$ .

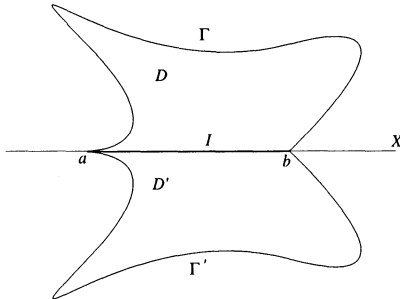


Fig. 1.4.3. Schwarz reflection principle.

**SCHWARZ REFLECTION PRINCIPLE:** If  $f(z)$  is analytic on a region containing a segment of the real axis and is real-valued on this segment, then  $\overline{f(z)} = f(\bar{z})$ . This leads to the concept of analytic continuation across the real axis when the function is known only on one side. Let  $I$  denote a segment  $a < x < b$ , and let  $\Gamma$  be a Jordan arc joining  $a$  and  $b$  and lying in  $\Re\{z\} > 0$ . Then  $C = I \cup \Gamma$  is a contour that encloses a region  $D$  lying entirely in  $\Re\{z\} > 0$ . If we reflect this region into the real axis, we get a region  $D'$  that lies in the lower half-plane and is bounded by  $I$  and  $\Gamma'$  which is the reflection of  $\Gamma$  into the real axis. Then the region  $I \cup D'$  is symmetric about the real axis. If  $f(z)$  is continuous on  $D \cup I$ , analytic on  $D$ , and real-valued on  $I$ , then the function  $F(z)$  defined by

$$F(z) = \begin{cases} f(z), & \text{if } z \in D \cup I, \\ \overline{f(\bar{z})}, & \text{if } z \in D' \end{cases}$$

is analytic on  $D \cup I \cup D'$  (see Fig. 1.4.3). If  $f$  is analytic on one side of a curve  $\Gamma$  and cannot be continued analytically across  $\Gamma$ , then  $\Gamma$  is called a *natural boundary* for  $f$ . For example, the unit circle  $|z| = 1$  is a natural boundary for the function  $f(z) = \sum_{n=0}^{\infty} z^{2^n}$ .

Let  $S^+$  ( $S^-$ ) denote the upper (lower) half-plane  $\Re\{z\} > 0$  ( $\Re\{z\} < 0$ ), respectively, or vice-versa, with  $L$  as their common boundary (i.e., the real axis,

Fig. 1.4.4). Let  $f(z)$  be a function defined at  $z \in S^+$ , and let it be connected with the function  $f^*(z)$  defined in  $S^-$  by the relation

$$f^*(z) = \overline{f(\bar{z})}, \quad (1.4.3)$$

i.e.,  $f(z)$  and  $f^*(z)$  take conjugate complex values at points symmetric with respect to the real axis, since the points  $z$  and  $\bar{z}$  are reflections of each other in  $L$ . We can rewrite the relation (1.4.3) as  $f^*(z) = \bar{f}(z)$ , i.e., if  $f(z) = u(x, y) + iv(x, y)$ , then  $\bar{f}(z) = u(x, -y) - iv(x, -y)$ . If  $f(z)$  is regular (or meromorphic) in  $S^+$ , then  $f^*(z) = \bar{f}(z)$  is regular (or meromorphic) in  $S^-$ , and the relation (1.4.3) is symmetric as regards  $f$  and  $f^*$ , i.e.,

$$f(z) = \overline{f^*(\bar{z})}, \quad (f^*(z))^* = f(z).$$

If  $f(z)$  is a rational function

$$f(z) = \frac{a_n z^n + a_{n-1} z^{n-1} + \cdots + a_0}{b_m z^m + b_{m-1} z^{m-1} + \cdots + b_0}, \quad (1.4.4)$$

then  $f^*(z) = \bar{f}(z)$  is obtained by simply replacing the coefficients by their conjugate complex values. Let  $t$  be a real number, and assume that  $f(z)$  takes a definite limit value  $f^+(t)$  as  $z \rightarrow t$  from  $S^+$ . Then  $f^{*-}(t)$  exists and

$$f^{*-}(t) = \bar{f}^-(t) = \overline{f^+(t)}, \quad (1.4.5)$$

because  $\bar{z} \rightarrow t$  from  $S^-$  as  $z \rightarrow t$  from  $S^+$ , and hence,  $f^*(z) = \overline{f(\bar{z})} \rightarrow \overline{f^+(t)}$ .

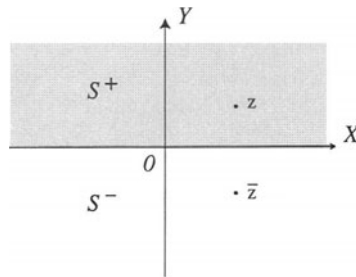


Fig. 1.4.4.

We shall assume that  $f(z)$  is regular on  $S^+$ , except possibly at infinity, and continuous on  $L$  from the left. Define a sectionally regular function  $F(z)$  by

$$F(z) = \begin{cases} f(z) & \text{for } z \in S^+, \\ f^*(z) & \text{for } z \in S^-. \end{cases} \quad (1.4.6)$$

Then, in view of (1.4.5)

$$F^-(t) = \overline{F^+(t)}, \quad F^+(t) = \overline{F^-(t)}. \quad (1.4.7)$$

These relations are useful when transforming the boundary conditions in any boundary problem containing  $f^+(t)$  and  $\overline{f^+(t)}$ , or  $f^-(t)$  and  $\overline{f^-(t)}$  into those involving  $F^+(t)$  and  $F^-(t)$ .

In view of the Schwarz reflection principle, another property is that of extending  $f(z)$ . If  $\Im\{f^*(t)\} = 0$  in any interval  $I$  of the real axis, then the function  $f^*(z)$  is the analytic continuation of  $f(z)$  through the interval  $I$  because  $f^{*-}(t) = f^+(t)$  on this interval.

A *conformal equivalence* between two regions  $D$  and  $G$  in the complex plane is a one-to-one analytic function  $f$  with  $f(D) = G$ . Thus,  $f'(z) \neq 0$  for all  $z$  in  $D$ . Conversely, if  $f : D \mapsto \mathbb{C}$  is analytic such that  $f'$  never vanishes, then  $f$  is not necessarily a conformal equivalence. As an example, consider  $f(z) = e^z$ . However, if  $f'(z) \neq 0$  on  $D$ , then  $f$  is locally one-to-one and conformal. The Riemann mapping theorem (Theorem 1.4.1) establishes the conformal equivalence of two regions. If  $f$  is a conformal equivalence between the open sets  $D$  and  $G$ , then

$$\text{Area}(G) = \iint_D |f'|^2 dz. \quad (1.4.8)$$

Note that if  $f$  is an analytic function, then the Jacobian of  $f$ , regarded as a mapping from  $\mathbb{R}^2$  into  $\mathbb{R}^2$ , is  $|f'|^2$ . Hence, if  $G$  is a simply connected region,  $g : D \mapsto G$  is a Riemann map, and  $g(z) = \sum_n a_n z^n$  in  $D$ , then from (1.4.8)

$$\text{Area}(G) = \iint_D |g'|^2 dz = \pi \sum_n n|a_n|^2. \quad (1.4.9)$$

In fact, since  $g'(z) = \sum_n n a_n z^{n-1}$ , then, for  $r < 1$ ,

$$\begin{aligned} |g'(re^{i\theta})|^2 &= \left( \sum_n n a_n r^{n-1} e^{i(n-1)\theta} \right) \overline{\left( \sum_m m a_m r^{m-1} e^{i(m-1)\theta} \right)} \\ &= \sum_{n,m} n m a_n \bar{a}_m r^{n+m-2} e^{i(n-m)\theta}, \end{aligned}$$

which converges uniformly in  $\theta$ . Since  $\int_0^{2\pi} e^{i(n-m)\theta} d\theta = 0$  for  $n \neq m$ ,

$$\begin{aligned}\iint_D |g'|^2 &= \sum_n n^2 |a_n|^2 2\pi \int_0^1 r^{2n-1} dr \\ &= 2\pi \sum_n n^2 |a_n|^2 \frac{1}{2n} \\ &= \pi \sum_n n |a_n|^2.\end{aligned}$$

This relation is useful in solving the minimum area problem in conformal mapping.

---

## 1.5. Problems

**PROBLEM 1.5.1.** Show that the function  $f(z) = \frac{x^4 - y^4}{x^3 + y^3} + i \frac{x^4 + y^4}{x^3 + y^3}$ ,  $f(0) = 0$ ,  $z \in \mathbb{C}$ , is not differentiable at the origin, although it satisfies the Cauchy–Riemann equations there. [Hint:  $u_x(0, 0) = 1 = v_x(0, 0) = v_y(0, 0)$ ,  $u_y(0, 0) = -1$ , but by limit definition,  $f'(0) = (1+i)/2$  along the line  $y = x$ .]

**PROBLEM 1.5.2.** Prove that if a function  $w = f(z)$  maps conformally a region  $D$  onto another region  $G$ , and if  $z_0$  is an isolated boundary point of  $D$ , then  $z_0$  is a removable singularity or a simple pole of  $f(z)$ . That is why we assume the regions to be without isolated boundary points. (Goluzin, 1969, p.205; Wen, 1992, p.95.)

**PROBLEM 1.5.3.** Show that the chain of mappings  $f_1 : z \mapsto z - 1$ ,  $f_2 : z \mapsto 2z$ ,  $f_3 : z \mapsto z + 3i/2$  maps the circle  $|z - 1| = 1$  onto the circle  $|w - 3i/2| = 2$ .

**PROBLEM 1.5.4.** Let  $w = f(z)$  be an analytic function, regular in a simply connected region  $D$ . Let  $\alpha$  be an interior point of  $D$  and a simple zero of  $f(z)$  such that  $f(\alpha) = 0$  and  $f'(\alpha) \neq 0$ . Moreover, let  $z_0 \in D$  be a first rough approximation of the zero  $\alpha$ , i.e.,  $z_0$  is close to  $\alpha$ . Show that

$$\alpha = \sum_{n=0}^{\infty} (-1)^n \frac{f(z_0)^n}{n!} \left[ \frac{d^n f^{-1}(w)}{dw^n} \right]_{w=f(z_0)}$$

$$= \exp \left\{ -f(z_0) \left[ \frac{df^{-1}(w)}{dw} \right]_{w=f(z_0)} \right\},$$

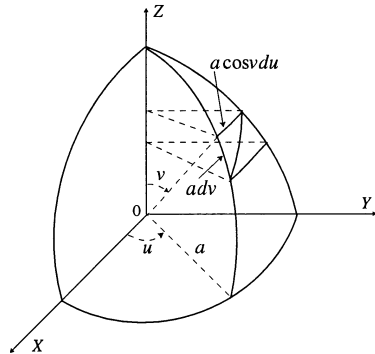
where  $z = f^{-1}(w)$  denotes the inverse function of  $f(z)$  and the exponential function operates symbolically on the differential symbol. (Blaschke and Scherdtfeger, 1945–46, p.266.)

**PROBLEM 1.5.5.** Prove the Schwarz lemma: If  $f(z)$  is analytic on the disk  $|z| < R$  such that  $f(0) = 0$ , and  $|f(z)| \leq M$ , where  $M > 0$  is a constant, then  $|f(z)| \leq \frac{M}{R} |z|$ ,  $|f'(0)| \leq \frac{M}{R}$  on this disk, where the equality holds only for  $f(z) = e^{i\alpha} \frac{M}{R} z$ ,  $\alpha$  real. (Wen, 1992, p.26–27.)

**PROBLEM 1.5.6.** Let  $\mathcal{S}$  denote the family of univalent functions analytic on the unit disk  $|z| < 1$ , which are of the form  $f(z) = z + \sum_{n=2}^{\infty} a_n z^n$ . Show that the coefficients  $a_n$  satisfy the inequality  $|a_n| \leq n$  for  $n = 2, 3, \dots$ , and this bound, known as de Branges estimate (see de Branges, 1985), is sharp for the Koebe function  $f(z) = \frac{z}{(1-z)^2}$ . (Wen, 1992, p.54.)

**PROBLEM 1.5.7.** If  $x = a u$  and  $y = a f(v)$ , where  $z = x + i y$  and  $w = u + i v$ , then the meridians and parallels of the earth will be mapped onto the coordinate lines in the  $(x, y)$ -plane. The equator will be mapped onto the  $x$ -axis if  $f(0) = 0$ . To make a rhumb line on the sphere, which cuts all the meridians at the same angle  $\alpha$  map onto a straight line in the  $z$ -plane cutting the lines  $x = \text{const}$  at the same angle  $\alpha$ , we must have

$\cot \alpha = \frac{dv}{\cos v du} = \frac{dy}{dx} = \frac{f'(v) dv}{du}$ , which yields  $f(v) = \int_0^v \sec v dv = \log \tan \left( \frac{v}{2} + \frac{\pi}{4} \right)$ . The resulting mapping is called Mercator's projection, given by  $z = a \left[ u + \log \tan \left( \frac{v}{2} + \frac{\pi}{4} \right) \right]$ . Show that this mapping is conformal in the sense that angles are preserved and lengths are multiplied by a factor depending on the latitude. Mercator's projection can also be written as  $z =$



$a [u + \text{gd}^{-1}v]$ , where gd denotes the Gudermannian of  $u$ . (Franklin, 1944, p.140–141.)

PROBLEM 1.5.8. Show that if a region whose boundary is a piecewise analytic Jordan contour is mapped conformally onto the unit disk, the mapping is continuous on the boundary. (Nevanlinna and Paatero, 1969, pp.339–340.)

REFERENCES USED: Ahlfors (1966), Betz (1964), Blaschke and Scherdtfeger (1945–46), Boas (1987), Carathéodory (1969), Carrier, Krook and Pearson (1966), Franklin (1944), Gaier (1964), Goluzin (1969), Jeffrey (1992), Kober (1945–48), Lawrentjew and Schabat (1965), Marsden and Hoffman (1987), Muskhelishvili (1948, 1992), Nehari (1952), Wen (1992).

# Chapter 2

---

## Conformal Mappings

---

The central problem in the theory of conformal mapping is determining a function  $f$  which maps a given region  $D \subset \mathbb{C}$  conformally onto another region  $G \subset \mathbb{C}$ . The function  $f$  does not always exist, and it is not always uniquely determined. The Riemann mapping theorem (§1.4) guarantees the existence and uniqueness of a conformal map of  $D$  onto the unit disk  $U$  under certain specific conditions. Besides some elementary mappings we shall study linear, bilinear, and Schwarz–Christoffel transformations.

---

### 2.1. Polynomials

The general *complex polynomial*  $P_n(z)$  of degree  $n$  is an entire function for all  $z \in \mathbb{C}$  and has derivatives of all orders such that  $P_n^{(k)}(z) = 0$  for  $k > n$ . If  $P_n(z)$  has a zero of multiplicity  $p$  at  $z_0$ , then  $P_n(z) = (z - z_0)^p g(z)$ , where  $g(z)$  is a polynomial of degree  $n - p$ ,  $g(z_0) \neq 0$ . The special cases  $P_1(z) = az + b$ , where  $a$  and  $b$  are complex constants, represent a magnification (or dilatation) by  $|a|$  and a rotation by  $\arg a$ , followed by a translation by  $b$ . A *rational function*, as the quotient of two complex polynomials  $P_n(z)$  and  $Q_m(z)$  of degree  $n$  and  $m$ , respectively,  $n \leq m - 1$ , with no common factors, is analytic for all  $z$  that is not a zero of  $Q_m(z)$ . If the polynomial  $Q_m(z)$  has a zero  $z_0$  of multiplicity  $p$ , then the partial fraction development of the rational function corresponding to this zero has the form

$$\frac{A_1}{z - z_0} + \frac{A_2}{(z - z_0)^2} + \cdots + \frac{A_p}{(z - z_0)^p}. \quad (2.1.1)$$

Under the mapping  $w = P_n(z)$ ,  $n > 1$ , there are at most  $n$  points  $w_0$  in the extended  $w$ -plane with fewer than  $n$  distinct inverse images. In fact, the point  $w = \infty$  has just one inverse image. If  $w_0 \neq \infty$  has fewer than  $n$  distinct inverse images, then the equation

$$P_n(z) = w_0, \quad (2.1.2)$$

where  $w_0 = P_n(z_0)$ , must have multiple roots which satisfy the equation  $P'(z) = 0$ . But since the polynomial  $P'(z)$  is of degree at most  $(n - 1)$  and has at most  $n - 1$  distinct zeros  $z'_\nu$ ,  $1 \leq \nu \leq n - 1$ . Hence Eq (2.1.2) can have a multiple root only at the numbers  $P_n(z'_1)$ ,  $P_n(z'_2), \dots, P_n(\infty)$ , at most  $n$  of which are distinct.

Let  $z_0$  be a root of multiplicity  $k > 1$  of Eq (2.1.2). Then under the mapping  $w = P_n(z)$ , every angle with its vertex at  $z_0$  is enlarged  $k$ -times, whereas every angle with vertex at  $z = \infty$  is enlarged  $n$ -times.

Now we shall study the mapping

$$w = (z - a)^n, \quad n > 1. \quad (2.1.3)$$

This function maps the extended  $z$ -plane into the extended  $w$ -plane such that every point  $w$  has  $n$  distinct inverse images, except at the two points  $w = 0$  and  $w = \infty$ , for which the  $n$  inverse images coalesce into a single point  $z = a$  and  $z = \infty$ , respectively. For  $w \neq 0$  and  $w \neq \infty$ , the  $n$  inverse images of  $w$  are obtained by solving (2.1.3) for  $z$ , which yields

$$z = a + \sqrt[n]{w} = a + \sqrt[n]{|w|} \cdot \left( \cos \frac{\arg\{w\}}{n} + i \sin \frac{\arg\{w\}}{n} \right). \quad (2.1.4)$$

Thus, the  $n$  distinct points  $z$ , defined by (2.1.4), are situated at the vertices of a regular  $n$ -gon with center at  $z = a$ . The mapping (2.1.3) is conformal at all points except  $z = a$  and  $z = \infty$ , and every angle with the vertex at one of these two points is enlarged  $n$ -times. In fact, since  $|w| = |z - a|^n$ ,  $\arg\{w\} = n \arg\{z - a\}$ , the circle  $|z - a| = r$  is mapped into the circle  $|w| = r^n$ . Also, as the point  $z$  traverses once around the circle  $|z - a| = r$ , the image point  $w$  traverses the circle  $|w| = r^n$   $n$ -times in the same direction, since  $\arg\{w\}$  increases continuously by  $2n\pi$ . Moreover, the ray  $\arg\{z - a\} = \theta_0 + 2k\pi$  ( $k$  an integer) in the  $z$ -plane going from  $a$  to  $\infty$  is mapped into the ray  $\arg\{w\} = n\theta_0 + 2m\pi$  ( $m$  an integer) in the  $w$ -plane going from 0 to  $\infty$ .

Let  $D$  denote the region  $\{z : \theta_0 + 2k\pi < \arg\{z - a\} < \theta_1 + 2k\pi\}$ , where  $k$  is an integer and  $0 < \theta_1 - \theta_0 \leq 2\pi/n$ . This region  $D$  is called the *interior* of

the angle  $(\theta_1 - \theta_0)$  which is bounded by the two rays  $\arg\{z - a\} = \theta_0 + 2k\pi$  and  $\arg\{z - a\} = \theta_1 + 2k\pi$ ,  $k = 0, \pm 1, \pm 2, \dots$ . Then the function (2.1.3) maps the region  $D$  onto the region  $G = \{n\theta_0 + 2m\pi < \arg\{w\} < n\theta_1 + 2m\pi\}$ ,  $m = 0, \pm 1, \pm 2, \dots$ , which is the interior of the angle  $n(\theta_1 - \theta_0)$  with vertex at  $w = 0$  (Fig 2.1.1).

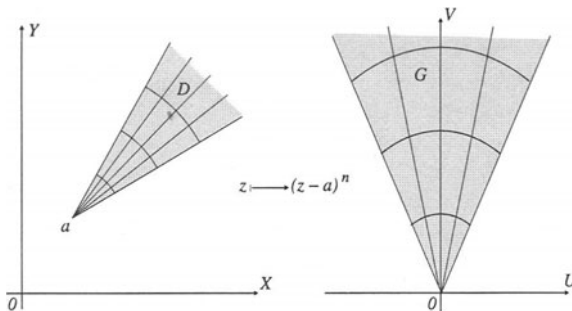


Fig. 2.1.1. The mapping  $w = (z - a)^n$ .

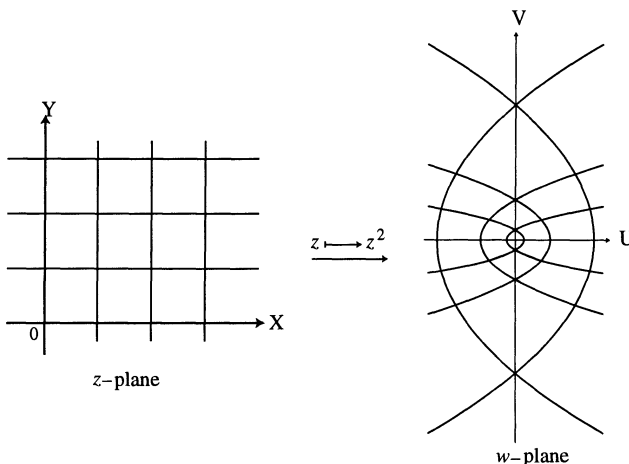


Fig. 2.1.2. The mapping  $w = z^2$ .

The mapping function (2.1.3) produces a conformal and one-to-one map of the interior of an angle onto the interior of another angle which is  $n$ -times wider. However, it does not map every circle into a circle (in the extended sense). For example, for  $n = 2$ ,  $a = 0$ , the map  $w = z^2$  maps every vertical

straight line  $z = b + it$ , where  $b \neq 0$  is real and  $-\infty < t < \infty$ , onto the parabola  $v^2 = 4b^2(b^2 - u)$  which opens to the left, and every horizontal line  $z = t + ic$ , where  $c \neq 0$  is real and  $-\infty < t < \infty$ , onto the parabola  $v^2 = 4c^2(c^2 + u)$  which opens to the right (Fig. 2.1.2). This mapping is conformal except at  $z = 0$ , but it is not one-to-one, since every point in the  $w$ -plane except  $w = 0$  and  $w = \infty$  has two inverse images.

The multiple-valued function  $w = \sqrt[n]{z}$  has the inverse  $z = w^n$  which has been discussed above with reverse roles of  $w$  and  $z$ . Under the mapping  $z = w^n$ , the interiors  $G_1, \dots, G_n$  of the  $n$  angles, each equal to  $2\pi/n$  radians, formed by the  $n$  rays emanating from the point  $w = 0$  lead to the  $n$  single-valued branches  $(\sqrt[n]{z})_1, \dots, (\sqrt[n]{z})_n$  of the function  $w = \sqrt[n]{z}$ , all defined on the region  $D$ . These branches, which have nonzero derivatives on  $D$ , map  $D$  one-to-one and continuously onto  $G_k$ ,  $k = 1, \dots, n$  (Fig. 2.1.3).

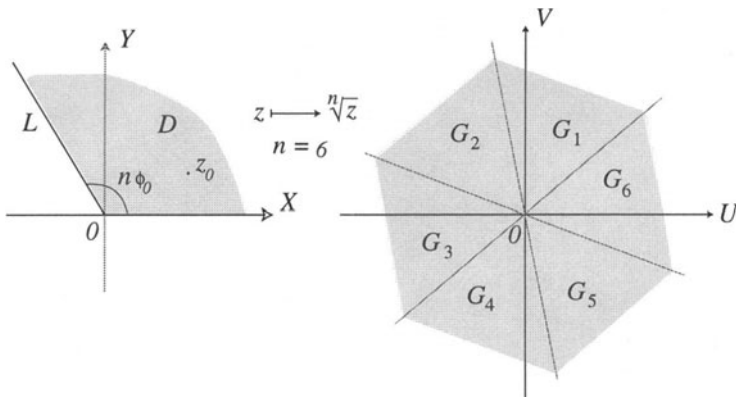


Fig. 2.1.3. The map  $w = \sqrt[n]{z}$ .

The inverse image in the  $z$ -plane of the regions  $G_k$ , whose boundaries are marked by solid lines, is the single ray  $L$  emanating from  $z = 0$  and inclined at an angle  $n\phi_0$ . The manner in which a branch  $(\sqrt[n]{z})_k$  changes into the next branch  $(\sqrt[n]{z})_{k+1}$  can be explained by letting a point  $z_0 \neq 0$  in  $D$  make a complete circle with center at  $z = 0$ . We choose the value of  $\sqrt[n]{z}$  that is associated with the branch  $(\sqrt[n]{z})_k$  and represented by the value  $w_0 = \sqrt[n]{|z_0|} e^{i\theta_0/n} \in G_k$ . Then, as the point  $z_0$  moves continuously along the circle  $|z| = |z_0|$  in the positive direction, the value of  $w = \sqrt[n]{|z_0|} e^{i\theta/n}$  varies continuously with  $\theta$  such that as the point  $z$  returns to its original value  $z_0$ , the value of  $w$  goes to

the value  $w_1 = \sqrt[n]{|z_0|} e^{i(\theta_0+2\pi)/n}$ , where  $w_1$  is the value associated with the branch  $(\sqrt[n]{z})_{k+1}$  on the adjacent region  $G_{k+1}$ , where  $G_k \cap G_{k+1} = \emptyset$  for  $k = 1, \dots, n$ . Proceeding in this manner through  $n$  windings around  $z = 0$ , the  $n$  branches  $(\sqrt[n]{z})_k$  undergo the following chain of transformations:

$$\begin{aligned} (\sqrt[n]{z})_k &\rightarrow (\sqrt[n]{z})_{k+1}, (\sqrt[n]{z})_{k+1} \rightarrow (\sqrt[n]{z})_{k+2}, \dots, \\ (\sqrt[n]{z})_n &\rightarrow (\sqrt[n]{z})_1, (\sqrt[n]{z})_1 \rightarrow (\sqrt[n]{z})_2, \dots, (\sqrt[n]{z})_{k-1} \rightarrow (\sqrt[n]{z})_k. \end{aligned}$$

The points  $z = 0$  and  $z = \infty$  are the algebraic branch points for the mapping  $w = \sqrt[n]{z}$ .

---

## 2.2. Bilinear Transformations

The *bilinear (linear-fractional, or Möbius) transformation* has the form

$$w = f(z) = \frac{az + b}{cz + d}, \quad (2.2.1)$$

where  $a, b, c, d$  are complex constants such that  $ad - bc \neq 0$  (otherwise the function  $f(z)$  would be identically constant). If  $c = 0$  and  $d = 1$ , or if  $a = 0$ ,  $d = 0$  and  $b = c$ , then the function (2.2.1) reduces to a linear transformation  $w = az + b$ , or an inversion  $w = \frac{1}{z}$ , respectively. The transformation (2.2.1) can also be written as

$$w = \frac{a}{c} + \frac{bc - ad}{c(cz + d)}, \quad (2.2.2)$$

that can be viewed as composed of the following three successive functions:

$$z_1 = cz + d, \quad z_2 = \frac{1}{z_1}, \quad w = \frac{a}{c} + \frac{bc - ad}{c} z_2.$$

This shows that the mapping (2.2.1) is a linear transformation, followed by an inversion followed by another linear transformation. The bilinear transformation (2.2.1) maps the extended  $z$ -plane conformally onto the extended  $w$ -plane such that the pole at  $z = -d/c$  is mapped into the point  $w = \infty$ . The inverse transformation

$$z = f^{-1}(w) = \frac{b - dw}{-a + cw} \quad (2.2.3)$$

is also bilinear defined on the extended  $w$ -plane, and maps it conformally onto the extended  $z$ -plane such that the pole at  $w = a/c$  is mapped into the point  $z = \infty$ . Note that  $f'(z) = \frac{ad - bc}{(cz + d)^2} \neq 0$ ; also  $[f^{-1}(w)]' = \frac{-ad + bc}{(cw - a)^2} \neq 0$ . A bilinear transformation carries circles into circles (in the extended sense\*).

A cross-ratio between four distinct finite points  $z_1, z_2, z_3, z_4$  is defined by

$$(z_1, z_2, z_3, z_4) = \frac{z_1 - z_2}{z_1 - z_4} \cdot \frac{z_3 - z_4}{z_3 - z_2}. \quad (2.2.4)$$

If  $z_2, z_3$ , or  $z_4$  is a point at infinity, then (2.2.4) reduces to

$$\frac{z_3 - z_4}{z_1 - z_4}, \quad \frac{z_1 - z_2}{z_1 - z_4}, \quad \text{or} \quad \frac{z_1 - z_2}{z_3 - z_2},$$

respectively. The cross-ratio  $(z, z_1, z_2, z_3)$  is invariant under bilinear transformations.

**THEOREM 2.2.1.** *A bilinear transformation is uniquely defined by a correspondence of the cross-ratios*

$$(w, w_1, w_2, w_3) = (z, z_1, z_2, z_3), \quad (2.2.5)$$

*which maps any three distinct points  $z_1, z_2, z_3$  in the extended  $z$ -plane into three prescribed points  $w_1, w_2, w_3$  in the extended  $w$ -plane.*

The cross-ratio  $(z, z_1, z_2, z_3)$  is the image of  $z$  under a bilinear transformation that maps three distinct points  $z_1, z_2, z_3$  into  $0, 1, \infty$ .

The points  $z$  and  $z^*$  are said to be *symmetric* with respect to a circle  $C$  (in the extended sense) through three distinct points  $z_1, z_2, z_3$  iff

$$(z^*, z_1, z_2, z_3) = \overline{(z, z_1, z_2, z_3)}. \quad (2.2.6)$$

The mapping that carries  $z$  into  $z^*$  is called a *reflection* with respect to  $C$ . Two reflections obviously yield a bilinear transformation.

---

\*There is no distinction between circles and straight lines in the theory of bilinear transformations.

If  $C$  is a straight line, then we choose  $z_3 = \infty$ , and the condition for symmetry (2.2.6) gives

$$\frac{z^* - z_1}{z_1 - z_2} = \frac{\bar{z} - \bar{z}_1}{\bar{z}_1 - \bar{z}_2}. \quad (2.2.7)$$

Let  $z_2$  be any finite point on the line  $C$ . Then, since  $|z^* - z_1| = |z - z_1|$ , the points  $z$  and  $z^*$  are equidistant from the line  $C$ . Moreover, since  $\Im\left\{\frac{z^* - z_1}{z_1 - z_2}\right\} = -\Im\left\{\frac{z - z_1}{z_1 - z_2}\right\}$ , the line  $C$  is the perpendicular bisector of the line segment joining  $z$  and  $z^*$ . If  $C$  is the circle  $|z - a| = R$ , then

$$\begin{aligned} \overline{(z, z_1, z_2, z_3)} &= \overline{(z - a, z_1 - a, z_2 - a, z_3 - a)} \\ &= \left( \bar{z} - \bar{a}, \frac{R^2}{z_1 - a}, \frac{R^2}{z_2 - a}, \frac{R^2}{z_3 - a} \right) \\ &= \left( \frac{R^2}{\bar{z} - \bar{a}}, z_1 - a, z_2 - a, z_3 - a \right) \\ &= \left( \frac{R^2}{\bar{z} - \bar{a}} + a, z_1, z_2, z_3 \right). \end{aligned}$$

Hence, in view of (2.2.6), we find that the points  $z$  and  $z^* = \frac{R^2}{\bar{z} - \bar{a}} + a$  are symmetric, i.e.,

$$(z^* - a)(\bar{z} - \bar{a}) = R^2. \quad (2.2.8)$$

Note that  $|z^* - a||z - a| = R^2$ ; also, since  $\frac{z^* - a}{z - a} > 0$ , the points  $z$  and  $z^*$  are on the same ray from the point  $a$  (Fig 2.2.1). Note that the point symmetric to  $a$  is  $\infty$ .

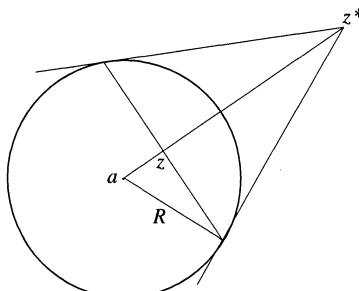


Fig. 2.2.1. Symmetry with respect to a circle.

A generalization of this result is as follows: If  $\Gamma$  denotes an analytic Jordan curve with parametric equation  $z = \gamma(s)$ ,  $s_1 < s < s_2$ , then for any point  $z$  sufficiently close to  $\Gamma$ , the point

$$z^* = \gamma(\overline{\gamma^{[-1]}(z)}) \quad (2.2.9)$$

defines a symmetric point of  $z$  with respect to  $\Gamma$  (Sansone and Gerretsen, 1969, p.103; Papamichael, Warby and Hough, 1986). Some examples are as follows:

(i) If  $\Gamma$  is the circle  $x^2 + y^2 = a^2/9$ , then  $z^* = a^2/9\bar{z} = z^*$ .

(ii) If  $\Gamma$  is the ellipse  $\frac{(x+a/2)^2}{a^2} + y^2 = 1$ , then

$$z^* = -\frac{a}{2} + \frac{(a^2+1)(\bar{z}+a/2) + 2ia\sqrt{a^2-1-(\bar{z}+a/2)}}{a^2-a}.$$

(iii) If  $\Gamma_1$  is a cardioid defined by  $z = \gamma(s) = \left(\frac{1}{2} + \cos \frac{s}{2}\right) e^{is}$ ,  $-\pi < s \leq \pi$ , then from (2.2.9) we cannot write an explicit expression for symmetric points with respect to  $\Gamma_1$ . However, for any real  $t$

$$\gamma(\pm it) = \left(\frac{1}{2} + \cosh \frac{t}{2}\right) e^{\mp t}$$

defines two real symmetric points with respect to  $\Gamma_1$ , provided the parameter  $t$  satisfies the equation  $\gamma(it)\gamma(-it) = a^2$ , i.e.,  $\frac{1}{2} + \cosh \frac{t}{2} = a$  which has the roots

$$t = 2 \cosh^{-1}(a - 1/2) = \pm 2 \log \rho, \quad (2.2.10)$$

where  $\rho = a - \frac{1}{2} + \sqrt{\left(a - \frac{1}{2}\right)^2 - 1}$ .

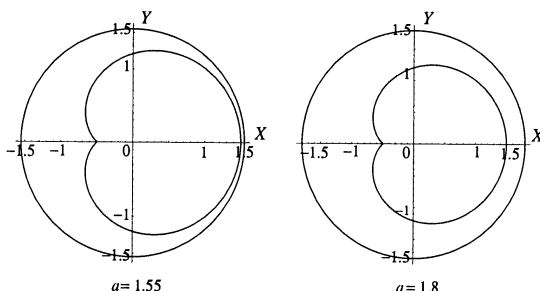


Fig. 2.2.2. Cardioid inside a Circle.

(iv) If a doubly connected region  $\Omega$  is bounded outside by the circle  $\Gamma_2 = \{z : |z| = a, a > 1.5\}$  and inside by the cardioid  $\Gamma_1$  defined above in (iii) (see Fig. 2.2.2), then it follows from (2.2.10) that there is one pair of real common symmetric points  $\zeta_1 \in \text{Int}(\Gamma_1)$  and  $\zeta_2 \in \text{Ext}(\Gamma_2)$  such that  $\zeta_1 = a/\rho^2$  and  $\zeta_2 = a\rho^2$ , where  $\rho$  is defined in (2.2.10).

The *symmetry principle* states that if a bilinear transformation maps a circle  $C_1$  onto a circle  $C_2$ , then it maps any pair of symmetric points with respect to  $C_1$  into a pair of symmetric points with respect to  $C_2$ . This means that bilinear transformations preserve symmetry.

A practical application of the symmetry principle is finding bilinear transformations which map a circle  $C_1$  onto a circle  $C_2$ . We already know that the transformation (2.2.5) can always be determined by requiring that the three points  $z_1, z_2, z_3 \in C_1$  map onto three points  $w_1, w_2, w_3 \in C_2$ . But a bilinear transformation is also determined if a point  $z_1 \in C_1$  should map into a point  $w_1 \in C_2$  and a point  $z_2 \notin C_1$  should map into a point  $w_2 \notin C_2$ . Then, by the symmetry principle, the point  $z_2^*$  which is symmetric to  $z_2$  with respect to  $C_1$  is mapped into the point  $w_2^*$  which is symmetric to  $w_2$  with respect to  $C_2$ , and then the desired bilinear transformation is given by

$$(w, w_1, w_2, w_2^*) = (z, z_1, z_2, z_2^*). \quad (2.2.11)$$

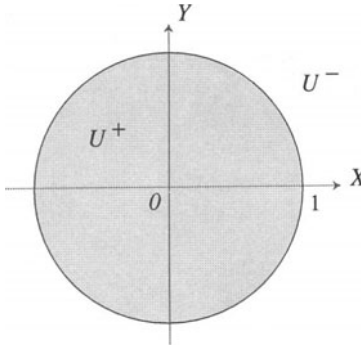


Fig. 2.2.3.

Let  $U^+$  denote the region  $|z| < 1$ ,  $U^-$  the region  $|z| > 1$ , and let  $C = \{|z| = 1\}$  be their common boundary (Fig. 2.2.3). Let  $f(z)$  be a function defined on  $U^+$ . Then this function can be related to the function  $f^*(z)$  defined

in  $U^-$  in the same manner as in (1.4.3) for half-planes, except that now the conjugate complex points are replaced by points inverse with respect to the circle  $C$  according to the relation (2.2.8). Thus,

$$\overline{f^*(z)} = \overline{f\left(\frac{1}{\bar{z}}\right)} = \bar{f}\left(\frac{1}{z}\right). \quad (2.2.12)$$

This relation is symmetrical, i.e.,

$$f(z) = \overline{f^*\left(\frac{1}{\bar{z}}\right)}, \quad (f^*(z))^* = f(z). \quad (2.2.13)$$

If  $f(z)$  is regular or meromorphic in  $U^+$ , then  $f^*(z)$  is regular or meromorphic in  $U^-$ . Also, if  $f(z)$  is a rational function defined by (1.4.4), then

$$f^*(z) = \frac{\bar{a}_n z^{-n} + \bar{a}_{n-1} z^{-n+1} + \cdots + \bar{a}_0}{\bar{b}_m z^{-m} + \bar{b}_{-m+1} z^{m-1} + \cdots + \bar{b}_0}. \quad (2.2.14)$$

Moreover, if  $f(z)$  has the power series expansion

$$f(z) = \sum_{k=-\infty}^{\infty} a_k z^k \quad z \in U^+,$$

then

$$f^*(z) = \sum_{k=-\infty}^{\infty} \bar{a}_k z^{-k}, \quad z \in U^-. \quad (2.2.15)$$

If  $f(z)$  has a zero (pole) of order  $k$  at  $z = \infty$  ( $z = 0$ ), so does  $f^*(z)$ . Let us assume that  $f(z)$  approaches a definite limit value  $f^+(t)$  as  $z \rightarrow t \in C$  from  $U^+$ . Then  $f^{*-}(t)$  exists and

$$f^{*-}(t) = \bar{f}^-\left(\frac{1}{t}\right) = \overline{f^+(t)}, \quad (2.2.16)$$

because  $1/\bar{z} \rightarrow t$  from  $U^+$  as  $z \rightarrow t$  from  $U^-$ , and hence  $f^*(z) = \bar{f}\left(\frac{1}{z}\right) = \overline{f\left(\frac{1}{\bar{z}}\right)} \rightarrow \overline{f^+(t)}$ . If  $f(z)$  is regular in  $U^+$  except possibly at infinity and continuous on  $C$  from the left, then let  $F(z)$  be sectionally regular and be defined by

$$F(z) = \begin{cases} f(z) & \text{for } z \in U^+, \\ f^*(z) & \text{for } z \in U^-. \end{cases} \quad (2.2.17)$$

Then,  $F^*(z) = F(z)$ , and, as in (1.4.7),

$$F^-(t) = \overline{F^+(t)}, \quad F^+(t) = \overline{F^-(t)}. \quad (2.2.18)$$

Moreover, in view of the Schwarz reflection principle, if  $\Im\{f^+(t)\} = 0$  on some part of the circle  $C$ , then  $f^*(z)$  is the analytic continuation of  $f(z)$  through this part of  $C$ .

### 2.3. Schwarz-Christoffel Transformations

The *Schwarz-Christoffel formula* helps solve an important class of boundary value problems that involve regions with polygonal boundaries. This formula has an integral representation and is used to map conformally the upper half-plane  $\Im\{z\} > 0$  or the unit disk  $U$  in the  $z$ -plane onto the interior of a given  $n$ -gon ( $n \geq 2$ ) in the  $w$ -plane. Let  $\Gamma = \bigcup_{i=1}^n \Gamma'_i$  in the  $w$ -plane with vertices  $w_i$  and exterior angles  $\pi\alpha_i$ ,  $|\alpha_i| < 1$ , and  $\sum_{i=1}^n \alpha_i = 2$  for  $i = 1, \dots, n$  (Fig. 2.3.1).

Then the conformal map from the upper half-plane  $D = \{z : \Im\{z\} > 0\}$  onto  $G$ , which is the interior of  $\Gamma$ , is given by

$$w = f(z) = A + B \int_{z_0}^z \prod_{i=1}^n (\zeta - x_i)^{-\alpha_i} d\zeta, \quad (2.3.1)$$

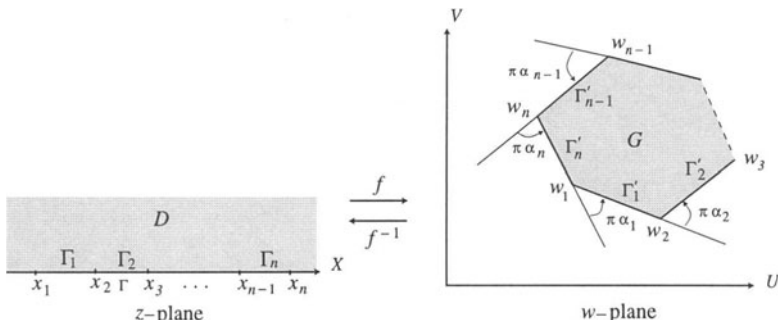


Fig. 2.3.1. Schwarz-Christoffel transformation.

where  $A$  and  $B$  are constants that determine the size and position of the polygon  $\Gamma$ , and integration is carried out along any path in  $D$  that joins  $z_0 \in D$  to  $z$ , and the principal branch is used for the multiple-valued function  $(\zeta - x_i)^{-\alpha_i}$  in the integrand such that  $0 < \arg\{\zeta - x_i\} < \pi$ ,  $i = 1, \dots, n$ , for  $\Im\{z\} > 0$ . These branches are a direct analytic continuation into the upper half-plane of the real-valued functions  $(x - x_i)^{-\alpha_i}$ , where  $x > x_i$ . Then the integral (2.3.1) is a single-valued analytic function in the upper half-plane  $\Im\{z\} > 0$ , and the points  $x_i$  lying on the  $x$ -axis are the singularities of the Schwarz–Christoffel integral (2.3.1). This function  $w = f(z)$  defines a conformal mapping of  $D$  onto  $G$  provided the points  $x_i$  are suitably chosen.

Thus, if all the numbers  $x_i$  are finite, then the function  $f(z)$  defined by (2.3.1) remains bounded in the neighborhood of the singularities  $x_i$ . To see that the Schwarz–Christoffel integral (2.3.1) remains bounded as  $z \rightarrow \infty$ , we rewrite this integral as

$$\begin{aligned} w = f(z) &= A + B \int_{z_0}^z \zeta^{-(\alpha_1 + \dots + \alpha_n)} \left(1 - \frac{x_1}{\zeta}\right)^{-\alpha_1} \dots \left(1 - \frac{x_n}{\zeta}\right)^{-\alpha_n} d\zeta \\ &= a + B \int_{z_0}^z \frac{1}{\zeta^2} \prod_{i=1}^n \left(1 - \frac{x_i}{\zeta}\right)^{-\alpha_i} d\zeta, \end{aligned} \tag{2.3.2}$$

which shows that the integral is convergent as  $z \rightarrow \infty$ . Hence, the Schwarz–Christoffel integral (2.3.1) defines a univalent function of  $z$  in  $D$  that maps  $D$  conformally onto the bounded polygon  $G$  in the  $w$ -plane. If  $G$  is convex, then  $\alpha_i > 0$ . Thus, there are  $(n - 1)$  independent numbers  $\alpha_i$ , and  $(n - 3)$  independent numbers  $x_i$ .

In order to see the structure of the boundary  $\Gamma = \bigcup_{i=1}^n \Gamma_i$  of the polygon  $G$ , consider the derivative of the Schwarz–Christoffel integral (2.3.1), which is

$$f'(z) = B(z - x_1)^{-\alpha_1} \dots (z - x_n)^{-\alpha_n}.$$

Notice that  $f' \neq 0$  everywhere in  $\Im\{z\} \geq 0$  except at the singularities  $x_i$  where it vanishes or becomes unbounded. As  $z$  varies along every interval  $x_k < x < x_{k+1}$ ,  $k = 1, \dots, n - 1$ , the value of  $\arg\{f'(z)\}$  does not change, since

$$\arg\{(x - x_k)^{-\alpha_k}\} = \begin{cases} -\pi\alpha_k, & \text{if } x < x_k, \\ 0, & \text{if } x > x_k. \end{cases}$$

Geometrically,  $\arg\{f'(z)\}$  determines the size of the angle through which the tangent to a Jordan curve passing through  $x_k$  must be rotated in order to obtain

the tangent of the image of this curve at the point  $w_k = f(x_k)$ . Hence the segments  $x_k < x < x_{k+1}$ ,  $k = 1, \dots, n - 1$ , of the real axis are mapped by  $f(z)$  into rectilinear segments in the  $w$ -plane. The points  $x_k$  of the real axis are transformed into the vertices  $w_k$  in the  $w$ -plane, where the polygon  $\Gamma$  is made up of the polygonal lines through  $w_1, w_2, \dots, w_n$  with straight line segments as sides. As the point  $z$  traverses the entire real  $x$ -axis in the positive sense, the corresponding point  $w$  travels completely through the polygonal lines of  $\Gamma$  which, in general, can have a self-intersecting point.

The size of the angle between adjacent segments of the polygon  $\Gamma$  can be determined as follows: Consider the variation of  $\arg\{f'(z)\}$  as  $z$  passes through the point  $x_i$  in the positive direction (Fig. 2.3.2). Then the angle between the vectors  $\overrightarrow{w_{i-1} w_i}$  and  $\overrightarrow{w_i w_{i+1}}$  is equal to  $\pi\alpha_i$ . For  $\mu_i < 1$ , where  $\mu_i = 1 - \alpha_i$ , the transition from the vector  $\overrightarrow{w_{i-1} w_i}$  to the direction of the vector  $\overrightarrow{w_i w_{i+1}}$  occurs in the positive sense (Fig. 2.3.2a), whereas for  $\mu_i > 1$  it occurs in the negative sense (Fig. 2.3.2b), although the angle of transition in the positive sense in both cases from the direction of the vector  $\overrightarrow{w_{i-1} w_i}$  to the direction of the vector  $\overrightarrow{w_i w_{i+1}}$  is  $\pi\alpha_i$ . If a polygonal line does not intersect itself, it becomes the boundary of a closed polygon. Also the sum of all interior angles of this closed polygon is equal to  $\sum_{i=1}^n \pi\mu_i = \sum_{i=1}^n \pi(1 - \alpha_i) = (n - 2)\pi$ .

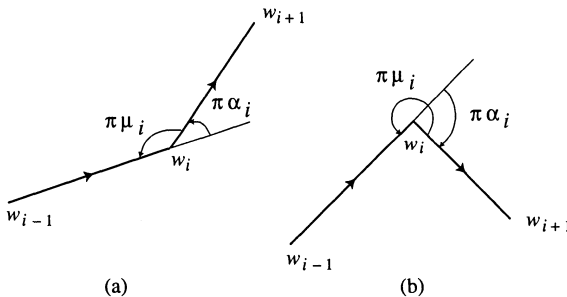


Fig. 2.3.2.

For practical purposes, while constructing a conformal map of  $D$  onto  $G$  one can specify any three points  $x_i, x_j, x_k$  of the real axis that go into the three prescribed vertices  $w_i, w_j, w_k$  of the polygon  $\Gamma$ .

When one of the points  $x_i$ , say  $x_n$ , coincides with the point at infinity, the

vertices of the polygon  $\Gamma$  correspond to the points  $x'_1, \dots, x'_{n-1}, \infty$ , and the formula (2.3.1) becomes

$$w = f(z) = A + B' \int_{z_0}^z \prod_{i=1}^{n-1} (\zeta - x'_i)^{-\alpha_i} d\zeta. \quad (2.3.3)$$

Note that formula (2.3.3) is similar to (2.3.1) except that the term corresponding to the point  $x_n = \infty$  has been dropped. The inverse Schwarz–Christoffel transformation is given by

$$z = f(w) = C_0 + C \int_{w_0}^w \prod_{i=1}^n (\zeta - w_i)^{-\mu_i} d\zeta. \quad (2.3.4)$$

**CASE STUDY 2.3.1** To map the upper half-plane  $\Im\{z\} > 0$  onto a triangle  $A_1A_2A_3$  with interior angles  $\mu_1\pi$ ,  $\mu_2\pi$  and  $\mu_3\pi$ , respectively, such that the vertex  $A_1$  corresponds to  $x_1 = 0$ ,  $A_2$  to  $x_2 = 1$  and  $A_3$  to  $x_3 = \infty$ , we get, by using (2.3.1), the mapping function

$$w = A + B \int_0^z \zeta^{-\alpha_1} (1 - \zeta)^{-\alpha_2} d\zeta. \quad (2.3.5)$$

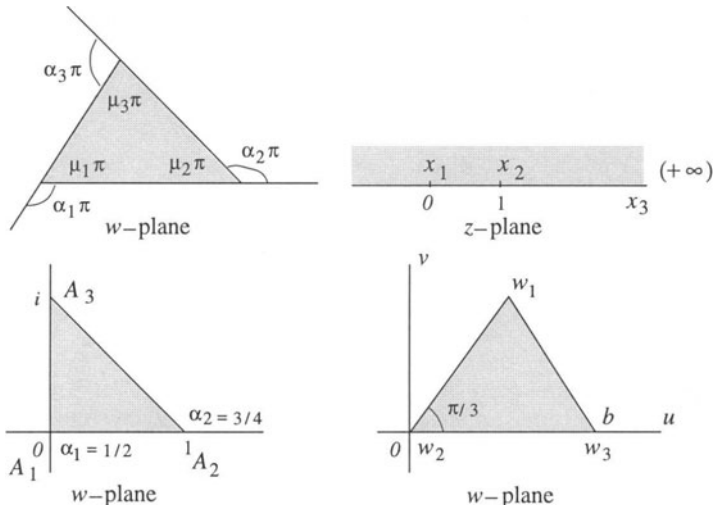


Fig. 2.3.3.

If the triangle is isosceles such that the vertices  $A_1, A_2, A_3$  are at  $w = 0$ ,  $w = 1$ , and  $w = i$ , respectively (Fig 2.3.3), then from (2.3.5) the transformation becomes

$$w = A + B \int_0^z \zeta^{-1/2} (1 - \zeta)^{-3/4} d\zeta. \quad (2.3.6)$$

Since  $w = 0$  corresponds to  $z = 0$ , we get  $A = 0$ , and since  $w = 1$  corresponds to  $z = 1$ , we find from (2.3.6) that

$$B = \frac{1}{\int_0^1 \zeta^{-1/2} (1 - \zeta)^{-3/4} d\zeta}. \quad (2.3.7)$$

For an equilateral triangle of side  $b$  (see Fig. 2.3.3), let  $x_1 = -1$  correspond to the vertex  $w_1$ ,  $x_2 = 1$  to  $w = 0$ , and  $x_3 = \infty$  to  $w_3 = b$ . Since  $\alpha_1 = \alpha_2 = \alpha_3 = 2/3$ , the transformation is given by

$$w = \int_1^z (\zeta + 1)^{-2/3} (\zeta - 1)^{-2/3} d\zeta. \quad (2.3.8)$$

When  $z = -1$ , we set  $\zeta = x$ . Then for  $-1 < x < 1$ , we have  $x + 1 > 0$  and  $\arg\{x + 1\} = 0$ , but  $|x - 1| = 1 - x$ , and  $\arg\{x - 1\} = \pi$ . Thus,

$$\begin{aligned} w_1 &= \int_{-1}^1 (x + 1)^{-2/3} e^{-2i\pi/3} (1 - x)^{-2/3} dx = e^{i\pi/3} \int_{-1}^1 \frac{dx}{(1 - x^2)^{2/3}} \\ &= 2e^{i\pi/3} B\left(\frac{1}{2}, \frac{1}{3}\right) = b e^{i\pi/3}, \end{aligned} \quad (2.3.9)$$

where  $b = 2B\left(\frac{1}{2}, \frac{1}{3}\right)$ , and  $B$  denotes the beta function of its arguments. For the vertex  $w_3$  note that it is on the positive  $u$ -axis, i.e.,

$$w_3 = \int_1^\infty (x + 1)^{-2/3} (x - 1)^{-2/3} dx = \int_1^\infty \frac{dx}{(x^2 - 1)^{2/3}}.$$

But  $w_3$  is also defined by (2.3.8) when  $z$  goes to  $\infty$  along the negative  $u$ -axis, i.e.,

$$\begin{aligned} w_3 &= \int_1^\infty (x + 11)^{-2/3} (x - 1)^{-2/3} dx \\ &= w_1 + e^{-4i\pi/3} \int_{-1}^{-\infty} [|x + 1| |x - 1|]^{-2/3} dx \quad \text{using (2.3.9)} \\ &= b e^{i\pi/3} + e^{-i\pi/3} \int_1^\infty \frac{dx}{(x^2 - 1)^{2/3}} \\ &= b e^{i\pi/3} + w_3 e^{-i\pi/3}, \end{aligned}$$

which yields  $w_3 = b$ . A numerical evaluation of the improper integral in (2.3.7) is given in Case Study 3.3.1. ■

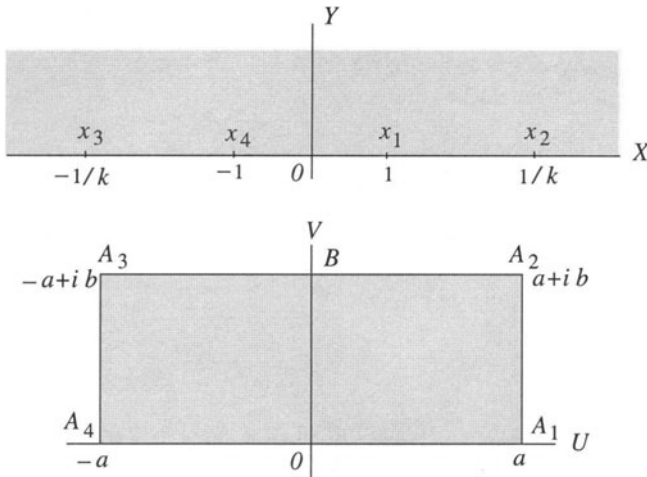


Fig. 2.3.4.

CASE STUDY 2.3.2 To map the upper half-plane  $\Im\{z\} > 0$  onto a rectangle  $A_1 A_2 A_3 A_4$  with vertices at the points  $w = \pm a$ ,  $\pm a + ib$ , where  $2a$  and  $b$  are the width and the height of the rectangle (Fig. 2.3.4), note that in the formula (2.3.1) with  $n = 4$ , only three of the four points  $x_1, x_2, x_3, x_4$  may be chosen arbitrarily. Since the rectangle is symmetric about the *v*-axis, we can choose the *x*'s symmetrically. Thus, for the right-half rectangle  $O A_1 A_2 B$  let  $w = 0, a, ib$  correspond to  $z = 0, 1, \infty$ , respectively, and let the preimage of  $A_2$  be  $z = 1/k$ ,  $0 < k < 1$ . Similarly, for the left-half rectangle  $O B A_3 A_4$  let  $w = 0, -a, ib$  correspond to  $z = 0, -1, -\infty$ , respectively, with the preimage of  $A_3$  as  $-1/k$ . Then the formula (2.3.1) yields

$$\begin{aligned} w &= A + B \int^z \prod_{i=1}^4 (\zeta - x_i)^{-\alpha_i} d\zeta \\ &= B \int_0^z \frac{d\zeta}{\sqrt{\zeta-1} \sqrt{\zeta+1} \sqrt{\zeta-1/k} \sqrt{\zeta+1/k}} \\ &= B \int_0^z \frac{d\zeta}{\sqrt{\zeta^2-1} \sqrt{\zeta^2-1/k^2}} = B \int_0^z \frac{d\zeta}{\sqrt{\zeta^2-1} \sqrt{1-k^2\zeta^2}}, \end{aligned} \quad (2.3.10)$$

where  $A = 0$  since  $z = 0$  goes into  $w = 0$ , and  $B$  is an arbitrary constant.

Now, to evaluate the constants  $B$  and  $k$ , note that since  $z = 1$  goes into  $w = a$ , we get from (2.3.10)

$$a = B \int_0^1 \frac{d\zeta}{\sqrt{1 - \zeta^2} \sqrt{1 - k^2 \zeta^2}}. \quad (2.3.11)$$

Also, since  $z = 1/k$  goes into  $w = a + ib$ , using (2.3.11) we find that

$$\begin{aligned} a + ib &= B \int_0^{1/k} \frac{d\zeta}{\sqrt{1 - \zeta^2} \sqrt{1 - k^2 \zeta^2}} \\ &= B \left( \int_0^1 + \int_1^{1/k} \right) \frac{d\zeta}{\sqrt{1 - \zeta^2} \sqrt{1 - k^2 \zeta^2}} \\ &= a + i B \int_1^{1/k} \frac{d\zeta}{\sqrt{1 - \zeta^2} \sqrt{1 - k^2 \zeta^2}}, \end{aligned}$$

where  $B$  is an arbitrary complex constant. Thus, with  $B = 1$

$$b = \int_1^{1/k} \frac{d\zeta}{\sqrt{1 - \zeta^2} \sqrt{1 - k^2 \zeta^2}}. \quad (2.3.12)$$

Hence, we can determine  $B$  and  $k$  from (2.3.11) and (2.3.12) if  $a$  and  $b$  are prescribed. But if  $k$  is preassigned and we take  $B = 1$ , then the values of  $a$  and  $b$  are determined from (2.3.11) and (2.3.12). Then the mapping function becomes

$$w = \int_0^z \frac{d\zeta}{\sqrt{1 - \zeta^2} \sqrt{1 - k^2 \zeta^2}}, \quad (2.3.13)$$

which is known as the elliptic integral of the first kind. The inverse function is called the elliptic sine function  $z = \operatorname{sn} w = \operatorname{sn}(w; k)$  which is a Jacobian elliptic function. The function  $\operatorname{sn}$  is a  $2a$ - and  $2ib$ -periodic function. For more material on the function  $\operatorname{sn}$  and other Jacobian elliptic functions, see Whittaker and Watson (1927, p.491 ff.), Nehari (1952, p.280 ff.), or Andersen et al. (1962, p.159ff), and see Case Study 3.3.2 for numerical evaluation of improper integrals in (2.3.13). If we denote the value of  $a$ , given by (2.3.11), by  $K(k)$ , where  $0 < k < 1$ , then the ratio  $a/b$  of the sides of the rectangle is given by

$$\frac{a}{b} = 2 \frac{K(k)}{K(\sqrt{1 - k^2})}. \quad (2.3.14)$$

An evaluation of  $K(k)$  is accomplished by the Landen transformation: Set  $k_1 = \sqrt{1 - k^2}$ , and  $k' = \frac{1 - k_1}{1 + k_1}$ . Then

$$K(k) = \frac{2}{1 + k_1} K(k'). \quad (2.3.15)$$

In fact, by separating the integral (2.3.11) into two parts, we get

$$K(k) = \left( \int_0^{1/\sqrt{1+k_1}} + \int_{1/\sqrt{1+k_1}}^1 \right) \frac{d\zeta}{\sqrt{(1-\zeta^2)(1-k^2\zeta^2)}} \equiv I_1 + I_2.$$

If we set  $\zeta = \sqrt{\frac{1-t^2}{1-k^2t^2}}$ , where  $1/\sqrt{1+k_1} \leq \zeta \leq 1$ , and  $t = \sqrt{\frac{1-\zeta^2}{1-k^2\zeta^2}}$ ,  $0 \leq t \leq 1/\sqrt{1+k_1}$ , then

$$I_2 = \int_{1/\sqrt{1+k_1}}^1 \frac{d\zeta}{\sqrt{(1-\zeta^2)(1-k^2\zeta^2)}} = \int_0^{1/\sqrt{1+k_1}} \frac{dt}{\sqrt{(1-t^2)(1-k^2t^2)}}.$$

Moreover, if we set  $\tau = (1+k_1) \frac{\zeta\sqrt{1-\zeta^2}}{\sqrt{1-k^2\zeta^2}}$ ,  $0 \leq \zeta \leq 1/\sqrt{1+k_1}$ , then  $0 \leq \tau \leq 1$ , and

$$I_1 = \frac{1}{1+k_1} K\left(\frac{1-k_1}{1+k_1}\right).$$

Hence,

$$I_1 + I_2 = 2I_1 = \frac{2}{1+k_1} K\left(\frac{1-k_1}{1+k_1}\right),$$

which proves (2.3.15). Since

$$k' = \frac{1-k_1}{1+k_1} = \frac{1-k_1^2}{(1+k_1)^2} = \frac{k^2}{(1+k^2)^2} < k^2 < 1,$$

after  $n$  applications of the Landen transformation we find that the quantities  $k'^{(n)} \rightarrow 0$  very rapidly as  $n \rightarrow \infty$ . This means that we can use the Landen transformation to evaluate the integral in (2.3.11) step-by-step with smaller and smaller values of  $k$ , so that after a finite number of steps the value of the integral (2.3.11) becomes equal to  $\sin^{-1}(1) = \pi/2$ . However, for values of  $k$  closer to 1, the convergence becomes very slow. In that case we can use the inverse Landen transformation

$$K(k') = \frac{1}{2} (1+k_1) K(k), \quad (2.3.16)$$

where  $k_1 = \frac{1-k'}{1+k'}$ ,  $k = \sqrt{1-k_1^2} = \frac{2\sqrt{k'}}{1+k'}$ , and then we can evaluate  $K(k)$  approximately with sufficient accuracy from the asymptotic formula

$$K(k) \approx \ln \frac{4}{k_1} = \frac{1}{2} \ln \frac{16}{1-k^2} \quad \text{for } k \text{ close to 1.} \quad (2.3.17)$$

Further, if we set  $\zeta = \sin \phi$  in (2.3.11), then

$$K(k) = \int_0^{\pi/2} \frac{d\phi}{\sqrt{1 - k^2 \sin^2 \phi}} = \frac{2}{1 + k_1} \int_0^{\pi/2} \frac{d\phi}{\sqrt{1 - k'^2 \sin^2 \phi}},$$

or

$$\begin{aligned} K(k) &= \int_0^{\pi/2} \frac{d\phi}{\sqrt{\cos^2 \phi + k_1^2 \sin^2 \phi}} \\ &= \frac{2}{1 + k_1} \int_0^{\pi/2} \frac{d\phi}{\sqrt{\cos^2 \phi + (1 + k'^2) \sin^2 \phi}}. \end{aligned}$$

Let  $k_1 = \frac{d_0}{c_0}$ , where  $c_0 = 1$  and  $d_0 = k_1$ . Then

$$1 - k'^2 = 1 - \left( \frac{1 - k_1}{1 + k_1} \right)^2 = \left( \frac{2\sqrt{k_1}}{1 + k_1} \right)^2 = \left( \frac{2\sqrt{c_0 d_0}}{c_0 + d_0} \right)^2 = \left( \frac{d_1}{c_1} \right)^2,$$

where  $d_1 = \sqrt{c_0 d_0}$ , and  $c_1 = (c_0 + d_0)/2$ , which yields

$$\begin{aligned} K(k) &= \int_0^{\pi/2} \frac{d\phi}{\sqrt{c_0^2 \cos^2 \phi + d_0^2 \sin^2 \phi}} \\ &= \frac{2}{1 + d_0/c_0} \int_0^{\pi/2} \frac{d\phi}{\sqrt{\cos^2 \phi + (d_1/c_1)^2 \sin^2 \phi}} \\ &= \int_0^{\pi/2} \frac{d\phi}{\sqrt{c_1^2 \cos^2 \phi + d_1^2 \sin^2 \phi}}. \end{aligned}$$

Repeating this process  $n$ -times, we get

$$K(k) = \int_0^{\pi/2} \frac{d\phi}{\sqrt{c_n^2 \cos^2 \phi + d_n^2 \sin^2 \phi}}, \quad (2.3.18)$$

where  $c_n$  and  $d_n$  are determined recursively from

$$c_n = \frac{1}{2} (c_{n-1} + d_{n-1}), \quad d_n = \sqrt{c_{n-1} d_{n-1}}.$$

Hence, as  $n \rightarrow \infty$ , the sequences  $\{c_j\}$  and  $\{d_j\}$  for  $j = 0, 1, 2, \dots$ , and  $c_0 > d_0$ , converge to the same limit, i.e.,

$$\lim_{n \rightarrow \infty} c_n = \lim_{n \rightarrow \infty} d_n = M(k), \quad (2.3.19)$$

which yields

$$K(k) = \frac{\pi}{2 M(k)}.$$

Proof of this result is given in Andersen et al. (1962, p.163). Hence, from (2.3.14) the ratio between the sides of the rectangle is given by

$$\frac{a}{b} = 2 \frac{K(k)}{K(k_1)} = 2 \frac{M(k_1)}{M(k)}, \quad (2.3.20)$$

where  $M(k_1)$  is obtained in the same manner as (2.3.19) by applying the above recursion to  $k_1 = \sqrt{1 - k^2}$ . For more on elliptic integrals and Jacobian elliptic functions, see Phillips (1957, Ch. 1 and 2). ■

**CASE STUDY 2.3.3** To map the upper half-plane  $\Im\{z\} > 0$  onto an arbitrary quadrilateral  $A_1 A_2 A_3 A_4$  with interior angles  $\mu_1\pi$ ,  $\mu_2\pi$ ,  $\mu_3\pi$ , and  $\mu_4\pi$ , respectively, such that the angle  $\mu_1\pi$  at  $A_1$  is the smallest and the ratio of the side  $A_4 A_1$  to the side  $A_1 A_2$  is  $\lambda$ . Without loss of generality, let the vertices  $A_1, A_2, A_3, A_4$  correspond to the points  $x_1 = -1, x_2 = 1, x_3 = k, x_4 = 3$ . Then, by (2.3.1), the transformation is given by

$$w = f(z) = A + B \int_1^z (\zeta + 1)^{-\alpha_1} (\zeta - 1)^{-\alpha_2} (\zeta - k)^{-\alpha_3} (\zeta - 3)^{-\alpha_4} d\zeta. \quad (2.3.21)$$

Newton's method for numerical evaluation of improper integrals in (2.3.21) and an approximate value of  $k$  is given in §3.2. ■

**CASE STUDY 2.3.4** To map a horizontal parallel strip with a rectilinear horizontal cut onto the upper half-plane (Fig. 2.3.5), note that the given strip is equivalent to a quadrilateral with vertices at  $A_1, A_2$  and  $A_3$ , all at infinity, and  $A_4$  at the origin. For the vertices at  $A_1, A_2, A_3$  we have  $\alpha_1 = \alpha_2 = \alpha_3 = 1$ , and for  $A_4$  we have  $\alpha_4 = -1$ . We choose  $x_1 = 1, x_2 = \infty, x_4 = 0$ , and let  $w = 0$  correspond to  $z = 0$ . Then  $A$  in (2.3.1) is zero. With this choice the point  $A_3$  would correspond to some point  $x_3 = -k$  on the negative  $x$ -axis ( $k > 0$ ). Then from (2.3.1) the required transformation with proper choice of

principal values for the integrand is given by

$$\begin{aligned} w &= B \int_0^z \frac{\zeta d\zeta}{(1-\zeta)(k+\zeta)} \\ &= B \int_0^z \frac{1}{1+k} \left( \frac{1}{1-\zeta} - \frac{k}{k+\zeta} \right) d\zeta \\ &= B \left[ \log(1-z) + k \log \left( 1 + \frac{z}{k} \right) \right], \end{aligned} \quad (2.3.22)$$

where  $B$  is an arbitrary constant. To determine  $B$  and  $k$  if  $a$  and  $b$  are given, let  $z = 1 - \varepsilon e^{i\theta}$ ,  $-\pi \leq \theta < 0$ ,  $\varepsilon > 0$  and small, and define a half-circle  $C_\varepsilon$ . Then, as  $z$  moves along  $C_\varepsilon$ , its image point  $w$  varies from the ray  $A_4 A_1$  to the line  $A_1 A_2$ . Thus, for the end point of the image curve the difference  $\Delta w$  in the values of  $w$  on  $A_4 A_1$  and  $A_1 A_2$  is

$$\Delta w = -ia + o(1). \quad (2.3.23)$$

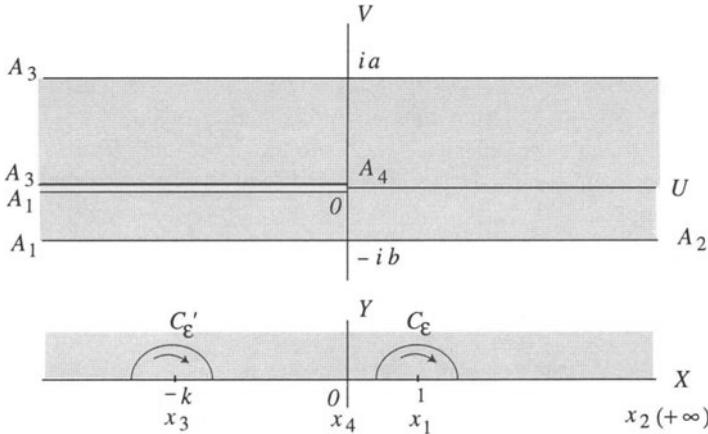


Fig. 2.3.5.

But the difference  $\Delta w$  given by the right side of (2.3.22) is given by

$$\Delta w = B(-i\pi) + o(1). \quad (2.3.24)$$

Hence, comparing (2.3.23) and (2.3.24), we find that  $B = a/\pi$ . Similarly, as  $z$  moves on the other half-circle  $C'_\varepsilon$  with center at  $z = -k$ , i.e.,  $z + k = \varepsilon e^{i\theta}$ , the value of  $w$  varies from its value on  $A_2 A_3$  to  $A_3 A_4$ , and in this case the

difference is  $\Delta w = -ib + o(1)$ , which from (2.3.22) is equal to  $-Bki\pi + o(1)$ . This yields  $b = Bk\pi = ka$ , or  $k = b/a$ . Thus, the required mapping is given by

$$w = \frac{a}{\pi} \log(1-z) + \frac{b}{\pi} \log\left(1 + \frac{a}{b}z\right). \blacksquare \quad (2.3.25)$$

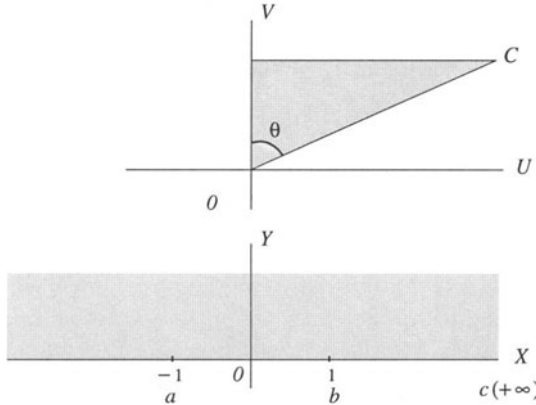


Fig. 2.3.6.

**CASE STUDY 2.3.5** Map the semi-infinite strip  $u > 0, 0 < v < a$ , as the limit of the triangle  $OCA$  as  $\theta \rightarrow \pi/2$  onto the upper half-plane  $\Im\{z\} > 0$  (Fig. 2.3.6), such that  $z = -1, 1$  correspond to  $w = ia, 0$ , respectively. The transformation (2.3.1) yields

$$\begin{aligned} w = f(z) &= A + \lim_{\theta \rightarrow \pi/2} B \int^z \frac{d\zeta}{(\zeta+1)^{1/2}(\zeta-1)^{1-\theta/\pi}} \\ &= B \int_1^z \frac{d\zeta}{\sqrt{\zeta^2-1}} = B \cosh^{-1} z, \end{aligned} \quad (2.3.26)$$

where  $A = 0$  since  $w = 0$  corresponds to  $z = 1$ . From (2.3.26) we have  $w/B = \cosh^{-1} z$ , which gives  $z = \cosh(w/B)$ , and since  $w = ia$  corresponds to  $z = -1 = \cosh i\pi$ , we get  $B = a/\pi$ . Hence, from (2.3.26)

$$w = \frac{a}{\pi} \cosh^{-1} z,$$

and the required transformation is given by

$$z = \cosh \frac{\pi w}{a}. \blacksquare \quad (2.3.27)$$

CASE STUDY 2.3.6 To map the region in the  $z$ -plane, shown in Fig. 2.3.7, onto the upper half-plane  $\Im\{w\} > 0$ , formula (2.3.4) gives

$$z = C \int_1^w \frac{d\zeta}{\zeta^{1-k} (\zeta - 1)^k}, \quad 0 < k < 1. \quad (2.3.28)$$

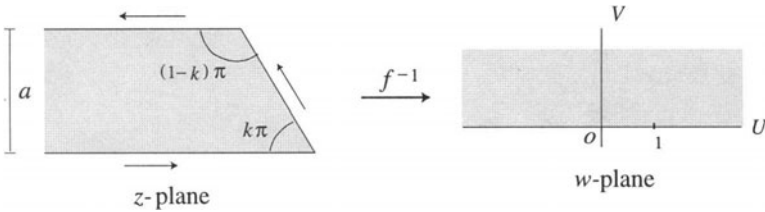


Fig. 2.3.7.

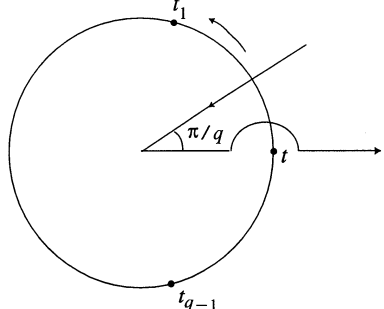
To determine the constant  $C$ , we integrate along the half-circle  $w = Re^{i\theta}$ ,  $0 < \theta < \pi$ . Since the residue of the integrand at  $\zeta = \infty$  is  $-1$ , we find from (2.3.28), as  $R \rightarrow \infty$ , that  $ai = -Ci\pi$ , i.e.,  $C = -a/\pi$  (see figure on the right).

The integral in (2.3.28) can be evaluated in terms

of known functions if  $k$  is rational. Let  $k = p/q$ ,  $p < q$ , where  $p, q \in \mathbb{R}^+$ .

$$\text{Set } \left( \frac{\zeta - 1}{\zeta} \right)^{1/q} = t.$$

Then,  $d\zeta = \frac{qt^{q-1}}{(1-t^q)^2} dt$ , and (2.3.28) becomes



$$z = \frac{a q}{\pi} \int_0^t \frac{t^{-p+q-1}}{t^q - 1} dt. \quad (2.3.29)$$

Now, the  $q$  poles of the integrand in (2.3.29) are the  $q$ -th zeros of  $(t^q - 1)$ , i.e., they are at  $t_n = e^{2ni\pi/q}$ ,  $n = 0, 1, \dots, q-1$ . Thus,

$$\frac{t^{-p+q-1}}{t^q - 1} = \sum_{n=0}^{q-1} \frac{t_n^{-p+q-1}}{q t_n^q - 1} \frac{1}{t - t_n} = \frac{1}{q} \sum_{n=0}^{q-1} \frac{1}{t_n^p} \frac{1}{t - t_n},$$

and

$$\int_0^t \frac{1}{t - t_n} dt = \ln |t - t_n| + \text{const} = \ln \left( 1 - \frac{t}{t_n} \right),$$

where the constant is zero because the integrand is zero at  $t = 0$  and the principal value of the logarithm is taken. Thus, the required transformation becomes

$$z = \frac{a}{\pi} \sum_{n=0}^{q-1} \frac{1}{t_n^q} \ln \left( 1 - \frac{t}{t_n} \right). \quad (2.3.30)$$

As a special case, if  $\mu = 1/2$ , i.e., if  $p = 1, q = 2$ , the transformation (2.3.30) reduces to

$$z = \frac{a}{\pi} \ln \frac{1-t}{1+t}, \quad t = \left( \frac{\zeta-1}{\zeta} \right)^{1/2}. \blacksquare \quad (2.3.31)$$

In the next chapter we shall discuss the problem of approximately computing the values of the  $(2n+2)$  parameters involved in the Schwarz–Christoffel formula (2.3.1) or (2.3.4). This discussion involves numerical solution of improper integrals known as Schwarz–Christoffel integrals. ■

## 2.4. Catalog of Conformal Maps

The mathematical theory of conformal mapping has produced extensive information about mapping classes. Some classes of elementary mappings are available in most textbooks on the subject of complex analysis. Although Mathematica can be used very effectively to produce cartesian, polar, parametric, and conformal maps (see Maeder, 1991, and Wolfram, 1996), and there is a DOS software *conform* (Ivanov and Trubetskoy, 1995). Besides, there are two catalog-style collections of conformal mappings, one by Koppenfels (1937) and the other by Kober (1957), which are very practical and useful for applications of computational conformal mapping. Both of these publications also contain a number of formulas and properties of various different kinds of conformal mappings; Kober's work, however, lists these formulas and properties, without proof, although it explains the method of Schwarz–Christoffel transformations.

Although the choice of a collection of conformal mappings is a matter of personal interest and each reader is directed in making this collection by the type and scope of the study one is involved in, yet there are some very basic and useful conformal mappings that need to be pointed out. A listing of some such mappings can be found in Appendix E.

## 2.5. Problems

PROBLEM 2.5.1. Show that the Schwarzian derivative (also called Schwarz differential operator)

$$\{w, z\} = \left( \frac{w''}{w'} \right)' - \frac{1}{2} \left( \frac{w''}{w'} \right)^2 = \frac{w'''}{w'} - \frac{3}{2} \left( \frac{w''}{w'} \right)^2$$

is invariant under bilinear transformations. (Nehari, 1952, p.199; Wen, 1992, p.76.)

PROBLEM 2.5.2. Show that the Schwarzian derivative of the function  $w = w(z)$  that maps the upper half-plane  $\Im\{z\} > 0$  conformally onto a circular triangle with interior angles  $\alpha\pi$ ,  $\beta\pi$  and  $\gamma\pi$  is given by

$$\{w, z\} = \frac{1 - \alpha^2}{2z^2} + \frac{1 - \beta^2}{2(1-z)^2} + \frac{1 - \alpha^2 - \beta^2 + \Gamma^2}{2z(1-z)}.$$

(Nevanlinna and Paatero, 1969, p.342.)

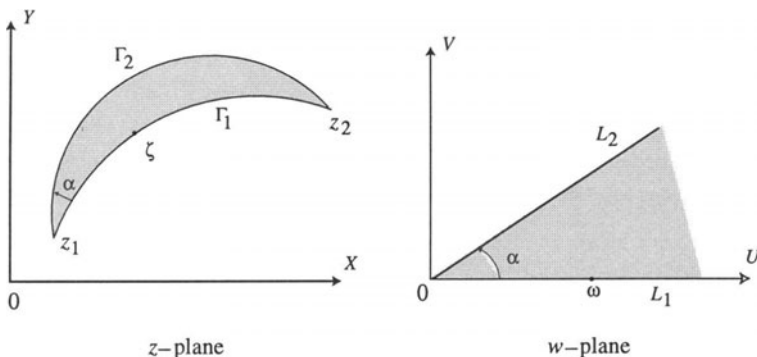


Fig. 2.5.1.

PROBLEM 2.5.3. Show that the function  $f(z) = \rho e^{i\alpha_0} \frac{z - z_1}{z - z_2}$  maps the region enclosed by two arcs onto the region enclosed by the sector shown in Fig. 2.5.1, such that a fixed point  $\zeta \neq z_{1,2}$  on  $\Gamma_1$  goes into a point  $\omega$  on the  $u$ -axis, where  $\alpha_0 = \arg \left\{ \frac{\zeta - z_1}{\zeta - z_2} \right\}$  and  $\rho = \omega \left| \frac{\zeta - z_1}{\zeta - z_2} \right|$ . (Pennisi, 1963, p.321.)

**PROBLEM 2.5.4.** Show that the bilinear transformation  $w = f(z) = \frac{z}{2z - 8}$  maps the region  $\text{Int}(\Gamma)$ , where  $\Gamma = \{|z - 2| = 2\}$  conformally onto the region  $\Re\{w\} < 0$ , such that the point  $z = 2$  goes into  $w = -1/2$ .

**PROBLEM 2.5.5.** Show that the bilinear transformation  $w = f(z)$  that transforms the three points  $z_k$  into the points  $w_k$ ,  $k = 1, 2, 3$ , can be expressed as

$$\begin{vmatrix} 1 & z & w & zw \\ 1 & z_1 & w_1 & z_1 w_1 \\ 1 & z_2 & w_2 & z_2 w_2 \\ 1 & z_3 & w_3 & z_3 w_3 \end{vmatrix} = 0.$$

**PROBLEM 2.5.6.** Show that the function  $w = f(z) = \frac{z}{z - (1+i)}$  maps the lens-shaped region bounded by the circles  $|z - 1| = 1$  and  $|z - i| = 1$  onto the region bounded by the rays  $\arg\{w\} = 3\pi/4$  and  $\arg\{w\} = 5\pi/4$  such that  $f(0) = 0$  and  $f(1+i) = \infty$ .

**PROBLEM 2.5.7.** Show that the Schwarz–Christoffel transformation  $w = f(z) = \frac{2}{\pi} \sin^{-1} z$  maps the upper half-plane  $\Im\{z\} > 0$  onto the semi-infinite strip  $|\Re\{w\}| < 1$ ,  $\Im\{w\} > 0$ , such that  $f(0) = 0$  and  $f(1) = 1$ .

**PROBLEM 2.5.8.** Show that the Schwarz–Christoffel transformation

$$w = f(z) = \frac{1}{\pi} \sqrt{2(1-z)} + \frac{1}{\pi} \log \frac{\sqrt{1-z} - \sqrt{2}}{\sqrt{1-z} + \sqrt{2}} - i$$

maps the upper half-plane  $\Im\{z\} > 0$  onto the region consisting of the fourth quadrant plus the strip  $0 < v < 1$  in the  $w$ -plane,  $w = u + iv$ , such that  $f(1) = 0$ .

**PROBLEM 2.5.9.** Let  $z$  be fixed and let  $\Re\{z\} \geq 0$ . Define a sequence of bilinear transformations

$$T_0(w) = \frac{a_0}{z + a_0 + b_1 + w}, \quad T_k(w) = \frac{a_k}{z + b_{k+1} + w}, \quad k = 1, \dots, n-1,$$

such that each  $a_j > 0$  is real and each  $b_j$  is zero or purely imaginary,  $j = 0, 1, \dots, n-1$ . Use induction to prove that the chain of transformations defined by  $\zeta = S(w) = (T_0 \circ T_{n-2} \cdots \circ T_{n-1})(w)$  maps the half-plane  $\Re\{w\} > 0$

onto a region contained in the disk  $|\zeta - 1/2| < 1/2$ . [Hint: Use Wallis criterion: If  $P(z) = z^n + c_1 z^{n-1} + c_2 z^{n-2} + \cdots + c_n$  is a polynomial of degree  $n > 0$  with complex coefficients  $c_k = p_k + i q_k$ ,  $k = 1, 2, \dots, n$ , if  $Q(z) = p_1 z^{n-1} + i q_2 z^{n-2} + p_3 z^{n-3} + i q_4 z^{n-4} + \cdots$ , and if  $Q(z)/P(z)$  can be written as a continued fraction

$$\frac{Q(z)}{P(z)} = \cfrac{a_0}{z + a_0 + b_1 + \cfrac{a_1}{z + b_2 + \cfrac{a_2}{z + b_3 + \cdots + \cfrac{a_{n-1}}{z + b_n}}}},$$

then  $Q(z)/P(z) = (T_0 \circ T_{n-2} \cdots \circ T_{n-1})(0)$ .] (Saff and Snider, 1976, p.330.)

REFERENCES USED: Ahlfors (1966), Andersen et al. (1962), Betz (1964), Boas (1987), Carathéodory (1969), Carrier, Krook and Pearson (1966), Gaier (1964), Kantorovich and Krylov (1958), Koppenfels (1937, 1959), Ivanov and Trubetskoy (1995), Kober (1957), Mader (1991), Nehari (1952), Nevanlinna and Paatero (1969), Pennisi (1963), Phillips (1943), Saff and Snider (1976), Sansone and Gerretsen (1969), Silverman (1967), Wen (1992), Whittaker and Watson (1927), Wolfram (1996).

# Chapter 3

---

## Schwarz–Christoffel Integrals

---

In practical applications of conformal mapping of a standard region (the half-plane or the unit disk) onto a problem region which is in the form of a polygon, it becomes necessary to determine approximately the  $(2n + 2)$  parameters  $\alpha_1, \dots, \alpha_n, x_1, \dots, x_n$ , and the constants  $A$  and  $B$  that appear in the Schwarz–Christoffel formula (2.3.1). Evaluation of these quantities is known as the parameter problem. We have seen in case studies in §2.3 that the mapping functions obtained by using the Schwarz–Christoffel formula involve certain improper integrals which are known as Schwarz–Christoffel integrals. We shall discuss methods for numerical solution of these integrals and present Newton’s method for the general case of mapping the upper half-plane onto a quadrilateral.

---

### 3.1. Parameter Problem

If the values of all  $(2n + 2)$  parameters in the Schwarz–Christoffel formula (2.3.1) or (2.3.4) are known, then the polygon is uniquely defined, and the coordinates  $w_k$  of the vertices  $w_k$  are given by

$$w_k = A + B \int_0^{x_k} \prod_{i=1}^n (\zeta - x_i)^{-\alpha_i} d\zeta, \quad k = 1, \dots, n. \quad (3.1.1)$$

The length of the side joining the vertices  $w_k$  and  $w_{k+1}$  of the polygon is determined by

$$|w_k, w_{k+1}| = |w_{k+1} - w_k| = |B| \int_{x_k}^{x_{k+1}} \prod_{i=1}^n (\zeta - x_i)^{-\alpha_i} d\zeta. \quad (3.1.2)$$

Therefore, it is very easy to figure out the behavior of the  $(2n + 2)$  parameters in the formula (2.3.1) or (2.3.4). Thus, the parameters  $\alpha_1, \dots, \alpha_n$  are related to the quantities  $\mu_1, \dots, \mu_n$  which are the ratios of the interior angles of the polygon to  $\pi$ . The parameter  $A$  affects the location of the vertices of the polygon. Any change in  $A$  changes the coordinates of every vertex by the same amount through homothety and translation and displaces the polygon as a unit. The parameter  $B$  that is a factor in the formula (3.1.2) affects the lengths of the sides of the polygon. Any change in  $B$  changes all sides of the polygon by the same amount and rotates the polygon as a unit. Any change in the parameters  $x_1, \dots, x_n$  also produces relative change in the lengths of the sides of the polygon.

Let the ratio of the second, third,  $\dots$ ,  $(n - 2)$ -th side of the polygon to the first side be denoted by  $\lambda_2, \lambda_3, \dots, \lambda_{n-2}$ , i.e.,

$$\lambda_j = \frac{|w_{j+1} - w_j|}{|w_2 - w_1|}, \quad j = 2, 3, \dots, n - 2. \quad (3.1.3)$$

Consider the function

$$\tilde{w} = \int_0^z \prod_{i=1}^n (\zeta - x_i)^{-\alpha_i} d\zeta. \quad (3.1.4)$$

If we choose the numbers  $x_1, \dots, x_n$  in this function such that the relations (3.1.3) are satisfied, where  $\alpha_i = 1 - \mu_i$ , the function  $\tilde{w}$  will define a conformal mapping of the upper half-plane onto a polygon  $\tilde{G}$ . In order to pass from the polygon  $\tilde{G}$  to  $G$ , we use the linear transformation

$$w = C_1 \tilde{w} + C_2, \quad (3.1.5)$$

which does the following: It transfers any vertex, say  $\tilde{w}_k$ , of the polygon  $\tilde{G}$  to the corresponding vertex  $w_k$  of the polygon  $G$ , then rotates the polygon  $\tilde{G}$  about the vertex  $\tilde{w}_k$  so that its sides become parallel to the sides of the polygon  $G$ , and finally, without changing the position of the vertex  $\tilde{w}_k$ , it changes the lengths of all sides of the polygon  $\tilde{G}$  such that the polygon  $\tilde{G}$  coincides with  $G$ . The constants  $C_1$  and  $C_2$  in (3.1.3) can be determined by comparing the location and sides of the polygons  $\tilde{G}$  and  $G$ .

In order to determine the parameters  $x_1, \dots, x_n$ , there are only  $(n - 3)$  equations, since three of these points can be chosen arbitrarily. We can use a Möbius transformation to carry the upper half-plane onto itself such that

the three points of the  $x$ -axis go into three preassigned points of the  $u$ -axis. Let these three preassigned points be denoted by  $p_1, p_2, p_3$ . Let us denote the improper integrals thus obtained from the formula (2.3.1) by  $I_m$ ,  $m = 1, 2, \dots, n - 2$ , and define them as

$$\begin{aligned} I_1 &= \int_{p_1}^{p_2} (\zeta - p_1)^{-\alpha_1} (p_2 - \zeta)^{-\alpha_2} (x_3 - \zeta)^{-\alpha_3} \cdots (x_{n-1} - \zeta)^{-\alpha_{n-1}} \\ &\quad (p_3 - \zeta)^{-\alpha_n} d\zeta, \\ I_2 &= \int_{p_2}^{x_3} (\zeta - p_1)^{-\alpha_1} (\zeta - p_2)^{-\alpha_2} (x_3 - \zeta)^{-\alpha_3} \cdots (x_{n-1} - \zeta)^{-\alpha_{n-1}} \\ &\quad (p_3 - \zeta)^{-\alpha_n} d\zeta, \\ &\vdots \\ I_{n-2} &= \int_{x_{n-2}}^{x_{n-1}} (\zeta - p_1)^{-\alpha_1} (\zeta - p_2)^{-\alpha_2} (\zeta - x_3)^{-\alpha_3} \cdots (\zeta - x_{n-2})^{-\alpha_{n-1}} \\ &\quad (p_3 - \zeta)^{-\alpha_n} d\zeta. \end{aligned} \tag{3.1.6}$$

These integrals are known as *Schwarz-Christoffel integrals*. Then, in view of (3.1.3),

$$I_j(x_3, x_4, \dots, x_{n-1}) = \lambda_j I_1(x_3, x_4, \dots, x_{n-1}), \quad j = 2, 3, \dots, n - 2. \tag{3.1.7}$$

In view of the Riemann mapping theorem (§1.4), once the three points  $x_1, x_2, x_3$  are chosen arbitrarily, the system of equations (3.1.7) has a unique solution.

In order to solve the system (3.1.7) numerically, we use Newton's method which is as follows: Let  $\tilde{x}_3, \tilde{x}_4, \dots, \tilde{x}_{n-1}$  denote the solution. Let us take the initial guess for these values as  $x_3^{(0)}, x_4^{(0)}, \dots, x_{n-1}^{(0)}$  which are assumed to be sufficiently close to  $\tilde{x}_3, \tilde{x}_4, \dots, \tilde{x}_{n-1}$ . If we expand each equation of the system (3.1.7) in a Taylor series in powers of the difference  $\tilde{x}_\nu - x_\nu^{(0)}$ ,  $\nu = 3, 4, \dots, n - 1$ , and, as the first approximation, truncate these Taylor series after the first power of the differences, then we obtain a system of equations

$$I_j^{(0)} + \sum_{\nu=3}^{n-1} h_\nu^{(1)} \frac{\partial I_j^{(0)}}{\partial x_\nu} = \lambda_j \left[ I_1^{(0)} + \sum_{\nu=3}^{n-1} h_\nu^{(1)} \frac{\partial I_1^{(0)}}{\partial x_\nu} \right], \quad j = 2, \dots, n - 2, \tag{3.1.8}$$

with a nonzero determinant, where  $h_\nu^{(1)}$ , known as the corrections of the first order, are the perturbed values of the differences  $\tilde{x}_\nu - x_\nu^{(0)}$ . Then the system

(3.1.8) is reduced and solved for  $x_\nu^{(1)}$ ,  $\nu = 3, 4, \dots, n - 1$ . Then using the initial values of  $h_\nu^{(0)}$ , the first approximations are given by

$$x_\nu^{(1)} = x_\nu^{(0)} + h_\nu^{(1)}, \quad \nu = 3, 4, \dots, n - 1. \quad (3.1.9)$$

Next, the system (3.1.8) is expanded in Taylor series in powers of the differences

$$\tilde{x}_\nu - x_\nu^{(1)}, \quad \nu = 3, 4, \dots, n - 1, \quad (3.1.10)$$

and these series are truncated after the first powers of these differences. Thus, a new system, analogous to (3.1.8), is constructed with unknowns  $x_\nu^{(2)}$ ,  $\nu = 3, 4, \dots, n - 1$ , with the perturbed values of the differences (3.1.10), except that now the new system is computed using the known values of  $x_\nu^{(1)}$ . It yields the values of  $x_\nu^{(2)}$ , and the second approximations are given by

$$x_\nu^{(2)} = x_\nu^{(1)} + h_\nu^{(2)}, \quad \nu = 3, 4, \dots, n - 1. \quad (3.1.11)$$

This process is continued until we reach arbitrarily close to the solutions  $\tilde{x}_\nu$ , such that the difference between two consecutive approximate values is within a prescribed tolerance.

Once the system (3.1.8) is solved, we are able to approximate the coordinates of the vertices of the polygon and the lengths of its sides. But in doing so, we must compute the Schwarz–Christoffel integrals of the form

$$E = \int_{x_k}^{x_{k+1}} (\zeta - p_1)^{-\alpha_1} (\zeta - p_2)^{-\alpha_2} (\zeta - x_3)^{-\alpha_3} \cdots (\zeta - x_k)^{-\alpha_k} \\ (x_{k+1} - \zeta)^{-\alpha_{k+1}} \cdots (p_3 - \zeta)^{-\alpha_n} d\zeta, \quad (3.1.12)$$

which are improper because the integrand of each integral becomes unbounded at two points where  $\zeta = x_k$ ,  $x_{k+1}$  which are the limits of integration. These integrals exist because each  $\alpha_k > 0$ . The Kantorovich method to solve these integrals is as follows: Let the integrand in (3.1.12) be denoted by  $F(\zeta)$ . Then

$$F(\zeta) = (\zeta - p_1)^{-\alpha_1} (\zeta - p_2)^{-\alpha_2} (\zeta - x_3)^{-\alpha_3} \cdots (\zeta - x_k)^{-\alpha_k} \\ (x_{k+1} - \zeta)^{-\alpha_{k+1}} \cdots (p_3 - \zeta)^{-\alpha_n} \\ = (\zeta - x_k)^{-\alpha_k} [\phi(x_k) + \phi'(x_k)(\zeta - k_k)] \\ + (x_{k+1} - \zeta)^{-\alpha_{k+1}} [\psi(x_{k+1}) - \psi'(x_{k+1})(x_{k+1} - \zeta)] \\ + \left\{ F(\zeta) - (\zeta - x_k)^{-\alpha_k} [\phi(x_k) + \phi'(x_k)(\zeta - k_k)] \right. \\ \left. - (x_{k+1} - \zeta) [\psi(x_{k+1}) - \psi'(x_{k+1})(x_{k+1} - \zeta)] \right\}, \quad (3.1.13)$$

where

$$\begin{aligned}\phi(\zeta) &= (\zeta - p_1)^{-\alpha_1} (\zeta - p_2)^{-\alpha_2} (\zeta - x_3)^{-\alpha_3} \cdots (\zeta - x_{k-1})^{-\alpha_{k-1}} \\ &\quad (x_{k+1} - \zeta)^{-\alpha_{k+1}} \cdots (p_3 - \zeta)^{-\alpha_n},\end{aligned}\tag{3.1.14}$$

$$\begin{aligned}\psi(\zeta) &= (\zeta - p_1)^{-\alpha_1} (\zeta - p_2)^{-\alpha_2} (\zeta - x_3)^{-\alpha_3} \cdots (\zeta - x_k)^{-\alpha_k} \\ &\quad (x_{k+2} - \zeta)^{-\alpha_{k+2}} \cdots (p_3 - \zeta)^{-\alpha_n}.\end{aligned}\tag{3.1.15}$$

Let  $E = E_1 + E_2$ , where

$$\begin{aligned}E_1 &= \int_{x_k}^{x_{k+1}} \left\{ (\zeta - x_k)^{-\alpha_k} [\phi(x_k) + \phi'(x_k)(\zeta - x_k)] \right. \\ &\quad \left. + (x_{k+1} - \zeta)^{-\alpha_{k+1}} [\psi(x_{k+1}) - \psi'(x_{k+1})(x_{k+1} - \zeta)] \right\} d\zeta\end{aligned}\tag{3.1.16a}$$

$$\begin{aligned}E_2 &= \int_{x_k}^{x_{k+1}} \left\{ F(\zeta) - (\zeta - x_k)^{-\alpha_k} [\phi(x_k) + \phi'(x_k)(\zeta - x_k)] \right. \\ &\quad \left. - (x_{k+1} - \zeta) [\psi(x_{k+1}) - \psi'(x_{k+1})(x_{k+1} - \zeta)] \right\} d\zeta.\end{aligned}\tag{3.1.16b}$$

The integral  $E_1$  can be evaluated directly in a finite form, and since  $E_2$  has no singularities it can be approximated by any formula for numerical integration of definite integrals, like Simpson's rule.

## 3.2. Newton's Method

We shall discuss Newton's method for mapping the upper half-plane onto an arbitrary quadrilateral (see Case Study 2.3.3). In fact, in order to determine  $k$  in (2.3.14), we have only one equation from (3.1.8)

$$I_4(k) = \lambda I_1(k),\tag{3.2.1}$$

where

$$\begin{aligned}I_4(k) &= \int_3^\infty (\zeta + 1)^{-\alpha_1} (\zeta - 1)^{-\alpha_2} (\zeta - k)^{-\alpha_3} (\zeta - 3)^{-\alpha_4} d\zeta \\ &\quad + \int_{-\infty}^{-1} (-1 - \zeta)^{-\alpha_1} (1 - \zeta)^{-\alpha_2} (k - \zeta)^{-\alpha_3} (3 - \zeta)^{-\alpha_4} d\zeta,\end{aligned}\tag{3.2.2}$$

and

$$I_1(k) = \int_{-1}^1 (\zeta + 1)^{-\alpha_1} (1 - \zeta)^{-\alpha_2} (k - \zeta)^{-\alpha_3} (3 - \zeta)^{-\alpha_4} d\zeta. \quad (3.2.3)$$

In  $I_4(k)$ , set  $\zeta = 2 + 1/t$  in the first integral and  $\zeta = -1/t$  in the second. Then

$$\begin{aligned} I_4(k) &= \int_0^1 (1 + 3t)^{-\alpha_1} (1 + t)^{-\alpha_2} (1 + (2 - k)t)^{-\alpha_3} (1 - t)^{-\alpha_4} dt \\ &\quad + \int_0^1 (1 - t)^{-\alpha_1} (1 + t)^{-\alpha_2} (1 + kt)^{-\alpha_3} (1 + 3t)^{-\alpha_4} d\zeta. \end{aligned} \quad (3.2.4)$$

Let  $F(k) = I_4(k) - \lambda I_1(k)$ . Then  $F'(k) > 0$ . To see this, we have from (3.1.13)

$$\begin{aligned} F'(k) &= \alpha_3 \int_0^1 t(1 + 3t)^{-\alpha_1} (1 + t)^{-\alpha_2} (1 + (2 - k)t)^{-\alpha_3 - 1} (1 - t)^{-\alpha_4} dt \\ &\quad - \alpha_3 \int_0^1 t(1 - t)^{-\alpha_1} (1 + t)^{-\alpha_2} (1 + kt)^{-\alpha_3 - 1} (1 + 3t)^{-\alpha_4} dt \\ &\quad + \lambda \alpha_3 \int_{-1}^1 (\zeta + 1)^{-\alpha_1} (1 - \zeta)^{-\alpha_2} (k - \zeta)^{-\alpha_3 - 1} (3 - \zeta)^{-\alpha_4} d\zeta. \end{aligned} \quad (3.2.5)$$

Note that  $F'(1)$  and  $F'(3)$  do not exist because they are not finite. Since

$$\begin{aligned} F''(k) &= \alpha_3 (1 + \alpha_3) \left\{ \int_0^1 t^2(1 + 3t)^{-\alpha_1} (1 + t)^{-\alpha_2} \right. \\ &\quad (1 + (2 - k)t)^{-\alpha_3 - 2} (1 - t)^{-\alpha_4} dt \\ &\quad + \int_0^1 t^2(1 - t)^{-\alpha_1} (1 + t)^{-\alpha_2} (1 + kt)^{-\alpha_3 - 2} (1 + 3t)^{-\alpha_4} dt \\ &\quad \left. - \lambda \int_{-1}^1 (\zeta + 1)^{-\alpha_1} (1 - \zeta)^{-\alpha_2} (k - \zeta)^{-\alpha_3 - 2} (3 - \zeta)^{-\alpha_4} d\zeta \right\}, \end{aligned} \quad (3.2.6)$$

we find that  $F''(k) > 0$  for  $1 < k < 3$ , and  $F''(1) = -\infty$  and  $F''(3) = +\infty$ . Hence, as  $k$  varies from 1 to 3, both  $F(k)$  and  $F''(k)$  increase continuously from  $-\infty$  to  $+\infty$  (for details, see Kantorovich and Krylov, 1958). Hence, the function  $F(k)$  has a zero in  $(1, 3)$ . Let the zero of  $F(k)$  be denoted by  $k^*$ , and that of  $F''(k)$  by  $k^{**}$ . Now we shall solve the equation  $F(k) = 0$  by Newton's method. Although the initial guess for the value of  $k$  is important in this method, yet we shall show that it can be chosen arbitrarily from below or from above in the interval  $(1, 3)$ . Let  $k_0$  denote an arbitrary initial guess for the value of  $k$ . Then

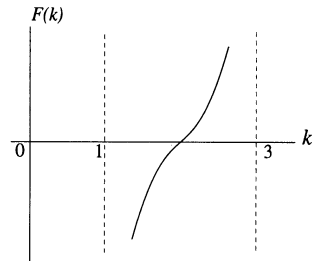
**THEOREM 3.2.1.** *In order to solve the equation  $F(k) = 0$  by Newton's method, the value of  $k_0 \in (1, 3)$  can be chosen arbitrarily, independent of the values of  $k^*$  and  $k^{**}$ .*

**PROOF.** There are three cases to analyze:

CASE 1: If  $K^{**} = k^*$ , then the initial value  $k_0$  is any number in the interval  $(1, 3)$  (see figure on the right).

In fact, let  $k_0$  be an approximation of  $k^*$  from below. Then  $F(k) < 0$ , and  $F''(k) < 0$  for all  $k \in (k_0, k^*)$ . Hence, there is an  $M$  such that  $F'(k) < M$  for all  $k_0 \leq k \leq k^*$ . The first correction is given by

$$\delta^{(1)} = -\frac{F(k_0)}{F'(k_0)} > 0. \quad (3.2.7)$$



Thus, the exact first correction  $h_1$  is positive and satisfies the equation

$$F(k_0) + h_1 F'(k_0) + \frac{h_1^2}{2} F''(\tilde{k}) = 0, \quad k_0 < \tilde{k} < k^*. \quad (3.2.8)$$

Hence, from (3.2.7) and (3.2.8), we have

$$\left[ h_1 - \delta^{(1)} \right] F'(k_0) = -\frac{h_1^2}{2} F''(\tilde{k}),$$

which yields

$$h_2 = h_1 - \delta^{(1)} = -\frac{h_1^2}{2} \frac{F''(\tilde{k})}{F'(k_0)}, \quad (3.2.9)$$

which is positive in view of (3.2.8). Thus, the first approximation  $k_1$ , like  $k_0$ , is an approximation from below, and, therefore, all subsequent approximations will be very small. It is the basic property of Newton's method that the exact corrections  $h$  are always positive and decreasing. In fact, we can show that if the difference between  $h_n$  and  $h_{n+1}$  is sufficiently small, then  $h_n$  is itself very small. Assume that

$$h_n - h_{n+1} < \frac{K}{M} \varepsilon, \quad (3.2.10)$$

where  $\varepsilon > 0$  is arbitrarily small. Since  $h_n - h_{n+1} = \delta^{(n)}$ , we have  $\delta^{(n)} < \frac{K}{M} \varepsilon$ . Also,

$$\delta^{(n)} = -\frac{F(k_{n-1})}{F'(k_{n-1})} = \frac{|F(k_{n-1})|}{F'(k_{n-1})},$$

or

$$|F(k_{n-1})| = \delta^{(n)} F'(k_{n-1}). \quad (3.2.11)$$

But  $h_n$  can be evaluated from the equation

$$F(k_{n-1}) + h_n F'(\tilde{k}), \quad k_{n-1} < \tilde{k} < k^*. \quad (3.2.12)$$

Hence, from (3.2.11) and (3.2.12)

$$h_n = \frac{|F(k_{n-1})|}{F'(\tilde{k})} = \frac{\delta^{(n)} F'(k_{n-1})}{F'(\tilde{k})}, \quad h_n < \frac{K}{M} \varepsilon \frac{M}{K} = \varepsilon.$$

This shows that the sequence  $\{h_1, h_2, \dots, h_n, \dots\} \searrow 0$ . This analysis leads to the same conclusion if  $k_0$  is an approximation from above.

CASE 2: If  $k^{**} > k^*$ , then for any initial guess  $k_0 < k^*$  the convergence is the same as in case 1. Also,  $F(k) < 0$ , and  $F'(k) < 0$  for  $k_0 < k < k^*$  (as in case 1). Now, let  $k_0$  be such that  $k^* < k_0 < k^{**}$ . Then  $F(k_0) > 0$ , and  $F''(k) < 0$  for all  $k \leq k_0$ . Moreover,  $\delta^{(1)} < 0$ , and  $h_1 < 0$ . Now,

$$h_2 = -\frac{1}{2} h_1^2 \frac{F''(\tilde{k})}{F'(k_0)} F''(\tilde{k}) < 0,$$

and thus,  $h_2 > 0$ . This means that the first approximation is an approximation from below, and all subsequent approximations will converge from below to  $k^*$  (as in case 1). In the case when  $k_0 > k^{**}$ , we have  $F(k) > 0$  for all  $k \in (k^*, k_0)$ ;  $F'(k) \begin{cases} < 0 & \text{for all } k \in (k^*, k^{**}) \\ > 0 & \text{for all } k \in (k^{**}, k_0) \end{cases}$ ;  $\delta^{(1)} < 0$ , and  $h_1 < 0$ . Thus,  $k_1$  can be in any one of the three intervals  $(1, k^*)$ ,  $(k^*, k^{**})$ , and  $(k^{**}, k_0)$ . If  $k_1$  is in the first two intervals, then we have convergence from below to  $k^*$ . But if  $k_1$  is in the third interval, then all approximations, although decreasing continuously, still remain greater than  $k^{**}$  and approach some limiting value  $k_1 \geq k^{**}$ . The difference between  $h_n$  and  $h_{n+1}$  would be sufficiently small for sufficiently large  $n$ , and  $h_n - h_{n+1} < \frac{K}{M} \frac{k^{**} - k^*}{2}$ , where  $M = \max_{k \in (k^*, k_0)} |F'(k)|$ . As in case 1, it can be shown that  $|h_n| < \frac{k^{**} - k^*}{2}$ . But, by assumption, we have

$|h_n| \geq k^{**} - k^*$ . This contradiction shows that if Newton's method starts with  $k_0 > k^{**}$ , then the approximation will cross  $k^{**}$  and fall in the interval where the convergence is established as in case 1.

CASE 3: If  $k^{**} < k^8$ , then this case can be analyzed by taking  $k_0$  in any one of the intervals discussed in cases 1 and 2. We shall apply this method in Case Study 3.3.3.

---

### 3.3. Numerical Computations

Now we shall solve some parameter problems.

CASE STUDY 3.3.1. Consider the integral in the denominator in (2.3.7) Denoting it by  $E$ , we have  $B = 1/E$ , where

$$E = \left( \int_0^{1/2} + \int_{1/2}^1 \right) \zeta^{-1/2} (1 - \zeta)^{-3/4} d\zeta = E_1 + E_2.$$

Then, by (3.1.16),

$$\begin{aligned} E_1 &= \lim_{t \rightarrow 0} \int_t^{1/2} \zeta^{-1/2} (1 - \zeta)^{-3/4} d\zeta \\ &= \lim_{t \rightarrow 0} \int_t^{1/2} \left\{ \zeta^{-1/2} \left( 1 + \frac{3}{4}\zeta \right) + \zeta^{-1/2} \left[ (1 - \zeta)^{-3/4} - 1 - \frac{3}{4}\zeta \right] \right\} d\zeta \\ &= E_{11} + E_{12} \approx 1.59099 + 0.0708022 = 1.66179; \\ E_2 &= \lim_{t \rightarrow 1} \int_{1/2}^t \zeta^{-1/2} (1 - \zeta)^{-3/4} d\zeta \\ &= \lim_{t \rightarrow 1} \int_{1/2}^t \left\{ (1 - \zeta)^{-3/4} \left[ 1 + \frac{1}{2}(1 - \zeta) \right] \right. \\ &\quad \left. + (1 - \zeta)^{-3/4} \left[ \zeta^{-1/2} - 1 - \frac{1}{2}(1 - \zeta) \right] \right\} d\zeta \\ &= E_{21} + E_{22} \approx 3.53176 + 0.0505577 = 3.58232. \end{aligned}$$

Hence  $E = E_1 + E_2 \approx 5.24412$ , and the constant  $B = 1/E \approx 0.19069$ . Note that the exact value of  $E = \frac{\sqrt{\pi} \Gamma(1/4)}{\Gamma(3/4)} \approx 0.19068994$ . The hypotenuse of the

triangle is given by

$$|w_3 - w_2| = B \int_1^\infty \zeta^{-1/2} (1 - \zeta)^{-3/4} d\zeta \approx 1.41421356 \approx \sqrt{2}$$

with an error of  $O(10^{-10})$ . ■

CASE STUDY 3.3.2. In order to determine  $k$  in (2.3.10) such that the ratio  $\frac{w_2 - w_1}{w_3 - w_2} = 2$ , note that the system (3.1.7) reduces to only one equation  $I_2 = 2 I_1$ , i.e.,

$$\int_{-1}^1 (1 - \zeta^2)^{-1/2} (1 - k^2 \zeta^2)^{-1/2} d\zeta = 2 \int_1^{1/k} (\zeta^2 - 1)^{-1/2} (1 - k^2 \zeta^2)^{-1/2} d\zeta, \quad (3.3.1)$$

which is solved by Newton's method as follows: We have only one correction which we shall denote by  $h$  with subscript to denote the appropriate number of approximation. Let us take the initial guess  $k = 1/2$ , and determine  $h_1$  from (3.1.8) which is

$$I_2\left(\frac{1}{2}\right) + h_1 \frac{dI_2\left(\frac{1}{2}\right)}{dk} = I_1\left(\frac{1}{2}\right) + h_1 \frac{dI_1\left(\frac{1}{2}\right)}{dk}. \quad (3.3.2)$$

The free term  $I_2(1/2) = \int_0^1 (1 - \zeta)^{-1/2} \psi(\zeta) d\zeta$ , where  $\psi(\zeta) = (1 + \zeta)^{-1/2} + (1 - \zeta^2/4)^{-1/2}$ , which yields  $I_2(1/2) \approx 2.15652$  on integration. Also,

$$\begin{aligned} \frac{dI_2\left(\frac{1}{2}\right)}{dk} &= \frac{1}{2} \int_0^1 \frac{\zeta^2}{(1 - \zeta^2)^{1/2}} \left(1 - \frac{\zeta^2}{4}\right)^{3/2} d\zeta \approx 0.541732, \\ \frac{dI_1(1/2)}{dk} &\approx -1.79181. \end{aligned}$$

Substituting these values in (3.3.2) we find that  $h_1 \approx 0.201739$ . Hence, the first approximation for  $k \approx 0.5 + 0.201739 \approx 0.7$ . Now, for the second approximation, first we compute  $h_2$  from (3.1.8), i.e.,

$$I_2(0.7) + h_2 \frac{dI_2(0.7)}{dk} = I_1(0.7) + h_2 \frac{dI_1(0.7)}{dk}, \quad (3.3.3)$$

which gives  $h_2 \approx 0.00668985$ , and the second approximation for  $k \approx 0.7 + 0.00668985 \approx 0.70669$ . However, the exact value of  $k$  can be determined in this case by setting  $\zeta = \frac{1}{\sqrt{1 - (1 - k^2)x^2}}$  in  $I_2(k)$ . Then

$$I_2(k) = \int_0^1 (1 - x^2)^{-1/2} (1 - k'^2 x^2)^{-1/2} dx,$$

where  $k'^2 = 1 - k^2$ . Hence, Eq (3.3.1) gives

$$\int_0^1 (1 - \zeta^2)^{-1/2} (1 - k^2 \zeta^2)^{-1/2} d\zeta = \int_0^1 (1 - x^2)^{-1/2} (1 - k'^2 x^2)^{-1/2} dx.$$

Thus,  $k = k'$ , which gives  $k = 1/\sqrt{2} \approx 0.7071$ . A comparison of this value of  $k$  with the second approximation for  $k$  shows that the error is about 0.04%. ■

**CASE STUDY 3.3.3.** Map the trapezoid  $A_1 A_2 A_3 A_4$  in the  $z$ -plane onto the upper half-plane (Fig. 3.3.1). From (2.3.14) the mapping function is given by

$$w = A + B \int_0^z (\zeta + 1)^{-1/6} (\zeta - 1)^{-1/3} (\zeta + k)^{-2/3} (\zeta - 3)^{-5/6} d\zeta. \quad (3.3.4)$$

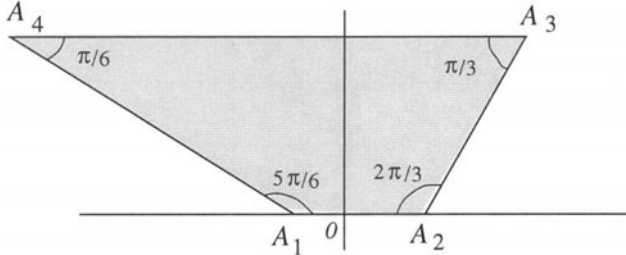


Fig. 3.3.1.

In order to determine the value  $k$ , we have from Eq (3.1.8)

$$I_4(k) = 3 I_1(k), \quad (3.3.5)$$

where from (3.2.4)

$$\begin{aligned} I_4(k) &= \int_0^1 (1 + 3t)^{-1/6} (1 + t)^{-1/3} (1 + (2 - k)t)^{-2/3} (1 - t)^{-5/6} dt \\ &\quad + \int_0^1 (1 - t)^{-1/6} (1 + t)^{-1/3} (1 + kt)^{-2/3} (1 + 3t)^{-5/6} dt \\ &= I_{41}(k) + I_{42}(k), \end{aligned} \quad (3.3.6)$$

and from (3.2.3)

$$\begin{aligned} I_1(k) &= \int_{-1}^1 (\zeta + 1)^{-1/6} (1 - \zeta)^{-1/3} (k - \zeta)^{-2/3} (3 - \zeta)^{-5/6} d\zeta \\ &= \left( \int_{-1}^0 + \int_0^1 \right) (\zeta + 1)^{-1/6} (1 - \zeta)^{-1/3} (k - \zeta)^{-2/3} (3 - \zeta)^{-5/6} d\zeta \\ &= I_{11}(k) + I_{12}(k). \end{aligned}$$

Let  $k = 2$  be the initial guess. Then we find that  $\delta^{(1)} \approx -0.650694$ ,  $k_1 \approx 1.34931$ ,  $\delta^{(2)} \approx 0.0150829$ ,  $k_2 \approx 1.36439$ ,  $\delta^{(3)} \approx 0.0005$ , and  $k_3 \approx 1.36554$ . Now, in order to compute  $A$  and  $B$ , note that the function

$$w = \int_0^z (\zeta + 1)^{-1/6} (\zeta - 1)^{-1/3} (\zeta + k)^{-2/3} (\zeta - 3)^{-5/6} d\zeta \quad (3.3.7)$$

maps the upper half-plane onto a trapezoid  $A_1^* A_2^* A_3^* A_4^*$  similar to the given  $A_1 A_2 A_3 A_4$ . To determine the complex coordinate  $w_1^*$  of the vertex  $A_1^*$  which corresponds to  $z = -1$ , we have

$$\begin{aligned} w_1^* &= \int_0^{-1} (\zeta + 1)^{-1/6} (\zeta - 1)^{-1/3} (\zeta + k)^{-2/3} (\zeta - 3)^{-5/6} d\zeta \\ &\approx -(-1)^{1/6} (0.24631) = -0.24631 i. \end{aligned}$$

Similarly,  $w_2^* \approx 0.90311 i$ . Hence  $w = A + B w^*$  yields

$$-\frac{1}{2} = A - 0.24631 i B, \quad \frac{1}{2} = A + 0.90311 i B,$$

which gives  $A = -0.2851$ , and  $B = -0.87 i$ , and the required transformation is given by

$$w \approx -0.2851 - 0.87 i \int_0^z (\zeta + 1)^{-1/6} (\zeta - 1)^{-1/3} (\zeta + k)^{-2/3} (\zeta - 3)^{-5/6} d\zeta. \blacksquare \quad (3.3.8)$$

**CASE STUDY 3.3.4 (SCHWARZ-CHRISTOFFEL INTEGRAL FOR THE UNIT DISK).** In view of (2.3.2), the integral in the Schwarz-Christoffel formula (2.3.1) is approximately equal to  $\zeta^{-2}$  when  $\zeta$  is close to infinity, whereas the integrand in the formula (2.3.3) is approximately  $\zeta^{-\alpha_n}$ . These quantities are significant when the region is infinite. However, we can avoid an infinite region by mapping the upper half-plane  $\Im\{z\} > 0$  onto the unit disk by the chain of

mappings  $z_1 = \frac{z-i}{z+i}$  and  $z = i \frac{1+z_1}{1-z_1}$ , where  $dz = \frac{2i}{(1-z_1)^2} dz_1$ . Then the integrand in the formula (2.3.1) becomes

$$\begin{aligned} \prod_{j=1}^n (z = x_j)^{-\alpha_j} dz &= \prod_{j=1}^n \left( i \frac{1+z_1}{1-z_1} - x_j \right)^{-\alpha_j} \frac{2i}{(1-z_1)^2} dz_1 \\ &= 2i \prod_{j=1}^n \left( \frac{z_1(x_j+i)-(x_j-i)}{1-z_1} \right)^{-\alpha_j} \frac{1}{(1-z_1)^2} dz_1 \\ &= 2i \prod_{j=1}^n (x_j+i)^{-\alpha_j} \left( z_1 - \frac{x_j-i}{x_j+i} \right)^{-\alpha_j} \frac{dz_1}{(1-z_1)^{2-\alpha_j}} \\ &= C_1 \prod_{j=1}^n (z_1 - b_j)^{-\alpha_j} dz_1, \end{aligned} \tag{3.3.9}$$

where  $b_j = (a_j - i)/(a_j + i)$ , and the exponent  $2 - \alpha_j$  is zero in the product. Thus, formula (2.3.1) becomes

$$w = C_2 \int_{z_{10}}^{z_1} \prod_{j=1}^n (z_1 - b_j) dz_1 + z_0, \tag{3.3.10}$$

where the points  $b_j$  lie on the unit circle  $|z_1| = 1$ . The lower limit  $z_{10}$  may be chosen as the center of this circle or a point on its circumference. Then there are two cases to consider:

CASE 1. If  $z_{10} = 0$ , then the integration is carried out along the ray  $z_1 = r e^{i\theta}$ ,  $0 \leq r \leq R$ ,  $\theta = \text{const}$ , and  $b_j = e^{i\phi_j}$ ,  $j = 1, \dots, n$ . Then the mapping function (3.3.10) reduces to

$$\begin{aligned} w &= C_2 e^{i\theta} \int_0^R \prod_{j=1}^n (r e^{i\theta} - e^{i\phi_j})^{-\alpha_j} r dr + z_0 \\ &= C_2 e^{i\theta} \int_0^R \prod_{j=1}^n e^{-i\theta\phi_j} \left( r - e^{i(\phi_j-\theta)} \right)^{-\alpha_j} r dr + z_0 \\ &= C_2 e^{-i\theta} \int_0^R \prod_{j=1}^n \left( r - e^{i(\phi_j-\theta)} \right)^{-\alpha_j} r dr + z_0. \end{aligned} \tag{3.3.11}$$

CASE 2. If  $z_{10} = 1$ , we choose the path of integration along the circumference.

Thus, for a point  $z_1 = e^{i\theta}$  the mapping function (3.3.10) becomes

$$\begin{aligned}
 w &= C_2 \int_0^\theta \prod_{j=1}^n (e^{i\theta} - e^{i\phi_j})^{-\alpha_j} ie^{i\theta} d\theta + z_0 \\
 &= iC_2 \int_0^\theta \prod_{j=1}^n e^{-(\sum \phi_j \alpha_j)/2} \left( e^{i(\theta-\phi_j)/2} - e^{-i(\theta-\phi_j)/2} \right)^{-\alpha_j} d\theta + z_0 \\
 &= i(2i)^{-2} C_2 \int_0^\theta \prod_{j=1}^n \left( \sin \frac{\theta - \phi_j}{2} \right)^{-\alpha_j} d\theta + z_0 \\
 &= K \int_0^\theta \prod_{j=1}^n \left( \sin \frac{\theta - \phi_j}{2} \right)^{-\alpha_j} d\theta + z_0.
 \end{aligned} \tag{3.3.12}$$

If  $\sin \frac{\theta - \phi_j}{2} < 0$ , then we choose the branch

$$\sin \left( \frac{\theta - \phi_j}{2} \right)^{-\alpha_j} = \exp \left\{ -\alpha_j \log \left| \sin \frac{\theta - \phi_j}{2} \right| - i\pi\alpha_j \right\}.$$

There is no problem for  $\sin \frac{\theta - \phi_j}{2} \geq 0$ . Thus, there exists a constant argument in (3.3.12) in each interval  $\phi_{j-1} < \theta < \phi_j$ ,  $j = 1, \dots, n$ , and the length  $l_j = |z_{j-1}, z_j| = |z_j - z_{j-1}|$  is given by

$$l_j = |K| \int_{\phi_{j-1}}^{\phi_j} \prod_{j=1}^n \left| \sin \frac{\theta - \phi_j}{2} \right|^{-\alpha_j} d\theta, \quad j = 1, \dots, n. \tag{3.3.13}$$

Therefore, the parameter problem for the unit circle is solved by carrying out the integration in (3.3.13) over a finite interval. ■

**CASE STUDY 3.3.5 (REMOVAL OF SINGULARITIES).** The computation of the improper integrals in the formulas (2.3.1) or (2.3.3) can be easily carried out by removing the singularities in the integrand. There are two analytical methods to do this.

**METHOD 1.** We shall consider the exponent  $-\alpha_1$ ; others can be handled similarly. If  $\alpha_1 > 0$  in (2.3.1), we set

$$K_1 = (x_1 - x_2)^{-\alpha_1} \cdots (x_1 - x_n)^{-\alpha_n}$$

and rewrite the integrand in (2.3.1) as

$$\begin{aligned}
 \int_{z_0}^z &\left[ (\zeta - x_1)^{1-\alpha_1} (\zeta - x_2)^{-\alpha_2} \cdots (\zeta - x_n)^{-\alpha_n} - (\zeta - x_1)^{-\alpha_1} K_1 \right] d\zeta \\
 &+ \frac{K_1}{1 - \alpha_1} \left[ (\zeta - x_1)^{1-\alpha_1} - (z_0 - x_1)^{1-\alpha_1} \right].
 \end{aligned} \tag{3.3.14}$$

The integrand in (3.3.14) in the neighborhood of  $z = z_1$  is approximately equal to  $(\zeta - x_1)^{-\alpha_1}$ . In fact, it consists of two factors, the first of which goes to  $\infty$  and the second to 0 as  $\zeta \rightarrow x_1$ . Hence, the product is bounded or even goes to zero.

If we use (3.3.14) for Case 2 of Case Study 3.3.4, then we get integrals of the form

$$I = \int_{\phi_1}^{\theta} \left( \sin \frac{\theta - \phi_1}{2} \right)^{-\alpha_1} d\theta = 2 \int_0^{(\theta - \phi_1)/2} (\sin t)^{-\alpha_1} dt,$$

where we have set  $\theta = \phi_1 + 2t$ . Now, let  $\phi_1 < \theta < \phi_1 + \pi$ . Then, by setting  $t = \sin^{-1} u$ ,  $u = \sqrt{x}$ , we obtain

$$I = 2 \int_0^{u_0} u^{-\alpha_1} \frac{1}{\sqrt{1-u^2}} du = \int_0^{x_0} x^{-\alpha_1/2} (1-x)^{-1/2} dx, \quad x_0 < 1, \quad (3.3.15)$$

which is the incomplete beta function.

METHOD 2. If  $\alpha_1 > 0$  in (2.3.1), then we remove the singularity at  $\zeta = x_1$  by using the transformation  $z_1 = (z - x_1)^{1-\alpha_1}$ , i.e.,

$$z = x_1 + z_1^{1/(1-\alpha_1)}. \quad (3.3.16)$$

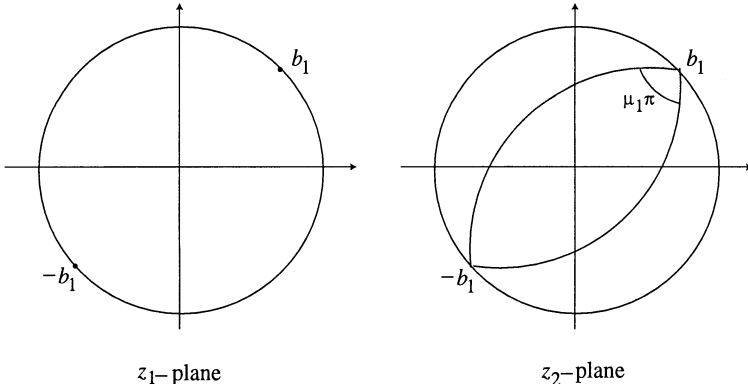


Fig. 3.3.2.

Then the integral (2.3.1) becomes

$$w = z_0 + \frac{C}{\alpha_1} \int_{z_{10}}^{z_1} \left( z_1^{\alpha_1/(1-\alpha_1)} + x_1 - x_2 \right)^{-\alpha_2} \cdots \left( z_1^{-\alpha_1/(1-\alpha_1)} x_1 - x_n \right)^{-\alpha_n} dz_1, \quad (3.3.17)$$

which does not have infinity for  $\alpha_1$ . The transformation (3.3.16) transforms the half-plane  $\Im\{z\} > 0$  onto an angular sector of argument  $(1 - \alpha_j)\pi = \mu_j\pi$ . Note that the mapping (3.3.16) is not suitable for the case of the circle. However, the transformation that maps the circle onto a region bounded by two circles is given by

$$z_1 = b_1 \frac{(b_1 + z_2)^{1/\mu_1} - (b_1 - z_2)^{1/\mu_1}}{(b_1 + z_2)^{1/\mu_1} + (b_1 - z_2)^{1/\mu_1}}, \quad (3.3.18)$$

which is represented in Fig. 3.3.2. ■

---

### 3.4. Kirchhoff Flow Problem

The classical Kirchhoff flow problem (Kirchhoff, 1869) deals with the flow of an ideal incompressible fluid past an obstacle and around a stationary wake bounded by free streamlines (see Problem 3.5.5). It is known that a plane Kirchhoff flow past a solid polygonal obstacle composed of an open polygonal line facing the flow, in theory, can be determined by constructing its conformal mapping onto an  $n$ -gon in the log-hodograph plane and then onto the upper half-plane by using the Schwarz–Christoffel transformation. In practice, however, this approach is fraught with computational difficulties as we shall soon see.

The geometry of a plane Kirchhoff flow is as follows: A solid obstacle with a open polygonal boundary  $\Gamma$ , composed of  $n$  straight line segments  $\Gamma_k = (z_{k-1}, z_k)$ ,  $k = 1, \dots, n$ , lies in the region  $G_z$  in the  $z$ -plane (physical plane) as shown in Fig. 3.4.1(a). The ideal incompressible fluid flow, flowing past the obstacle  $\Gamma$ , is assumed to be irrotational. Let the complex velocity be denoted by  $v(z)$  and normalized by  $v(\infty) = 1$ . The flow divides between an upper and a lower part at an unspecified stagnation point  $z_*$  where the upper flow passes over  $z_n$  and the lower over  $z_0$ . Then the flow continues smoothly forward past  $z_n$  and  $z_0$  with finite acceleration around a wake in which  $v \equiv 0$ . The two streamlines,  $\Gamma^+$  and  $\Gamma^-$  denote the curves of discontinuity which separate the wake from the rest of the flow, and the stream function is zero on  $\Gamma^\pm$ . The shape of  $\Gamma^\pm$  is not known but must be determined by using the condition that  $|v(z)| = 1$  along them (this condition follows from Bernoulli's equation ( $p + 0.5|v|^2 = \text{const}$ ) and the fact that the pressure must remain constant throughout the wake and continuous on  $\Gamma^\pm$ ).

Now the Kirchhoff flow problem can be stated as follows: Given the obstacle  $\Gamma$  in the physical region  $G_z$  in the  $z$ -plane, determine the velocity field  $v(z)$ , the streamlines  $\Gamma^\pm$ , and the location of the stagnation point  $z_*$  for the above flow. Also compute the associated lift and drag coefficients. A conformal mapping solution of this problem can be stated as follows: Let  $\tau$  denote the hodograph (or conjugate velocity) plane so that the complex conjugate velocity is defined by  $\tau(z) = \bar{v}(z)$ . Since the flow is incompressible and irrotational, the velocity  $v = \nabla\phi$ , where  $\phi(z)$  is the real part of the complex velocity potential  $\zeta(z) = \phi(z) + i\psi(z)$  such that  $\nabla^2\phi = 0$  and  $\psi(z)$  is the stream function. Thus,

$$\tau(z) = \frac{d\zeta}{dz}. \quad (3.4.1)$$

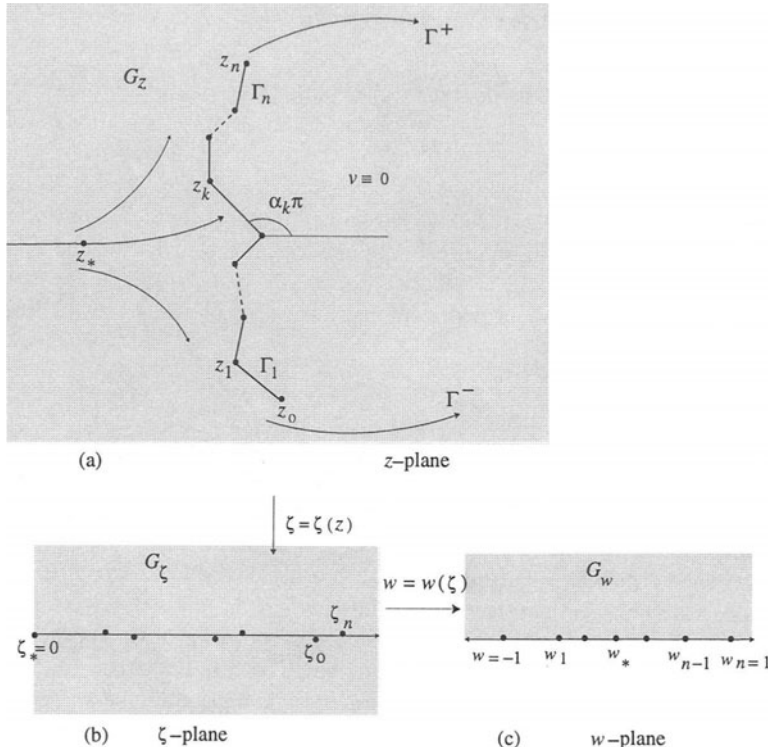


Fig. 3.4.1.

The function  $\zeta(z)$ , regular in  $G_z$ , maps the region  $G_z$  conformally onto a slit

region  $G_\zeta$  in the  $\zeta$ -plane, where the slit begins at  $\zeta_* = \zeta(z_*)$  at which point the flow separates to go around the polygonal obstacle (Fig. 3.4.1(b)). Without loss of generality we take  $\zeta_* = 0$ . Let a new complex variable  $w$  be defined by

$$w = \sqrt{\frac{2\zeta}{W}} + w_*, \quad \zeta = \frac{W}{2} (w - w_*)^2, \quad (3.4.2)$$

where  $W$  is real and  $w_* \in (-1, 1)$  (Fig. 3.4.1(b) in which  $w_k = w(\zeta_k)$  is marked),  $G_w$  is the upper half-plane where  $[-1, 1]$  is the image of  $\Gamma$ , and  $(1, \infty)$  and  $-\infty, -1)$  that of  $\Gamma^+$  and  $\Gamma^-$ , respectively. We shall discuss two methods.

**CLASSICAL HODOGRAPH METHOD.** In this method the upper half-plane  $G_w$  in the  $w$ -plane is mapped onto the hodograph region  $G_\tau = \tau(G_\zeta)$  in the  $\tau$ -plane. The technique leads to a solution, at least theoretically, for the general Kirchhoff flow problem, because although  $G_z$  is unknown due to the presence of unknown free streamlines, the region  $G_\tau$  is almost known in the following sense: Since the flow must be tangential on the solid boundary  $\Gamma$ , we know  $\arg\{\tau(z)\}$  depending on whether the point on  $\Gamma$  is downstream of  $z_*$  toward  $z_0$  or upstream toward  $z_n$ , respectively, i.e.,

$$\arg\{\tau(z)\} = \begin{cases} (1 - \alpha_k)\pi & \text{for } z \in \Gamma_k, w < w_*, \\ -\alpha_k\pi & \text{for } z \in \Gamma_k, w > w_*. \end{cases} \quad (3.4.3)$$

Also

$$|\tau(z)| = 1 \quad \text{for } z \in \Gamma^\pm. \quad (3.4.4)$$

The region  $G_\tau$  is ‘gearlike’, bounded by circular arcs and subsets of rays passing through the origin. By introducing the log-hodograph variable

$$\Omega(z) = -\log \tau(z), \quad (3.4.5)$$

the region  $G_\tau$  is mapped onto a region  $G_\Omega$  which is bounded by vertical and horizontal line segments. Then we can use a Schwarz–Christoffel transformation to map  $G_w$  onto  $G_\Omega$ . This method establishes a relation between  $\tau$  and  $\zeta$  and then integrates (3.4.1) to obtain  $\zeta$  and  $\tau$  as functions of  $z$ .

However, in practice only a few simple cases involving a flat plate (Kirchhoff, 1869; for the classical case see Problem 3.5.5) and certain wedges (Birkhoff and Zarantonello, 1957; Gurevich, 1965; Robertson, 1965; Elcrat, 1982) have been solved by this method because the complexity of the conformal mappings grows as the number of sides of the polygonal obstacle increases. Then the resulting parameter problem inherent in the Schwarz–Christoffel integrals must

be determined numerically which is not an easy task. Another difficulty stems from the fact that although the vertices in the  $w$ -plane are known, those in the  $\Omega$ -plane must be computed by integrating (3.4.1), which can be very time consuming. Finally, the most serious difficulty with this method is that, in general,  $G_\Omega$  is a Riemann surface with slits or branch points of unknown dimensions rather than just a polygon.

**ELCRAT-TREFETHEN METHOD.** This method, developed by Elcrat and Trefethen (1986), for computing flows past an arbitrary obstacle with a high degree of accuracy, uses a modified Schwarz-Christoffel integral to map the upper half-plane  $\Im\{w\} > 0$  directly onto the physical domain  $G_z$  rather than onto the log-hodograph plane. The Schwarz-Christoffel formula (2.3.5) is modified as follows: Let the polygonal line  $\Gamma = \bigcup_{k=1}^n \Gamma_k$  in the  $z$ -plane (the obstacle in the physical plane) have vertices  $z_k$ , sides  $\Gamma_k = (z_{k-1}, z_k)$ , interior angles  $\alpha_k \pi$  (counterclockwise),  $k = 1, \dots, n$ , and exterior angles  $\mu_k$ , where  $\mu_k = \alpha_{k-1} - \alpha_k$  for  $k = 1, \dots, n-1$ , and  $\mu_n = \alpha_1 - \alpha_n + 2$ , thus  $\sum_{k=1}^n \mu_k = 2$ . Let  $z = F(w)$  be the conformal mapping of the upper half-plane  $\Im\{w\} > 0$  onto the  $G_z$  such that the point  $w = \infty$  goes into a point on  $\Gamma_1$ . Let  $W_k = w(\Gamma_k)$  denote the intervals  $(w_{k-1}, w_k)$ , where  $w_k = F(z_k)$ . Then  $\arg\left\{\frac{dz}{dw}\right\}$  has a constant value  $\alpha_\pi$  on each  $W_k$  and a jump of  $\mu_k \pi$  at  $w_k$ , i.e.,

$$\arg\left\{\frac{dz}{dw}\right\} = \alpha_1 \pi \quad \text{for } w \in (w_n, \infty), \quad (3.4.6)$$

$$\Delta \arg\left\{\frac{dz}{dw}\right\} = \mu_k \pi \quad \text{at } w = w_k. \quad (3.4.7)$$

Let  $g_k(w) = (w - w_k)^{-\mu_k}$  denote the factors in the formula (2.3.5), where the branch of  $g_k(w)$  is chosen such that  $g_k(w) > 0$  for  $w > w_k$ . Then  $\arg\{g_k(w)\} = \text{const}$  except for a jump of  $\mu_k \pi$  at  $w_k$ . It means that the function  $g_k(w)$  maps  $\Im\{w\} > 0$  onto the sector bounded by the rays  $e^{-i\mu_k \pi} \mathbb{R}^+$  and  $\mathbb{R}^+$  in the  $z$ -plane (Fig. 3.4.2(a)). Hence,

$$\frac{dz}{dw} = C e^{i\alpha_1 \pi} \prod_{k=1}^n g_k(w) = C e^{i\alpha_1 \pi} \prod_{k=1}^n (w - w_k)^{-\mu_k}, \quad C > 0, \quad (3.4.7)$$

and the modified Schwarz-Christoffel formula is

$$z = F(w) = C_0 + C e^{i\alpha_1 \pi} \int^w (\zeta - w_k)^{-\mu_k} d\zeta, \quad (3.4.8)$$

where  $C_0$  is a complex constant (cf. this formula with (2.3.4)).

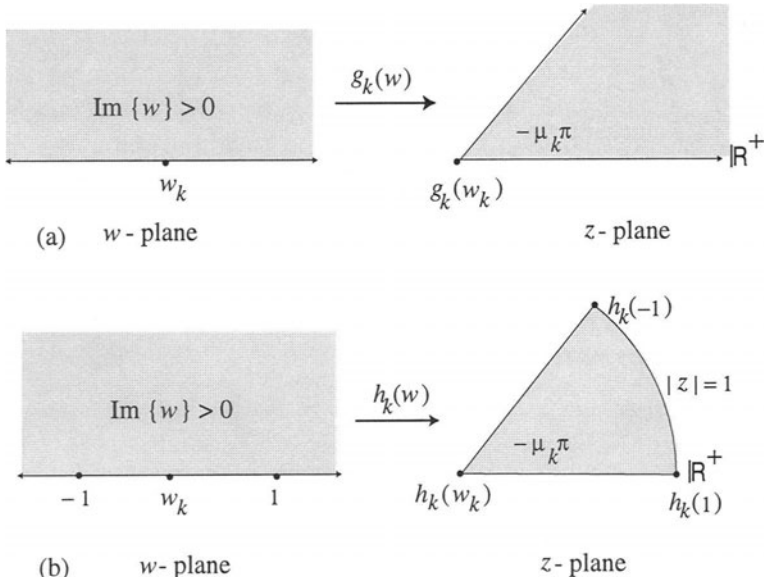


Fig. 3.4.2.

Now, consider the function  $z = F_1(\zeta)$  which maps the slit region  $G_\zeta$  in the  $\zeta$ -plane onto the region  $G_z$  in the  $z$ -plane (Fig. 3.4.1). Since we know  $\arg \left\{ \frac{dz}{d\zeta} \right\}$  for  $w \in [-1, 1]$  and  $\left| \frac{dz}{d\zeta} \right|$  elsewhere, we have

$$\begin{aligned}
 \arg \left\{ \frac{dz}{d\zeta} \right\} &= \alpha_k \pi \quad \text{for } w = w_k, \\
 \Delta \arg \left\{ \frac{dz}{d\zeta} \right\} &= \mu_k \pi \quad \text{at } w = w_k \text{ for } k = 1, \dots, n-1, \\
 \left| \frac{dz}{d\zeta} \right| &= 1 \quad \text{for } w \in W_{\pm}, \text{i.e., } |w| > 1, \\
 \arg \left\{ \frac{dz}{d\zeta} \right\} &= 0 \quad \text{at } w = \infty.
 \end{aligned} \tag{3.4.9}$$

Thus, the Kirchhoff flow problem is a modification of the Schwarz–Christoffel problem (3.4.6) in the sense that a constant-modulus condition, instead of the constant-argument condition, is applied over the boundary. Define a function

$h_k(w)$  by

$$h_k(w) = \left[ \frac{w - w_k}{1 - w_k w + \sqrt{(1 - w^2)(1 - w_k^2)}} \right]^{-\mu_k}, \quad (3.4.10)$$

where the branch is chosen such that  $h_k(w) > 0$  for  $w \in (w_k, 1)$ . The function  $h_k$  has singularity at  $w_k$  (like the function  $g_k$ ) and also at  $w = \pm 1$ , and it maps the half-plane  $\Im\{w\} > 0$  onto the closed circular sector bounded by the rays  $e^{-i\mu_k\pi} \mathbb{R}^+$ ,  $\mathbb{R}^+$  and the unit circle  $|z| = 1$  (Fig. 3.4.2(b)). Since  $|h_k(w)| = 1$  for  $|w| > 1$ , we have

$$\frac{dz}{d\zeta} = \frac{1}{\tau} = e^{i\alpha_n \pi} \prod_* h_k(w), \quad (3.4.11)$$

where  $\prod$  denotes the product over  $k = 1, \dots, n-1$  and  $k = *$  ( $\sum_*$  defined analogously) and  $w_*$  is the preimage of  $z_*$ . Note that the function defined by (3.4.11) satisfies all the conditions in (3.4.9) except the last one. In order to satisfy this last condition we must choose  $w_*$  properly. Thus, from (3.4.10) we find that  $\arg\{h_k(w)\} = -\mu_k \cos^{-1}(-w_k)$ , and hence,

$$\arg \left\{ e^{i\alpha_n \pi} \prod_* h_k(w) \right\} = \alpha_n \pi - \sum_* \mu_k \cos^{-1}(w_k).$$

Hence, the last condition in (3.4.9) implies that

$$\alpha_n \pi = \alpha_n \pi - \sum_* \mu_k \cos^{-1}(w_k) = 0,$$

and thus,

$$w_* = -\cos \left( \alpha_n \pi - \sum_{k=1}^{n-1} \mu_k \cos^{-1}(w_k) \right). \quad (3.4.12)$$

Then Eq (3.4.11) yields the Kirchhoff flow as the Schwarz-Christoffel integral

$$\begin{aligned} z &= C + e^{i\alpha_n \pi} \int^\zeta \prod_* h_k(t) dt \\ &= C + e^{i\alpha_n \pi} W \int^w (t - w_*) \prod_* h_k(t) dt \\ &= C + W e^{i\alpha_n \pi} \int^w \left( 1 - w_* t + \sqrt{(1 - t^2)(1 - w_*^2)} \right) \\ &\quad \times \prod_{k=1}^{n-1} \left( \frac{t - w_k}{1 - w_* t + \sqrt{(1 - t^2)(1 - w_*^2)}} \right)^{-\mu_k} dt, \end{aligned} \quad (3.4.13)$$

where we replaced the integration with respect to  $\zeta$  by that with respect to  $w$  by setting  $d\zeta = W (w - w_*) dw$  and in the last step canceling the common factor  $(t - w_*)$ . The above formula basically matches the formula derived by Monakov (1983, Eq (5) on p.185, where he erroneously takes  $w_* = 0$ ). A Fortran package for the Kirchhoff flow problem, containing the files `scpack.exe` and `kirch1.exe`, can be obtained from the second author in Elcrat and Trefethen (1986).

---

### 3.5. Problems

**PROBLEM 3.5.1.** Let the field of an infinite two-dimensional capacitor be as shown in the Fig. 3.5.1, with the values of the potential on the curves  $\Gamma_1$  and  $\Gamma_2$  as 0 and 1. Show that the function  $w = f(z)$  that maps the upper half-plane onto the triangle  $A_1 A_2 A_3$  is given by

$$w = C_0 \int_{-1}^z \zeta^{-1} (1 + \zeta)^\alpha d\zeta + C_1,$$

where  $C_1 = ih$  and  $C_0 = h/\pi$ . (Sveshnikov and Tikhonov, 1978, pp.217–218.)

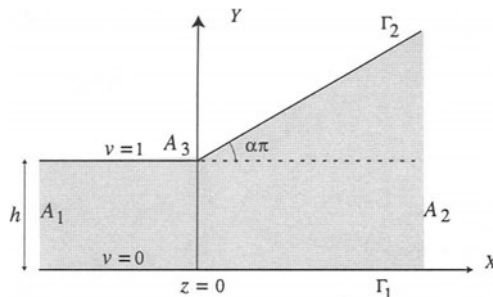


Fig. 3.5.1.

**PROBLEM 3.5.2.** Show that the function  $w = \int_0^z \frac{dt}{\sqrt{t(1-t^2)}}$  maps the upper half-plane  $\Im\{z\} > 0$  onto the interior of the square of side  $\frac{\Gamma^2(1/4)}{2\sqrt{2\pi}}$ . (Phillips, 1966, p.65.)

PROBLEM 3.5.3. Show that the function  $\pi w = \cosh^{-1} z - \sin^{-1}(1/z) + \pi/2$  maps the region in the positive quadrant of the  $w$ -plane bounded by the lines  $u = 0$ ,  $v = 0$ ,  $u = 1$  ( $v > 1$ ), and  $v = 1$  ( $u > 1$ ), onto the upper half-plane  $\Im\{z\} > 0$ . (Phillips, 1966, p.66.)

PROBLEM 3.5.4. Show that the Schwarz-Christoffel transformation that maps the region (shaded) in Fig. 3.5.2 onto the upper half-plane  $\Im\{w\} > 0$  such that  $z = 0$  goes into  $w = 0$  is given by

$$z = \frac{a}{\mu\pi} \int_1^w \left( \frac{\zeta - 1}{\zeta} \right)^\mu d\zeta.$$

Let  $\mu = p/q$ ,  $p < q$  ( $p, q \in \mathbb{R}^+$ ), and set  $t = \left( \frac{\zeta - 1}{\zeta} \right)^{1/q}$ , as in Case Study 2.3.6. Show that the mapping function becomes

$$z = \frac{a}{\pi} \left[ -\frac{1}{\mu} \frac{t^p}{t^q - 1} + \sum_{n=0}^{q-1} t_n^p \log \left( 1 - \frac{t}{t_n} \right) \right],$$

where  $t_n = e^{2i\pi n/q}$ ,  $n = 0, 1, \dots, q-1$ , are the  $q$  zeros of  $t^q - 1$ . [Use  $\frac{t^{p-1}}{t^q - 1} = \frac{1}{q} \sum_{n=0}^{q-1} \frac{t_n^p}{t - t_n}$ .] In particular, for  $\mu = 1/2$ ,  $p = 1$ ,  $q = 2$ , show that

the mapping function is given by  $z = \frac{a}{\pi} \left[ \frac{2t}{1-t^2} + \log \frac{1-t}{1+t} \right]$ . (Koppenfels, 1959, pp.210–211.)

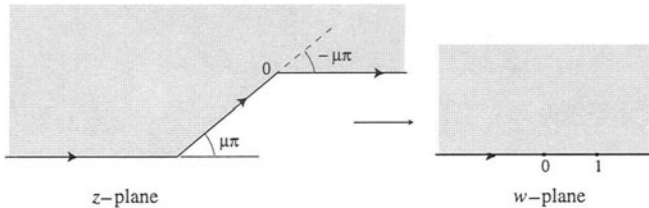


Fig. 3.5.2.

PROBLEM 3.5.5. The original Kirchhoff's problem deals with an irrotational flow of a weightless, ideal, incompressible fluid past a flat plate  $AB$  with separation of the jet, such that the modulus of flow velocity is equal to the modulus of the approaching stream  $v_0$  on the surfaces of the jets  $AD$  and  $BD$  (Fig. 3.5.3). The region of constant pressure behind the plate extends to

infinity and the plate  $AB$  is perpendicular to the flow. This problem deals with the determination of the function  $\zeta(w)$  such that  $v_0 \frac{dz}{dw} = \zeta(w)$ . Show that the function

$$\zeta(w) = -\sqrt{\frac{u_0}{w}} - \sqrt{\frac{u_0}{w} - 1},$$

where  $u_0$  is a real constant maps the  $w$ -plane cut along the positive real axis from  $C$  to  $+\infty$  onto the upper half-plane  $\Im\{\zeta\} > 0$  from which a semicircle of unit radius is removed (Fig. 3.5.4). [Use the following conformal maps:  $\tau = \frac{\zeta - 1}{\zeta + 1}$ ,  $\tau_1 = \tau^2$ ,  $t = \sqrt{\frac{w}{u_0}}$ , and  $t_1 = \frac{1+t}{1-t}$ .] (Gurevich, 1965, pp.15–20.)

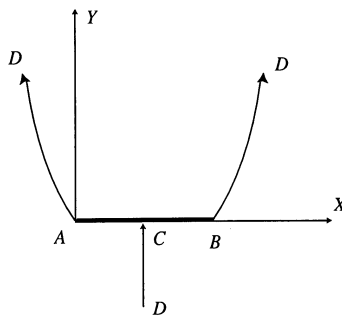


Fig. 3.5.3.

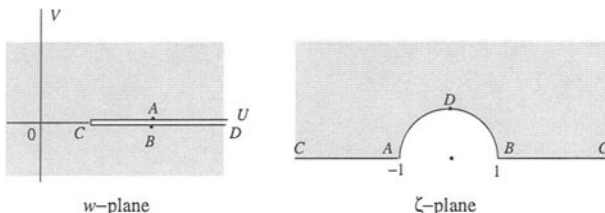


Fig. 3.5.4.

REFERENCES USED: Ahlfors (1966), Betz (1964), Birkoff and Zarantonello (1957), Boas (1987), Carathéodory (1969), Carrier, Krook and Pearson (1966), Elcrat (1982), Elcrat and Trefethen (1986), Gaier (1964), Gilbarg (1949, 1960), Gurevich (1965), Kantorovich and Krylov (1958), Koppenfels (1959), Monakov (1983), Robertson (1965), Sveshnikov and Tikhonov (1978).

# Chapter 4

---

## Polynomial Approximations

---

Gaier's variational method is used to solve two extremal problems in the theory of conformal mapping. The first deals with the conformal mapping of a simply connected region onto a disk, and the second with that of the boundary of the region onto the circumference of the disk. Both problems use the Ritz method for approximating the minimal mapping function by polynomials. This mapping function in the first problem is represented in terms of the Bergman kernel function, and in the second problem in terms of the Szegö kernel. Another important problem deals with an investigation into the nature and location of boundary singularities and poles of the mapping function close to the boundary, which is presented in Chapter 12.

---

### 4.1. Minimum Area Problem

An extremal property in the conformal mapping of a simply connected region  $D$  onto a disk is connected with the minimum area problem. This problem, which we shall denote as Problem I, is known as the Bieberbach minimizing principle. The mapping function possesses an extremal property which provides a method to compute an approximate solution for the map. Let  $\mathcal{K}^1(D)$  denote the class of all functions  $f \in L^2(D)$  with  $f(a) = 1$ , where  $a \in D$ . Similarly, let  $\mathcal{K}^0(D)$  denote the class of all functions  $f \in L^2(D)$  such that  $f(a) = 0$ . Note that the classes  $\mathcal{K}^1(D)$  and  $\mathcal{K}^0(D)$  are, respectively, a closed

convex subset and a closed subspace of  $L^2(D)$ . Let the function

$$w = f(z) = \sum_{n=0}^{\infty} a_n (z - a)^n, \quad |z - a| < R, \quad (4.1.1)$$

which is regular in  $D$ , map  $D$  onto the disk  $B(0, R)$  in the  $w$ -plane. Without loss of generality, we shall sometimes take the point  $a$  as the origin.

PROBLEM I: In the class  $\mathcal{K}^1$  minimize the integral

$$I = \iint_D |f'(z)|^2 dS_z. \quad (4.1.2)$$

The Riemann mapping theorem (Theorem 1.4.1) guarantees the existence and uniqueness of the solution of this extremal problem.

**THEOREM 4.1.1.** *Problem I (minimum area problem) has a unique solution  $f_0(z) = f'(z)$ . The minimum is  $\pi R^2$ .*

PROOF. If  $f_0(a) = 0$  and  $f'_0(a) = 1$ , then in view of (1.4.9)

$$\begin{aligned} \text{area}(D) &= \iint_D |f'(z)|^2 dS_z = \int_0^R \int_0^{2\pi} |f' (r e^{i\theta})|^2 r dr d\theta \\ &= \int_0^R \sum_{n=0}^{\infty} |a_n|^2 n^2 2\pi r^{2n-1} dr \\ &= \pi R^2 |a_1|^2 + \pi \sum_{n=2}^{\infty} n |a_n|^2 R^{2n}. \end{aligned} \quad (4.1.3)$$

The above result implies that in the problem of mapping by the function (4.1.1), which is regular in  $B(0, R)$  and is such that  $f'(a) = a_1$ , the area of the mapped region  $D$  is always greater than  $\pi R^2 |a_1|^2$ . It is exactly equal to this value if the map  $f(z)$  is linear, i.e., if  $w = a_0 + a_1 z$ . A particular case is when  $a_1 = 1$ . Then the mapping function is  $w = a_0 + z$ . If this linear transformation is excluded, then the mapping function can be normalized by the conditions  $f(a) = 0$  and  $f'(a) = 1$ , by considering the function  $f(z)/a_1$ . In either case the minimum area of  $D$  is  $\pi R^2$ . ■

Before we solve Problem I, we shall examine the minimal function  $f_0(z)$  closely.

**THEOREM 4.1.2.** *The function  $f_0(z)$  is orthogonal to every function  $f \in L^2(D)$  with  $g(a) = 0$ , i.e.,*

$$\langle f_0, g \rangle = \iint_D f_0(z) \overline{g(z)} dS_z = 0. \quad (4.1.4)$$

**PROOF.** For every  $\varepsilon > 0$  and  $0 \leq \theta \leq 2\pi$ , the function  $f_0(z) + \varepsilon g(z)$  belongs to the class  $\mathcal{K}^1$ . Then

$$\begin{aligned} \iint_D |f_0(z)|^2 dS_z &\leq \iint |f_0(z) + \varepsilon g(z)|^2 dS_z \\ &= \iint_D |f_0(z)|^2 dS_z + 2\varepsilon \Re \left\{ \iint_D f_0(z) \overline{g(z)} dS_z \right\} \\ &\quad + \varepsilon^2 \iint_D |g(z)|^2 dS_z, \end{aligned}$$

which implies that

$$\Re \left\{ \iint_D f_0(z) \overline{g(z)} dS_z \right\} + \frac{\varepsilon}{2} \iint_D |g(z)|^2 dS_z \geq 0.$$

If (4.1.4) were false, then the above expression would be negative for sufficiently small  $\varepsilon > 0$ . ■

**4.1.1. Bergman Kernel.** If we take  $g(z) = f_0(z) - f_0(a)$ , then from (4.1.4) for  $f \in \mathcal{K}^1(D)$  we have

$$\iint_D f_0(z) \overline{f(z)} dS_z = \overline{f(a)} \iint_D f_0(z) dS_z,$$

and if  $f = f_0$ , then

$$\|f_0\|^2 = \iint_D |f_0(z)|^2 dS_z = \overline{f_0(a)} \iint_D f_0(z) dS_z.$$

If we introduce the Bergman kernel

$$K(z, a) = \frac{f_0(z)}{\|f_0\|^2}, \quad (4.1.5)$$

where  $f_0(z)$  minimizes Problem I, then for every  $f \in \mathcal{K}^1(D)$

$$\iint_D \overline{K(z, a)} f(z) dS_z = f(a). \quad (4.1.6)$$

Hence, every function  $f \in L^2(D)$  is the eigenfunction of the integral equation (4.1.6) with eigenvalue  $\lambda = f_0(a) = 1$ . Then the minimal function  $f_0(z)$  is, in view of (4.1.5), given by

$$f_0(z) = \frac{K(z, a)}{K(a, a)}, \quad (4.1.7)$$

where

$$K(a, a) = \iint_D |K(z, a)|^2 dS_z = \frac{1}{\|f_0\|^2}. \quad (4.1.8)$$

Note that we cannot find  $f_0(z)$  directly. We can find  $f'(z)$  since it appears in the integrand in (4.1.2). Then the mapping function  $f$  is related to the Bergman kernel of  $D$  by

$$f(z) = \frac{\iint_D K(z, a) dS_z}{K(a, a)}. \quad (4.1.9)$$

## 4.2. Numerical Methods for Problem I

We shall study the Ritz method (RM) and the Bergman kernel method (BKM) but postpone until Chapter 12 the investigation into the nature and location of boundary singularities and poles of the mapping function that are close to the boundary.

**4.2.1. Ritz Method.** The Ritz method is used to find the solution of the above extremal problem approximately in the form of a polynomial. Consider an arbitrary system of linearly independent functions  $u_0(z), u_1(z), \dots$ , which are regular in  $D$  and are such that  $\iint_D |u_k(z)|^2 dx dy < +\infty$  for  $k = 0, 1, \dots$ .

We assume that one of these functions, say  $u_0(z)$ , is such that  $u_0(a) \neq 0$ . Without loss of generality, we take  $a = 0$ . Let  $\{\phi_n(z)\}$  be a complete set of  $L^2(D)$ , and denote by  $\mathcal{K}_n^0$  and  $\mathcal{K}_n^1$  the  $n$ -dimensional counterparts of  $\mathcal{K}^0$  and  $\mathcal{K}^1$ , respectively, i.e., if

$$\phi_n(z) = \sum_{k=0}^n c_k u_k(z), \quad (4.2.1)$$

then  $\phi_n \in \mathcal{K}_n^0$  if  $\phi(0) = 0$ , and  $\phi_n \in \mathcal{K}_n^1$  if  $\phi_n(0) = 1$ , where  $c_k = \alpha_k + i\beta_k$ ,  $c_0 \neq 0$ , are complex numbers. Now we shall consider the integral

$$I(\phi_n) = \iint_D |\phi_n(z)|^2 dS_z, \quad (4.2.2)$$

which is the same as (4.1.1) except that the integrand in (4.2.2) is  $\phi_n(z)$  instead of  $f'(z)$ .

PROBLEM I<sub>n</sub>: In the class  $\mathcal{K}_n^1$  minimize the integral  $I(\phi_n)$ , defined by (4.2.2).

Now we shall discuss the existence and uniqueness of the minimal polynomial  $\phi_n(z)$ , determine  $\phi_n(z)$ , and approximate  $f_0(z)$  by the minimal polynomial  $\phi_n(z)$ . The numerical value of the integral (4.2.2) is equal to the area of the image of the region  $D$ . Then the problem reduces to a choice of the coefficients  $c_k$  so that this value is a minimum among the values of the same integral for any other linear combination  $\psi_n$  of the functions  $u_k(z)$ ,  $k = 0, 1, \dots, n$ , subject to the condition  $\psi_n(0) = 1$ . Suppose that

$$\psi_n(z) = \phi_n(z) + \varepsilon \gamma_n(z), \quad (4.2.3)$$

where  $\varepsilon$  is a complex number and  $\gamma_n(z)$  is a linear combination of  $u_k(z)$ ,  $k = 0, 1, \dots, n$ . The requirement that  $\psi_n(0) = 1$  for all  $\varepsilon$  implies that  $\gamma_n(0) = 0$ . Now

$$\begin{aligned} I(\psi_n) &= \iint_D |\phi_n|^2 dx dy + \bar{\varepsilon} \iint_D \phi_n \bar{\gamma}_n dx dy \\ &\quad + \varepsilon \iint_D \bar{\phi}_n \phi_n dx dy + |\varepsilon|^2 \iint_D |\gamma_n|^2 dx dy. \end{aligned} \quad (4.2.4)$$

The sign of the difference  $I(\psi_n) - I(\phi_n)$  for small  $\varepsilon$  will depend on the linear terms in  $\varepsilon$  and  $\bar{\varepsilon}$  because the last term in (4.2.4) is of order  $O(\varepsilon^2)$ . Thus,  $I(\psi_n) - I(\phi_n) \geq 0$  iff the following orthogonality relations hold:

$$\iint_D \phi_n \bar{\gamma}_n dx dy = 0 \quad \text{and} \quad \iint_D \bar{\phi}_n \gamma_n dx dy = 0 \quad (4.2.5)$$

for any linear combination  $\gamma_n$  that satisfies the condition  $\gamma_n(0) = 0$ . Otherwise, we can always choose an  $\varepsilon$  which will make  $I(\psi_n) < I(\phi_n)$ , and this will contradict the minimal properties of  $\phi_n(z)$ . Note that the integrands in (4.2.5) are complex conjugates of each other, so we can use either as needed.

Conversely, if  $\phi_n(z)$  satisfies the orthogonality relations (4.2.5), then  $\phi_n(z)$  imparts the integral  $I(\phi_n)$  its minimum value among the values imparted by all linear combinations of  $\psi_n(z)$  with  $\psi_n(0) = 1$ . Thus, from (4.2.4) and (4.2.5) we get

$$I(\psi_n) - I(\phi_n) = |\varepsilon|^2 \iint_D |\gamma_n|^2 dx dy. \quad (4.2.6)$$

Hence, the polynomial  $\phi_n(z)$  will be unique if it exists, since the integral on the right side of (4.2.6) is equal to zero only when  $\gamma_n = 0$ , i.e., when  $\psi_n = \phi_n$ . Thus, the orthogonality relations (4.2.5) constitute necessary and sufficient conditions for  $\phi_n(z)$  to be the minimal polynomial.

We shall rewrite the conditions (4.2.5) in a different but equivalent form. Let

$$v_k(z) = u_k(z) - \frac{u_k(0)}{u_0(0)} u_0(z), \quad k = 1, \dots, n. \quad (4.2.7)$$

Then each of the functions  $v_k(z)$  satisfies the requirements imposed on  $\gamma_k(z)$ , and the conditions (4.2.5) become

$$\sum_{j=0}^n A_{kj} c_j = 0, \quad (4.2.8)$$

where

$$A_{kj} = \iint_D \bar{u}_j v_k dx dy = \iint_D u_j \bar{v}_k dx dy, \quad k = 1, \dots, n. \quad (4.2.9)$$

Also, since

$$\sum_{k=0}^n u_k(0) c_k = 1, \quad (4.2.10)$$

Eqs (4.2.8) and (4.2.10) provide us with a system of  $(n + 1)$  equations to determine the numbers  $c_0, c_1, \dots, c_n$  uniquely.

Note that the functions  $u_k(z)$ , though linearly independent, are still undetermined and are not subject to limitation. However, it becomes very easy to determine the integrals in (4.2.9) if all  $u_k(z)$  are suitably chosen beforehand such that  $u_0(0) = 1$ , and  $u_k(0) = 0$  for  $k = 1, \dots, n$ . Then  $v_k(z) = u_k(z)$ , and the integral

$$\iint_D u_j \bar{v}_k dx dy = \iint_D u_j \bar{v}_k dx dy.$$

Also, Eq (4.2.10) degenerates to  $c_0 = 1$ , which reduces the number of unknowns by one. Moreover, if the system of functions  $u_0(z), u_1(z), \dots$  is orthogonal in  $D$ , i.e., if

$$\iint_D u_j \bar{u}_k dx dy = 0 \quad \text{for } k \neq j,$$

then

$$\iint_D u_j \bar{v}_k dx dy = 0 \quad \text{for } j \neq 0 \text{ and } k \neq j,$$

and

$$\iint_D u_0 \bar{v}_k dx dy = -\frac{\overline{u_k(0)}}{\overline{u_0(0)}} \iint_D u_0 \bar{u}_0 dx dy,$$

$$\iint_D u_k \bar{v}_k dx dy = \iint_D u_k \bar{u}_k dx dy.$$

Then Eqs (4.2.8)–(4.2.10) simplify to

$$c_k \iint_D |u_k|^2 dx dy - c_0 \frac{\overline{u_k(0)}}{\overline{u_0(0)}} \iint_D |u_0|^2 dx dy = 0. \quad (4.2.11)$$

Thus, we have proved

**THEOREM 4.2.1.** *The problem  $I_n$  has a unique solution. The coefficients of the minimal polynomial  $\phi_n(z)$ , defined by (4.2.1), are determined by the system of linear equations (4.2.8)–(4.2.9). The coefficients  $A_{kj}$ , defined by (4.2.9), are hermitian.*

Let the system  $\{u_k\}_{k=0}^n$  be taken as the complete set  $\{1, z, z^2, \dots, z^n\}$ . Then for the minimal polynomial

$$\phi_n(z) = 1 + c_1 z + c_2 z^2 + \dots + c_n z^n, \quad (4.2.12)$$

the system of equations (4.2.8)–(4.2.9), which determine the  $n$  coefficients  $c_k$ , becomes

$$\begin{bmatrix} A_{10} & A_{11} & A_{12} & \cdots & A_{1n} \\ A_{20} & A_{21} & A_{22} & \cdots & A_{2n} \\ \cdots & \cdots & \cdots & \cdots & \cdots \\ A_{n0} & A_{n1} & A_{n2} & \cdots & A_{nn} \end{bmatrix} \begin{Bmatrix} 1 \\ c_1 \\ c_2 \\ \vdots \\ c_n \end{Bmatrix} = \{0\}, \quad (4.2.13)$$

where the coefficients  $A_{kj}$  are given by

$$A_{kj} = \iint_D z^k \bar{z}^j dS_z, \quad A_{kj} = \bar{A}_{jk}. \quad (4.2.14)$$

Note that if  $a \neq 0$ , then the coefficients  $A_{kj}$  are determined from

$$A_{kj} = \iint_D (z - a)^k \overline{(z - a)^j} dS_z, \quad A_{kj} = \bar{A}_{jk}. \quad (4.2.15)$$

The computation of the coefficients  $A_{kj}$  depends on the region  $D$ , although it may sometimes present difficulties.

**CASE STUDY 4.2.1** Let the region  $D$  be starlike with respect to a point  $a \neq 0 \in D$ , i.e., every ray emanating from the point  $a$  intersects the boundary in only one point. Let the equation of the boundary be  $r = r(\theta)$ . Using the polar coordinates  $z - a = r e^{i\theta}$ , we get

$$\begin{aligned} A_{kj} &= \int_0^{2\pi} \int_0^{r(\theta)} r^{j+k} e^{i(j-k)\theta} r dr d\theta \\ &= \frac{1}{j+k+2} \int_0^{2\pi} r^{j+k+2}(\theta) e^{i(j-k)\theta} d\theta \\ &= \frac{1}{j+k+2} \int_0^{2\pi} r^{j+k+2}(\theta) \cos(j-k)\theta d\theta \\ &\quad + \frac{i}{j+k+2} \int_0^{2\pi} r^{j+k+2}(\theta) \sin(j-k)\theta d\theta. \end{aligned} \quad (4.2.16)$$

Note that  $\Re \{A_{kj}\}$  and  $\Im \{A_{kj}\}$  differ from the coefficients of the Fourier series for  $r^{j+k+2}(\theta)$  by a factor  $\frac{\pi}{j+k+2}$ , and hence, they can be easily computed. ■

**DEFINITION 4.2.1.** The system of polynomials  $\{\phi_n\}$  is said to be *complete* in the Hilbert space  $L^2(D)$  if for every function  $f \in L^2(D)$  and every  $\varepsilon > 0$  there exists a polynomial  $\phi_n$  such that  $\|f - \phi_n\| < \varepsilon$ .

Now the question arises, under what additional assumptions on  $D$  the polynomials  $\phi_n(z)$  form a complete system in  $L^2(D)$ . Naturally,  $\|f_0 - \phi_n\| \searrow 0$  must hold, and thus also  $\phi_n(z) \rightarrow f_0(z)$  as  $n \rightarrow \infty$  in any closed subset  $\bar{G} \subset D$ .

**THEOREM 4.2.2.** *Let the polynomial  $p(z)$  belong to the class  $\mathcal{K}_n^1$ . Then*

$$\|f_0 - p\|^2 = \iint_D |f_0(z) - p(z)|^2 dS_z \quad (4.2.17)$$

*is minimal only if  $p(z) = \phi_n(z)$ .*

**PROOF.** In view of (4.1.4)

$$\langle f_0, p \rangle = \langle f_0, p - f_0 \rangle + \langle f_0, f_0 \rangle = \langle f_0, f_0 \rangle,$$

thus,

$$\langle f_0 - p, f_0 - p \rangle = \langle f_0, f_0 \rangle - 2 \langle f_0, f_0 \rangle + \langle p, p \rangle = \|p\|^2 - \|f_0\|^2,$$

and the result follows since  $\|p\|^2$  is minimal if  $p = \phi_n$ . ■

Hence, among all  $p \in \mathcal{K}_n^1$  the polynomial  $\phi_n$  yields the minimum norm  $\|f_0 - p\|$ , and since  $\mathcal{K}_{n+1}^1 \supset \mathcal{K}_n^1$ , then  $\|f_0 - p\| \searrow 0$  only if the system of polynomial  $\{\phi_n\}$  is complete in the space  $L^2(D)$ . Moreover, in Problem I<sub>n</sub> there exists a polynomial  $p = \phi_n$  which satisfies the additional condition  $p(a) = f(a)$ . Also note that the Bieberbach polynomial  $\pi_n(z)$  defined by

$$\pi_n(z) = \int_a^z \phi_{n-1}(\zeta) d\zeta \rightarrow f(z) \quad \text{as } n \rightarrow \infty \text{ in } \bar{G} \subset D. \quad (4.2.18)$$

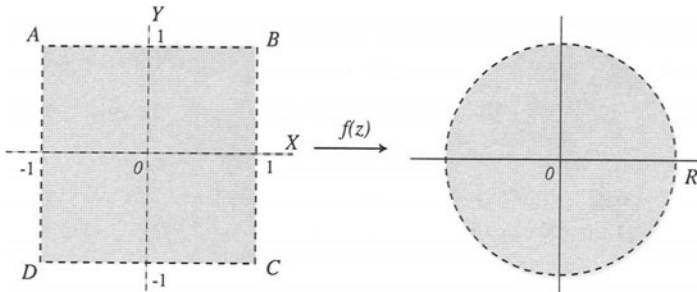


Fig. 4.2.1.

**CASE STUDY 4.2.2.** Determine the minimal polynomial  $\phi_n(z)$  and the approximate mapping function  $f(z)$  that maps the square region  $D = \{x, y :$

$-1 < x, y < 1\}$  conformally onto  $|w| < 1$  (Fig. 4.2.1). From `cs422.nb` (see Notes at the end of this chapter), the minimum polynomial is given by

$$\phi_8(z) = 1 + \frac{97402305}{266254834} z^4 + \frac{68765697}{2130038672} z^8,$$

which yields the approximate mapping function

$$\begin{aligned} f(z) &\approx \int_0^z \phi_8(t) dt \\ &= z + \frac{19480461}{266254834} z^5 + \frac{7640633}{2130038672} z^9 \\ &\approx z + 0.0731647 z^5 + 0.00358709 z^9. \blacksquare \end{aligned} \quad (4.2.19)$$

**4.2.2. Bergman Kernel Method.** In this method the mapping function  $f(z)$  is determined approximately from (4.1.19) by first approximating the kernel  $K(z, 0)$  by a finite Fourier sum. Let  $\{\phi_j^*(z)\}$  denote a complete orthonormal set of  $L^2(D)$ . Consider the Fourier series expansion of  $K(z, 0)$ . Then, in view of (4.1.6),

$$\langle K, \phi_j^* \rangle = \iint_D K(z, 0) \overline{\phi_j^*(z)} dS_z = \overline{\phi_j^*(0)}. \quad (4.2.19)$$

Thus, the kernel has a series expansion

$$K(z, 0) = \sum_{j=1}^{\infty} \overline{\phi_j^*(0)} \phi_j^*(z), \quad (4.2.20)$$

which converges in the mean of  $L^2(D)$ , i.e., the series (4.2.20) converges almost uniformly in  $D$ .

Hence, if we have a complete set  $\{\phi_j(z)\}$  of  $L^2(D)$ , then by using (4.1.19) and (4.2.20) we obtain an approximate mapping function  $f(z)$  as follows:

(i) Orthonormalize the set  $\{\phi_j(z)\}_{j=1}^n$  by using the Gram–Schmidt process which yields the set of orthonormal functions  $\{\phi_j^*(z)\}_{j=1}^n$ . Note that the Gram–Schmidt process requires evaluating  $\langle \phi_i, \phi_j \rangle$ , which, in view of Green's formula (1.1.29), is given by

$$\langle \phi_i, \phi_j \rangle = \iint_D \phi_i(z) \overline{\phi_j(z)} dS_z = \frac{1}{2i} \int_{\Gamma} \phi_i(z) \overline{\psi_j(z)} dz, \quad (4.2.21)$$

where  $\psi'_j(z) = \phi_j(z)$ . Then the integrals in (4.2.21) are computed by Gaussian quadrature.

(ii) Truncate the series (4.2.20) after  $n$  terms to obtain the approximation  $K_n(z, 0)$  of  $K(z, 0)$  as

$$K_n(z, 0) = \sum_{j=1}^n \overline{\phi_j^*(0)} \phi_j^*(z). \quad (4.2.22)$$

(iii) Use (4.1.19) to obtain the approximate mapping function  $f_n(z)$  as

$$f_n(z) = \frac{\int_0^z K_n(z, 0) dz}{K_n(0, 0)}. \quad (4.2.23)$$

(iv) The approximate radius  $R_n$  of the disk  $|w| < R$  is given by

$$R_n = \frac{1}{\sqrt{\pi K_n(0, 0)}}, \quad (4.2.24)$$

since  $\|f_0\|^2 = \pi R^2$  (because  $f_0 \in \mathcal{K}^1$ ).

(v) Thus, from (4.2.23) and (4.2.24) the approximation of the mapping function  $F(z)$  that maps  $D$  conformally onto the unit disk  $|w| < 1$  is given by

$$F_n(z) = \sqrt{\frac{\pi}{K_n(0, 0)}} \int_0^z K_n(z, 0) dz. \quad (4.2.25)$$

The maximum error estimate for  $|F_n(z)|$  is given by

$$E_n = \max_j |e_n(z_j)|,$$

where  $z_j \in \Gamma$  are the test points on the boundary and  $e_n(z) = 1 - |F_n(z)|$ . During the computation process the number  $n$  of the basis function is increased by one each time and this process is terminated when the inequality  $E_{n+1} < E_n$  no longer holds. Then such a number  $n$  is taken as the ‘optimum number’ for the basis functions.

Note that in both RM and BKM we have obtained approximations of the form

$$f_n(z) = \sum_{j=1}^n a_j u_j(z),$$

where  $u'_j(z) = \phi_j(z)$ . In both methods the set of monomials  $z^{j-1}$ ,  $j = 1, 2, \dots$ , which is a complete set in  $L^2(D \cup \Gamma)$  is the best choice of basis

functions in computation. Then this basis gives the polynomials  $\phi_j(z)$  defined in (4.2.13).

CASE STUDY 4.2.3. The function  $w = f(z)$  that maps the unit disk  $U$  onto itself such that the point  $z_0 \in U$  goes into the origin of the  $w$ -plane is given by

$$f(z) = \frac{z - z_0}{z - 1/\bar{z}_0}.$$

Thus, both  $f(z)$  and the associated Bergman kernel function  $K(z, z_0)$  have a pole at  $z = 1/\bar{z}_0$ . Since the polynomials  $\phi_j^*(z) = \sqrt{j/\pi} z^{j-1}$ ,  $j = 1, 2, \dots$ , form a complete orthonormal basis set of  $U$ , the kernel  $K(z, z_0)$  can, in view of (4.2.20), be represented by the polynomial series

$$K(z, z_0) = \frac{1}{\pi} \sum_{j=1}^{\infty} j (\bar{z}_0 z)^{j-1},$$

which converges rapidly when  $|z_0|$  is small, but the convergence becomes considerably slower the faster  $|z_0| \rightarrow 1$ , i.e., the closer the pole  $1/\bar{z}_0$  gets to the boundary of  $U$ . ■

### 4.3. Minimum Boundary Problem

An analogous minimum problem in the conformal mapping of a region  $D$  onto  $|w| < R$  leads to another characterization of the mapping function  $f(z)$  by considering the line integral

$$I = \int_{\Gamma} |f(z)|^2 ds, \quad (4.3.1)$$

where  $\Gamma$  is the boundary of  $D$ . This problem, studied by Julia (1931), is known as the minimum boundary problem which we shall call Problem II. Let  $\Gamma$  be a rectifiable Jordan curve, and let  $\mathcal{L}^1(\Gamma)$  denote the class of all functions  $f \in L^2(\Gamma)$  with  $f(a) = 1$ , where  $a \in D$  can be taken as the origin.

PROBLEM II: In the class  $\mathcal{L}^1(\Gamma)$  minimize the integral (4.3.1).

**THEOREM 4.3.1.** *Problem II has a unique solution  $f_0(z)$ , and it is  $f_0(z) = \sqrt{f'(z)}$ . The minimum is  $2\pi R$ .*

**PROOF.** For every function  $F \in L^2(\Gamma)$

$$\begin{aligned} \int_{\Gamma} |F(z)|^2 ds &= \lim_{r \rightarrow R} \int_{\Gamma_r} |F(z)|^2 ds \\ &= \lim_{r \rightarrow R} \int_{|w|=r} |F(g(w)) \sqrt{g'(w)}|^2 |dw| \\ &= \lim_{r \rightarrow R} r \int_0^{2\pi} |h(r e^{i\theta})|^2 d\theta, \end{aligned}$$

where  $h(w) = F(g(w)) \sqrt{g'(w)}$ ,  $h(0) = 1$ , and  $z = g(w)$  (see (1.1.26)). If  $h(w) = \sum_{n=0}^{\infty} a_n w^n$ ,  $a_0 = 1$ , then

$$\int_{\Gamma} |F(z)|^2 ds = 2\pi \sum_{n=0}^{\infty} |a_n|^2 R^{2n+1} \geq 2\pi R,$$

where the equality holds only for  $a_n = 0$ ,  $n > 0$ , which yields  $F(z) = \sqrt{f'(z)}$  for  $h(w) = 1$ . ■

This theorem implies that in the class of all conformal mappings  $w = \phi(z)$  of the region  $D$  with  $\phi(a) = 0$ ,  $\phi'(a) = 1$ , the integral  $\int_{\Gamma} |\phi'(z)| ds$  is minimum only when  $\phi(z) = f(z)$ . This is known as the principle of minimizing the image boundary.

The conformal map  $f$  of  $D$  onto  $|w| < R$ , normalized by  $f(a) = 0$ ,  $f'(a) = 1$ , is given by

$$f(z) = \int_a^z [f_0(\zeta)]^2 d\zeta.$$

The theory for Problem II is developed exactly on the same lines as in §4.1 and 4.2. Thus, as in (4.1.4), we have

**THEOREM 4.3.2.** *The function  $f_0(z)$  is orthogonal to every function  $g \in L^2(\Gamma)$  with  $g(a) = 0$ , i.e.,*

$$\langle f_0, g \rangle = \int_{\Gamma} f_0(z) \overline{g(z)} ds = 0. \quad (4.3.2)$$

For the minimal function  $f_0(z)$  of Problem II we introduce the Szegö kernel function

$$S(z, a) = \frac{f_0(z)}{\int_{\Gamma} |f_0(z)|^2 ds}, \quad (4.3.3)$$

with the properties

$$S(a, a) = \int_{\Gamma} |S(z, a)|^2 ds, \quad \text{and} \quad f_0(z) = \frac{S(z, a)}{S(a, a)}. \quad (4.3.4)$$

For any  $f \in L^2(\Gamma)$ , we apply (4.3.2) to  $f(z) - f(a)$  and get

$$\int_{\Gamma} f_0(z) \overline{f(z)} ds = \overline{f(a)} \int_{\Gamma} f_0(z) ds,$$

and if  $f = f_0$ , then, since  $h(w) = 1$  implies  $f(a) = 1 = \overline{f(a)}$ , we have

$$\int_{\Gamma} |f_0(z)|^2 ds = \int_{\Gamma} f_0(z) ds.$$

Thus, analogous to (4.1.6) we have: For every function  $f \in L^2(\Gamma)$

$$\int_{\Gamma} \overline{S(z, a)} f(z) ds = f(a). \quad (4.3.5)$$

Theorems 4.1.1 and 4.3.1 together with the definitions (4.1.5) and (4.3.3) yield

$$K(z, a) = 4\pi [S(z, a)]^2. \quad (4.3.6)$$

Thus,  $S(z, a)$  can be evaluated by the method of §4.2. A relation between the Cauchy and Szegö kernels and their application to the problem of conformal mapping is presented in §7.6.

## 4.4. Ritz Method for Problem II

Let  $\mathcal{L}_n^1$  denote the class of all polynomials  $p(z)$  of degree  $\leq n$  with  $p(a) = 1$ .

PROBLEM II<sub>n</sub>: In the class  $\mathcal{L}_n^1$  minimize the line integral  $\int_{\Gamma} |p(z)|^2 ds$ .

We shall discuss the existence and uniqueness of the minimal polynomial  $\phi_n(z)$ , determine  $\phi_n(z)$ , and approximate  $f_0(z)$  by the minimal polynomial  $\phi_n(z)$  and  $f(z)$  by the integral  $\int_a^z [\phi_n(\zeta)]^2 d\zeta$ , respectively. As in §4.2, it can be shown that a minimal polynomial  $\phi_n(z)$  exists for Problem II, that it is unique, and that it is characterized by

$$\langle \phi_n, g \rangle = 0 \quad (4.4.1)$$

for every polynomial  $g(z)$  of degree  $\leq n$  with  $g(a) = 0$ . The proof is analogous to that of (4.1.4).

In view of (4.4.1), the coefficients of the minimal polynomial

$$\phi_n(z) = 1 + a_1(z - a) + \cdots + a_n(z - a)^n \quad (4.4.2)$$

are determined by

$$\int_{\Gamma} \left( \sum_{k=0}^n a_k (z - a)^k \right) \overline{(z - a)^j} ds = 0, \quad j = 1, 2, \dots, n, \quad (4.4.3)$$

and  $a_0 = 1$ . If we set

$$B_{kj} = \int_{\Gamma} (z - a)^k \overline{(z - a)^j} ds, \quad k, j = 0, 1, \dots, \quad (4.4.4)$$

then the coefficients of the minimal polynomial  $\phi_n(z)$  defined by (4.4.2) are determined from the (consistent) system of equations

$$\sum_{k=0}^n B_{kj} a_k = 0, \quad a_0 = 1, \quad j = 1, \dots, n. \quad (4.4.5)$$

For any arbitrary polynomial  $p \in \mathcal{L}_n^1$ , we have, in view of (4.2.2),

$$\langle f_0 - p \rangle = \langle f_0, p - f_0 \rangle + \langle f_0, f_0 \rangle = \langle f_0, f_0 \rangle,$$

and hence

$$\|f_0 - p\|^2 = \|p\|^2 - \|f_0\|^2, \quad (4.4.6)$$

which implies that  $p(z)$  has the minimal property:

$$\int_{\Gamma} |f_0(z) - p(z)|^2 ds \quad \text{is minimum in } \mathcal{L}_n^1 \text{ for } p(z) = \phi_n(z). \quad (4.4.7)$$

Again, as in §4.2,  $\|f_0 - \phi_n\| \searrow 0$  as  $n \rightarrow \infty$ , since  $\mathcal{L}_{n+1}^1 \supset \mathcal{L}_n^1$ . Then we ask, under what assumptions on  $D$  is the system of polynomials  $\{\phi_n\}$  complete in the Hilbert space  $L^2(\Gamma)$ ? An answer was given by Smirnov (1928) as

**THEOREM 4.4.1.** *The system of polynomials in  $L^2(\Gamma)$  is complete iff the boundary  $\Gamma$  of the region  $D$  satisfies the condition*

$$\log |g'(w)| = \frac{1}{2\pi} \int_0^{2\pi} \log |g'(r e^{i\theta})| \frac{R^2 - r^2}{R^2 - 2Rr \cos(\alpha - \theta) + r^2} d\alpha, \quad (4.4.8)$$

for all  $r < R$ , where  $z = g(w)$  is the inverse mapping function which maps the region  $|w| < R$  onto the region  $D$  in the  $z$ -plane.

A proof of this theorem can be found in Goluzin (1957, p.396; or 1969, p.449). The condition (4.4.8) is known as the  $S$ -condition. This condition depends only on the region  $D$  and not on the normalization of  $g(w)$  or on the choice of  $a \in D$ . All such regions  $D$  whose mapping satisfy the  $S$ -condition (4.4.8) are said to belong to the Smirnov class  $\mathcal{S}$ . Not all regions with a rectifiable boundary belong to the class  $\mathcal{S}$ . Besides the rectifiability of  $\Gamma$ , however, it is sufficient for  $D \in \mathcal{S}$  if one of the following conditions is met: (i)  $D$  is convex or starlike with respect to a point in  $D$ ; (ii)  $\Gamma$  is piecewise smooth, and its smooth arcs  $\gamma_k$ ,  $k = 1, \dots, n$ , join one another with a nonzero interior angle; (iii) the ratio of the length of any arc  $\gamma_k$  of  $\Gamma = \cup \gamma_k$  to the length of its chord does not exceed a fixed limit; (iv) if  $D \notin \mathcal{S}$ , then the behavior of  $\|\phi_n\|^2$  and of  $\|f_0 - \phi_n\|^2 = \|\phi_n\|^2 - \|f_0\|^2$  is known; and (v) for any  $D$  with a rectifiable boundary  $\Gamma$ , the integral  $\int_{\Gamma} |\phi_n(z)|^2 ds \searrow 2\pi R\delta$ , where

$$\delta = \exp \left\{ \frac{1}{2\pi} \int_0^{2\pi} \log |g'(R e^{i\theta})| d\theta \right\}. \quad (4.4.9)$$

Thus, under the conditions (i), (ii), or (iii) we have  $\|f_0 - \phi_n\| \searrow 0$ , and, in view of Theorem 4.1.2,  $\phi_n(z) \rightarrow f_0(z)$  as  $n \rightarrow \infty$  for every region  $G \subset D$ . Hence, for  $z \in G \subset D$  the polynomial

$$\pi_{2n+1} = \int_a^z [\phi_n(\zeta)]^2 d\zeta \rightarrow f(z) \quad \text{as } n \rightarrow \infty. \quad (4.4.10)$$

Note that the polynomial  $\pi_{2n+1}(z)$  is different from the Bieberbach polynomial (4.2.18).

**THEOREM 4.4.2.** *For the system of polynomials to be complete in a region  $D$ , it is necessary and sufficient that an arbitrary function  $F(z) \in L^2(\Gamma)$  satisfies the condition*

$$\int_{\Gamma} |F(z)|^2 ds = \sum_{k=1}^n |a_k|^2, \quad (4.4.10)$$

where  $a_k$  are the Fourier coefficients of  $F(z)$ .

PROOF. Let  $p(z)$  be an arbitrary polynomial of degree  $n$ :

$$p(z) = \sum_{k=0}^n c_k u_k(z). \quad (4.4.11)$$

Then for  $F(z) \in L^2(\Gamma)$

$$\begin{aligned} \int_{\Gamma} |F(z) - p(z)|^2 ds &= \int_{\Gamma} |F(z)|^2 ds + \int_{\Gamma} |p(z)|^2 ds \\ &\quad - 2 \Re \left\{ \int_{\Gamma} F(z) \overline{p(z)} ds \right\} \\ &= \int_{\Gamma} |F(z)|^2 ds + \sum_{k=0}^n |c_k|^2 - 2 \Re \left\{ \sum_{k=0}^{\infty} a_k c_k \right\} \\ &= \int_{\Gamma} |F(z)|^2 ds - \sum_{k=0}^n |c_k|^2 + \sum_{k=0}^n |a_k - c_k|^2. \end{aligned} \quad (4.4.12)$$

Thus, the polynomial  $p(z)$  defined by (4.4.11) with  $c_k = a_k$  attains the minimum of the integral

$$\int_{\Gamma} |F(z) - p(z)|^2 ds, \quad (4.4.13)$$

and, in view of (4.4.11), this minimum yields

$$\int_{\Gamma} |F(z)|^2 ds - \sum_{k=0}^n |c_k|^2 = 0. \quad (4.4.14)$$

Hence, a system of polynomials is complete iff the difference (4.4.14) approaches zero as  $n \rightarrow \infty$  for an arbitrary function  $F \in L^2(\Gamma)$ . ■

**THEOREM 4.4.3.** *If the S-condition (4.4.8) is satisfied, then an arbitrary function  $F(z) \in L^2(\Gamma)$  can be represented in  $D$  by a Fourier series*

$$F(z) = \sum_{k=0}^{\infty} a_k u_k(z), \quad (4.4.15)$$

*which converges uniformly in  $D$ , where*

$$a_k = \int_{\Gamma} f(w) \overline{u_k(w)} ds. \quad (4.4.16)$$

PROOF. Since the minimum of the integral (4.4.13) is attained out of all polynomials  $p_n(z)$  by a polynomial defined by (4.4.11) with  $c_k = a_k$ ,  $k = 0, 1, \dots, n$ , then, if the  $S$ -condition is satisfied, we have

$$\lim_{n \rightarrow \infty} \int_{\Gamma} |F(\zeta) - p_n(\zeta)|^2 ds = 0. \quad (4.4.17)$$

But by Cauchy's formula in  $D$

$$F(z) - p_n(z) = \frac{1}{2i\pi} \int_{\Gamma} \frac{F(\zeta) - p_n(\zeta)}{\zeta - z} d\zeta.$$

If  $\bar{G}$  is a closed subset of  $D$  and  $\delta$  is the distance from  $G$  to  $\Gamma$ , then for  $z \in \bar{G}$

$$\begin{aligned} |F(z) - p_n(z)| &\leq \frac{1}{2\pi\delta} \int_{\Gamma} |F(\zeta) - p_n(\zeta)| ds \\ &\leq \frac{1}{2\pi\delta} \sqrt{l \int_{\Gamma} |F(\zeta) - p_n(\zeta)|^2 ds}, \end{aligned} \quad (4.4.18)$$

where  $l$  is the length of  $\Gamma$ , and this, in view of (4.4.17), implies that  $p_n(z) \rightarrow F(z)$  uniformly on  $\bar{G}$  as  $n \rightarrow \infty$ . But  $p_n(z)$  is a finite part of the Fourier series (4.4.15), which proves the theorem. ■

## 4.5. Orthogonal Polynomials

Functions analytic in a region  $D$  can always be represented by Taylor series only if  $D$  is a circular disk. If the boundary  $\Gamma$  of  $D$  is not a circle, such a series representation is not possible. Therefore, we must find a sequence of functions which depend only on the region  $D$  so that any analytic function in  $D$  can be expanded in the form of a series involving functions from this sequence. It turns out that all such functions are certain polynomials of a special form which are either orthogonal on the boundary  $\Gamma$  or in the region  $D$ . They not only provide a series expansion for analytic functions on  $D$  but also play a significant role in conformal mapping.

**4.5.1. Polynomials orthogonal on the boundary.** We shall analyze the structure of polynomials that are orthogonal on a contour. Let

$\Gamma$  be an arbitrary rectifiable curve (not necessarily closed) of length  $l$ . By using the Gram–Schmidt orthogonalization process (see Gaier, 1964, p.132, for an algorithm for this process) we construct a sequence of polynomials  $\{P_0(z), P_1(z), \dots, P_n(z), \dots\}$  with the following properties:

- (i)  $P_n(z)$  is a polynomial of degree  $n$  in  $z$ ;
- (ii) the coefficient of  $z^n$  in  $P_n(z)$  is positive; and
- (iii) the polynomials  $P_n(z)$  are orthonormal (orthogonal and normalized) along the curve  $\Gamma$ , i.e.,

$$\frac{1}{l} \int_{\Gamma} P_n(z) \overline{P_m(z)} ds = \delta_{nm}, \quad (4.5.1)$$

where  $\delta_{nm}$  is the Kronecker delta. We shall introduce the constants

$$h_{pq} = \frac{1}{l} \int_{\Gamma} z^p \bar{z}^q ds. \quad (4.5.2)$$

Note that  $ds = |dz|$  and  $h_{pq} = \bar{h}_{qp}$ . Consider the positive-definite hermitian quadratic forms

$$\begin{aligned} H_n(t) &= \sum_{p,q=0}^n h_{pq} t_p \bar{t}_q \\ &= \frac{1}{l} \int_{\Gamma} |t_0 + t_1 z + \dots + t_n z^n|^2 ds, \end{aligned} \quad (4.5.3)$$

with determinants  $D_n$  defined by

$$D_0 = 1, \quad D_n = \begin{vmatrix} h_{00} & h_{10} & \cdots & h_{n0} \\ h_{01} & h_{11} & \cdots & h_{n1} \\ \cdots & \cdots & \cdots & \cdots \\ h_{0n} & h_{1n} & \cdots & h_{nn} \end{vmatrix}. \quad (4.5.4)$$

Then the Szegö polynomials  $\sigma_n(z)$  are represented by

$$\sigma_n(z) = \frac{1}{\sqrt{D_{n-1} D_n}} \begin{vmatrix} h_{00} & h_{10} & \cdots & h_{n0} \\ h_{01} & h_{11} & \cdots & h_{n1} \\ \cdots & \cdots & \cdots & \cdots \\ h_{0,n-1} & h_{1,n-1} & \cdots & h_{n,n-1} \\ 1 & z & \cdots & z^n \end{vmatrix}. \quad (4.5.5)$$

It can be verified that these polynomials possess the above three properties. As regards the question of expansion of an arbitrary analytic function in a series involving Szegö polynomials, the following result due to Smirnov (1928) holds:

**THEOREM 4.5.1.** *Suppose that a function  $f(z)$  is analytic inside a region  $D$  bounded by a Jordan curve  $\Gamma$ , has almost everywhere boundary values on  $\Gamma$ , and can be represented in terms of these boundary values by Cauchy integrals. Then  $f(z)$  can be expanded in a series involving Szegö polynomials:*

$$f(z) = \sum_{n=0}^{\infty} A_n \sigma_n(z), \quad (4.5.6)$$

*which is uniformly convergent everywhere within  $\Gamma$ , and the coefficients  $A_n$  are determined by*

$$A_n = \frac{1}{l} \int_{\Gamma} f(z) \overline{\sigma_n(z)} ds. \quad (4.5.7)$$

For a proof of this theorem see Smirnov (1928).

As an application of Szegö polynomials to conformal mapping, let  $w = F(z)$  map the region  $D$  in the  $z$ -plane onto the disk  $|w| < R$  such that a point  $a \in D$  goes into the origin  $w = 0$ ,  $F(a) = 0$ , and  $F'(a) = 1$ . In view of Theorem 4.3.1, out of all functions  $F(z)$  analytic on  $D$  and normalized at  $a$  by  $F(a) = 1$ , the function  $\sqrt{f'(z)}$  minimizes the integral (4.3.1), i.e.,

$$I = \frac{1}{l} \int_{\Gamma} |F(z)|^2 ds \quad \text{in the class } \mathcal{L}^1. \quad (4.5.8)$$

Using the series expansion (4.5.6) for the function  $F(z)$  in terms of Szegö polynomials  $\sigma_n(z)$ , and using  $F(a) = 1$ , we find that

$$\sum_{j=0}^{\infty} A_j \sigma_j(a) = 1. \quad (4.5.9)$$

Then, from (4.5.8)

$$\frac{1}{l} \int_{\Gamma} F(z) \overline{F(z)} ds = \sum_{j=0}^{\infty} A_j \bar{A}_j. \quad (4.5.10)$$

Then the system of coefficients corresponding to the function  $F(z) = \sqrt{f'(z)}$  attains the minimum value for the sum in (4.5.10) such that the condition (4.5.9)

is satisfied. We shall denote these coefficients by  $\delta_j$ , and set  $A_j = \delta_j + \varepsilon \eta_j$ . Since, in view of (4.5.9), the condition

$$\sum_{j=0}^{\infty} \delta_j \sigma_j(a) = 1 \quad (4.5.11)$$

still holds, the numbers  $\eta_j$  must be such that

$$\sum_{j=0}^{\infty} \eta_j \sigma_j(a) = 0. \quad (4.5.12)$$

Then, from (4.5.10)

$$\begin{aligned} \frac{1}{l} \int_{\Gamma} F(z) \overline{F(z)} ds &= \sum_{j=0}^{\infty} \delta_j \bar{\delta}_j + \varepsilon \sum_{j=0}^{\infty} \eta_j \bar{\delta}_j \\ &\quad + \bar{\varepsilon} \sum_{j=0}^{\infty} \bar{\eta}_j \delta_j + |\varepsilon|^2 \sum_{j=0}^{\infty} \eta_j \bar{\eta}_j. \end{aligned} \quad (4.5.13)$$

Since the expression on the right side in (4.5.13) must be less than  $\sum_{j=0}^{\infty} \delta_j \bar{\delta}_j$ , which is the minimum value of the integral (4.5.8), it is necessary and sufficient that the coefficients of  $\varepsilon$  and  $\bar{\varepsilon}$  vanish for all  $\eta_j$  subject to the condition (4.5.12), i.e.,

$$\sum_{j=0}^{\infty} \eta_j \bar{\delta}_j = 0 = \sum_{j=0}^{\infty} \bar{\eta}_j \delta_j. \quad (4.5.14)$$

Now, from (4.5.12) we get  $\eta_0 = - \sum_{j=0}^{\infty} \eta_j \sigma_j(a)$ , since  $\sigma_0(z) = 1$ , and

$$\sum_{j=0}^{\infty} \eta_j [\bar{\delta}_j - \bar{\delta}_0 \sigma_j(a)] = 0, \quad (4.5.15)$$

which is valid for arbitrary  $\eta_1, \eta_2, \dots$  only if

$$\bar{\delta}_j = \bar{\delta}_0 \sigma_j(a). \quad (4.5.16)$$

Substituting the values of  $\delta_j$  from (4.5.16) and (4.5.11) we get

$$\delta_0 \sum_{j=0}^{\infty} \sigma_j(a) \overline{\sigma_j(a)} = 1. \quad (4.5.17)$$

Set

$$S(z, a) = \sum_{j=0}^{\infty} \overline{\sigma_j(a)} \sigma_j(z). \quad (4.5.18)$$

Then we have

$$\begin{aligned} \delta_0 &= \bar{\delta}_0 = \frac{1}{S(a, a)} = \frac{\overline{\sigma_0(a)}}{S(a, a)}, \\ \delta_j &= \frac{\overline{\sigma_j(a)}}{S(a, a)}, \\ \sqrt{f'(z)} &= \frac{1}{S(a, a)} \sum_{j=0}^{\infty} \overline{\sigma_j(a)} \sigma_j(z) = \frac{S(z, a)}{S(a, a)}, \\ f(z) &= \frac{1}{S^2(a, a)} \int_a^z S^2(z, a) dz, \end{aligned} \quad (4.5.19)$$

where  $S(z, a)$  is the Szegö kernel defined in §4.3. In order to derive an approximate formula for  $f(z)$ , we shall assume that only  $n$  Szegö polynomials  $\sigma_j(z)$  are known. Then

$$S_n(z, a) \approx \sum_{j=0}^n \overline{\sigma_j(a)} \sigma_j(z), \quad (4.5.20)$$

and

$$f(z) \approx \frac{1}{S(a, a)} \int_a^z S^2(z, a) dz. \quad (4.5.21)$$

The radius  $R$  of the disk  $|w| < R$  is given exactly by

$$\begin{aligned} R &= \frac{1}{2\pi} \int_{\Gamma} |f'(z)|^2 ds = \frac{1}{2\pi S^2(a, a)} \int_a^z S(z, a) \overline{S(z, a)} ds \\ &= \frac{1}{2\pi S^2(a, a)} \sum_{j=0}^{\infty} \overline{\sigma_j(a)} \sigma_j(a) = \frac{l}{2\pi S(a, a)}. \end{aligned} \quad (4.5.22)$$

Then obviously the function  $g(z)$  that maps the region  $D$  onto the unit disk  $U$  is given by

$$g(z) = \frac{2\pi}{l S^2(a, a)} \int_a^z S^2(z, a) dz. \quad (4.5.23)$$

**CASE STUDY 4.5.1.** We shall determine the mapping function  $F(z)$  that maps the square  $\{-1 \leq x, y \leq 1\}$  onto the disk  $|w| \leq R$  (see Fig. 4.2.1).

Since  $z = x + i$  on  $A B$ ,  $z = x - i$  on  $D C$ ,  $z = 1 + iy$  on  $C B$ , and  $z = -1 + iy$  on  $D A$ , the numbers

$$h_{pq} = \frac{1}{8} \left\{ \int_{-1}^1 [(x+i)^p(x-i)^q + (x-i)^p(x+i)^q] dx + [(1+iy)^p(1-iy)^q + (-1+iy)^p(-1-iy)^q] dy \right\} \quad (4.5.24)$$

are computed in `cs422.nb` for  $p, q = 0, 1, \dots, 8$ . If Mathematica is not used, then (4.5.24) can be written as

$$\begin{aligned} h_{pq} &= \frac{1}{8} \int_{-1}^1 \left\{ (x+i)^p(x-i)^q + (x-i)^p(x+i)^q \right. \\ &\quad \left. + i^{p-q} [(x+i)^p(x-i)^q + (x-i)^p(x+i)^q] \right\} dx \\ &= \frac{1+i^{p-q}}{8} \int_{-1}^1 [(x+i)^p(x-i)^q + (x-i)^p(x+i)^q] dx \quad (4.5.26) \\ &= \frac{1+i^{p-q}}{4} \Re \left\{ \int_{-1}^1 (x+i)^p(x-i)^q dx \right\} \\ &= \begin{cases} 0, & \text{if } p - q \neq 4k, \\ \frac{1}{2} \int_{-1}^1 (x^2 + 1)^q \Re \{(x+i)^{p-q}\} dx, & \text{if } p - q = 4k, \end{cases} \end{aligned}$$

and then the numbers  $h_{pq}$  can be evaluated with the same values as in (4.5.25). Now, from (4.5.5)

$$\begin{aligned} \sigma_0(z) &= 1, & \sigma_1(z) &= \frac{\sqrt{3}}{2} z, & \sigma_2(z) &= \frac{1}{2} \sqrt{\frac{15}{7}} z^2, \\ \sigma_3(z) &= \frac{1}{4} \sqrt{\frac{35}{6}} z^3, & \sigma_4(z) &= \frac{3}{16} \sqrt{\frac{7}{22}} (4 + 5z^4), \\ \sigma_5(z) &= \frac{3}{8} \sqrt{\frac{11}{379}} z(8 + 7z^4), & \sigma_6(z) &= \frac{1}{128} \sqrt{\frac{429}{3941}} z^2(220 + 147z^4), \\ \sigma_7(z) &= \frac{1}{8} \sqrt{\frac{65}{96222}} z^3(182 + 99z^4). \end{aligned}$$

Since all  $\sigma_j(0)$  are zero except for  $j = 1, 4$ , we find from (4.5.18) that

$$S(z, 0) = \sum_{n=0}^{\infty} \overline{\sigma_n(0)} \sigma_n(z) \approx 1 + \frac{63}{1408} (4 + 5z^4),$$

$S(0, 0) = \frac{415}{352}$ , and thus, from (4.5.19)

$$\begin{aligned} f(z) &\approx \frac{1}{S^2(0, 0)} \int_0^z S^2(z, 0) dz \\ &= z + \frac{63}{830} z^5 + \frac{441}{110224} z^9 \\ &\approx z + 0.0759036 z^5 + 0.004 z^9, \end{aligned} \quad (4.5.27)$$

which can be compared with (4.2.19). Let  $z = \phi(w)$  be the inverse function of  $w = f(z)$  such that  $\phi(w)$  maps the circle  $|w| = R$  onto the given square, and  $\phi(0) = 0$ ,  $\phi'(0) = 1$ . By using the Schwarz–Christoffel transformation analogous to Case Study 2.3.2, the function  $z = \phi(w)$  is represented by the elliptic integral

$$z = \int_0^w \frac{d\zeta}{\sqrt{1 + k^4 \zeta^4}} = w - \frac{k^4}{10} w^5 + \frac{k^8}{24} w^9 + \dots, \quad (4.5.28)$$

where

$$k = \int_0^1 \frac{d\zeta}{\sqrt{1 + \zeta^4}} \approx 0.927037. \quad (4.5.29)$$

On inversion, (4.5.28) yields

$$w = f(z) = z + \frac{k^4}{10} z^5 + \frac{k^8}{120} z^9 + \frac{11k^{12}}{15600} z^{13} + \dots, \quad (4.5.30)$$

(see, e.g., Gaier, 1964, p.148.) A comparison of (4.5.27) and (4.5.30) shows that  $\frac{k^4}{10} = \frac{63}{830}$ , or  $k = \sqrt[4]{\frac{63}{83}} \approx 0.933395$ , which, after comparing with the value of  $k$  in (4.5.29) shows that the polynomial approximation of  $f(z)$  has an error of 0.636%. This means that the polynomial  $f(z)$  maps the boundary of the square onto some curve that does not quite coincide with the circle  $|w| = R$ . In order to determine the closeness of this curve to the circle  $|w| = R$ , we evaluate  $|f(1)|$  and  $|f(1+i)|$ , which are given by  $|f(1)| = 1.0799036$ , and  $|f(1+i)| = 1.075368896$ , which shows that the radius of the circle onto which the square is mapped by the approximate polygon lies between these two values. However, from (4.5.22) we find that  $R = 1/k \approx 1.078705$ , which gives a maximum error of at most 0.5% of the value of  $R$ .

The polynomial that maps the given square onto the unit disk  $U$  can be determined from (4.5.23). The exact solution is given by the elliptic integral

$$\begin{aligned} z &= \frac{\int_0^w (1+t^4)^{-1/2} dt}{\int_0^1 (1+t^4)^{-1/2} dt} \\ &\approx 1.08 \left( w - \frac{1}{10} w^5 + \frac{1}{24} w^9 - \frac{5}{208} w^{11} + \dots \right). \blacksquare \end{aligned} \quad (4.5.31)$$

The exact mapping function is known in terms of Jacobian elliptic functions (see Case Study 2.3.2).

**4.5.2. Polynomials orthogonal to a region.** Let  $D$  be, as before, a simply connected region with a Jordan boundary  $\Gamma$  and area  $A$ . Using the Schmidt orthogonalization process, we construct a system of polynomials  $\{Q_0(z), Q_1(z), \dots, Q_n(z), \dots\}$ , with the following properties:

- (i)  $Q_n(z)$  is a polynomial of degree  $n$  in  $z$ ;
- (ii) the coefficient of  $z^n$  in  $Q_n(z)$  is positive; and
- (iii) the polynomials  $Q_n(z)$  are orthonormal (orthogonal and normalized) along the curve  $\Gamma$ , i.e.,

$$\frac{1}{A} \iint_D Q_n(z) \overline{Q_m(z)} dx dy = \delta_{nm}. \quad (4.5.32)$$

These properties are similar to those in §4.5.1, except that the line integral is now replaced by the surface integral. We introduce the constants

$$\gamma_{pq} = \frac{1}{A} \iint_D z^p \bar{z}^q dx dy, \quad (4.5.33)$$

and, analogous to (4.5.4), define the determinants  $\Delta_n$  by

$$\Delta_0 = 1, \quad \Delta_n = \begin{vmatrix} \gamma_{00} & \gamma_{10} & \cdots & \gamma_{n0} \\ \gamma_{01} & \gamma_{11} & \cdots & \gamma_{n1} \\ \cdots & \cdots & \cdots & \cdots \\ \gamma_{0n} & \gamma_{1n} & \cdots & \gamma_{nn} \end{vmatrix}. \quad (4.5.34)$$

Then the polynomials

$$\Pi_n(z) = \frac{1}{\sqrt{\Delta_{n-1} \Delta_n}} \begin{vmatrix} \gamma_{00} & \gamma_{10} & \cdots & \gamma_{n0} \\ \gamma_{01} & \gamma_{11} & \cdots & \gamma_{n1} \\ \cdots & \cdots & \cdots & \cdots \\ \gamma_{0n} & \gamma_{1n} & \cdots & \gamma_{nn} \\ 1 & z & \cdots & z^n \end{vmatrix} \quad (4.5.35)$$

are orthogonal in the region  $D$ , and form a complete closed system. Any function  $f(z)$  analytic on  $D$  such that the integral

$$\iint_D |f(z)|^2 dx dy < +\infty$$

can be uniquely expanded in a series involving the polynomials  $\Pi_n(z)$ , i.e.,

$$f(z) = \sum_{n=0}^{\infty} \alpha_n \Pi_n(z), \quad (4.5.36)$$

where the coefficients  $\alpha_n$  are determined by

$$\alpha_n = \frac{1}{A} \iint_D f(z) \overline{\Pi_n(z)} dx dy. \quad (4.5.37)$$

As an application, note that, in view of §4.1, the function  $F(z) = f_0(z) \in \mathcal{K}^1$  maps the region  $D$  conformally onto the disk  $|w| < R$  such that a point  $a \in D$  goes into  $w = 0$  and  $f'_0(a) = 1$ . Out of all analytic functions  $F(z) \in \mathcal{K}^1$  with  $F(a) = 0$  and  $F'(a) = 1$ , the function  $f_0(z)$  gives the minimum for the integral (4.1.2). Analogous to Theorem 4.5.1 the function  $f_0(z)$  can be represented in a series expansion involving the polynomials  $\Pi_j(z)$  as

$$f_0(z) = \frac{1}{K(a, a)} \int_a^z K(z, a) dz, \quad (4.5.38)$$

where, as in (4.1.5),

$$K(z, a) = \sum_{j=0}^{\infty} \overline{\Pi_j(a)} \Pi_j(z). \quad (4.5.39)$$

Then the area of the circle  $|w| = R$  is given by

$$\begin{aligned} \pi R^2 &= \iint_D |F'(z)|^2 dx dy \\ &= \frac{A}{K^2(a, a)} \sum_{j=0}^{\infty} \overline{\Pi_j(a)} \Pi_j(z) = \frac{A}{K(a, a)}, \end{aligned} \quad (4.5.40)$$

whence

$$R = \sqrt{\frac{A}{\pi K(a, a)}}, \quad (4.5.41)$$

and the mapping function is determined by

$$f_0(z) = \sqrt{\frac{A}{\pi K(a, a)}} \int_a^z K(a, a) dz. \quad (4.5.42)$$

## 4.6. Problems

PROBLEM 4.6.1. Let  $w = f(z)$  map a finite, simply connected region  $D$  onto the unit disk  $|w| < 1$ . Show that the functions

$$\phi_n(z) = \sqrt{\frac{n+1}{n}} [f(z)]^n f'(z), \quad n = 0, 1, \dots,$$

form a complete orthonormal set in  $D$ . (Nehari, 1952, p.247.)

PROBLEM 4.6.2. Show that the Bergman kernel  $K(z, a)$  can be expanded into the infinite series (4.2.20) which converges absolutely and uniformly in any closed region contained in  $D$ . (Nehari, 1952, p.251, 256.)

PROBLEM 4.6.3. Let  $E$  denote the ellipse  $\frac{x^2}{a^2} + \frac{y^2}{b^2} = 1$ . Show that the Bergman kernel for  $E$  has the form

$$K(z, a) = \frac{4}{\pi} \sum_{n=0}^{\infty} \frac{(n+1)U_n(z)\overline{U_n(a)}}{\rho^{n+1} - \rho^{-n-1}}, \quad \rho = (a+b)^2,$$

where  $U_n(z) = (1-z^2)^{-1/2} \sin((n+1)\cos^{-1}z)$  are the Chebyshev polynomials of the second kind and degree  $n$ . (Nehari, 1952, pp.258–259.)

PROBLEM 4.6.4. Prove that if  $\Gamma$  satisfies the  $S$ -condition, then

$$f'(z) = 2\pi \frac{\left[ \sum_{k=0}^{\infty} \overline{u_k(0)} u_k(z) \right]^2}{\sum_{k=0}^{\infty} |u_k(0)|^2}, \quad z \in D,$$

where the convergence of the series in the numerator is uniform in  $D$ . [Let  $F(z) = \sqrt{f'(z)}$ . Use (4.4.16) and show that  $a_n = 2\pi \overline{u_n(0)} \sqrt{f'(0)}$ .] (Goluzin, 1969, p.453.)

PROBLEM 4.6.5. Let the arc  $\Gamma$  be defined by the ellipse  $E : \frac{(x-x_c)^2}{a^2} + \frac{(y-y_c)^2}{b^2} = 1$ ,  $a > b$ , and let the parametric equation of  $\Gamma$  be  $z = \gamma(s) =$

$z_c + a e \cos(s - iq)$ ,  $0 \leq s_1 < s < s_2 < 2\pi$ , where  $z_c = x_c + iy_c$  is the center  $C$ ,  $e = \sqrt{1 - b^2/a^2}$  the eccentricity of the ellipse,  $\cosh q = 1/e$ , and  $s_2 - s_1 < 2\pi$ . Show that the function  $z = \gamma(\zeta)$ ,  $\zeta = s + it$ , is univalent in the strip  $\{\zeta : \zeta + s + it, s_1 < s < s_2, -\infty < t < q\}$ , and the region  $G^*$  is a symmetric subregion of the rectangle  $\{\zeta : \zeta = s + it, s_1 < s < s_2, -q < t < q\}$ . (Papamichael, Warby and Hough, 1983, p.157.)

PROBLEM 4.6.6. Show that the function

$$w = f(z) = \sqrt{k(q)} \operatorname{sn} \left( \frac{2K}{\pi} \sin^{-1} z, q \right), \quad q = \left( \frac{a-b}{a+b} \right)^2,$$

maps the interior of the ellipse  $\frac{x^2}{a^2} + \frac{y^2}{b^2} = 1$  onto the unit disk  $|w| < 1$ , such that the foci of the ellipse go into the points  $w = \pm\sqrt{k(q)}$ , and

$$\begin{aligned} f'(0) &= \frac{2}{a+b} \left( \sum_{n=0}^{\infty} q^{n(n+1)} \right) \cdot \left( 1 + 2 \sum_{n=1}^{\infty} q^n \right) \\ &= \begin{cases} 1.0165984 & \text{for } a/b = 1.2, \\ 1.2376223 & \text{for } a/b = 2, \\ 2.372368 & \text{for } a/b = 5. \end{cases} \end{aligned}$$

(Nehari, 1952, p. 296; Gaier, 1964, pp.160–161.)

NOTES. cs442.nb:

```
A[j_, k_] := Integrate[ Integrate[ (x+ I*y)^j * (x-I*y)^k,
{x, -1,1}], {y, -1,1}];

MatA = Table[A[j,k], {j,1,8}, {k,1,8}];

MatrixForm[MatA];

B=Table[A[j,0], {j,1,8}];

c=LinearSolve[MatA,- B];

(* These are the coefficients of phi_8[z] *)
phi8[z_] := 1 + c . Table[z^i, {i, 8}];

phi8[z];

(* The mapping function is given by f'[z]=phi8[z] *)
f[z_] := Integrate[phi8[t], {t, 0,z}];

f[z]
```

REFERENCES USED: Gaier (1964), Goluzin (1957, 1969), Kantorovich and Krylov (1958), Nehari (1952), Papamichael, Warby and Hough (1983).

# Chapter 5

---

## Nearly Circular Regions

---

We shall investigate methods for constructing a mapping function for conformal mapping of a simply connected nearly circular region onto a disk. A classical method that involves series expansion in powers of a small parameter for the interior and the exterior regions, known as the method of infinite systems, is presented with case studies, in which successive approximations are used to compute the approximate mapping function.

---

### 5.1. Small Parameter Expansions

Let a one-parameter family of Jordan curves  $\Gamma_\lambda$  in the  $z$ -plane be defined by

$$\Gamma_\lambda : z = z(t, \lambda), \quad (5.1.1)$$

where  $t$  and  $\lambda$  are real parameters (see §1.1). Let the origin  $z = 0$  lie inside all of these curves. Further, let the function

$$w = f(z, \lambda) \quad (5.1.2)$$

map the region  $D_\lambda$  bounded by the curve  $\Gamma_\lambda$  conformally onto a disk  $|w| < R$  in the  $w$ -plane, i.e. , the function (5.1.2) must also satisfy conditions

$$f(0, \lambda) = 0, \quad f'(0, \lambda) = 1. \quad (5.1.3)$$

Note that if the function  $z = z(t, \lambda)$  which defines the boundary curve  $\Gamma_\lambda$ , where the parameter  $t$  defines the position of the point  $z$  on  $\Gamma_\lambda$ , is an analytic

function of  $\lambda$  in the neighborhood of some value of  $\lambda$ , say  $\lambda = 0$ , then the mapping function (5.1.2) can also be regarded as an analytic function in that neighborhood. Thus, the function  $f(z, \lambda)$  for any  $z \in D_\lambda$  can be expanded in a power series in  $\lambda$  as

$$f(z, \lambda) = f_0(z) + \sum_{n=1}^{\infty} \lambda^n f_n(z), \quad (5.1.4)$$

which converges for sufficiently small  $|\lambda|$ . In order to compute the coefficients  $f_n(z)$ , we know from (5.1.3) that  $f_n(0) = 0$  for  $n = 0, 1, 2, \dots$ ,  $f'_0(0) = 1$  and  $f'_n(0) = 0$  for  $n = 1, 2, \dots$ . Thus,  $f_0(z) = f(z, 0)$ , which implies that the function  $w = f_0(z)$  maps the region  $D_0$  bounded by  $\Gamma_0$  exactly onto the disk  $|w| < R$ .

Now, to compute  $f_n(z)$  for  $n \geq 1$ , let us consider a system of functions  $\{u_n(z)\}_{n=1}^{\infty}$ , which are analytic in a region  $D$  containing all  $D_\lambda$  for sufficiently small  $|\lambda|$ , such that  $u_n(0) = 0$  for  $n = 1, 2, \dots$ ,  $u'_1(0) = 1$ , and  $u'_n(0) = 0$  for  $n = 2, 3, \dots$ . Then any function  $f(z, \lambda)$  analytic on  $D$  can be expanded in a series involving  $u_n(z)$ . Thus, let

$$f(z, \lambda) = u_1(z) + \sum_{n=2}^{\infty} \alpha_n(\lambda) u_n(z), \quad (5.1.4)$$

where the coefficients  $\alpha_n(\lambda)$  depend only on  $\lambda$ . Hence the problem of determining the function  $f(z, \lambda)$  reduces to that of computating the coefficients  $\alpha_n(\lambda)$ , which are, in fact, solutions of an infinite system of equations.

However, in practical problems, the function  $f(z, \lambda)$  is represented approximately by taking a finite sum in (5.1.4). Then the coefficients  $\alpha_n(\lambda)$  are determined by solving a finite system of equations. The details of computation are as follows (Kantorovich and Krylov, 1958): Let

$$U_n(z) = u_1(z) + \sum_{j=2}^n \alpha_j(\lambda) u_j(z) \quad (5.1.5)$$

denote a partial sum of the series (5.1.4). Then  $|U_n(z)|^2$  can be expanded in a trigonometric series in  $t \in [0, 2\pi]$ :

$$|U_n(z)|^2 = a_0 + \sum_{n=1}^{\infty} (a_n \cos nt + b_n \sin nt). \quad (5.1.6)$$

This means that the coefficients  $a_n$  and  $b_n$  in this expansion are quadratic functions of  $\alpha_j(\lambda)$ . We can choose that all coefficients  $a_n(\alpha_j)$  and  $b_n(\alpha_j)$  are zero for  $n = 1, 2, \dots$ , or that only the first  $(n - 1)$  coefficients  $a_n(\alpha_j)$  and  $b_n(\alpha_j)$  are zero. In the former case we get an exact determination of the function  $f(z, \lambda)$ . But in the second case we obtain a system of  $(2n - 2)$  equations

$$a_k(\alpha_j) = 0, \quad b_k(\alpha_j) = 0 \quad k = 1, 2, \dots, n - 1, \quad (5.1.7)$$

which shall determine the  $(n - 1)$  unknown complex coefficients  $\alpha_j(\lambda)$ . The form of the partial sum  $U_n(z)$ , defined by (5.1.5), depends on the choice of the system of the functions  $u_n(z)$ . If we take the system  $\{u_n(z)\} = \{z^n\}$ , then  $U_n(z)$  becomes a polynomial of degree  $n$ :

$$U_n(z) \equiv p_n(z) = z + \alpha_2(\lambda)z^2 + \dots + \alpha_n(\lambda)z^n. \quad (5.1.8)$$

Let us assume that the boundary  $\Gamma$  of the region  $D$  is nearly circular and is defined by

$$\Gamma : z(t) = e^{it} \{1 + \lambda F(e^{it}, \lambda)\}, \quad (5.1.9)$$

where  $F(\tau, \lambda)$ ,  $\tau = e^{it}$ , is an analytic function of its arguments for  $|\tau|$  close to 1 and  $\lambda$  close to 0. Then  $F(\tau, \lambda)$  can be expanded in a Laurent series in  $\tau$ :

$$F(\tau, \lambda) = \sum_{\nu=-\infty}^{\infty} \beta_{\nu}(\lambda) \tau^{\nu} = \sum_{\nu=-\infty}^{\infty} \beta_{\nu}(\lambda) e^{i\nu t},$$

where the coefficients  $\beta_{\nu}(\lambda)$  are analytic functions of  $\lambda$ . Then from (5.1.9) the boundary  $\Gamma$  is defined by

$$\begin{aligned} z(t) &= e^{it} \left\{ 1 + \lambda \sum_{\nu=-\infty}^{\infty} \beta_{\nu}(\lambda) e^{i\nu t} \right\} \\ &= \sum_{\nu=-\infty}^{\infty} \beta_{\nu}^{(1)}(\lambda) e^{i\nu t}, \end{aligned} \quad (5.1.10)$$

where

$$\beta_{\nu}^{(1)}(\lambda) = \begin{cases} \lambda \beta_{\nu-1}(\lambda) & \text{for } \nu \neq 1, \\ 1 + \lambda \beta_0(\lambda) & \text{for } \nu = 1. \end{cases} \quad (5.1.11)$$

The  $k$ -th power of  $z(t)$ , defined by (5.1.10), is given by

$$z^k(t) = \sum_{\nu=-\infty}^{\infty} \beta_{\nu}^{(k)}(\lambda) e^{i\nu t}, \quad (5.1.12)$$

where  $\beta_\nu^{(k)}(0) = \delta_{\nu k}$ . Thus, from (5.1.8) and (5.1.12)

$$\begin{aligned} |p_n(z)|^2 &= p_n(z), \overline{p_n(z)} \\ &= \sum_{k,j=1}^n \alpha_k \bar{\alpha}_j z^k \bar{z}^j, \quad (\text{where } \alpha_1 = 1) \\ &= \sum_{\nu=-\infty}^{\infty} \sum_{k,j=1}^n \alpha_k \bar{\alpha}_j \sum_{\substack{p,q=-\infty \\ p-q=\nu}}^{\infty} \beta_p^{(k)}(\lambda) \bar{\beta}_q^{(j)}(\lambda) e^{i\nu t}. \end{aligned} \quad (5.1.13)$$

Note that the right side of (5.1.13) represents a trigonometric series, whose coefficients depend on  $\alpha_k$ . If we denote the free term (corresponding to  $\nu = 0$ ) on the right side of (5.1.13) by  $R^2$ , we get

$$R^2 = \sum_{k,j=1}^n \alpha_k \bar{\alpha}_j \sum_{p=-\infty}^{\infty} \beta_p^{(k)}(\lambda) \bar{\beta}_p^{(j)}. \quad (5.1.14)$$

We will choose the coefficients  $\alpha_2, \dots, \alpha_n$ , such that the coefficients of  $e^{it}, e^{2it}, \dots, e^{(n-1)it}$  are zero, i.e.,

$$\sum_{k,j=1}^n \alpha_k \bar{\alpha}_j \sum_{m=-\infty}^{\infty} \beta_m^{(k)}(\lambda) \bar{\beta}_{m-m}^{(j)} = 0 \quad \text{for } m = 1, 2, \dots, n-1. \quad (5.1.15)$$

Note that the coefficients of  $e^{-it}, e^{-2it}, \dots, e^{-(n-1)it}$  are also zero. Hence, the system (5.1.15) should determine the coefficients  $\alpha_2, \dots, \alpha_n$ . Moreover, the difference between  $f(z)$  and  $U_n(z)$  decreases as  $n$  increases. The proof for the convergence of  $U_n(z)$  to  $f(z)$  through the method of successive approximations is given in Kantorovich and Krylov (1958, p.435). We shall look into some particular regions as case studies for which the system (5.1.15) provides simpler solutions.

**CASE STUDY 5.1.1.** In order to determine the function  $f(z, \lambda)$  that maps the interior of the ellipse  $x = (1 + \lambda^2) \cos t, y = (1 - \lambda^2) \sin t$  conformally onto the disk  $|w| < R$ , first note that the equation of the ellipse can be written as

$$z(t) = e^{it} (1 + \lambda^2 e^{-2it}). \quad (5.1.16)$$

We shall find the approximate mapping function  $U_n(z) = p_n(z)$  accurate to  $\lambda^{10}$ . Then the last coefficient in (5.1.8) shall be  $\alpha_{11}$ . Moreover, since the ellipse has two axes of symmetry, all  $\alpha_k$  are real and those with even indices shall be zero, thus

$$p_n(z) = z + \alpha_3 z^3 + \alpha_5 z^5 + \alpha_7 z^7 + \alpha_9 z^9 + \alpha_{11} z^{11},$$

and

$$\begin{aligned}
 |p_n(z)|^2 &= p_n(z) \overline{p_n(z)} \\
 &= z \bar{z} + \alpha_3 (z^3 \bar{z} + \bar{z}^3 z) + [\alpha_5 (z^5 \bar{z} + \bar{z}^5 z) + \alpha_3^2 z^3 \bar{z}^3] \\
 &\quad + [\alpha_7 (z^7 \bar{z} + \bar{z}^7 z) + \alpha_5 \alpha_3 (z^5 \bar{z}^3 + \bar{z}^5 z^3)] \\
 &\quad + [\alpha_9 (z^9 \bar{z} + \bar{z}^9 z) + \alpha_7 \alpha_3 (z^7 \bar{z}^3 + \bar{z}^7 z^3) + \alpha_5^2 z^5 \bar{z}^5] \\
 &\quad + [\alpha_{11} (z^{11} \bar{z} + \bar{z}^{11} z) + \alpha_9 \alpha_3 (z^9 \bar{z}^3 + \bar{z}^9 z^3) \\
 &\quad + \alpha_7 \alpha_5 (z^7 \bar{z}^5 + \bar{z}^7 z^5)] + [\alpha_{13} (z^{13} \bar{z} + \bar{z}^{13} z) \\
 &\quad + \alpha_{11} \alpha_3 (z^{11} \bar{z}^3 + \bar{z}^{11} z^3) + \alpha_9 \alpha_5 (z^9 \bar{z}^5 + \bar{z}^9 z^5) + \alpha_7^2 z^7 \bar{z}^7].
 \end{aligned} \tag{5.1.17}$$

The combinations  $z^k \bar{z}^j + \bar{z}^k z^j$  that appear in (5.1.17) are determined by Mathematica. Thus, substituting them into (5.1.17), equating the free term to  $R^2$ , and equating the coefficients of different cosines to zero, we obtain the following system of equations:

$$\begin{aligned}
 1 + \lambda^4 + 6\alpha_3 \lambda^2 (1 + \lambda^4) + 20\alpha_5 \lambda^4 + \alpha_3^2 (1 + 9\lambda^4) + 10\alpha_3 \alpha_5 \lambda^2 + \alpha_5^2 \\
 = R^2, \\
 \lambda^2 + \alpha_3 (1 + 6\lambda^4 + \lambda^8) + 5\alpha_3 \lambda^2 (1 + 4\lambda^4) + 3\alpha_3^2 \lambda^2 (1 + 3\lambda^4) \\
 + 21\alpha_7 \lambda^4 + \alpha_3 \alpha_5 (1 + 25\lambda^4) + 7\alpha_3 \alpha_7 \lambda^2 + 5\alpha_5^2 \lambda^2 + \alpha_3 \alpha_7 = 0, \\
 \alpha_3 \lambda^2 (1 + \lambda^4) + \alpha_5 (1 + 5\lambda^4) + 3\alpha_3^2 \lambda^4 + 7\alpha_7 \lambda^2 + 3\alpha_3 \alpha_5 \lambda^2 + \alpha_3 \alpha_7 = 0, \\
 \alpha_5 \lambda^2 + \alpha_3^2 \lambda^6 + \alpha_7 (1 + 7\lambda^4) + 3\alpha_3 \alpha_5 \lambda^4 + 9\alpha_9 \lambda^2 + 3\alpha_3 \alpha_7 \lambda^2 + \alpha_3 \alpha_9 = 0, \\
 \alpha_7 \lambda^2 + \alpha_9 = 0, \\
 \alpha_9 \lambda^2 + \alpha_{11} = 0.
 \end{aligned} \tag{5.1.18}$$

These equations, except the first, will be solved by the method of successive approximations. Thus, transposing  $\alpha_3, \alpha_5, \alpha_7, \alpha_9$  and  $\alpha_{11}$  we get

$$\begin{aligned}
 \alpha_3 &= -[\lambda^2 + \alpha_3 (6\lambda^4 + \lambda^8) + 5\alpha_3 \lambda^2 (1 + 4\lambda^4) + 3\alpha_3^2 \lambda^2 (1 + 3\lambda^4) \\
 &\quad + 21\alpha_7 \lambda^4 + \alpha_3 \alpha_5 (1 + 25\lambda^4) + 7\alpha_3 \alpha_7 \lambda^2 + 5\alpha_5^2 \lambda^2 + \alpha_3 \alpha_7], \\
 \alpha_5 &= -[\alpha_3 \lambda^2 (1 + \lambda^4) + 5\alpha_5 \lambda^4 + 3\alpha_3^2 \lambda^4 + 7\alpha_7 \lambda^2 + 3\alpha_3 \alpha_5 \lambda^2 + \alpha_3 \alpha_7], \\
 \alpha_7 &= -[\alpha_5 \lambda^2 + \alpha_3^2 \lambda^6 + 7\alpha_7 \lambda^4 + 3\alpha_3 \alpha_5 \lambda^4 + 9\alpha_9 \lambda^2 + 3\alpha_3 \alpha_7 \lambda^2 + \alpha_3 \alpha_9], \\
 \alpha_9 &= -\alpha_7 \lambda^2, \\
 \alpha_{11} &= -\alpha_9 \lambda^2.
 \end{aligned}$$

The values of the coefficients  $\alpha_3, \alpha_5, \alpha_7, \alpha_9$  and  $\alpha_{11}$  starting with initial values zero are computed up to the fifth successive approximation (see Table 1, Appendix D). Hence,

$$p(z) = z - (\lambda^2 + \lambda^6 + 4\lambda^{10}) z^3 + (\lambda^4 + 3\lambda^8) z^5 - (\lambda^6 + 5\lambda^{10}) z^7 + \lambda^8 z^9 + \lambda^{10} z^{11},$$

which is accurate to  $\lambda^{10}$ . The same fifth successive approximations for  $\alpha_3, \alpha_5, \alpha_7, \alpha_9$ , and  $\alpha_{11}$  when substituted in the first equation in (5.1.18) yield

$$R^2 = 1 - 4\lambda^4 + 10\lambda^8.$$

To check this result, note that  $z = 1 + \lambda^2$  for  $t = 0$ , thus  $p(z) = p(1 + \lambda^2) = 1 - 2\lambda^4 + 3\lambda^8$ , which coincides with  $R = (1 - 4\lambda^4 + 10\lambda^8)^{1/2} = 1 - 2\lambda^4 + 3\lambda^8$ . ■

## 5.2. Method of Infinite Systems

We shall present a general approach for the method of §5.1. This is known as the method of infinite systems, initially developed by Kantorovich and Krylov (1958) and later summarized in a systematic form with a computer program (in ALGOL) by Andersen et al. (1962).

Let the boundary  $\Gamma_\lambda$  of a nearly circular region  $D_\lambda$  in the  $z$ -plane, denoted by  $z = G(e^{it}, \lambda)$ , where  $\lambda$  is a small parameter, have a Laurent series expansion in  $e^{it}$  with suitable finite  $n$  and  $m$  as

$$\begin{aligned} z &= G(e^{it}, \lambda) = e^{it} \sum_{p=-n}^n C_p(\lambda) e^{ipt} = e^{it} \sum_{p=-n}^n \sum_{q=|p|}^m (k_{q,p} \lambda^q) e^{ipt} \\ &= e^{it} \cdot \left\{ \dots + e^{-2it} (0 + 0 + k_{2,-2} \lambda^2 + k_{3,-2} \lambda^3 + \dots) \right. \\ &\quad + e^{-it} (0 + k_{1,-1} \lambda + k_{2,-1} \lambda^2 + k_{3,-1} \lambda^3 + \dots) \\ &\quad + e^0 (1 + k_{1,0} \lambda + k_{2,0} \lambda^2 + k_{3,0} \lambda^3 + \dots) \\ &\quad + e^{it} (0 + k_{1,1} \lambda + k_{2,1} \lambda^2 + k_{3,1} \lambda^3 + \dots) \\ &\quad \left. + e^{2it} (0 + 0 + k_{2,2} \lambda^2 + k_{3,2} \lambda^3 + \dots) + \dots, \right\} \end{aligned} \tag{5.2.1}$$

where the nonzero coefficients  $k_{p,q}$  are known complex constants except  $k_{0,0}$ , which takes the value 1 because  $\lambda = 0$  must reduce the boundary  $\Gamma_\lambda$  to the circle  $z = e^{it}$ , and small values of  $\lambda$  produce nearly circular boundaries. Note that the expansion (5.2.1) is similar to (5.1.10).

Let the function  $w = f(z, \lambda)$  that maps the region  $D_\lambda$  onto the disk  $|w| < R$  (or 1) have a series representation

$$\begin{aligned} w = f(z, \lambda) &= \sum_{p=0}^{\infty} \lambda^p \left( \sum_{q=1}^{p+1} a_q^{(p)} z^q \right) \\ &= \sum_{p=0}^{\infty} \lambda^p \left[ a_1^{(p)} z + a_2^{(p)} z^2 + a_3^{(p)} z^3 + \cdots + a_{p+1}^{(p)} z^{p+1} \right] \\ &= a_1^{(0)} z + \lambda \left[ a_1^{(1)} z + a_2^{(1)} z^2 \right] + \lambda^2 \left[ a_1^{(2)} z + a_2^{(2)} z^2 + a_3^{(2)} z^3 \right] + \cdots . \end{aligned} \quad (5.2.2)$$

Since  $\lambda = 0$  gives the identity mapping, we have  $a_1^{(0)} = 1$ . Also, all coefficients  $a_q^{(p)}$  are real since  $f'(0, \lambda) = a_1^{(0)} + a_1^{(1)} \lambda + a_1^{(2)} \lambda^2 + \cdots$  is real for all  $\lambda$ . The problem of approximating  $f(z, \lambda)$  reduces to that of determining the unknown coefficients  $a_q^{(p)}$  from the fact that after  $z = G(e^{it}, \lambda)$  from (5.2.1) is substituted, we should have  $|w|^2 = w \cdot \bar{w} = R^2$  for all  $t$  and every  $\lambda$  up to the desired accuracy in powers of  $\lambda$ .

First, we determine  $z^q$ . Thus, from (5.2.1)

$$\begin{aligned} z^q &= e^{iqt} \cdot \left\{ \cdots + e^{-2it} \left( 0 + 0 + k_{2,-2}^{(q)} \lambda^2 + k_{3,-2}^{(q)} \lambda^3 + \cdots \right) \right. \\ &\quad + e^{-it} \left( 0 + k_{1,-1}^{(q)} \lambda + k_{2,-1}^{(q)} \lambda^2 + k_{3,-1}^{(q)} \lambda^3 + \cdots \right) \\ &\quad + e^0 \left( 1 + k_{1,0}^{(q)} \lambda + k_{2,0}^{(q)} \lambda^2 + k_{3,0}^{(q)} \lambda^3 + \cdots \right) \\ &\quad + e^{it} \left( 0 + k_{1,1}^{(q)} \lambda + k_{2,1}^{(q)} \lambda^2 + k_{3,1}^{(q)} \lambda^3 + \cdots \right) \\ &\quad \left. + e^{2it} \left( 0 + 0 + k_{2,2}^{(q)} \lambda^2 + k_{3,2}^{(q)} \lambda^3 + \cdots \right) + \cdots \right\} \end{aligned} \quad (5.2.3)$$

Note that the coefficients  $k_{q,p}^{(q)}$  in (5.2.3), though known, are different from  $k_{p,q}$  of (5.2.1).

Next, while computing  $|w|^2$ , we shall group together terms that have same powers of  $\lambda$ . Thus, the coefficients of  $\lambda^p$  includes only  $a_q^{(s)}$ ,  $s = 0, 1, 2, \dots, p$

( $s > p$  does not occur). This feature provides an application of the method of successive approximations to determine  $a_q^{(p)}$  under the condition that the coefficient of  $\lambda^p$  in  $|w|^2$  must vanish for  $p = 0, 1, 2, \dots$  (which yields a system of equations) and the free term (all terms without  $\lambda$ ) must be equal to  $R^2$  (or 1 if the region  $D_\lambda$  is mapped onto the unit disk).

Since  $a_p^{(q)}$  does not depend on  $a_q^{(s)}$  for  $s > p$ , any subsequent revision of (5.2.2) to include higher powers of  $\lambda$  than previously taken shall only entail determination of new terms that should be added to the free term and to each equation of the above system to be solved by successive approximations.

- An algorithm to compute (5.2.2) up to  $\lambda^N$  is as follows:
- Use all terms in (5.2.1) corresponding to  $\lambda^0, \lambda^1, \lambda^2, \dots, \lambda^N$ .
- Use all terms in  $z^2$  corresponding to  $\lambda^0, \lambda^1, \lambda^2, \dots, \lambda^{N-1}$ .
- Continue for  $z^3, \dots, z^p$ , i.e., use all terms in  $z^p$  corresponding to  $\lambda^0, \lambda^1, \lambda^2, \dots, \lambda^{N-p+1}$ .
- Continue until  $z^{N+1}$ , i.e., use all terms in  $z^N$  corresponding to  $\lambda^0, \lambda^1$ .
- Use all terms in  $z^{N+1}$  corresponding to  $\lambda^0$ .

Note that the sum of all coefficients of  $\lambda^0$  yields the free term, and the coefficients of  $\lambda^1, \lambda^2, \dots, \lambda^N$  equated to zero yield a system of  $N$  equations to determine  $a_q^{(s)}, s = 1, \dots, N$ , by successive approximations. This method will produce an approximate function that maps every single boundary (for a fixed  $\lambda$ ) by a power series in  $z$ , whose accuracy will depend on the manner in which  $a_q^{(p)}$  are computed.

CASE STUDY 5.2.1. Details for computation of  $a_1^{(0)}, a_1^{(1)}, a_2^{(1)}$  and  $a_1^{(2)}, a_2^{(2)}, a_3^{(2)}$  are given below. Without using any computational tools, we shall determine  $f(z, \lambda)$  up to  $\lambda^2$ .

$p = 0$  yields  $a_1^{(0)} = 1$ . Then

$$\begin{aligned} z &= e^{it}, \quad w = a_1^{(0)} z = z, \\ |w|^2 &= a_1^{(0)} e^{it} \cdot \overline{a_1^{(0)}} e^{-it} = R^2. \end{aligned}$$

$p = 1$  yields

$$z = e^{it} \left\{ 1 + \lambda \left[ k_{1,-1}^{(1)} e^{-it} + k_{1,0}^{(1)} + k_{1,1}^{(1)} e^{it} \right] \right\},$$

$$\begin{aligned}
z^2 &= e^{2it}, \\
w &= z + \lambda \left[ a_1^{(1)} z + a_2^{(1)} z^2 \right] \\
&= e^{it} \left\{ 1 + \lambda \left[ k_{1,-1}^{(1)} e^{-it} + k_{1,0}^{(1)} + k_{1,1}^{(1)} e^{it} \right] \right\} \\
&\quad + \lambda \left[ a_1^{(1)} e^{it} + a_2^{(1)} e^{2it} \right] \\
&= e^{it} \left\{ 1 + \lambda \left[ k_{1,-1}^{(1)} e^{-it} + \left( k_{1,0}^{(1)} a_1^{(1)} \right) + \left( k_{1,1}^{(1)} + a_2^{(1)} \right) e^{it} \right] \right\}, \\
|w|^2 &= 1 + \lambda \left[ \left( k_{1,-1}^{(1)} + \overline{k_{1,1}^{(1)}} + \overline{a_2^{(1)}} \right) e^{-it} + \left( k_{1,0}^{(1)} + a_1^{(1)} + \overline{k_{1,0}^{(1)}} \right. \right. \\
&\quad \left. \left. + \overline{a_1^{(1)}} \right) + \left( k_{1,1}^{(1)} + a_2^{(1)} + \overline{k_{1,-1}^{(1)}} \right) e^{it} \right] \\
&= 1 + \lambda \left[ \left( M_1^{(1)} + \overline{a_2^{(1)}} \right) e^{-it} + \left( M_0^{(1)} + \overline{M_0^{(1)}} + a_1^{(1)} + \overline{a_1^{(1)}} \right. \right. \\
&\quad \left. \left. + \left( M_1^{(1)} + a_2^{(1)} \right) e^{it} \right] = R^2.
\right.
\end{aligned}$$

Hence  $a_1 = -M_0^{(1)}$ ,  $a_2 = -M_1^{(1)}$ , and

$$w = f(z, \lambda) = z + \lambda \left[ L_{-1}^{(1)} + L_0^{(1)} z + L_1^{(1)} z^2 \right].$$

$p = 2$  yields

$$\begin{aligned}
z &= e^{it} \left\{ 1 + \lambda \left[ k_{1,-1}^{(1)} e^{-it} + k_{1,0} + k_{1,1} e^{it} \right] \right. \\
&\quad \left. + \lambda^2 \left[ k_{2,-2}^{(1)} e^{-2it} + k_{2,-1}^{(1)} e^{-it} + k_{2,0}^{(1)} + k_{2,1}^{(1)} e^{it} + k_{2,2}^{(1)} e^{2it} \right] \right\}, \\
z^2 &= e^{2it} \left\{ 1 + \lambda \left[ k_{1,-1}^{(2)} e^{-it} + k_{1,0}^{(2)} + k_{2,1}^{(2)} e^{it} \right] \right\}, \\
z^3 &= e^{3it}, \\
w &= z + \lambda \left[ a_1^{(1)} z + a_2^{(1)} z^2 \right] + \lambda^2 \left[ a_1^{(2)} z + a_2^{(2)} z^2 + a_3^{(2)} z^3 \right],
\end{aligned}$$

which gives

$$\begin{aligned}
w &= e^{it} \left\{ 1 + \lambda \left[ L_{-1}^{(1)} e^{-it} + L_0^{(1)} + L_1^{(1)} e^{it} \right] \right. \\
&\quad + \lambda^2 \left[ k_{2,-2}^{(1)} e^{-2it} + k_{2,-1}^{(1)} e^{-it} + k_{2,0}^{(1)} + k_{2,1}^{(1)} e^{it} + k_{2,2}^{(1)} e^{2it} \right. \\
&\quad + a_1^{(1)} k_{1,-1}^{(1)} e^{-it} + a_1^{(1)} k_{1,0}^{(1)} + a_1^{(1)} k_{2,1}^{(1)} e^{it} \\
&\quad + a_2^{(1)} k_{1,-1}^{(2)} + a_2^{(1)} k_{1,0}^{(2)} e^{it} + a_2^{(1)} k_{2,1}^{(2)} e^{2it} \\
&\quad \left. \left. + a_1^{(2)} + a_2^{(2)} e^{it} + a_3^{(2)} e^{it} \right] \right\}
\end{aligned}$$

$$\begin{aligned}
&= e^{it} \left[ 1 + \lambda \left[ L_{-1}^{(1)} e^{-it} + L_0^{(1)} + L_1^{(1)} e^{it} \right] \right. \\
&\quad + \lambda^2 \left[ K_{-2}^{(2)} e^{-2it} + K_{-1}^{(2)} e^{-it} + \left( K_0^{(2)} + a_1^{(2)} \right) \right. \\
&\quad \left. \left. + \left( K_1^{(2)} + a_2^{(1)} \right) e^{it} + \left( K_2^{(2)} + a_3^{(2)} \right) e^{2it} \right] \right\}
\end{aligned}$$

where

$$\begin{aligned}
K_{-2}^{(2)} &= k_{2,-2}^{(1)}, \\
K_{-1}^{(2)} &= k_{2,-1}^{(1)} + a_1^{(1)} k_{1,-1}^{(1)}, \\
K_0^{(2)} &= k_{2,0}^{(1)} + a_1^{(1)} k_{1,0}^{(1)} + a_2^{(1)} k_{1,-1}^{(2)} + a_1^{(2)}, \\
K_1^{(2)} &= k_{2,1}^{(1)} + a_1^{(1)} k_{1,1}^{(1)} + a_2^{(1)} k_{1,0}^{(2)} + a_2^{(2)}, \\
K_2^{(2)} &= k_{2,2}^{(1)} + a_2^{(1)} k_{1,1}^{(2)} + a_3^{(2)},
\end{aligned}$$

and  $K_{-j}^{(q)} = \overline{K_j^{(q)}} = K_j^{(q)}$ . Hence,

$$\begin{aligned}
|w|^2 &= 1 + \lambda^2 \left[ \left( M_2^{(2)} + a_3^{(2)} \right) e^{-2it} + \left( M_1^{(2)} + a_2^{(2)} \right) e^{it} \right. \\
&\quad + 2 \left( M_0^{(2)} + a_1^{(2)} \right) + \left( M_1^{(2)} + a_2^{(2)} \right) e^{it} \\
&\quad \left. + \left( M_2^{(2)} + a_3^{(2)} \right) e^{2it} \right] = R^2,
\end{aligned}$$

where  $M_{-j}^{(q)} = \overline{M_j^{(q)}} = M_j^{(q)}$ , and

$$\begin{aligned}
M_2^{(2)} &= K_{-2}^{(2)} + \overline{K_2^{(2)}} + L_{-1}^{(1)} L_1^{(1)} = 2 \left( K_1^{(2)} + L_1^{(1)} \right), \\
M_1^{(2)} &= K_1^{(2)} + \overline{K_{-1}^{(2)}} + L_0^{(1)} \overline{L_{-1}^{(1)}} + \overline{L_0^{(1)}} L_1^{(1)} = 2 \left( K_1^{(2)} + L_0^{(1)} L_1^{(1)} \right), \\
M_0^{(2)} &= K_0^{(2)} + L_{-1}^{(1)} \overline{L_{-1}^{(1)}} + L_0^{(1)} \overline{L_0^{(1)}} = K_0^{(2)} + 2 \left( L_0^{(1)} + L_1^{(1)} \right).
\end{aligned}$$

Hence,  $a_1^{(2)} = -M_0^{(2)}$ ,  $a_2^{(2)} = -M_1^{(2)}$ ,  $a_3^{(2)} = -M_2^{(2)}$ , and

$$w = f(z, \lambda) = z - \lambda \left[ M_0^{(2)} + M_1^{(2)} \right] - \lambda^2 \left[ M_0^{(2)} z + M_1^{(2)} z^2 + M_2^{(2)} z^3 \right]. \blacksquare$$

CASE STUDY 5.2.2. We shall consider the same problem as in Case Study 5.1.1, where the contour  $\Gamma_\lambda$  is given by (5.1.16), i.e.,

$$\begin{aligned}
z(t, \lambda) &= e^{it} \left( 1 + \lambda [0 \cdot e^{-it} + 0 + 0 \cdot e^{it}] \right. \\
&\quad \left. + \lambda^2 [1 \cdot e^{-2it} + 0 \cdot e^{-it} + 0 + 0 \cdot e^{it} + 0 \cdot e^{2it}] \right).
\end{aligned}$$

The coefficients  $a_q^{(p)}$  for  $N = 8$  are given by

| $p \setminus q$ | 1 | 2 | 3  | 4 | 5 | 6 | 7  | 8 | 9 |
|-----------------|---|---|----|---|---|---|----|---|---|
| 0               | 1 |   |    |   |   |   |    |   |   |
| 1               | 0 | 0 |    |   |   |   |    |   |   |
| 2               | 0 | 0 | -1 |   |   |   |    |   |   |
| 3               | 0 | 0 | 0  | 0 |   |   |    |   |   |
| 4               | 2 | 0 | 0  | 0 | 1 |   |    |   |   |
| 5               | 0 | 0 | 0  | 0 | 0 | 0 |    |   |   |
| 6               | 0 | 0 | -3 | 0 | 0 | 0 | -1 |   |   |
| 7               | 0 | 0 | 0  | 0 | 0 | 0 | 0  | 0 |   |
| 8               | 1 | 0 | 0  | 0 | 5 | 0 | 0  | 0 | 1 |

Hence, the mapping function is given by

$$w = f(z, \lambda) = z - \lambda^2 z^3 + \lambda^4 (2z + z^5) - \lambda^6 (3z^3 + z^7) + \lambda^8 (z + 5z^5 + z^9). \blacksquare \quad (5.2.4)$$

This method can be improved as follows: Since

$$[z(t, \lambda)]^2 = e^{2it} [1 + 2\lambda^2 e^{-2it} + \lambda^4 e^{-4it}], \quad (5.2.5)$$

we can redefine the contour  $\Gamma_\lambda$  by

$$\Gamma_\mu : Z(\tau, \mu) = e^{i\tau} [1 + 2\mu e^{-i\tau} + \mu^2 e^{-2i\tau}], \quad (5.2.6)$$

where  $\mu = \lambda^2$  and  $\tau = 2t$ . The new contour  $\Gamma_\mu$  yields the mapping function  $w = \phi(Z, \mu)$  such that  $\phi(z^2, \lambda^2) \equiv [f(z, \lambda)]^2$ , since  $f(z, \lambda)$  has the form  $z \cdot g(z^2, \lambda^2)$ , i.e.,

$$[f(z, \lambda)]^2 = z^2 [g(z^2, \lambda^2)]^2 = Z [g(Z, \mu)]^2.$$

Also, since  $f(z(t, \lambda), \lambda) = e^{i\theta}$  implies that  $[f(z(t, \lambda), \lambda)]^2 = e^{2i\theta}$ , we find that

$$Z(\tau, \mu) \cdot [g(Z(\tau, \lambda), \lambda)]^2 = e^{2i\theta},$$

and for  $z^2 = Z = 0$  we get  $[f(z, \lambda)]^2 = 0$ , where  $\frac{\partial}{\partial z} [f(z, \lambda)]^2$  is real. Hence, the functions  $\phi(Z, \mu)$  and  $Z \cdot [g(Z, \mu)]^2$  yield the same mapping function of the contour  $\Gamma_\mu$  onto the unit circle for  $0 \leq \tau < 2\pi$  for every fixed  $\mu = \lambda^2$  as the function  $[z(t, \lambda)] \cdot [g(z^2(t, \lambda), \lambda^2)]^2$  for  $0 \leq t < \pi$ . An advantage of this

technique is that the computation of  $\phi(z^2, \lambda^2)$  up to the power  $\mu^N$  provides the function  $f(z^2, \lambda^2)$  up to the power  $\lambda^{2N}$ , which while computing  $\sqrt{\phi(z^2, \lambda^2)}$  will yield a mapping function with power up to  $\lambda^{16}$  instead of  $\lambda^8$  as in (5.2.4).

CASE STUDY 5.2.3. We shall again consider the contour (5.1.16) for the ellipse, which we rewrite as

$$\begin{aligned} Z = & e^{i\tau} [1 + \mu [2 \cdot e^{-i\tau} + 0 + 0 \cdot e^{i\tau}]] \\ & + \mu^2 [1 \cdot e^{-2i\tau} + 0 \cdot e^{it\tau} + 0 + 0 \cdot e^{i\tau} + 0 \cdot e^{2i\tau}]. \end{aligned}$$

Taking  $N = 8$  we obtain the coefficients  $a_q^{(p)}$  as follows:

| $p \setminus q$ | 1 | 2   | 3  | 4    | 5  | 6   | 7 | 8  |
|-----------------|---|-----|----|------|----|-----|---|----|
| 0               | 1 |     |    |      |    |     |   |    |
| 1               | 0 | -2  |    |      |    |     |   |    |
| 2               | 4 | 0   | 3  |      |    |     |   |    |
| 3               | 0 | -10 | 0  | -4   |    |     |   |    |
| 4               | 6 | 0   | 20 | 0    | 5  |     |   |    |
| 5               | 0 | -28 | 0  | -34  | 0  | -6  |   |    |
| 6               | 8 | 0   | 77 | 0    | 52 | 0   | 7 |    |
| 7               | 0 | -62 | 0  | -164 | 0  | -74 | 0 | -8 |

Thus, after replacing  $\mu$  by  $\lambda^2$  and  $\tau$  by  $2t$ , we have

$$\begin{aligned} [f(z, \lambda)]^2 = & z^2 + \lambda^2 (-2z^4) + \lambda^4 (4z^2 + 3z^6) + \lambda^6 (-10z^4 - 4z^8) \\ & + \lambda^8 (6z^2 + 20z^6 + 5z^{10}) + \lambda^{10} (-28z^4 - 34z^8 - 6z^{12}) \\ & + \lambda^{12} (8z^2 + 77z^6 + 52z^{10} + 7z^{14}) \\ & + \lambda^{14} (-62z^4 - 164z^8 - 74z^{12} - 8z^{16}). \end{aligned}$$

An application of the binomial expansion to the above expression yields the mapping function as

$$\begin{aligned} f(z, \lambda) = & z + \lambda^2 (-z^3) + \lambda^4 (2z + z^5) + \lambda^6 (-3z^3 - z^7) \\ & + \lambda^8 (z + 5z^5 + z^9) + \lambda^{10} (-7z^3 - 7z^7 - z^{11}) \\ & + \lambda^{12} (2z + 16z^5 + 9z^9 + z^{13}) \\ & + \lambda^{14} (-12z^3 - 29z^7 - 11z^{11} - z^{15}). \blacksquare \quad (5.2.7) \end{aligned}$$

### 5.3. Three Special Cases

In the case of conformal mapping of the unit disk  $|z| < 1$  onto a simply connected region  $D$  in the  $w$ -plane, the mapping function  $z = F(w)$  can be represented by a Taylor series

$$z = x + i y = \sum_{n=0}^{\infty} c_n w^n, \quad c_n = a_n + i b_n. \quad (5.3.1)$$

In particular when the region  $D$  is also the unit disk, bounded by  $|w| = 1$ , we set  $w = e^{i\phi}$  in (5.3.1) and obtain

$$z = \sum_{n=0}^{\infty} c_n e^{i n \phi}, \quad (5.3.2)$$

which, when separated into real and imaginary parts, gives

$$\begin{aligned} x = f(\phi) &= \sum_{n=0}^{\infty} (a_n \cos n\phi - b_n \sin n\phi), \\ y = g(\phi) &= \sum_{n=0}^{\infty} (b_n \sin n\phi + a_n \cos n\phi). \end{aligned} \quad (5.3.3)$$

Thus, the mapping function (5.3.1) can be represented in the form of a Cauchy integral as

$$z = \frac{1}{2\pi} \int_0^{2\pi} \frac{f(\phi) + i g(\phi)}{e^{i\phi}} e^{i\phi} d\phi. \quad (5.3.4)$$

The method of infinite systems is useful when the boundary  $\Gamma$  is defined by an implicit function.

CASE 1. Let  $\Gamma$  be defined implicitly by

$$\gamma(x, y) = 0, \quad (5.3.5)$$

where  $\gamma(x, y) = \gamma(z)$  is an analytic function for  $z \in \Gamma = \partial B(0, 1)$ . Then, by substituting  $x$  and  $y$  from (5.3.4) in (5.3.5) and expanding the result in a Fourier series, we obtain

$$\begin{aligned} \gamma(x, y) &= \gamma(f(\phi), g(\phi)) \\ &= \gamma_0(a_j, b_j) + \sum_{n=1}^{\infty} \{\gamma_n(a_j, b_j) \cos n\phi + \gamma_n^*(a_j, b_j) \sin n\phi\}, \end{aligned} \quad (5.3.6)$$

where  $\gamma_0, \gamma_n, \gamma_n^*$  are the Fourier coefficients, and  $a_j, b_j$  denote the dependence of  $\gamma$  and  $\gamma^*$  on  $a_0, b_0, a_1, b_1, \dots$ . Now, by equating the coefficients of  $\cos n\phi$  and  $\sin n\phi$  to zero, we obtain an infinite system of equations for  $a_j, b_j$ :

$$\gamma_0(a_j, b_j) = 0, \quad \gamma_n(a_j, b_j) = 0, \quad \gamma_n^*(a_j, b_j) = 0, \quad n = 1, 2, \dots \quad (5.3.7)$$

CASE 2. Let  $\Gamma$  be defined by an implicit complex function

$$\psi(z, \bar{z}) = 0. \quad (5.3.8)$$

Then, by substituting the series (5.3.2) for  $z$  in (5.3.8), we find that

$$\psi \left( \sum_{n=0}^{\infty} c_n e^{in\phi}, \sum_{n=0}^{\infty} \bar{c}_n e^{-in\phi} \right) = \sum_{n=-\infty}^{\infty} \psi_n(a_j, b_j) e^{in\theta}, \quad (5.3.9)$$

which leads to an infinite system

$$\psi_n(a_j, b_j) = 0, \quad n = \dots, -1, 0, 1, \dots \quad (5.3.10)$$

In order to obtain a solution for the unknowns  $a_0, b_0, a_1, b_1, \dots$  from the system (5.3.7) and (5.3.10) it is necessary that all related series converge and the derivative  $\frac{dz}{dw} \Big|_{|w|=1} > 0$ .

METHOD. Let a nearly circular boundary  $\Gamma_\lambda$  be represented by

$$x^2 + y^2 + \lambda P(x, y) = 1 \quad \text{in Case 1}, \quad (5.3.11)$$

or by

$$z\bar{z} + \lambda \Pi(z, \bar{z}) = 1 \quad \text{in Case 2}, \quad (5.3.12)$$

where  $\lambda$  is a small real parameter and  $P(x, y)$  and  $\Pi(x, y)$  satisfy the same conditions as the functions  $\gamma(x, y)$  and  $\psi(x, y)$ , respectively. Note that both equations (5.3.11) and (5.3.12) are equivalent since  $2x = z + \bar{z}$  and  $2iy = z - \bar{z}$ . Hence, we can use either equation. Suppose we consider Eq (5.3.12). Then

$$\begin{aligned} z\bar{z} &= \dots + (c_0\bar{c}_1 + c_1\bar{c}_2 + \dots) e^{-i\theta} + (c_0\bar{c}_0 + c_1\bar{c}_1 + \dots) \\ &\quad + (c_1\bar{c}_0 + c_2\bar{c}_1 + \dots) e^{i\theta} + \dots \end{aligned} \quad (5.3.13)$$

In  $\Pi(z, \bar{z})$  the coefficients of conjugate quantities  $e^{in\theta}$  and  $e^{-in\theta}$  must also be conjugate. Also,  $\Pi(z, \bar{z})$  must be real since in Eq (5.3.12) both  $z\bar{z}$  and  $\lambda$  are real. Thus, after substituting the values of  $z$  and  $\bar{z}$  from (5.3.2), we get

$$\Pi(z, \bar{z}) = \sum_{n=0}^{\infty} \tau_n(a_j, b_j) e^{in\theta} + \sum_{n=0}^{\infty} \overline{\tau_n(a_j, b_j)} e^{-in\theta}, \quad (5.3.14)$$

where

$$\tau_n(a_j, b_j) = t_n(a_j, b_j) + i t_n^*(a_j, b_j), \quad t_0^*(a_j, b_j) = 0. \quad (5.3.15)$$

Substituting the quantities (5.3.13) and (5.3.14) in (5.3.12) and comparing the coefficients of positive powers of  $e^{i\theta}$ , we obtain the infinite system of equations

$$\begin{aligned} c_0\bar{c}_0 + c_1\bar{c}_1 + c_2\bar{c}_2 + \cdots + \lambda t_0(a_j, b_j) &= R^2, \\ c_1\bar{c}_0 + c_2\bar{c}_1 + c_3\bar{c}_2 + \cdots + \lambda \tau_1(a_j, b_j) &= 0, \\ c_2\bar{c}_0 + c_3\bar{c}_1 + c_4\bar{c}_2 + \cdots + \lambda \tau_2(z_j, b_j) &= 0, \\ &\dots \quad \dots \quad \dots \quad \dots \quad \dots. \end{aligned} \quad (5.3.16)$$

Note that we will obtain an infinite system conjugate to (5.3.16) if we compare the coefficients of negative powers of  $e^{i\theta}$  in Eq (5.3.12). The system (5.3.16), except for the first equation, can be rewritten as

$$\begin{aligned} c_1\bar{c}_1 &= 1 - c_0\bar{c}_0 - c_2\bar{c}_2 - \cdots - \lambda t_0(a_j, b_j), \\ c_2 &= -\frac{c_1\bar{c}_0}{\bar{c}_1} - \frac{c_3\bar{c}_2}{\bar{c}_1} - \cdots - \frac{\lambda}{\bar{c}_1} \tau_1(a_j, b_j), \\ c_3 &= -\frac{c_2\bar{c}_0}{\bar{c}_1} - \frac{c_4\bar{c}_2}{\bar{c}_1} - \cdots - \frac{\lambda}{\bar{c}_1} \tau_2(z_j, b_j), \\ &\dots \quad \dots \quad \dots \quad \dots \quad \dots. \end{aligned} \quad (5.3.17)$$

**CASE STUDY 5.3.1.** We shall use the above method to obtain the function that maps the unit disk onto the interior of the ellipse

$$(1 + \lambda)x^2 + (1 - \lambda)y^2 = 1, \quad (5.3.18)$$

with semimajor and semiminor axes as  $(1 + \lambda)^{-1/2}$  and  $(1 - \lambda)^{-1/2}$ , respectively, such that center  $w = 0$  goes into the center  $z = 0$  and the real axis into the real axis. Then  $c_0 = 0$ , and  $c_1$  shall be real. Because of the symmetry of the ellipse about the  $x$ -axis, all  $b_j$ ,  $j = 1, 2, \dots$  will be zero. The symmetry of the  $y$ -axis also implies that all  $a_j$  with even  $j$  shall be zero. The equation of the ellipse (5.3.18) in the complex form is

$$z\bar{z} + \lambda \frac{z^2 + \bar{z}^2}{2} = 1.$$

Hence,

$$\Pi(z, \bar{z}) = \frac{z^2 + \bar{z}^2}{2}.$$

Now, on  $\Gamma_\lambda (\tau = e^{i\theta})$ ,

$$\begin{aligned} z^2 &= (a_1 e^{i\theta} + a_3 e^{3i\theta} + \dots)^2, \\ &= a_1^2 e^{2i\theta} + 2a_1 a_3 e^{4i\theta} + (2a_1 a_5 + a_3^2) e^{6i\theta} \\ &\quad + 2(a_1 a_7 + a_3 a_5) e^{8i\theta} + (2a_1 a_9 + 2a_3 a_7 + a_5^2) e^{10i\theta} + \dots, \end{aligned}$$

which yields ( $\tau_n = e^{in\theta}$ )

$$\begin{aligned} \tau_0 &= \tau_1 = \tau_3 = \tau_5 = \dots = 0, \\ \tau_2 &= -\frac{1}{2}a_1^2, \quad \tau_4 = -a_1 a_3, \quad \tau_6 = -(a_1 a_5 + \frac{1}{2}a_3^2), \\ \tau_8 &= -(a_1 a_7 + a_3 a_5), \quad \tau_{10} = a_1 a_9 + a_3 a_7 + \frac{1}{2}a_5^2, \end{aligned}$$

and so on. Thus, the system (5.3.17) becomes

$$\begin{aligned} a_1^2 &= 1 - a_3^2 - a_5^2 - a_7^2 - a_9^2 - \dots, \\ a_3 &= -\frac{1}{a_1} \left( a_5 a_3 + a_7 a_5 + a_9 a_7 + \dots + \frac{\lambda}{2} a_1^2 \right), \\ a_5 &= -\frac{1}{a_1} (a_7 a_3 + a_9 a_5 + a_{11} a_7 + \dots + \lambda a_1 a_3), \\ a_7 &= -\frac{1}{a_1} \left( a_9 a_3 + a_{11} a_5 + \dots + \lambda (a_1 a_5 + \frac{1}{2} a_3^2) \right), \\ a_9 &= -\frac{1}{a_1} (a_{11} a_3 + \dots + \lambda (a_1 a_7 + a_3 a_5)), \\ a_{11} &= -\frac{1}{a_1} \left( a_{13} a_3 + \dots + \lambda (a_1 a_9 + a_3 a_7) \frac{1}{2} a_5^2 \right), \quad \dots. \end{aligned} \tag{5.3.19}$$

If we introduce the notation  $A_0 = a_1$ ,  $A_j = \frac{a_{2j} + 1}{a_1}$  for  $j = 1, 2, \dots$ , then the system (5.3.19) reduces to

$$\begin{aligned} A_0 &= \left( 1 + \sum_{j=1}^{\infty} A_j^2 \right)^{-1/2}, \\ A_1 &= -\frac{\lambda}{2} - \sum_{j=1}^{\infty} A_j A_{j+1}, \\ A_2 &= -\lambda A_1 - \sum_{j=1}^{\infty} A_j A_{j+2}, \end{aligned}$$

$$\begin{aligned} A_3 &= -\lambda (A_2 + A_1^2) - \sum_{j=1}^{\infty} A_j A_{j+3}, \\ A_4 &= -\lambda (A_3 + A_1 A_2) - \sum_{j=1}^{\infty} A_j A_{j+4}, \\ A_5 &= -\lambda \left( A_4 + A_1 A_3 + \frac{1}{2} A_2^2 \right) - \sum_{j=1}^{\infty} A_j A_{j+5}, \quad \dots \end{aligned}$$

Holding the first equation of the above system, thus treating  $A_0$  as undetermined, we shall use the method of §5.2 and solve the remaining equations in this system by successive approximations. Let the initial values be taken as  $A_j = 0$  for  $j = 1, 2, \dots$ . The fifth approximations for  $A_1, A_2, A_3, A_4$ , and  $A_5$  are available in Table 2 (Appendix D). Then the first equation of the above system yields

$$\begin{aligned} A_0 &= 1 - \frac{1}{2} (A_1^2 + A_2^2 + \dots) + \frac{\frac{1}{2} \cdot \frac{3}{2}}{2!} (A_1^2 + A_2^2 + \dots)^2 + \dots \\ &= 1 - \frac{1}{8} \lambda^2 + \frac{3}{128} \lambda^4, \end{aligned} \tag{5.3.20}$$

which is accurate to  $\lambda^5$ . Hence, the mapping function is given by

$$\begin{aligned} z &= A_0 w \left[ 1 + \sum_{n=1}^{\infty} A_n w^{2n} \right] \\ &= \left( 1 - \frac{1}{8} \lambda^2 + \frac{3}{128} \lambda^4 \right) \left\{ w - \left( \frac{\lambda}{2} - \frac{\lambda^3}{4} + \frac{3\lambda^5}{32} \right) w^3 \right. \\ &\quad \left. + \left( \frac{\lambda^2}{2} - \frac{9\lambda^4}{16} \right) w^5 - \left( \frac{5\lambda^3}{8} - \frac{9\lambda^5}{8} \right) w^7 + \frac{7\lambda^4}{8} w^9 + \frac{21\lambda^5}{16} w^{11} \right\}, \end{aligned} \tag{5.3.21}$$

which is accurate to  $\lambda^5$ . ■

**CASE STUDY 5.3.2.** We shall compute the function that maps the unit circle  $|w| = 1$  onto the family of squares

$$z \bar{z} + k \left( \frac{z^2 - \bar{z}^2}{4} \right)^2 = 1 \tag{5.3.22}$$

in the  $z$ -plane such that the point  $w = 0$  goes into the point  $z = 0$ . Note that for  $k = 1$ , Eq (5.3.22) reduces to  $(x^2 - 1)(y^2 - 1) = 0$  which represents the sides of the square of Fig. 4.2.1. Obviously,  $c_0 = 0$ , and since the real axes are preserved,  $\arg\{c_1\} = 0$ . The square (5.3.22) is symmetric about the  $x$  and  $y$

axes and also about the lines  $y = \pm x$ . Hence,  $b_j = 0$ ,  $a_{2j} = 0$ , and  $a_{4j-1} = 0$  for  $j = 1, 2, \dots$ . Then, from (5.3.2)

$$z = \sum_{n=1}^{\infty} a_{4n-3} e^{i(4n-3)\theta}, \quad (5.3.23)$$

which gives

$$\begin{aligned} \Pi(z, \bar{z}) &= \left( \frac{z^2 - \bar{z}^2}{4} \right)^2 \\ &= \frac{1}{16} [a_1^2 e^{2i\theta} + 2a_1 a_5 e^{6i\theta} + (2a_1 a_9 + a_5^2) e^{10i\theta} + \dots \\ &\quad - a_1^2 e^{-2i\theta} - 2a_1 a_5 e^{-6i\theta} + (2a_1 a_9 + a_5^2) e^{-10i\theta} + \dots]^2. \end{aligned}$$

Thus,

$$\begin{aligned} \tau_0(a_j, b_j) &= -\frac{1}{2} \left[ \left( \frac{a_1^2}{2} \right)^2 \right. \\ &\quad \left. + (a_1 a_5)^2 + \left( a_1 a_9 + \frac{1}{2} a_5^2 \right)^2 (a_1 a_{13} + a_5 a_9)^2 + \dots \right], \\ \tau_4(a_j, b_j) &= -\frac{1}{2} \left[ \frac{a_1^4}{8} + \frac{a_1^3 a_5}{2} + \left( a_1 a_5 a_9 + \frac{1}{2} a_1 a_5^3 \right) + \dots \right], \\ \tau_8(a_j, b_j) &= -\frac{1}{2} \left[ -\frac{a_1^3 a_5}{2} + \left( \frac{a_1^3 a_9}{2} + \frac{a_1^2 a_5^2}{2} \right) + \left( a_1^2 a_5 a_9 + \frac{a_1 a_5^3}{2} \right) + \dots \right], \\ \tau_{12}(a_j, b_j) &= -\frac{1}{2} \left[ -\left( \frac{a_1^3 a_9}{2} + \frac{a_1^2 a_5^2}{4} \right) - \frac{a_1^2 a_5^2}{2} + \left( \frac{a_1^3 a_{13}}{2} + a_1^2 a_5 a_9 \right) + \dots \right], \end{aligned}$$

which yields the system (5.3.19) as

$$\begin{aligned} a_1^2 &= 1 - a_5^2 - a_9^2 - a_{13}^2 - \dots, \\ &\quad + \frac{k}{2a_1} \left[ \frac{a_1^4}{4} + a_1^2 a_5^2 + \left( a_1 a_9 + \frac{a_5^2}{2} \right)^2 + (a_1 a_{13} + a_5 a_9)^2 + \dots \right], \\ a_5 &= -\frac{a_5 a_9}{a_1} - \frac{a_9 a_{13}}{a_1} - \dots + \frac{k}{2a_1} \left[ -\frac{a_1^4}{8} + \frac{a_1^3 a_5}{2} + \left( a_1^2 a_9 + \frac{1}{2} a_1 a_5^3 \right) \right. \\ &\quad \left. + (a_1 a_{13} + a_5 a_9) \left( a_1 a_9 + \frac{1}{2} a_1 a_5^2 \right) + \dots \right], \\ a_9 &= -\frac{a_5 a_{13}}{2} - \dots + \frac{k}{2a_1} \left[ -\frac{a_1^3 a_5}{2} + \frac{a_1^3 a_9}{2} + \frac{a_1^2 a_5^2}{4} \right] \end{aligned}$$

$$a_{13} = -\frac{a_5 a_{17}}{2} - \dots + \frac{k}{2a_1} \left[ -\frac{a_1^3 a_9}{2} - \frac{a_1^2 a_5^2}{2} - \frac{a_1^2 a_5^2}{2} \right. \\ \left. + \frac{1}{2} (a_1^3 a_{13} + a_1^2 a_5 a_9) + \dots \right].$$

If we take the initial values as  $a_1 = 1$ ,  $a_5 = a_9 = \dots = 0$ , then computing up to the third successive approximations (see Table 3, Appendix D), we get the approximate mapping function as

$$z = \left( 1 + \frac{k}{16} + \frac{3k^2}{256} + \frac{3k^2}{1024} \right) w - \left( \frac{k}{16} + \frac{7k^2}{256} + \frac{11k^2}{1024} \right) w^5 \\ + \left( \frac{k^2}{64} + \frac{27k^3}{2048} \right) w^9 - \frac{11k^3}{2048} w^{13}. \quad (5.3.24)$$

For  $k = 1$ , this becomes

$$z = 1.077 w - 0.1006 w^5 + 0.0288 w^9 - 0.0054 w^{13},$$

which compares with the exact solution (4.5.31) with a maximum error of the order of  $10^{-3}$ . ■

CASE 3. If the boundary  $\Gamma_\lambda$  is defined by the parametric equations

$$x = g(t, \lambda), \quad y = h(t, \lambda), \quad (5.3.25)$$

then we can expand the functions  $g$  and  $h$  as trigonometric series

$$g(x, \lambda) = \alpha_0 + \sum_{n=1}^{\infty} (\alpha_n \cos nt + \beta_n \sin nt), \\ h(t, \lambda) = \gamma_0 + \sum_{n=1}^{\infty} (\gamma_n \cos nt - \delta_n \sin nt). \quad (5.3.26)$$

Since the series in (5.3.26) are conjugate, we obtain the complex form for the equation of  $\Gamma_\lambda$  as

$$z = x + iy = \pi_0 + \sum_{n=1}^{\infty} (\pi_n \cos nt + \rho_n \sin nt) \\ = \pi_0 + \sum_{n=1}^{\infty} \left\{ \frac{\pi_n - i\rho_n}{2} e^{int} + \frac{\pi_n + i\rho_n}{2} e^{-int} \right\}, \quad (5.3.27)$$

where  $\pi_n = \alpha_n + i\gamma_n$ , and  $\rho_n = \beta_n - i\delta_n$ . We shall assume that the curve (5.3.27) has the same form as (5.2.1), where the coefficients  $\pi_n$  and  $\rho_n$  depend on  $\lambda$ . If we take  $\lambda = 0$  in (5.3.27), then this equation for  $\Gamma_\lambda$  reduces to

$$z = G(e^{it}, \lambda) = \pi_0 + \sum_{n=1}^{\infty} \frac{\pi_n - i\rho_n}{2} e^{int}. \quad (5.3.28)$$

The function  $w = G(e^{it}, \lambda)$ , where  $e^{it}$  is a point on the unit circle is assumed to be analytic in  $w$  and  $\lambda$  near the values  $\lambda = 0$ . The parameter  $t$  represents the polar angle of the point in the  $w$ -plane such that  $w = |w|e^{it}$  for any  $w \in U$ . However, the parameter  $t$ , in general, does not coincide with the argument  $\theta$  taken for the values of  $x$  and  $y$  in (5.3.3). Therefore, we shall substitute in (5.3.28)

$$t = \theta + \lambda \psi_1(\theta) + \lambda^2 \psi_2(\theta) + \dots, \quad (5.3.29)$$

where  $\psi_j(\theta)$ ,  $j = 1, 2, \dots$ , are real, periodic functions, yet to be determined. Note that for  $\lambda = 0$ , the series (5.3.29) reduces to  $t = \theta$ . Now, the functions  $\psi_j(\theta)$  must be determined for  $j = 1, 2, \dots$  such that the coefficient of  $\lambda^j$  in the series (5.3.27) does not contain any term in negative powers of  $e^{i\theta}$ . This process is explained in the next case study.

CASE STUDY 5.3.3. Let the boundary  $\Gamma_\lambda$  be defined in the parametric form by  $x = \cos t + \frac{\lambda}{2} \cos 2t$ ,  $y = \sin t + \frac{\lambda}{2} \sin 2t$  (Fig. 5.3.1), which in the complex form is

$$z = e^{it} + \frac{\lambda}{2} [e^{i(n+1)t} + e^{-i(n-1)t}]. \quad (5.3.30)$$

Substituting for  $t$  from (5.3.29), we obtain

$$\begin{aligned} z &= e^{i\theta} + \lambda \left[ i\psi_1 e^{i\theta} + \frac{1}{2} \left\{ e^{i(n+1)\theta} + e^{-i(n+1)\theta} \right\} \right] \\ &\quad + \lambda^2 \left[ \left( i\psi_2 - \frac{1}{2} \psi_1^2 \right) e^{i\theta} + \frac{1}{2} i(n+1)\psi_1 e^{i(n+1)\theta} \right. \\ &\quad \left. - \frac{1}{2} i(n-1)\psi_1 e^{i(n-1)\theta} \right] + \dots. \end{aligned} \quad (5.3.31)$$

It is obvious from this expression that  $z$  will contain only positive powers of  $e^{i\theta}$  if

$$\begin{aligned} i\psi_1 e^{i\theta} + \frac{1}{2} \left\{ e^{i(n+1)\theta} + e^{-i(n+1)\theta} \right\} &= e^{i(n+1)\theta}, \\ \left( i\psi_2 - \frac{1}{2} \psi_1^2 \right) e^{i\theta} + \frac{i}{2} \psi_1 [(n+1) e^{i(n+1)\theta} - (n-1) e^{i(n-1)\theta}] &= e^{i(2n+1)\theta}, \end{aligned}$$

which yields

$$\begin{aligned}\psi_1 &= \frac{i}{2} (e^{-in\theta} - e^{in\theta}) = \sin n\theta, \\ \psi_2 &= i \frac{2n-1}{8} (e^{-2in\theta} - e^{2in\theta}) = \frac{2n-1}{4} \sin 2n\theta.\end{aligned}$$

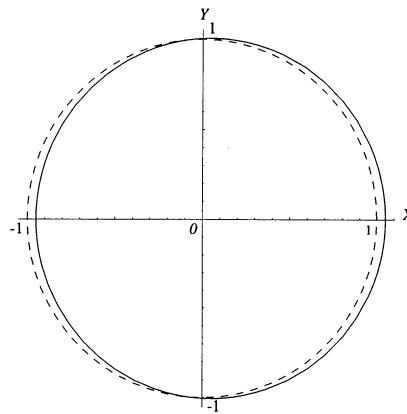


Fig. 5.3.1.

Substituting these values in (5.3.31), we get

$$z = e^{i\theta} + \lambda e^{i(n+1)\theta} + \frac{2n+1}{4} \lambda^2 [e^{i(2n+1)\theta} - e^{i\theta}], \quad (5.3.32)$$

which is accurate up to  $O(\lambda^2)$ . Hence, the approximate mapping function is given by

$$z = \left(1 - \frac{2n+1}{4} \lambda^2\right) w + \lambda w^{n+1} + \frac{2n+1}{4} \lambda^2 w^{2n+1}. \blacksquare \quad (5.3.33)$$

## 5.4. Exterior Regions

We shall approximate the function that maps the region exterior to the boundary (5.1.9) or (5.2.1) onto the exterior or interior of the circle  $|w| = R$ , assuming

that the point at infinity  $z = \infty$  goes into the point  $w = \infty$  or into the origin  $w = 0$ , respectively. There are two cases to consider:

CASE 1. In the case of mapping onto the exterior  $\{|w| > R\}$ , the mapping function  $w = f(z)$  with  $f(\infty) = 1$  has an expansion

$$w = z + a_0 + \frac{a_1}{z} + a_2 + z^2 + \dots \quad (5.4.1)$$

CASE 2. In this case of mapping onto the interior  $\{|w| < R\}$ , the mapping function with  $f(\infty) = 0$  has the expansion

$$w = \frac{1}{z} + \frac{a_2}{z^2} + \frac{a_3}{z^3} + \dots \quad (5.4.2)$$

In both cases we shall use the method of infinite systems to approximate  $w = f(z)$ .

In Case 1, the mapping function can be approximated by taking the first  $n$  terms in (5.4.1) :

$$w = z + a_0 + \frac{a_1}{z} + \dots + \frac{a_{n-2}}{z^{n-2}}. \quad (5.4.3)$$

In order to find  $|w|^2$  on the boundary (5.1.9), we represent  $1/z$  in the form of the series (5.1.10). Thus,

$$\frac{1}{z} = \sum_{\nu=-\infty}^{\infty} \beta_{\nu}^{(-1)}(\lambda) e^{i\nu t}, \quad (5.4.4)$$

where the coefficients  $\beta_{\nu}^{(-1)}(\lambda)$  are regular functions of the parameter  $\lambda$ , such that

$$\beta_{\nu}^{(-1)}(0) = \begin{cases} 0 & \text{for } \nu \neq -1 \\ 1 & \text{for } \nu = -1. \end{cases}$$

First we compute  $|w|^2$  from (5.4.1) and substitute in it the value of  $z$  from (5.1.10) and the value of  $1/z$  from (5.4.4). This will yield a trigonometric series, in which we equate the free terms to  $R^2$  (i.e., those terms which are independent of trigonometric functions), and set the coefficients of the first  $n$  terms of this series to zero. This will yield a system of equations exactly as in §5.1, which can be solved by the method of successive approximations to determine approximate values of  $a_0, a_1, \dots, a_n$ , and  $R$ .

**Case Study 5.4.1.** We shall consider the mapping of the region exterior to the ellipse

$$z(t) = e^{it} (1 + \lambda e^{-2it})$$

onto the exterior  $|w| > R$ . Since the region is symmetric about the coordinate axes, the mapping function has an expansion about the point at infinity

$$w = z + \frac{a_1}{z} + \frac{a_3}{z^3} + \cdots, \quad (5.4.5)$$

where all  $a_j$  are real and  $w(\infty) = \infty$ . Let us approximate  $w$  by a polynomial of the form

$$w = z + \frac{a_1}{z} + \frac{a_3}{z^3} + \frac{a_5}{z^5} + \frac{a_7}{z^7} + \frac{a_9}{z^9}.$$

Then

$$\begin{aligned} |w|^2 &= z\bar{z} + a_1 \left( \frac{z}{\bar{z}} + \frac{\bar{z}}{z} \right) + \left[ a_3 \left( \frac{z}{\bar{z}^3} + \frac{\bar{z}}{z^3} \right) + a_1^2 \frac{1}{z\bar{z}} \right] \\ &\quad + a_5 \left[ \left( \frac{z}{\bar{z}^5} + \frac{\bar{z}}{z^5} \right) + a_1 a_3 \left( \frac{1}{z^3 \bar{z}} + \frac{1}{z \bar{z}^3} \right) \right] \\ &\quad + a_7 \left[ \left( \frac{z}{\bar{z}^7} + \frac{\bar{z}}{z^7} \right) + a_1 a_5 \left( \frac{1}{z^5 \bar{z}} + \frac{1}{z \bar{z}^5} \right) + a_3^2 \frac{1}{z^3 \bar{z}^3} \right] \quad (5.4.6) \\ &\quad + a_9 \left[ \left( \frac{z}{\bar{z}^9} + \frac{\bar{z}}{z^9} \right) + a_1 a_7 \left( \frac{1}{z^7 \bar{z}} + \frac{1}{z \bar{z}^7} \right) \right. \\ &\quad \left. + a_3 a_5 \left( \frac{1}{z^5 \bar{z}} + \frac{1}{z \bar{z}^5} \right) \right]. \end{aligned}$$

$$z\bar{z} = 1 + \lambda^2 + 2\lambda \cos 2t,$$

$$\frac{z}{\bar{z}} + \frac{\bar{z}}{z} = -2 [(\lambda - \lambda^3) - \cos 2t - (\lambda - \lambda^3) \cos 4t],$$

$$\frac{z}{\bar{z}^3} + \frac{\bar{z}}{z^3} = 2 [6\lambda^2 - 3\lambda \cos 2t + (1 - 3\lambda^2) \cos 4t + \lambda \cos 6t],$$

$$\frac{1}{z\bar{z}} = (1 + \lambda^2) - 2\lambda \cos 2t + 2\lambda^2 \cos 4t,$$

$$\frac{z}{\bar{z}^5} + \frac{\bar{z}}{z^5} = -2 (5\lambda \cos 4t - \cos 6t - \lambda \cos 8t),$$

$$\frac{1}{z^3 \bar{z}} + \frac{1}{z \bar{z}^3} = -2 (3\lambda - \cos 2t + \lambda \cos 4t),$$

$$\frac{z}{\bar{z}^7} + \frac{\bar{z}}{z^7} = 2 \cos 8t,$$

$$\frac{1}{z^5 \bar{z}} + \frac{1}{z \bar{z}^5} = 2 \cos 4t,$$

$$\frac{1}{z^3 \bar{z}^3} = 1.$$

Hence, substituting these values in (5.4.6), equating the terms independent of  $e^{it}$  to  $R^2$ , and equating the coefficient of cosines to zero, we obtain

$$\begin{aligned} 1 + \lambda^2 - 2(\lambda - \lambda^3)a_1 + 12\lambda^2a_3 + (1 + \lambda^2)a_1^2 - 6\lambda a_1 a_3 + a_3^2 &= R^2, \\ \lambda + a_1 - 3\lambda a_3 - \lambda a_1^2 + a_1 a_3 &= 0, \\ (\lambda - \lambda^3)a_1 + (1 - 3\lambda^2)a_3 + \lambda^2 a_1^2 - 5\lambda a_5 - \lambda a_1 a_3 + a_1 a_5 &= 0, \\ \lambda a_3 + a_5 &= 0, \\ \lambda a_5 + a_7 &= 0, \end{aligned} \tag{5.4.7}$$

which except for the first equation is rewritten as

$$\begin{aligned} a_1 &= -\lambda + 3\lambda a_3 + \lambda a_1^2 - a_1 a_3, \\ a_3 &= 3\lambda^2 a_3 - (\lambda - \lambda^3)a_1 - \lambda^2 a_1^2 + 5\lambda a_5 + \lambda a_1 a_3 - a_1 a_5, \\ a_5 &= -\lambda a_3, \\ a_7 &= -\lambda a_5. \end{aligned}$$

Choosing the initial values for  $a_1, a_3, a_5, a_7$  as zero, the successive approximations for these coefficients are available in Table 4 (Appendix D), where we have retained the values up to the fourth approximation. Hence, the mapping function accurate up to  $\lambda^4$  is given by

$$w = z - \frac{\lambda - 5\lambda^3}{z} + \frac{\lambda^2 - 11\lambda^4}{z^3} - \frac{\lambda^3}{z^5} + \frac{\lambda^4}{z^7},$$

and the approximate value of  $R^2$  from the first equation in (5.4.7) is  $R^2 = 1 - 4\lambda^2 - 2\lambda^8$ , which yields the radius  $R = 1 + 2\lambda^2 - 3\lambda^4$  (compare this value of  $R$  with that obtained in Case Study 5.1.1). ■

Case 2 can be analyzed analogously by taking the approximate function as

$$w = \frac{a_1}{z} + \frac{a_2}{z^2} + \cdots + \frac{a_n}{z^n}, \tag{5.4.8}$$

and following the above method step-by-step, where  $a_1 = 1$  for a nearly circular boundary of the type (5.1.9) or (5.2.1).

**CASE STUDY 5.4.2.** We shall map the exterior of the square  $\{-1 \leq x, y \leq 1\}$  onto the disk  $|w| < R$ . The equation of the square in complex form is

$$z\bar{z} + \frac{z^2 - \bar{z}^2}{4} = 1.$$

We shall, however, analyze the family of curves

$$z\bar{z} + \lambda \frac{z^2 - \bar{z}^2}{4} = 1, \quad (5.4.9)$$

where  $\lambda = 1$  gives the above square. Since the squares are symmetric about the coordinate axes and about the diagonals  $y = \pm x$ , the function  $w$  has, from (5.4.8), the form

$$z = a_1 e^{-i\theta} + a_5 e^{3i\theta} + a_9 e^{7i\theta} + \dots, \quad (5.4.10)$$

where  $a_j$  are real. Now,

$$\begin{aligned} \frac{z^2 - \bar{z}^2}{4} &= \frac{1}{2} \left\{ - \left( \frac{1}{2} a_9^2 + \dots \right) e^{-14i\theta} - (a_5 a_9 + \dots) e^{-10i\theta} \right. \\ &\quad - \left( a_1 a_9 + \frac{1}{2} a_5^2 \right) e^{-6i\theta} - \left( a_1 a_5 - \frac{1}{2} a_1^2 \right) e^{-2i\theta} \\ &\quad + \left( a_1 a_5 - \frac{1}{2} a_1^2 \right) e^{2i\theta} - \left( a_1 a_9 - \frac{1}{2} a_5^2 \right) e^{6i\theta} \\ &\quad \left. + (a_5 a_9 + \dots) e^{10i\theta} - \left( \frac{1}{2} a_9^2 + \dots \right) e^{14i\theta} \right\}. \end{aligned} \quad (5.4.11)$$

After substituting (5.4.10) and (5.4.11) in Eq (5.4.9) and comparing the coefficients of different exponential powers, we get

$$\begin{aligned} a_1^2 + a_5^2 + a_9^2 + \dots &= R^2 + \frac{\lambda}{2} \left[ \left( a_1 a_5 - \frac{1}{2} a_1^2 \right)^2 + \left( a_1 a_9 + \frac{1}{2} a_5^2 \right)^2 \right. \\ &\quad \left. + a_5^2 a_9^2 + \frac{1}{4} a_9^4 + \dots \right], \\ a_1 a_5 + a_5 a_9 + \dots &= -\frac{\lambda}{2} \left[ \frac{1}{2} \left( a_1 a_5 - \frac{1}{2} a_1^2 \right)^2 - \left( a_1 a_9 + \frac{1}{2} a_5^2 \right) \right. \\ &\quad \times \left( a_1 a_5 + \frac{1}{2} a_1^2 \right)^2 - a_5 a_9 \left( a_1 a_9 + \frac{1}{2} a_5^2 \right) - \frac{1}{2} a_9^2 a_5 a_9 - \dots \left. \right], \\ a_1 a_9 + \dots &= -\frac{\lambda}{2} \left[ \left( a_1 a_5 - \frac{1}{2} a_1^2 \right) \left( a_1 a_9 + \frac{1}{2} a_5^2 \right) - a_5 a_9 \left( a_1 a_5 + \frac{1}{2} a_1^2 \right) \right. \\ &\quad \left. - \frac{1}{2} a_9^2 \left( a_1 a_9 + \frac{1}{2} a_5^2 \right) - \dots \right]. \end{aligned}$$

Taking the initial value of  $a_1 = 1$ , and  $a_3 = a_5 = \dots = 0$  and using the method of successive approximations up to the third approximation (see Table 5, Appendix D), we find that the approximate mapping function is given by

$$w = \left( 1 + \frac{\lambda}{16} + \frac{7\lambda^2}{256} + \frac{9\lambda^3}{1024} \right) \frac{1}{z} - \left( \frac{\lambda}{16} + \frac{7\lambda^2}{256} + \frac{9\lambda^3}{1024} \right) z^3 + \frac{\lambda^3}{2048} z^7.$$

If we set  $\lambda = 1$ , we obtain

$$w = \frac{1125}{1024} \frac{1}{z} - \frac{203}{2048} z^3 + \frac{1}{2048} z^7. \blacksquare$$

## 5.5. Problems

**PROBLEM 5.5.1.** Let  $E$  denote the nearly circular ellipse  $b^2 u^2 + a^2 v^2 = a^2 b^2$ , where  $b = 1$  and  $a = 1 + \varepsilon$ . Show that the function  $f(z) = z + \frac{\varepsilon}{2} z (1 + z^2) + o(\varepsilon)$  maps the unit disk  $|z| < 1$  onto the region  $\text{Int}(E)$ . (Nehari, 1952, p.265.)

**PROBLEM 5.5.2.** Show that the function

$$w = f(z) = z + \frac{\varepsilon z}{2\pi} \int_0^{2\pi} \frac{e^{it} + z}{e^{it} - z} p(t) dt + o(\varepsilon)$$

maps the unit disk  $|z| < 1$  onto a nearly circular region whose boundary has the polar equation  $r = 1 + \varepsilon p(\theta)$ , where  $p(\theta)$  is bounded and piecewise continuous and  $\varepsilon > 0$  is a small parameter. (Nehari, 1952, p.263.)

**PROBLEM 5.5.3.** Let the boundary  $\Gamma$  of a simply connected region be defined in polar coordinates by  $r = 1 + \varepsilon g(\theta)$ ,  $\varepsilon > 0$ , where  $g(\theta)$  has a finite Fourier series expansion of the form

$$g(\theta) = a_0 + \sum_{j=1}^n (a_j \cos j\theta + b_j \sin j\theta).$$

Show that the function

$$f(z) = z + \varepsilon z + \left[ a_0 + \sum_{j=1}^n (a_j - i b_j) z^j \right] + o(\varepsilon)$$

maps the unit disk  $|z| < 1$  onto the nearly circular region  $\text{Int}(\Gamma)$ . (Nehari, 1952, p.265.)

**PROBLEM 5.5.4.** The ellipse defined by (5.1.16) can be written as  $z = a \cos t + i b \sin t$ , where  $a = 1 + \lambda^2$  and  $b = 1 - \lambda^2$ . Determine the mapping function  $f(z, \lambda)$  in the following cases: (i)  $\lambda^2 = 1/11$ , i.e.,  $a/b = 1.2$ ; (ii)  $\lambda^2 = 1/5$ , i.e.,  $a/b = 1.5$ ; and (iii)  $\lambda^2 = 1/3$ , i.e.,  $a/b = 2$ . What does the value of  $f'(0, \lambda)$  signify in each case? [Hint: Show that the mapping function is

- (i)  $f(z, \lambda) = 1.0165984 z - 0.0932071 z^3 + 0.008615 z^5 - 0.0007963 z^7 + 0.0000734 z^9 - 0.0000068 z^{11} + 0.0000006 z^{13} + 0.00000005 z^{15}$ ;
- (ii)  $f(z, \lambda) = 1.081728 z - 0.226394 z^3 + 0.049024 z^5 - 0.010611 z^7 + 0.002176 z^9 - 0.000461 z^{11} + 0.000064 z^{13} + 0.000013 z^{15}$ ;
- (iii)  $f(z, \lambda) = 1.2373 z - 0.4787 z^3 + 0.1948 z^5 - 0.0791 z^7 + 0.0247 z^9 - 0.0091 z^{11} + 0.0014 z^{13} + 0.00046 z^{15}$ .] (Andersen et al., 1962, pp.254-255.)

**REFERENCES USED:** Andersen et al. (1962), Goluzin (1937), Kantorovich and Krylov (1958), Nehari (1952).

# Chapter 6

---

## Green's Functions

---

Green's functions are useful in solving the first boundary value problem (Dirichlet problem) of potential theory in itself and in the case of conformal mapping of a region onto a disk. In the latter case a relationship is needed between the conformal map and Green's function for the region. An approximate determination of Green's functions is an important numerical tool in solving both the Dirichlet problem for different types of regions and the related mapping problem. An integral representation of Green's function for the disk leads to the Poisson integral. The Dirichlet problem is a special case of the Riemann–Hilbert problem which is discussed in Appendix C. Analogous to Green's functions, the solution of the second boundary value problem (Neumann problem) of potential theory is the Neumann function which also possesses an integral representation.

---

### 6.1. Mean–Value Theorem

The mean–value theorem for harmonic functions is discussed in §1.3. Thus, if we integrate in (1.3.2) on the circle  $|z - z_0| = r_0$  and if the function  $u(z)$  is harmonic on  $|z - z_0| \leq r_0$ , then this integral must vanish, i.e., in polar coordinates

$$\frac{1}{2\pi} \int_0^{2\pi} \frac{\partial u}{\partial r} r_0 d\theta = 0. \quad (6.1.1)$$

After multiplying the integral (6.1.1) by  $\frac{dr}{r_0}$  and integrating from  $r_1$  and  $r_2$ ,

we get

$$\int_{r_1}^{r_2} \int_0^{2\pi} \frac{\partial u}{\partial r} d\theta dr = \int_0^{2\pi} u(r_2, \theta) d\theta - \int_0^{2\pi} u(r_1, \theta) d\theta = 0, \quad (6.1.2)$$

or

$$\frac{1}{2\pi} \int_0^{2\pi} u(r_1, \theta) d\theta = \frac{1}{2\pi} \int_0^{2\pi} u(r_2, \theta) d\theta. \quad (6.1.3)$$

These are the mean values of  $u(z)$  taken on both circles  $|z - z_0| = r_1$  and  $|z| = r_2$ , where  $r_1 < r_2$ . So long as  $u(z)$  is harmonic on the larger circle, these mean values are equal. For  $r_1 \rightarrow 0$  the left side of (6.1.3) takes the value  $u(z_0)$  at the center, so that we finally obtain

$$u(z_0) = \frac{1}{2\pi} \int_0^{2\pi} u(r, \theta) d\theta. \quad (6.1.4)$$

This is the mean-value theorem of potential theory which states that for every function harmonic on a circle the value at the center is equal to the mean value of the function on the circumference (see (1.3.3)). An important consequence of the mean-value theorem is that a nonconstant function  $u(z)$  harmonic in a region  $D$  takes neither a maximum nor a minimum value in the interior of  $D$ . Since the real and imaginary part of a regular analytic function  $w = f(z) = u(z) + iv(z)$  are harmonic functions, the mean-value theorem also holds for analytic functions, and Cauchy's integral formula (1.2.2) remains valid, i.e.,

$$f(z_0) = \frac{1}{2i\pi} \oint_{|z|=r} \frac{f(z)}{z - z_0} dz. \quad (6.1.5)$$

## 6.2. Dirichlet Problem

Let  $z_0 \in D$  be a fixed point (known as the source point). Green's function for the Dirichlet problem in the region  $D$  with a logarithmic singularity at  $z_0$  is the function  $\mathcal{G}(z, z_0)$  with the following properties:

- (i) As a function of  $z$ ,  $\mathcal{G}(z, z_0)$  is harmonic everywhere in  $D$  except at the point  $z_0$ .
- (ii) At the point  $z_0$  the function  $\mathcal{G}(z, z_0)$  is defined by

$$\mathcal{G}(z, z_0) = \frac{1}{2\pi} \log \frac{1}{r} + \mathcal{G}(z, z_0), \quad r = |z - z_0|, \quad (6.2.1)$$

where  $\mathcal{G}(z, z_0)$  is harmonic everywhere in  $D$ .

(iii)  $\mathcal{G}(z, z_0) = 0$  if the point  $z_0$  lies on the boundary  $\Gamma$ .

The Dirichlet problem for the region  $D$  can be solved in an explicit form by using Green's function. Since, in view of the property (ii), the function  $\mathcal{G}$  becomes unbounded at  $z = z_0$ , we can indent the point  $z_0$  by a circle  $\Gamma_\varepsilon$  of small radius  $\varepsilon$  (see Fig.B.1(a)). Then the functions  $u$  and  $\mathcal{G}$  become continuous in the region  $D_\varepsilon$  bounded by  $\Gamma$  and  $\Gamma_\varepsilon$ . An application of Green's second identity (B.5) (with  $g = \mathcal{G}$ ) yields

$$\int_{\Gamma + \Gamma_\varepsilon} \left( u \frac{\partial \mathcal{G}}{\partial n} - \mathcal{G} \frac{\partial u}{\partial n} \right) ds = 0, \quad (6.2.2)$$

where  $n$  denotes the outward normal to the boundary which will be normal to  $\Gamma$ , exterior to  $D_\varepsilon$ , and interior to  $\Gamma_\varepsilon$ . Separating the integral (6.2.2) over two contours  $\Gamma$  and  $\Gamma_\varepsilon$  and using (6.2.1), we find that

$$\begin{aligned} \int_{\Gamma} \left( u \frac{\partial \mathcal{G}}{\partial n} - \mathcal{G} \frac{\partial u}{\partial n} \right) ds &= \frac{1}{2\pi} \int_{\Gamma_\varepsilon} u \frac{\partial \log \frac{1}{r}}{\partial n} ds + \int_{\Gamma_\varepsilon} u \frac{\partial \mathcal{G}}{\partial n} ds \\ &- \frac{1}{2\pi} \int_{\Gamma_\varepsilon} \log \frac{1}{r} \frac{\partial u}{\partial n} ds - \int_{\Gamma_\varepsilon} \mathcal{G} \frac{\partial u}{\partial n} ds \equiv I_1 + I_1 + I_2 + I_3 + I_4. \end{aligned} \quad (6.2.3)$$

The interior normal to  $\Gamma_\varepsilon$  is along the radius  $r$  with its direction opposite to that of increasing  $r$ , and hence,  $\frac{\partial}{\partial n} = -\frac{\partial}{\partial r}$ , which yields

$$\frac{\partial \log \frac{1}{r}}{\partial n} = -\frac{\partial \log \frac{1}{r}}{\partial r} = \frac{1}{r}.$$

Also, since  $r = \varepsilon$  on the circle  $\Gamma_\varepsilon$ , we get, in view of (6.1.4),

$$I_1 = \frac{1}{2\pi\varepsilon} \int_{\Gamma_\varepsilon} u ds = u(z_0)$$

for any  $\varepsilon$  by the mean value theorem. In  $I_3$ , since  $r = \varepsilon$  and  $u$  is harmonic, we have

$$I_3 = \frac{1}{2\pi} \log \frac{1}{\varepsilon} \int_{\Gamma_\varepsilon} \frac{\partial u}{\partial n} ds = 0 \quad \text{for any } \varepsilon.$$

The remaining two integrals  $I_2$  and  $I_4$  tend to zero as  $\varepsilon \rightarrow 0$ . In fact, since  $u, \mathcal{G}, \frac{\partial u}{\partial n}$  and  $\frac{\partial \mathcal{G}}{\partial n}$  are bounded in the neighborhood of the point  $z_0$ , we find that

$$|I_2| \leq \max_{\Gamma_\varepsilon} \left| u \frac{\partial \mathcal{G}}{\partial n} \right| \cdot 2\pi\varepsilon, \quad \text{and} \quad |I_4| \leq \max_{\Gamma_\varepsilon} \left| \mathcal{G} \frac{\partial u}{\partial n} \right| \cdot 2\pi\varepsilon.$$

Hence, as  $\varepsilon \rightarrow 0$ , the relation (6.2.3) yields

$$\frac{1}{2\pi} \int_{\Gamma} \left( u \frac{\partial \mathcal{G}}{\partial n} - \mathcal{G} \frac{\partial u}{\partial n} \right) ds = u(z_0). \quad (6.2.4)$$

Moreover, by condition (iii) the function  $\mathcal{G}$  vanishes on  $\Gamma$ , and hence, from (6.2.5) we obtain

$$u(z_0) = \frac{1}{2\pi} \int_{\Gamma} u \frac{\partial \mathcal{G}}{\partial n} ds. \quad (6.2.5)$$

Note that this equation is also a consequence of Green's third identity (B.8). If Green's function is known for the region  $D$ , then formula (6.2.5) can be used to solve the Dirichlet problem for any continuous or piecewise continuous, boundary values of the harmonic function  $u(z)$ . An alternate form of formula (6.2.5) is

$$u(z_0) = \frac{1}{2\pi} \int_{\Gamma} u d\mathcal{G}(z, z_0). \quad (6.2.6)$$

The relationship between Green's function and conformal mapping is established as follows: Let  $w = f(z) = \rho e^{i\theta}$  map a simply connected region  $D$  conformally onto the unit disk  $|w| < 1$  such that the point  $z_0 \in D$  goes into the point  $w = 0$ , i.e.,  $f(z_0) = 0$ . If  $f(z)$  has a simple zero at  $z_0$ , the function  $F(z) = \frac{f(z)}{z - z_0} \neq 0$  for all  $z \in D$  and is regular everywhere in  $D$ . Thus,  $\log F(z)$  is also regular analytic in  $D$ . Let us denote  $\log F(z) = U + iV$ . Then

$$f(z) = (z - z_0) e^{U+iV},$$

which yields, with  $z - z_0 = r e^{i\phi}$ ,

$$\frac{1}{2\pi} \log \frac{1}{|f(z)|} = \frac{1}{2\pi} \left( \log \frac{1}{r} - U \right). \quad (6.2.7)$$

It can easily be verified that the function  $\frac{1}{2\pi} \log \frac{1}{|f(z)|}$  satisfies all three properties for the Green's function  $\mathcal{G}(z, z_0)$ , namely, this function with a simple pole at  $z_0$  is harmonic in  $D$  except at  $z_0$ , where it has a logarithmic singularity, and it is equal to

$$\frac{1}{2\pi} \log \frac{1}{r} + g(z),$$

where  $g(z) = -\frac{1}{2\pi} U$ . Moreover,  $|f(z)| = 1$  on the boundary  $\Gamma$ , and, therefore,  $\frac{1}{2\pi} \log \frac{1}{|f(z)|} = 0$  there. Thus, we have shown that Green's function

$\mathcal{G}(z, z_0)$  and the mapping function  $f(z)$  which produces the conformal map of the region  $D$  onto the unit disk are related to each other by

$$\mathcal{G}(z, z_0) = \frac{1}{2\pi} \log \frac{1}{|f(z)|}. \quad (6.2.8)$$

If Green's function for a region  $D$  is known, we can use (6.2.8) and construct the function  $f(z)$  which maps the region  $D$  conformally onto the unit disk. The method of accomplishing this is as follows: For each term in (6.2.7), we determine the respective conjugate harmonic function. The conjugate harmonic function for  $\frac{1}{2\pi} \log \frac{1}{r}$  is  $-\frac{\phi}{2\pi}$ , where  $\phi = \arg\{z - z_0\}$ . Let  $h(z)$  be conjugate to the function  $g(z)$ . Then, in view of (1.3.2),

$$h(z) = \int_{z_0}^z \left( \frac{\partial U}{\partial x} dy - \frac{\partial U}{\partial y} dx \right) + C, \quad (6.2.9)$$

where  $C$  is an arbitrary constant, which corresponds to the rotation of the unit disk about  $w = 0$ . Hence, the required mapping function is given by

$$w = f(z) = r e^{i\phi} e^{-2\pi(g+i h)} = (z - z_0) e^{-2\pi(g+i h)}. \quad (6.2.10)$$

Note that the construction of the Green's function  $\mathcal{G}(z, z_0)$  involves determining the harmonic function  $g(z)$ , whose boundary values are determined from the third property, namely, that  $\mathcal{G}(z, z_0) = 0$  on the boundary  $\Gamma$ . This means that  $g(z)$  must take the values  $-\frac{1}{2\pi} \log \frac{1}{r}$  on  $\Gamma$ . Hence, the conformal mapping problem of transforming the region  $D$  onto the unit disk reduces to the solution of the Dirichlet problem with the boundary condition

$$g(x, y)|_{\Gamma} = \frac{1}{2\pi} \log r. \quad (6.2.11)$$

If  $D$  can be mapped conformally onto the unit disk, then the dependence of Green's function on  $z_0$  can be given explicitly. Thus, if  $w = f(z)$  is any function that maps  $D$  onto the unit disk, then we can use the mapping

$$z \mapsto e^{i\gamma} \frac{w - w_0}{1 - \bar{w}w_0},$$

where  $\gamma$  is an arbitrary real constant, which maps the unit disk onto itself such that the point  $w(z_0)$  goes into the origin and  $w_0 = f(z_0)$ . Hence,

$$\mathcal{G}(z, z_0) = \log \frac{w - w_0}{1 - \bar{w}w_0}. \quad (6.2.12)$$

For practical applications, once Green's function  $\mathcal{G}(z, z_0)$  is known for a region, we can use formula (6.2.5) and determine the solution of the Dirichlet problem at the point  $z_0$ . Now, to compute the solution of the Dirichlet problem at another point, say  $z_1$ , we must recompute Green's function with a pole at  $z_1$ . Let this new Green's function be denoted by  $\mathcal{G}(z, z_1)$ . Now we shall establish a relation which connects the two Green's functions  $\mathcal{G}(z, z_0)$  and  $\mathcal{G}(z, z_1)$ . Assuming that  $\mathcal{G}(z, z_0)$  is known, the other Green's function  $\mathcal{G}(z, z_1)$  can be determined as follows: By the method presented above, first we determine the conformal mapping function  $w = f(z)$  from the known Green's function  $\mathcal{G}(z, z_0)$ . This mapping function transforms the region  $D$  into the unit disk such that the point  $z = z_0$  goes into the origin  $w = 0$ . Under this mapping, the point  $z_1$  is transformed into some point, say,  $w_1 = f(z_1)$ , which is known because the function  $f(z)$  is known. Next, to determine  $\mathcal{G}(z, z_1)$  by formula (6.2.6), we must find the function  $w = f_1(z)$  that would map the region  $D$  onto the unit disk such that the point  $z = z_1$  goes into the origin  $w = 0$ . If  $f(z)$  is known, then  $f_1(z)$  can be determined by mapping the unit disk onto itself, i.e., we use the transformation  $w \mapsto \frac{w - w_1}{1 - w\bar{w}_1}$ . Hence,

$$f_1(z) = \frac{f(z) - w_1}{1 - \bar{w}_1 f(z)}, \quad (6.2.13)$$

which yields the required Green's function

$$\mathcal{G}(z, z_1) = \frac{1}{2\pi} \log \frac{1}{|f_1(z)|} = \frac{1}{2\pi} \log \frac{|1 - w\bar{w}_1|}{|f(z) - w_1|}. \quad (6.2.14)$$

### 6.3. Numerical Computation

Green's function  $\mathcal{G}(z, z_0)$  with a pole at  $z_0$  can be determined from (6.2.1), provided that the harmonic function  $g(z) = \frac{1}{2\pi} \log r$ , defined by (6.2.11), is determined for  $z \in \Gamma$ . An interpolation method for numerically computing the function  $g(z)$  is as follows: In the polar coordinate system let  $z_0$  be taken as the pole, and let the polar axis be directed parallel to the  $x$ -axis. Thus,  $z - z_0 = r e^{i\theta}$ . Let  $g(z)$  have the series representation

$$g(z) = \sum_{k=0}^{\infty} c_k (z - z_0)^k, \quad c_k = a_k + i b_k. \quad (6.3.1)$$

Then we take the harmonic polynomial  $P_n(r, \theta) = \Re \left\{ \sum_{k=0}^n c_k (z - z_0)^k \right\}$ , i.e.,

$$P_n(r, \theta) = a_0 + \sum_{k=1}^n r^k (a_k \cos k\theta - b_k \sin k\theta). \quad (6.3.2)$$

Since this polynomial has  $(2n + 1)$  coefficients, we take  $(2n + 1)$  arbitrary points  $z_1, \dots, z_{2n+1}$  on  $\Gamma$  and choose the coefficients  $a_k, b_k$  such that at the points  $z_j, j = 1, \dots, 2n + 1$ , the polynomial  $P_n(r, \theta)$  has the same values as  $g(z_j)$ , respectively. Noting that  $g(z)$  has the boundary value defined by (6.2.11), the coefficients  $a_k, b_k$  are determined from the system of equations

$$\begin{aligned} a_0 + \sum_{k=1}^n r_1^k (a_k \cos k\theta_1 - b_k \sin k\theta_1) &= \frac{1}{2\pi} \log r_1, \\ a_0 + \sum_{k=1}^n r_2^k (a_k \cos k\theta_2 - b_k \sin k\theta_2) &= \frac{1}{2\pi} \log r_2, \\ &\dots &&\dots \\ a_0 + \sum_{k=1}^n r_{2n+1}^k (a_k \cos k\theta_{2n+1} - b_k \sin k\theta_{2n+1}) &= \frac{1}{2\pi} \log r_{2n+1}, \end{aligned} \quad (6.3.3)$$

where  $z_j - z_0 = r_j e^{i\theta_j}, j = 1, \dots, 2n + 1$ . The determinant of the system (6.3.3) depends on the choice of the points  $z_j$ . Let us assume that these points lie on an equipotential line of a harmonic polynomial  $Q_n(r, \theta)$  of degree at most  $n$ :

$$Q_n(r, \theta) = a_0 + \sum_{k=1}^n r^k (a_k \cos k\theta - b_k \sin k\theta) = 0, \quad (6.3.4)$$

where the coefficients  $a_k$  and  $b_k$  are not zero at the same time. Then this line exists iff the homogeneous system of  $(2n + 1)$  equations

$$a_0 + \sum_{k=1}^n r_j^k (a_k \cos k\theta_j - b_k \sin k\theta_j) = 0, \quad j = 1, \dots, 2n + 1, \quad (6.3.5)$$

has a nonzero solution for  $a_0, a_1, b_1, \dots$ . Hence, if the determinant of the system (6.3.5) is zero, there exists a nonzero solution, which implies that the points  $z_j$  lie on an equipotential line. However, if this determinant is not zero, then the system (6.3.5) has a trivial solution, and there is no curve that passes through the points  $z_j$ . Since this determinant of the system (6.3.5) is the same

as that of the system (6.3.3), a zero determinant of the latter system implies that all  $(2n + 1)$  chosen points  $z_j$  lie on the said equipotential line. Thus, first we solve the system (6.3.3) for the unknown coefficients  $a_0, a_1, b_1, \dots$ . Then their values are substituted in  $P_n(r, \theta)$ . This harmonic polynomial so constructed has the property that at the  $(2n + 1)$  points  $z_j$  it takes the same values as the harmonic function  $g(z)$ . Hence, in view of (6.2.1), Green's function has the approximate representation

$$\mathcal{G}(z, z_0) \approx \frac{1}{2\pi} \log \frac{1}{r} + a_0 + \sum_{k=1}^n r^k (a_k \cos k\theta - b_k \sin k\theta). \quad (6.3.6)$$

It is assumed here that the difference between  $P_n(r, \theta)$  and  $g(z)$  decreases as  $n$  increases and the above interpolation method becomes justified, provided

$$\lim_{n \rightarrow \infty} P_n(r, \theta) = g(z).$$

**CASE STUDY 6.3.1.** We shall approximate Green's function for the square  $\{(x, y) : -1 \leq x, y \leq 1\}$  in the  $z$ -plane with the pole  $z_0$  at the origin (see Fig. 4.2.1). In view of the symmetry about both coordinate axes, we shall approximate  $g(z)$  by the harmonic polynomial  $P_n(r, \theta)$  defined by (6.3.2). Since the values of  $g(z) = g(x, y)$  are arranged symmetric to the  $y$ -axis, all  $b_k = 0$ . Also, since the values of  $g(x, y)$  are symmetric to  $x$ -axis and bisectors of coordinate angles, the series (6.3.2) will contain cosine terms of angles  $4n\theta$ ,  $n = 0, 1, 2, \dots$ . Hence, the series expansion for  $g(x, y)$  becomes

$$g(x, y) \approx a_0 + a_4 r^4 \cos 4\theta + a_8 r^8 \cos 8\theta + \dots. \quad (6.3.7)$$

We shall consider the points  $z_j$  on the boundary defined as follows:  $z_1 = 1$ ,  $z_2 = \frac{2}{\sqrt{3}} e^{i\pi/6}$ ,  $z_3 = \sqrt{2} e^{i\pi/4}$ . Then the coefficients  $a_0, a_4$ , and  $a_8$  are determined from the system

$$\begin{bmatrix} 1 & 1 & \frac{1}{81} \\ 1 & -\frac{8}{9} & -\frac{128}{81} \\ 1 & -4 & 16 \end{bmatrix} \begin{Bmatrix} a_0 \\ a_4 \\ a_8 \end{Bmatrix} = \frac{1}{2\pi} \begin{Bmatrix} 0 \\ \ln \frac{2}{\sqrt{3}} \\ \ln \sqrt{2} \end{Bmatrix},$$

whose solution is as follows:

$$\begin{aligned} a_0 &= 0.12648 = \frac{0.075578}{2\pi}, \\ a_4 &= -0.012244 = -\frac{0.0740122}{2\pi}, \\ a_8 &= -0.000404057 = -\frac{0.00156583}{2\pi}. \end{aligned}$$

Note that additional points  $z_4 = \frac{2}{\sqrt{3}} e^{i\pi/3}$  and  $z_4 = e^{i\pi/2}$  add nothing to the solution. The approximate Green's function is given by

$$\begin{aligned}\mathcal{G}(z, 0) &= \frac{1}{2\pi} \log \frac{1}{r} + g(z) \\ &\approx \frac{1}{2\pi} \left[ \log \frac{1}{r} + 0.075578 - 0.0740122 r^4 \cos 4\theta \right. \\ &\quad \left. - 0.00156583 r^8 \cos 8\theta \right] \\ &= \frac{1}{2\pi} \Re \left\{ \log \frac{1}{z} + 0.075578 - 0.0740122 z^4 - 0.00156583 z^8 \right\}.\end{aligned}$$

Then, in view of (6.2.8) the mapping function  $w = f(z)$  that maps the square onto the unit disk is found from

$$\begin{aligned}\log |f(z)| &= -2\pi \mathcal{G}(z, 0) \\ &= \Re \left\{ \log z - 0.075578 + 0.0740122 z^4 + 0.00156583 z^8 \right\}\end{aligned}$$

up to a purely imaginary additive constant which we shall ignore. Hence,

$$f(z) = z e^{-0.075578+0.0740122 z^4+0.00156583 z^8}. \quad (6.3.7)$$

Note that

$$f'(0) = e^{-0.075578} = 0.927207.$$

The exact value from (4.5.29) is  $f'(0) = \int_0^1 \frac{d\zeta}{\sqrt{1+\zeta^4}} \approx 0.927037$  which shows that the error in the approximate value for  $f(z)$  is about 0.017

**CASE STUDY 6.3.2.** In order to approximate Green's function for the ellipse (5.1.16), let the points  $z_j$  be taken for  $t = 0, \pi/8, \pi/4, 3\pi/8$ , and  $\pi/2$ . Then, we have

$$\begin{aligned}g(z) &\approx \Re \left\{ -0.0025 + 0.063 z^2 - 0.0038 z^4 + 0.0034 z^6 - 0.000035 z^8 \right\} \\ &= \frac{1}{2\pi} \Re \left\{ -0.0158 + 0.396 z^2 - 0.0238 z^4 + 0.00215 z^6 - 0.0002 z^8 \right\}.\end{aligned}$$

Thus,

$$\begin{aligned}\mathcal{G}(z, 0) &= \frac{1}{2\pi} \Re \left\{ \log \frac{1}{z} - 0.0158 + 0.396 z^2 - 0.0238 z^4 \right. \\ &\quad \left. + 0.00215 z^6 - 0.0002 z^8 \right\},\end{aligned}$$

which gives

$$f(z) = z e^{0.0158 - 0.396 z^2 + 0.0238 z^4 - 0.00215 z^6 + 0.0002 z^8}.$$

Note that  $f'(0) = e^{0.0158} \approx 1.0159$ , which matches with the value of  $p'(0)$  in Case Study 5.1.1. ■

CASE STUDY 6.3.3. We shall consider the curve

$$F(x, y, \alpha) = [(x - 0.5)^2 + (y - \alpha)^2] [1 - y^2 - (x - 0.5)^2] = 0.1.$$

The graphs for  $\alpha = \infty, 1, 0.5, 0.3$ , and  $0.2746687749$  can be plotted as suggested in `cs633.nb` (Notes, end of chapter). For  $\alpha = \infty$  it represents the unit circle with center at  $(0.5, 0)$ . The region does not remain simply connected for  $\alpha = 0.2746687749$ . We shall approximate Green's function for the region at  $\alpha = 1$  which is a nearly circular cardioid (see Fig. 6.3.1).

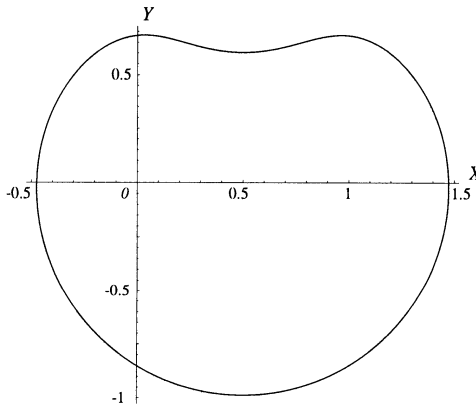


Fig. 6.3.1. The curve for  $\alpha = 1$ .

Since the region is symmetric about the line  $x = 0.5$ , we shall choose seven boundary points  $z_j$  as follows:  $z_1 = 0.5 - 0.98725 i$ ,  $z_2 = 0.8 - 0.92024 i$ ,  $z_3 = 1.2 - 0.69296 i$ ,  $z_4 = 1.474$ ,  $z_5 = 1.2 + 0.5972 i$ ,  $z_6 = 0.8 + 0.65589 i$ , and  $z_7 = 0.5 + 0.60343 i$ . Unlike previous case studies, we have computed the radii and arguments for each of these points (see Notes, `cs633.nb`, end of chapter). Green's function is given by

$$\begin{aligned} \mathcal{G}(z, 0.5) &\approx \frac{1}{2\pi} \log \frac{1}{r} - 0.0431944 + 0.0404596 r \cos \theta \\ &+ 0.0107145 r^2 \cos 2\theta - 0.0114393 r^3 \cos 3\theta + 0.0569173 r \sin \theta \\ &- 0.039137 r^2 \sin 2\theta + 0.00477567 r^3 \sin 3\theta, \end{aligned}$$

where  $r = |z - 0.5|$ . Then the mapping function  $f(z)$  can easily be obtained with  $f'(0.5) = e^{-0.0431944} = 0.957725$ . ■

CASE STUDY 6.3.4. We shall consider the Cassini's ovals

$$F(x, y, \alpha) = [(x + \alpha)^2 + y^2] [(x - \alpha)^2 + y^2] = 1.$$

The graphs for  $\alpha = 0, 0.5, 0.9, 0.99$ , and 1 are plotted in Fig. 6.3.2. For  $\alpha = 0$  the curve becomes the unit circle. The region does not remain simply connected for  $\alpha = 1$ . We shall approximate Green's function for the region at  $\alpha = 0.5$  which is bounded by a nearly circular ellipse (see also Fig. 9.2.1).

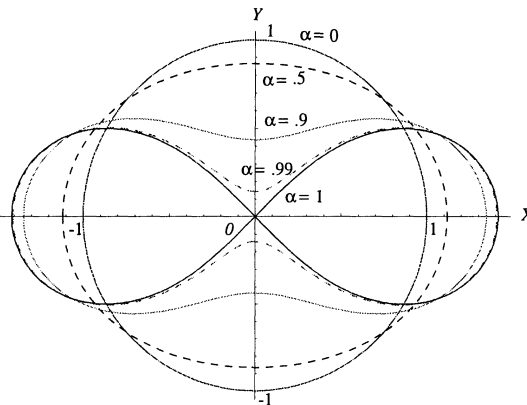


Fig. 6.3.2. Cassini's ovals.

Because of the symmetry of the region about the axes of coordinates, the function  $g(z)$  has a series expansion of the form

$$g(z) = a_0 + a_2 r^2 \cos 2\theta + a_4 r^4 \cos 4\theta + \dots$$

Let the points  $z_j$  on the boundary be chosen as  $z_1 = 1.11803$ ,  $z_2 = 1.04942 e^{i\pi/6}$ ,  $z_3 = 0.98399 e^{i\pi/4}$ ,  $z_4 = 0.92265 e^{i\pi/3}$ , and  $z_5 = 0.866 e^{i\pi/2}$ . Then, as in the previous Case Study, we can compute  $a_0 = -0.00513$ ,  $a_2 = 0.02124$ ,  $a_4 = -0.00282$ ,  $a_6 = 0.0005$ ,  $a_8 = -0.000096$ . Thus, Green's function is given by

$$\begin{aligned} \mathcal{G}(z, 0) \approx & \frac{1}{2\pi} \Re \left\{ \log \frac{1}{z} - 0.0322236 + 0.133465 z^2 - 0.0177425 z^4 \right. \\ & \left. + 0.0031616 z^6 - 0.000605 z^8 \right\}, \end{aligned}$$

and the mapping function by

$$f(z) \approx z e^{0.0322236 - 0.133465 z^2 + 0.0177425 z^4 - 0.0031616 z^6 + 0.000605 z^8},$$

with  $f'(0) \approx 1.03276$ . ■

---

## 6.4. Schwarz Formula

We shall consider specially the case when  $D$  is a circle with center at the origin and radius  $R$ . In this case we carry out the mapping onto the unit disk by

$$w = \frac{z}{R}, \quad (6.4.1)$$

and Green's function (6.2.12) becomes

$$\mathcal{G}(z, z_0) = \log \frac{R(z - z_0)}{R^2 - z\bar{z}_0}. \quad (6.4.2)$$

Then

$$d\mathcal{G}(z, z_0) = \left( \frac{1}{z - z_0} + \frac{\bar{z}_0}{R^2 - z\bar{z}_0} \right) dz. \quad (6.4.3)$$

Since  $|z|^2 = z\bar{z} = R^2$  on the boundary of the circle and  $dz = iz d\theta$ , so

$$d\mathcal{G}(z, z_0) = i \left( \frac{z}{z - z_0} + \frac{\bar{z}}{\bar{z} - \bar{z}_0} - 1 \right) d\theta. \quad (6.4.4)$$

Setting  $z = R e^{i\theta}$  and  $z_0 = \rho e^{i\phi}$ , we find that

$$d\mathcal{G}(z, z_0) = i \frac{R^2 - \rho^2}{R^2 + \rho^2 - 2R\rho \cos(\theta - \phi)} d\theta. \quad (6.4.5)$$

If we substitute (6.4.5) in (6.2.5), we obtain the Poisson integral

$$u(\rho e^{i\phi}) = \frac{1}{2\pi} \int_0^{2\pi} u(R e^{i\phi}) \frac{R^2 - \rho^2}{R^2 + \rho^2 - 2R\rho \cos(\theta - \phi)} d\theta. \quad (6.4.6)$$

By a similar integral representation we can determine the harmonic function  $v(z)$  which is conjugate to  $u(z)$ . In view of (1.3.2)

$$v(z) - v(0) = \int_0^z \frac{\partial u}{\partial n} ds. \quad (6.4.7)$$

When we apply this operation on (6.4.6) and follow through the corresponding integrations and differentiations, we get

$$\begin{aligned} v(\rho e^{i\phi}) - v(0) \\ = \frac{1}{2\pi} \int_0^{2\pi} u(R e^{i\phi}) \int_0^{\rho e^{i\phi}} \frac{\partial}{\partial u} \left[ \frac{R^2 + \rho^2}{R^2 + \rho^2 - 2R\rho \cos(\theta - \phi)} \right] ds d\theta, \end{aligned} \quad (6.4.8)$$

where the inner integral is taken on an arbitrary path that lies entirely in the interior of the circle. Note that

$$\begin{aligned} \frac{R^2 - \rho^2}{R^2 + \rho^2 - 2R\rho \cos(\theta - \phi)} &= \frac{z}{z - z_0} + \frac{\bar{z}}{\bar{z} - \bar{z}_0} - 1 \\ &= \Re \left\{ \frac{2z}{z - z_0} - 1 \right\} = \Re \left\{ \frac{z + z_0}{z - z_0} \right\}. \end{aligned} \quad (6.4.9)$$

Thus,

$$\Im \left\{ \frac{z + z_0}{z - z_0} \right\} = \frac{-2R\rho \sin(\theta - \phi)}{R^2 + \rho^2 - 2R\rho \cos(\theta - \phi)}, \quad (6.4.10)$$

and hence

$$v(\rho e^{i\phi}) = v(0) - \frac{1}{2\pi} \int_0^{2\pi} u(R e^{i\theta}) \frac{2R \sin(\theta - \phi)}{R^2 + \rho^2 - 2R\rho \cos(\theta - \phi)} d\theta. \quad (6.4.11)$$

If we combine (6.4.6) and (6.4.11), we obtain the Schwarz formula:

$$w(\rho e^{i\phi}) = i v(0) + \frac{1}{2\pi} \int_0^{2\pi} u(R e^{i\phi}) \frac{R e^{i\theta} + \rho e^{i\phi}}{R e^{i\theta} - \rho e^{i\phi}} d\theta, \quad (6.4.12)$$

which allows us to determine the value of a complex potential function  $f(z) = u(z) + i v(z)$  in a circle with prescribed boundary values  $u(z)$  and  $v(0)$ .

## 6.5. Neumann Problem

With the help of the above formulas, we can find an explicit solution for the Neumann problem, for a disk, and thereby for all regions whose conformal mapping onto the disk is known. In this case the value of the normal derivative  $\frac{\partial u}{\partial n}$  on the boundary of the region is prescribed, and we seek a function harmonic

on  $D$  whose normal derivative takes this boundary value. This problem has a solution and, as in (6.1.1), we require that

$$\oint_{\Gamma} \frac{\partial u}{\partial n} ds = 0. \quad (6.5.1)$$

Since, in view of (1.3.2),

$$v(z_2) = v(z_1) - \int_{z_1}^{z_2} \frac{\partial u}{\partial n} ds, \quad (6.5.2)$$

the value of  $v(z)$  is determined on the boundary up to an additive constant. With this boundary value  $v(z)$  the value of  $u(z)$ , which is a harmonic function conjugate to  $v(z)$ , can be determined in the interior of  $D$  by the formula (6.4.11). Thus,

$$\begin{aligned} u(\rho e^{i\phi}) &= u(0) + \frac{1}{2\pi} \int_0^{2\pi} v(R e^{i\theta}) \frac{2R\rho \sin(\theta - \phi)}{R^2 + \rho^2 - 2R\rho \cos(\theta - \phi)} d\theta \\ &= u(0) + \frac{1}{2\pi} [v(R e^{i\theta}) \log(R^2 + \rho^2 - 2R\rho \cos(\theta - \phi))]_0^{2\pi} \\ &\quad - \frac{1}{2\pi} \int_0^{2\pi} \frac{\partial v(R e^{i\theta})}{\partial \theta} \log(R^2 + \rho^2 - 2R\rho \cos(\theta - \phi)) d\theta. \end{aligned} \quad (6.5.3)$$

Since  $v(R e^{i\theta})$  and  $\log(R^2 + \rho^2 - 2R\rho \cos(\theta - \phi))$  are periodic, the second term on the right side of (6.5.3) vanishes. Also,

$$\frac{\partial v}{\partial \theta} d\theta = dv = \frac{\partial u}{\partial n} ds = \frac{\partial u}{\partial n} R d\theta, \quad (6.5.4)$$

so that we finally obtain the following integral formula:

$$u(R e^{i\theta}) = u(0) - \frac{1}{2\pi} \int_0^{2\pi} \frac{\partial u}{\partial n} R \log(R^2 + \rho^2 - 2R\rho \cos(\theta - \phi)) d\theta, \quad (6.5.5)$$

which establishes a relationship between the boundary values of  $\frac{\partial u}{\partial n}$  and the values of  $u(z)$ . We shall denote the expression

$$\log(R^2 + \rho^2 - 2R\rho \cos(\theta - \phi)) = \log\{(z - z_0)(\bar{z} - \bar{z}_0)\} \equiv \mathcal{N}(z, z_0) \quad (6.5.6)$$

and call  $\mathcal{N}(z, z_0)$  the Neumann function. It plays the same role for the second boundary value problem as Green's function does for the first. This

function represents a regular analytic function of  $z$  in  $D$  except for logarithmic singularities. Since  $\bar{z} = \frac{R^2}{z}$ , we have

$$\log \{(z - z_0)(\bar{z} - \bar{z}_0)\} = \log \frac{(z - z_0)(R^2 - z\bar{z}_0)}{z}. \quad (6.5.7)$$

This function can be regarded as a complex potential function for a flow, which has a source at  $z_0$  and a sink at  $z$  and for which the circle  $|z| = R$  acts as an impermeable wall (see figure on the right).

As in the case of Green's function, for general domains the Neumann function  $\mathcal{N}(z, z_0)$  can be characterized by the following conditions:

(i)  $\mathcal{N}(z, z_0)$  is a regular analytic function of  $z$  on a region  $D$  except for a logarithmic singularity at  $z = z_0$  and at another fixed point  $z = z^*$ , i.e.,

$$\mathcal{N}(z, z_0) = \log \frac{z - z_0}{z - z^*} + \mathcal{N}(z, z_0), \quad (6.5.8)$$

where  $\mathcal{N}(z, z_0)$  is a regular analytic function on  $D$ .

(ii)  $\mathcal{N}(z, z_0)$  as a function of  $z$  has a boundary value which is continuous everywhere on the boundary  $\Gamma$  of  $D$ , and

$$\Im \mathcal{N}(z, z_0) = 0 \quad \text{on } \Gamma. \quad (6.5.9)$$

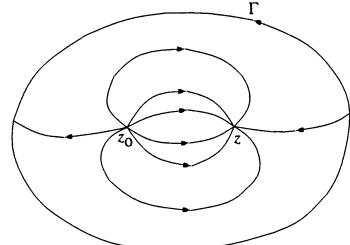
If these conditions are satisfied, then

$$u(z_0) = u(z^*) - \frac{1}{2\pi} \oint_{\Gamma} \mathcal{N}(z, z_0) \frac{\partial u}{\partial u} ds. \quad (6.5.10)$$

If the region  $D$  is mapped conformally onto the unit disk by the function  $w = f(z)$ , then  $\mathcal{N}(z, z_0)$  can also be defined by

$$\mathcal{N}(z, z_0) = \log \frac{[f(z) - f(z_0)]\overline{f(z_0)}}{f(z)}, \quad (6.5.11)$$

where  $z^*$  under this map goes into  $f(z^*) = 0$ .



Note that the Neumann problem is solvable only if the condition (6.5.1) is satisfied. For a multiply connected region the contour  $\Gamma$  in (6.5.1) must include the exterior and all interior paths. The reason why this condition does not hold for each individual path is that the function  $u$  may be multiple-valued, which does not let the integral of  $\partial u / \partial n$  around  $\Gamma$  vanish.

---

## 6.6. Series Representations

To obtain a series representation for Schwarz formula (6.4.12), we shall develop a series expansion for the kernel function

$$\frac{Re^{i\theta} + \rho e^{i\phi}}{Re^{i\theta} - \rho e^{i\phi}} = \frac{z + z_0}{z - z_0} \quad (6.6.1)$$

into a geometric series in  $\frac{z_0}{z}$  by using

$$\frac{2}{1 - z_0/z} - 1 = 1 + 2 \sum_{k=1}^{\infty} \left(\frac{z_0}{z}\right)^k = 1 + 2 \sum_{k=1}^{\infty} \left(\frac{z_0}{z}\right)^k e^{ik(\phi-\theta)}. \quad (6.6.2)$$

This series converges absolutely and uniformly for  $\left|\frac{z_0}{z}\right| < 1$ , i.e., for  $|z_0| < R$ , and thus, we can integrate (6.4.12) term-by-term, which yields

$$\begin{aligned} w(\rho e^{i\phi}) &= \frac{1}{2\pi} \int_0^{2\pi} u(Re^{i\theta}) d\theta + iv(0) \\ &\quad + \frac{1}{\pi} \sum_{k=1}^{\infty} \left(\frac{z_0}{z}\right)^k e^{ik\phi} \int_0^{2\pi} u(Re^{i\theta}) e^{-ik\theta} d\theta. \end{aligned} \quad (6.6.3)$$

If we separate this expression into real and imaginary parts and set for  $k = 1, 2, \dots$

$$\begin{aligned} a_0 &= \frac{1}{2\pi} \int_0^{2\pi} u(Re^{i\theta}) d\theta, & b_0 &= -v(0), \\ a_k &= \frac{1}{\pi} \int_0^{2\pi} u(Re^{i\theta}) \cos k\theta d\theta, & b_k &= \frac{1}{\pi} \int_0^{2\pi} u(Re^{i\theta}) \sin k\theta d\theta, \end{aligned} \quad (6.6.4)$$

which are the Fourier coefficients for the function  $u(R e^{i\theta})$ , then

$$\begin{aligned} u(\rho e^{i\phi}) &= \sum_{k=0}^{\infty} \left(\frac{z}{R}\right)^k (a_k \cos k\phi + b_k \sin k\phi), \\ v(\rho e^{i\phi}) &= \sum_{k=0}^{\infty} \left(\frac{z}{R}\right)^k (-b_k \cos k\phi + a_k \sin k\phi). \end{aligned} \quad (6.6.5)$$

Since the Fourier coefficients (6.6.4) can easily be computed and the series (6.6.5) converges inside the circle, this series expansion represents the most convenient way to solve the first boundary value problem for the circle. The second boundary value problem can also be handled analogously. Thus,

$$\frac{\partial u}{\partial n} = \frac{\partial u}{\partial \rho} \Big|_{\rho=R} = \sum_{k=0}^{\infty} k(a'_k \cos k\theta + b'_k \sin k\theta), \quad (6.6.6)$$

where the Fourier coefficients  $a'_k$  and  $b'_k$  are defined by

$$\begin{aligned} a'_k &= \frac{1}{k\pi} \int_0^{2\pi} \frac{\partial u}{\partial n} \cos k\theta d\theta, \\ b'_k &= \frac{1}{k\pi} \int_0^{2\pi} \frac{\partial u}{\partial n} \sin k\theta d\theta, \quad \text{for } k = 1, 2, \dots, \end{aligned} \quad (6.6.7)$$

and the coefficients corresponding to  $a_0, b_0$  are not needed in this case.

These series expansions show that every harmonic function on a disk and, hence an analytic function, can be represented by a series (6.6.5). Since  $u(z_0)$  and  $v(z_0)$  are real and imaginary parts of a complex function  $w = f(z_0)$ , respectively, we obtain from (6.6.5) the Taylor series

$$f(z_0) = \sum_{k=0}^{\infty} c_k z_0^k, \quad (6.6.8)$$

where

$$c_k = \frac{a_k - ib_k}{R^k}. \quad (6.6.9)$$

This representation leads to the Liouville theorem: Every analytic function that is regular and bounded in the entire plane is constant. In fact, if  $f(z)$  is such a function, then its real part  $u(z)$  must be bounded and so must the Fourier coefficients  $a_k$  and  $b_k$  for any large circle. On the other hand since  $R$  can be chosen arbitrarily large, the quantity  $|c_k|$  for every  $k$  can be made, in view of

(6.6.9), smaller than an arbitrarily small positive number, so it must vanish, which implies that  $f(z) = c_0 = \text{constant}$ , and the theorem is proved.

We obtain yet another integral representation for the Taylor coefficients  $c_k$  by using Cauchy's integral formula (1.2.2) which we write as

$$f(z_0) = \frac{1}{2i\pi} \oint \frac{f(z)}{z - z_0} dz, \quad (6.6.10)$$

where the path of integration is arbitrary and can be fixed so long as  $z_0$  lies inside a region bounded by it. Now we use the series expansion

$$\frac{1}{z - z_0} = \frac{1}{z} \frac{1}{1 - \frac{z_0}{z}} = \frac{1}{z} \sum_{k=0}^{\infty} \left(\frac{z_0}{z}\right)^k \quad (6.6.11)$$

and integrate term-by-term. If we equate the result to the representation (6.6.8), we obtain

$$c_k = \frac{1}{2i\pi} \oint \frac{f(z)}{z^{k+1}} dz. \quad (6.6.12)$$

On the other hand, by differentiating (6.6.8) term-by-term, we can show that

$$c_k = \frac{1}{k!} \left[ \frac{\partial f}{\partial z} \right]_{z=0}. \quad (6.6.13)$$

Thus, we get the series expansion

$$f(z) = \sum_{k=0}^{\infty} c_k (z - z_0)^k, \quad (6.6.14)$$

where the coefficients  $c_k$  can be determined from (6.6.12) or from (6.6.4) and (6.6.9) with the path of integration as the circle  $|z - z_0| = R$ . The function  $f(z)$  is regular on the disk  $|z - z_0| < R$ . Thus, we can expand every regular analytic function at a point  $z = z_0$  into the series (6.6.14) and this series converges in every neighborhood  $B(z_0, R)$  about  $z_0$ , where the function is regular analytic.

Conversely, every potential series (6.6.14), which converges in a neighborhood  $B(z_0, R)$ , represents a regular analytic function. Moreover, we define two potential series of the same function  $f(z)$ :

$$\sum_{k=0}^{\infty} c_k^* (z - z_0)^k = \sum_{k=0}^{\infty} c_k^{**} (z - z_0)^k = f(z), \quad (6.6.15)$$

if  $c_k^* = c_k^{**}$  for all  $k$ . In fact, if we compute the coefficients of  $f(z)$  by using (6.6.12) or (6.6.4)–(6.6.9), and substitute them in the series (6.6.15), then we obtain  $c_k = c_k^* = c_k^{**}$  (this proves the uniqueness of  $c_k$ ).

---

## 6.7. Problems

PROBLEM 6.7.1. Approximate Green's function for the regions bounded by the following curves:

(a) Cassini's oval  $[(x+1)^2 + y^2][(x-1)^2 + y^2] = a^4$  (Fig. 9.2.1) for  $a = 1.1, 1.2$ , and  $1.5$ .

(b)  $z = 2 \cos t + i (\sin t + 2 \cos^3 t)$ ,  $0 \leq t < 2\pi$  (Fig. 9.4.1).

(c) Square with round corners  $x^4 + y^4 = 1$  (Fig. 9.4.2).

(d) Limaçon  $r = a - \cos \theta$ ,  $a = 1.5, 2$ ,  $0 \leq \theta < 2\pi$  (Fig. 9.6.1).

(e) Bean-shaped curve (Fig. 12.5.4)

$$z = 2.25 [0.2 \cos s + 0.1 \cos 2s - 0.1 \\ + i (0.35 \sin s + 0.1 \sin 2s - 0.02 \sin 4s)], \quad -\pi \leq s \leq \pi.$$

(f) Two hyperbolic arcs of Problem 12.7.4 (Fig. 12.7.2).

(h) Quadrilateral of Problem 12.7.5 (Fig. 12.7.3).

(i) Octagonal curve of Problem 12.7.6 (Fig. 12.7.4).

PROBLEM 6.7.2. Show that Green's function for the upper half-plane  $D = \{\Im\{z\} \geq 0\}$  is given by

$$\mathcal{G}(z, z_0) = \log \left| \frac{z + \bar{z}_0}{z - z_0} \right|.$$

(Wayland, 1970, p.333.)

NOTES. cs633.nb

```

<<Graphics`ImplicitPlot`
f[x_,y_,a_]:= ((x-1/2)^2+(y-a)^2)*(1-y^2-(x-1/2)^2)-1/10;
ImplicitPlot[f[x,y,1]== 0, {x, -1, 2}];
ImplicitPlot[f[x,y,0.5]== 0, {x, -1, 2}];
ImplicitPlot[f[x,y, 0.3]== 0, {x, -1, 2}];
ImplicitPlot[f[x,y,0.2746687749]== 0, {x, -1, 2}];
(* Plot at a=infinity *)
ImplicitPlot[1-y^2-(x-1/2)^2 == 0, {x, -1, 2}]

(* To find Green's function for a=1, by A. Buzing *)
N[NSolve[f[0.5,y,1]== 0,y], 10];
N[NSolve[f[0.8,y,1]== 0, y],10];
N[NSolve[f[1.2,y,1]== 0, y],10];
N[NSolve[f[x,0,1]== 0, x],10]

(* Seven points on the boundary *)
points = {
{0.5, -0.9872580108}, {0.5, 0.6034331769},
{0.8, -0.9402428315}, {0.8, 0.6558861255},
{1.2, -0.6929674261}, {1.2, 0.5972261642},
{1.474003746, 0} };
r[l_] := Sqrt[ (l[[1]]-0.5)^2+l[[2]]^2]
radii = Map[r, points] th[l_] := ArcTan[ l[[1]]-0.5, l[[2]] ];
theta = Map[th, points];
rhs = Map[(Log[#]/(2*Pi))&, radii];
lhs = Table[ If[j==1,
1,
If[j>1 && j<5,
radii[[i]]^(j-1)*Cos[theta[[i]]*(j-1)],
radii[[i]]^(j-4)*Sin[theta[[i]]*(j-4)] ]
], {i,1,7},{j,1,7}];
coeff = LinearSolve[lhs, rhs];
GreensFunction[rr_,tt_] :=
(Log[1/rr]/(2*Pi))+
coeff[[1]]+Sum[rr^k * coeff[[k+1]] * Cos[k*tt],{k,1,3}]
- Sum[rr^k * coeff[[k+4]] * Sin[k*tt], {k,1,3}];
GreensFunction[rr,tt]

(* fp=f'(0)=e^(-0.0431944) *)

```

```
fp = Exp[-0.0431944]


$$\text{cs634.nb}$$

<<Graphics`ImplicitPlot`
f[a_] := ((x+a)^2+y^2)*((x-a)^2)+y^2== 1;
ImplicitPlot[f[0], {x, -1.5, 1.5}];
ImplicitPlot[f[0.5], {x, -1.5, 1.5}];
ImplicitPlot[f[0.9], {x, -1.5, 1.5}];
ImplicitPlot[f[0.99], {x, -1.5, 1.5}];
ImplicitPlot[f[1], {x, -1.5, 1.5}];
```

REFERENCES USED: Andersen et al. (1962), Carrier, Krook and Pearson (1966), Gaier (1964), Kantorovich and Krylov (1958), Goluzin (1969), Lawrentjew and Schabat (1965), Muskhelishvili (1948, 1992), Nehari (1952), Koppenfels (1959), Wayland (1970).

# Chapter 7

---

## Integral Equation Methods

---

We shall discuss certain integral equations that arise in the problem of computing the function  $w = f(z)$  that maps a simply connected region  $D$ , with boundary  $\Gamma$  and containing the origin, conformally onto the interior or exterior of the unit circle  $|w| = 1$ . In the case when  $\Gamma$  is a Jordan contour, we obtain Fredholm integral equations of the second kind  $\phi(s) = \pm \int_{\Gamma} N(s, t) \phi(t) dt + g(s)$ , where  $\phi(s)$ , known as the boundary correspondence function, is to be determined and  $N(s, t)$  is the Neumann kernel. We shall discuss an iterative method for numerical computation of the Lichtenstein–Gershgorin equation and present the case of a degenerate kernel and also of the Szegő kernel. The case when  $\Gamma$  has a corner yields Stieltjes integral equations and is presented in Chapter 12.

---

### 7.1. Neumann Kernel

Let  $\Gamma : z = \gamma(s)$ ,  $0 \leq s \leq L$ , be a Jordan contour with continuously turning tangent and positive orientation with respect to a simply connected region  $D = \text{Int}(\Gamma)$ . We say that  $\Gamma$  belongs to the class  $\Gamma'_{\alpha}$  (and write  $\Gamma \in \Gamma'_{\alpha}$ ) if  $z'(s)$  satisfies a Hölder condition of order  $\alpha$ ,  $0 < \alpha \leq 1$ . Similarly,  $\Gamma \in \Gamma''_{\alpha}$  if  $z''(s)$  satisfies a Hölder condition of order  $\alpha$ . We assume that  $w = f(z)$  maps the region  $D$  univalently onto the unit disk  $|w| < 1$ , such that a point  $z_0 \in D$  goes into  $w = 0$  and a boundary point  $z = e^{i\theta}$  goes into a point  $w = e^{i\phi}$ . The

Neumann kernel  $N(s, t)$  is defined for  $t \neq s$  by

$$N(s, t) = \frac{\sin(\tau - \theta_s)}{\pi r_{st}} = \frac{1}{\pi} \frac{\partial}{\partial t} \theta_s(t) = -\frac{1}{\pi} \frac{\partial r_{st}}{\partial n_t}, \quad (7.1.1)$$

where  $\tau = \tau(t)$  is the tangent angle,  $\theta_s = \theta_s(t) = \arg\{\gamma(t) - \gamma(s)\}$ ,  $r_{st} = |\gamma(t) - \gamma(s)|$ , and  $n_t$  is the interior normal at  $\gamma(t)$  (Fig. 7.1.1).

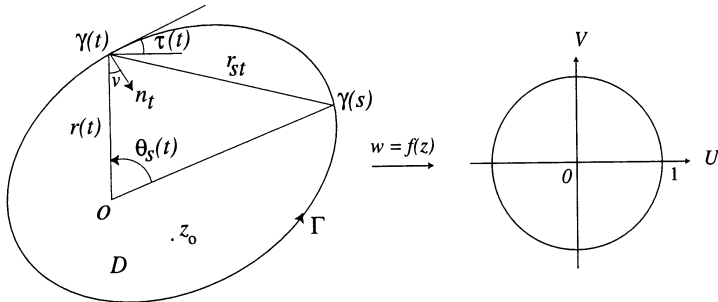


Fig. 7.1.1.

This kernel first appeared in the solution of the Dirichlet problem by Carl Neumann (1877). Some of its properties are as follows:

1.  $N(s, t)$  is continuous for  $t \neq s$ , but, in general, it is not bounded as  $t \rightarrow s$ .
2. If  $\Gamma \in \Gamma'_\alpha$ , then  $N(s, t) |s - t|^{1-\alpha}$  and  $\frac{\partial}{\partial s} N(s, t) |s - t|^{2-\alpha}$  are bounded for  $0 \leq s, t \leq L$ .
3. If  $\Gamma \in \Gamma''_\alpha$ , then  $\frac{\partial}{\partial s} N(s, t) |s - t|^{1-\alpha}$  is bounded for  $0 \leq s, t \leq L$ .
4. If  $\Gamma$  has a continuous curvature, then for every  $s_0$

$$\lim_{s, t \rightarrow s_0, s_0} N(s, t) = \frac{1}{2} \kappa(s_0), \quad (7.1.2)$$

where  $\kappa(s_0)$  is the curvature of  $\Gamma$  at the point  $\gamma(s_0)$ .

5. The kernel is normalized by

$$\int_{\Gamma} N(s, t) dt = 1, \quad \text{or} \quad \int_{\Gamma} N(t, s) dt = -1, \quad (7.1.3)$$

since an application of the formula (1.2.9) to  $f(z) \equiv 1$  gives

$$1 = \frac{1}{\pi} \int_{\Gamma} \frac{\sin(\tau - \theta_s)}{r_{st}} dt - \frac{i}{\pi} \int_{\Gamma} \frac{\cos(\tau - \theta_s)}{r_{st}} dt. \quad (7.1.4)$$

The integral in (7.1.3) takes a Cauchy p.v.

6. From (7.1.1) we have

$$\begin{aligned}\frac{\partial}{\partial s} N(s, t) &= \frac{1}{\pi} \frac{\partial}{\partial s} \frac{\partial}{\partial t} \arg\{\gamma(t) - \gamma(s)\} = \frac{1}{\pi} \frac{\partial}{\partial t} \frac{\partial}{\partial s} \arg\{\gamma(t) - \gamma(s)\} \\ &= \frac{1}{\pi} \frac{\partial}{\partial t} \frac{\partial}{\partial s} \arg\{\gamma(s) - \gamma(t)\} = \frac{\partial}{\partial t} N(t, s),\end{aligned}\tag{7.1.5}$$

where  $\frac{\partial}{\partial s} \frac{\partial}{\partial t} = \frac{\partial}{\partial t} \frac{\partial}{\partial s}$  is permitted because these mixed derivatives exist and are continuous for  $t \neq s$ .

The proofs of these properties can be constructed as in Gaier (1964, p.4). This kernel plays an important role in certain integral equations that arise in conformal mapping.

Let  $\delta$  denote the length of  $\Gamma$ . Then for all functions  $f(s) \in C[0, L]$ , the quadratic functional

$$\langle f, f \rangle = \int_{\Gamma} \int_{\Gamma} f(s) f(t) \log \frac{\delta}{r_{st}} ds dt,\tag{7.1.6}$$

is positive-definite. For a fixed  $\delta$  we introduce the Hilbert space  $H$  which is obtained by completing the set of all functions  $f(s) \in C[0, L]$  with the norm  $\|f(s)\|^2$  defined by (7.1.6). Let  $T$  denote an operator on  $H$  such that for a continuous function  $f(t) \in H$

$$T f = \int_{\Gamma} N(s, t) f(t) dt.\tag{7.1.7}$$

The kernel  $N(s, t)$  can be made symmetric by  $\log \frac{\delta}{r_{st}}$ . Thus,

$$M(s, t) = \int_{\Gamma} N(s, x) \log \frac{\delta}{r_{st}} dx\tag{7.1.8}$$

is symmetric, i.e.,  $M(s, t) = M(t, s)$ . This implies that the operator  $T$  is hermitian:  $\langle T f, g \rangle = \langle f, T g \rangle$ . It can also be shown that  $T$  is a completely continuous operator on  $H$ . This means that if  $\lambda_i$ ,  $i = 1, 2, \dots$ , denote all eigenvalues of an equation  $\phi = \lambda T \phi$ , where each  $\lambda_i$  is counted according to its multiplicity, and if  $h_i$  is a set of associated eigenfunctions such that  $\langle \phi_i, \phi_j \rangle = \delta_{ij}$ , where  $\delta_{ij}$  is the Kronecker delta, then

$$\lambda_1 = 1 < |\lambda_2| \leq |\lambda_3| \leq \dots,\tag{7.1.9}$$

and

$$\frac{1}{|\lambda_2|} \leq \sup \frac{\langle T\phi, \phi \rangle}{\|\phi\|} \quad (7.1.10)$$

for all  $\phi \in H$  with  $\langle \phi, \phi_1 \rangle = 0$ , which implies that  $\int_{\Gamma} \phi(s) ds = 0$  since  $\phi_1(s) = \text{const.}$

---

## 7.2. Interior Regions

First, we shall derive the three following integral equations when the function  $w = f(z)$  maps  $\text{Int}(\Gamma)$  conformally onto the unit disk  $|w| < 1$ .

**7.2.1. Lichtenstein's Integral Equation.** Let  $w = f(z)$ ,  $f(0) = 0$ , map a simply connected region  $D$  conformally onto the unit disk  $|w| < 1$  such that a boundary point  $z = e^{i\theta}$  goes into a boundary point  $w = e^{i\phi}$ . We shall consider the function

$$F(z) = \log \frac{f(z)}{z}, \quad (7.2.1)$$

which is analytic in  $D$  and continuous on  $\bar{D}$ , where

$$\arg\{F(z)\} = \arg\{f(e^{i\theta})e^{-i\theta}\} = \phi(s) - \theta(s).$$

An application of Cauchy's formula (1.2.9) on  $F(z)$  yields

$$\log \frac{f(z)}{z} = \frac{1}{i\pi} \int_{\Gamma} \log \frac{f(\zeta)}{\zeta} \frac{d\zeta}{\zeta - z}, \quad z \in \Gamma. \quad (7.2.2)$$

If we set  $\zeta = \gamma(t)$ ,  $z = \gamma(s)$ , then  $\frac{d\zeta}{\zeta - z} = \frac{e^{i(\phi(t) - \theta_s(t))}}{r_{st}} dt$ . Thus, equating the imaginary parts on both sides of (7.2.2), we obtain

$$\begin{aligned} \phi(s) - \theta(s) &= \frac{1}{\pi} \int_{\Gamma} [\phi(s) - \theta(s)] \frac{\sin [\phi(t) - \theta_s(t)]}{r_{st}} dt \\ &\quad + \frac{1}{\pi} \int_{\Gamma} \log r(t) \frac{\cos [\phi(t) - \theta_s(t)]}{r_{st}} dt, \end{aligned}$$

which gives *Lichtenstein's integral equation*

$$\phi(s) - \theta(s) = \frac{1}{\pi} \int_{\Gamma} N(s, t) [\phi(t) - \theta(t)] dt + g(s), \quad (7.2.3)$$

where

$$g(s) = \frac{1}{\pi} \int_{\Gamma} \log r(t) \frac{\cos [\phi(t) - \theta_s(t)]}{r_{st}} dt, \quad (7.2.4)$$

and  $r(t) = |\gamma(t)|$ . The integrals in (7.2.3) and (7.2.4) take Cauchy p.v.'s. The integral equation (7.2.3), derived by Lichtenstein (1917), is periodic in the angular deformation  $\phi(s) - \theta(s)$ .

**7.2.2. Gershgorin's Integral Equation.** Let  $D'$  denote the region obtained from  $D$  by indenting a disk  $B(0, \varepsilon)$  whose boundary is denoted by  $\Gamma'$  (Fig. 7.2.1). The function  $F(z)$ , with  $F(\gamma(0+)) = i\phi(0)$ , is single-valued on  $D'$ . Then, in view of (1.2.9), for  $z = \gamma(s)$ ,  $s \neq 0$ , we have

$$\log f(z) = \frac{1}{i\pi} \int_{\Gamma + \Gamma'} \frac{\log f(\zeta)}{\zeta - z} d\zeta. \quad (7.2.5)$$

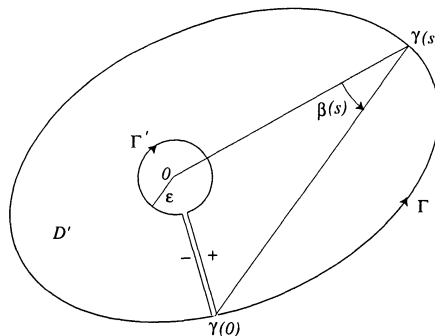


Fig. 7.2.1.

Since  $|f(\zeta)| \leq A|\zeta|$ , where  $A > 0$  is a constant, the contribution of the integral over  $\Gamma'$  is of order  $O(\varepsilon \log \varepsilon) = o(1)$ . Also, along the cut the integral has the value  $\log f(z^+) = \log f(z^-) - 2i\pi$ . Thus, as  $\varepsilon \rightarrow 0$ , the integral along the cut approaches  $-2i\pi \frac{1}{i\pi} \int_{\zeta=0}^{\zeta=\gamma(0)} \frac{d\zeta}{\zeta - z}$ , whose imaginary part is equal

to  $-2 \arg \left\{ \frac{\gamma(0) - \gamma(s)}{0 - \gamma(s)} \right\} = -2\beta(s)$  (see Fig. 7.2.1). Hence, equating the imaginary parts on both sides of (7.2.5) we get

$$\phi(s) = \Im \left\{ \frac{1}{i\pi} \int_{\Gamma} \frac{i\phi(t) \cdot e^{i(\phi(t) - \theta_s(t))}}{r_{st}} dt \right\} - 2\beta(s)$$

or

$$\phi(s) = \int_{\Gamma} N(s, t) \phi(t) dt - 2\beta(s). \quad (7.2.6)$$

This is known as *Gershgorin's integral equation* (Gershgorin, 1933).

**7.2.3. Carrier's Integral Equation.** Carrier (1947) considered the problem when  $w = f(z)$  maps the region  $D$  conformally onto  $|w| < 1$  such that two interior points  $P$  and  $Q$  in  $D$  go into two points  $w = \pm a$ ,  $0 < a < 1$ , respectively, i.e.,  $f(P) = a$  and  $f(Q) = -a$ . The function  $f(z)$  and the quantity  $a$  are uniquely determined. In fact, if we consider the function

$$F(z) = \log \left\{ \frac{f(z) - a}{f(z) + a} - \frac{f(z) - a^{-1}}{f(z) + a^{-1}} \right\} - i\pi \quad (7.2.7)$$

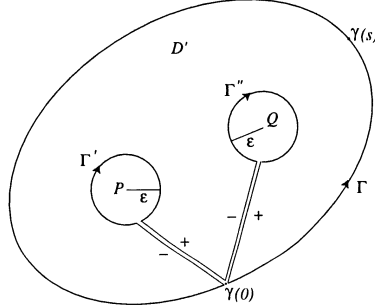


Fig. 7.2.2.

in the region  $D'$  bounded by  $\Gamma$ ,  $\Gamma'$  and  $\Gamma''$  (Fig. 7.2.2), then, in the case when the boundary of  $D'$  is a Jordan contour (i.e., it has no corners), we find by (1.2.9) that

$$\begin{aligned} F(z) &= \frac{1}{i\pi} \int_{\Gamma+\Gamma'+\Gamma''} \frac{F(\zeta)}{\zeta - z} d\zeta, \quad z = \gamma(s), \quad s \neq 0, \\ &= \frac{1}{i\pi} \int_{\Gamma} \frac{F(\zeta)}{\zeta - z} d\zeta - 2 \int_{\zeta=P}^{\zeta=\gamma(0)} \frac{d\zeta}{\zeta - z} + 2 \int_{\zeta=Q}^{\zeta=\gamma(0)} \frac{d\zeta}{\zeta - z} \quad (7.2.8) \\ &\equiv I_1 + I_2 + I_3, \end{aligned}$$

because the value of  $F(z)$  is given by  $F(z^+) = F(z^-) - 2i\pi$  along the cut from  $P$  to  $\gamma(0)$ , and by  $F(z^+) = F(z^-) + 2i\pi$  along the cut from  $Q$  to  $\gamma(0)$ . Since  $I_1 + I_2 = 2 \log \left| \frac{P - \gamma(s)}{Q - \gamma(s)} \right|$  which is real, we find that  $\Im\{F(z)\} = 0$  for  $z \in \Gamma$ . In fact, on  $|w| = 1$ , we have from (7.2.7)

$$\arg \left\{ \frac{w-a}{w+a} \cdot \frac{w-a^{-1}}{w+a^{-1}} \right\} = \pi.$$

Hence, taking  $\Phi(s) = \Re\{F(z)\}$ , we find from (7.2.8) that

$$\Phi(s) = \int_{\Gamma} N(s, t) \Phi(t) dt + 2 \log \left| \frac{P - \gamma(s)}{Q - \gamma(s)} \right|, \quad s \neq 0, \quad (7.2.9)$$

which is known as *Carrier's integral equation*. This equation describes the problem of the potential flow of an inviscid fluid past a periodic array of airfoils of arbitrary shape (more on this problem in Chapter 10).

---

### 7.3. Exterior Regions

Although the problem of conformally mapping the region  $\text{Ext}(\Gamma)$  onto  $|w| > 1$  can be reduced to that of the interior regions of §7.2 by applying the reflection principle (§1.4), the following direct method produces faster converging results in numerical computations. As before, we assume that  $\Gamma$  is a Jordan contour, the arc length  $s$  is measured in the positive sense, and at  $z = \infty$  the mapping function has the series representation

$$f_E(z) = A z + a_0 + \frac{a_1}{z} + \frac{a_2}{z^2} + \cdots, \quad A > 0. \quad (7.3.1)$$

First, as in §7.2.1, by considering the function  $F(z) = \log \frac{f_E(z)}{z}$  and applying the formula (1.2.11), we obtain the integral equation

$$\phi_E(s) - \theta(s) = - \int_{\Gamma} N(s, t) [\phi_E(t) - \theta(t)] dt - g(s). \quad (7.3.2)$$

Secondly, as in §7.2.2, we consider the function  $F(z) = \log f_E(z)$ . Then, for a fixed  $z = \gamma(s)$ ,  $s \neq 0$ , and sufficiently large  $R > 0$ , we consider the

region between  $\Gamma$  and the circle  $|\zeta - z| = R$  with a cut from the point  $z = a$  to  $z = \gamma(s) + R = \zeta_R$  (Fig. 7.3.1). Let  $\Gamma^*$  denote the boundary of the resulting simply connected region. Obviously,  $F(z^-) = F(z^+) + 2i\pi$ , so that by (1.2.11) we have

$$\begin{aligned} \log f_E(z) &= -\frac{1}{i\pi} \int_{\Gamma^*} \frac{\log f_E(\zeta)}{\zeta - z} d\zeta \\ &= -\frac{1}{i\pi} \int_{\Gamma} \frac{\log f_E(\zeta)}{\zeta - z} d\zeta - 2 \int_{\zeta=a}^{\zeta=\zeta_R} \frac{d\zeta}{\zeta - z} \\ &\quad + \frac{1}{i\pi} \int_{|\zeta-z|=R} \frac{\log f_E(\zeta)}{\zeta - z} d\zeta \\ &\equiv I_1 + I_2 + I_3. \end{aligned} \quad (7.3.3)$$

Note that  $\Im\{I_2\} = 2[\arg\{(z-a) - \pi\}]$ . Since, in view of (7.3.1), with  $\zeta - z = Re^{i\phi_E}$ ,

$$\frac{1}{i\pi} \int_{|\zeta-z|=R} \log \frac{f_E(\zeta)}{\zeta - z} \frac{d\zeta}{\zeta - z} = 2 \log A,$$

which is real, we get

$$\Im\{I_3\} = \Im \left\{ \frac{1}{i\pi} \int_{|\zeta-z|=R} \frac{\log(\zeta - z)}{\zeta - z} d\zeta \right\} = 2\pi.$$

Hence, equating the imaginary parts on both sides of (7.3.3), we obtain the integral equation

$$\phi_E(s) = - \int_{\Gamma} N(s, t) \phi_E(t) dt + 2 \arg\{\gamma(s) - a\}. \quad (7.3.4)$$

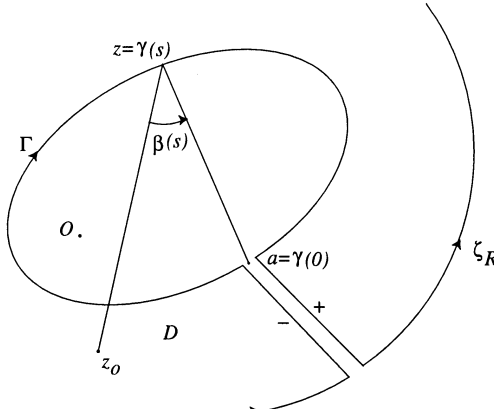


Fig. 7.3.1.

If  $f_E(z_0) = \infty$  for a finite point  $z_0 \in D$  and  $f_E(\infty) = \rho_\infty e^{i\varphi_\infty}$ , then the mapping of  $D$  onto  $|w| > 1$  is univalent only if  $f_E(a) = 1$ . In this case we obtain the integral equation

$$\phi_E(s) = - \int_{\Gamma} N(s, t) \phi_E(t) dt + 2 \arg\{\beta(s) - \varphi_\infty\}. \quad (7.3.5)$$

For the external regions under consideration, Eqs (7.3.2) and (7.3.5) are analogues of the integral equations (7.2.3) and (7.2.6).

Now we shall derive two integral equations for  $\phi'_E(s)$ , one from (7.3.4) and the other from (7.2.6). These integral equations will involve the kernel  $N(t, s)$  which is conjugate to the Neumann kernel  $N(s, t)$ . These equations are interesting from a numerical standpoint. As opposed to  $\phi_E(s)$ , the function  $\phi'_E(s)$  is periodic with period  $L$ , and hence, an application of the quadrature formula to  $\phi'_E(s)$  increases computational precision.

**7.3.1. Banin's Integral Equation.** Let  $\Gamma \in \Gamma'_\alpha$  be a Jordan contour. If the function  $f_E(z)$ , with the series expansion (7.3.1) at  $z = \infty$ , maps  $\text{Ext}(\Gamma)$  conformally onto  $|w| > 1$ , then we can rewrite (7.3.4) as

$$\phi_E(s) = - \int_{\Gamma} N(s, t) [\phi_E(t) - \phi_E(s)] dt - \phi_E(s) + 2 \arg\{\gamma(s) - a\}. \quad (7.3.6)$$

Since  $|\phi_E(t) - \phi_E(s)| = O(|t - s|)$ , and  $|t - s|^{2-\alpha} \left| \frac{\partial}{\partial s} N(s, t) \right|$  is bounded by property 2 of §7.1, we find after differentiating (7.3.6) with respect to  $s$  that

$$\phi'_E(s) = - \int_{\Gamma} \frac{\partial}{\partial s} N(s, t) [\phi_E(t) - \phi_E(s)] dt + 2 \arg\{\gamma(s) - a\}, \quad (7.3.7)$$

where the differentiation under the integral sign is justified in view of the Lebesgue convergence theorem. Then, using (7.1.5) and integrating (7.3.7), we get

$$\begin{aligned} \phi'_E(s) &= - \int_{\Gamma} \frac{\partial}{\partial t} N(t, s) [\phi_E(t) - \phi_E(s)] dt + 2 \frac{\partial}{\partial s} \arg\{\gamma(s) - a\} \\ &= -N(0, s) [\phi_E(L) - \phi_E(0)] + \int_{\Gamma} N(t, s) \phi'_E(t) dt \\ &\quad + 2 \frac{\partial}{\partial s} \arg\{\gamma(s) - a\} \\ &= -\frac{1}{\pi} \frac{\partial}{\partial s} \theta_0(s) \cdot 2\pi + \int_{\Gamma} N(t, s) \phi'_E(t) dt + 2 \frac{\partial}{\partial s} \arg\{\gamma(s) - a\}, \end{aligned}$$

which yields *Banin's integral equation*

$$\phi'_E(s) = \int_{\Gamma} N(t, s) \phi'_E(t) dt, \quad (7.3.8)$$

since  $\frac{\partial}{\partial s} \theta_0(s) = \arg\{\gamma(s) - \gamma(0)\}$ .

**7.3.2. Warschawski–Stiefel's Integral Equation.** If we apply the method outlined above in §7.3.1 to Gershgorin's integral equation (7.2.6), we obtain the following integral equation:

$$\phi'_E(s) = - \int_{\Gamma} N(t, s) \phi'_E(t) dt + 2 \frac{d\theta(s)}{ds}, \quad (7.3.9)$$

which was established independently by Warschawski (1955) and Stiefel (1956). If we set  $\tau(s) = \phi_E(s) - \theta(s)$  in (7.3.9), then the integral equation for  $\tau'(s)$  is

$$\tau'(s) = - \int_{\Gamma} N(t, s) \tau'(t) dt + k(s), \quad (7.3.10)$$

where

$$k(s) = - \int_{\Gamma} N(t, s) \theta'(t) dt + \theta'(s). \quad (7.3.11)$$

**7.3.3. Interior and Exterior Maps.** In §7.2 we have considered the problem of determining the mapping function  $w = f(z)$  which maps the region  $D = \text{Int}(\Gamma)$  univalently onto the unit disk  $U = \{|w| < 1\}$  such that  $f(0) = 0$  and  $f'(0) > 0$ . In §7.3.1 and 7.3.2 we have considered the problem of finding the mapping function  $w = f_E(z)$  which maps the region  $D^* = \text{Ext}(\Gamma)$  univalently onto the region  $U^* = \{|w| > 1\}$  such that  $f_E(\infty) = \infty$  and  $\lim_{z \rightarrow \infty} f'_E(z) > 0$ . These two problems are related to each other by the inversion transformation  $z \mapsto z^{-1}$ , which transforms the boundary  $\Gamma$  into a Jordan contour  $\hat{\Gamma}$  and maps  $D$  onto  $\hat{D}^* = \text{Ext}(\hat{\Gamma})$  and  $D^*$  onto  $\hat{D} = \text{Int}(\hat{\Gamma})$ . Let  $\hat{f}$  and  $\hat{f}_E$  be the interior and exterior univalent maps associated with  $\hat{\Gamma}$ . Then

$$\begin{aligned} f_E(z) &= \left\{ \hat{f}(z^{-1}) \right\}^{-1}, \\ f(z) &= \left\{ \hat{f}_E(z^{-1}) \right\}^{-1}. \end{aligned} \quad (7.3.12)$$

Hence, there is no need to consider the interior and exterior mappings as separate problems. From the computational point of view, it is convenient first

to determine  $f(z)$  and then use the relations (7.3.12) to compute  $f_E(z)$ . But in integral equation methods it is advantageous to determine  $f(z)$  and  $f_E(z)$  separately.

In each case the conformal maps are determined from the respective boundary correspondence function  $\phi(s)$  and  $\phi_E(s)$ .

---

## 7.4. Iterative Method

As seen from §7.2 and 7.3, the function  $\phi(s) = \arg\{f(\gamma(s))\}$ ,  $0 \leq s \leq L$ , in general, satisfies the integral equation

$$\phi(s) = \lambda \int_0^L N(s, t) \phi(t) dt + g(s), \quad (7.4.1)$$

where  $\lambda = 1$  corresponds formally to the integral equations (7.2.3), (7.2.6) and (7.2.9) for the interior regions, whereas  $\lambda = -1$  corresponds to equations (7.3.8) and (7.3.10) for the exterior regions. We shall present an iterative scheme for the numerical solution of Eq (7.4.1) for  $\lambda = 1$ ; the case  $\lambda = -1$  can be handled by similar iterations. Note that  $\lambda = 1$  is the smallest eigenvalue of the kernel  $N(s, t)$ . The associated eigenfunction for the homogeneous equation (7.4.1) is a constant. The eigenfunction for the conjugate kernel  $N(t, s)$  is the equilibrium distribution  $\mu(t)$  with  $\int_{\Gamma} \mu(t) dt = 1$ . Since  $\lambda = 1$  is the only simple pole of  $N(s, t)$  on  $|\lambda| = 1$  and its principal part at this pole is  $\frac{\mu(t)}{1 - \lambda}$ , the function

$$\gamma(s, t; \lambda) = \sum_{i=1}^{\infty} \lambda^i [N_{i+1}(s, t) - \mu(t)], \quad (7.4.2)$$

where  $N_{i+1}(s, t)$  denote the iterated kernels with  $N_1(s, t) = N(s, t)$ , is analytic for  $|\lambda| < |\lambda_2|$ , where  $\lambda_2$  is the next eigenvalue close to 1 ( $|\lambda_2| > 1$ ). Then the series

$$\sum_{i=1}^{\infty} \lambda^i [N_{i+1}(s, t) - \mu(t)]$$

converges for  $|\lambda| < |\lambda_2|$ . Since  $\int_0^L g(t) \mu(t) dt = 0$ , by the Fredholm theory, it follows that the Neumann series

$$\sum_{i=1}^{\infty} \lambda^i [N_{i+1}(s, t) - \mu(t)] + g(s) \quad (7.4.3)$$

converges for  $|\lambda| < |\lambda_2|$ , and for  $\lambda = 1$  it represents a solution  $\phi(s)$  of Eq (7.4.1). The main result due to Warschawski (1956) is the following:

**THEOREM 7.4.1.** *Let  $\Gamma \in \Gamma'_\alpha$ ,  $0 < \alpha \leq 1$ . Suppose that  $\phi_0(t) \in C[0, L]$  and that  $\phi_0(L) - \phi_0(0) = 2\pi$ . Then the iterations  $\phi_n(s)$  defined by*

$$\phi_{n+1}(s) = \int_{\Gamma} N(s, t) \phi_n(t) dt + g(s), \quad n = 0, 1, 2, \dots, \quad (7.4.4)$$

*converge uniformly to the solution  $\phi(s)$  of Eq (7.4.1) with  $\lambda = 1$ , such that  $\int_{\Gamma} \phi(s) \mu(s) ds = \int_{\Gamma} \phi_0(s) \mu(s) ds$ . More precisely,*

$$|\phi_{n+1}(s) - \phi_n(s)| \leq \frac{1}{\pi |\lambda_2|^n} \|N(s, t)\| \|\phi'_0 - \phi'\| \sqrt{\frac{\lambda_2^2}{\lambda_2^2 - 1}}. \quad (7.4.5)$$

In fact, by the Schwarz inequality,

$$\|\phi'_0 - \phi'\| \leq \sqrt{\int_{\Gamma} \int_{\Gamma} \left( \log \frac{\delta}{r_{st}} \right)^2 ds dt} \cdot \sqrt{\int_{\Gamma} (\phi'_0 - \phi')^2 dt}.$$

The factor  $\|\phi'_0 - \phi'\|$  in the error estimate (7.4.5) must be small which happens when  $\max_{0 \leq s \leq L} |\phi'_0 - \phi'|$  is small or when  $\int_{\Gamma} (\phi'_0(t) - \phi'(t)) dt$  is small. Thus, the factor  $\|\phi'_0 - \phi'\|$  in the error estimate (7.4.5) plays a useful role.

To prove the uniform convergence of the iterations  $\phi_n(s)$  to the solution  $\phi(s)$ , it suffices to assume that  $\phi(s)$  exists and satisfies the condition  $\int_{\Gamma} g(s) \phi(s) ds = 0$ , and that  $\phi_n(s) \in C[0, L]$  for all  $n = 0, 1, 2, \dots$ , where  $\phi_0(L) - \phi_0(0) = 2\pi$ . Then

$$|\phi_{n+1}(s) - \phi_n(s)| \leq \frac{1}{\pi |\lambda_2|^{n-1}} \|N(s, t)\| \|\phi'_1 - \phi'_0\| \sqrt{\frac{\lambda^2}{\lambda^2 - 1}}, \quad (7.4.6)$$

which leads to the solution

$$\phi(s) = \phi_0(s) + \sum_{n=0}^{\infty} [\phi_{n+1}(s) - \phi_n(s)]. \quad (7.4.7)$$

**ESTIMATES FOR  $|\lambda_2|$ :** The inequality (7.4.6) gives an estimate for the rate of convergence. A result on the convergence of the derivatives  $\phi'_n(s)$ , which is due to Warschawski (1956), is as follows:

**THEOREM 7.4.2.** *If  $\Gamma \in \Gamma''_\alpha$ ,  $0 < \alpha \leq 1$ , then the derivatives  $\phi'_n(s)$  converge uniformly to  $\phi'(s)$ ,  $0 \leq s \leq L$ . More precisely, the following estimate holds:*

$$|\phi_{n+1}(s) - \phi_n(s)| \leq \frac{1}{\pi |\lambda_2|^{n-1}} \left\| \frac{\partial N(s, t)}{\partial s} \right\| \sqrt{\frac{\lambda_2^2}{\lambda_2^2 - 1}}. \quad (7.4.8)$$

Let  $\Gamma_0$  be a Jordan contour and  $N_0(s, t)$  denote the associated Neumann kernel. Suppose that the second eigenvalue  $\Lambda_2$  of  $N_0(s, t)$  is known. For example, for an ellipse  $b^2x^2 + a^2y^2 = a^2b^2$ ,  $\Lambda_2 = \frac{a+b}{a-b}$ ; for a circle  $x^2 + y^2 = a^2$ ,  $\Lambda_2 = \infty$ . Then estimates for  $\lambda_2$  can be given in terms of  $\Lambda_2$  in the following cases:

(a) Let  $\Gamma_0$  be close to  $\Gamma \in \Gamma''_\alpha$ ,  $0 < \alpha \leq 1$ , in the sense that either  $\Gamma_0 \subset \text{Int } \Gamma$  or  $\Gamma \subset \text{Int } \Gamma$ . The former situation corresponds to the case of the interior regions (§7.2) when  $w = f(z)$  maps  $\text{Int } (\Gamma)$  onto the unit disk  $|w| < 1$ , whereas the latter corresponds to the case of the exterior regions (§7.3) when  $w = f(z)$  maps  $\text{Ext } (\Gamma)$  onto the unit disk  $|w| > 1$  such that  $z = \infty$  goes into  $w = \infty$ . Let

$$q = \frac{\max_{|w|=1} |f'(z)|}{\min_{|w|=1} |f'(z)|}, \quad \text{and} \quad M = \int_{\Gamma} \left\| \frac{\partial N(s, t)}{\partial t} \right\|^2 dt.$$

If  $d$  is the Fréchet distance\* of  $\Gamma$  and  $\Gamma_0$ , then

$$c_1 \leq \frac{1}{|\lambda_2|} \leq \frac{1}{\Lambda_2} + a d \lambda_2^2, \quad (7.4.9)$$

where  $a = 2 q M / \pi$ , and  $c_1$  is the real root of the cubic equation  $d a x^3 + x / \Lambda_2 = 1$ .

(b) Let  $\Gamma \in \Gamma''_\alpha$  and  $\Gamma_0 \in \Gamma'_\alpha$ , and let contours  $\Gamma$  and  $\Gamma_0$  have the same length  $\delta$ . Suppose that for some choice of the points corresponding to  $s = 0$  on each contour

$$\begin{aligned} \int_{\Gamma} \int_{\Gamma} (N(s, t) - N_0(s, t))^2 ds dt &= \varepsilon^2, \\ \int_{\Gamma} \int_{\Gamma} \left( \log \frac{1}{r_{st}} - \log \frac{1}{\rho_{st}} \right)^2 ds dt &= \nu^2, \end{aligned}$$

---

\*See (1.1.20) for its definition.

where  $\rho_{st} = |z_0(s) - z_0(t)|$ ,  $N_0(s, t)$  is the Neumann kernel associated with  $\Gamma_0$ , and  $z_0(s)$  is the parametric representation of  $\Gamma_0$  in terms of the arc length parameter  $s$ ,  $0 \leq s \leq L$ . Then

$$c_2 \leq \frac{1}{|\lambda_2|} \leq \frac{1}{\Lambda_2} + \frac{a \lambda^2}{2\pi} \left[ \nu^2 \left( \frac{1}{\lambda_2} + \frac{1}{\Lambda_2} \right) + \varepsilon B \right], \quad (7.4.10)$$

where  $B = \sqrt{\int_{\Gamma} \int_{\Gamma} \left( \log \frac{1}{\rho_{st}} \right)^2 ds dt}$ ,  $c_2$  is the real root of the cubic equation

$$\left( \frac{a \delta}{2\pi \Lambda_2} + \varepsilon B \right) x^3 + \frac{a \delta}{2\pi} x^2 + \frac{x}{\Lambda_2} = 1,$$

and  $a$  is the same as in (7.4.9).

(c) If  $\Gamma \in \Gamma'_\alpha$  for  $1/2 < \alpha < 1$ , i.e.,  $\Gamma$  is the boundary of a nearly circular region, then

$$\frac{1}{\lambda_2} \leq \frac{1}{2} \left[ \int_{\Gamma} N_2(s, t) ds - 1 \right], \quad (7.4.11)$$

where, by the Schwarz inequality,

$$N_2(s, t) = \int_{\Gamma} \int_{\Gamma} N(s, x) N(x, t) dx ds \leq \int_{\Gamma} \int_{\Gamma} N^2(s, x) dx ds,$$

and

$$\frac{1}{\lambda_2^2} \leq \frac{1}{2} \left[ \int_{\Gamma} \int_{\Gamma} N^2(s, x) dx ds - 1 \right] = \frac{1}{2} \left[ \int_{\Gamma} \int_{\Gamma} \left( N(s, x) - \frac{1}{\delta} \right)^2 dx ds \right]. \quad (7.4.12)$$

Since the kernel  $N_0(s, t) = \frac{1}{\delta}$  for a circle of circumference  $\delta$ , the condition that the last integral in (7.4.12) be less than unity implies that  $\Gamma$  is a near circle.

(d) Neumann's lemma states that if  $\Gamma$  is a convex Jordan contour, then  $N(s, t) \geq 0$  and there exists a constant  $\kappa$ ,  $0 < \kappa < 1$ , known as the *Neumann constant*, which depends only on  $\Gamma$  and has the following property: Let  $g^*(s) = \int_{\Gamma} N(s, t) g(t) dt$ , where the function  $g(t)$  is bounded and integrable on  $\Gamma$ ,  $0 \leq t \leq L$ . Let  $m \leq g(t) \leq M$  on  $[0, L]$  and  $m^* \leq g^*(s) \leq M^*$  on  $[0, L]$ . Then

$$M^* - m^* \leq (M - m)(1 - \kappa). \quad (7.4.13)$$

A Jordan contour is said to be *nearly convex* if it satisfies the following criterion: There exists a convex Jordan contour  $\Gamma_0$  such that (i)  $\Gamma_0$  has the same length as  $\Gamma$ , and (ii) if  $N(s, t)$  and  $N_0(s, t)$  are the kernels associated with  $\Gamma$  and  $\Gamma_0$ , respectively, then for all  $s \in [0, L]$

$$\int_{\Gamma} |N(s, t) - N_0(s, t)| dt \leq \varepsilon < \kappa.$$

If  $\Gamma$  is nearly convex, and if  $\phi_0(s) \in C[0, L]$  is an arbitrary function, then the iterations (7.4.4) satisfy the inequality

$$|\phi_{n+1}(s) - \phi_n(s)| \leq (1 + \varepsilon) V (1 + \varepsilon - \kappa)^n, \quad (7.4.14)$$

where  $V$  is a constant;  $V \leq \omega_0 + 2\pi$ , and  $\omega_0$  is the oscillation of  $\phi_0(s)$  in  $[0, L]$ . If  $\phi_0(s)$  is nondecreasing and  $\omega_0 = 2\pi$ , then  $V = 2\pi$ . Finally, if  $\phi_0(s)$  is an approximation of the solution of Eq (7.4.1), i.e., if it is known a priori that  $|\phi_0(s) - \phi(s)| \leq \eta$ ,  $0 \leq s \leq L$ , for some solution of (7.4.1), then  $V \leq 2\eta$ . If  $\Gamma_0$  is a circle, then  $\kappa = 1$ . The Neumann constant  $\kappa$  characterizes a nearly circular region in a manner different from that presented in Chapter 5.

For computational purposes, the best method for numerically solving the integral equation (7.4.1) is to discretize the integral and replace the equation by a matrix equation. Thus, the problem becomes one of matrix inversion. To do this, we partition the boundary  $\Gamma$  into  $n$  parts at the points

$$t_j = j \frac{L}{n}, \quad j = 0, 1, \dots, n, \quad (t_0 = t_n),$$

and obtain for the values  $\phi(t_j)$  of  $\phi(s)$  at the  $n$  points  $t_k = kL/n$ ,  $k = 1, 2, \dots, n$ , the following system of  $n$  linear equations where the integral in (7.4.1) is replaced by a sum:

$$\phi(t_k) = \sum_{j=1}^n N(t_k, t_j) \phi(t_j) \frac{L}{n} + g(t_k),$$

or

$$\sum_{j=1}^n [\delta_{jk} - N(t_k, t_j)] \phi(t_j) = \frac{n}{L} g(t_k). \quad (7.4.15)$$

In practical applications, since the boundary  $\Gamma$  cannot be divided into partitions of equal length, it is useful to take more partition points on those portions of  $\Gamma$  where the curvature is positive and larger. This is accomplished by transforming

the arc length parameter  $t$  into an integration variable  $\tau$  such that  $t = \psi(\tau)$ ,  $s = \psi(\sigma)$ ,  $\psi'(\tau) > 0$ ,  $0 \leq s, t \leq L$ ,  $0 \leq \tau \leq l$ , and  $\psi(\tau)$  is small (large) according as the curvature is large (small). This substitution transforms Eq (7.4.1) into

$$\phi(\psi(\tau)) = \int_0^l N^*(\sigma, \tau) \phi^*(\tau) d\tau + g^*(\sigma), \quad (7.4.16)$$

which, after discretization with partitions of equal length in  $\tau$ , yields the matrix equation

$$\sum_{j=1}^n [\delta_{jk} - N^*(\sigma_k, \tau_j)] \phi^*(\tau_j) = \frac{n}{L} g^*(\tau_k), \quad (7.4.15')$$

which is similar to (7.4.15).

In this method the matrix inversion is of  $O(n^3)$ , which becomes considerably large if  $n$  is large. To overcome this difficulty, an iterative method is used where the computations are of order  $O(mn^2)$ ,  $m$  being the number of iterations. This iteration starts with a function  $\phi(s) = \phi_0(s)$ , called the initial guess, that is taken close to the correct solution. Then, with this function the right side of Eq (7.4.1) is computed, which yields

$$\phi_1(s) = \int_0^L N(s, t) \phi_0(t) dt + g(s),$$

and the iterative process is repeated  $n$  times. It leads to Eq (7.4.4) for  $n = 1, 2, \dots$ , which, by Theorem 7.4.1, converges uniformly to the solution  $\phi(s)$ .

In numerical computation, the rate of convergence is fast only if the region  $D$  is nearly circular, i.e., if it can be approximated in polar coordinates by the function  $r = r(\theta)$ ,  $0 \leq \theta \leq 2\pi$ ,  $r(0) = r(2\pi)$ , which belongs to the class  $C^2[0, 2\pi]$ , is almost constant for all  $\theta$ , i.e.,  $r(\theta) \approx \text{const}$ , and has a small first derivative  $r'(\theta) \ll 1$ . Thus, the algorithm for solving Eq (7.4.1) is as follows:

1. Check if  $\Gamma$  is a Jordan contour with no corners. In case  $\Gamma$  has corners, they should be first analyzed by the methods of Chapter 12.
2. Use elementary conformal mapping (like, log, exp, sin, cos functions) to make the region  $D$  “circular” (see Fig. 7.4.1).
3. Carry out the iterations (7.4.4) using the discretized formula (7.1.15) or (7.1.16).
4. Stop the iterations when the difference  $|\phi_m(s) - \phi_{m-1}(s)| < \varepsilon$ , where

$\varepsilon > 0$  is a preassigned quantity (called the tolerance).

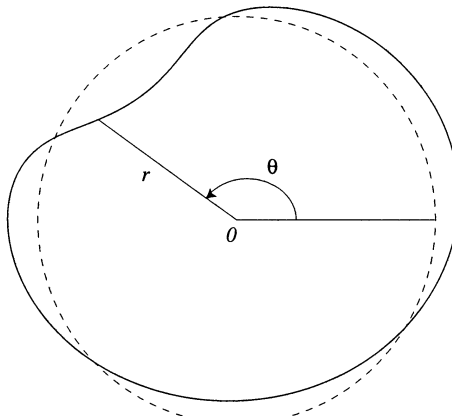


Fig. 7.4.1.

If  $c$  denotes the rate of convergence, i.e., if it is the largest number greater than unity such that

$$|\phi_{n+1}(s) - \phi_n(s)| \leq \frac{1}{c} |\phi_n(s) - \phi_{n-1}(s)|$$

for all  $s$  and  $n$ , then an upper bound for the error made by taking  $\phi_m(s) \approx \phi(s)$  is given by

$$|\phi(s) - \phi_m(s)| \leq \frac{\varepsilon}{c} + \frac{\varepsilon}{c^2} + \dots = \frac{\varepsilon}{c-1}. \quad (7.4.17)$$

The value of  $c$  may be approximately estimated during the iteration process. Since  $c > 1$ , we find from (7.4.17) that the error is smaller than  $\varepsilon$ . However, in the entire computation, besides this error, we have the discretization as well as round-off errors.

The eigenvalue  $\lambda_1$  is important in numerical computations. Ahlfors (1952) has given a simple estimate for  $1/\lambda_1$  which is called the convergence factor. If the boundary  $\Gamma$  is defined in polar coordinates, as above, by  $r = r(\theta)$  and if  $v_0 = \max v$ , where  $v$  is the angle between the radius vector and the normal (Fig. 7.1.1), then the Ahlfors estimate is given by

$$\lambda_1 \geq \frac{1}{\sin v_0}. \quad (7.4.18)$$

This estimates for an ellipse  $E$ , defined in the  $z$ -plane by

$$x = a \cos t, \quad y = b \sin t, \quad 0 \leq t \leq 2\pi, \quad (7.4.19)$$

with foci  $\pm 1$ , semi-axes  $a$  and  $b$ ,  $a > b$ ,  $a^2 - b^2 = 1$ , and axes-ratio  $k = a/b$ , and for Cassini's oval  $|z^2 - 1| = k$  (see §6.3) are given below (Andersen et al., 1962, p.190):

FOR THE ELLIPSE:

$$k = 1.2 : \csc v_0 = 5545, \text{ and } C = -11.0,$$

$$k = 1.6 : \csc v_0 = 2282, \text{ and } C = -4.4,$$

$$k = 2.0 : \csc v_0 = 1667, \text{ and } C = -3.0.$$

FOR CASSINI'S OVAL:

$$k = 1.2 : \csc v_0 = 1.2, \text{ and } C = -2.0,$$

$$k = 2.0 : \csc v_0 = 2.0, \text{ and } C = -3.8,$$

$$k = 5.0 : \csc v_0 = 5.0, \text{ and } C = -10.0,$$

where  $|C|$  denotes the rate of convergence which is sufficiently large for nearly circular regions. The negative sign for  $C$  indicates that the iterations "oscillate".

CASE STUDY 7.4.1. Let  $\Gamma$  be the boundary of an ellipse  $E$  defined in the  $z$ -plane by (7.4.19). It is well known that the function  $2z = w + w^{-1}$  maps the circle  $|w| = R = a + b$ ,  $R > 1$ , conformally onto  $E$ . Then the function  $f(z)$ , which is univalent in  $\text{Int}(E)$  and  $|f(z)| = 1$  on  $E$ , is regular in  $\text{Int}(E)$  (real at  $z = 0$ ) and maps the ellipse  $E$  conformally onto the circle  $|w| = R$  such that it satisfies (Szegö, 1950)

$$\log \frac{f(z)}{z} = \log \frac{2}{R} + \sum_{n=1}^{\infty} \frac{(-1)^n}{n} \frac{2R^{-2n}}{R^{2n} + R^{-2n}} T_{2n}(z), \quad (7.4.20)$$

where  $T_n(z) = \frac{w^n + w^{-n}}{2}$  are the Chebyshev polynomials of the first kind.

(a) To prove that the function  $w = f(z)$  maps  $\text{Int}(E)$  univalently onto  $|w| < R$ , we shall use the argument principle and show that as  $z$  goes around the ellipse  $E$ , the point  $w$  describes the circle  $|w| = R$  exactly once and in the same direction, i.e.,  $\frac{d}{d\phi} \Im \{\log f(z)\} > 0$ . We find from (7.4.20), with  $w = Re^{i\phi}$ , that

$$\begin{aligned} \Im \{\log f(z)\} &= \Im \{\log z\} + \sum_{n=1}^{\infty} \frac{(-1)^n}{n} \frac{2R^{-2n}}{R^{2n} + R^{-2n}} \Im \{T_{2n}(z)\} \\ &= \Im \left\{ \log \frac{Re^{i\phi} + R^{-1}e^{-i\phi}}{2} \right\} \\ &\quad + \sum_{n=1}^{\infty} \frac{(-1)^n}{n} \frac{2R^{-2n}}{R^{2n} + R^{-2n}} \frac{R^{2n} - R^{-2n}}{2} \sin 2n\phi. \end{aligned}$$

Thus,

$$\begin{aligned}\frac{d}{d\phi} \Im \{\log f(z)\} &= \Im \left\{ \frac{i (R e^{i\phi} - R^{-1} e^{-i\phi})}{R e^{i\phi} + R^{-1} e^{-i\phi}} \right\} \\ &\quad + 2 \sum_{n=1}^{\infty} (-1)^n \frac{R^{2n} - R^{-2n}}{R^{2n} + R^{-2n}} R^{-2n} \cos 2n\phi \\ &\equiv A_1 + A_2.\end{aligned}$$

Since  $A_1 = \Re \left\{ \frac{1 - R^{-2} e^{-2i\phi}}{1 + R^{-2} e^{-2i\phi}} \right\} = 1 + 2 \sum_{n=1}^{\infty} (-1)^n R^{-2n} \cos 2n\phi$ , we get

$$\begin{aligned}\frac{d}{d\phi} \Im \{\log f(z)\} &= A_1 + A_2 = 1 + 2 \sum_{n=1}^{\infty} (-1)^n R^{-2n} \cos 2n\phi \\ &\quad + 2 \sum_{n=1}^{\infty} (-1)^n \frac{R^{2n} - R^{-2n}}{R^{2n} + R^{-2n}} R^{-2n} \cos 2n\phi \\ &= 1 + 2 \sum_{n=1}^{\infty} (-1)^n \frac{2}{R^{2n} + R^{-2n}} \cos 2n\phi \\ &= \lim_{\rho \rightarrow 1^-} \left\{ 1 + 2 \sum_{n=1}^{\infty} (-1)^n \frac{2\rho^n}{R^{2n} + R^{-2n}} \cos 2n\phi \right\}.\end{aligned}$$

If we define  $R^2 = e^{\alpha\pi}$ , then since  $\int_0^\infty \frac{\cos \alpha x}{\cosh(x/2)} dx = \frac{\pi}{\cosh \alpha\pi}$ , we have for  $n = 0, 1, \dots$

$$\frac{2}{R^{2n} + R^{-2n}} = \frac{2}{e^{n\alpha\pi} + e^{-n\alpha\pi}} = \frac{1}{\cosh n\alpha\pi} = \frac{1}{\pi} \int_0^\infty \frac{\cos n\alpha x}{\cosh(x/2)} dx.$$

Hence,

$$\begin{aligned}1 + 2 \sum_{n=1}^{\infty} (-1)^n \frac{2\rho^n}{R^{2n} + R^{-2n}} \cos 2n\phi &= \frac{1}{\pi} \int_0^\infty \frac{1}{\cosh(x/2)} \left( 1 + 2 \sum_{n=1}^{\infty} (-\rho)^n \cos n\alpha x \cos 2n\phi \right) dx \\ &= \frac{1}{2\pi} \int_0^\infty \frac{1}{\cosh(x/2)} \left( \frac{1 - \rho^2}{1 + 2\rho \cos(\alpha x + 2\phi) + \rho^2} \right. \\ &\quad \left. + \frac{1 - \rho^2}{1 + 2\rho \cos(\alpha x - 2\phi) + \rho^2} \right) dx > 0,\end{aligned}$$

by (6.4.9) and (6.4.10).

(b). We shall determine the exact solution for the boundary map  $f(z)$ . Let  $w = e^{i(\pi/2-x)} = i e^{-ix}$ , and  $z = \cos(\pi/2 - x) = \sin x$ . Then

$$\log \frac{f(z)}{z} = \log \frac{2}{R} + \sum_{n=1}^{\infty} \frac{1}{n} \frac{2 R^{-2n}}{R^{2n} + R^{-2n}} \cos 2nx.$$

Since

$$\begin{aligned} \sum_{n=1}^{\infty} \frac{1}{n} \frac{2 R^{-2n}}{R^{2n} + R^{-2n}} \cos 2nx &= \log \operatorname{sn} \left( \frac{2Kx}{\pi}, k \right) - \log \left( 2q^{1/4} \right) \\ &\quad + \frac{1}{2} \log k - \log \sin x, \end{aligned}$$

(see Whittaker and Watson, 1927, p.509, Ex. 3), where  $q = R^{-4}$ ,  $\operatorname{sn}$  is a Jacobian elliptic function of modulus  $k$ ,  $0 < k < 1$  (see §2.3), we find that

$$f(z) = \sqrt{k} \operatorname{sn} \left( \frac{2Kx}{\pi}, k \right) = \sqrt{k} \operatorname{sn} \left( \frac{2K}{\pi} \sin^{-1} z, k \right), \quad (7.4.21)$$

which is the Schwarz formula.

(c) For the interior regions (§7.2) the boundary correspondence function is given by

$$\begin{aligned} \phi(t) &= \arg\{f(z)\} = \arg\{z\} + \sum_{n=1}^{\infty} \frac{(-1)^n}{n} R^{-2n} \frac{R^{4n} - 1}{R^{4n} + 1} \sin 2nt \\ &= \tan^{-1} \left\{ \frac{(R^2 - 1)^2 - 2 \cos^2 t}{(R^2 + 1)^2 - 2 \sin^2 t} \tan t \right\} - 2 \sum_{n=1}^{\infty} \frac{(-1)^n}{n} R^{-2n} \frac{\sin 2nt}{R^{4n} + 1}. \end{aligned} \quad (7.4.22)$$

If we set  $L_j = 2 \sum_{n=j}^{\infty} \frac{(-1)^n}{n} R^{-2n} \frac{\sin 2nt}{R^{4n} + 1}$ , then

$$|L_j| \leq \frac{2R^6}{R^6 - 1} \frac{1}{jR^{6j}}, \quad (7.4.23)$$

and the function  $\phi(t)$ , defined by (7.4.22), can be approximated by

$$\phi(t) \approx \phi_j(t)$$

$$= \tan^{-1} \left\{ \frac{(R^2 - 1)^2 - 2 \cos^2 t}{(R^2 + 1)^2 - 2 \sin^2 t} \tan t \right\} - 2 \sum_{n=1}^{j-1} \frac{(-1)^n}{n} R^{-2n} \frac{\sin 2nt}{R^{4n} + 1}, \quad (7.4.24)$$

with an error (uniform in  $t$ ,  $0 \leq t \leq 2\pi$ ) given by (7.4.23). In computations  $j$  in (7.4.24) is usually estimated so that

$$\frac{2R^6}{R^6 - 1} \frac{1}{j R^{6j}} < 10^{-12}.$$

Thus,  $j$  becomes larger, the closer  $R$  is taken to 1. Todd and Warschawski (1955) have taken the minimum value of  $R$  in their computations as  $R = \sqrt{1.5}$ ; then  $j = 22$ . The function actually computed is  $\phi_{22} - \pi$  for the values of  $t = 0^\circ$  ( $3^\circ$ )  $90^\circ$ . Since these values are symmetric about the  $y$ -axis, they are extended in other quadrants. Then the results obtained by computation from (7.4.24) are compared with those from (7.4.21).

(d) In the case of exterior regions (§7.3),  $\phi(t) = t$ . Note that  $\lambda_2 = \frac{a+b}{a-b}$  for the ellipse  $E$ . The function

$$\mathcal{G}(z, 0) = \Re \left\{ \log \frac{1}{f(z)} \right\} = \log \frac{1}{|f(z)|}$$

is Green's function of  $\text{Int}(E)$  with respect to the origin. ■

**CASE STUDY 7.4.2.** We shall determine the correspondence between the boundaries in the case of mapping the ellipse  $E$ , defined by (7.4.19), onto the unit circle. The boundary correspondence function  $\phi$  is normalized so that the origin is preserved and  $\phi(0) = -\pi$ . Using the parameter  $t$  instead of the arc length  $s$ , we find from (7.4.19) that

$$\frac{ds}{dt} = \sqrt{a^2 \sin^2 t + b^2 \cos^2 t} = b \sqrt{k^2 \sin^2 t + \cos^2 t}.$$

Then, Gershgorin's integral equation (7.2.6) can be written as

$$\phi(\tau) = \frac{1}{\pi} \int_0^{2\pi} N(\tau, t) \phi(t) dt + g(\tau), \quad (7.2.25)$$

where

$$g(\tau) = -2 \beta(s(\tau)) = 2 \tan^{-1} \left\{ \frac{k \sin \tau}{k^2 (\cos \tau - \cos^2 \tau) - \sin^2 \tau} \right\}, \quad (7.4.26)$$

and

$$\begin{aligned}
 N(\tau, t) &= \frac{k/2}{\sqrt{k^2 \sin^2 \frac{t-\tau}{2} + \left[ k^2 \sin t \sin \frac{t-\tau}{2} + \cos t \cos \frac{t-\tau}{2} \right]^2}} \\
 &\quad \times \sqrt{\frac{k^2 \sin^2 t + \cos^2 t}{k^2 \sin^2 \frac{t-\tau}{2} + \cos^2 \frac{t-\tau}{2}}} \\
 &= \frac{k}{(k^2 + 1) - (k^2 - 1) \cos(t + \tau)}. \tag{7.4.27}
 \end{aligned}$$

The branch of arctan in (7.4.26) is chosen such that  $g(0) = \lim_{\tau \rightarrow 0^+} g(\tau) = -\pi$  and  $g(2\pi) = \lim_{\tau \rightarrow 2\pi^-} g(\tau) = \pi$ . Since  $\phi(2\pi - \tau) = -\phi(\tau)$ , we can write Eq (7.4.25) as

$$\begin{aligned}
 \phi(\tau) &= \frac{k}{\pi} \int_0^\pi \left[ \frac{k_1 \phi(t)}{1 - k_2 \cos(t + \tau)} - \frac{k_1 \phi(t - \tau)}{1 + k_2 \cos(t + \tau)} \right] dt \\
 &\quad + 2 \tan^{-1} \left\{ \frac{\sin \tau}{k(1 - \cos \tau)(k_3 \cos \tau - k^{-2})} \right\}, \tag{7.4.28}
 \end{aligned}$$

where

$$k_1 = \frac{1}{k^2 + 1}, \quad k_2 = \frac{k^2 - 1}{k^2 + 1}, \quad k_3 = 1 - \frac{1}{k^2}.$$

Eq (7.4.28) can be represented in the operator form as

$$\phi(\tau) = T \phi + g(\tau), \tag{7.4.29}$$

where  $T$  is the integral operator in (7.4.28) and  $g(\tau)$  is the arctan term. If the initial guess is taken as  $\phi_0 = g(\tau)$ , then the iterations

$$\phi_{n+1}(\tau) = T \phi_n + g(\tau), \tag{7.4.30}$$

lead to the equation

$$\phi_{n+1} = g_0 + g_1 + \cdots + g_n, \quad g_0 = g, \quad T g_n = g_{n+1}. \tag{7.4.31}$$

Thus, first we must compute  $\phi_0 = g(\tau)$ , and then compute the integrals  $T g_n$  which are replaced by an appropriate approximate quadrature. For  $k = 1.2$  Todd and Warschawski (1955) found that at a fixed  $t$  the functions  $g(\tau)$  and  $N(\tau, t)$  behave approximately like  $g(\tau) \approx 1.5(1 + \cos \tau)$  and  $N(\tau, t) \approx$

$0.5 + 0.1 \cos \tau$ . Weddle's rule was used for quadrature (see Birkoff et al., 1950, 1951). The results for  $\phi_n$  for  $k = 1.2$  are computed against  $t$  at a step-size of  $3^\circ$  from  $t = 0^\circ$  to  $t = 180^\circ$  and presented in Fig. 7.4.2 ( $t$  along the horizontal axis). Similar computations can also be carried out for  $k = 2$  and 5. The results match the exact value given by (7.4.22). These computations, though carried out for an ellipse, are well suited for other types of nearly circular regions.

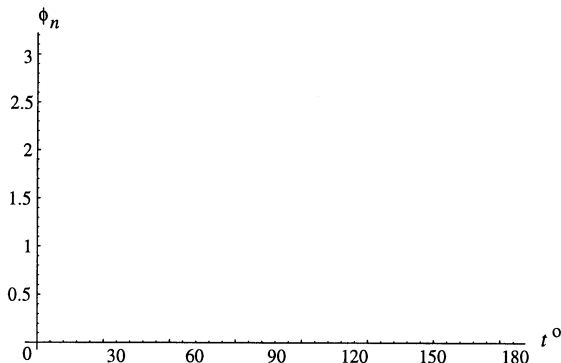


Fig. 7.4.2.

CASE STUDY 7.4.3. The integral equation for the dipole distribution is given by

$$\mu(s) = \int_0^L N(s, t) \mu(t) dt + g(s), \quad (7.4.32)$$

where the dipole strength on the boundary  $\Gamma$  is  $2\pi \mu(s)$ ,  $g(s)$  denotes the boundary value of the potential function, and  $t$ ,  $0 \leq t \leq L$ , is the arc length parameter along the positive direction of  $\Gamma$ . The integral equation (7.4.32) has the same form as (7.4.1). Let us assume that the distribution  $\mu(s)$  has already been determined by solving Eq (7.4.25). Then the Dirichlet problem and hence the problem of conformal mapping is reduced to that of quadratures. To see this, note that the potential  $u(P)$  at a point  $P = (x, y) \in D$  is given by

$$u(P) = \int_0^L N(P, t) \mu(t) dt, \quad (7.4.33)$$

where  $N(P, t) = -\frac{\partial}{\partial n_t} r_{Pt}$  (Fig. 7.4.3). The kernel  $N(P, t)$  becomes unbounded as  $P$  approaches the boundary  $\Gamma$ . To avoid this difficulty, we proceed

as follows: Consider a point  $P'$  near  $\Gamma$  (Fig. 7.4.3). Let  $t'$  be a point on  $\Gamma$  such that the normal  $n_{t'}$  passes through the point  $P'$ . Then, we can rewrite (7.4.33) as

$$\begin{aligned} u(P) &= \mu(t') + \int_0^L N(P, t) [\mu(t) - \mu(t')] dt \\ &= \mu(t') + \int_{-L/2}^{L/2} N(P, t + t') [\mu(t + t') - \mu(t')] dt, \end{aligned} \quad (7.4.34)$$

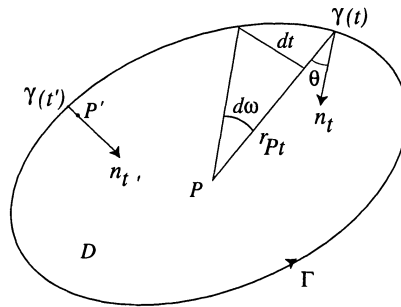


Fig. 7.4.3.

where  $t$  is replaced by  $t' + t$ , and  $N(P, t' + t) = -\frac{\partial}{\partial n_{t'+t}} r_{Pt}$ . The integral in (7.4.34) is finite for all  $t$ , and  $\mu(t' + t) - \mu(t') \approx t \mu'(t')$  for numerically small values of  $t$ . Then (7.4.34) can be written as

$$\begin{aligned} u(P) &= \mu(t') - \int_{-L/2}^{L/2} \left\{ [\mu(t' + t) - \mu(t')] \frac{\partial}{\partial n_{t'+t}} r_{Pt} \right. \\ &\quad \left. + [\mu(t' - t) - \mu(t')] \frac{\partial}{\partial n_{t'-t}} r_{Pt} \right\} dt, \end{aligned} \quad (7.4.35)$$

since  $\int_0^L \frac{\partial}{\partial n_t} r_{Pt} = \int_0^{2\pi} d\omega = 2\pi$ , and  $\int_0^L \frac{\partial}{\partial n_t} \log r_{Pt} = \int_0^\pi d\omega = \pi$  for  $\gamma(s) \in \Gamma$  (Fig. 7.4.3). ■

CASE STUDY 7.4.4. If  $U$  and  $U^*$  denote the region  $|z| < 1$  and  $|z| > 1$ , respectively,  $z = e^{i\theta}$ , and if  $D = \text{Int}(\Gamma)$ , as before, then for certain curves the following data is useful (Gaier, 1964, p.264):

1. Eccentric circle in the  $w$ -plane: Let  $D : |w - a| < b$ ,  $b > a > 0$ . Then

$$\Gamma : \rho = \rho(\phi) = a \cos \phi + \sqrt{b^2 - a^2 \sin^2 \phi};$$

$$\text{Mapping } D \mapsto U : z = \frac{b w}{a w + b^2 - a^2};$$

$$\text{Boundary correspondence function : } \tan \theta = \frac{\sin \phi}{c \rho(\phi) + \cos \phi}, c = \frac{a}{b^2 - a^2}.$$

2. Inverted ellipses: The region  $D$  is formed by inverting the exterior of the ellipse with half-axes  $1/p$  and  $1$  into the unit circle.

$$\text{Mapping } U \mapsto D : w = \frac{2 p z}{(1+p) + (1-p) z^2};$$

$$\Gamma : \rho = \rho(\phi) = \sqrt{1 - (1-p)^2 \cos^2 \phi}, 0 < p < 1;$$

$$\text{Boundary correspondence function : } \tan \phi = p \tan \theta.$$

3. Ellipses, with boundary  $\Gamma : z = a \cos t + i b \sin t, a^2 - b^2 = 1$ ;

For the mapping  $\text{Int}(\Gamma) \mapsto U$ , the boundary correspondence function is defined by (7.4.22);

For the mapping  $\text{Ext}(\Gamma) \mapsto U^*$ , the boundary correspondence function is defined by  $\phi(t) = t$ .

The boundary correspondence function determines the correspondence between the boundaries of the two regions where one is the problem region and the other the image region. It is denoted by  $\phi$  when a given simply connected region in the  $z$ -plane is mapped onto a region in the  $w$ -plane ( $z = r e^{i\theta} \mapsto w = \rho e^{i\phi}$ , which is the notation used in this book), but by  $\theta$  if  $w = \rho e^{i\phi} \mapsto z = r e^{i\theta}$ . This function is usually normalized in so that the origin is preserved. ■

## 7.5. Degenerate Kernel

A kernel is said to be degenerate if it can be represented in the semi-discrete form of a finite sum of products. A degenerate Neumann kernel can be expressed as

$$N(s, t) = \sum_{k=1}^n \alpha_k(s) \beta_k(t), \quad (7.5.1)$$

where it is assumed that the functions  $\alpha_k(s)$  are linearly independent. Otherwise the number of terms in the expression for the kernel in (7.5.1) would reduce. For such a kernel we can determine a complete solution of the Fredholm integral

equation of the form

$$\phi(s) = \lambda \int_0^L N(s, t) \phi(t) dt + g(s). \quad (7.5.2)$$

Let us assume the required solution of Eq (7.5.2) with  $\lambda = 1$  in the form

$$\phi(s) = g(s) + \sum_{i=1}^n A_i \alpha_i(s), \quad (7.5.3)$$

where  $A_i$  are constants yet to be determined. We shall use the notation:

$$\int_0^L \beta_i(t) g(t) dt = f_i, \quad \int_0^L \alpha_i(t) \beta_j(t) dt = b_{j,i}. \quad (7.5.4)$$

Then substituting (7.5.3) for  $\phi(s)$  in Eq (7.5.2), we get

$$\begin{aligned} \sum_{i=1}^n A_i \alpha_i(s) - \lambda \int_0^L \left( \sum_{i=1}^n \alpha_i(s) \beta_i(t) \right) g(t) dt \\ - \lambda \int_0^L \sum_{i=1}^n \sum_{j=1}^n A_j \alpha_i(s) \beta_i(t) \alpha_j(t) dt = 0. \end{aligned} \quad (7.5.5)$$

Equating the coefficients of  $\alpha_i(s)$  and using the notation (7.5.4), we find that

$$A_i - \lambda \sum_{j=1}^n A_j b_{i,j} = \lambda f_i, \quad i = 1, 2, \dots, n. \quad (7.5.6)$$

The determinant of the system (7.5.6) in the unknowns  $A_i$  is

$$D(\lambda) = \begin{vmatrix} 1 - \lambda b_{1,1} & -\lambda b_{1,2} & \cdots & -\lambda b_{1,n} \\ -\lambda b_{2,1} & 1 - \lambda b_{2,2} & \cdots & -\lambda b_{2,n} \\ \cdots & \cdots & \cdots & \cdots \\ -\lambda b_{n,1} & -\lambda b_{n,2} & \cdots & 1 - \lambda b_{n,n} \end{vmatrix}. \quad (7.5.7)$$

Then, by Cramer's rule,

$$A_i = \lambda \frac{\sum_{k=1}^n D_{i,k} f_k}{D(\lambda)}, \quad i = 1, 2, \dots, n, \quad (7.5.8)$$

where  $D_{i,k}$  is the algebraic complement of the  $k$ -th row and  $i$ -th column. Hence, from (7.5.3) the approximate solution  $\tilde{\phi}(s)$  of Eq (7.5.2) is given by

$$\begin{aligned}\tilde{\phi}(s) &= g(s) + \lambda \sum_{i=1}^n \frac{\sum_{k=1}^n D_{i,k} f_k}{D(\lambda)} \alpha_i(s) \\ &= g(s) + \lambda \frac{\sum_{k=1}^n \left( \sum_{i=1}^n D_{i,k} \alpha_i(s) \right) \int_0^L \beta_k(t) g(t) dt}{D(\lambda)} \\ &= g(s) + \lambda \int_0^L \frac{\sum_{k=1}^n \sum_{i=1}^n D_{i,k} \alpha_i(s) \beta_k(t)}{D(\lambda)} g(t) dt \\ &= g(s) + \lambda \int_0^L \frac{D(s, t, \lambda)}{D(\lambda)} g(t) dt,\end{aligned}\tag{7.5.9}$$

where

$$D(s, t, \lambda) = \sum_{i=1}^n \sum_{k=1}^n D_{i,k} \alpha_i(s) \beta_k(t).\tag{7.5.10}$$

Thus, the resolvent  $\gamma(s, t, \lambda)$  of Eq (7.5.2) is given by

$$D(s, t, \lambda) = \frac{D(s, t, \lambda)}{D(\lambda)}.\tag{7.5.11}$$

In practical applications an arbitrary kernel  $N(s, t)$  can be replaced approximately by a degenerate kernel  $\tilde{N}(S, t)$ , which will help solve the resulting approximate equation

$$\tilde{\phi}(s) - \lambda \int_0^L \tilde{N}(s, t) \tilde{\phi}(t) dt = g(s),\tag{7.5.12}$$

rather than the original equation (7.5.2). A suitable degenerate kernel close to the one given in an integral equation can always be found by taking it as a finite part of its Taylor series (as in Case Study 6.5.1 and 6.5.2), of its Fourier series, or by an trigonometric interpolation scheme (see §8.7). An error estimate in replacing the given kernel by an approximate degenerate kernel is contained in the following result:

**THEOREM 7.5.1.** *Given two kernels  $N(s, t)$  and  $\tilde{N}(s, t)$  such that*

$$\int_0^L |N(s, t) - \tilde{N}(s, t)| dt < h,$$

let the resolvent  $\gamma(s, t, \lambda)$  of Eq (7.5.2) satisfy the inequality

$$\int_0^L |\gamma(s, t, \lambda)| dt < B.$$

If the conditions  $|g(s) - \tilde{g}(s)| < \varepsilon$  and  $1 - |\lambda| h(1 + \lambda B) > 0$  are satisfied where  $\tilde{g}(s)$  is an approximation of  $g(s)$ , then Eq (7.5.2) has a unique solution  $\phi(s)$ , and

$$|\phi(s) - \tilde{\phi}(s)| < \frac{M |\lambda| (1 + |\lambda| B)^2}{1 - |\lambda| h(1 + \lambda B)} + \varepsilon (1 + |\lambda| B), \quad (7.5.13)$$

where  $M$  is the maximum modulus of  $g(s)$ .

A proof of this result can be found in Kantorovich and Krylov (1958, p.143), or Berezin and Zhidkov (1965, p.647).

CASE STUDY 7.5.1. (a) Solve the integral equation

$$\phi(s) = \int_0^{1/2} \sin st \phi(t) dt + g(s), \quad (7.5.14)$$

with no assumptions on  $g(s)$  at this time. Expanding  $\sin st$  in its Taylor series we get

$$\sin st = st - \frac{s^3 t^3}{3!} + \frac{s^5 t^5}{5!} - \dots$$

If we replace  $\sin st$  in (7.5.14) by the first two terms of this series expansion, then Eq (7.5.14) reduces to

$$\tilde{\phi}(s) = \int_0^{1/2} \left( st - \frac{s^3 t^3}{6} \right) \tilde{\phi}(t) dt + g(s), \quad (7.5.15)$$

which has an algebraic kernel. We shall assume a solution of the form

$$\tilde{\phi}(s) = as + bs^3 + g(s).$$

Then substituting it in (7.5.12) we get

$$as + bs^3 - sf_1 - s^3 f_2 - \frac{as}{24} - \frac{bs}{160} + \frac{as^3}{768} + \frac{bs^3}{5376} = 0,$$

where

$$f_1 = \int_0^{1/2} t g(t) dt, \quad f_2 = -\frac{1}{6} \int_0^{1/2} t^3 g(t) dt.$$

Equating the coefficients of  $a$  and  $b$  to zero, we obtain

$$\begin{aligned} \frac{23a}{24} - \frac{b}{160} - f_1 &= 0, \\ \frac{a}{160} + \frac{5377b}{5376} - f_2 &= 0, \end{aligned}$$

and

$$\tilde{\phi}(s) = g(s) + as + bs^3 = g(s) + \int_0^{1,2} \gamma(s, t, 1) dt, \quad (7.5.16)$$

where the resolvent  $\gamma(s, t, 1)$  is given by

$$\begin{aligned} \gamma(s, t, 1) &= 1.043277 (1.000186 s t - 0.0010416 s^3 t - 0.0010416 s t^3 \\ &\quad - 0.1597222 s^3 t^3). \end{aligned}$$

Since  $\int_0^{1/2} |\gamma(s, t, 1)| dt < \frac{1}{12}$ , we can take  $B = 1/12$  in the above estimate (7.5.16). Also, since

$$\int_0^{1/2} |N(s, t) - \tilde{N}(s, t)| dt \leq \int_0^{1/2} \frac{s^5 t^5}{120} dt \leq \frac{1}{46080} \left(\frac{1}{2}\right)^5 < \frac{1}{1474560},$$

we can take  $h = \frac{1}{1474560} \approx \frac{3}{4 \cdot 10^6}$ . Then

$$|\phi(s) - \tilde{\phi}(s)| < M \frac{\frac{3}{4 \cdot 10^6} (1 + 1/12)}{1 - \frac{3}{4 \cdot 10^6} (1 + 1/12)} < \frac{M}{10^6}.$$

In particular, if  $g(s) = 1 + \frac{1}{s} \left( \cos \frac{s}{2} - 1 \right) = 1 - \frac{s}{8} + \frac{s^3}{384} - \dots$ , then  $M = 1$ , and the approximate solution is

$$\phi(s) \approx 1 + 0.0000009 s - 0.0000002 s^3,$$

which has an error of  $O(10^6)$ .

(b) To solve the equation

$$\phi(s) = \int_0^1 \sin st \phi(t) dt + g(s), \quad (7.5.17)$$

we take  $\tilde{\phi}(s) = a s + b s^3 + g(s)$ . Then

$$a s + b s^3 = \int_0^1 \left( s t - \frac{s^3 t^3}{6} \right) (a s + b s^3 + g(s)) dt$$

yields the system of equations  $\frac{2a}{3} - \frac{b}{5} - f_1 = 0$ ,  $\frac{a}{30} + \frac{43b}{42} - f_2 = 0$ . The resolvent is

$$\gamma(s, t, 1) = \frac{3225}{2171} s t - \frac{105}{2171} s t^3 - \frac{105}{2171} s^3 t - \frac{350}{2171} s^3 t^3.$$

Since  $\int_0^1 |\gamma(s, t, 1)| dt \leq \frac{445}{668} < 1$ , we take  $B = 1$ . Also, since

$$\int_0^1 |N(s, t) - \tilde{N}(s, t)| dt \leq \frac{1}{720},$$

we take  $h = 1/720$ . Then

$$|\phi(s) - \tilde{\phi}(s)| < M \frac{\frac{1}{720} (2)}{1 - \frac{1}{720} (2)} < \frac{M}{10^3}.$$

In particular, if  $g(s) = 1 + \frac{1}{s} (1 - \cos s) = 1 - \frac{s}{2} + \frac{s^3}{24} - \dots$ , then  $M = 1$ , and the approximate solution is

$$\phi(s) \approx 1 + 0.001545 s,$$

which has an error of  $O(10^3)$ . ■

CASE STUDY 7.5.2. To solve

$$\phi(s) + \int_0^1 s (e^{st} - 1) \phi(t) dt = e^s - s,$$

we take

$$\tilde{N}(s, t) = s (e^{st} - 1) = s^2 t + \frac{1}{2} s^3 t^2 + \frac{1}{6} s^4 t^3.$$

Then we shall solve the equation

$$\tilde{\phi}(s) + \int_0^1 \tilde{N}(s, t) \tilde{\phi}(t) dt = e^s - s,$$

where we have

$$\tilde{\phi}(s) = e^s - s + as^2 + bs^3 + cs^4.$$

Substituting this expression for  $\tilde{\phi}(s)$  into the above equation, we obtain the system

$$\begin{aligned} \frac{5}{4}a - \frac{1}{5}b + \frac{1}{6}c &= -\frac{2}{3}, \\ \frac{1}{5}a - \frac{13}{6}b + \frac{1}{7}c &= \frac{9}{4} - e, \\ \frac{1}{6}a - \frac{1}{7}b + \frac{49}{8}c &= 2e - \frac{29}{5}, \end{aligned}$$

whose solution is  $a = -0.501019$ ,  $b = -0.167126$ ,  $c = 0.0418054$ . Thus

$$\tilde{\phi}(s) = e^s - s - 0.501019 s^2 - 0.167126 s^3 - 0.0418054 s^4.$$

The exact solution of the given equation is  $\phi(s) \equiv 1$ . Note that  $\tilde{\phi}(0) = 1$ ,  $\tilde{\phi}(1/2) = 0.999963$ , and  $\tilde{\phi}(1) = 1.00833$ . ■

## 7.6. Szegö Kernel

Let  $D$  be a bounded simply connected region with a Jordan boundary  $\Gamma$ . The Cauchy kernel

$$H(z, a) = \frac{1}{2i\pi} \frac{1}{z-a} \quad a \in D, \quad (7.6.1)$$

defined by (1.2.3), represents an analytic function  $f(z)$  on  $D$  with

$$f(a) = \frac{1}{2i\pi} \int_{\Gamma} \frac{f(z)}{z-a} dz = \frac{1}{2i\pi} \int_0^L \frac{f(z)}{z-a} \gamma'(s) ds, \quad a \in D, \quad (7.6.2)$$

where  $z = \gamma(s)$ ,  $dz = \gamma'(s) ds$ ,  $0 \leq s \leq L$ , is the parametrization of  $\Gamma$  in terms of the boundary arc  $s$ . The Szegö kernel, defined by (4.3.3), also represents an analytic function  $f$  on  $D$  with

$$f(a) = \int_{\Gamma} S(z, a) f(z), dz, \quad a \in D. \quad (7.6.3)$$

Let  $\mathcal{H}^2(\Gamma)$  denote a closed subspace of  $L^2(\Gamma)$ , containing boundary values of analytic functions on  $D$ , and let  $\mathcal{S} : L^2(\Gamma, ds) \mapsto \mathcal{H}^2(\Gamma)$  denote the orthogonal projection. Then for any  $f \in L^2(\Gamma)$

$$\mathcal{S} f(a) = \int_{\Gamma} S(z, a) f(z), dz, a \in D. \quad (7.6.4)$$

This relation implies (7.6.3) because  $f = \mathcal{S} f$  in (7.6.3). The Szegö kernel coincides with the Cauchy kernel

$$H(z, a) = \frac{1}{2i\pi} \frac{1}{z - a} \gamma'(s), \quad (7.6.5)$$

iff  $D$  is a disk. In fact, the Szegö kernel for the unit disk  $U$ , denoted by  $S_U(z, a)$ , is given by

$$S_U(z, a) = \frac{1}{2\pi} \frac{1}{1 - a\bar{z}}, \quad |a| < 1, |z| = 1. \quad (7.6.6)$$

The following result holds for an analytic function  $f : D \mapsto U$  such that  $f(a) = 0$  and  $f'(a) > 0$  real, where  $a \in D$ . Such a function is called the Riemann mapping function (see Theorem 1.4.1).

**THEOREM 7.6.1.** *For a given  $a \in D$  let an analytic function  $w = f(z)$  be the Riemann mapping function. Then*

$$f'(z) = \frac{2\pi}{S(a, a)} S^2(z, a), \quad z \in D. \quad (7.6.7)$$

**PROOF.** The following transformation connects  $S$  to  $S_U$ :

$$S(z, \zeta) = \sqrt{f'(\zeta)} S_U(f(\zeta), f(z)) \overline{\sqrt{f'(z)}} \quad \text{for } z, \zeta \in D. \quad (7.6.8)$$

Set  $\zeta = a$ . Then  $f(a) = 0$ , and (7.6.6) yields

$$S(z, a) = \frac{1}{2\pi} \sqrt{f'(z)} \overline{\sqrt{f'(a)}},$$

which implies (7.6.7). ■

We use (7.6.7) to compute the Riemann mapping function by the formula

$$f(z) = \frac{1}{i} \frac{f'(z)}{|f'(z)|} \gamma'(s). \quad (7.6.9)$$

This formula is used by Kerzman and Trummer (1986) for numerical computation of  $f(z)$ . Now we shall define the Kerzman–Stein kernel  $A(z, a)$  in terms of the Cauchy kernel by

$$\begin{aligned} A(z, a) &= \bar{H}(z, a) - H(z, a) \in C^\infty(\Gamma \times \Gamma) \\ &= -\frac{1}{2i\pi} \Re \left\{ \frac{\gamma''(s)}{\gamma'(s)} \right\}. \end{aligned} \quad (7.6.10)$$

Note that  $A(z, z) = 0$  since  $\gamma''(s)$  is orthogonal to  $\gamma'(s)$ . Let  $\mathcal{A} : L^2(\Gamma) \mapsto L^2(\Gamma)$  define the integral operator

$$\mathcal{A} f(a) = \int_{\Gamma} A(z, a) f(z) ds, \quad a, z \in \Gamma, z = \gamma(s). \quad (7.6.11)$$

This operator is compact, and  $i\mathcal{A}$  is self-adjoint. The operator  $(1 - \mathcal{A})$  is bijective on  $L^2(\Gamma) \mapsto L^2(\Gamma)$ , and hence it has a bounded inverse  $(1 - \mathcal{A})^{-1} : L^2(\Gamma) \mapsto L^2(\Gamma)$ . The geometric interpretation of the kernel  $A(z, a)$  is as follows: Let both  $z$  and  $a$  lie on a closed contour in  $\Gamma$ , with tangent vectors (complex numbers)  $\gamma'(s)$  and  $\gamma'(t)$ ,  $z = \gamma(s)$  and  $a = \gamma(t)$ , respectively. Then the vector (complex number)  $\overline{\gamma'(s)}$  is the reflection of  $\gamma'(a)$  in the chord joining  $z$  and  $a$  (Fig. 7.6.1). Then

$$A(z, a) = \frac{1}{2i\pi} \frac{1}{z - a} [\gamma'(s) - \gamma'(t)].$$

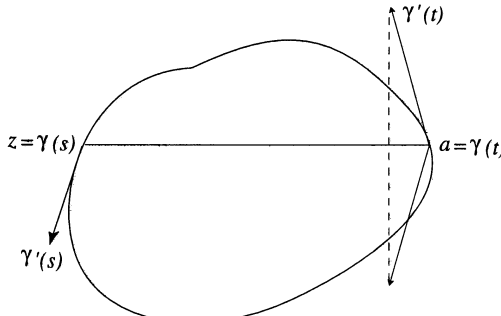


Fig. 7.6.1.

This relation is obvious if  $\arg \{z - a\} = 0$  or  $\pi$ , i.e., if the chord joining  $z$  and  $a$  is horizontal. Otherwise, it is proved by rotation. Since a circle is the only closed contour where a chord joining any two boundary points meets the circumference at the same angle at both points, we have  $A(z, a) \equiv 0$  for all  $z, a$  on the boundary iff the boundary is a circle. If we expand  $z = \gamma(s)$  in a Taylor series at  $a = \gamma(t)$ , we obtain

$$z = \gamma(s) = \gamma(t) + \gamma'(t)(s-t) + \frac{1}{2}\gamma''(t)(s-t)^2 + O(h^3), \quad h = s-t, \quad (7.6.12)$$

which yields

$$z - a = \gamma'(t)(s-t) \left[ 1 + \frac{1}{2} \frac{\gamma''(t)}{\gamma'(t)} (s-t) + O(h^2) \right],$$

and

$$\frac{1}{z-a} = \frac{1}{\gamma'(t)(s-t)} \left[ 1 - \frac{1}{2} \frac{\gamma''(t)}{\gamma'(t)} (s-t) + O(h^2) \right].$$

By differentiating (7.6.12), we get

$$\gamma'(s) = \gamma'(t) + \gamma''(t)(s-t) + O(h^2),$$

which together with (7.6.13) gives

$$\frac{\gamma'(s)}{z-a} = \frac{1}{s-t} + \frac{1}{2} \frac{\gamma''(t)}{\gamma'(t)} + O(h). \quad (7.6.13)$$

Similarly,

$$\frac{\gamma'(t)}{z-a} = \frac{1}{s-t} - \frac{1}{2} \frac{\gamma''(t)}{\gamma'(t)} + O(h). \quad (7.6.14)$$

Subtracting (7.6.13) and (7.6.14) we find that the singularities (which are real) of  $1/(s-t)$  cancel, and then using (7.6.5), we obtain the Kerzman–Stein kernel  $A(z, a)$  defined by (7.7.10). This kernel is continuous and skew-symmetric, i.e.,  $A(z, a) = -\overline{A(z, a)}$ . The following result (Kerzman and Stein, 1986) is useful:

**THEOREM 7.6.2.** *The Szegö kernel  $S(z, a)$ , as a function of  $z$ , is the unique solution of the integral equation*

$$S(z, a) + \int_{\Gamma} A(z, a) S(z, a) d\gamma_{\zeta} = \overline{H(a, z)}, \quad z, \zeta \in \Gamma, \quad (7.6.15)$$

where  $\gamma$  denotes the arc length on  $\Gamma$ .

If we use a parametrization  $z = \gamma(s)$  on  $\Gamma$ ,  $0 \leq s \leq L$ , the integral equation (7.6.15) becomes

$$\theta(s) + \int_0^L k(s, t) \theta(t) dt = g(s), \quad 0 \leq s \leq L, \quad (7.6.16)$$

where

$$\begin{aligned} \theta(s) &= |\gamma'(s)|^{1/2} S(\gamma(s), a), \\ g(s) &= |\gamma'(s)|^{1/2} \overline{H(a, \gamma(s))}, \\ k(s, t) &= |\gamma'(s)|^{1/2} A(\gamma(s), \gamma(t)) |\gamma'(t)|^{1/2}. \end{aligned} \quad (7.6.17)$$

This integral equation is solved by Nyström method (see Atkinson, 1976; Delves and Mohamed, 1985) which is as follows: Since all functions in this equation are periodic, we take  $n$  equispaced collocation points  $s_j = (j - 1)L/n$ ,  $j = 1, \dots, n$ , and use the trapezoidal rule. This gives

$$\theta(s_j) + \frac{L}{n} \sum_{m=1}^n k(s_j, s_m) = g(s_j). \quad (7.6.18)$$

Let  $B_{jm} = \frac{L}{n} k(s_j, s_m)$  define the skew-hermitian matrix  $\mathbf{B}$ , and let  $x_j = \theta(s_j)$ , be written in matrix form as

$$(I + \mathbf{B}) \mathbf{x} = \mathbf{y}, \quad (7.6.19)$$

which is solved by an iterative method based on the generalized conjugate gradient method (GCM), the details of which can be found in Trummer (1986).

The discretized form (7.6.18) of Eq (7.6.16) gives the interpolation formula

$$\theta(s) = g(s) - \frac{L}{n} \sum_{m=1}^n k(s, s_m) x_m. \quad (7.6.20)$$

Once the solution  $\theta$  of Eq (7.6.16) is computed, the boundary correspondence function  $\phi(s)$ , defined by  $f(z) = f(\gamma(s)) = e^{i\phi(s)}$ ,  $z = r, e^{i\theta}$ , can be computed from the formula

$$\phi(s) = \arg \{ -i \theta^2(s) \gamma'(s) \}. \quad (7.6.21)$$

Trummer (1986) has applied this method to the following six conformal mapping problems:

1.  $\Gamma$  is the inverted ellipse, defined by  $z(s) = e^{is} \sqrt{1 - (1 - p^2) \cos^2 s}$ ,  $0 < p \leq 1$ , where  $\tan s = p \tan \phi(s)$  (see §7.4).
2.  $\Gamma$  is the ellipse  $z(s) = e^{is} - \varepsilon e^{-is}$ ,  $0 \leq \varepsilon < 1$ , with eccentricity  $= (1 - \varepsilon)/(1 + \varepsilon)$ , where  $\phi(s) = s + 2 \sum_{n=1}^{\infty} \frac{1}{n} \frac{\varepsilon^n}{1 + \varepsilon^{2n}} \sin 2ns$ .
3.  $\Gamma$  is the epitrochoid ('apple')  $z(s) = e^{is} + \frac{\alpha}{2} e^{2is}$ ,  $0 \leq \alpha < 1$ , where  $\phi(s) = s$ .
4.  $\Gamma$  is Cassini's oval  $|z - \alpha||z + \alpha| = 1$ ,  $0 \leq \alpha < 1$ , or

$$z(s) = e^{is} \sqrt{\alpha^2 \cos 2s + \sqrt{1 - \alpha^4 \sin^2 2s}},$$

where  $\phi(s) = s - 0.5 \arg\{h(s)\}$ ,  $h(s) = \sqrt{1 - \alpha^4 \sin^2 2s}$ .

5.  $\Gamma$  is the unit square, where  $\cos \phi(s) = \operatorname{dn}(Ky)$ .
6.  $\Gamma$  is the stadium with boundary composed of two semicircles joined by two line segments, all of the same length.

This method requires some programming. For details see Trummer (1986).

CASE STUDY 7.6.1. The results for the ellipse with eccentricity 0.5 are presented in Fig. 7.6.2. ■

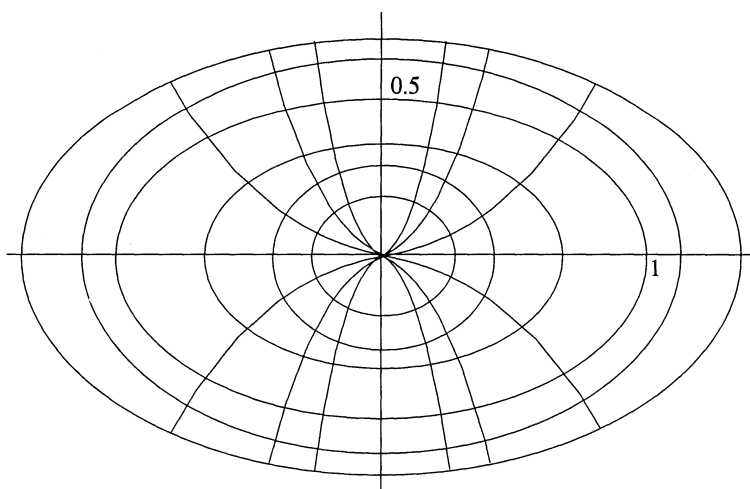


Fig. 7.6.2.

## 7.7. Problems

PROBLEM 7.7.1. Find the approximate solution of the integral equation

$$\phi(x) - \int_0^{1/2} \sin xy \phi(y) dy = f(x),$$

$\sin xy \approx xy - \frac{x^3 y^3}{6} + \frac{x^5 y^5}{120}$ . Then taking  $f(x) = 1 + \frac{1}{x} \left( \cos \frac{x}{2} - 1 \right)$ , show that the approximate solution is  $\phi(x) \approx 1 + 0.0000009 x - 0.0000002 x^3$ . [Note that the exact solution is  $\phi(x) = 1$ .] (Kantorovich and Krylov, 1958, p.145.)

PROBLEM 7.7.2. Show that the approximate solution of the integral equation

$$y(x) + \int_0^1 x (e^{xs} - 1) y(s) ds = e^x - x$$

is  $y(x) \approx e^x - x - 0.501 x^2 - 0.1671 x^3 - 0.0422 x^4$ . Compare it with the exact solution  $y(x) \equiv 1$ . (Berezin and Zhidkov, 1965, p.653.)

PROBLEM 7.7.3. Show that the first two eigenvalues and corresponding eigenfunctions of the homogeneous integral equation

$$u(x) - \lambda \int_0^1 K(x, s) u(s) ds = 0,$$

where

$$K(x, s) = \begin{cases} x(1-s) & 0 \leq x \leq s \leq 1, \\ s(1-x) & 0 \leq s \leq x \leq 1. \end{cases}$$

are  $\lambda_1 = \pi^2$ ,  $\lambda_2 = 4\pi^2$  and  $u_1(x) = \sqrt{2} \sin \pi x$ ,  $u_2(x) = \sqrt{2} \sin 2\pi x$ , and the approximate solutions are  $\lambda_1 \approx 9.8751$ ,  $\lambda_2 \approx 40$ ,  $u_1(x) \approx -0.0684 + 5.817x(1-x)$ ,  $u_2(x) \approx 14.49x(1-x)(1-2x)$ . (Berezin and Zhidkov, 1965, p.657.)

PROBLEM 7.7.4. Consider the function  $u = \log 1/r$ ,  $|z| = r$ , which is a potential function, regular for  $r \neq 0$ . Show that

- (i) this function yields the force flux of  $2\pi$  at  $r = 0$ . [Hint: Evaluate  $\lim_{\epsilon \rightarrow 0} \frac{\partial u}{\partial n} ds$ , where  $n$  is the outward normal.]

(ii) Define a source of strength  $q$  at a point  $\zeta = (\xi, \eta)$  on the boundary  $\Gamma$  of a simply connected region  $D$  by

$$u(\xi, \eta) = \frac{q}{2\pi} \log \frac{1}{\sqrt{(x - \xi)^2 + (y - \eta)^2}}.$$

A source of strength  $-q$  is called a sink of strength  $q$ . By combining a source and a sink of the same strength  $q$  and letting the distance between them tend to zero while keeping the moment constant, show that the potential

$$u(\zeta) = \frac{qx}{2\pi(x^2 + y^2)} = \frac{q \cos r}{2\pi r}.$$

Note that this potential is known as a dipole of strength  $q$  which is also the moment along the  $x$ -axis. (Andersen et al., 1962, p.173.)

**PROBLEM 7.7.5.** If  $s$  denotes the arc length on the boundary  $\Gamma$  of a simply connected region  $D$ ,  $0 \leq s \leq L$ , and if the dipole density of  $\Gamma$  is  $2\pi\nu(s)$ , then the potential  $u(z)$  is defined in  $D$  and in  $D^* = \text{Ext } (\Gamma)$  by

$$u(z) = \int_{\Gamma} \nu(s) \frac{\partial}{\partial n_s} \left( \log \frac{1}{r_{sz}} \right) ds, \quad z \in D, \quad (7.7.1)$$

where  $n_s$  is the inward normal at a point  $\zeta \in \zeta(s)$  and  $r_{sz} = |z - \zeta|$ . The function  $u(z)$  is regular in  $D$  and  $D^*$  but is discontinuous on  $\Gamma$ . If the unknown potential function  $u(z)$  is determined by the boundary values  $u_{\Gamma}(s) = g(s)$  from (7.7.1), then show that the dipole distribution  $\nu(s)$  satisfies the integral equation

$$\nu(s) = \frac{1}{\pi} \left[ g(s) - \int_0^L \nu(t) \frac{\partial}{\partial n_t} \left( \log \frac{1}{r_{tz}} \right) dt \right],$$

where  $n_t$  is the inward normal at a point  $\zeta = \zeta(t)$ ,  $0 \leq t \leq L$ ,  $t \neq s$ . (Andersen et al., 1962, p.173.)

**PROBLEM 7.7.6.** Let  $f(z) = u(z) + i v(z)$ ,  $u$  and  $v$  real, be continuous and regular in  $|z| < 1$ . Show that

$$v(r^{i\phi}) = v(0) + \frac{1}{2\pi} \int_0^{2\pi} u(e^{i\theta}) \cot \frac{\phi - \theta}{2} d\theta.$$

For  $\theta = \phi$ , the integral takes the Cauchy p.v. If  $f(z) = z^n$ ,  $n = 0, 1, \dots$ , then show that

$$\frac{1}{2\pi} \int_0^{2\pi} \begin{Bmatrix} \sin n\theta \\ \cos n\theta \end{Bmatrix} \cot \frac{\phi - \theta}{2} d\theta = \begin{cases} -\cos n\phi & \text{for } n = 1, 2, \dots, \\ \sin n\phi & \text{for } n = 0, 1, \dots. \end{cases}$$

(Gaier, 1964, p.62.)

**PROBLEM 7.7.7.** Prove the transformation relation (7.6.8) between  $S(z, a)$  and  $S_U(z, a)$ . (Kerzman and Stein, 1978, p.87; 1986, p.111.)

**PROBLEM 7.7.8.** Develop the details of the conjugate gradient method. (Trummer, 1986, p.857.)

**REFERENCES USED:** Ahlfors (1952), Andersen et al. (1962), Atkinson (1976), Banin (1943), Berezin and Zhidkov (1965), Birkoff et al. (1950, 1951), Carrier (1947), Carrier, Krook and Pearson (1966), Gaier (1964), Gershgorin (1933), Kerzman and Stein (1978, 1986), Lichtenstein (1917), Kantorovich and Krylov (1958), Neumann (1877), Stiefel (1956), Szegö (1950), Trummer (1986), Todd and Warschawski (1955), Warschawski (1955, 1956), Whittaker and Watson (1927).

# Chapter 8

---

## Theodorsen's Integral Equation

---

The problem of conformally mapping an almost circular region onto the interior or exterior of a circular disk by the the method of infinite systems was discussed in Chapter 5. In this chapter we shall present Theodorsen's integral equation and establish the convergence of the related iterative method for the standard case of mapping the unit circle onto the interior (or exterior) of almost circular and starlike regions, both containing the origin. A trigonometric interpolation scheme is presented, and Wegmann's iterative and Newton's method for numerically solving this equation are discussed. The last two methods are based on a certain Riemann–Hilbert problem, which turns out to be a linearized form of a singular integral equation of the second kind. Unlike the classical iterative method, the solution of the linearized problem in Wegmann's method for the conformal map of the unit circle can be represented explicitly in terms of integral transforms, which leads to a quadratic convergent Newton–like method that avoids the numerical solution of a system of linear equations and thus becomes more economical. Theodorsen's integral equation has specific significance in the theory of airfoils.

---

### 8.1. Classical Iterative Method

Let  $\Gamma$  denote a Jordan curve defined in the polar coordinate system by  $\rho = \rho(\phi)$ ,  $0 \leq \phi \leq 2\pi$ , where  $\rho(\phi) \in C^1$ , such that for some  $\varepsilon$  ( $0 < \varepsilon < 1$ ) and a constant  $a > 0$

$$\frac{a}{1 + \varepsilon} \leq \rho(\phi) \leq a(1 + \varepsilon), \quad (8.1.1)$$

and

$$\left| \frac{\rho'(\phi)}{\rho(\phi)} \right| \leq \varepsilon. \quad (8.1.2)$$

Any Jordan curve  $\Gamma$  that satisfies these two conditions is called a nearly circular contour or a near circle. Let us assume that a function  $w = f(z) = \rho e^{i\phi}$ ,  $z = e^{i\theta}$ , with  $f(0) = 0$  and  $f'(0) > 0$ , maps the unit disk  $U = \{|z| < 1\}$  onto  $\text{Int}(\Gamma)$  which is starlike with respect to the origin. Then  $f(e^{i\theta}) = \rho(\phi(\theta)) e^{i\phi(\theta)}$  defines the boundary correspondence function  $\phi : [0, 2\pi] \mapsto \mathbb{R}$ . If  $\phi$  is known, then  $f$  is known. Consider the function

$$F(z) = \log \frac{f(z)}{z} = \log \left| \frac{f(z)}{z} \right| + i \arg \left\{ \frac{f(z)}{z} \right\}, \quad (8.1.3)$$

which, defined as real-valued  $\log f'(0)$  for  $z = 0$ , is single-valued and analytic in  $U$ , and continuous on  $U \cup \partial U$ . If we set  $z = e^{i\theta}$ , then  $\arg \left\{ \frac{f(z)}{z} \right\} = \arg \{f(e^{i\theta}) e^{-i\theta}\} = \phi(\theta) - \theta$ . Thus,

$$F(e^{i\theta}) = \log \rho[\phi(\theta)] + i[\phi(\theta) - \theta]. \quad (8.1.4)$$

Then, in view of the Schwarz formula (6.4.12) with  $\rho = R = 1$  and  $v(0) = 0$ , we obtain

$$\phi(\theta) - \theta = \frac{1}{2\pi} \int_0^{2\pi} \log \rho(\phi(\theta)) \cot \frac{\phi - \theta}{2} d\theta. \quad (8.1.5)$$

Note that not only the mapping function  $f(z)$  is defined in the form  $\rho = \rho(\phi)$  on  $\Gamma$ , but the relation (8.1.5) represents an integral equation for the unknown function  $\phi(\theta)$ , i.e.,

$$\phi(\theta) - \theta = -\frac{1}{2\pi} \int_0^\pi [\log \rho(\phi(\theta+t)) - \log \rho(\phi(\theta-t))] \cot \frac{t}{2} dt. \quad (8.1.6)$$

This is known as *Theodorsen's integral equation*. Once the function  $\phi(\theta)$  is determined, the function  $F(z)$  and then the mapping function  $f(z)$  can be computed. The term  $\arg \left\{ \frac{f(z)}{z} \right\}_{z=0} = \arg \{f'(0)\}$  is not added to the right side of (8.1.6) because it is zero. Theodorsen (1931) showed that  $\phi$  is a solution of Eq (8.1.6). Gaier (1964, p.66) proved that this equation has exactly one solution which is continuous and strongly monotone. The Riemann mapping theorem (§1.4) guarantees the existence of a continuous solution of this integral equation. We shall also show that this solution is unique.

Theodorsen's method for solving the integral equation (8.1.6) for nearly circular regions is based on the iterations

$$\begin{aligned}\phi_0(\theta) &= 0, \\ \phi_n(\theta) - \theta &= -\frac{1}{2\pi} \int_0^\pi \{\log \rho[\phi_{n-1}(\theta + t)] - \log \rho[\phi_{n-1}(\theta - t)]\} \cot \frac{t}{2} dt, \\ n &= 1, 2, \dots.\end{aligned}\tag{8.1.7}$$

The functions  $\phi_n(\theta)$  are absolutely continuous, and  $\phi'_n(\theta) \in L^2[0, 2\pi]$ . In fact, this is obviously true for  $n = 0$ . Suppose that this statement is true for some  $n \geq 0$ . Since, in view of (8.1.2), the function  $\log \rho(\phi)$  has a bounded difference quotient and  $\phi_n(\theta)$  is absolutely continuous, it follows that  $\log \rho(\phi_n(\theta))$  is also absolutely continuous. Also, since

$$\left( \frac{\rho'(\phi_n(\theta))}{\rho(\phi_n(\theta))} \phi'_n(\theta) \right)^2 \leq \varepsilon^2 [\phi'_n(\theta)]^2,\tag{8.1.8}$$

the integral  $\int_0^{2\pi} \left[ \frac{\rho'(\phi_n(\theta))}{\rho(\phi_n(\theta))} \phi'_n(\theta) \right]^2 d\theta$  exists. Hence, the function  $\phi_n(\theta) - \theta$  which is the conjugate of  $\log \rho(\phi_n(\theta))$  exists and is absolutely continuous. The integrands in (8.1.7) are singular at  $t = 0$  where the integrals take the Cauchy p.v.'s. In what follows we shall use the notation

$$\sigma(\phi(\theta)) = \frac{\rho'(\phi(\theta))}{\rho(\phi(\theta))}, \quad \text{and} \quad p(\phi) = \frac{d}{d\phi} \left[ \frac{\rho'(\phi)}{\rho(\phi)} \right].\tag{8.1.9}$$

Both  $\sigma$  and  $p$  are Hölder-continuous.

## 8.2. Convergence

The following result holds for the convergence of Theodorsen's iterative method (8.1.7).

**THEOREM 8.2.1.** *The sequences  $\{\phi_n(\theta)\}$  and  $\{\phi'_n(\theta)\}$  converge uniformly to  $\phi(\theta)$  and  $\phi'(\theta)$ , respectively, as  $n \rightarrow \infty$ .*

This result will in turn establish that  $\log \rho[\phi_n(\theta)]$  converges uniformly to  $\log \rho[\phi(\theta)]$  as  $n \rightarrow \infty$ , so that the functions

$$F_0(e^{i\theta}) = \log a, \quad F_n(e^{i\theta}) = \log \rho[\phi_{n-1}(\theta)] + i(\phi_n(\theta) - \theta), \quad n \geq 1, \quad (8.2.1)$$

will compute  $f(e^{i\theta})$  to any desired accuracy. Let the functions  $F_n(z)$  be analytic on  $U$  and assume boundary values  $F_n(e^{i\theta})$  on  $|z| = 1$ . In view of the maximum modulus principle, the uniform convergence of  $F_n(e^{i\theta})$  to  $F(e^{i\theta})$  implies the uniform convergence of  $F_n(z)$  to  $F(z)$  on  $|z| \leq 1$ . Hence, the functions  $f_n(z) = z e^{F_n(z)}$  converge uniformly to the mapping function  $f(z) = z e^{F(z)}$ .

To prove the above theorem, we shall first derive the estimates for the differences  $|\phi_n(\theta) - \phi(\theta)|$  and  $|\phi'_n(\theta) - \phi'(\theta)|$  in terms of  $\varepsilon$  and  $n$ , and show that these differences approach zero as  $n \rightarrow \infty$ .

**THEOREM 8.2.2.** *If  $\Gamma$  is a near circle and if  $\phi_n(\theta)$  and  $\phi(\theta) = \arg\{f(r e^{i\theta})\}$  are defined by (8.1.7) and (8.1.4), then*

$$|\phi_n(\theta) - \phi(\theta)| \leq 2 \left( \frac{\pi}{1 - \varepsilon^2} \right)^{1/4} \varepsilon^{(n+2)/2}. \quad (8.2.2)$$

Note that the bound in (8.2.2) goes to zero as  $n \rightarrow \infty$  since  $0 < \varepsilon < 1$ . This will establish the convergence of  $\phi_n(\theta)$  to  $\phi(\theta)$ .

**THEOREM 8.2.3.** *If  $\Gamma$  is a near circle and if  $\sigma \in H^1$ , then*

$$|\phi_n(\theta) - \phi(\theta)| \leq \sqrt{2\pi A(n+1)} \varepsilon^{n+1}, \quad (8.2.3)$$

where  $A = 4^\varepsilon e^{\varepsilon^2}$ .

This result provides a bound that converges to zero more rapidly as  $n \rightarrow \infty$ .

**THEOREM 8.2.4.** *If  $\Gamma$  is a near circle and if  $\sigma \in H^1$  and  $p(\phi) \in H^1$ , then*

$$|\phi'_n(\theta) - \phi'(\theta)| \leq \sqrt{2\pi c_n} [A(n+1)]^{3/2} \varepsilon^{n+1}, \quad (8.2.4)$$

where

$$c_1 = 1 + \varepsilon, \quad c_n = (1 + \varepsilon) \prod_{k=2}^n \left( 1 + \varepsilon^k \sqrt{2\pi Ak} \right), \quad (8.2.5)$$

and for all  $n$

$$c_n \leq (1 + \varepsilon) e^{2\varepsilon^2 \sqrt{\pi A} (1 - \varepsilon)^{-3/2}}. \quad (8.2.6)$$

The last inequality shows that  $c_n$  is bounded if  $0 < \varepsilon < 1$ . The proofs for these theorems are given in Warschawski (1945). We shall outline these proofs in the next section. It should be noted that the estimates for the difference  $|F_n(z) - F(z)|$  for  $|z| \leq 1$  are obtained from those for  $|\phi_n(\theta) - \phi(\theta)|$  given above. Thus, in view of (8.1.2), we have

$$|F_n(e^{i\theta}) - F(e^{i\theta})| \leq \sqrt{\varepsilon^2 [\phi_{n-1}(\theta) - \phi(\theta)]^2 + [\phi_n(\theta) - \phi(\theta)]^2},$$

and

$$|F_n(z) - F(z)| \leq \max_{\theta} |F_n(e^{i\theta}) - f(e^{i\theta})| \quad \text{for } |z| \leq 1.$$

In the case of Theorem 8.2.2 this yields

$$|F_n(z) - f(z)| \leq 2 \left( \frac{\pi^2}{1 - \varepsilon} \right)^{1/4} \varepsilon^{(n+2)/2} \sqrt{1 + \varepsilon},$$

and in the case of Theorem 8.2.3

$$|F_n(z) - f(z)| \leq 2 \varepsilon^{n+1} \sqrt{\pi A \left( n + \frac{1}{2} \right)}.$$

Hence, for  $0 < \varepsilon < 1$  the iterations  $F_n(z)$  converge uniformly to  $F(z) = \log \frac{f(z)}{z}$  for  $|z| \leq 1$ . The above theorems constitute the classical theory for the convergence of the numerical method for solving Theodorsen's integral equation by iterations in terms of the boundary correspondence function  $\phi$ , which provides the required boundary map  $f$ .

### 8.3. Proofs

Theodorsen's method converges strongly like a geometric series. First, we obtain the bounds for the square means

$$\begin{aligned} M_n^2 &= \frac{1}{2\pi} \int_0^{2\pi} [\phi_n(\theta) - \phi(\theta)]^2 d\theta, \quad M_n'^2 = \frac{1}{2\pi} \int_0^{2\pi} [\phi'_n(\theta) - \phi'(\theta)]^2 d\theta, \\ M_n''^2 &= \frac{1}{2\pi} \int_0^{2\pi} [\phi''_n(\theta) - \phi''(\theta)]^2 d\theta. \end{aligned} \quad (8.3.1)$$

Then the results of these theorems are obtained by using the inequalities

$$|\phi_n(\theta) - \phi(\theta)| \leq \sqrt{2\pi M_n M'_n}, \quad |\phi'_n(\theta) - \phi'(\theta)| \leq \sqrt{2\pi M'_n M''_n}. \quad (8.3.2)$$

The following results are also needed:

LEMMA 8.3.1. *If the function  $g(\theta) \in L^2[0, 2\pi]$  is real-valued,  $2\pi$ -periodic, and square-integrable (in Lebesgue's sense) on  $0 \leq \theta \leq 2\pi$ , and if  $\bar{g}(\theta)$  is a conjugate function of  $g(\theta)$ , then*

$$\frac{1}{2\pi} \int_0^{2\pi} [\bar{g}(\theta)]^2 d\theta + \alpha^2 = \frac{1}{2\pi} \int_0^{2\pi} [g(\theta)]^2 d\theta + \beta^2, \quad (8.3.3)$$

where

$$\alpha^2 = \frac{1}{2\pi} \int_0^{2\pi} g(\theta) d\theta, \quad \beta^2 = \frac{1}{2\pi} \int_0^{2\pi} \bar{g}(\theta) d\theta.$$

LEMMA 8.3.2. *If  $g(\theta) \in L^2[0, 2\pi]$  is a real-valued, absolutely continuous,  $2\pi$ -periodic and square integrable function, then for any  $\theta_0$*

$$[g(\theta)]^2 - [g(\theta_0)]^2 \leq 2\pi M M', \quad (8.3.4)$$

where

$$M^2 = \frac{1}{2\pi} \int_0^{2\pi} [g(\theta)]^2 d\theta, \quad M'^2 = \frac{1}{2\pi} \int_0^{2\pi} [g'(\theta)]^2 d\theta.$$

The factor  $2\pi$  in (8.3.4) is the best possible.

LEMMA 8.3.3. *If  $\Gamma$  is nearly circular, then the function  $\phi(\theta) = \arg\{f(r e^{i\theta})\}$ , defined by (8.1.4), is absolutely continuous and  $[\phi'(\theta)]^2 \in L^2[0, 2\pi]$  in Lebesgue's sense such that*

$$\frac{1}{2\pi} \int_0^{2\pi} [\phi'(\theta)]^2 d\theta \leq \frac{1}{1 - \varepsilon^2}. \quad (8.3.5)$$

LEMMA 8.3.4. *If  $g(\theta) \in H^\alpha$ ,  $0 < \alpha \leq 1$ , is a  $2\pi$ -periodic function, then any conjugate function of  $g(\theta)$  also satisfies a Hölder condition.*

LEMMA 8.3.5. *If  $\Gamma$  is a near circle and if  $\sigma(\phi) \in H^1$ , then*

$$\frac{1}{A\sqrt{1+\varepsilon^2}} \leq \phi'(\theta) \leq A, \quad (8.3.6)$$

$$\sqrt{\frac{1}{2\pi} \int_0^{2\pi} [\phi''(\theta)]^2 d\theta} \leq A^{3/2} \varepsilon \min(1 + \varepsilon; \sqrt{2}). \quad (8.3.7)$$

LEMMA 8.3.6. *If  $u(t) \in C^1[0, 2\pi]$  is a  $2\pi$ -periodic function and if  $v(t) \in C^1[0, 2\pi]$  is a function conjugate to  $u(t)$ , then for every  $\theta$*

$$\int_0^{2\pi} \left( \frac{u(t) - u(\theta)}{\sin \frac{t-\theta}{2}} \right)^2 dt = \int_0^{2\pi} \left( \frac{v(t) - v(\theta)}{\sin \frac{t-\theta}{2}} \right)^2 dt.$$

Proof of Lemma 8.3.1 is available in Zygmund, 1935, p.76 (Eq (4)); of Lemma 8.3.4 in Privaloff (1916) or Zygmund (1935, p.156); of Lemma 8.3.5 in Warschawski (1950); and of Lemma 8.3.6 (on conjugate functions) in Warschawski (1945).

PROOF OF LEMMA 8.3.2. Note that for  $0 \leq \theta \leq 2\pi$ ,  $0 \leq \theta_0 \leq 2\pi$ ,

$$g^2(\theta) - g^2(\theta_0) = 2 \int_{\theta_0}^{\theta} g(t) g'(t) dt = 2 \int_{\theta_0}^{\theta-2\pi} g(t) g'(t) dt. \quad (8.3.8)$$

Since

$$\left| \int_{\theta_0}^{\theta} |g g'| dt \right| + \left| \int_{\theta_0}^{\theta-2\pi} |g g'| dt \right| = \int_{\theta-2\pi}^{\theta} |g g'| dt = \int_0^{2\pi} |g g'| dt,$$

one of the two integrals in (8.3.8) does not exceed  $\frac{1}{2} \int_0^{2\pi} |g g'| dt$ . Hence, by the Schwarz inequality,

$$[g(\theta)]^2 - [g(\theta_0)]^2 \leq \int_0^{2\pi} |g g'| dt \leq 2\pi M M'.$$

Also, applying (8.3.4) with  $g(\theta) = \cos^n \theta$  ( $\theta_0 = \pi/2$ ) and letting  $n \rightarrow \infty$ , we find that the constant  $2\pi$  cannot be replaced by any smaller one. ■

PROOF OF LEMMA 8.3.3. Since  $\Gamma$  is rectifiable, the function  $F(e^{i\theta})$  is absolutely continuous (this follows from a theorem of F. and M. Riesz, 1923). Hence,

$$\frac{d}{d\theta} F(e^{i\theta}) - i = \sigma(\phi(\theta)) \phi'(\theta) + i \phi'(\theta)$$

exists a.e. for  $0 \leq \theta \leq 2\pi$  and is integrable. Moreover, the function  $\frac{\partial}{\partial\theta} F(z) - i = u(z) + i v(z)$ ,  $z = r e^{i\theta}$ , has the Poisson integral representation in the unit disk as

$$u(z) + i v(z) = \frac{1}{2\pi} \int_0^{2\pi} [u(r e^{it}) + i v(r e^{it})] \frac{1 - r^2}{1 + r^2 - 2r \cos(t - \theta)} dt, \quad (8.3.9)$$

(see (6.4.6)). For almost all  $\theta \in [0, 2\pi]$  we have

$$\begin{aligned} \lim_{r \rightarrow 1} u(r e^{i\theta}) &= \sigma(\phi(\theta)) \phi'(\theta) = u(e^{i\theta}), \\ \lim_{r \rightarrow 1} v(r e^{i\theta}) &= \phi'(\theta) = v(e^{i\theta}), \end{aligned}$$

and since  $\text{Int}(\Gamma)$  is starlike (see §8.5),  $\phi'(\theta) \geq 0$ . Then by (8.1.2)

$$v(e^{i\theta}) \pm u(e^{i\theta}) \geq \phi'(\theta)(1 - \varepsilon) \geq 0.$$

Thus, in view of (8.3.9) we have  $v(z) + u(z) \geq 0$  and  $v(z) - u(z) \geq 0$  for  $|z| < 1$ . Hence,  $v^2(z) - u^2(z) \geq 0$  for  $|z| < 1$ . Also,

$$\frac{1}{2\pi} \int_0^{2\pi} [v^2(r e^{i\theta}) - u^2(r e^{i\theta})] d\theta = 1.$$

Then, taking the limit as  $r \rightarrow 1$  and using Fatou's lemma, we get

$$\frac{1}{2\pi} \int_0^{2\pi} [\phi'(\theta)]^2 \left\{ [1 - \sigma(\phi(\theta))]^2 \right\} d\theta \leq 1,$$

which, in view of (8.1.2), yields (8.3.5). ■

PROOF OF THEOREM 8.2.2. (a) First we determine an estimate for  $M_n$ . In view of (8.1.4) and (8.1.7), we have

$$\int_0^{2\pi} [\phi(\theta) - \theta] d\theta = 0, \quad \int_0^{2\pi} [\phi_n(\theta) - \theta] d\theta = 0. \quad (8.3.10)$$

Now, applying Lemma 8.3.1 with  $g(\theta) + i\bar{g}(\theta) = F_n(e^{i\theta}) - F(e^{i\theta})$  and noting that  $\beta = 0$  because of (8.3.10), we get

$$\begin{aligned} M_n^2 &= \frac{1}{2\pi} \int_0^{2\pi} [\phi_n(\theta) - \phi(\theta)]^2 d\theta \\ &\leq \frac{1}{2\pi} \int_0^{2\pi} [\log \rho(\phi_{n-1}(\theta)) - \log \rho(\phi(\theta))]^2 d\theta. \end{aligned} \quad (8.3.11)$$

Since by (8.1.2)

$$|\log \rho(\phi_{n-1}(\theta)) - \log \rho(\phi(\theta))| \leq \varepsilon |\phi_{n-1}(\theta) - \phi(\theta)|,$$

from (8.3.11) we obtain

$$M_n^2 \leq \varepsilon^2 \frac{1}{2\pi} \int_0^{2\pi} [\phi_{n-1}(\theta) - \phi(\theta)]^2 d\theta \leq \varepsilon^2 M_{n-1}^2,$$

or

$$M_n \leq \varepsilon M_{n-1}, \quad M_n \leq \varepsilon^n M_0.$$

For  $n = 0$  we find from (8.3.3) by using (8.1.1) that

$$M_0^2 = \frac{1}{2\pi} \int_0^{2\pi} [\phi(\theta) - \theta]^2 d\theta \leq \frac{1}{2\pi} \int_0^{2\pi} \left[ \log \frac{\rho(\phi(\theta))}{a} \right]^2 d\theta \leq \varepsilon^2,$$

which yields the estimate

$$M_n \leq \varepsilon^{n+1}. \quad (8.3.12)$$

(b) Now we determine an estimate for  $M'_n$ . Since  $F_n(e^{i\theta})$  and  $F(e^{i\theta})$  are absolutely continuous and  $\frac{d}{d\theta} F_n(e^{i\theta})$  and  $\frac{d}{d\theta} F(e^{i\theta})$  belong to the class  $L^2[0, 2\pi]$ , the imaginary part of  $\frac{d}{d\theta} [F_n(e^{i\theta}) - F(e^{i\theta})]$  is a conjugate function of the real part. Then

$$\int_0^{2\pi} \frac{d}{d\theta} F(e^{i\theta}) d\theta = F(e^{i\theta}) \Big|_{\theta=0}^{2\pi} = 0, \quad \int_0^{2\pi} \frac{d}{d\theta} F_n(e^{i\theta}) d\theta = 0. \quad (8.3.13)$$

Hence, using Lemma 8.3.1 with  $g(\theta) + i\bar{g}(\theta) = \frac{d}{d\theta} [F_n(e^{i\theta}) - F(e^{i\theta})]$ , we obtain

$$\begin{aligned} M'_n &= \frac{1}{2\pi} \int_0^{2\pi} [\phi'_n(\theta) - \phi'(\theta)]^2 d\theta \\ &= \frac{1}{2\pi} \int_0^{2\pi} \{ \sigma(\phi_{n-1}(\theta)) \phi'_{n-1}(\theta) - \sigma(\phi(\theta)) \phi'(\theta) \}^2 d\theta. \end{aligned} \quad (8.3.14)$$

In view of (8.1.2), then

$$M_n'^2 \leq 2\varepsilon^2 \frac{1}{2\pi} \int_0^{2\pi} [\phi_{n-1}'^2(\theta) - \phi'^2(\theta)]^2 d\theta. \quad (8.3.15)$$

By Lemma 8.3.3, we have  $\frac{1}{2\pi} \int_0^{2\pi} \phi'^2(\theta) d\theta \leq \frac{1}{1-\varepsilon^2}$ . Moreover, again using Lemma 8.3.1 with  $g(\theta) + i\bar{g}(\theta) = \frac{d}{d\theta} F_n(e^{i\theta})$ , and (8.1.2), we get

$$\begin{aligned} \frac{1}{2\pi} \int_0^{2\pi} [\phi_n'(\theta) - 1]^2 d\theta &= \frac{1}{2\pi} \int_0^{2\pi} [\sigma(\phi_{n-1}(\theta)) \phi_{n-1}'(\theta)]^2 d\theta \\ &\leq \varepsilon^2 \frac{1}{2\pi} \int_0^{2\pi} \phi_{n-1}'^2(\theta) d\theta, \end{aligned}$$

or, after suppressing the argument  $\theta$  in the integrands,

$$\frac{1}{2\pi} \left\{ \int_0^{2\pi} [\phi_n' - 1]^2 d\theta - 2 \int_0^{2\pi} \phi_n' d\theta + 2\pi \right\} \leq \varepsilon^2 \frac{1}{2\pi} \int_0^{2\pi} \phi_{n-1}'^2 d\theta.$$

Since  $\int_0^{2\pi} \phi_n' d\theta = 2\pi$ , we have

$$\frac{1}{2\pi} \int_0^{2\pi} \phi_n'^2 d\theta - 1 \leq \varepsilon^2 \frac{1}{2\pi} \int_0^{2\pi} \phi_{n-1}'^2 d\theta.$$

If we set  $m_n^2 = \frac{1}{2\pi} \int_0^{2\pi} \phi_n'^2 d\theta$ , then  $m_n^2 \leq 1 + m_{n-1}^2$ , and hence,  $m_n^2 \leq 1 + \varepsilon^2 + \varepsilon^4 + \dots + \varepsilon^{2n} m_0^2$ . Since  $m_0^2 = \frac{1}{2\pi} \int_0^{2\pi} d\theta = 1$ , we get

$$m_n^2 \leq (1 - \varepsilon^2)^{-1}. \quad (8.3.16)$$

Thus, from (8.3.15), (8.3.5) and (8.3.16) we find that

$$M_n'^2 \leq \frac{4\varepsilon^2}{1 - \varepsilon^2}. \quad (8.3.17)$$

(c) Finally, we determine an estimate for  $|\phi_n(\theta) - \phi(\theta)|$ . We set  $g(\theta) = \phi_n(\theta) - \phi(\theta)$  in Lemma 8.3.2. Then, since  $\int_0^{2\pi} g(\theta) d\theta = 0$ , there exists a value  $\theta_0$  such that  $g(\theta_0) = 0$ , which yields

$$|\phi_n(\theta) - \phi(\theta)| \leq \sqrt{2\pi M_n M_n'}.$$

This gives (8.2.2) after using (8.3.12) and (8.3.17), which completes the proof of Theorem 8.2.2. ■

PROOF OF THEOREM 8.2.3. (a) First, we determine an estimate for  $M'_n$ . Using (8.3.14), we have by Minkowsky's inequality for  $n \geq 1$

$$\begin{aligned} M'_n &= \sqrt{\frac{1}{2\pi} \int_0^{2\pi} [(\sigma(\phi_{n-1}) - \sigma(\phi)) \phi' + \sigma(\phi_{n-1})(\phi'_{n-1} - \phi')]^2 d\theta} \\ &\leq \sqrt{\frac{1}{2\pi} \int_0^{2\pi} [\sigma(\phi_{n-1}) - \sigma(\phi)]^2 \phi'^2 d\theta} \\ &\quad + \sqrt{\frac{1}{2\pi} \int_0^{2\pi} (\phi'_{n-1} - \phi')^2 [\sigma(\phi_{n-1})]^2 d\theta}. \end{aligned}$$

Since  $0 < \phi'(\theta) \leq A$  (Lemma 8.3.5) and  $\sigma(\phi) \in H^1$ , from (8.1.2) we obtain

$$M'_n \leq \varepsilon A \sqrt{\frac{1}{2\pi} \int_0^{2\pi} (\phi_{n-1} - \phi)^2 d\theta} + \varepsilon M'_{n-1} = \varepsilon (AM_{n-1} + M'_{n-1}),$$

and, then by (8.3.12)

$$M'_n \leq \varepsilon (A\varepsilon^n + M'_{n-1}) \quad \text{for } n \geq 1. \quad (8.3.18)$$

For  $n = 0$  from (8.1.2) and Lemma 8.3.1 we get

$$\begin{aligned} M'_0^2 &= \frac{1}{2\pi} \int_0^{2\pi} (\phi' - 1)^2 d\theta = \frac{1}{2\pi} \int_0^{2\pi} [\sigma(\phi)\phi']^2 d\theta \\ &\leq \varepsilon^2 \frac{A}{2\pi} \int_0^{2\pi} \phi' d\theta = \varepsilon^2 A. \end{aligned} \quad (8.3.19)$$

Now we shall prove by induction that

$$M'_n \leq A(n+1)\varepsilon^{n+1}. \quad (8.3.20)$$

In fact, since (8.3.19) holds for  $n = 0$ , we assume that (8.3.20) is true for some  $n > 0$ . Then from (8.3.18)

$$M'_{n+1} \leq \varepsilon [A\varepsilon^{n+1} + A(n+1)\varepsilon^{n+1}] = A(n+2)\varepsilon^{n+2},$$

which proves (8.3.20) for  $(n+1)$ .

(b) Next, we determine an estimate for  $|\phi_n(\theta) - \phi(\theta)|$ . In fact, by using Lemma 8.3.2, (8.3.12), and (8.3.20)

$$|\phi_n(\theta) - \phi(\theta)| \leq \sqrt{2\pi M_n M'_n} \leq \varepsilon^{n+1} \sqrt{2\pi A(n+1)}. \blacksquare \quad (8.3.21)$$

PROOF OF THEOREM 8.2.4. Since  $p \in H^1$ , the function  $F(e^{i\theta}) \in C^2[0, 2\pi]$  (see Warschawski, 1935, Theorem III). Similarly, all functions  $F_n(e^{i\theta}) \in C^2[0, 2\pi]$ , where  $F_n(e^{i\theta})$  are defined by (8.2.1). Also,

$$\begin{aligned} \frac{dF}{d\theta} &= \sigma(\phi) \phi' + i(\phi' - 1), \\ \frac{d^2F}{d\theta^2} &= p(\phi) \phi'^2 + \sigma(\phi) \phi'' + i \phi'', \\ \frac{dF_n}{d\theta} &= \sigma(\phi_{n-1}) \phi'_{n-1} + i(\phi'_n - 1), \\ \frac{d^2F_n}{d\theta^2} &= p(\phi_{n-1}) \phi'_{n-1}^2 + \sigma(\phi_{n-1}) \phi''_{n-1} + i \phi''_n. \end{aligned} \quad (8.3.22)$$

(a) Now we shall estimate

$$M''_n = \sqrt{\frac{1}{2\pi} \int_0^{2\pi} (\phi''_n - \phi'')^2 d\theta},$$

and prove that

$$M''_n \leq A^2(n+1)^2 c_n \varepsilon^{n+1} \quad \text{for } n \geq 1. \quad (8.3.23)$$

Proof of (8.3.23) is as follows: Since, by (8.3.13),

$$\frac{1}{2\pi} \int_0^{2\pi} \frac{d^2}{d\theta^2} [F_n(e^{i\theta}) - F(e^{i\theta})] d\theta = 0,$$

we find by applying Lemma 8.3.1 that

$$\begin{aligned} M''_{n+1}^2 &= \frac{1}{2\pi} \int_0^{2\pi} \left\{ (p(\phi_n) - p(\phi)) \phi'^2 + p(\phi_n) (\phi'^2 - \phi'^2) \right. \\ &\quad \left. + (\sigma(\phi_n) - \sigma(\phi)) \phi'' + \sigma(\phi_n) (\phi'' - \phi'') \right\}^2 d\theta. \end{aligned} \quad (8.3.24)$$

Since  $\sigma(\phi) \in H^1$ , we have  $|p(\phi)| \leq \varepsilon$ , and since  $\phi'(\theta) \leq A$  (Lemma 8.3.5) and  $p \in H^1$ , we find from (8.1.2) that

$$\begin{aligned} M''_{n+1}^2 &\leq \frac{\varepsilon^2}{2\pi} \int_0^{2\pi} [A^2 |\phi_n - \phi| + |\phi'^2 - \phi'^2| \\ &\quad + |\phi''| |\phi_n - \phi| + |\phi'' - \phi''|]^2 d\theta, \end{aligned}$$

which, by Minkowski's inequality, yields

$$\begin{aligned} M''_{n+1} &\leq \varepsilon \left[ A^2 M_n + \sqrt{\frac{1}{2\pi} \int_0^{2\pi} (\phi'_n)^2 - \phi'^2)^2 d\theta} \right. \\ &\quad \left. + \sqrt{\frac{1}{2\pi} \int_0^{2\pi} (\phi'')^2 (\phi_n - \phi)^2 d\theta} + M''_n \right], \end{aligned} \quad (8.3.25)$$

where  $M_n$  and  $M'_n$  are defined in (8.3.1). Since  $\sqrt{\frac{1}{2\pi} \int_0^{2\pi} (\phi''(\theta))^2 d\theta} \leq \varepsilon A^{3/2} \min(1 + \varepsilon; \sqrt{2})$  (Lemma 8.3.5), we have

$$M''_0 = \sqrt{\frac{1}{2\pi} \int_0^{2\pi} (\phi'')^2 d\theta} \leq \sqrt{2} \varepsilon A^{3/2},$$

and since  $|\phi_n(\theta) - \phi(\theta)| \leq \varepsilon^{n+1} \sqrt{2\pi A(n+1)}$  by (8.2.3), we get

$$\begin{aligned} \sqrt{\frac{1}{2\pi} \int_0^{2\pi} (\phi_n - \phi)^2 (\phi'')^2 d\theta} &\leq \sqrt{2} \varepsilon^{n+2} A^{3/2} \sqrt{2\pi A(n+1)} \\ &= 2 \varepsilon^{n+2} A^2 \sqrt{\pi(n+1)}. \end{aligned} \quad (8.3.26)$$

Thus, using Lemma 8.3.2 with  $g(\theta) = \phi'_n(\theta) - \phi'(\theta)$ , we find that

$$(\phi'_n - \phi')^2 \leq 2\pi M'_n M''_n,$$

which, after taking the square root and using  $\phi'(\theta) \leq A$ , yields  $|\phi'_n + \phi| \leq |\phi'_n - \phi'| + 2|\phi'| \leq \sqrt{2\pi M'_n M''_n} + 2A$ . Hence,

$$\sqrt{\frac{1}{2\pi} \int_0^{2\pi} (\phi'_n)^2 - \phi'^2)^2 d\theta} \leq M'_n \left( \sqrt{2\pi M'_n M''_n} + 2A \right). \quad (8.3.27)$$

Now, integration by parts gives

$$\begin{aligned} \frac{1}{2\pi} \int_0^{2\pi} (g'(\theta))^2 d\theta &= \left| g(\theta) g'(\theta) \right|_0^{2\pi} - \int_0^{2\pi} g(\theta) g''(\theta) d\theta \\ &\leq \int_0^{2\pi} |g(\theta) g''(\theta)| d\theta \\ &\leq \sqrt{\int_0^{2\pi} (g(\theta))^2 d\theta \cdot \int_0^{2\pi} (g''(\theta))^2 d\theta}, \end{aligned}$$

which, after setting  $g(\theta) = \phi_n(\theta) - \phi(\theta)$ , yields the inequality  $M'_n \leq \sqrt{M'_n M''_n}$ . Applying this inequality to (8.3.27), we get

$$\sqrt{\frac{1}{2\pi} \int_0^{2\pi} (\phi'_n)^2 - \phi'^2)^2 d\theta} \leq 2AM'_n + M''_n \sqrt{2\pi M_n M'_n}. \quad (8.3.28)$$

Hence, from (8.3.25) we find, after using (8.3.12), (8.3.28), (8.3.26), and (8.3.20), that for  $n \geq 2$

$$\begin{aligned} M''_{n+1} &\leq \varepsilon \left\{ A^2 \varepsilon^{n+1} + 2A^2(n+1)\varepsilon^{n+1} + 2A^2\varepsilon^{n+2} \sqrt{\pi(n+1)} \right. \\ &\quad \left. + \left(1 + \varepsilon^{n+1} \sqrt{2\pi A(n+1)}\right) M''_n \right\} \\ &= A^2 \varepsilon^{n+2} \left\{ 1 + 2(n+1) + 2\varepsilon \sqrt{\pi(n+1)} \right. \\ &\quad \left. + \left(1 + \varepsilon^{n+1} \sqrt{2\pi A(n+1)}\right) \frac{M''_n}{A^2 \varepsilon^{n+1}} \right\} \\ &\leq A^2 \varepsilon^{n+2} \left\{ 1 + 2(n+1) + 2\varepsilon \sqrt{\pi(n+1)} \right. \\ &\quad \left. + \left(1 + \varepsilon^{n+1} \sqrt{2\pi A(n+1)}\right) (n+1)^2 c_n \right\} \quad \text{by (8.3.23)} \\ &\leq A^2 \varepsilon^{n+2} c_{n+1} \{1 + 2(n+1) + (n+1)^2\} \\ &= A^2(n+2)^2 c_{n+1} \varepsilon^{n+2}, \end{aligned} \quad (8.3.29)$$

because

$$1 + 2(n+1) + 2\varepsilon \sqrt{\pi(n+1)} < [1 + 2(n+1)](1 + \varepsilon) < [1 + 2(n+1)] c_{n+1}$$

for  $n \geq 2$ , where we have assumed that (8.3.20) is true for  $n \geq 2$ . To show that (8.3.23) is true for  $n = 1$ , note that from (8.3.24) for  $n = 0$

$$\begin{aligned} M''_1 &= \sqrt{\frac{1}{2\pi} \int_0^{2\pi} [p(\theta) - p(\phi(\theta))] \phi'^2 + p(\theta) (1 - \phi'^2) + \sigma(\phi(\theta)) \phi'']^2 d\theta} \\ &\leq \varepsilon \left[ A^2 M_0 + \sqrt{\frac{1}{2\pi} \int_0^{2\pi} (1 - \phi'^2)^2 d\theta} + M''_0 \right], \end{aligned}$$

by Minkowski's inequality and (8.1.2), where  $\phi_0 = \theta$ ,  $\sigma(\phi) \in H^1$  and  $p \in H^1$ . Since  $M_0'' \leq A^2 \varepsilon (1 + \varepsilon)$ , and  $\phi'(\theta) \leq A$  by Lemma 8.3.5, we get, in view of (8.3.12) and (8.3.20),

$$M_1'' \leq \varepsilon^2 [A^2 + (1 + A)A + A^2(1 + \varepsilon)] = A^2 \varepsilon^2 \left( 2 + \frac{1 + A}{A} + \varepsilon \right).$$

Since  $A \geq 1$  and  $\frac{1 + A}{A} \leq 2$ , we find that

$$M_1'' \leq A^2 \varepsilon^2 (4 + \varepsilon) < 4A^2 \varepsilon^2 (1 + \varepsilon). \quad (8.3.30)$$

We shall establish that (8.3.23) holds for  $n = 2$ . In fact, by applying (8.3.29) with  $n = 1$  and replacing  $M_1''$  by  $A^2 \varepsilon^2 (4 + \varepsilon)$  from (8.3.30), we get

$$M_2'' \leq A^2 \varepsilon^3 \left[ 5 + 2\varepsilon \sqrt{2\pi} + \left( 1 + 2\varepsilon^2 \sqrt{\pi A} \right) (4 + \varepsilon) \right]. \quad (8.3.31)$$

Since  $2\sqrt{2\pi} < 6$  and  $1 + 2\varepsilon^2 \sqrt{\pi A} > 1$ , we find from (8.3.31) that

$$\begin{aligned} M_2'' &\leq A^2 \varepsilon^3 (5 + 6\varepsilon + 4 + \varepsilon) \left( 1 + 2\varepsilon^2 \sqrt{\pi A} \right) \\ &< 9(1 + \varepsilon) \left( 1 + 2\varepsilon^2 \sqrt{\pi A} \right) A^2 \varepsilon^3 \\ &= 9A^2 c_2 \varepsilon^3. \end{aligned} \quad (8.3.32)$$

(b) Next, we determine an estimate for  $|\phi_n'(\theta) - \phi'(\theta)|$ . By applying Lemma 8.3.1 with  $g(\theta) = \phi_n'(\theta) - \phi'(\theta)$ , we find from (8.3.20) and (8.3.23) that

$$|\phi_n'(\theta) - \phi'(\theta)| \leq \sqrt{2\pi c_n} [A(n + 1)]^{3/2} \varepsilon^{n+1}. \quad (8.3.33)$$

(c) Finally, we estimate  $c_n$ . Note that

$$\prod_{k=2}^n \left( 1 + \varepsilon^k \sqrt{2\pi A k} \right) \leq e^{\sqrt{2\pi A} \sum_{k=2}^n \varepsilon^k \sqrt{k}}.$$

Then, by the Schwarz inequality

$$\begin{aligned} \sum_{k=2}^n \varepsilon^k \sqrt{k} &= \varepsilon \sum_{k=2}^n \varepsilon^{(k-1)/2} \left( \sqrt{k} \varepsilon^{(k-1)/2} \right) \\ &\leq \varepsilon \sqrt{\sum_{k=2}^n \varepsilon^{k-1} \sum_{k=2}^n k \varepsilon^{k-1}}. \end{aligned}$$

Hence,

$$\sum_{k=2}^n \varepsilon^k \sqrt{k} \leq \varepsilon \sqrt{\frac{\varepsilon}{1-\varepsilon} \left( \frac{1}{1-\varepsilon^2} - 1 \right)} < \frac{\varepsilon^2 \sqrt{2}}{(1-\varepsilon)^{3/2}},$$

which yields (8.2.6). This completes the proof of Theorem 8.2.4. ■

**PROOF OF THE UNIQUENESS OF THE SOLUTION OF THEODORSEN'S INTEGRAL EQUATION:** We shall show that if  $\Gamma$  is a near circle, then the integral equation (8.1.6) has at most one continuous solution. Let us assume that there exist two such solutions  $\phi_1(\theta)$  and  $\phi_2(\theta)$ . Since

$$\int_0^{2\pi} [\phi_1(\theta) - \theta] d\theta = 0, \quad \int_0^{2\pi} [\phi_2(\theta) - \theta] d\theta = 0,$$

we have by Lemma 8.3.1

$$\begin{aligned} M^2 &= \frac{1}{2\pi} \int_0^{2\pi} [\phi_1(\theta) - \phi_2(\theta)]^2 d\theta \\ &\leq \frac{1}{2\pi} \int_0^{2\pi} [\log \rho(\phi_1(\theta)) - \log \rho(\phi_2(\theta))]^2 d\theta. \end{aligned}$$

Since, in view of (8.1.2),

$$|\log \rho(\phi_1(\theta)) - \log \rho(\phi_2(\theta))| \leq \varepsilon |\phi_1(\theta) - \phi_2(\theta)|,$$

we find that  $M^2 \leq \varepsilon^2 M^2$ , which yields  $M = 0$  because  $0 < \varepsilon < 1$ . Hence,  $\phi_1(\theta) = \phi_2(\theta)$ . ■

## 8.4. Integral Representation

An integral representation for the function  $\phi'_n(\theta)$  is given by the following result.

**THEOREM 8.4.1.** *If  $\Gamma$  is a near circle and if the function  $\rho(\phi)$  which defines  $\Gamma$  satisfies the condition  $H^1$ , then  $\phi'(\theta)$  is continuous and*

$$\phi'_1(\theta) - 1 = -\frac{1}{2\pi} \int_{\theta-\pi}^{\theta+\pi} [\sigma(t) - \sigma(\theta)] \cot \frac{t-\theta}{2} dt, \quad (8.4.1)$$

and for  $n \geq 1$

$$\begin{aligned}\phi'_{n+1}(\theta) - 1 &= -\frac{1}{2\pi} \int_{\theta-\pi}^{\theta+\pi} [\sigma(\phi_{n-1}(t)) - \sigma(\phi_{n-1}(\theta))] \phi'_{n-1}(t) \\ &\quad \times \cot \frac{t-\theta}{2} dt - \sigma(\phi_{n-1}(\theta)) \sigma(\phi_{n-2}(\theta)) \phi'_{n-2}(\theta).\end{aligned}\quad (8.4.2)$$

PROOF. The integrand in (8.4.1) is continuous in both  $t$  and  $\theta$ , except at  $t = \theta$ , and is bounded because  $\sigma \in H^1$ . Hence, the integral (8.4.1) is a continuous function of  $\theta$ , represents a conjugate function of  $\sigma(\theta)$ , and is equal to  $(\phi'_1(\theta) - 1)$  at least for almost all  $\theta$  and, because of continuity, for all  $\theta$ . This proves (8.4.1).

We shall prove (8.4.2) by induction. Let us assume that  $\phi'_k(\theta)$  is a continuous function for  $k = 1, 2, \dots, n$ . We shall prove that (8.4.2) holds for  $(n + 1)$  and that  $\phi'_{n+1}(\theta)$  is continuous.

The absolute continuity of  $F_{n+1}(e^{i\theta}) = \log \rho(\phi_n(\theta)) + i(\phi_{n+1}(\theta) - \theta)$  implies that  $(\phi'_{n+1}(\theta) - 1)$  is conjugate of  $\sigma(\phi_n(\theta)) \phi'_n(\theta)$ , and for almost all  $\theta$  we have

$$\begin{aligned}\phi'_{n+1}(\theta) - 1 &= -\frac{1}{2\pi} \int_0^\pi \sigma(\phi_n(\tau)) \Big|_{\tau=\theta-t}^{\theta+t} \cot \frac{t}{2} dt \\ &= -\frac{1}{2\pi} \int_0^\pi [\sigma(\phi_n(\theta+t)) - \sigma(\phi_n(\theta))] \phi'_n(\theta+t) \cot \frac{t}{2} dt \\ &\quad + \frac{1}{2\pi} \int_0^\pi [\sigma(\phi_n(\theta-t)) - \sigma(\phi_n(\theta))] \phi'_n(\theta-t) \cot \frac{t}{2} dt \\ &\quad - \sigma(\phi_n(\theta)) \frac{1}{2\pi} \int_0^\pi [\phi'_n(\theta+t) - \phi'_n(\theta-t)] \cot \frac{t}{2} dt \\ &\equiv I_1 + I_2 + I_3.\end{aligned}$$

Note that, since  $\sigma(\phi) \in H^1$  and  $\phi'(\theta)$  is continuous, the integrals  $I_1$  and  $I_2$  represent continuous functions of  $\theta$ . The integral  $I_3$ , without the factor  $\sigma(\phi_n(\theta))$ , is equal to  $\sigma(\phi'_{n-1}(\theta)) \phi'_{n-1}(t)$ , since  $(\phi'_n(\theta) - 1)$  is conjugate to this function. If we set  $\tau = \theta + t$  in  $I_1$  and  $\tau = \theta - t$  in  $I_2$ , we get

$$\begin{aligned}\phi'_{n+1}(\theta) - 1 &= -\frac{1}{2\pi} \int_{\theta-\pi}^{\theta+\pi} [\sigma(\phi_n(\tau)) - \sigma(\phi_n(\theta))] \phi'_n(\tau) \cot \frac{t-\theta}{2} d\tau \\ &\quad - \sigma(\phi_n(\theta)) \sigma(\phi_{n-1}(\theta)) \phi'_{n-1}(\theta),\end{aligned}$$

which defines a continuous function of  $\theta$ . ■

Theorem 8.4.1 establishes conditions under which the images  $\Gamma_n$  of the unit circle under the mapping function  $w = f_n(z) = z e^{F_n(z)}$  are starlike with respect to the origin. We shall discuss starlike regions in the next section. The advantage in assuming starlike contours is that  $\phi_n(\theta)$  becomes a monotone increasing function and, therefore, possesses a unique inverse function  $\theta = \theta(\phi)$ . This helps us compute the approximate inverse mapping function  $z = e^{i\theta_n(\phi)}$  that maps the unit circle onto  $\Gamma_n$ .

---

## 8.5. Starlike Regions

A region  $D$  is said to be *starlike* with respect to a point  $z_0 \in D$  if every ray from the point  $z_0$  intersects  $\partial D$  in exactly one point. The functions  $f_n(z) = z e^{F_n(z)}$  map the unit circle  $|z| = 1$  onto Jordan curves  $\Gamma_n$ . Since the functions  $f_n(z)$  are approximations of the mapping function  $f(z)$ , it is important to assume that the contours  $\Gamma_n$  enclose regions that are starlike with respect to the origin, as we have done in §8.3 in the proof of Lemma 8.2.3 and remarked about the advantage of such an assumption at the end of §8.4. The functions  $f_n(z)$  are starlike with respect to the origin if  $\Re \left\{ \frac{zf'_n(z)}{f_n(z)} \right\} > 0$ , which, in view of (8.3.22), leads to the condition  $(\phi'_n - 1) < 1$ .

**CASE STUDY 8.5.1.** We shall determine the conditions on  $\varepsilon$  under which the regions bounded by  $\Gamma_n$  are starlike. In fact, we shall show that if  $\Gamma$  is a near circle and if  $\sigma(\phi) \in H^1$ , then the region bounded by the contour  $\Gamma_1$  is starlike with respect to the origin if  $\varepsilon \leq (2 \log 2)^{-1} \approx 0.72$ , by  $\Gamma_2$  if  $\varepsilon \leq 0.34$ , by  $\Gamma_3$  if  $\varepsilon \leq 0.31$ , and by  $\Gamma_n$  for  $n \geq 4$  if  $\varepsilon \leq 0.295$ .

These results are obtained by evaluating the values of  $\varepsilon$  for which  $|\phi'_n(\theta) - 1| \leq 1$ , so that  $\phi'(\theta) \geq 0$ , which implies that  $\phi_n(\theta)$  is a monotone increasing function. Thus, since  $\sigma(\phi) \in H^1$ , we have, in view of (8.4.1),

$$\begin{aligned} |\phi_1(\theta) - 1| &\leq \frac{1}{2\pi} \int_{\theta-\pi}^{\theta+\pi} |\sigma(t) - \sigma(\theta)| \cot \left| \frac{t-\theta}{2} \right| dt \\ &\leq \frac{\varepsilon}{2\pi} \int_{\theta-\pi}^{\theta+\pi} (t-\theta) \cot \frac{t-\theta}{2} dt = 2\varepsilon \log 2, \end{aligned}$$

where  $\sigma$  is defined by (8.1.9). Then the region bounded by  $\Gamma_1$  is starlike if  $\phi'_1(\theta) \geq 0$ , i.e., if  $2\varepsilon \log 2 \leq 1$ , which gives  $\varepsilon \leq (2 \log 2)^{-1}$ .

Assuming that  $\phi'_n(\theta) \geq 0$  for some  $n \geq 1$ , provided that  $\varepsilon \leq \varepsilon_0 < 1$ , we shall evaluate  $\phi'_{n+1}(\theta)$ . Thus, since  $\sigma(\phi) \in H^1$ , we have by (8.4.2) and (8.1.2),

$$\begin{aligned} |\phi'_{n+1}(\theta) - 1| &\leq \frac{\varepsilon}{2\pi} \int_{\theta-\pi}^{\theta+\pi} [\phi_n(t) - \phi_n(\theta)] \phi'_n(t) \cot \frac{t-\theta}{2} dt \\ &\quad + \varepsilon^2 |\phi'_{n-1}(\theta)| \equiv \varepsilon m_n^2 + \varepsilon^2 |\phi'_{n-1}(\theta)|. \end{aligned} \quad (8.5.1)$$

Note that  $\phi_n(t) - \phi_n(\theta)$  has the same sign as  $(t - \theta)$  since  $\phi'_n(t) \geq 0$ . Now, integrating by parts, we find that

$$\begin{aligned} m_n^2 &= \frac{1}{2\pi} \int_{\theta-\pi}^{\theta+\pi} [\phi_n(t) - \phi_n(\theta)] \phi'_n(t) \cot \frac{t-\theta}{2} dt \\ &= \frac{1}{2\pi} \int_{\theta-\pi}^{\theta+\pi} \left( \frac{\phi_n(t) - \phi_n(\theta)}{2 \sin \frac{t-\theta}{2}} \right)^2 dt \\ &= \frac{1}{2\pi} \int_{\theta-\pi}^{\theta+\pi} \left( \frac{\phi_n(t) - t - [\phi_n(\theta) - \theta] + t - \theta}{2 \sin \frac{t-\theta}{2}} \right)^2 dt, \end{aligned}$$

which, by Minkowski's inequality, yields

$$\begin{aligned} m_n &\leq \sqrt{\frac{1}{2\pi} \int_{\theta-\pi}^{\theta+\pi} \left( \frac{\phi_n(t) - t - [\phi_n(\theta) - \theta]}{2 \sin \frac{t-\theta}{2}} \right)^2 dt} \\ &\quad + \sqrt{\frac{1}{2\pi} \int_{\theta-\pi}^{\theta+\pi} \left( \frac{t - \theta}{2 \sin \frac{t-\theta}{2}} \right)^2 dt} \equiv \sqrt{J_1} + \sqrt{J_2}. \end{aligned} \quad (8.5.2)$$

Now, by Lemma 8.3.6,

$$\begin{aligned} J_1 &= \frac{1}{2\pi} \int_{\theta-\pi}^{\theta+\pi} \left( \frac{\log \rho(\phi_{n-1}(t)) - \log \rho(\phi_{n-1}(\theta))}{2 \sin \frac{t-\theta}{2}} \right)^2 dt \\ &\leq \frac{\varepsilon}{2\pi} \int_{\theta-\pi}^{\theta+\pi} \left( \frac{\phi_{n-1}(t) - \phi_{n-1}(\theta)}{2 \sin \frac{t-\theta}{2}} \right)^2 dt \\ &= \varepsilon^2 m_{n-1}^2. \end{aligned}$$

Also, integrating by parts, we get  $J_2 = 2 \log 2 \equiv c^2$ . Hence, from (8.5.2)

$$m_n \leq \varepsilon m_{n-1} + c. \quad (8.5.3)$$

Since  $c = m_0$ , we find that

$$m_n \leq c \left( 1 + \varepsilon + \varepsilon^2 + \cdots + \varepsilon^n \right) = c \frac{1 - \varepsilon^{n+1}}{1 - \varepsilon}.$$

Thus, by (8.5.1),

$$\begin{aligned} |\phi'_{n+1}(\theta) - 1| &\leq \varepsilon m_n^2 + \varepsilon^2 |\phi'_{n-1}(\theta)| \\ &\leq 2\varepsilon \left( \frac{1 - \varepsilon^{n+1}}{1 - \varepsilon} \right)^2 \log 2 + \varepsilon^2 |\phi'_{n-1}(\theta)|. \end{aligned} \quad (8.5.4)$$

Set  $n = 1$  in (8.5.4). Then, since  $\phi'_0(t) = 1$ , we find that

$$|\phi'_2(t) - 1| \leq 2\varepsilon (1 + \varepsilon)^2 \log 2 + \varepsilon^2, \quad (8.5.5)$$

which is less than 1 if  $\varepsilon \leq 0.34$ . If we set  $n = 2$  in (8.5.4), then, since  $\phi'_1(\theta) \leq 1 + 2\varepsilon \log 2$ , and  $\phi'_1(\theta) > 0$  for  $\varepsilon < (2 \log 2)^{-1}$ , we find that

$$|\phi'_3(\theta) - 1| \leq 2\varepsilon (1 + \varepsilon + \varepsilon^2)^2 \log 2 + \varepsilon (1 + 2\varepsilon \log 2),$$

which is less than 1 if  $\varepsilon \leq 0.31$ . Note that, by (8.5.5),  $|\phi'_2(\theta)| \leq 1.7927$  if  $\varepsilon = 0.3$ . Hence, setting  $n = 3$  in (8.5.4) and using this estimate for  $\phi'_2(\theta)$ , we find that  $|\phi'_4(\theta)| \leq 1$  if  $\varepsilon \leq 0.3$ . Let us assume that  $0 < \phi'_{n-1}(\theta) \leq 2$  for some  $n \geq 1$ . Then, from (8.5.4),

$$|\phi'_{n+1}(\theta) - 1| \leq \varepsilon \frac{2 \log 2}{(1 - \varepsilon)^2} + 2\varepsilon^2 < 1,$$

if  $\varepsilon \leq 0.295$ . Since this assumption is obviously valid for  $n = 1$  and  $n = 2$  if  $\varepsilon \leq 0.295$ , it follows that  $|\phi'_{n+1}(\theta) - 1| < 1$  for all  $n \geq 4$  if  $\varepsilon \leq 0.295$ . ■

## 8.6. Exterior Regions

Theodorsen (1931) considered the case where the exterior of the circle  $|\zeta| = R$  is mapped onto the exterior of a nearly circular region  $D$  bounded by  $\Gamma$ . In this

case the mapping function  $\omega = g(\zeta)$  is normalized such that  $\lim_{\zeta \rightarrow \infty} \frac{\omega}{\zeta} = 1$ . This case reduces to that analyzed in §8.1 if we use the transformations  $w = 1/\omega$  and  $z = R/\zeta$ . Let the boundary  $\Gamma$  be defined by  $r = r(\Phi)$ ,  $0 \leq \Phi \leq 2\pi$ , where, analogous to (8.1.1) and (8.1.2), for some  $b > 0$  and  $0 < \varepsilon < 1$ ,

$$\frac{b}{1 + \varepsilon} \leq r(\Phi) \leq b(1 + \varepsilon), \quad (8.6.1)$$

and

$$\left| \frac{r'(\Phi)}{r(\Phi)} \right| \leq \varepsilon. \quad (8.6.2)$$

Thus, the function  $w = f(z) = \frac{1}{g(\zeta)}$ ,  $\zeta = R/z$ , maps the unit disk  $|z| < 1$  onto  $\text{Int}(\Gamma)$ , where  $\Gamma$  is represented by the equation

$$\rho = \rho(\phi) = \frac{1}{r(\Phi)},$$

such that  $\phi = -\Phi$ ,  $\rho(\phi)$  satisfies the conditions (8.1.1) and (8.1.2), and  $a = 1/b$ . Then, for  $\zeta = R e^{i\psi}$ , we have

$$\arg \{g(\zeta)/\zeta\} = \Phi(\psi) - \psi,$$

where we take  $\arg \{g(\zeta)/\zeta\}_{\zeta=\infty} = 0$ . Thus, for  $\zeta = R e^{i\psi}$  and  $z = e^{i\theta}$ , where  $\theta = -\psi$ , we have

$$\begin{aligned} \log \frac{g(\zeta)}{\zeta} &= \log r[\Phi(\psi)] + i[\Phi(\psi) - \psi] - \log R \\ &= -\log \frac{f(z)}{z} - \log R \\ &= -\log \rho[\phi(\theta)] - i[\phi(\theta) - \theta] - \log R. \end{aligned} \quad (8.6.3)$$

Thus,  $\Phi_n(\psi) = -\phi(\theta)$ ,  $\psi = -\theta$ , and we can form the iterations in this case, analogous to (8.1.7), as

$$\begin{aligned} \Phi_0(\psi) &= 0, \\ \Phi_n(\psi) - \psi &= \frac{1}{2\pi} \int_0^\pi \{\log r(\phi_{n-1}(\psi + t)) - \log r(\phi_{n-1}(\psi - t))\} \\ &\quad \times \cot \frac{t}{2} dt, \quad n = 1, 2, \dots. \end{aligned} \quad (8.6.4)$$

Hence, the estimates for  $|\phi_n(\theta) - \phi(\theta)|$  and for derivatives of these differences obtained in §8.3 also hold for  $|\Phi_n(\psi) - \Phi(\psi)|$  and derivatives of these differences. See §10.4 for more on Theodorsen's method and its convergence problems.

---

## 8.7. Trigonometric Interpolation

In practice, computations are specially simple if functions are expanded in Fourier series and then the method of trigonometric interpolation is applied. We fix  $2N$  points on the unit circle in the  $z$ -plane by

$$\theta_k = \frac{k\pi}{n}, \quad k = 0, 1, \dots, 2N-1,$$

and denote

$$\phi_k^{(\nu)} = \phi^{(\nu)}(\theta_k), \quad w_k^{(\nu)} = \log \rho(\phi^{(\nu)}(\theta_k)). \quad (8.7.1)$$

Using the Fourier polynomial

$$w_k^{(\nu)} = \frac{\alpha_0^{(\nu)}}{2} + \sum_{n=1}^N \left( \alpha_n^{(\nu)} \cos n\theta_k + \beta_n^{(\nu)} \sin n\theta_k \right), \quad (8.7.2)$$

where

$$\begin{aligned} \alpha_n^{(\nu)} &= \frac{1}{N} \sum_{k=0}^{2N-1} w_k^{(\nu)} \cos n\theta_k, \quad n = 0, 1, \dots, N, \\ \beta_n^{(\nu)} &= \frac{1}{N} \sum_{k=0}^{2N-1} w_k^{(\nu)} \sin n\theta_k, \quad n = 0, 1, \dots, N-1. \end{aligned} \quad (8.7.3)$$

Then, in view of (5.4.17), the harmonic function

$$\phi_k^{(\nu+1)} - \theta_k = \sum_{n=1}^N \left( \alpha_n^{(\nu)} \sin n\theta_k - \beta_n^{(\nu)} \cos n\theta_k \right) \quad (8.7.4)$$

is conjugate to  $w_k^{(\nu)}$ . If we substitute the values of  $\alpha_n^{(\nu)}$  and  $\beta_n^{(\nu)}$  from (8.7.3), then we obtain the formula

$$\phi_k^{(\nu+1)} - \theta_k = -\frac{1}{N} \sum_{n=1}^N \left( w_{k+n}^{(\nu)} - w_{k-n}^{(\nu)} \right) \cot \frac{\theta_n}{2}, \quad (8.7.5)$$

where we set  $w_{1\pm 2N} = w_1$ . Taking the initial value  $\phi_k^{(0)} = \theta_k$ , formula (8.7.5) together with (8.7.1) provides an iterative technique to compute the quantities  $\phi_k^{(\nu)}$  and  $w_k^{(\nu)}$ . Note that the finite sum (8.7.5) has a form that corresponds to the integral in (8.1.6). Since the method converges, we can determine the Fourier coefficients  $\alpha_n$  and  $\beta_n$  by taking the limiting processes  $\phi_k = \lim_{\nu \rightarrow \infty} \phi_k^{(\nu)}$  and  $w_k = \lim_{\nu \rightarrow \infty} w_k^{(\nu)}$ , which yields an approximation  $\tilde{F}(z)$  for the function  $F(z)$  as

$$\tilde{F}(z) = \frac{\alpha_0}{2} + \sum_{n=1}^{N-1} (\alpha_n - i\beta_n) z^n + \alpha_N z^N, \quad (8.7.6)$$

and an approximation  $\tilde{f}(z)$  for the mapping function as

$$\tilde{f}(z) = z e^{\tilde{F}(z)}. \quad (8.7.7)$$

The function  $\tilde{f}(z)$  maps the unit disk onto a region  $\tilde{D}$  with a boundary  $\tilde{\Gamma}$  which cuts the curve  $\Gamma$  in  $2N$  points determined by  $z = e^{i\theta_k}$ . The quality of the approximation depends on the closeness of the two curves  $\Gamma$  and  $\tilde{\Gamma}$  between these  $2N$  points. For better closeness, even  $4N$  points can be chosen where the values of  $\phi_k$  and  $w_k$  already computed can be used as the first approximation. This approximation method with Fourier series is suitable for regions with smooth boundaries.

## 8.8. Wegmann's Method

This quadratic convergence method deals with the general problem of conformal mapping between any two simply connected regions  $D$  and  $G$  bounded by Jordan contours  $\Gamma$  and  $\Delta$ , respectively. Let this conformal map be denoted by  $f : D \mapsto G$  such that all such maps  $f$  can be extended to  $\bar{D}$  together with the homeomorphism  $f : \Gamma \mapsto \Delta$ . The function  $f$  is uniquely defined if  $f(z_0) = a_0$  for  $z_0 \in D$  and  $f(\zeta) = a_1$  for  $\zeta \in \Gamma$ . Since the mapping function is fully determined by its boundary values, the problem of computing  $f$  can be reduced to that of finding the boundary map  $f : \Gamma \mapsto \Delta$ . Thus, if a parametrization  $\gamma(s)$  of  $\Delta$  is prescribed, then there exists a real function  $S(\zeta)$  which satisfies

$$f(\zeta) = \gamma(S(\zeta)), \quad (8.8.1)$$

where  $\zeta = \zeta(t)$  is a parametric representation of the boundary  $\Gamma$ ,  $\gamma(s)$  is assumed to be a  $2\pi$ -periodic function, and  $S$  is a continuous, multiple-valued

function that changes by  $2\pi$  while winding around  $\Gamma$  once, i.e.,

$$[S(\gamma)]_\Gamma = 2\pi. \quad (8.8.2)$$

This mapping problem can be generalized to the case when the boundary  $\Delta$  is not necessarily a Jordan contour. In that case, let  $\gamma(s) \in C^1[0, 2\pi]$  with  $\gamma'(s) \neq 0$ , where prime denotes differentiation with respect to  $s$ , and let  $\kappa (\geq 1)$  be the winding number of  $\gamma'$  with respect to the origin. Then a function  $f$  analytic in the region  $D$  and continuous on  $\bar{D}$  and satisfying (8.8.1) and (8.8.2) maps  $D$  onto a  $\kappa$ -sheeted Riemann surface with  $\kappa - 1$  branch points. Since these branch points cannot be determined by the boundary  $\Gamma$  alone, we can fix  $\kappa - 1$  additional parameters through  $\kappa - 1$  interpolation functions. Then  $f$  can be determined if the following additional conditions are satisfied:

$$f(z_j) = a_j, \quad j = 0, 1, \dots, \kappa, \quad (8.8.3)$$

where  $z_0 \in \Gamma$ ,  $a_0 \in \Delta$ , and  $z_1, \dots, z_\kappa \in D$ .

The iterative method to determine the approximate function  $\tilde{f}$  that maps the boundary  $\Gamma$  conformally onto the boundary  $\Delta$  requires that  $\tilde{f}_\nu(\zeta) = \gamma(S_\nu(\zeta))$  prior to the  $\nu$ -th iteration. Then at the  $\nu$ -th step this map is updated by shifting the function values along the tangent to the boundary curve, i.e., by determining a real-valued function  $u_\nu(\zeta)$  such that

$$\gamma(S_\nu(\zeta)) - u_\nu(\zeta) \gamma'(S_\nu(\zeta)) = h_{\nu+1}(\zeta), \quad (8.8.4)$$

where the function  $h_{\nu+1}$  is analytic in  $D$  and continuous on  $\bar{D}$  with  $h_{\nu+1}(z_\nu) = a_\nu$ ,  $\nu = 1, 2, \dots, n$ . For the boundary point  $z_0 \in \Gamma$  (the case  $\nu = 0$ ) the prescribed value  $a_0$  lies on  $\Delta$ , i.e.,  $a_0 = \gamma(s_0)$ . But since  $h_{\nu+1}(z_0)$  lies on the tangent through the point  $\gamma(S_\nu(z_0))$ , the condition  $h_{\nu+1}(z_0) = a_0$ , in general, is not satisfied. Therefore, we replace this condition by

$$u_\nu(z_0) = s_0 - S_\nu(z_0). \quad (8.8.5)$$

Note that the function  $h_{\nu+1}$  is an approximation of the boundary map  $f$ , although the values that it takes on  $\Gamma$ , in general, do not lie on  $\Delta$ . The function  $h_{\nu+1}$ , however, yields a new approximation for the parameter mapping function  $S$  as

$$S_{\nu+1}(\zeta) = S_\nu(\zeta) + u_\nu(\zeta). \quad (8.8.6)$$

Thus, after starting with an arbitrary function  $S_1(\zeta)$ , the conditions  $S_\nu(z_0) = s_0$  and  $u_\nu(z_0) = 0$  are satisfied for all  $\nu \geq 2$ , and hence, the condition  $h_{\nu+1}(z_0) = a_0$  is satisfied.

If we multiply (8.8.4) by  $\frac{1}{2i\pi} \frac{d\zeta}{\zeta - z}$  and integrate over  $\Gamma$ , we get

$$\begin{aligned} & \frac{1}{2i\pi} \int_{\Gamma} \frac{\gamma(S_{\nu}(\zeta)) + u_{\nu}(\zeta) \gamma'(S_{\nu}(\zeta))}{\zeta - z} d\zeta \\ &= \begin{cases} 0 & \text{for } z \notin \bar{D}, \\ \frac{1}{2} [\gamma(S_{\nu}(z)) + u_{\nu}(z) \gamma'(S_{\nu}(z))] & \text{for } z \in \Gamma, \\ a_{\nu} & \text{for } z = z_{\nu}, \nu = 1, \dots, \kappa. \end{cases} \quad (8.8.7) \end{aligned}$$

Note that the formula (8.8.7) is a linearization of the equation

$$\frac{1}{2i\pi} \int_{\Gamma} \frac{\gamma(S(\zeta))}{\zeta - z} d\zeta = \begin{cases} 0 & \text{for } z \notin \bar{D}, \\ \frac{1}{2} \gamma(S(z)) & \text{for } z \in \Gamma, \\ a_{\nu} & \text{for } z = z_{\nu}, \nu = 1, \dots, \kappa. \end{cases} \quad (8.8.8)$$

The middle part of Eq (8.8.8) is a nonlinear singular integral equation of the second kind for the parameter function  $S$  associated with the boundary map  $f$ . The method of solution for this equation is linearization and the use of Newton's method. This fact is used to prove convergence which is locally quadratic. A proof is available in Wegmann (1984).

The numerical computation of the iterative method begins with the discretization (8.8.7) of Eq (8.8.8) for the boundary  $\Gamma$  which is used to compute the updates  $u_{\nu}$ . However, in the particular case when  $\Gamma$  is the unit circle, explicit representations of the solution in terms of integrals can be obtained. Details for this case are as follows: All functions are discretized at  $n = 2N$  equidistant points  $\zeta_i = e^{i\phi_i} \in \Gamma$ ,  $\phi_i = \phi_0 + i\pi/N$ ,  $i = 1, \dots, n$ . The integrals are evaluated by trigonometric interpolation. Thus, for example, if

$$F(z) = \frac{1}{2i\pi} \int_{\Gamma} \frac{\phi(\zeta)}{\zeta - z} d\zeta, \quad (8.8.9)$$

then the function  $\phi$  is represented as a polynomial in  $\zeta$  and  $\zeta^{-1}$ , i.e.,

$$\phi(\zeta_i) = \sum_{i=-N}^N \alpha_j \zeta_i^j = F^+(\zeta_i) + F^-(\zeta_i), \quad (8.8.10)$$

where

$$F^+(\zeta_i) = \sum_{i=0}^N \alpha_j \zeta_i^j, \quad F^-(\zeta_i) = \sum_{i=-N}^N \alpha_j \zeta_i^j. \quad (8.8.11)$$

If we define

$$G(z) = \begin{cases} e^{F(z)-F(0)/2} & \text{for } |z| < 1, \\ z^{2\kappa} e^{F(z)-F(0)/2} & \text{for } |z| > 1, \end{cases} \quad (8.8.12)$$

$$\psi(z) = \frac{G(z)}{2i\pi} \int_{\Gamma} \frac{\hat{g}(\zeta) \Im \left\{ \frac{\hat{f}(\zeta)}{\hat{g}(\zeta)} \right\}}{G^+(\zeta)} \frac{d\zeta}{\zeta - z}, \quad (8.8.13)$$

where the function  $\hat{f}(\zeta) = \gamma(S(\zeta))$  and  $\hat{g}(\zeta) = \gamma'(S(\zeta))$  are Hölder-continuous, and

$$h_0(z) = \frac{1}{2} \left[ \psi^+(\zeta) + \overline{\psi^-(\zeta)} \right], \quad (8.8.14)$$

then Wegmann (1984) has proved the following:

**THEOREM 8.8.1.** *Let  $\zeta$  and  $\gamma$  be Hölder-continuous functions with  $\zeta(t) \neq 0$  and  $\gamma'(s) \neq 0$  for all  $s$  and  $t$ , where  $\zeta = \zeta(t)$  and  $\gamma = \gamma(s)$  are parametric representations of the boundaries  $\Gamma$  and  $\Delta$ , respectively, of simply connected regions  $D$  and  $G$ . Let  $S(\zeta)$  be a Hölder-continuous function satisfying (8.8.1). Let the winding number  $\kappa$  of  $\gamma'$  be positive, and let the points  $z_1, \dots, z_\kappa \in D$  and  $z_0 \in \Gamma$  and the complex numbers  $a_1, \dots, a_\kappa$  and a real number  $u_0$  be given. Then there exists a unique Hölder-continuous real function  $u(\zeta)$  defined on  $\Gamma$  and a unique complex function  $h$  analytic in  $D$  and continuous on  $\bar{D}$  such that*

$$\gamma(S(\zeta)) + u(\zeta) \gamma'(S(\zeta)) = h(\zeta), \quad (8.8.15)$$

satisfying the conditions

$$h(z_\nu) = a_\nu \quad \text{for } \nu = 1, 2, \dots, \kappa, \quad (8.8.16)$$

and

$$u(z_0) = a_0, \quad (8.8.17)$$

In the case when  $\Gamma$  is the unit circle, the solution of the linearized integral equation in (8.8.7) can be represented explicitly in terms of integral transforms.

Thus, the integrals are computed by using the discrete Fourier transform. Note that if FFT is used instead, then the transformation of  $\phi$  to  $F^\pm$  takes  $O(n \log n)$  operations. The foregoing outline of the method and this theorem show how this iterative method differs from that discussed in §8.1 and 8.2.

The iterative process is carried out in the following two steps:

STEP 1: Assuming that the functions  $\gamma(s)$ ,  $\gamma'(s)$  and  $\phi_0(s) = \arg\{\gamma'(s)\}$  are defined explicitly and the initial value of  $S_1(\zeta_0)$  is available (initial guess), once  $S_\nu$  has been computed for some  $\nu \geq 1$ , then compute

$$\begin{aligned}\hat{f}_\nu(\zeta_i) &= \gamma(S_\nu(\zeta_i)), \quad \hat{g}_\nu(\zeta_i) = \gamma'(S_\nu(\zeta_i)), \\ \phi(\zeta_i) &= 2\phi_0(S_\nu(\zeta_i)) - 2\kappa\theta_i.\end{aligned}\quad (8.8.18)$$

STEP 2: Use one of the methods described below.

METHOD 1: Determine  $\psi$  and  $h_0$  from (8.8.13) and (8.8.14), and set

$$h_{\nu+1}(z) = h_0(z) + P(z)G(z), \quad (8.8.19)$$

where the polynomial  $P$  is chosen such that

$$\begin{aligned}P(z_0)G^+(z_0) &= (s_0 - S_\nu(z_0))\hat{g}_\nu(z_0) + \hat{f}_\nu(z_0) - h_0(z_0), \\ P(z_i)G(z_i) &= a_i - h_0(z_i) \quad \text{for } i = 1, \dots, \kappa.\end{aligned}\quad (8.8.20)$$

Note that in this discretization  $z_0$  is equal to one of the  $\zeta_i$ . Then use Cauchy's formula (1.2.2) and integral representation (8.8.9) to compute  $h_0(z_i)$  and  $F(z_i)$  for  $i \geq 1$ . Thus,  $G(z_i) = e^{F(z_i)-F(0)/2} \neq 0$ , and  $P$  is taken as an interpolation polynomial. Finally, set

$$S_{\nu+1}(\zeta_i) = S_\nu(\zeta_i) + \Re \left\{ \frac{h_{\nu+1}(\zeta_i) - \hat{f}_\nu(\zeta_i)}{\hat{g}_\nu(\zeta_i)} \right\}. \quad (8.8.21)$$

METHOD 2: Instead of (8.8.13), compute  $\psi$  for  $\nu \geq 2$  by the formula

$$\psi(z) = \frac{G(z)}{\pi} \int_{\Gamma} \frac{\hat{g}_\nu(\zeta) \Im \left\{ (\hat{f}_\nu(\zeta) - h_\nu(\zeta)) \hat{g}_\nu(\zeta) \right\}}{G^+(\zeta)} \frac{d\zeta}{\zeta - z}. \quad (8.8.22)$$

Then  $h_0$  is computed from (8.8.14), which leads to

$$h_{\nu+1}(z) = h_\nu(z) + h_0(z) + P(z)G(z), \quad (8.8.23)$$

where the polynomial  $P$  is computed from

$$P(z_i) = -\frac{h_0(z_i)}{G(z_i)} \quad \text{for } i = 0, 1, \dots, \kappa. \quad (8.8.24)$$

As noted by Wegmann (1986), the first method gives more accurate results than the second.

CASE STUDY 8.8.1. The result of the conformal mapping of the unit circle  $\zeta(t) = e^{it}$  onto the inverted ellipses (see Case Study 7.4.4), defined by  $\rho(s) = \sqrt{1 - (1 - p^2) \cos^2 s}$ ,  $0 < p < 1$ , are shown in Wegmann (1986) for  $p = 0.4, 0.6$ , and  $0.8$ , where the error after the 10-th iteration is  $\|S_{11} - S\| \approx 1.8 \times 10^{-2}$ ,  $5.7 \times 10^{-5}$ , and  $10^{-8}$ , respectively, for the above values of  $p$  with  $n = 40$ . The exact boundary correspondence function is given by  $\tan s = p \tan \theta$ , where  $\theta = \arg\{z\}$ , and the boundary map is defined by  $w = \frac{2pz}{(1+p)+(1-p)z^2}$ . ■

---

## 8.9. Newton's Method

As explained in §8.1 and 8.8, the function  $f(r e^{i\theta}) = \rho(\phi(\theta)) e^{i\phi(\theta)}$  defines the boundary correspondence function  $\phi : [0, 2\pi] \mapsto \mathbb{R}$  for the boundary map  $f$ . Let  $\mathcal{K}$  denote the conjugation operator

$$\mathcal{K}[h](\theta) = \frac{1}{2\pi} \int_0^{2\pi} h(\theta) \cot \frac{\theta - t}{2} dt, \quad (8.9.1)$$

where the integral takes a Cauchy p.v. Then Theodorsen's integral equation (8.1.5) can be written as

$$\phi(\theta) = \theta + \mathcal{K}[\log \rho(\phi(\theta))](\theta), \quad (8.9.2)$$

or, if we set  $\Psi(\theta) = \phi(\theta) - \theta$ , then as

$$\Psi(\theta) = \mathcal{K}[\log \rho(\Psi(\theta) + \theta)](\theta), \quad (8.9.3)$$

which, according to Gaier (1964) and Wegmann (1984), has a unique  $2\pi$ -periodic solution  $\Psi^*(\theta)$ . Wegmann (1984) has also proved that for  $f \in L^2$  and  $\mathcal{K}f \in L^\infty$

$$\|\mathcal{K}f\|_\infty \leq \sqrt{\frac{\pi}{6} \int_0^\pi |f'(x)|^2 dx} = \sqrt{\frac{\pi}{3}} \|f\|_2 < 2 \|f\|_2. \quad (8.9.4)$$

We shall assume that the  $2\pi$ -periodic function  $\rho$  is absolutely continuous on  $\mathbb{R}$  and  $|\sigma| = < \varepsilon$  a.e. (we say that  $\rho$  satisfies the  $\varepsilon$ -condition), where  $\sigma$  is defined in (8.1.9). The solution  $\Psi^*(\theta)$  of Eq (8.9.3) is given explicitly as a consequence

of the Riemann–Hilbert problem (see Appendix C). As we have seen in §8.1 and 8.3, a numerical solution of the integral equation (8.9.3) can be obtained by first discretizing this equation and then applying an iterative method. The convergence of this method depends on the  $\varepsilon$ -condition ( $\varepsilon < 1$ ), except in the case of certain symmetric curves with corners and pole singularities. Thus, it can be shown, as in Gaier (1964), Warschawski (1955), Hübner (1979) and Gutknecht (1981, 1983), that  $\|\Psi_n - \Psi^*\|_2 \rightarrow 0$  and  $\|\Psi_n - \Psi^*\|_\infty \rightarrow 0$  as  $n \rightarrow \infty$ .

Let  $\mathcal{F} : W \mapsto W$ , where  $W$  is the Sobolev space of  $2\pi$ -periodic and absolutely continuous functions  $f$  with  $f' \in L^2$  (see §1.1). Define the operator

$$\mathcal{F}(\Psi(\theta)) = \Psi(\theta) - (\mathcal{K}[\log \rho(\Psi(\theta) + \theta)]) (\theta). \quad (8.9.5)$$

Then Newton's method for solving the equation (8.9.3) is

$$\begin{aligned} \Psi_0 &\in W, \\ \mathcal{F}'(\Psi_n)[\Psi_{n+1} - \Psi_n] &= -\mathcal{F}(\Psi_n), \quad n = 0, 1, \dots, \end{aligned} \quad (8.9.6)$$

where  $\mathcal{F}'(\Psi_n)$  is the  $F$ -derivative\* of  $\mathcal{F}$  in the Banach space  $(W, \|\cdot\|)$  at  $\Psi_n$ . The operator  $\mathcal{F}(\Psi)$  has an inverse for any  $\Psi \in W$ . Using the solution of a Riemann–Hilbert problem (see §C.3), Hübner (1986) has shown that

$$\Psi_{n+1} - \psi_n = -(\mathcal{F}'(\Psi_n))^{-1} \mathcal{F}(\Psi_n). \quad (8.9.7)$$

Thus, to determine  $\Psi_{n+1}$  from  $\Psi_n$  in formula (8.9.7), we require two applications of the conjugation operator  $\mathcal{K}$ . For numerical computation, we discretize (8.9.7) instead of (8.9.3). Then by using FFT we first approximate  $\Psi_n$  by a vector in  $\mathbb{R}^{2n}$  and then compute an approximate value of  $\Psi_{n+1}$  in the same space. This method, however, is different from Wegmann's (§8.8) as shown in Case Study 8.9.1.

Hübner (1986) has proved the following two results on the convergence of Newton's method.

---

\*If  $p$  is Hölder-continuous and  $\Psi \in W$ , then the  $F$ -derivative of  $\mathcal{F}$  at  $\Psi$  in  $(W, \|\cdot\|)$  exists and is given by

$$(\mathcal{F}'(\Psi)\Omega)(\theta) = \Omega(\theta) - (\mathcal{K}[\sigma(\Psi(\theta) + \theta) \cdot \Omega(\theta)]) (\theta)$$

for some  $\Omega \in W$ .

**THEOREM 8.9.1.** *If  $p$  is  $2\pi$ -periodic and Lipschitz-continuous, then Newton's method for Theodorsen's integral equation (8.9.3) converges locally and quadratically in  $(W, \|\cdot\|)$ .*

**THEOREM 8.9.2.** *If  $|\sigma| < 1/3$  and  $p \in L^\infty$ , then Newton's method for Theodorsen's equation (8.9.3) converges globally in  $(W, \|\cdot\|_2)$ .*

Proofs of these theorem are given in Hübner (1986).

**CASE STUDY 8.9.1.** Wegmann's and Newton's methods are not identical for boundary curves defined in polar coordinates. As an example, take  $\rho(\phi) \equiv 1$  and  $\Psi_0 = \sin \theta$ . Then  $\mathcal{F}(\Psi_0(\theta)) = \Psi_0 - \mathcal{K}[1] = \sin \theta$ . Hence,  $\Psi_1 = 1$ , which is the exact solution of Eq (8.9.3). ■

---

## 8.10. Problems

**PROBLEM 8.10.1.** Prove Theorem 8.8.1. (For a proof see Wegman, 1986, p.9.)

**PROBLEM 8.10.2.** Prove Theorems 8.9.1 and 8.9.2. (For a proof see Hübner, 1986, p.25.)

**PROBLEM 8.10.3.** Develop an algorithm for Newton's method as developed in Hübner (1986), pp.19–30.

**REFERENCES USED:** Carrier, Krook and Pearson (1966), Gaier (1964), Gutknecht (1981, 1983), Hübner (1979, 1986), Koppenfels (1959), Privaloff (1916), F. and M. Riesz (1923), Theodorsen (1931), Theodorsen and Garrick (1934), Warschawski (1935, 1945, 1950, 1955), Wegmann (1984, 1986), Zygmund (1935).

# Chapter 9

---

## Symm's Integral Equation

---

A potential-theoretic formulation of the problem of conformally mapping a simply connected region (or its complement) onto the unit disk leads to a Fredholm integral equation of the first kind, known as Symm's integral equation, which has a kernel with a logarithmic singularity. Unlike Fredholm integral equations of the second kind, e.g., Theodorsen's equation, in which the singularity of the kernel at points near but not on the boundary creates computational difficulties, Symm's integral equation is found easily solvable by numerical methods, such as the orthonormal polynomials method or its modified form, Lagrange's interpolation method, and spline approximations which are discussed in this chapter. Numerical evaluation of Green's functions, as developed in Chapter 6, is another viable alternative to obtain the approximate mapping function.

---

### 9.1. Symm's Integral Equation

We shall derive Symm's integral equation for both interior and exterior regions.

**9.1.1. Interior Regions.** The function  $w = f(z)$  that maps a given simply connected region  $D$  with a Jordan boundary  $\Gamma$  onto the unit disk  $U$  such that  $f(z_0) = 0$  is given by

$$w = f(z) = e^{\log(z-z_0)+g(z-z_0)+i h(z-z_0)}, \quad (9.1.1)$$

(see (6.2.10); also Gram, 1962), such that  $\nabla^2 g = 0$ ,  $z \in D$ , which yields  $g(z) = -\log |z - z_0|$ ,  $z \in \Gamma$ , and  $h$  is the conjugate of  $g$ . Without loss of generality, we shall take  $z_0$  as the origin. Then  $f(z) = e^{\log z + g(x,y) + i h(x,y)}$ ,  $z = x + iy$ , where

$$\begin{aligned}\nabla^2 g &= 0, \quad z \in D, \\ g(x, y) &= -\frac{1}{2} \log (x^2 + y^2), \quad z \in \Gamma.\end{aligned}\tag{9.1.2}$$

If  $w = u + iv$ , then from (9.1.1), we get

$$\begin{aligned}u(x, y) &= e^{\log |z| + g} \cos (\arg\{z\} + h), \\ v(x, y) &= e^{\log |z| + g} \sin (\arg\{z\} + h).\end{aligned}\tag{9.1.3}$$

Thus, the conformal mapping problem reduces to that of determining the harmonic functions  $g$  and  $h$ . We shall represent the harmonic function  $g(x, y)$  as a single-layer logarithmic potential

$$g(x, y) = \int_{\Gamma} \log |x - \zeta| \mu(\zeta) d\zeta,\tag{9.1.4}$$

where  $\mu(\zeta)$  is a suitable source density function on the boundary  $\Gamma$  (see Kythe, 1996, p.21; Maiti, 1968). The harmonic conjugate of the representation (9.1.4) is given by

$$h(x, y) = \int_{\Gamma} \theta(z - \zeta) \mu(\zeta) d\zeta,\tag{9.1.5}$$

(see Jawson, 1963), where  $\theta(z - \zeta) = \arg\{z - \zeta\}$ . Hence, the problem further reduces to that of finding the density function  $\mu(\zeta)$  such that  $g$  satisfies (9.1.2) on  $\Gamma$ . Once  $\mu(\zeta)$  is known, the functions  $g$  and  $h$  can be determined by quadrature at any point in  $D$ . Since the function  $\mu(\zeta)$  is continuous in  $\bar{D}$ , it satisfies the integral equation

$$\int_{\Gamma} \log |z - \zeta| \mu(\zeta) d\zeta = -\log |z|, \quad z \in D, \quad \zeta \in \Gamma,\tag{9.1.6}$$

which is known as *Symm's integral equation* for interior regions. This equation has a unique solution provided  $\text{cap}(\Gamma) \neq 1$  (for the existence of the solution, see Jawson, 1963).

Note that although the function  $g(x, y)$  is single-valued, the function  $h(x, y)$ , in general, is multiple-valued. In fact, suppose that some Jordan contour  $\Gamma^*$  is

contained in  $D$  such that  $0 \in \text{Int}(\Gamma^*)$  and  $\int_{\Gamma^*} \frac{\partial g}{\partial n} ds = A$ , where  $n$  denotes the inward normal to  $\Gamma^*$ , and  $A \neq 0$  is a constant. Then, in view of the Cauchy–Riemann equations, the value of  $h$  will increase by an amount  $A$  whenever  $z$  traverses  $\Gamma^*$  in a clockwise direction. Hence,  $h$  will be single-valued on the contour  $\Gamma^*$  only if  $A = 0$ , i.e., for any such  $\Gamma^*$  we require that

$$\int_{\Gamma^*} \frac{\partial g}{\partial n} ds = 0, \quad (9.1.7)$$

as a condition for the function  $h$  to be single-valued.

**9.1.2. Exterior Regions.** For conformal mapping of the region  $D^* = \text{Ext}(\Gamma)$  onto the region  $U^* = \{w : |w| > 1\}$  such that  $f(0) = 1$  and  $f(\infty) = \infty$ , the mapping function  $w = f_E(z)$  is unique up to a rotation. Let  $C = \text{diam}(D) = \lim_{z \rightarrow \infty} |f'(z)|^{-1} > 0$  denote the transfinite diameter of  $D$  (see §1.1). Then the required mapping function  $f_E(z)$  must satisfy the condition

$$f'_E(z) \rightarrow \frac{1}{C} \quad \text{as } z \rightarrow \infty. \quad (9.1.8)$$

Assuming that  $0 \in D$ , the function  $\frac{f_E(z)}{z}$  is regular in  $D^*$ , including the point  $z = \infty$ . Hence, we take

$$f_E(z) = e^{\log z + \psi(z)}, \quad (9.1.9)$$

where  $\psi(z)$  is regular in  $D^*$ , and in view of (9.1.8),  $\psi(z) \rightarrow -\log C = \gamma$  as  $z \rightarrow \infty$ , where  $\gamma$  is Robin's constant (§1.3). Let  $\psi(z) = \beta(z) + \gamma$ . Then  $\beta(z)$  is regular in  $D^*$ , and  $\beta(z) \rightarrow 0$  as  $z \rightarrow \infty$ . Hence,  $\beta(z)$  can be represented as

$$\beta(z) = \hat{g}(x, y) + i \hat{h}(x, y), \quad z = x + iy,$$

where  $\hat{g}$  and  $\hat{h}$  are conjugate harmonic functions in  $D^*$  such that  $\hat{g} \rightarrow 0$  and  $\hat{h} \rightarrow 0$  as  $z \rightarrow \infty$ . Thus,

$$f_E(z) = e^{\log z + \gamma + \hat{g}(x, y) + i \hat{h}(x, y)}, \quad (9.1.10)$$

where the boundary condition  $|f_E(z)| = 1$  for  $z \in \Gamma$  becomes

$$\gamma + \hat{g}(x, y) = -\log |z|, \quad z \in \Gamma. \quad (9.1.11)$$

As in §9.1.1, the harmonic functions  $\hat{g}(x, y)$  and  $\hat{h}(x, y)$  can be represented in the form (9.1.4) and (9.1.5), respectively. Then the boundary condition (9.1.11) for the density function  $\mu(\zeta)$  becomes

$$\int_{\Gamma} \log(z - \zeta) \mu(\zeta) d\zeta + \gamma = -\log|z|, \quad z \in \Gamma, \quad (9.1.12)$$

and the condition  $g(\infty) = 0$  reduces to

$$\int_{\Gamma} \mu(\zeta) d\zeta = 0. \quad (9.1.13)$$

Eqs (9.1.12) and (9.1.13) are coupled integral equations for  $\mu(\zeta)$  and  $\gamma$ , and they have a unique solution (see Jawson, 1963, and Symm, 1967). Once  $\mu$  and  $\gamma$  are computed from (9.1.12)–(9.1.13), the mapping function  $f_E(z)$  can be determined from (9.1.10).

As explained in §7.3.3, the region  $D^*$  may be mapped onto  $U$  by using the inverse transformation  $z \mapsto z^{-1}$  such that the point  $z = \infty$  goes into  $w = 0$ .

## 9.2. Orthonormal Polynomial Method

The orthonormal polynomial (ONP) method, developed by Rabinowitz (1966), is used to compute the density function  $\mu(\zeta)$  numerically. The basic idea is to approximate  $\mu(\zeta)$  by a step-function. To do this, we partition the boundary  $\Gamma$  into  $N$  sections  $\Gamma_1, \dots, \Gamma_N$ , and assume that  $\mu(\zeta) \equiv \mu_j (= \text{const})$  for any point  $\zeta \in \Gamma_j$ ,  $j = 1, \dots, N$ .

(a) INTERIOR REGIONS. Then Eq (9.1.6) reduces to

$$\sum_{j=1}^N \left\{ \int_{\Gamma_j} \log|z - \zeta| |d\zeta| \right\} \mu_j = -\log|z|, \quad z \in \Gamma. \quad (9.2.1)$$

If we take  $z \in \Gamma$  with each of the  $N$  nodes  $z_k = x_k + i y_k$ ,  $k = 1, \dots, N$ , then we obtain a system of  $N$  linear equations in  $N$  unknowns  $\mu_j$ :

$$\sum_{j=1}^N \left\{ \int_{\Gamma_j} \log|z_k - \zeta| |d\zeta| \right\} \mu_j = -\frac{1}{2} \log(x_k^2 + y_k^2), \quad k = 1, \dots, N. \quad (9.2.2)$$

The solution  $\mu_j, j = 1, \dots, N$ , of this system gives the approximate values of  $g$  and  $h$  from (9.1.4) and (9.1.5), respectively, as

$$G(x, y) = \sum_{j=1}^N \left\{ \int_{\Gamma_j} \log |z - \zeta| |d\zeta| \right\} \mu_j, \quad z \in \bar{D}, \quad (9.2.3)$$

$$H(x, y) = \sum_{j=1}^N \left\{ \int_{\Gamma_j} \theta(z - \zeta) |d\zeta| \right\} \mu_j, \quad z \in \bar{D}, \quad (9.2.4)$$

and then the approximate mapping function  $f(z)$  can be determined from (9.1.3).

The details for selecting the nodes  $z_j$  and evaluating the integrals in (9.2.3) and (9.2.4) are as follows: A convenient way to partition  $\Gamma$  is to take the sections  $\Gamma_j$  with end points  $z_{j-1/2}$  and  $z_{j+1/2}$  and to take the nodes  $z_k$  as any point in each  $\Gamma_j$ . Then, for any  $z \in \bar{D} \setminus \{\Gamma_j\}$ , we take

$$\begin{aligned} \int_{\Gamma_j} \log |z - \zeta| |d\zeta| &= \frac{l_j}{6} [\log |z_k - z_{j-1/2}| + 4 \log |z_k - z_j| \\ &\quad + \log |z_k - z_{j+1/2}|], \end{aligned} \quad (9.2.5)$$

$$\begin{aligned} \int_{\Gamma_j} \theta(z - \zeta) |d\zeta| &= \frac{l_j}{6} [\theta(z_k - z_{j-1/2}) + 4 \theta(z_k - z_j) \\ &\quad + \theta(z_k - z_{j+1/2})], \end{aligned} \quad (9.2.6)$$

where  $l_j$  is the length of  $\Gamma_j$ . If  $\Gamma$  is a simple Jordan contour, the length  $l_j$  for each  $\Gamma_j$  is the arc length which can be easily evaluated analytically, and if  $z_j$  is the mid-point of  $\Gamma_j$ , the formulas (9.2.5) and (9.2.6) correspond to Simpson's rule. However, if the boundary  $\Gamma$ , in general, is analytic, the length  $l_j$  can be approximated by

$$l_j = |z_j - z_{j-1/2}| + |z_j - z_{j+1/2}|, \quad (9.2.7)$$

where  $z_j$  need not be a midpoint of  $\Gamma_j$ .

When  $z \in \Gamma_j$ , formulas (9.2.5)–(9.2.6) cannot be used because  $\log |z - \zeta|$  has a singularity at  $z = \zeta$  and  $\theta(z - \zeta)$  is undefined at  $z = \zeta$ . However, in each case the integrals exist and can be computed approximately. In particular, for  $z = z_j$  we take

$$\begin{aligned} \int_{\Gamma_j} \log |z_j - \zeta| |d\zeta| &= |z_j - z_{j-1/2}| (\log |z_j - z_{j-1/2}| - 1) \\ &\quad + |z_j - z_{j+1/2}| (\log |z_j - z_{j+1/2}| - 1), \end{aligned} \quad (9.2.8)$$

and for  $z = z_{j \pm 1/2}$  we take

$$\int_{\Gamma_j} \log |z_{j \pm 1/2} - \zeta| |d\zeta| = |z_{j+1/2} + z_{j-1/2}| (\log |z_{j+1/2} - z_{j-1/2}| - 1), \quad (9.2.9)$$

and

$$\int_{\Gamma_j} \theta(z_{j \pm 1/2} - \zeta) |d\zeta| = l_j \theta(z_{j \pm 1/2} - z_j). \quad (9.2.10)$$

Thus, formula (9.2.5) with  $z = z_k$  for  $j \neq k$ , and formula (9.2.8) for  $j = k$  give the coefficients of  $\mu_j$  in (9.2.2), whereas the coefficients of  $\mu_j$  in (9.2.3) and (9.2.4) are given by (9.2.5) and (9.2.6), respectively.

To estimate the error involved in this method, let  $F(z)$  denote the approximate mapping function. Then, by hypothesis,  $|F(z)| = 1$  at each node  $z_j \in \Gamma_j$ . The maximum error  $E_M$  can be estimated by computing the values of  $||F(z)| - 1|$ ,  $z \in \Gamma$ , such that

$$E_M = \sup_{z \in \Gamma} ||F(z)| - 1|. \quad (9.2.11)$$

In view of the maximum modulus theorem (§1.2),  $|F(z) - f(z)|$  assumes its maximum value somewhere on the boundary  $\Gamma$ . Also for any  $z$ ,

$$\begin{aligned} |F(z) - f(z)| &\leq ||F(z)| - |f(z)|| + |f(z)| |\arg\{F(z)\} - \arg\{f(z)\}| \\ &= ||F(z)| - |f(z)|| + |f(z)| |H(x, y) - h(x, y)| \\ &\leq \max_{z \in \Gamma} \left\{ ||F(z)| - 1| + |H(x, y) - h(x, y)| \right\} \\ &\leq E_M + \max_{z \in \Gamma} |H(x, y) - h(x, y)|, \end{aligned} \quad (9.2.12)$$

where we have used (9.1.5) and (9.2.4). This inequality implies that if  $h$  is known on  $\Gamma$ , then the absolute error in the approximate mapping function  $F(z)$  can be determined at any point. But  $h$ , in general, is not known for any  $z$ , except when the region  $D$  has symmetry. In that case  $h$  is known at some points of  $\Gamma$ . In fact, if  $\theta(z - \zeta)$  is so defined that the axes of symmetry are mapped onto themselves, then  $h = 0$  on such axes. Also, we may expect maximum error at some of these points on  $\Gamma$ , which are, e.g., the end points of the major and minor axes of an ellipse or corners of a rectangle or square. Therefore, we take the largest value attained by  $|H|$  at such points as an estimate of maximum error in  $|H(z) - h(z)|$  for  $z \in \Gamma$ , which, in view of (9.2.12), accounts for maximum error in  $\arg\{F(z)\}$ ,  $z \in \Gamma$ . We denote this estimate by  $E_A$ . Then,

from (9.2.12), the sum  $E_M + E_A$  gives an estimate for the upper bound on absolute error in the ONP method.

CASE STUDY 9.2.1. Consider Cassini's oval

$$\Gamma : [(x+1)^2 + y^2] [(x-1)^2 + y^2] = a^4,$$

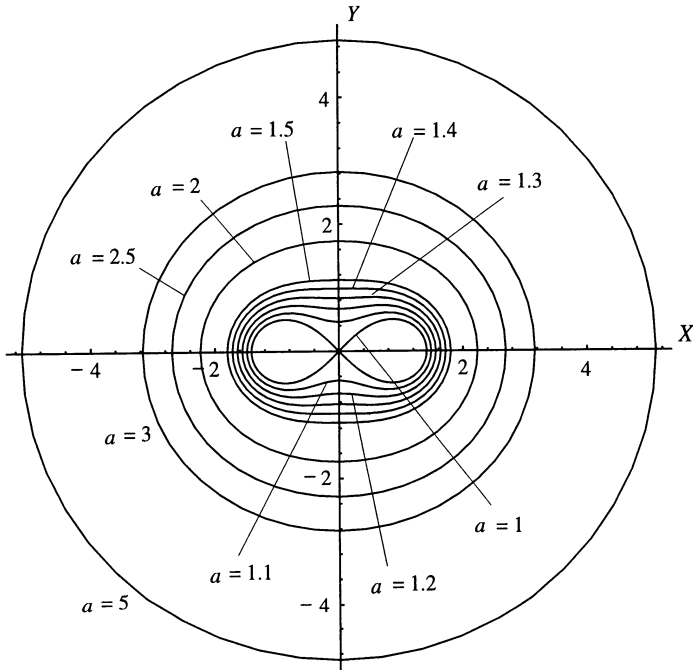


Fig. 9.2.1. Cassini's oval for  $a = 1, 1.1, 1.2, 1.3, 1.4, 1.5, 2, 2.5, 3, 5$ .

which is represented in Fig. 9.2.1 for different values of  $a$  (also see Fig 6.3.1). The region  $D$  is not univalent for  $a = 1$ . Each contour  $\Gamma$  is symmetric about both coordinate axes, so we shall consider the first quadrant. The exact mapping function is given by (Rabinowitz, 1966)

$$f(z) = \frac{az}{\sqrt{a^4 - 1 + z^2}}.$$

Tabular data for the approximate mapping function, using the ONP method, are given in Symm (1966) for  $a = 1.2$ . The functions  $U(x, y)$  and  $V(x, y)$

computed for  $a = 1.3$  are given below in Table 1. ■

Table 1. Cassini's oval,  $a = 1.3$

| $x$       | $y$      | $U(x, y)$ | $V(x, y)$ |
|-----------|----------|-----------|-----------|
| 0.00      | 0.830662 | 0.00000   | 0.99999   |
| 0.05      | 0.830937 | 0.09541   | 0.99491   |
| 0.10      | 0.831741 | 0.18887   | 0.98201   |
| 0.15      | 0.833019 | 0.27838   | 0.96047   |
| 0.20      | 0.834681 | 0.36248   | 0.93199   |
| 0.25      | 0.836608 | 0.44009   | 0.89795   |
| 0.30      | 0.838659 | 0.51061   | 0.85981   |
| 0.35      | 0.840675 | 0.57384   | 0.81897   |
| 0.40      | 0.842488 | 0.62991   | 0.77667   |
| 0.45      | 0.843923 | 0.67921   | 0.73395   |
| 0.50      | 0.844805 | 0.72227   | 0.69161   |
| 0.55      | 0.844960 | 0.75971   | 0.65026   |
| 0.60      | 0.844218 | 0.79217   | 0.61029   |
| 0.65      | 0.842412 | 0.82026   | 0.57199   |
| 0.70      | 0.839382 | 0.84456   | 0.53546   |
| 0.75      | 0.834966 | 0.86559   | 0.50075   |
| 0.80      | 0.829006 | 0.88381   | 0.46783   |
| 0.85      | 0.821342 | 0.89963   | 0.43665   |
| 0.90      | 0.811805 | 0.91338   | 0.40709   |
| 0.95      | 0.800220 | 0.92538   | 0.37903   |
| 1.00      | 0.786394 | 0.93587   | 0.35234   |
| 1.05      | 0.770111 | 0.94507   | 0.32686   |
| 1.10      | 0.751122 | 0.95317   | 0.30245   |
| 1.15      | 0.729135 | 0.96031   | 0.27895   |
| 1.20      | 0.703789 | 0.96662   | 0.25619   |
| 1.25      | 0.674634 | 0.97223   | 0.23401   |
| 1.30      | 0.641080 | 0.97723   | 0.21219   |
| 1.35      | 0.602324 | 0.98169   | 0.19049   |
| 1.40      | 0.557216 | 0.98568   | 0.16862   |
| 1.45      | 0.503985 | 0.98973   | 0.14612   |
| 1.50      | 0.439623 | 0.99251   | 0.12225   |
| 1.55      | 0.358101 | 0.99542   | 0.09562   |
| 1.60      | 0.242597 | 0.99806   | 0.06228   |
| 1.6401219 | 0.000000 | 1.00001   | 0.00000   |

(b) EXTERIOR REGIONS. In this case we solve the coupled equations (9.1.12)–(9.1.13) by the ONP method as follows: With the partitions  $\Gamma_j$ ,  $j = 1, \dots, N$ , Eq (9.1.12) reduces to the system of linear equations

$$\sum_{j=1}^N \left\{ \int_{\Gamma_j} \log |z_k - \zeta| |d\zeta| \right\} \mu_j + \hat{\gamma} = -\frac{1}{2} \log (x^2 + y^2), \quad k = 1, \dots, N, \quad (9.2.13)$$

where  $\hat{\gamma}$  approximates  $\gamma$  and Eq (9.1.13) becomes

$$\sum_{j=1}^N \left\{ \int_{\Gamma_j} |d\zeta| \right\} \mu_j = 0. \quad (9.2.14)$$

Thus, Eqs (9.2.13)–(9.2.14) form a system of  $(N + 1)$  linear equations which are solved to determine the  $(N + 1)$  unknowns  $\mu_1, \dots, \mu_N$  and  $\hat{\gamma}$ . The solution for  $\hat{\gamma}$  determines the approximate transfinite diameter  $\hat{C}$  of the region  $D$ , where  $\hat{C} = e^{-\hat{\gamma}}$ . The approximations  $\hat{G}$  and  $\hat{H}$  for the functions  $g$  and  $h$  are given by

$$\begin{aligned} \hat{G}(x, y) &= \sum_{j=1}^N \left\{ \int_{\Gamma_j} \log |z - \zeta| |d\zeta| \right\} \mu_j, \\ \hat{H}(x, y) &= \sum_{j=1}^N \left\{ \int_{\Gamma_j} \arg \{z - \zeta\} |d\zeta| \right\} \mu_j, \end{aligned}$$

where  $z = x + iy \in D^* \cup \Gamma$ . Then the approximate mapping function  $F_E(z)$  is computed from (9.1.10) as

$$f_E(z) \approx F_E(z) = U + iV = \frac{z}{\hat{C}} e^{\hat{G}(x,y) + i\hat{H}(x,y)}. \quad (9.2.15)$$

The choice of the nodes and evaluation of integrals is performed in the same manner as in part (a) above, except for the integral in (9.2.14) which is evaluated by

$$\int_{\Gamma_j} |d\zeta| \approx |z_j - z_{j-1/2}| + |z_j - z_{j+1/2}|, \quad (9.2.16)$$

where  $z_{j \pm 1/2}$  denote the end points of  $\Gamma_j$ .

**ERROR ESTIMATE.** Since  $f_E(\infty) = \infty$  and  $f_E(z) \neq 0$  for  $z \in D$ , the relative error is given by

$$\frac{|F_E(z) - f_E(z)|}{|f_E(z)|} = \left| \frac{F_E(z)}{f_E(z)} - 1 \right|.$$

By the maximum modulus theorem, the maximum value of this error is attained on the boundary  $\Gamma$  or at  $z = \infty$ . In view of Symm (1967), the error at  $z = \infty$  is considerably less than the maximum error on  $\Gamma$ . Thus, for  $z \in \Gamma$

$$\left| \frac{F_E(z)}{f_E(z)} - 1 \right| = \left| |F_E(z)| e^{i(\hat{H} - h)} - 1 \right| \leq \left| \left| \frac{F_E(z)}{f_E(z)} \right| - 1 \right| + |\hat{H} - h|.$$

Since  $|\hat{H} - h|$  is generally not known on  $\Gamma$ , although it is of the same order as  $|\hat{G} - g|$ , and since, by hypothesis,  $\left| |F_E(z_j)| - 1 \right| = 0$ , the maximum error  $E$  in  $F_E(z)$  can be measured by

$$E = \max_j \left| |F_E(z_{j-1/2})| - 1 \right|. \quad (9.2.17)$$

**CASE STUDY 9.2.2.** Consider the ellipse  $x^2/a^2 + y^2 = 1$ ,  $a = 1.5$ , and  $N = 100$  in the first quadrant because of the symmetry about both axes. The values of  $U(x, y)$  and  $V(x, y)$  are given in Table 2 on page 247. The transfinite diameter  $C = (a + 1)/2$  (Pólya and Szegö, 1951), and the exact mapping function is given by (Phillips, 1966)

$$f_E(z) = \frac{z + \sqrt{z^2 - a^2 + 1}}{a + 1}. \blacksquare$$

### 9.3. Modified ONP Method

The ONP method, discussed in §9.2, for numerically solving Eqs (9.1.4), (9.1.5), and (9.1.6) has been modified by Hayes, Kahaner and Kellner (1972) as follows: Let the parametric representation of the boundary  $\Gamma$  be  $\zeta = \zeta(t) = x(t) + i y(t)$ ,  $0 \leq t \leq L$ . Then Eq (9.1.4) and (9.1.5) can be written as

$$g(z) = \int_0^L \mu(t) \log |z - \zeta(t)| dt, \quad (9.3.1)$$

$$h(z) = \int_0^L \mu(t) \arg \{z - \zeta(t)\} dt, \quad (9.3.3)$$

where  $\mu(t) = \mu(\zeta(t))$  and  $z \in \bar{D}$ . We shall assume that  $\mu(t) \in C^3(-\infty, +\infty)$  and the boundary  $\Gamma$  has no corners (for corner singularities, see §9.5 and 12.2).

Table 2. Ellipse,  $a = 1.5$ 

| $x$  | $y$      | $U(x, y)$ | $V(x, y)$ |
|------|----------|-----------|-----------|
| 0.00 | 1.000000 | 0.00000   | 0.88989   |
| 0.05 | 0.999444 | 0.03633   | 0.88936   |
| 0.10 | 0.997775 | 0.07267   | 0.88774   |
| 0.15 | 0.994987 | 0.10903   | 0.88503   |
| 0.20 | 0.991071 | 0.14542   | 0.88123   |
| 0.25 | 0.986013 | 0.18184   | 0.87633   |
| 0.30 | 0.979796 | 0.21831   | 0.87032   |
| 0.35 | 0.972397 | 0.25483   | 0.86317   |
| 0.40 | 0.963789 | 0.29142   | 0.85487   |
| 0.45 | 0.953939 | 0.32808   | 0.84540   |
| 0.50 | 0.942809 | 0.36483   | 0.83472   |
| 0.55 | 0.930352 | 0.40167   | 0.82278   |
| 0.60 | 0.916515 | 0.43862   | 0.80961   |
| 0.65 | 0.901234 | 0.47567   | 0.79509   |
| 0.70 | 0.884433 | 0.51285   | 0.77918   |
| 0.75 | 0.866025 | 0.55019   | 0.76184   |
| 0.80 | 0.845905 | 0.58761   | 0.74296   |
| 0.85 | 0.823947 | 0.62521   | 0.72248   |
| 0.90 | 0.800000 | 0.66296   | 0.70025   |
| 0.95 | 0.773879 | 0.70088   | 0.67614   |
| 1.00 | 0.745356 | 0.73896   | 0.64997   |
| 1.05 | 0.714143 | 0.77722   | 0.62152   |
| 1.10 | 0.679869 | 0.81565   | 0.59048   |
| 1.15 | 0.642045 | 0.85425   | 0.55647   |
| 1.20 | 0.600000 | 0.89303   | 0.51892   |
| 1.25 | 0.552771 | 0.93198   | 0.47703   |
| 1.30 | 0.498888 | 0.97110   | 0.42959   |
| 1.35 | 0.435890 | 1.01039   | 0.37452   |
| 1.40 | 0.359011 | 1.04983   | 0.30778   |
| 1.45 | 0.256038 | 1.08942   | 0.21902   |
| 1.50 | 0.000000 | 1.12915   | 0.00000   |

We partition  $\Gamma$  into an even number  $n$  of uniform sections  $\Gamma_j$ ,  $j = 1, \dots, n$ , of length  $\alpha = L/n$  each. Then the nodes on the section  $\Gamma_j$  are uniform as regards the arc length of each  $\Gamma_j$ . First, we define a set of piecewise polynomials  $p_j(t)$ ,

$j = 1, \dots, n$ , by

$$\begin{aligned} p_1(t) &= \begin{cases} \frac{1}{2\alpha^2} (t + \alpha)(t + 2\alpha), & -2\alpha \leq t \leq 0, \\ \frac{1}{2\alpha^2} (t - \alpha)(t - 2\alpha), & 0 \leq t \leq 2\alpha, \\ 0, & \text{otherwise,} \end{cases} \\ p_2(t) &= \begin{cases} -\frac{1}{2\alpha^2} t(t - 2\alpha), & 0 \leq t \leq 2\alpha, \\ 0, & \text{otherwise,} \end{cases} \\ p_{2k+1}(t) &= p_1(t - 2k\alpha), \quad k = 1, 2, \dots, \frac{n}{2} - 1, \\ p_{2m}(t) &= p_2(t - 2(m-1)\alpha), \quad m = 1, 2, \dots, \frac{n}{2}. \end{cases} \quad (9.3.3)$$

The graphs of some of these polynomials are presented in Fig. 9.3.1 for  $\alpha = 0.1$ .

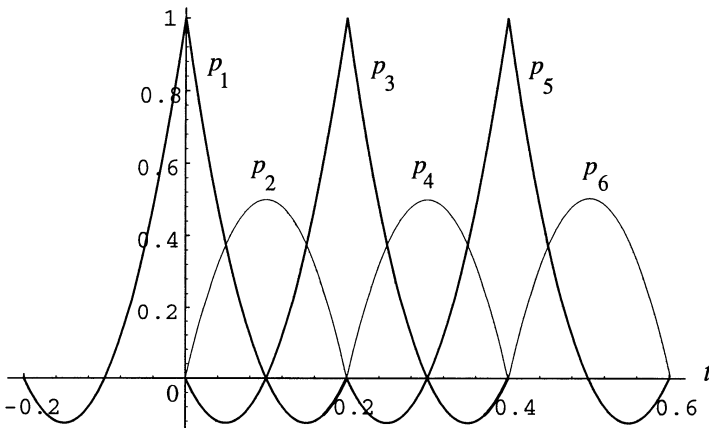


Fig. 9.3.1.

Next, we define the function

$$\tilde{\mu}(t) = \sum_{j=1}^n \mu(j\alpha) p_j(t). \quad (9.3.4)$$

The following results hold:

- (i)  $\tilde{\mu}(t)$  is a polynomial of degree two on  $[j\alpha, (j+2)\alpha]$ ,  $j = 0, 2, 4, \dots, n-2$ ,
- (ii)  $\tilde{\mu}(t) = \mu(t)$  at  $t = j\alpha$ ,  $j = 0, 1, 2, \dots, n$ .

$$(iii) \quad \mu(t) = \tilde{\mu}(t) + O(\alpha^3) = \sum_{j=1}^n \mu_j p_j(t) + O(\alpha^3), \quad (9.3.5)$$

where  $\mu_j = \mu(j\alpha)$  for  $j = 1, \dots, n$ . Using the approximation (9.3.5) for  $\mu(t)$  in (9.3.1), we obtain an approximation for  $g$  as

$$\sum_{j=1}^n \mu_j \int_0^L p_j(t) \log |z - \zeta(t)| dt = g(z) + O(\alpha^3). \quad (9.3.6)$$

The function  $g(z) = -\log |z - z_0|$  for  $z \in \Gamma$ . Thus, we can evaluate Eq (9.3.6) at the points  $z = j\alpha$  for  $j = 1, \dots, n$ , which yields a system of  $n$  linear equations with constant coefficients for the unknowns  $\mu_1, \mu_2, \dots, \mu_n$ . Set  $A = (a_{jk})$  and  $B = (b_j)$ , where

$$\begin{aligned} a_{jk} &= \int_0^L p_j(t) \log |\zeta(j\alpha) - \zeta(t)| dt \quad \text{for } j, k = 1, \dots, n, \\ b_j &= -\log |\zeta(j\alpha) - z_0|, \quad \text{for } j = 1, \dots, n. \end{aligned} \quad (9.3.7)$$

Using this matrix notation Eq (9.3.6) becomes the linear system

$$A \mu = B + O(\alpha^3), \quad (9.3.8)$$

where  $O(\alpha^3)$  is a vector (column matrix). Thus, each component of Eq (9.3.8) is bounded by  $O(\alpha^3)$ , and  $\mu = (\mu_1, \dots, \mu_n)^T$ , where  $T$  denotes the transpose of a matrix. Hence, we solve the matrix equation

$$\tilde{A} \tilde{\mu} = B, \quad (9.3.9)$$

where  $\tilde{A} = (\tilde{a}_{jk})$  is the approximation of the matrix  $A$  and  $\tilde{\mu}$  that of the vector  $\mu$ . To evaluate  $\tilde{A}$ , however, we must compute the elements  $\tilde{a}_{jk}$  which contain integrals of the form

$$\int_{(j-1)\alpha}^{j\alpha} t^j \log |z - \zeta(t)| dt \quad (9.3.10)$$

for  $j = 1, \dots, n$ . Also, for each fixed  $x, y$ , and  $j$ , we approximate  $|z - \zeta(t)|$  by a polynomial  $q(t)$  of degree two on the interval  $((j-1)\alpha, j\alpha)$ , where  $q(t)$  is chosen such that  $q(t) = |z - \zeta(t)|^2$  for  $t = (j-1)\alpha, (j-1/2)\alpha, j\alpha$ . Then

$$\int_{(j-1)\alpha}^{j\alpha} t^j \log |z - \zeta(t)| dt \approx \frac{1}{2} \int_{(j-1)\alpha}^{j\alpha} t^j \log [q(t)] dt, \quad (9.3.11)$$

which can be evaluated explicitly. In some particular cases, e.g., when  $|z - \zeta(t)| = 0$  on  $[(j-1)\alpha, j\alpha]$ , the integral (9.3.10) is computed with a polynomial of higher order.

Then the matrix equation (9.3.9) is solved for the vector  $\tilde{\mu} = (\tilde{\mu}_1, \dots, \tilde{\mu}_n)^T$  which is the approximation for the density function  $\mu$ , with an error estimate

$$\|\tilde{\mu} - \mu\| \leq \|(\tilde{A}^{-1} - A^{-1}) B\| + \|A^{-1}\| O(\alpha^3), \quad (9.3.12)$$

where the error due to the term  $\tilde{A}^{-1} - A^{-1}$  seldom dominates the  $\|A^{-1}\| O(\alpha^3)$  term, an observation made by Hayes et al. (1972) from certain examples. Once  $\tilde{\mu}$  is computed, the functions  $g(z)$  and  $h(z)$  are obtained from

$$\begin{aligned} g(z) &= \int_0^L \mu(t) \log |z - \zeta(t)| dt \\ &= \sum_{k=1}^n \tilde{\mu}_k \int_0^L p_k(t) \log |z - \zeta(t)| dt, \end{aligned} \quad (9.3.13)$$

and

$$\begin{aligned} h(z) &= \int_0^L \mu(t) \arg \{z - \zeta(t)\} dt \\ &\approx \sum_{j=1}^n \mu(j\alpha) \int_0^L p_j(t) \arg \{z - \zeta(t)\} dt \\ &= \sum_{j+1}^n \mu(j\alpha) [p_j(t) \eta_1(t) - p'_j(t) \eta_2(t) + p''_j(t) \eta_3(t)], \end{aligned} \quad (9.3.14)$$

by integration by parts, where

$$\begin{aligned} \eta_1(t) &= \int_0^L \arg \{z - \zeta(t)\} dt, \quad \eta_2(t) = \int_0^L \arg \{z - \zeta(t)\} dt, \\ \eta_3(t) &= \int_0^L \arg \{z - \zeta(t)\} dt. \end{aligned}$$

Note that  $p''_j(t)$  is constant. Thus, (9.3.14) involves integrals of the form (9.3.10).

Hayes et al. (1972) have a Fortran IV computer program for this method. This program can easily be adapted to any modern operating system. As examples, they investigated cases of Cassini's oval (Case Study 9.2.1; Problem 9.6.3), an ellipse (Problem 9.6.2), a rectangle (Problem 9.6.4), and an isosceles triangle (Case Study 9.3.1).

CASE STUDY 9.3.1. Consider an isosceles triangle with corners at the points  $(0, 1)$ ,  $(2, -1)$  and  $(-2, 1)$  such that the point  $(0, 0)$  goes into the point  $w = 0$  under the conformal mapping  $w = f(z)$ . The partition is taken with equal number of nodes on each side. The error  $E_M$ , defined by (9.2.11) is found as follows:

$$E_m = \begin{cases} 2 \times 10^{-4} & \text{for } n = 17, \\ 2 \times 10^{-5} & \text{for } n = 33, \\ 10^{-6} & \text{for } n = 65. \blacksquare \end{cases}$$

## 9.4. Lagrange Interpolation

The choice of a suitable basis set used in the RM, BKM or ONP methods is an important aspect of any numerical technique for polynomial approximation of the mapping function. Gautschi (1977, 1978, 1979) investigated numerical conditions of various bases for polynomial approximation on the real axis. Reichel (1985) observed that a well-conditioned basis depends on the shape of the simply connected region  $D$  bounded by a Jordan contour  $\Gamma$ . For example, the monomials  $\phi_j(z) = (z/r)^j$ ,  $j = 0, 1, \dots$ , are well-conditioned for disks  $B(0, r)$ , but this basis becomes ill-conditioned for ellipses (see Case Study 9.4.1 below where a criterion for well-conditioned bases is developed and applied to these cases).

CASE STUDY 9.4.1 (*Gautschi criterion*). Let  $p_j(z)$ ,  $j = 0, 1, \dots, n$ , denote polynomials such that  $\text{span} \{p_j\}_{j=0}^n = \text{span} \{z^j\}_{j=0}^n$ . We shall determine the sensitivity of the functions

$$P_n(z) = \sum_{j=0}^n a_j p_j(z), \quad z \in \bar{D}, \quad (9.4.1)$$

subject to the perturbations in the coefficients  $a_j$ . Let  $M_n : \mathcal{C}^{n+1} \rightarrow \Pi_n$  denote the mapping of the coefficient space  $\mathcal{C}^{n+1}$  onto the space  $\Pi_n$  of polynomials of degree  $\leq n$ . Let  $\mathbf{a} = (a_0, a_1, \dots, a_n) \in \mathcal{C}^{n+1}$  denote a vector. Then we define

$$(M_n \mathbf{a})(z) = \sum_{k=0}^n a_k p_k(z), \quad z \in \bar{D}. \quad (9.4.2)$$

Note that  $M_n^{-1} P_n(z) = \mathbf{a}$ . The maximum norm in  $\mathcal{C}^{n+1}$  and  $\Pi_n$  is defined, respectively, by  $\|\mathbf{a}\|_\infty = \max_{0 \leq k \leq n} |a_k|$ , and  $\|\Pi_n\|_\Gamma = \sup_{z \in \Gamma} |P_n(z)|$ . Let  $\|M_n\|$  and  $\|M_n^{-1}\|$  be the induced operator norms. We are interested in determining how the condition of the map  $M_n$  defined by

$$\text{cond } (M_n) = \|M_n\| \|M_n^{-1}\| \quad (9.4.3)$$

grows with  $n$  for different choices of the polynomial  $p_j(z)$ . We shall examine two choices:

(a) Let  $D$  be the unit disk  $U$  and  $p_j(z) = z^j$ ,  $j = 0, 1, \dots$ . Then

$$\|M_n\| = \max_{\|\mathbf{a}\|_\infty=1} \left\| \sum_{j=0}^n a_j z^j \right\|_\Gamma = n + 1,$$

and

$$\|M_n^{-1}\| = \left( \min_{\|\mathbf{a}\|_\infty=1} \left\| \sum_{j=0}^n a_j z^j \right\|_\Gamma \right)^{-1} \geq 1.$$

Since

$$\|P_n\|_\Gamma \geq \sqrt{\frac{1}{2\pi} \int_0^{2\pi} |P_n(e^{i\theta})|^2 d\theta} = \sqrt{\sum_{j=0}^n |a_j|^2},$$

we find that

$$\|M_n^{-1}\| \leq \left( \min_{\|\mathbf{a}\|_\infty=1} \sqrt{\sum_{j=0}^n |a_j|^2} \right)^{-1} = 1.$$

Hence,  $\text{cond } (M_n) = n + 1$ , which shows that the monomial basis  $\{z^j\}_{j=0}^n$  is well-conditioned for the unit disk. Thus, this basis is well-conditioned for the disk  $B(0, r)$ .

(b) Let  $\Gamma$  denote the ellipse  $E(a, b) = \{(x, y) : x^2/a^2 + y^2/b^2 = 1\}$ ,  $z = x + iy$ , and  $a \geq b$ . Using the scaling factor  $1/a$ , this ellipse is transformed into the ellipse  $E(1, b/a) = \{Z : Z = z/a\}$  which has foci at  $\pm\xi$ , where  $\xi = \sqrt{1 - (b/a)^2}$ . We use the Chebyshev polynomials  $T_n$  of the first kind

$$\begin{aligned} T_n(Z, \xi) &= \frac{\xi^n}{2^{n-1}} T_n(Z/\xi) = \frac{1}{2^n} \left[ \left( Z + \sqrt{Z^2 - \xi^2} \right)^n \right. \\ &\quad \left. + \left( Z - \sqrt{Z^2 - \xi^2} \right)^n \right], \quad n = 0, 1, \dots \end{aligned} \quad (9.4.4)$$

Let the points  $Z \in E(1, b/a)$  be taken as

$$Z = \frac{1}{2} \left[ \left( 1 + \frac{b}{a} \right) e^{i\theta} + \left( 1 - \frac{b}{a} \right) e^{-i\theta} \right], \quad 0 \leq \theta \leq 2\pi.$$

Substituting them in (9.4.4), we obtain

$$\begin{aligned} T_n(Z, \xi) &= \left[ \frac{1}{2} \left( 1 + \frac{b}{a} \right) \right]^n e^{in\theta} + \left[ \frac{1}{2} \left( 1 - \frac{b}{a} \right) \right]^n e^{-in\theta} \\ &\sim \left[ \frac{1}{2} \left( 1 + \frac{b}{a} \right) \right]^n e^{in\theta} \quad \text{as } n \rightarrow \infty. \end{aligned} \quad (9.4.5)$$

Let  $\beta^{(n)} = (\beta_0^{(n)}, \beta_1^{(n)}, \dots, \beta_{[n/2]}^{(n)})^T$  denote the coefficient vector of  $T_n(Z, \xi)$ , i.e.,

$$T_n(Z, \xi) = \sum_{k=0}^{[n/2]} \beta_k^{(n)} Z^{n-2k}, \quad (9.4.6)$$

where  $[n/2]$  is the greatest integer  $\leq n/2$ . If  $\xi = 0$  (the case of the circle  $|z| = a$ ), then  $\beta_0^{(n)} = 1$  and  $\beta_k^{(n)} = 0$  for all  $k \geq 1$ . We shall not discuss this case because it has been examined in part (a) above. Let  $\xi > 0$ . Then

$$\|M_n\|^{-1} = \left[ \min_{\|\mathbf{a}\|_\infty=1} \left\| \sum a_k Z^k \right\|_{E(1, b/a)} \right]^{-1} \geq \frac{\|\beta^{(n)}\|_\infty}{\|T_n\|_{E(1, b/a)}}. \quad (9.4.7)$$

From Gautschi (1979) we have

$$\|\beta^{(n)}\| \sim \sqrt{\frac{2}{n\pi}} \frac{(1+\xi^2)^{3/4}}{\xi} \left( \frac{1+\sqrt{1+\xi^2}}{2} \right)^n \quad \text{as } n \rightarrow \infty. \quad (9.4.8)$$

Hence, from (9.4.5), (9.4.7) and (9.4.8) we find that

$$\|M_n^{-1}\| \geq \sqrt{\frac{2}{n\pi}} \frac{(1+\xi^2)^{3/4}}{\xi} \left( \frac{1+\sqrt{1+\xi^2}}{1+\frac{b}{a}} \right)^n \quad \text{as } n \rightarrow \infty.$$

Since  $\|M_n\| = n+1$ , we have

$$\text{cond}(M_n) \geq \sqrt{\frac{2n}{\pi}} \frac{(1+\xi^2)^{3/4}}{\xi} \left( \frac{1+\sqrt{1+\xi^2}}{1+\frac{b}{a}} \right)^n \quad \text{as } n \rightarrow \infty.$$

If we set  $\rho = b/a$  and

$$F(\rho) = \frac{1 + \sqrt{1 + \xi^2}}{1 + \frac{b}{a}} = \frac{1 + \sqrt{2 - \rho^2}}{1 + \rho},$$

then

$$\begin{aligned} F(0) &= 1 + \sqrt{2}, \quad \text{which corresponds to } \Gamma = [-a, a], \\ F(1) &= 1, \\ F'(\rho) &< 0, \quad 0 \leq \rho \leq 1, \end{aligned}$$

which imply that in the case of a nondegenerate ellipse ( $\xi > 0$ ) the condition number  $\text{cond}(M_n)$  increases exponentially with  $n$  for the monomial basis and the growth rate increases with  $\rho$ . Hence, if the region is not circular or nearly circular, the choice of the monomial basis is ill-conditioned for the ellipse and may produce computational inaccuracy. ■

Reichel (1985) has shown that Lagrange's interpolation functions

$$l_k(z) = \prod_{\substack{j=0 \\ j \neq k}}^n \frac{z - z_j}{z_k - z_j}, \quad k = 0, 1, \dots, n, \quad (9.4.9)$$

where  $z_k$  are Fejér points on the boundary  $\Gamma$ , provide a well-conditioned basis which is simple to compute for boundaries that are not circular or nearly circular. In fact, he has proved the following:

**THEOREM 9.4.1.** *For Lagrange's functions  $l_k(z)$ , defined by (9.4.9),*

$$\text{cond}(M_n) \leq \frac{2}{\pi} \log n + \alpha, \quad (9.4.10)$$

where the constant  $\alpha$  depends on the shape of the analytic boundary  $\Gamma$ .

Let  $w = f_E(z)$  map the region  $\text{Ext}(\Gamma)$  conformally onto  $U^* = \{w : |w| > 1\}$  such that  $f_E(\infty) = \infty$  and  $f_E(z_1) = 1$ , where  $z_1$  is an arbitrary point on  $\Gamma$ . By analytic continuation the function  $f_E(z)$  can be continued to a bijective map from  $D^* \cup \Gamma$  onto  $|w| \geq 1$ . The points  $z_k$ ,  $k = 1, \dots, n$ , are called the *Fejér points* if

$$f_E(z_k) = e^{2i(k-1)\pi/n}, \quad k = 1, \dots, n. \quad (9.4.11)$$

To determine a set of Fejér points  $\{z_k\}_{k=1}^n$  to be used in (9.4.9), we must restrict  $f_E$  to  $\Gamma$ . This restriction, however, leads to a modified Symm's integral equation which has a unique solution, is solvable for all scalings of the boundary  $\Gamma$ , and differs only in their righthand sides from Eqs (9.1.12)–(9.1.13) in the case of exterior regions (and from Eq (9.1.6) in the case of interior regions). For exterior regions we have the following (Reichel, 1985):

**THEOREM 9.4.2.** *Let  $\phi(z) = \arg \{f_E(z)\}$ , and let  $\gamma = \text{cap}(\Gamma)$ . Then the unique solution  $(C^*, \mu^*)$  of the modified Symm's integral equations*

$$\begin{aligned} \int_{\Gamma} \log |z - \zeta| \mu(\zeta) |d\zeta| + q &= 0, \quad z \in \Gamma, \\ \int_{\Gamma} \mu(\zeta) |d\zeta| &= 1, \end{aligned} \tag{9.4.12}$$

where  $\mu^* = \mu^*(s) \in L^2(\Gamma)$  and  $C^*$  is a constant, satisfies

$$\phi(z) = 2\pi \int_{z_1}^z \mu^*(\zeta) |d\zeta|, \quad C^* = -\log \gamma, \tag{9.4.13}$$

where integration in (9.4.13) is carried out in the positive direction.

**PROOF.** Let the boundary  $\Gamma$  have the parametric representation  $s \mapsto \zeta(s)$ ,  $0 \leq s < L$ ,  $\zeta(0) = z_1$ , where  $s$  is the arc length of  $\Gamma$ . Then the boundary correspondence function  $\phi(\zeta)$  may be regarded as a function of  $s$ , i.e., we write  $\phi(s) = \phi(\zeta(s))$ . It is shown in Gaier (1976) that for a rectifiable curve  $\Gamma$  and  $\gamma \neq 1$ , the integral equation

$$\int_{\Gamma} \log |z - \zeta| \mu(\zeta) |d\zeta| = 1 \tag{9.4.14}$$

has a.e. a unique, integrable solution

$$\mu(\zeta) = \frac{1}{2\pi} \frac{1}{\log \gamma} \phi'(s), \quad \zeta = \zeta(s), \tag{9.4.15}$$

where the prime denotes differentiation with respect to  $s$ . Thus, Eq (9.4.12) has a unique solution

$$\begin{aligned} \mu^*(\zeta) &= \frac{1}{2\pi} \phi'(s), \quad \zeta = \zeta(s), \\ C^* &= -\log \gamma. \end{aligned} \tag{9.4.16}$$

It is also known (Reichel, 1984) that Eq (9.4.12) has a unique solution for any scaling of  $\Gamma$ , and that  $\mu^*$  is invariant under scaling and  $C^*$  varies continuously with scaling. Hence, (9.4.16) is also a unique solution for  $\gamma = 1$ . ■

Let  $w = f(z)$  map the region  $\text{Int}(\Gamma)$  conformally onto the unit disk  $U$ . Then for interior regions we have the following (Reichel, 1985):

**THEOREM 9.4.3.** *Let  $\phi_j(z) = \arg\{f(z)\}$  for  $z \in \Gamma$  with  $\phi_j(z_1) = 0$ . Then the unique solution  $(C_j^*, \mu_j^*)$  of the system of modified Symm's equations*

$$\begin{aligned} \int_{\Gamma} \log |z - \zeta| \mu_j(\zeta) |d\zeta| + C_j^* &= \log |z|, \quad z \in \Gamma, \\ \int_{\Gamma} \mu_j(\zeta) |d\zeta| &= 1, \end{aligned} \tag{9.4.17}$$

where  $\mu_j^* = \mu_j^*(z) \in L^2(\Gamma)$  and  $C_j^*$  are constants, satisfies

$$\phi_j(z) = 2\pi \int_{z_1}^z \mu_j^*(\zeta) |d\zeta|, \quad C_j^* = 0, \tag{9.4.18}$$

where the integration in (9.4.18) is taken in the positive direction of  $\Gamma$ .

**PROOF.** As in the above proof, we shall use Gaier's result. Let  $\gamma = \text{cap}(\Gamma)$ , and assume that  $\gamma \neq 1$ . Then

$$\int_{\Gamma} \log |z - \zeta| \mu(\zeta) |d\zeta| = \log |z|, \quad z \in \Gamma, \tag{9.4.19}$$

has a unique solution  $\mu^*(\zeta)$  such that  $\int_{\Gamma} \mu^*(\zeta) |d\zeta| = 1$ . Thus,  $\mu_j^* = \mu^*$ , and  $C^* = 0$  is a solution of (9.4.17), and, as in the proof of the previous theorem, this solution is unique and invariant under scaling. Hence, (9.4.18) holds for boundaries for which  $\gamma = 1$ . ■

To approximate the mappings  $f(z)$  and  $f_E(z)$  numerically, the following algorithm is used:

1. Compute  $\phi(z)$  and  $\phi_j(z)$  as defined in Theorem 9.4.2 and 9.4.3.
2. Determine the  $(n+1)$  Fejér points  $z_k$  by solving the system of equations

$$\phi(z_k) = \frac{2k\pi}{n+1}, \quad k = 0, 1, \dots, n.$$

3. Compute the images  $w_k$  of  $z_k$  under  $f$  by evaluating

$$w_k = e^{i\phi_j(z_k)}, \quad k = 0, 1, \dots, n.$$

4. Determine a polynomial approximation  $p_k(z)$  of  $\frac{f(z)}{z}$  of degree  $\leq n$  by interpolating  $\frac{f(z)}{z}$  at the Fejér points  $z_k$ ,  $k = 0, 1, \dots, n$ .

Then an approximation of  $f(z)$  is given by

$$f_{n+1}(z) = z p_n(z). \quad (9.4.20)$$

The accuracy of  $f_{n+1}$  depends on that of  $\phi_j(z)$ ,  $\phi(z)$  and the interpolation error. Reichel (1985) has found no computational problems with polynomials  $p_j(z)$  of degree 80–100, since the basis with Lagrange's interpolation functions is well-conditioned.

CASE STUDY 9.4.2. Consider the region  $D$  bounded by the contour  $\Gamma = \{z = 2 \cos t + i(\sin t + 2 \cos^3 t), 0 \leq t < 2\pi\}$  (see Fig. 9.4.1), where the Fejér points are marked with dots. The following data for the error  $E = |||f_n(z)| - 1||_\Gamma$  is from Reichel (1985):

| $n$ | Basis    | $E$                |
|-----|----------|--------------------|
| 16  | Monomial | $3 \times 10^{-2}$ |
| 32  | Monomial | $3 \times 10^{-3}$ |
| 64  | Lagrange | $9 \times 10^{-6}$ |

and  $\text{cond}(M_{32}) = 5 \times 10^9$ . ■

CASE STUDY 9.4.3. Consider the ellipse  $\Gamma = \{z = \cos t + i b \sin t, 0 \leq t < 2\pi\}$ . The mapping function  $f(z)$  onto  $U$  with  $f(0) = 0$  is known in terms of the elliptic sine function (see Kober, 1957, p.177)

$$f(z) = \sqrt{k} \operatorname{sn} \left( \frac{2K}{\pi} \sin^{-1} \frac{z}{\sqrt{1-b^2}} \right),$$

which shows that the singularities of  $f(z)$  close to the boundary are the poles at the points  $\zeta_{1,2} = \pm \frac{2ib}{\sqrt{1-b^2}}$ . We use a Möbius transformation  $f_M$  (§2.2), with  $f_M(0) = 0$ , such that  $f_M(z)$  maps the circle of curvature through  $ib$  onto the unit circle. It has a pole at  $\zeta_1^* = 2ib \frac{1-b^2/2}{1-b^2}$ . Note that  $\zeta_1^* = \zeta_1 + O(b^4)$

as  $b \rightarrow 0$ . Hence, we approximate the function  $f(z)(z - \zeta_1^*)(z - \bar{\zeta}_1^*)$  by the polynomials defined with Lagrange's interpolation functions as the basis. The nature and location of singularities adjacent to the boundary are studied in detail in Chapter 12. As shown above, the use of the Möbius transformation in such cases generally provides good approximations of the singularities by locally approximating  $f$  by  $f_M$ . ■

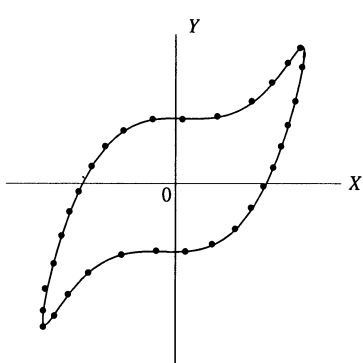


Fig. 9.4.1.

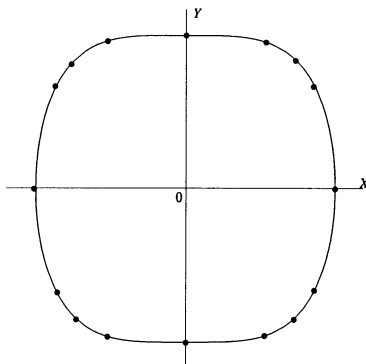


Fig. 9.4.2.

CASE STUDY 9.4.4. Consider the region (square with round corners) bounded by  $\Gamma = \{z = x + iy, x^4 + y^4 = 1\}$  (see Fig. 9.4.2, where 16 Fejér points are marked). In this case the error  $E = \||f_{16}(z)| - 1\|_\Gamma = 6 \times 10^{-4}$  (see Reichel, 1985). ■

## 9.5. Spline Approximations

Spline functions of various degrees can be used effectively to approximate the source density  $\mu(\zeta)$  at corner singularities of the boundary  $\Gamma$ . In fact, the singular functions are combined with splines and together they approximate  $\mu$  over the entire boundary. In previous sections we have evaluated  $\mu$  and the functions  $g$  and  $h$  to approximate the mapping function  $w = f(z)$  for any point  $z \in \bar{D}$ . If  $f(z)$  is required only at the boundary points, then the function  $h$  can be determined by simple integration of  $\mu$  as follows: Let  $\phi$  denote the boundary

correspondence function defined by

$$\phi(t) = \arg \{f(\zeta(t))\} = \frac{1}{2i} (\log w - \log \bar{w}), \quad z \in \Gamma. \quad (9.5.1)$$

Then, since  $|w| = 1$  for  $z \in \Gamma$ , we have (see Gautschi, 1976)

$$\mu(t) = -\frac{1}{2\pi} \frac{d\phi}{dt} = \frac{1}{4i\pi} \left( w \frac{\partial \bar{w}}{\partial t} - \bar{w} \frac{\partial w}{\partial t} \right). \quad (9.5.2)$$

Let  $z_0$  be a corner of the polygonal boundary  $\Gamma$  with interior angle  $\alpha\pi$ ,  $0 < \alpha < 2$ . Then the Schwarz–Christoffel formula (2.3.1) implies that in a neighborhood of  $z_0$

$$f(z) = f(z_0) + \sum_{j=1}^{\infty} A_j (z - z_0)^{j/\alpha}. \quad (9.5.3)$$

For any point  $z = \zeta(t)$  on adjacent sides of the polygon at a corner point  $z_0 = \zeta(t_0)$ , we may take

$$z - z_0 = \begin{cases} t - t_0, & \text{if } t \geq t_0, \\ (t - t_0) e^{i\alpha\pi}, & \text{if } t < t_0. \end{cases} \quad (9.5.4)$$

Then (9.5.2)–(9.5.4) give

$$\mu(t) = \begin{cases} \sum_{j=1}^{\infty} a_j (t - t_0)^{-1+j/\alpha}, & t > t_0, \\ \sum_{j=1}^{\infty} (-1)^{j+1} a_j (t_0 - t)^{-1+j/\alpha}, & t < t_0, \end{cases} \quad (9.5.5)$$

where

$$a_j = \frac{1}{2\alpha\pi} \Im \left\{ \sum_{k=1}^j k A_{j-k} \bar{A}_k \right\}, \quad (9.5.6)$$

and  $A_0 = f(z_0)$ . Hence, we conclude that

- (i) If  $\alpha = 1/q$ , where  $q \geq 1$  is an integer, then (9.5.5) has no fractional powers of  $(t - t_0)$ , and
  - (a) if  $q$  is odd, then  $\mu$  has no singularity at  $t = t_0$ ;
  - (b) if  $q$  is even, then  $\frac{d^{q-1}\mu}{dt^{q-1}}$ , in general, has a finite jump discontinuity at  $t = t_0$ ;
- (ii) If  $\frac{1}{q+1} < \alpha < \frac{1}{q}$ ,  $q \geq 1$  an integer, then  $\frac{d^q\mu}{dt^q}$  is unbounded at  $t = t_0$ ; and
- (iii) If  $1 < \alpha < 2$  (re-entrant corner), then  $\mu$  is unbounded at  $t = t_0$ . For more on corner singularities, see §12.2.

The spline approximation of  $\mu$  is generally carried out by using spline functions of degree  $n$  for most boundaries. However, in a neighborhood of a corner point  $z_0$  with interior angle  $\alpha\pi$  where  $\mu$  exhibits the behavior mentioned in (i)–(iii) above, we use either of the two schemes: (a) continue the spline approximation through  $z_0$  or (b) use a special function which reflects the known asymptotic behavior of  $\mu$  near  $z_0$  to approximate  $\mu$  in the neighborhood of this point. In the latter scheme the special functions are combined with the spline approximation subject to appropriate continuity conditions through the point  $z_0$ . This yields an augmented spline of degree  $n$ . The choice between scheme (a) or (b) depends on the nature and location of the singularity of  $\mu$  and on the degree of the splines used to approximate  $\mu$  over the rest of the boundary. Thus, for example, scheme (b) should always be used if  $1 < \alpha < 2$  (case (iii) above). However, if  $\alpha = 1/2$  (case (i)(b) above) where there is a jump discontinuity in  $\frac{d\mu}{dt}$ , scheme (a) for splines of degree 0 or 1 and scheme (b) for splines of degree  $n \geq 2$  should be used.

The details of the numerical method for augmented spline approximations are as follows (Hough and Papamichael, 1981): Assume that  $\mu$  is an  $L$ -periodic function of the real parameter  $t$ . Let the corner point  $z_0$ , where scheme (b) is to be used, be designated as a singular corner point, and assume that there are  $N \geq 1$  such points with arc lengths  $t = \tau_m$ ,  $m = 1, \dots, N$ , where  $0 < \tau_1 < \dots < \tau_n < L$ . Let each  $[\tau_m, \tau_{m+1}]$  for  $m = 1, \dots, N$  be divided into  $(k_m + 3)$  intervals,  $m = 1, \dots, N$ , where  $k_m \geq 0$  and  $\tau_{N+1} = \tau_1 + L$ . The end points of these intervals are denoted by  $t_{mj}$ , where

$$\tau_m = t_{m0} < t_{m1} < \dots < t_{m,k_m+3} = \tau_{m+1}, \quad m = 1, \dots, N. \quad (9.5.7)$$

We shall also use the notation

$$t_{1,-1} = t_{N,k_N+2} - L, \quad t_{m,-1} = t_{m-1,k_{m-1}+2}, \quad m = 1, \dots, N. \quad (9.5.8)$$

We shall assume that every corner point on the boundary  $\Gamma$  is an end point in the partition (9.5.7) which may not be uniform (i.e., may have unequal arc lengths). Then the source density  $\mu$  is approximated by

$$\tilde{\mu}(t) = \begin{cases} r_m(t), & t_{m,-1} < t < t_{m1}, \\ s_m(t), & t_{m1} < t < t_{m,k_m+2}, \end{cases} \quad (9.5.9)$$

where  $r_m(t)$  is an appropriate singular function which depends on the nature of the boundary singularity, and  $s_m(t)$  is a spline of degree  $n$  with knots  $t_{mj}$ ,  $j = 1, \dots, k_m + 2$ . Thus, for example, if the singular corner point at  $\tau_m = t_{m0}$

has an interior angle  $\alpha_m \pi$ ,  $0 < \alpha_m < 2$ , then the series (9.5.5) for  $\mu$  is truncated, and we use

$$r_m(t) = \begin{cases} \sum_{j=1}^{n_m} a_{mj} (t - t_{m0})^{-1+j/\alpha_m}, & t_{m0} \leq t < t_{m1}, \\ \sum_{j=1}^{n_m} (-1)^{j+1} a_{mj} (t_{m0} - t)^{-1+j/\alpha_m}, & t_{m,-1} < t \leq t_{m0}, \end{cases} \quad (9.5.10)$$

and

$$s_m(t) = \sum_{j=0}^n b_{mj} (t - t_{m1})^j + \sum_{j=2}^{k_m+1} c_{mj} (t - t_{mj})^n \chi(t - t_{mj}), \quad (9.5.11)$$

where

$$\chi(t - t_{mj}) = \begin{cases} 0, & \text{if } t \leq t_{mj}, \\ 1, & \text{if } t > t_{mj}. \end{cases} \quad (9.5.12)$$

The total number of unknown parameters needed to compute  $\tilde{\mu}$  is determined from (9.5.9)–(9.4.10) to be equal to  $M_0 = (n+1)N + \sum_{m=1}^N (k_m + n_m)$ . These parameters are determined by the collocation method at a number of points on  $\Gamma$  and also by subjecting  $\tilde{\mu}$  to certain continuity conditions.

The collocation equations are formulated as follows: For splines  $s_m(t)$  of odd degree  $n$  we collocate at the end points (9.5.7) of each interval. For splines of even degree  $n$  we collocate at the midpoints of each of these intervals. We can always reduce the number collocation equations in the case of any symmetry of the boundary. Thus, let  $z_i$ ,  $i = 1, \dots, M_1$ , denote the chosen collocation points. Then from (9.5.7) we find that  $M_1 = 3N + \sum_{m=1}^N k_m$ , and Symm's integral equation (9.1.6) yields the following collocation equations:

$$\int_0^L \log |z_i - \zeta(t)| \tilde{\mu}(t) dt = -\log |z_i|, \quad i = 1, \dots, M_1, \quad (9.5.13)$$

which in view of (9.5.9)–(9.4.11) reduce to

$$\sum_{m=1}^N \left[ \sum_{j=1}^{n_m} A_{mij} a_{mj} + \sum_{j=0}^n B_{mij} b_{mj} + \sum_{j=2}^{k_m+1} C_{mij} c_{mj} \right] = -\log |z_i|, \\ i = 1, \dots, M_1, \quad (9.5.14)$$

where

$$\begin{aligned} A_{mij} &= (-)^{j+1} \int_{t_{m,-1}}^{t_{m0}} (t_{m0} - t)^{-1+j/\alpha_m} \log |z_i - \zeta(t)| dt \\ &\quad + \int_{t_{m0}}^{t_{m1}} (t - t_{m0})^{-1+j/\alpha_m} \log |z_i - \zeta(t)| dt, \\ B_{mij} &= \int_{t_{m1}}^{t_{m,k_m+2}} (t - t_{m1})^j \log |z_i - \zeta(t)| dt \\ C_{mij} &= \int_{t_{m,j}}^{t_{m,k_m+2}} (t - t_{mj})^n \log |z_i - \zeta(t)| dt. \end{aligned} \tag{9.5.15}$$

The continuity conditions to be imposed on  $\tilde{\mu}$  are based on the assumption that the first  $l_m$  derivatives of  $\tilde{\mu}$  must be continuous at the points  $t_{m,-1}$  and  $t_{m1}$  where the type of approximation changes. This leads to

$$\begin{aligned} r_m^{(k)} &= \begin{cases} s_{m-1}^{(k)} & \text{at } t = t_{m,-1}, \text{ where } m = 2, \dots, N, \\ s_m^{(k)} & \text{at } t = t_{m1}, \text{ where } m = 1, \dots, N, \end{cases} \\ r_1^{(k)}(t_{1,-1}) &= s_N^{(k)}(t_{N,k_N+2}), \quad k = 1, \dots, l_m, \end{aligned} \tag{9.5.16}$$

which, in view of (9.5.10) and (9.5.11) yield the continuity equations

$$\begin{aligned} \sum_{j=1}^{n_m} a_{mj} \left( -1 + \frac{j}{\alpha_m} \right) \left( -2 + \frac{j}{\alpha_m} \right) \cdots \left( -k + \frac{j}{\alpha_m} \right) \\ \times (t_{m1} - t_{m0})^{-1-k+j/\alpha_m} = k! b_{mk}, \\ \sum_{j=1}^{n_m} a_{mj} (-1)^{j+k-1} \left( -1 + \frac{j}{\alpha_m} \right) \left( -2 + \frac{j}{\alpha_m} \right) \cdots \left( -k + \frac{j}{\alpha_m} \right) \\ \times (t_{m0} - t_{m,-1})^{-1-k+j/\alpha_m} \\ = \sum_{j=0}^n b_{m-1,j} j(j-1) \cdots (j-k+1) (t_{m,-1} - t_{m-1,j})^{j-k} \\ + \sum_{j=2}^{k_{m-1}+1} c_{m-1,j} n(n-1) \cdots (n-k+1) (t_{m,-1} - t_{m-1,j})^{n-k}, \\ b_{0j} = b_{Nj}, \quad c_{0j} = c_{Nj}, \quad t_{0j} = t_{Nj} - L, \end{aligned} \tag{9.5.17}$$

where  $m = 1, \dots, N$ , and  $k = 0, 1, \dots, l_m$ . The total number of these continuity equations is  $M_2 = 2 \sum_{m=1}^N (1 + l_m)$ . Combining the collocation

equations (9.5.14) and the continuity equations (9.5.17), we obtain a linear system of  $(M_1 + M_2)$  equations which is solved for the unknown parameters  $a_{mj}$ ,  $b_{mj}$ , and  $c_{mj}$ , which in turn determines

$$\tilde{g}(z) + i \tilde{h}(z) = \int_0^L \log(z - \zeta(t)) \tilde{\mu}(t) dt, \quad (9.5.18)$$

so that the approximate mapping function  $f(z)$  can be evaluated from (9.1.1) (with  $z_0 = 0$ ). In fact, substituting (9.5.10)–(9.5.12) in (9.5.18) we get

$$\tilde{g}(z) + i \tilde{h}(z) = \sum_{m=1}^N \left\{ \sum_{j=1}^{n_m} a_{mj} A_{mj}(z) + \sum_{j=0}^n b_{mj} B_{mj}(z) + \sum_{j=2}^{k_m+1} c_{mj} C_{mj}(z) \right\}, \quad (9.5.19)$$

where

$$\begin{aligned} A_{mj}(z) &= (-1)^{m+j} \int_{t_{m,-1}}^{t_{m,0}} (t_{m0} - t)^{-1+j/\alpha_m} \log(z - \zeta(t)) dt \\ &\quad + \int_{t_{m0}}^{t_{m1}} (t - t_{m0})^{-1+j/\alpha_m} \log(z - \zeta(t)) dt, \\ B_{mij}(z) &= \int_{t_{m1}}^{t_{m,k_m+2}} (t - t_{m1})^j \log(z - \zeta(t)) dt, \\ C_{mij}(z) &= \int_{t_{m,j}}^{t_{m,k_m+2}} (t - t_{mj})^n \log(z - \zeta(t)) dt. \end{aligned} \quad (9.5.20)$$

Note that the coefficients in (9.1.14) are related to (9.1.19) by  $A_{mij} = \Re\{A_{mj}(z)\}$ ,  $B_{mij} = \Re\{B_{mj}(z)\}$  and  $C_{mij} = \Re\{C_{mj}(z)\}$ . The error  $E$  is defined by

$$E = \max_{j=1,\dots,M_1} \left| |\tilde{f}(z_{j+1/2})| - 1 \right|, \quad (9.5.21)$$

where  $M_1$  is the number of collocation points used, and  $z_{j+1/2} \in \Gamma$  denotes the end point or midpoint of the interval depending on whether the degree  $n$  of splines is even or odd.

Certain reduction in the number of splines occurs in some particular cases. For example, if a corner has interior angle  $\pi/q$ , where  $q$  is an odd positive integer, then the corner is treated as a singular corner with (i)  $n_m = 2$ , when  $n = 0$ ; (ii)  $n_m = 2$ , when  $n = 2, 4$  and  $q \geq 2$ ; (iii)  $n_m = 4$ , when  $n = 2, 4$  and  $q < 2$ ; and (iv)  $n_m = 3$ , when  $n = 1, 3, 5$ . Symmetry of any kind always reduces the size of the linear system.

CASE STUDY 9.5.1. Consider the rectangles  $\Gamma_a = \{(x, y) : |x| < 1, |y| < a\}$  for  $a = 1, 0.5, 0.2, 0.1$ . The exact mapping function is known (see Case Study 2.3.2). Take  $M_1 = 128$ . The boundary is partitioned into sections of uniform length on each side with 32, 20, 10, and 6 intervals on the side  $x = \pm 1$ . Because of the symmetry about both coordinate axes, the total number of equations in the linear system reduces to  $(17 + n)$  ( $n$  even) and  $(18 + n)$  ( $n$  odd) when  $a = 1$ , and  $(32 + 2n)$  ( $n$  even) and  $(33 + 2n)$  ( $n$  odd) when  $a \neq 1$ . Hough and Papamichael (1981) have computed the error  $E$  as follows:

| $n$                    | $a = 1$             | $a = 0.5$           | $a = 0.2$          | $a = 0.1$          |
|------------------------|---------------------|---------------------|--------------------|--------------------|
| 0                      | $2 \times 10^{-4}$  | $1 \times 10^{-4}$  | $4 \times 10^{-4}$ | $3 \times 10^{-3}$ |
| 1                      | $9 \times 10^{-6}$  | $2 \times 10^{-5}$  | $2 \times 10^{-4}$ | $1 \times 10^{-3}$ |
| 2                      | $4 \times 10^{-8}$  | $3 \times 10^{-7}$  | $1 \times 10^{-5}$ | $3 \times 10^{-4}$ |
| 3                      | $9 \times 10^{-9}$  | $6 \times 10^{-8}$  | $3 \times 10^{-6}$ | $7 \times 10^{-5}$ |
| 4                      | $3 \times 10^{-9}$  | $3 \times 10^{-9}$  | $6 \times 10^{-7}$ | $8 \times 10^{-5}$ |
| 5                      | $3 \times 10^{-11}$ | $5 \times 10^{-10}$ | $1 \times 10^{-7}$ | $2 \times 10^{-2}$ |
| Symm<br>(1966)         | $4 \times 10^{-4}$  | $2 \times 10^{-4}$  | $4 \times 10^{-4}$ | $3 \times 10^{-3}$ |
| Hayes et al.<br>(1972) | $1 \times 10^{-6}$  | $2 \times 10^{-5}$  | $5 \times 10^{-4}$ | $5 \times 10^{-3}$ |
| Global cubic<br>spline | $9 \times 10^{-5}$  | $6 \times 10^{-5}$  | $3 \times 10^{-6}$ | $7 \times 10^{-5}$ |

Their conclusions on the effectiveness of this method are as follows:

- (i) For splines and augmented splines of degree  $n \leq 3$  there is no ill-conditioning effect, as is found in other polynomial basis methods, in solving the linear system for parameters used in the approximation.
- (ii) If  $n \geq 4$ , there is a possible loss of significance in computations, which indicates that for higher degree splines the use of  $B$ -splines instead of (9.5.11) may be necessary if the knot spacing is not uniform.
- (iii) Augmented cubic splines with three singular terms for each singular corner provide the best results in most problems.
- (iv) Every corner of a polygonal boundary must be treated like a singular corner. This makes the method easy to implement because it introduces appropriate terms from (9.5.10) at every corner.
- (v) This method can be generalized to regions with curved boundaries. In such cases, the integrals in (9.5.20) must be evaluated by numerical quadrature, like

Gauss quadrature, which gives good approximations for nonsingular integrals, but any logarithmic and fractional power singularities need special treatment.

(vi) Besides the corner singularities, any poles of  $f(z)$  that lie very close to the boundary may also introduce inaccuracies in numerical computations (see §12.3). In such cases a suitable choice of knot spacing which may not be equi-spaced is recommended.

(vii) The corner singularity in narrow rectangles ( $a \ll 1$ ) does not produce any computational difficulty. The difficulty arises from the location of the poles of the mapping function  $f(z)$ .

## 9.6. Problems

PROBLEM 9.6.1. Using complex variable methods, prove that either the equation

$$\int_{\Gamma} \log |z - \zeta| \mu(\zeta) d\zeta = 1$$

or the equation

$$\int_{\Gamma} \log |z - \zeta| \mu(\zeta) d\zeta = 0$$

has a solution for any Jordan contour  $\Gamma$ , where  $z$  and  $\zeta$  are distinct points on  $\Gamma$ . (Muskhelishvili, 1953, p.184.)

PROBLEM 9.6.2. Consider the Limaçon  $r = a - \cos \theta$ , where  $r = 0$  corresponds to  $z = 1/2$  for  $a = 1$ , and to  $z = 0$  for  $a > 1$  (Fig. 9.6.1). The ray  $\theta = 0$  is the direction of the polar axis which is the axis of symmetry. The partitions  $\Gamma_j$ ,  $j = 1, \dots, N$ , are taken for  $\theta = 0 (\pi/N) 2\pi$ ,  $N = 2n$ . Show that the errors in the OPN method are:

|     | For $n = 16$ |        | For $n = 32$ |        |
|-----|--------------|--------|--------------|--------|
| $a$ | $E_M$        | $E_A$  | $E_M$        | $E_A$  |
| 1.0 | 0.0723       | 0.0029 | 0.0408       | 0.0014 |
| 1.1 | 0.0800       | 0.0002 | 0.0215       | 0.0003 |
| 1.2 | 0.0261       | 0.0004 | 0.0048       | 0.0004 |
| 1.3 | 0.0116       | 0.0006 | 0.0019       | 0.0004 |
| 1.4 | 0.0064       | 0.0006 | 0.0011       | 0.0004 |

Note that  $E_A \ll E_M$  and the maximum error in each case occurs at the interval point on the polar axis when  $r = a - 1$  and the boundary is concave. For  $a = 1$ , there is a singularity at the point, but the concavity of the boundary decreases with an increase in  $a$ , and so does the error. An increase in  $N$  results in a decrease in error. (Symm, 1966.)

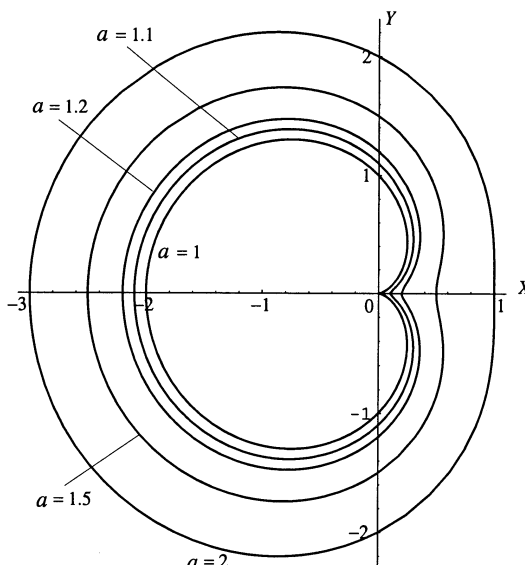


Fig. 9.6.1. Limaçons for  $a = 1, 1.1, 1.2, 1.5$ , and 2.

**PROBLEM 9.6.3.** Consider the ellipse  $x^2/a^2 + y^2 = 1$ . Take the partitions  $\Gamma_j, j = 1, \dots, N$  for  $\theta = 0 (\pi/N) 2\pi, N = 4n$ . Show that the errors in the OPN method are as follows:

| For $n = 16$ |         |        | For $n = 32$ |        |
|--------------|---------|--------|--------------|--------|
| $a$          | $E_M$   | $E_A$  | $E_M$        | $E_A$  |
| 1.25         | 0.00002 | 0.0024 | 0.0001       | 0.0012 |
| 2.5          | 0.0010  | 0.0005 | 0.0002       | 0.0003 |
| 5            | 0.0079  | 0.0003 | 0.0012       | 0.0001 |
| 10           | 0.0525  | 0.0003 | 0.0083       | 0.0001 |
| 20           | 0.2135  | 0.0018 | 0.0530       | 0.0001 |

Note that  $E_A > E_M$  for small  $a$ , but as  $a$  increases, the error on the whole

increases, and  $E_M$  becomes prominent. The maximum error occurs at the end points of the minor axis where the nodes are widely spread. The error decreases as  $N$  increases. (Symm, 1966.)

**PROBLEM 9.6.4.** Consider Cassini's oval

$$[(x + \alpha)^2 + y^2] [(x - \alpha)^2 - y^2] = 1$$

of Fig. 6.3.1. Take  $\alpha = 5/6$  (the near circle case), and determine the errors in the OPN method for  $N = 16$  and  $N = 32$  for both interior and exterior regions.

**PROBLEM 9.6.5.** Consider the rectangle  $-1 \leq x \leq 1, -a \leq y \leq a$  (see Case Study 2.3.2 and 3.3.2 and compare it with Case Study 4.5.1). Determine the error in mapping problems for the interior and exterior regions. Note that  $C = \frac{a}{2} (E' - k^2 K') = \frac{a}{2} (E - k'^2 K)$ , where  $E$  and  $E'$  are complete elliptic integrals and  $k' = \sqrt{1 - k^2}$ ,  $k$  being the modulus of elliptic functions (Bickley, 1932), such that  $E(k, \phi) = \int_0^{\pi/2} \sqrt{1 - k^2 \sin^2 \phi} d\phi = \int_0^K dn u du$ .

**PROBLEM 9.6.6.** Consider the ellipse  $\Gamma : z(t) = e^{it} (1 + \lambda^2 e^{-2it})$ , where  $|\lambda|$  is taken sufficiently small for the region  $D$  to be nearly circular (see Case Study 5.1.1). The approximate mapping function obtained by the method of infinite systems is given by (5.2.7). Take  $\lambda = 0.1$ , obtain the approximate solution by the ONP method, and compare it with the solution (5.2.7).

**PROBLEM 9.6.7.** Develop the numerical method for evaluating Green's functions (of §6.3) by using the spline approximations discussed in §9.5.

**PROBLEM 9.6.8.** It is known that the unique solution  $\mu$  of Symm's integral equations generates an interior harmonic function

$$g_{\text{int}}(z) = \int_{\Gamma} \log |z - \zeta| \mu(\zeta) d\zeta, \quad z \in D,$$

and an exterior harmonic function

$$g_{\text{ext}}(z) = \int_{\Gamma} \log |z - \zeta| \mu(\zeta) d\zeta, \quad z \in D^*,$$

each of which reduces to  $g(z)$ , defined by (9.1.4), on  $\Gamma$ .

(a) Show that  $g'_{\text{int}} + g'_{\text{ext}} = 2\pi\mu$ , where the prime denotes the normal derivative

into the respective regions.

- (b) Take  $g_{\text{int}} = r \sin \psi$  and  $g_{\text{ext}} = a^2 \cos \psi/r$ , where  $(r, \psi)$  are polar coordinates, and, by using the result of part (a), show that  $\mu = -\cos \psi/\pi$ .
- (c) If  $g(z)$  is constant in  $\bar{D}$ , then show that its complex conjugate function  $h(z)$ , defined by (9.1.5), is also constant in  $\bar{D}$ . (Maiti, 1968.)

REFERENCES USED: Bickley (1932), Gaier (1976), Gram (1962), Gautschi (1977, 1978, 1979), Gutknecht (1986), Hayes, Kahaner and Kellner (1972), Jawson (1963), Hough and Papamichael (1981), Kober (1957), Kythe (1996), Maiti (1968), Muskhelishvili (1953), Phillips (1966), Pólya and Szegö (1951), Rabinowitz (1966), Reichel (1984, 1985), Symm (1963, 1966, 1967).

# Chapter 10

---

## Airfoils

---

The research developed by Joukowski to determine the force exerted by a flow on a body around which it is flowing eventually led to the theoretical foundation for practical aircraft construction, and the methods of conformal mapping played an important role in modern aviation. During the 1930s Theodorsen's iterative method became a pioneer in transforming the exterior of the unit circle onto the exterior of an almost circular contour. But in the potential flow analysis of airfoils, James's method developed in 1971 turns out to be more successful for all types of contours which do not have corner singularity. We shall develop Joukowski mapping functions, compare numerical solutions of single-element airfoils by both Theodorsen's and James's iterative methods, unfold the mechanism of divergence of Theodorsen's method in the cases where the image boundary is not almost circular, and finally analyze multiple-element airfoils by using von Karman–Treffitz transformations and FFT with Garrick's method of conjugate functions.

---

### 10.1. Joukowski Function

The Joukowski function

$$w = f(z) = \frac{1}{2} (z + z^{-1}) \quad (10.1.1)$$

is a second order rational function which satisfies the condition  $f(z) = f(1/z)$ . It means that every point of the  $w$ -plane except  $w = \pm 1$  has only

two distinct inverse images  $z_1$  and  $z_2$  such that

$$z_1 z_2 = 1, \quad (10.1.2)$$

since the two points  $z + 1 \neq z_2$  are transformed by (10.1.1) into one and the same point in the  $w$ -plane, i.e.,  $z_1 + \frac{1}{z_1} = z_2 + \frac{1}{z_2}$ , and then  $z_1 - z_2 = \frac{z_1 - z_2}{z_1 z_2}$  only if  $z_1 z_2 = 1$ . The function (10.1.1) is analytic in  $\mathbb{C}_\infty$  except at  $z = 0$  which is a simple pole for this function. The derivative

$$f'(z) = \frac{1}{2} \left( 1 - \frac{1}{z^2} \right) \quad (10.1.3.)$$

is nonzero at all points except  $z = \pm 1$ . Thus, the mapping by this function is conformal everywhere except at  $z = \pm 1$ . The regions of univalence for the Joukowski function are  $U = \{|z| < 1\}$  and  $U^* = \{|z| > 1\}$ , both of which are mapped conformally by this function onto one and the same region in the  $w$ -plane which is determined as follows: Consider the mapping of the circle  $|z| = r$  by the function (10.1.1). With  $z = r e^{i\theta}$   $0 \leq \theta < 2\pi$ , we find that

$$u(r, \theta) = \frac{1}{2} (r + r^{-1}) \cos \theta, \quad v(r, \theta) = \frac{1}{2} (r - r^{-1}) \sin \theta. \quad (10.1.4)$$

If we eliminate  $\theta$  in (10.1.4), we get

$$\frac{4u^2}{(r + r^{-1})^2} + \frac{4v^2}{(r - r^{-1})^2} = 1. \quad (10.1.5)$$

Hence, the function (10.1.1) maps concentric circles  $|z| = r$  conformally onto confocal ellipses with semiaxes  $(r \pm r^{-1})/2$  and foci at  $\pm 1$  on the  $u$ -axis (Fig. 10.1.1).

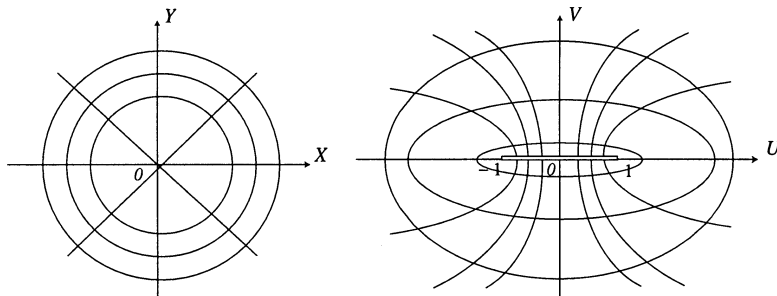


Fig. 10.1.1.

Moreover, as  $r \rightarrow 1$ , the ellipse (10.1.5) reduces to the segment  $[-1, 1]$  of the  $u$ -axis traversed twice. As  $r \rightarrow 0$ , the ellipse is transformed into a circle of infinitely large radius. Hence, the Joukowski function (10.1.1) maps the region  $U$  in the  $z$ -plane conformally onto the  $w$ -plane cut along the segment  $[-1, 1]$  of the  $u$ -axis. The boundary  $|z| = 1$  is mapped onto this segment such that the upper semicircle is mapped onto the lower edge of the cut and the lower semicircle onto the upper edge of the cut. The region  $U^*$  in the  $z$ -plane is mapped onto the second sheet of the  $w$ -plane cut along the segment  $[-1, 1]$  of the  $u$ -axis, the upper semicircle  $|z| = 1, \Im\{z\} > 0$  onto the upper edge, and the lower semicircle  $|z| = 1, \Im\{z\} < 0$  onto the lower edge of the cut. Thus, the Joukowski function (10.1.1) maps the extended  $z$ -plane conformally onto the Riemann surface of the inverse function

$$z = g(w) = w + \sqrt{w^2 - 1}, \quad (10.1.6)$$

which is a two-sheeted surface made up of two sheets of the  $w$ -plane cut along the segment  $[-1, 1]$  of the real axis.

To determine the image of a rays  $\arg\{z\} = \theta_0$ , we eliminate  $r$  in Eqs (10.1.4) and replace  $\theta$  by  $\theta_0$ . This gives

$$\frac{u^2}{\cos^2 \theta_0} - \frac{v^2}{\sin^2 \theta_0} = 1, \quad (10.1.7)$$

which shows that the rays  $\arg\{z\} = \theta_0$  are transformed into branches of the hyperbola (10.1.7) with foci at  $\pm 1$  (Fig. 10.1.1). The Joukowski function defines the orthogonal system of polar coordinates in the  $z$ -plane in terms of an orthogonal system in the  $w$ -plane such that the confocal families of ellipses and hyperbolae in the  $w$ -plane are orthogonal. For  $\theta = 0$ , we find from (10.1.4) that  $u = (r + r^{-1})/2, v = 0, 0 \leq r < 1$ , which represents the interval  $1 < u \leq +\infty$ . The infinite interval  $-\infty \leq u < 1$  is the image of the ray  $\theta = \pi$ . For  $\theta = \pi/2$ , we have  $u = 0, v = -(r - r^{-1})/2, 0 \leq r < 1$ , which represents the negative imaginary axis  $-\infty \leq v < 0$ . The positive imaginary axis  $0 < v \leq +\infty$  is the image of the ray  $\theta = -\pi/2$ . Thus, the horizontal diameter of the unit disk  $U$  is mapped onto the real axis going from  $-1$  to  $+1$  through the point at infinity and excluding the points  $\pm 1$ . The vertical diameter of  $U$  is mapped onto the entire imaginary axis including the point at infinity but excluding the origin.

The geometrical interpretation of the mapping

$$w = z + z^{-1} \quad (10.1.8)$$

is as follows: If  $\Gamma$  is a circle in the  $z$ -plane passing through the point  $z = -1$ , such that the point  $z = 1$  lies inside  $\Gamma$ , then the function (10.1.8) conformally maps the region exterior to  $\Gamma$  onto the region exterior to the Joukowski profile  $C$  (Fig. 10.1.2). The shape of the curve  $C$  is obtained from the circle  $\Gamma$  by making the point  $z$  trace out the circle  $\Gamma$  and adding the vectors  $z$  and  $1/z$ .

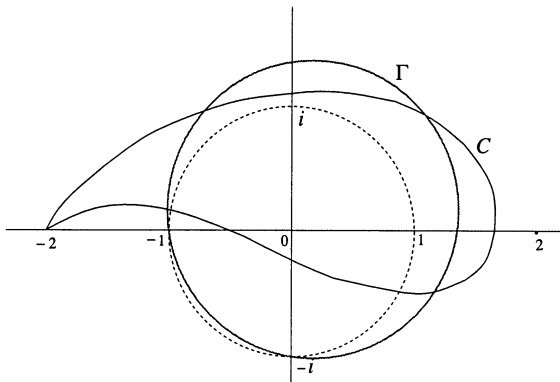


Fig. 10.1.2.

**CASE STUDY 10.1.1.** Consider the irrotational plane flow of an ideal fluid around an infinite plate. Let the  $(x, y)$ -plane intersect the plate along the segment  $-a \leq x \leq a$  and the velocity vector of the flow lie in the  $(x, y)$ -plane and have a prescribed complex value  $w_\infty$ . Since the Joukowski function

$$z = F(\zeta) = \frac{a}{2} \left( \zeta + \frac{1}{\zeta} \right) \quad (10.1.9)$$

conformally maps the exterior of the unit circle in the  $\zeta$ -plane onto the  $z$ -plane cut along the segment  $-a \leq x \leq a$ , we have  $F(\infty) = \infty$ , and  $F'(\infty) = a/2$ . Hence, the flow problem reduces to that of an irrotational flow around a circular cylinder of unit radius in the  $\zeta$ -plane with complex velocity  $W_\infty = \frac{a}{2} w_\infty$  at infinity. The complex potential of this latter problem is given by

$$\psi(\zeta) = \frac{a}{2} \left( \bar{w}_\infty \zeta + \frac{w_\infty}{\zeta} \right). \quad (10.1.10)$$

If we set  $\zeta = \frac{z + \sqrt{z^2 - a^2}}{a}$  and  $\frac{1}{\zeta} = \frac{z - \sqrt{z^2 - a^2}}{a}$ , which are obtained from (10.1.9) such that  $\sqrt{z^2 - a^2} > 0$  for  $z = x > a$ , and separate  $w_\infty$  into real and imaginary parts ( $w_\infty = (v_x)_\infty + i(v_y)_\infty$ ), where the vector

$\mathbf{v}_\infty = (v_x) \mathbf{i} + (v_y) \mathbf{j}$  and  $v_x$  and  $v_y$  are related to  $w = u + iv$  by the Cauchy–Riemann equations  $v_x = \frac{\partial u}{\partial x} = \frac{\partial v}{\partial y}$  and  $v_y = \frac{\partial u}{\partial y} = -\frac{\partial v}{\partial x}$ , then the complex potential of the original problem from (10.1.10) is given by

$$f(z) = (v_x)_\infty z - i (v_y)_\infty \sqrt{z^2 - a^2}. \quad (10.1.11)$$

Now, since the force of pressure acting on an element  $ds$  of any contour  $C$  is proportional to the hydrodynamic pressure  $p$  at the given point of flux and is directed along the inward normal  $\mathbf{n}$  such that  $-d\mathbf{n} = \mathbf{j} dx - \mathbf{i} dy$ , we find that the components of the force acting on the contour  $C$  are given by  $R = R_x + i R_y$ , where  $R_x = - \int_C p dy$  and  $R_y = \int_C p dx$ . Since  $p = A - \frac{\rho v^2}{2}$  from Bernoulli's integral, where  $A$  is a constant and  $\rho$  is the fluid density, we obtain the pressure force with which the flow acts on the plate as

$$R = \frac{\rho}{2} \int_C \mathbf{v}^2 (dx - i dy) = -\frac{\rho}{2} \int_C \mathbf{v}^2 \overline{dz}, \quad (10.1.12)$$

where the integral of the constant  $A$  around the contour  $C$  is zero. Since the velocity acts tangentially to  $C$  at points of  $C$ , the complex velocity  $w$  of the flow is related to  $\mathbf{v}$  by  $w = \mathbf{v} e^{i\phi}$ , where  $\phi$  is the angle that the tangent makes with the  $x$ -axis. Then, since in view of the Cauchy–Riemann equations  $w = v_x + i v_y = \frac{\partial u}{\partial x} + i \frac{\partial u}{\partial y} = \frac{\partial u}{\partial x} - i \frac{\partial v}{\partial x} = \overline{f'(z)}$ , we have  $\mathbf{v} e^{i\phi} = f'(z)$ , and  $\overline{dz} = e^{-i\phi} ds$ . Thus,  $\mathbf{v}^2 dz = \mathbf{v}^2 e^{-2i\phi} e^{i\phi} ds = f'^2(z) dz$ , and (10.1.12) becomes

$$R = -\frac{\rho}{2} \int_C f'^2(z) dz, \quad (10.1.13)$$

which is known as *Chaplygin's formula* that expresses the force exerted by a flow on a body around which it flows in terms of the derivative of the complex potential.

If we use the formula

$$f(z) = \bar{w}_\infty z + \frac{\Gamma_\infty}{2i\pi} \log z + \sum_{n=0}^{\infty} \frac{c_n}{z^n},$$

which defines the complex potential in the neighborhood of the point at infinity, where  $\Gamma_\infty$  is the circulation of the flow at infinity, we find that

$$f'(z) = \bar{w}_\infty z + \frac{\Gamma_\infty}{2i\pi} \frac{1}{z} + \sum_{n=2}^{\infty} \frac{c_n}{z^n},$$

$$f'^2(z) = \frac{\bar{w}_\infty \Gamma_\infty}{i\pi} \frac{1}{z} + \sum_{n=2}^{\infty} \frac{b_n}{z^n},$$

and thus,  $\int_C f'^2(z) dz = 2\bar{w}_\infty \Gamma_\infty$ . Then (10.1.13) yields  $R = \rho (v_y)_\infty \Gamma_\infty - \rho (v_x)_\infty \Gamma_\infty$ , or

$$|R| = \rho |\mathbf{v}_\infty| |\Gamma_\infty|, \quad (10.1.14)$$

known as *Joukowski's theorem* on lifting force, which states that the force of pressure of an irrotational flow with velocity  $\mathbf{v}_\infty$  at infinity and flowing around a contour  $C$  with circulation  $\Gamma$  is given by the formula  $R = \rho |\mathbf{v}_\infty| |\Gamma|$ . The direction of the force is obtained by rotating the vector  $\mathbf{v}_\infty$  through an angle  $\pi/2$  in the direction of the circulation. ■

---

## 10.2. Generalized Joukowski Mappings

A generalized Joukowski mapping has the form

$$w = f(z) = z \sum_{j=0}^{\infty} \frac{c_j}{z^j}, \quad (10.2.1)$$

where  $c_j$  may be complex and  $c_0 \neq 0$  ( $c_0$  is usually taken as 1). Assume that the series in (10.2.1) converges for  $|z| \geq a$  and  $f'(z)$  has no zero outside the circle  $\Gamma : \{|z| = a\}$ . Then the mapping (10.2.1) is conformal in the region  $\text{Ext}(\Gamma)$  and maps the circle  $\Gamma$  onto a Jordan contour  $C$ . But if  $f'(z)$  has a simple zero at a point  $z_1 \in \Gamma$ , then the contour  $C$  will have a cusp at  $w_1 = f(z_1) \in C$ .

The inverse mapping  $z = F(w) = w \sum_{j=0}^{\infty} \frac{b_j}{w^j}$  is a single-valued function for

sufficiently large  $w$ . If we set  $z = a e^\zeta$ ,  $a$  real, in (10.2.1), then the region  $\text{Ext}(C)$  is mapped onto the semi-strip  $S : \{\xi \geq 0, 0 \leq \eta < 2\pi, \zeta = \xi + i\eta\}$  of the  $\zeta$ -plane, and the contour corresponding to  $\xi = 0$  will have the parametric equations

$$u + i v = a e^{i\eta} \sum_{j=0}^{\infty} \frac{c_j}{a^j} e^{-ij\eta}. \quad (10.2.2)$$

For example, consider

$$w = \frac{1}{2} \left( \frac{a+b}{a} z + \frac{a(a-b)}{z} \right). \quad (10.2.3)$$

Then for  $z = a e^{i\theta}$  on the circle  $\Gamma$  we have  $u + i v = a \cos \theta + i b \sin \theta$ , i.e., the contour  $C$  is an ellipse with semi-axes  $a$  and  $b$  and eccentric angle  $\theta$ . If the

mapping is taken as

$$w = z + \frac{a^2}{z}, \quad (10.2.4)$$

which is obtained by setting  $b = 0$  in (10.2.3), then  $u = a \cos \theta$ ,  $v = 0$ , i.e., the circle  $\Gamma$  is mapped onto the two sides of the straight line from  $(2a, 0)$  to  $(-2a, 0)$  and back. This mapping can be written as

$$\frac{w+2a}{w-2a} = \left( \frac{z+a}{z-a} \right)^2, \quad (10.2.5)$$

which yields  $\frac{dw}{dz} = 1 - \frac{z^2}{a^2}$ . Now consider

$$\frac{dw}{dz} = \prod_{k=1}^n \left( 1 - \frac{z_k}{z} \right), \quad (10.2.6)$$

where  $\sum z_k = 0$ ,  $|z_1| = a$ ,  $|z_k| < a$  if  $k \neq 1$ . The mapping (10.2.5) is a special case of (10.2.6) for  $n = 2$ ,  $z_1 = a$ , and  $z_2 = -a$ . Then the contour  $C$  has a cusp at  $w_1$ , and in the neighborhood of this point we have  $\frac{dw}{dz} = (z - z_1) g(z)$ , where  $g(z)$  is regular,  $g(z_1) \neq 0$ . Thus,  $w - w_1 = \frac{1}{2} g(z_1) (z - z_1)^2 + \dots$ , which means that, as  $z$  traverses the circle  $\Gamma$  and passes through  $z_1$ ,  $w$  approaches  $w_1$  and then recedes along a curve with the same tangent. If instead of  $\Gamma$  we take a larger circle that passes through  $z = a$  but slightly beyond  $z = -a$ , and transform this circle, then we have the mapping in Fig. 10.1.2 (in which  $a$  is at  $x = -1$ ), with a cusp at  $w = 2a$  and a rounded end at  $w$  a little less than  $-2a$ .

**10.2.1. Glauert's Modification.** Since Joukowski airfoils are mappings of the type (10.2.1), they all have cusps. But an airplane wing is not a cusp. Glauert (1948) removed this problem as follows: Consider the mapping

$$\frac{w - (2-n)a \cos \beta}{w + (2-n)a \cos \beta} = \left( \frac{z - a e^{-i\beta}}{z + a e^{i\beta}} \right)^{2-n}, \quad (10.2.7)$$

where  $n$  and  $\beta$  are positive and small. Set

$$\begin{aligned} \arg \{z - a e^{-i\beta}\} &= \theta_1, & \arg \{w - (2-n)a \cos \beta\} &= \phi_1, \\ \arg \{z + a e^{i\beta}\} &= \theta_2, & \arg \{w + (2-n)a \cos \beta\} &= \phi_2, \end{aligned}$$

where all arguments are defined to be zero when  $z$  is on  $AB$  (produced) but vary continuously as  $z$  traverses a contour outside the circle (see Fig. 10.2.1).

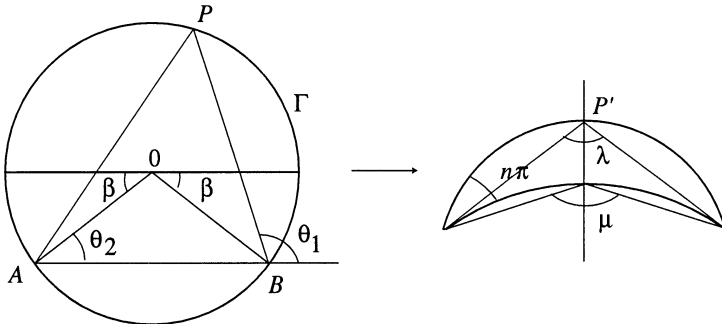


Fig. 10.2.1.

Then at  $P$ ,  $\theta_1 - \theta_2 = \frac{\pi}{2} - \beta$ , and  $\phi_1 - \phi_2 = (2 - n)(\theta_1 - \theta_2)$  for points outside  $\Gamma$ . The image point  $P'$  in the  $w$ -plane is on a circular arc through the points  $\pm(2 - n)a \cos \beta$ , subtending an angle  $\lambda = (2 - n)\left(\frac{\pi}{2} - \beta\right)$ . In the case when  $P$  moves near  $B$  and then travels around a small semicircle about  $B$ , then  $\theta_2$  increases by  $\pi$ , and in this case  $\phi_1 - \phi_2 = (2 - n)\left[\left(\frac{\pi}{2} - \beta\right) - \pi\right] = -(2 - n)\left(\frac{\pi}{2} + \beta\right) < 0$ . We add  $2\pi$  to this angle to make it positive. Then the lower arc of  $\Gamma$  is mapped onto the lower circular arc in the  $w$ -plane that subtends an angle  $\mu = 2\pi + (\phi_1 - \phi_2) = 2\pi - (2 - n)\left(\frac{\pi}{2} + \beta\right)$ . If  $\mu < \pi$ , the lower arc in the  $w$ -plane is concave downward. The two circular arcs in the  $w$ -plane intersect at an angle  $n\pi$  (see Fig. 10.2.1). If instead of  $\Gamma$ , we take a circle passing through  $A$  but a little beyond  $B$ , then we obtain a rounded leading edge. For large  $z$  the Glauert mapping (10.2.7) can be approximated by

$$w = z + i a \sin \beta + \frac{(1 - n)(3 - n)}{3} \cos^2 \beta \frac{a^2}{z} + \dots \quad (10.2.8)$$

**10.2.2. Symmetric Joukowski Airfoil.** Let  $a > 0$ . Consider the circles

$$\Gamma : \{|z| = a\}, \quad \Gamma_1 : \left\{ |z + a| = a - c, -\infty < c < a, c \neq 0, \frac{a}{2} \right\},$$

$$\Gamma_2 : \left\{ \left| z + \frac{a}{2} \right| = \frac{a}{2} \right\}.$$

(See Fig. 10.2.2; Kober, 1957, p.67). Then the mapping (10.2.4) for  $a > 0$ ,

- (i) maps the circle  $\Gamma_1$  onto the symmetric airfoil  $\Gamma'_1 : A'G'F'D'A'$  with cusp at  $A'$ ;
- (ii) maps the circle  $\Gamma_2$  and the line  $x = -c$  onto the circle  $\Gamma'_2 : O'B'A'C'O'$  with a cusp at  $A'$  and the line  $u = -a$  as its asymptote, respectively; and
- (iii) maps the region  $\text{Int}(\Gamma_1)$  bijectively, with  $0 < c < a/2$ , onto the region  $\text{Ext}(\Gamma'_1)$ .

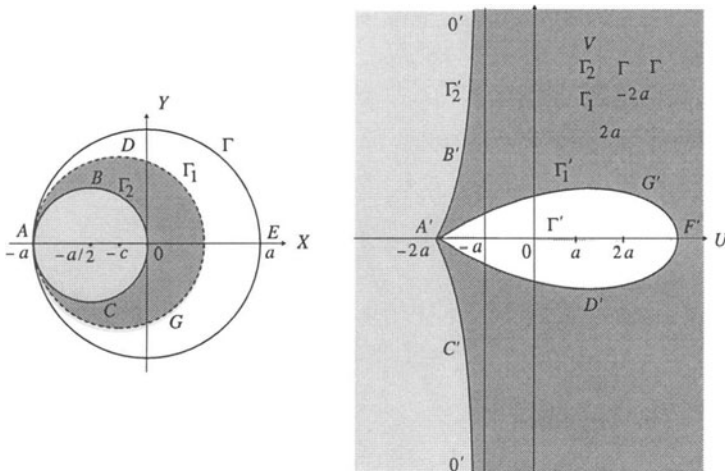


Fig. 10.2.2.

### 10.3. Nearly Circular Approximations

In practical applications airfoils are not exactly defined by the Joukowski function (10.1.1). They are often approximated by nearly circular regions. This idea can be explained as follows: Let  $D$  denote the region bounded by two circular arcs  $\gamma_1$  and  $\gamma_2$  with end points  $a$  and  $b$ . Let  $\theta$  ( $0 < \theta < 2\pi$ ) denote the angle between the arcs  $\gamma_1$  and  $\gamma_2$ . The region  $D$  has a central arc  $\gamma_c$  connecting points  $a$  and  $b$  and bisecting the angle  $\theta$  (see Fig. 10.3.1(a) if  $D$  is the interior

region and Fig. 10.3.1(b) if  $D$  is the exterior region). The region  $D$  is mapped onto the unit disk  $U$  by a chain of mappings  $f^{-1} \circ g \circ f$  (Fig 10.3.2), where

$$f(z) = e^{i\alpha} \frac{z - a}{z - b}, \quad (10.3.1)$$

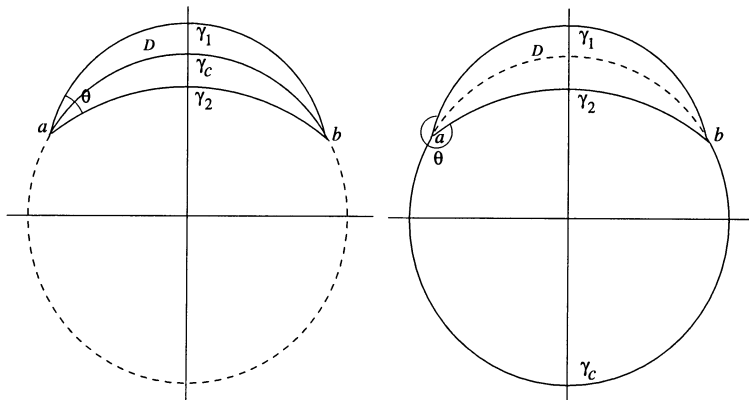


Fig. 10.3.1.

$\alpha$  is a real number chosen such that the central arc  $\gamma_c$  is mapped onto the positive real axis in  $D_1$ , and

$$g(z) = z^{\pi/\theta}. \quad (10.3.2)$$

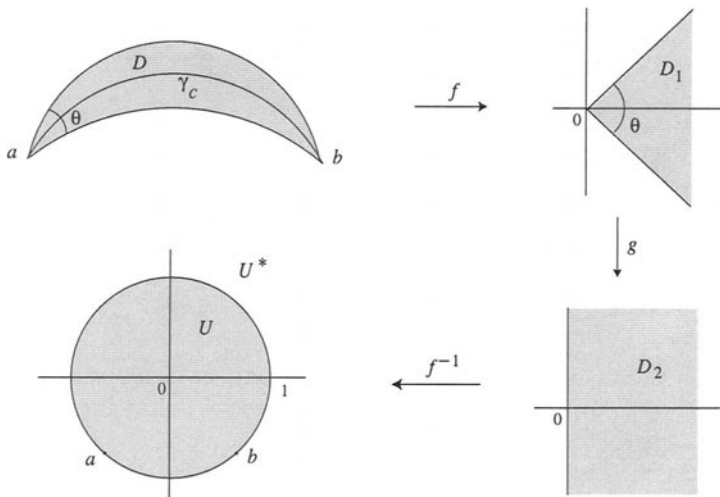


Fig. 10.3.2.

Note that the function  $f^{-1}$  maps the right half-plane  $D_2$  onto a region similar to  $D$  except that the angle between the arcs now becomes  $\pi$ . Thus,  $f^{-1}$  maps  $D_2$  onto  $U$  which is bounded by the unit circle through  $a$  and  $b$  and orthogonal to the central arc. Similarly, the chain of mappings  $f^{-1} \circ (-g) \circ f$  will map the region  $D$  onto the region  $U^*$  exterior to the unit circle. These mappings have points  $a$  and  $b$  as fixed points. In the case of Fig. 10.3.1(b), where  $D$  is the exterior region, a circle slightly larger than the boundary of  $U$  and touching  $U$  at point  $b$  is the map of the curve that looks like an airfoil (the curve on the left in Fig. 10.3.3).

Although airfoils are shaped slightly differently than regions like  $D$  considered above, yet they can be approximated by such regions. The idea is to map an airfoil approximately onto a nearly circular region such as  $D$  which can then be mapped onto the unit disk.

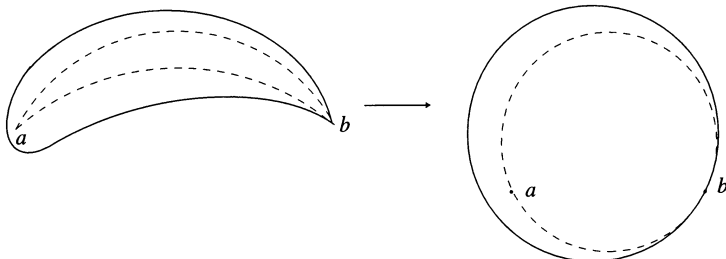


Fig. 10.3.3.

## 10.4. James's Method

As we have seen in §8.6, Theodorsen's method starts with the conformal map of the the exterior of the unit circle  $|z| > 1$  onto the exterior of a physical boundary in the  $\zeta$ -plane. The iterations in this method are convergent only if the image boundary is a near circle. An analysis of two-element airfoils using Theodorsen's method is given in Case Study 10.4.1. However, the limitation of Theodorsen's method do not apply in James's method (James, 1971) which will be presented below in §10.4.1. Note that every multi-element potential flow analysis makes use of the single-element mapping methods at some stage during the computations.

The single-element mapping deals with the problem of conformally mapping the exterior of the unit circle onto the region outside (or inside) a Jordan contour  $\Gamma$ . Contours  $\Gamma$  with corners or boundary curves that do not close can be considered by using preliminary transformations or by including singular functions in the series for the mapping function with augmented bases, as in the RM, BKM or ONP method. A further assumption often made during the approximation process is that the image curve maintains its proper scale and orientation whereas the distant regions are left undisturbed. Mappings are generally made, however, without any prior knowledge as to the scale factor or rotation of the boundary.

**10.4.1. Single-Element Airfoils.** Let the mapping be represented by a function of the form

$$z = \zeta + a_0 + \frac{c_1}{\zeta} + \frac{a_2}{\zeta^2} + \cdots, \quad (10.4.1)$$

where  $z = e^{i\theta}$  and  $\zeta = \rho e^{i\phi}$  denote the complex coordinates on the unit circle and the physical plane, respectively, and  $a_j$ ,  $j = 0, 1, \dots$ , are complex constants. Both Theodorsen (1931) and James (1971) use series closely related to (10.4.1). Their methods can be called the *method of successive conjugates* (Garrick, 1949).

**THEODORSEN'S METHOD.** This method uses the truncated series of the form

$$\log \left( \frac{z}{\zeta} \right) = b_0 + \frac{b_1}{\zeta} + \frac{b_2}{\zeta^2} + \cdots + \frac{b_{N-1}}{\zeta^{N-1}}, \quad (10.4.2)$$

which is applied at equispaced points  $j$  on the unit circle (clockwise along the perimeter). This yields

$$\log \left( \frac{z}{\zeta} \right)_j = \sum_{k=0}^{N-1} b_k e^{i2\pi j k / N}. \quad (10.4.3)$$

The terms on the left side of (10.4.3) are related to the geometric variables by the relation

$$\log \left( \frac{z}{\zeta} \right)_j = \log \rho_j + i (\phi_j - \theta_j), \quad (10.4.4)$$

where  $\rho_j$  is the radial coordinate of the point  $j$  in the  $\zeta$ -plane and  $\phi_j$  and  $\theta_j$  are the arguments (positive clockwise) of the points in the  $\zeta$ - and  $z$ -plane, respectively. The real and imaginary parts of  $\log(z/\zeta)$  are conjugate harmonic

functions, so that if one is known the other can be computed efficiently by Fourier transforms. Thus, the iterations are carried out step-by-step as follows:

- STEP 1. Compute the values of  $\theta_j$  at the defining points in the  $z$ -plane.
- STEP 2. Approximate the values of  $\phi_j$  at the points in the  $\zeta$ -plane corresponding to the equispaced points in the  $z$ -plane ( $\phi_j = \theta_j$  is often assumed).
- STEP 3. Use the curve-fit coefficients to determine the values of  $\log \rho_j$  corresponding to the estimated values of  $\phi_j$ .
- STEP 4. Compute the conjugate harmonic function corresponding to the latest values of  $\log \rho_j$ , and use them to update the estimated values of  $\phi_j$ .
- STEP 5. Repeat steps 3 and 4 until the values of  $\phi_j$  converge.
- STEP 6. Determine the coefficients of the mapping function from the converged data.

JAMES'S METHOD. This method uses the truncated series of the form

$$\log \left( \frac{dz}{d\zeta} \right) = c_0 + \frac{c_1}{\zeta} + \frac{c_2}{\zeta^2} + \cdots + \frac{c_{N-1}}{\zeta^{N-1}}, \quad (10.4.5)$$

which is applied at equispaced points on the circle. This yields

$$\log \left( \frac{dz}{d\zeta} \right)_j = \sum_{k=0}^{N-1} c_k e^{i2\pi j k / N}. \quad (10.4.6)$$

The term on the left side is related to the geometric variables by the relation

$$\log \left( \frac{dz}{d\zeta} \right)_j = \log \left| \frac{dz}{d\zeta} \right|_j + i \arg \left\{ \frac{dz}{d\zeta} \right\}_j, \quad (10.4.7)$$

$$s_j = \int_0^{\theta_j} \left| \frac{dz}{d\zeta} \right| d\theta, \quad (10.4.8)$$

$$\arg \left\{ \frac{dz}{d\zeta} \right\}_j = \tau_j + \theta_j - \frac{3\pi}{2}, \quad (10.4.9)$$

where  $s_j$  is the arc length on the contour  $\Gamma$  in the  $\zeta$ -plane and  $\tau_j$  is the angle on that contour (for the convention, see Fig. 10.4.1). Then the iterations are performed as follows:

- STEP 1. Compute the values of  $s$  and  $\tau$  at the defining points in the  $z$ -plane, and determine the curve-fit coefficients of  $\tau$  vs  $s$ .

- STEP 2. Approximate the values of  $\left| \frac{dz}{d\zeta} \right|_j$  at equispaced points on the circle

( $\left| \frac{dz}{d\zeta} \right|_j = 1.0$  is usually assumed).

STEP 3. Integrate (10.4.8), and obtain approximate values of  $s_j$ .

STEP 4. Use the curve-fit coefficients to determine the values of  $\tau_j$  corresponding to the approximate values of  $s_j$ , and compute  $\arg \left\{ \frac{dz}{d\zeta} \right\}_j$  from (10.4.9).

STEP 5. Compute the conjugate function to determine the values of  $\log \left| \frac{dz}{d\zeta} \right|_j$  corresponding to the latest values of  $\arg \left\{ \frac{dz}{d\zeta} \right\}_j$ , and take the exponential to update the values of  $\left| \frac{dz}{d\zeta} \right|_j$ .

STEP 6. Repeat steps 3 through 5 until the values of  $\left| \frac{dz}{d\zeta} \right|_j$  converge.

STEP 7. Compute the coefficients of the mapping function from the converged data.

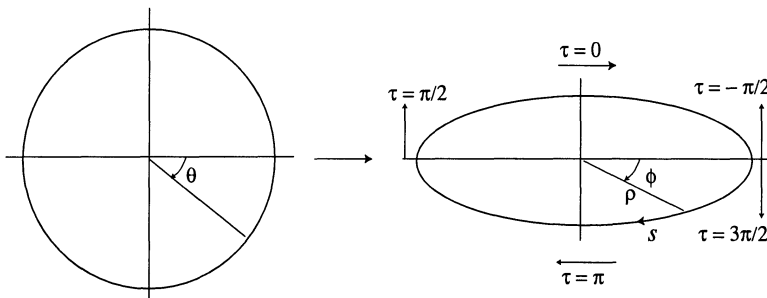


Fig. 10.4.1.

Halsey (1982) found, by comparing the numerical data and convergence properties of both of these methods, that James's method is more suitable than Theodorsen's for a larger class of single- and multi-element boundaries. For example, an application of Theodorsen's method to a slightly complicated boundary, such as a cambered ellipse, where polar coordinates are used ( $\log \rho$  and  $\phi$ ), leads to functions with multiple values. This makes numerical interpolation inaccurate, if not impossible. On the contrary, in James's method the use of intrinsic coordinates ( $\tau$  and  $s$ ) always yields a family of interpolated functions so long as the boundary has no corner singularity. Thus, James's method is more suited for mapping complicated boundaries. The three-element looped boundary shown in Fig. 10.4.2 failed to be mapped by Theodorsen's method, but James's method presented no computational difficulty. Even when the use of polar coordinates is not appropriate, James's method still works smoothly in many cases where Theodorsen's method fails. These include elliptic boundaries of different ratios  $b/a$  of the minor and major axes. For example, for  $b/a = 0.9$

both methods require 10 iterations to reduce the residuals to less than  $10^{-5}$ ; for  $b/a = 0.4$  Theodorsen's method requires 25 iterations, but James's 15, to reduce the residuals to  $10^{-5}$ ; and for  $b/a = 0.3$  Theodorsen's method fails to converge, whereas James's method succeeds even down to  $b/a = 0.005$  with only a maximum of 25 iterations.

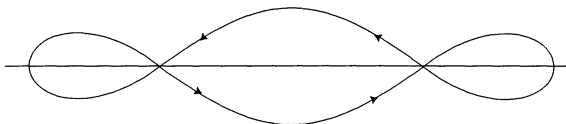


Fig. 10.4.2. Three-element loop.

Halsey (1982) has found that both methods fail to satisfy Warschawski's sufficient conditions (8.2.5)–(8.2.6) for convergence established in §8.2.

A detailed examination of all computed data has revealed the mechanism for the failure of iterations to converge in Theodorsen's method. In general, equispaced points on the circle transform into more closely spaced points on the boundary  $\Gamma$  for values of  $\left| \frac{dz}{d\zeta} \right| < 1$  and into more sparsely spaced points on the boundary for values of  $\left| \frac{dz}{d\zeta} \right| > 1$ . Thus, the thinner a boundary gets, the smaller some the values of  $\left| \frac{dz}{d\zeta} \right|$  become and the more closely spaced some of the points become. As such, computation of the conjugate harmonic function in Theodorsen's method is an approximation to the difference in arguments between the corresponding points in the  $z$ - and  $\zeta$ -plane, which leads to computation of arguments in the  $\zeta$ -plane. For boundaries where the points are very closely spaced, small errors in the computed arguments cause a breakdown in the ordering of the points where the argument at a point number  $j$  becomes smaller than that at the point number  $j - 1$ . Hence, subsequent computations contain large errors, and the iterations fail to converge. Moreover, this kind of failure of Theodorsen's method is more likely if a larger number of points is used. For example, if the number of points is increased to 257, the iterations fail to converge in the case of an ellipse with  $b/a = 0.4$ , whereas with only 17 iterations the iterations do converge even with  $b/a = 0.2$ . This mechanism of failure of convergence is absent in James's method.

**10.4.2. von Karman–Treffitz Transformations.** These transformations are useful in analyzing potential flow over multi-element airfoils. First,

we shall consider a single-element airfoil and modify Theodorsen's method by using a von Karman transformation and FFT. There are four basis procedural steps in the problem of conformally mapping any airfoil onto a circle: (i) remove the effects of slope discontinuities in the airfoil contour, and expand the regions of rapid flow changes (e.g., the nose region) by conformally mapping the airfoil point-by-point onto a nearly circular contour; (ii) translate the coordinate system so as to place the centroid of the nearly circular region on or near the origin; (iii) use interpolation and obtain a continuous representation of the nearly circular contour and thus of the airfoil; and (iv) map the nearly circular contour onto a circle.

The analytical and computational tools to perform these four steps are as follows. For step (i) a von Karman–Trefftz transformation is used. Let  $z$  denote a complex coordinate in the airfoil plane ( $z$ -plane), and  $\zeta$  a complex coordinate in the nearly circular contour plane ( $\zeta$ -plane). Then the von Karman–Trefftz transformation is given by

$$\frac{z - \zeta}{z + \zeta} = \left( \frac{z - z_s - \kappa z_l}{z + z_s - \kappa z_l} \right)^{1/\kappa}, \quad (10.4.10)$$

where  $z_s$  and  $z_l$  are complex constants,  $\kappa = 1 - \tau/\pi$ , and  $\tau$  is the trailing edge included angle. This transformation is singular at

$$z = z_s + \kappa z_l \equiv z_{T1}, \quad \text{and} \quad z = z_s - \kappa z_l \equiv z_{N1}, \quad (10.4.11)$$

where the firmer point is at the trailing edge and the latter at a point midway between the nose of the airfoil and its center of curvature (Fig. 10.4.3). Since  $z_{T1}$  and  $z_{N1}$  are known, we can determine  $z_s$  and  $z_l$  from (10.4.11). If the angle  $\tau$  is opened up to  $\pi$  (see Fig. 10.3.2), then the airfoil is mapped into a near circle in the  $\zeta$ -plane where the circle (dotted) is drawn for comparison, 0 is the origin of the coordinates and  $C$  is the approximate centroid which is the origin of the  $\zeta'$ -plane. Since the transformation (10.4.10) contains a rational exponent, the proper branch should be chosen by 'tracking' the transformation from a point where it is known to the point of interest. A proper choice of the branch in (10.4.10) implies continuity of the argument of the base (the expression within parentheses) along a path that does not cross the boundary of the airfoil. Note that this argument approaches zero as  $z \rightarrow \infty$ .

In step (ii) the origin of the coordinate system is translated to the centroid  $C$  of the nearly circular region. First an approximate centroid  $C$  is determined by connecting adjacent points of the line segment. This translation is given by

$$\zeta' = \zeta - C. \quad (10.4.12)$$

It will be used to improve the convergence of a series expression used in step (iv).

In step (iii) a continuous representation of the airfoil image, which has so far been defined pointwise, is obtained. To do this, a polar coordinate system is defined in the  $\zeta$ -plane (Fig. 10.4.3), where  $\log \rho$  as a function of  $\psi$  is fitted with a periodic cubic spline (see §9.5 for more on splines). This curve fitting technique leads to a smooth definition of the airfoil image in the  $\zeta$ -plane with a high degree of accuracy.

In step (iv) the Theodorsen–Garrick transformation is used to map the near circle in the  $\zeta$ -plane onto a circle in the  $\zeta'$ -plane, where instead of Theodorsen's integral equation (8.1.6) with a cotangent kernel we shall use the Fourier series analysis to eventually use FFT. That is how Theodorsen's method is modified.

Thus, the Theodorsen–Garrick transformation can be written as

$$\zeta'_j = \zeta \exp \left\{ \sum_{j=0}^N (A_j + i B_j) \zeta^j \right\}. \quad (10.4.13)$$

Note that the near circle in the  $\zeta$ -plane is represented by

$$\zeta = \rho(\psi) e^{i\psi}. \quad (10.4.14)$$

We shall finally map the circle in the  $\zeta'$ -plane onto the unit circle  $w = e^{i\phi}$ . Thus, substituting these polar representations in (10.4.14), taking logarithms on both sides, and equating real and imaginary parts, we obtain the following set of equations:

$$\log \rho = A_0 + \sum_{j=1}^N (A_j \cos j\phi + B_j \sin j\phi), \quad (10.4.15)$$

$$\psi = \phi + B_0 + \sum_{j=1}^N (B_j \cos j\phi - A_j \sin j\phi). \quad (10.4.16)$$

Since  $\log \rho$  on the near circle is known as a function of  $\psi$  from the periodic cubic spline fit, the problem reduces to determining the coefficients  $A_j$  and  $B_j$  by FFT and an iterative scheme, as follows: Choose  $2N$  equispaced points on the unit circle in the  $w$ -plane, starting at the image of the trailing edge. Thus,

$$\phi_k = \frac{(k-1)\pi}{N}, \quad k = 1, \dots, 2N. \quad (10.4.17)$$

To place the trailing edge at  $\phi = 0$  in the  $w$ -plane, set

$$B_0 + \sum_{j=1}^N B_j = \psi_T, \quad (10.4.18)$$

where  $\psi_T$  is the value of  $\psi$  at the trailing edge in the  $\zeta'$ -plane. Take  $B_N = 0$  to make a closed system. Then,  $\psi_k$  is given by

$$\psi_k - \phi_k = \psi_T - \sum_{j=1}^{N-1} (B_j + A_j \sin j\phi_k - B_j \cos j\phi_k), \quad (10.4.19)$$

which can be evaluated by the Fourier technique as follows (assuming  $A_j$  and  $B_j$  are given for  $j = 1, \dots, N-1$ ):

$$\begin{aligned} y_1 &= \frac{1}{2} \left( \psi_T - \sum_{j=1}^{N-1} B_j \right), \\ y_{j+1} &= \frac{1}{2} (B_j + i A_j), \quad j = 1, \dots, N-1, \\ y_{2N-j+1} &= \bar{y}_j, \quad j = 1, \dots, N, \end{aligned} \quad (10.4.20)$$

where the bar denotes the complex conjugate. Then

$$\psi_k - \phi_k = \sum_{j=1}^{2N} y_j \exp \left\{ \frac{i\pi(j-1)(k-1)}{N} \right\}, \quad (10.4.21)$$

which is known as a discrete Fourier transform (Cooley and Tukey, 1965; Cooley, Lewis and Welch, 1970) and is evaluated by FFT technique in  $O(N \log_2 N)$  operations for  $k = 1, \dots, N$ . Note that a direct evaluation of Eq (10.4.21) takes  $O(N^2)$  operations.

We can apply a similar FFT technique to solve Eq (10.4.15) and obtain  $A_j$  and  $B_j$  by using a trigonometric series fit through the points  $(\log \rho_k)$  for  $k = 1, \dots, 2N$  as follows: Define

$$y_j = \frac{1}{2N} \sum_{k=1}^{2N} (\log \rho)_k \exp \left\{ -\frac{i\pi(j-1)(k-1)}{N} \right\}, \quad (10.4.22)$$

where  $(\log \rho)_k$  is the value of  $\log \rho$  at the  $k$ -th point given by Eq (10.4.17). Then

$$\begin{aligned} A_j &= 2 \Re \{ y_{k+1} \}, \quad j = 0, 1, \dots, N, \\ B_j &= -2 \Re \{ y_{j+1} \}, \quad j = 1, \dots, N-1. \end{aligned} \quad (10.4.23)$$

This evaluation takes  $O(N \log_2 N)$  operations.

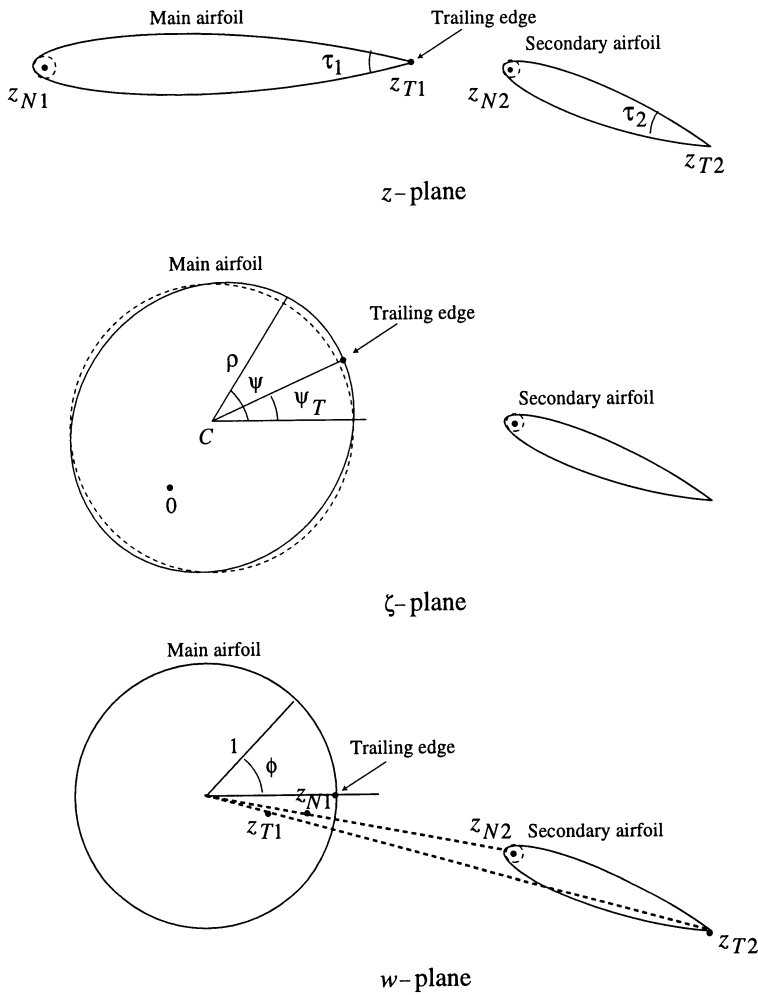


Fig. 10.4.3. Single-element airfoil mappings.

Now, we can summarize the iterative method by the following five-step algorithm:

1. Set  $A_j = B_j = 0$  for  $j = 1, \dots, N - 1$ .
2. Evaluate  $\psi_j$  from (10.4.21) by using (10.4.20).
3. Evaluate  $(\log \rho)_k$  for  $k = 1, \dots, 2N$ , using  $\psi_k$  and the cubic spline fit coefficients.
4. Solve for  $A_0$ ,  $A_N$ , and  $A_j$ ,  $B_j$  for  $j = 1, \dots, N - 1$ , using (10.4.22)–(10.4.23).

5. Using the latest computed values of  $A_j$  and  $B_j$  repeat the steps 2 through 4 until the values converge.

Warschawski's sufficient conditions for convergence (§8.2) for the above algorithm imply that

$$\sqrt{\frac{\rho_{\max}}{\rho_{\min}}} - 1 < \varepsilon, \quad \left| \left( \frac{\partial \log \rho}{\partial \psi} \right)_{\max} \right| < \varepsilon,$$

where  $\varepsilon = 0.2954976$ , and the maximum and minimum values are taken on the nearly circular contour. Note that the composite accuracy of this method depends on the accuracy at each step. Since (10.4.20) involves trigonometric functions, the computation of  $A_j$ ,  $B_j$  in step 4 may not produce accurate results. However, an error analysis in step 4 must be carried out to determine the terms that should be taken to approximate the trigonometric functions involved in this step. It is known (Abramovici, 1973) that about 100 terms are enough to approximate  $\log \rho$  in terms of the trigonometric series in  $\psi$ . Another source of errors lies in step 3 where a periodic cubic spline is used to interpolate  $\log \rho$  as a function of  $\psi$ . These errors, though small, are due to the definition of the airfoil only at finitely many points  $j$  which are mapped onto the circle with an accuracy limited only by the round-off error of the computer.

**10.4.3. Two-Element Airfoils.** We shall use Garrick's approach (Garrick, 1936, 1949), together with the von Karman–Treffitz transformation and FFT, to map a two-element airfoil onto the unit circle conformally. A two-element airfoil mapping is initially identical to a single-element airfoil mapping except that there is a secondary airfoil which is carried through the four steps (i)–(iv) mentioned in §10.4.2. Then the airfoil-like shape of the secondary airfoil is mapped onto the near circle whereas the mapping of the main airfoil remains a circle (Fig. 10.4.3). The von Karman–Treffitz transformation for a simultaneous conformal mapping of the two airfoils (main and secondary) is  $g(\zeta) = f(z)$ , where

$$g(\zeta) = \frac{\zeta - \zeta_T}{\zeta - \zeta_N} \cdot \frac{\zeta - \zeta_T^*}{\zeta - \zeta_N^*}, \quad f(z) = \left( \frac{z - z_{T2}}{z - z_{N2}} \cdot \frac{z - z_{T2}^*}{z - z_{N2}^*} \right)^{1/\kappa_2}, \quad (10.4.24)$$

and  $\kappa_2 = 2 - \tau_2/\pi$ ,  $\tau_2$  is the trailing edge angle for the secondary airfoil;  $z_{N2}$ ,  $\zeta_N$ , and  $\zeta_T$  are complex constants, and  $z_{N2}^*$ ,  $z_{T2}^*$  denote the symmetric points to  $z_{N2}$ ,  $z_{T2}$  with respect to the unit circle, i.e.,  $z_{N2}^* = 1/\bar{z}_{N2}$ ,  $z_{T2}^* = 1/\bar{z}_{T2}$ , and  $\zeta_N^*$ , and  $\zeta_T^*$  are symmetric points to  $\zeta_N$ , and  $\zeta_T$  with respect to the

circle  $|\zeta| = R$ , i.e.,  $\zeta_N^* = R^2/\bar{\zeta}_N$ , and  $\zeta_T^* = R^2/\bar{\zeta}_T$  (see §2.2). Moreover,

$$\frac{\zeta_T \zeta_N^*}{\zeta_N \zeta_T^*} = \left( \frac{z_{T2} z_{N2}^*}{z_{N2} z_{T2}^*} \right)^{1/\kappa_2}, \quad (10.4.25)$$

where  $z_{T2}$  and  $z_{N2}$  are the points at the trailing edge and at a point midway between the nose and the center of curvature of the secondary airfoil. From (10.4.24) we find that  $\frac{d\zeta}{dz} \rightarrow 1$  as  $\zeta \rightarrow \infty$  only if

$$\zeta_T + \zeta_T^* - \zeta_N - \zeta_N^* = \frac{1}{\kappa_2} (z_{T2} + z_{T2}^* - z_{N2} - z_{N2}^*). \quad (10.4.26)$$

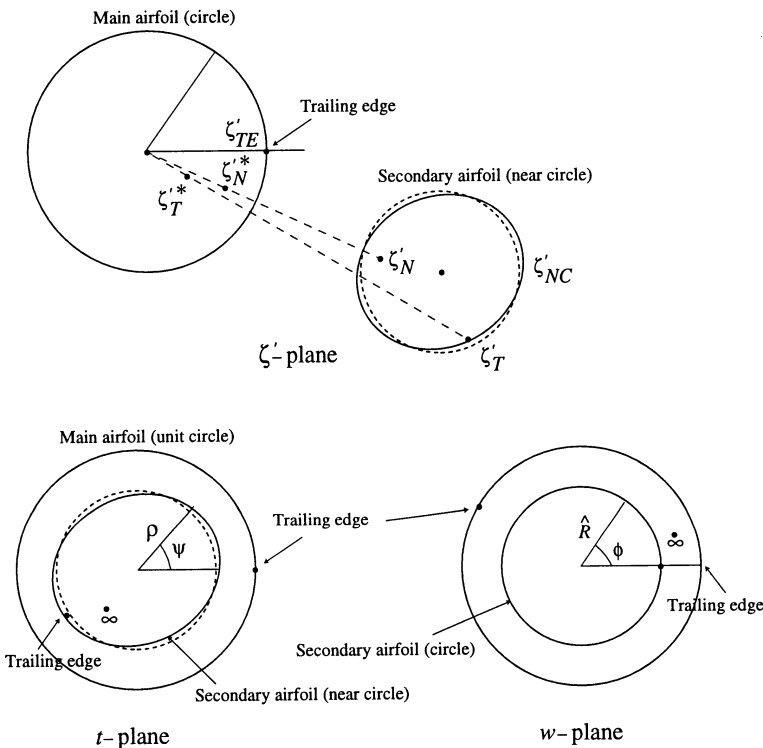


Fig. 10.4.4. Two-element airfoil mappings.

Also,  $\frac{dz}{df} \rightarrow \infty$  when

$$\frac{1}{z - z_{N2}} + \frac{1}{z - z_{T2}} - \frac{1}{z - z_{N2}^*} - \frac{1}{z - z_{N2}^*} = 0, \quad (10.4.27)$$

and  $\frac{d\zeta}{dg} \rightarrow \infty$  when

$$\frac{1}{\zeta - \zeta_N} + \frac{1}{\zeta - \zeta_T} - \frac{1}{\zeta - \zeta_N^*} - \frac{1}{\zeta - \zeta_N^*} = 0. \quad (10.4.28)$$

Let the (simple) roots of Eqs (10.4.27) and (10.4.28) be denoted by  $z_{01}, z_{02}$  and  $\zeta_{01}, \zeta_{02}$ , respectively. A further analysis shows that  $\arg\{f\} = \arg\{g\}$  at these roots which are singular points, although the magnitudes of these roots, in general, are different. Thus, we have

$$\left| \frac{z_{0m} - z_{T2}}{z_{0m} - z_{N2}} \cdot \frac{z_{0m} - z_{T2}^*}{z_{0m} - z_{N2}^*} \right|^{1/\kappa_2} = \left| \frac{\zeta_{0m} - \zeta_T}{\zeta_{0m} - \zeta_{N2}} \cdot \frac{\zeta_{0m} - \zeta_T^*}{\zeta_{0m} - \zeta_N^*} \right|, \quad m = 1, 2, \quad (10.4.29)$$

in order that  $|dz/d\zeta|$  or its inverse is regular at these singular points. In this analysis all quantities except a real  $R$  and the complex variable  $\zeta_N$  can be computed from (10.4.24) and (10.4.25). The two unknowns  $R$  and  $\zeta_N$  can be computed from (10.4.25) by using  $\bar{\zeta}_T = R^2/\zeta_T^*$ .

The above mapping transforms the secondary airfoil into a near circle and at the same time transforms the main airfoil into a circle of radius  $\hat{R}$  ( $w$ -plane, Fig. 10.4.4). This mapping is nonsingular at all points except  $z_N, z_T, z_N^*, z_T^*, \zeta_N, \zeta_T, \zeta_N^*$  and  $\zeta_T^*$ . The near circle is mapped onto the unit circle by the Möbius transformation

$$t = a \frac{\zeta' + b}{\zeta' + c}, \quad (10.4.30)$$

where the trailing edge image  $\zeta'_{TE}$  of the main airfoil is mapped into  $w = 1$  if

$$a \frac{\zeta'_{TE} + b}{\zeta'_{TE} + c} = 1. \quad (10.4.31)$$

The image of the near circle of the secondary airfoil in the  $t$ -plane should be mapped onto  $|w| = r$ ,  $r < 1$ , such that its center lies at the origin so that a Fourier series used later will converge rapidly. Also the point  $\zeta'_N$  in the  $\zeta'$ -plane is mapped into  $t = 0$  so that

$$\zeta'_N + b = 0. \quad (10.4.32)$$

The Möbius transformation that maps the circle  $\zeta' = R$  onto the circle  $|t| = 1$  with their centers at the origin is given by

$$\frac{1}{\zeta'_N} + c = 0. \quad (10.4.33)$$

Then the complex constants  $a$ ,  $b$  and  $c$  are determined as follows:

- 1) Set  $\zeta_N$  equal to the centroid of the near circle in the  $\zeta$ -plane.
- 2) Solve (10.4.31)–(10.4.33) for  $a$ ,  $b$ , and  $c$ .
- 3) Use (10.4.30) to transform the near circle from the  $\zeta'$ -plane to the  $t$ -plane.
- 4) Approximate the centroid of the near circle, denoted by  $\zeta'_{NC}$ , by connecting adjacent points with straight lines and calculating the centroid of the resulting region.
- 5) Compute a new value for  $\zeta'_N$  from (10.4.30), using  $\zeta'_{NC}$ ,  $a$ ,  $b$ , and  $c$ .
- 6) Use the latest value of  $\zeta'_N$ , and repeat steps 2 through 5 until convergence is achieved.

The region infinitely far from the airfoil is mapped into the point  $\infty$  in the  $t$ -plane. The near circle in the  $t$ -plane is determined only point-by-point, and thus a periodic cubic spline can be used to interpolate  $\log \rho$  on the near circle as a function of  $\psi$  (as in the single-element airfoils). The mapping from the near circle to the circle  $|w| = \hat{R}$  is carried out by the function

$$w = \sum_{j=1}^N \left[ (-A_{2j} + i B_{2j}) (\hat{R}t)^j + (A_{2j} + i B_{2j}) \left(\frac{\hat{R}}{t}\right)^j \right], \quad (10.4.34)$$

where  $\hat{R} < 1$  is the image of the nearly circular contour of the secondary airfoil in the  $w$ -plane. Note that since  $w$  is purely imaginary for  $t = e^{i\beta}$  for any real  $\beta$ , the mapping (10.4.34) maps the  $\zeta'$ -plane onto itself in the  $t$ -plane.

**10.4.4. Multi-Element Airfoils.** The von Karman–Treffitz transformation for simultaneous conformal mapping of  $n$  airfoils in the  $z$ -plane is given by  $g(\zeta) = f(z)$ , where

$$g(\zeta) = \prod_{j=1}^n \frac{\zeta - \zeta_{Tj}}{\zeta - \zeta_{Nj}}, \quad f(z) = \prod_{j=1}^n \left( \frac{z - z_{Tj}}{z - z_{Nj}} \right)^{1/\kappa_j}, \quad (10.4.35)$$

where  $\kappa_j = 2 - \tau_j/\pi$ ,  $\tau_j$  is the trailing edge included angle of the  $j$ -th airfoil;  $z_{Tj}$  and  $z_{Nj}$  denote the complex coordinates of the trailing edge and the point midway between the nose and the center of curvature of the  $j$ -th airfoil, and  $\zeta_{Tj}$  and  $\zeta_{Nj}$  are suitably chosen complex coefficients. The condition  $\lim_{\zeta \rightarrow \infty} |dz/d\zeta| = 1$  is satisfied only if

$$\sum_{j=1}^n \left[ \zeta_{Tj} - \zeta_{Nj} - \frac{1}{\kappa_j} (z_{Tj} - z_{Nj}) \right] = 0. \quad (10.4.36)$$

The coordinate system in the  $\zeta$ -plane is defined by  $\zeta_{T1} + \zeta_{N1} = 0$ . Note that  $dz/d\zeta$  becomes unbounded when

$$\sum_{j=1}^n \frac{1}{\kappa_j} \left( \frac{1}{z - z_{Tj}} - \frac{1}{z - z_{Nj}} \right) = 0, \quad (10.4.37)$$

and  $d\zeta/dg$  becomes unbounded when

$$\sum_{j=1}^n \left( \frac{1}{\zeta - \zeta_{Tj}} - \frac{1}{\zeta - \zeta_{Nj}} \right) = 0. \quad (10.4.38)$$

In general, there exist  $(2n - 2)$  finite roots of Eq (10.4.37), all different from  $z_{Tj}$  and  $z_{Nj}$ . There are also  $(2n - 2)$  finite roots of Eq (10.4.38), all different from  $\zeta_{Tj}$  and  $\zeta_{Nj}$ . Let these roots (which are also singularities) be denoted by  $z_{0j}$  and  $\zeta_{0j}$ ,  $j = 1, \dots, 2n - 2$ . Then  $dz/d\zeta$  and its inverse will be finite at all these singular points only if

$$g(\zeta_{0j}) = f(z_{0j}), \quad j = 1, \dots, 2n - 2. \quad (10.4.39)$$

The  $2n$  complex quantities  $\zeta_{Tj}$  and  $\zeta_{Nj}$ ,  $j = 1, \dots, n$ , are uniquely determined from (10.4.35)–(10.4.39) by using an  $n$ -dimensional complex Newton–Raphson iteration scheme. For  $n = 1$  this mapping reduces to that of the single-element airfoils defined by (10.4.10).

---

## 10.5. Problems

PROBLEM 10.5.1. Show that the conformal mapping

$$w = \frac{lz^2 + 2mz + n}{pz^2 + 2qz + r} \quad (10.5.1)$$

degenerates to a bilinear transformation if  $(lr - np)^2 = 4(mr - nq)(lq - mp)$ . If this condition is not satisfied, then the above mapping can be reduced to the

following forms:

$$\begin{aligned} \frac{w - \beta}{w - \alpha} &= k \left( \frac{z - \mu}{z - \lambda} \right)^2 \quad \text{when } q^2 \neq pr, lq \neq mp; \\ \frac{w - \beta}{w - \alpha} &= k (z - \mu)^2 \quad \text{when } q^2 \neq pr, lq \neq mp, p \neq 0; \\ w - \beta &= k \left( \frac{z - \mu}{z - \lambda} \right)^2 \quad \text{when } q^2 = pr, lq \neq mp, p \neq 0; \\ w - \beta &= \frac{k}{(z - \lambda)^2} \quad \text{when } q^2 = pr, lq = mp, p \neq 0; \\ w - \beta &= k (z - \mu)^2 \quad \text{when } p = 0, q = 0, \end{aligned} \quad (10.5.2)$$

where  $\alpha$  and  $\beta$  are two unequal roots of  $lz^2 + 2mz + n - w (pz^2 + 2qz + r) = 0$ ,  $z = \lambda$  and  $z = \mu$  are the two real values that correspond to  $w = \alpha$  and  $w = \beta$ , respectively, and  $\lambda \neq \mu$  since  $\alpha \neq \beta$ . (Piaggio and Strain, 1947.)

**PROBLEM 10.5.2.** Let the circle  $\Gamma$  pass through the point  $z = ia$ ,  $a > 0$ , and let the point  $z = -i \in \text{Int}(\Gamma)$ . Show that the mapping (10.2.4) maps the circle  $\Gamma$  onto a Joukowski airfoil. (Pennisi et al., 1963, p.335.)

**PROBLEM 10.5. 3.** Show that under the mapping (10.2.4) one half of the unit circle  $|w| < 1$  is the image of the circle  $|z - i| = \sqrt{2}$ , and the other half that of the  $|z + i| = \sqrt{2}$ . (Pennisi et al., 1963, p.335.)

**PROBLEM 10.5.4.** Under the mapping (10.2.4) with  $a > 0$  show that  
(i) two distinct points  $z_1, z_2$  are mapped into the same point iff  $z_2 = a^2/z_1$ .  
(ii) a circle passing through the point  $z = -a$  and containing the point  $z = a$  in its interior is mapped bijectively in the  $w$ -plane;  
(iii) the circle  $|z| = (a + b)/2$ ,  $a > 0$ ,  $b > 0$ , is mapped onto an ellipse  $u = a \cos \phi$ ,  $v = b \sin \phi$  in the  $w$ -plane with foci at  $w = \pm 2a$ . (Pennisi et al., 1963, p.335.)

**PROBLEM 10.5.5.** Show that under the mapping  $w = \left( \frac{z^n + 1}{z^n - 1} \right)^2$ ,  $n > 0$  an integer, the image of the sector  $|z| < 1$ ,  $z = |z| e^{i\theta}$ ,  $0 < \theta < \pi/n$ , is the upper half-plane  $\Im\{w\} > 0$ . [Hint: Use the chain of mappings  $\zeta = z^n$  and  $w = \left( \frac{\zeta + 1}{\zeta - 1} \right)^2$ , in that order, to transform the sector onto the semi-circle  $|\zeta| \leq 1$  and  $\Im\{\zeta\} \geq 0$  onto  $\Im\{w\} \geq 0$ .] (Pennisi et al., 1963, pp.336–337.)

**PROBLEM 10.5.6.** Using the formula for density distribution  $\mu(s)$  of a charge on an ideally conducting circular cylinder, given by  $\mu(s) = \frac{e}{2\pi} \left| \frac{dz}{d\zeta} \right|_{|\zeta|=1}^{-1}$ , where  $e$  denotes the charge per unit length of the cylinder, show that the charge density in a strip of width  $2a$  in the  $(x, y)$ -plane along the segment  $-a < x < a$  is given by  $\mu(x) = \frac{e}{2\pi} \frac{1}{\sqrt{a^2 - x^2}}$ . [Hint: use the mapping (10.1.9).] (Sveshnikov and Tikhonov, 1978, p.216.)

**PROBLEM 10.5.7.** Apply Theodorsen's and James's methods to approximately transform the unit circle conformally onto the one-element boundary of

- (a) teardrop wing profile of NACA0010 shown in Fig. 10.5.1(a).
- (b) a composite elliptic wing profile composed of upper and lower curves from two ellipses with the same major axis but a different minor axis (Fig. 10.5.1(b)).

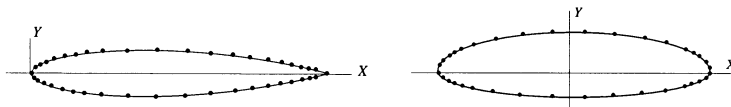


Fig. 10.5.1.(a), (b).

**REFERENCES USED:** Abramovici (1973), Andersen et al. (1962), Carathéodory (1969), Carrier, Krook and Pearson (1966), Cooley and Tukey (1965), Cooley, Lewis and Welch (1970), Gaier (1964), Garrick (1936, 1949), Glauert (1948), Halsey (1979, 1982), Ives (1976), James (1971), Kantorovich and Krylov (1958), Kober (1957), Piaggio and Strain (1947), Pennisi et al. (1963), Phillips (1943, 1966), Theodorsen (1931), von Karman and Trefitz (1918), Warschawski (1945).

# Chapter 11

---

## Doubly Connected Regions

---

Some well-known numerical methods for approximating conformal mapping of doubly regions onto an annulus or the unit disk are presented. There is a definite need for a simple yet accurate method for mapping a general doubly connected region onto a circular annulus. According to Kantorovich and Krylov (1958, p. 362) the problem of finding the conformal modulus is ‘one of the difficult problems of the theory of conformal transformation’. As such, analytic solutions have been determined for a very restricted class of doubly connected regions, like those mentioned in Muskhelishvili (1963, §48). Numerical solutions are also confined to a limited class of regions where either one boundary is circular or axisymmetric. Most common methods use integral equations, iterations, polynomial approximations, and kernels. We shall develop Symm’s integral equations and the related orthonormal polynomial method. A dipole formulation that leads to the method of reduction of connectivity shall be presented. Another useful method for multiply connected regions, based on Mikhlin’s integral equation, that also works for simply and doubly connected regions as well will be discussed in Chapter 13.

---

### 11.1. Conformal Modulus

Let  $\Gamma_1$  and  $\Gamma_0$  denote two Jordan contours such that  $\Gamma_1 \subset \text{Int}(\Gamma_0)$  and  $0 \in \text{Int}(\Gamma_1)$ . Let  $\Omega$  denote the doubly connected region

$$\Omega = \text{Ext}(\Gamma_1) \cap \text{Int}(\Gamma_0).$$

The conformal mapping problem is to determine the function  $w = f_\Omega(z)$  which maps  $\Omega$  univalently onto an annulus  $A(\rho_1, \rho_2) = \{w : \rho_1 < |w| < \rho_2\}$ , where  $\rho_{1,2}$  are real numbers such that  $0 < \rho_1 < \rho_2$ . Thus,  $\Gamma_1$  and  $\Gamma_0$  are mapped conformally onto two circles  $|w| = \rho_1$  and  $|w| = \rho_2$ , respectively. The ratio  $M = \rho_2/\rho_1 > 1$  is called the *conformal modulus* of  $\Omega$ . Let the parametric equation of the boundary  $\partial\Omega = \Gamma_1 \cup \Gamma_0$  be  $z = \gamma(s)$ ,  $0 \leq s \leq L$ , so that  $\Gamma_1 = \{\gamma(s) : 0 \leq s \leq l\}$  and  $\Gamma_0 = \{\gamma(s) : l \leq s \leq L\}$ . For simplicity, we shall write  $f$  instead of  $f_\Omega$  hereafter, and use the notation  $\gamma(0) = \gamma(0^+) = \gamma(l^-)$ , and  $\gamma(l) = \gamma(l^+) = \gamma(L^-) = \gamma(L)$ . Then the boundary correspondence function  $\Phi$  for the function  $f$  is defined by

$$\Phi(s) = \arg \{f(\gamma(s))\}, \quad (11.1.1)$$

where

$$f(\gamma(s)) = \rho(s) e^{i\Phi(s)}, \quad \text{and} \quad \rho(s) = \begin{cases} \rho_1, & 0 \leq s \leq l, \\ \rho_2, & l \leq s \leq L. \end{cases} \quad (11.1.2)$$

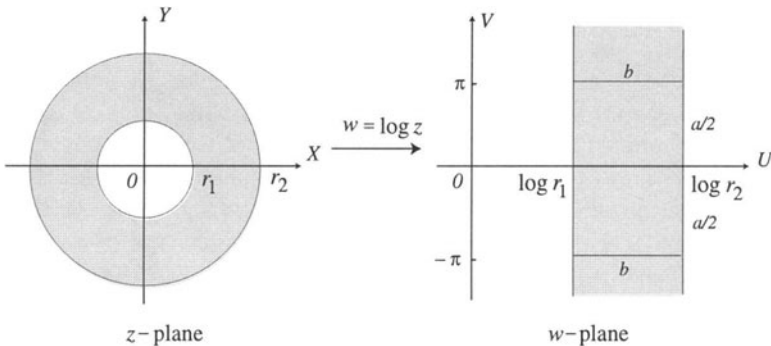


Fig. 11.1.1.

**11.1.1. Conformal Invariants.** If an annular region  $A(r_1, r_2)$ ,  $r_1 < |z| < r_2$ , is mapped conformally onto a parallel strip  $\{\log r_1 < u < \log r_2\}$  by the function  $w = \log z$ , then the annulus corresponds to an enumerable set of congruent rectangles, all with sides  $a$  and  $b$  such that  $b = \log \frac{r_2}{r_1}$ , and  $a = 2\pi$ . Since every doubly connected region can be mapped conformally onto an annulus of the type shown in Fig. 11.1.1 and since two annuli with different ratios  $r_2/r_1$  cannot be mapped conformally onto each other, the set of all doubly connected regions falls into classes of conformally equivalent regions

where every class is characterized by the ratio  $r_2/r_1$  of the radii belonging to that class (see §1.4). Hence, the ratio  $r_2/r_1$ , known as the *conformal invariant*, is related to the ratio  $a/b$  of the sides of the rectangles by

$$\frac{b}{a} = \frac{1}{2\pi} \log \frac{r_2}{r_1}, \quad \text{or} \quad \frac{r_2}{r_1} = e^{2\pi b/a}. \quad (11.1.3)$$

The linear transformation

$$\zeta = \frac{i - \sqrt{k} w}{1 + \sqrt{k} w}, \quad \text{or} \quad w = \frac{1}{i\sqrt{k}} \frac{\zeta - 1}{\zeta + 1}, \quad (11.1.4)$$

where  $k$  is defined by (2.3.11), maps the half-plane  $\Im\{w\} \geq 0$  onto the circular region  $|\zeta| \leq 1$  such that the four points corresponding to the points  $w = \pm 1, \pm \frac{1}{k}$  are the vertices of a rectangle whose center is at  $\zeta = 0$  (Fig. 11.1.2). Then the angle  $\psi$  between the diagonals of the rectangle is given by

$$\tan \frac{\psi}{2} = \frac{2\sqrt{k}}{1-k}. \quad (11.1.5)$$

Combining the mapping (11.1.4) and the mapping (2.3.13) of the upper half-plane  $\Im\{z\} > 0$  onto the rectangle, we obtain a conformal mapping of the rectangle onto the disk  $|\zeta| < 1$ . Thus, the angle  $\psi$  is another conformal invariant for doubly connected regions. A table of complete elliptic functions of the first kind for  $k$  from 0 to 1 and of  $k_1, K(k), K(k_1), a/b, r_2/r_1$  and  $\psi$  (see Fig. 11.1.2) is available in Andersen et al., 1962, pp.165–166 (also see §2.3).

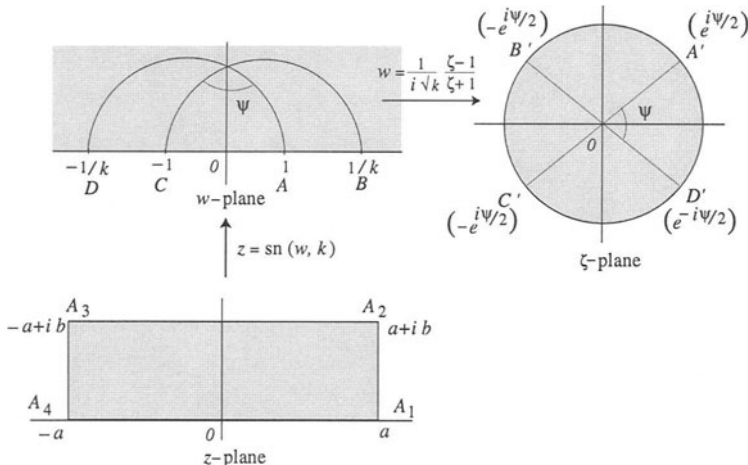


Fig. 11.1.2.

**11.1.2. Area Theorem.** The *star* of a region  $D$  is defined as the largest region contained in  $D$  that is starlike with respect to  $z = 0$  (see §8.5). Corresponding to the annulus  $A(\rho_1, \rho_2)$  in the  $w$ -plane, there exists a doubly connected region  $D$  in the  $z$ -plane, with  $\Gamma_1$  and  $\Gamma_0$  as the inner and outer boundaries such that  $\Gamma_1$  lies outside the disk  $|z| < r(1 - \delta_r)$ , where  $\delta_r \rightarrow 0$  as  $r \rightarrow 0$ . Let us partition the part of the star of  $D$  lying outside  $\Gamma_1$  by rays emanating from  $z = 0$  such that (i) the rays are mapped onto themselves by a rotation about  $z = 0$  through an angle  $2k\pi/n$ ,  $k = 1, \dots, n$ ; and (ii) the variations in  $|z|$  on the portion of  $\Gamma_1$  between two consecutive rays (excluding the rays themselves) is less than a preassigned quantity  $\varepsilon > 0$ . Since  $\Gamma_1$  is an analytic curve, such a system of rays exists. There are  $nm$  such rays, where  $m$  is an integer. We denote them in order by  $l_1, l_2, \dots, l_{nm}$ , where  $l_{mk+q}$  is obtained from  $l_q$  by a rotation through an angle  $2k\pi/n$ . Let  $r_k$ ,  $k = 1, 2, \dots, nm$ , denote the largest distance from  $z = 0$  to the part  $G_k$  of the star lying between the rays  $l_k$  and  $l_{k+1}$  and outside  $\Gamma_1$  for  $k = 1, 2, \dots, nm$ , where  $G_{nm+1} = G_1$  (Fig. 11.1.3). The function  $\zeta = \log \left( \frac{z}{r} \right)$  transforms this system of regions  $G_k$  into a system of regions  $H_k$  lying, respectively, in rectangles with sides of length  $\log \left( \frac{r_k}{r} \right)$  and  $\alpha_k$ , where  $\sum_{k=1}^{nm} \alpha_k = 2\pi$  and  $\alpha_{mk+j} \neq \alpha_j$ .

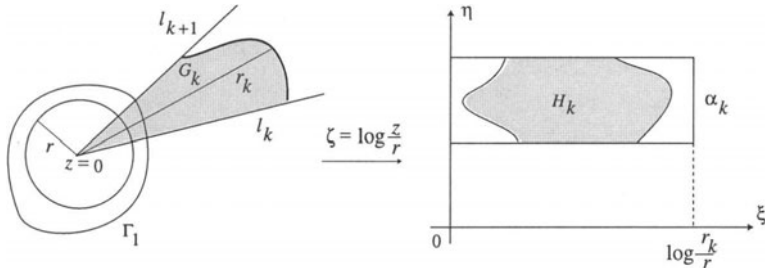


Fig. 11.1.3

If the region  $H_k$  is mapped onto a rectangle of sides  $a_k$  and  $b_k$  such that the boundary segments of  $H_k$  are mapped into the side of length  $b_k$ , then

$$\frac{a_k}{b_k} \geq \frac{\alpha_k}{\log \frac{r_k}{r}}, \quad (11.1.6)$$

which yields

$$\sum_{k=1}^{nm} \frac{a_k}{b_k} \geq \sum_{j=1}^m \sum_{k=0}^{n-1} \frac{\alpha_{mk+j}}{\log \frac{r_{mk+j}}{r}} = \sum_{j=1}^m \alpha_j \sum_{k=0}^{n-1} \frac{1}{\log \frac{r_{mk+j}}{r}}.$$

Since the system of regions  $G_k$  is the image of a system of strips contained in the annulus  $\rho_1 < |w| < \rho_2$  under the mapping  $w = f(z)$ , we have

$$\begin{aligned} \frac{2\pi}{\log \frac{\rho_2}{\rho_1}} &\geq \sum_{j=1}^m \alpha_j \cdot \min_j \sum_{k=0}^{n-1} \frac{1}{\log \frac{r_{mk+j}}{r}} \\ &= \frac{2\pi}{n} \cdot \min_j \sum_{k=0}^{n-1} \frac{1}{\log \frac{r_{mk+j}}{r}}. \end{aligned} \quad (11.1.7)$$

Using the inequality  $\frac{1}{n} \sum_{k=1}^n c_n \geq \sqrt[n]{\prod_{k=1}^n c_k}$ ,  $c_k \geq 0$ , twice, we find from (11.1.7) that

$$\sum_{k=0}^{n-1} \frac{1}{\log \frac{r_{mk+j}}{r}} \geq \frac{n}{\sqrt[n]{\prod_{k=1}^{n-1} \log \frac{r_{mk+j}}{r}}} \geq \frac{n^2}{\sum_{k=1}^{n-1} \log \frac{r_{mk+j}}{r}},$$

and hence, (11.1.7) yields

$$n \log \frac{\rho_2}{\rho_1} \leq \max_j \sum_{k=1}^{n-1} \log \frac{r_{mk+j}}{r},$$

or

$$M^n = \left( \frac{\rho_2}{\rho_1} \right)^n \leq \max_j \prod_{k=0}^{n-1} \frac{r_{mk+j}}{r}, \quad (11.1.8)$$

where  $M$  is the conformal modulus of the region  $A(\rho_1, \rho_2)$ .

Antonjuk (1958) has proved the following theorem for functions that are regular in an annulus:

**THEOREM 11.1.1.** *Suppose that the function  $w = f(z)$  is regular in the annulus  $A(1, M) = \{1 < |z| < M\}$  and satisfies the conditions  $|f(z)| \geq 1$  and  $\frac{1}{2i\pi} \int_C \frac{f'(z)}{f(z)} dz \geq 1$ , where  $C$  is a contour in  $A(1, M)$  which is not homologous to  $z = 0$ . Let  $A_f^*$  denote the star of a finite doubly connected Riemann surface  $A_f$  onto which the annulus  $A(1, m)$*

is mapped by the function  $w = f(z)$  with respect to the system of rays emanating from the point  $w = 0$ . Then

$$(P^* + \pi) (p^* + \pi) \geq \pi^2 M^4, \quad (11.1.9)$$

where  $P^*$  is the area of the star  $A_f^*$  and  $p^*$  the area of the preimage of  $A_f^*$ . The equality in (11.1.9) holds for functions of the form  $f(z) = cz$ ,  $|c| = 1$ .

CASE STUDY 11.1.1. The region  $A(\rho, 1) = \{\rho < |\zeta| < 1\}$  is mapped conformally onto the unit disk  $|t| < 1$ , slit from  $-L$  to  $+L$  (Fig. 11.1.4) by the function

$$t = L \operatorname{sn} \left( \frac{2iK}{\pi} \log \frac{\zeta}{\rho} + K, k \right), \quad k = L^2, \quad K = K(k), \quad (11.1.10)$$

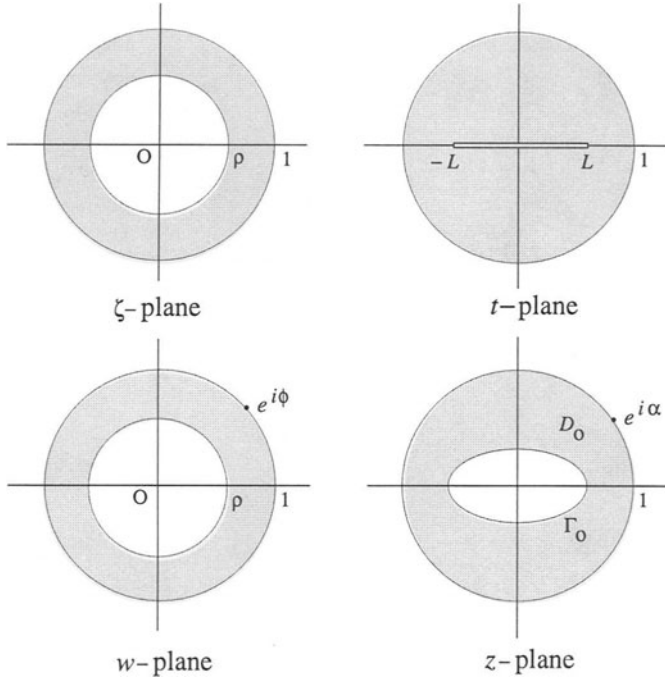


Fig. 11.1.4.

(Nehari, 1952, pp.293–295). Let

$$\zeta = \rho/w, \quad t = \frac{L}{2} (z + z^{-1}), \quad |z| = 1. \quad (11.1.11)$$

Then the circle  $|t| = 1$  is mapped onto the boundary  $\Gamma_0$  in the  $z$ -plane by the mapping (11.1.11), where  $\Gamma_0$  is in polar coordinates defined by

$$r = r(\theta) = \sqrt{\frac{1}{L^2} + \sin^2 \theta} - \sqrt{\frac{1}{L^2} - \cos^2 \theta}. \quad (11.1.12)$$

For example, if we take  $k = L^2 = \sin 46^\circ$ , as in Gaier (1964, p.222), then the values of  $r_n = r\left(\frac{n\pi}{18}\right)$  for  $n = 0, 1, 2, \dots, 9$  are given in the following table:

| $n$ | $r_n$     | $n$ | $r_n$     |
|-----|-----------|-----|-----------|
| 0   | 0.554 435 | 5   | 0.417 632 |
| 1   | 0.543 464 | 6   | 0.395 150 |
| 2   | 0.515 529 | 7   | 0.379 357 |
| 3   | 0.480 595 | 8   | 0.370 041 |
| 4   | 0.446 599 | 9   | 0.366 967 |

We find that

(i) The modulus  $M$  of the region  $D_0$  is given by (Nehari, 1952, p.294)

$$M = \frac{1}{\rho} = \exp\left\{\frac{\pi}{4} \frac{K'(k)}{K(k)}\right\} = \frac{1}{\sqrt[4]{q(k)}} \approx 2.166187,$$

for  $k = \sin 46^\circ$  (for the function  $\text{sn}$  and  $q$ , see §7.4).

(ii) Let  $w = e^{i\phi}$  be the map of  $z = e^{i\alpha}$ ,  $\alpha = \alpha(\phi)$ . Then

$$\zeta \mapsto t : t = L \text{sn}\left((1 + 2\phi/\pi) K, k\right), \quad (11.1.13)$$

$$z \mapsto t : t = L \cos \alpha, \quad (11.1.14)$$

where

$$\cos \alpha = \text{sn}\left((1 + 2\phi/\pi) K, k\right) = \text{sn}\left((1 - 2\phi/\pi) K, k\right).$$

Set  $\alpha' = \pi/2 - \alpha$ . Then  $(1 - 2\phi/\pi) K = F(\alpha', k)$ , where  $F$  is the hypergeometric function. In particular, let  $\phi_n = \frac{n\pi}{18}$ ,  $n = 1, 2, \dots, 8$ , and set  $r = 90 - 10n$ . Then  $F(\alpha', k) = rK/90$ ,  $r = 80, 70, \dots, 10$ , and  $k = \sin 46^\circ$ . This yields the values of  $\alpha'_n$ , and hence, of  $\alpha_n$ .

(iii) Let  $w = \rho e^{i\phi}$  map the  $z$ -plane onto the  $w$ -plane (Fig. 11.1.4). We shall determine  $\beta = \beta(\phi) - \arg\{z\}$ . First, we use the mapping

$$\zeta \mapsto t : t = L \text{sn}(K + i\kappa + v, k), \quad \kappa = \frac{2K \log M}{\pi}, \quad v = \frac{2K}{\pi} \phi. \quad (11.1.15)$$

Since  $t = e^{i\psi}$  maps  $t$  onto  $|t| = 1$ , we have  $1 = L \operatorname{sn}(K + i\kappa, k)$  for  $\phi \neq 0$ . Set  $u = K + i\kappa$ . Then  $\operatorname{sn} u = 1/L$ ,  $\operatorname{cn} u = \sqrt{1 - 1/L^2}$  which is purely imaginary, and  $\operatorname{dn} u = \sqrt{1 - L^2}$  which is real. Also,  $\operatorname{sn} v$ ,  $\operatorname{cn} v$ , and  $\operatorname{dn} v$  are real. Hence, from (11.1.15), by equating real parts, we get

$$\cos \psi = \frac{\operatorname{cn}(v, k) \operatorname{dn}(v, k)}{1 - L^2 [\operatorname{sn}(v, k)]^2}, \quad (11.1.16)$$

where  $v = v_n = nK/9$ ,  $n = 1, 2, \dots, 8$ . Since, in view of (11.1.14), the mapping  $z \mapsto t$  gives

$$\cos \psi = \frac{L}{2} \left( r + \frac{1}{r} \right) \cos \beta, \quad \sin \psi = \frac{L}{2} \left( r - \frac{1}{r} \right) \sin \beta,$$

we eliminate  $r$ , use (11.1.16), and obtain

$$\begin{aligned} \sin^2 \beta &= \frac{-(1 - L^2) + \sqrt{(1 - L^2)^2 + 4L^2 \sin^2 \psi}}{2L^2} \\ &= \frac{1 - l^2}{1 - L^2 \operatorname{sn}^2(v, k)} \operatorname{sn}^2(v, k). \end{aligned} \quad (11.1.17)$$

If we set  $v_n = nK/9$ ,  $n = 1, 2, \dots$ , then we determine the values of  $\beta_n = \beta(\phi_n)$  from the table given above. ■

**CASE STUDY 11.1.2** (Dirichlet problem for the annulus). Let two real-valued,  $2\pi$ -periodic and continuous functions  $u_1(\theta)$  and  $u_2(\theta)$  be defined on the boundary of the annulus  $A(r_1, r_2) = \{r_1 < |z| < r_2\}$ . The Dirichlet problem for this region deals with determining a function  $u(r, \theta)$  which is continuous in the closed region  $A(r_1, r_2) \cup \Gamma_1 \cup \Gamma_0 = \{r_1 \leq |z| \leq r_2\}$ , harmonic in  $A(r_1, r_2)$ , and takes the boundary value  $u_1(\theta)$  on  $\Gamma_1$  for  $z = r_1 e^{i\theta}$  and  $u_2(\theta)$  on  $\Gamma_0$  for  $z = r_2 e^{i\theta}$ . The harmonic function  $v(r, \theta)$ , conjugate to  $u(r, \theta)$ , is in general not single-valued, and thus the function  $f(z) = u + i v$  will have two summands. One is a single-valued function that can be expanded in a Laurent series for the annulus, and the other is  $\log z$  with a real coefficient  $A$ . Thus,

$$u + i v = \sum_{n=-\infty}^{\infty} \gamma_n z^n + A \log z, \quad \gamma_n = \alpha_n + i \beta_n, \quad (11.1.18)$$

which, after separating into real and imaginary parts, yields

$$\begin{aligned} u &= \alpha_0 + \sum_{n=1}^{\infty} [(\alpha_n r^n + \alpha_{-n} r^{-n}) \cos n\theta - (\beta_n r^n - \beta_{-n} r^{-n}) \sin n\theta] \\ &\quad + A \log r, \\ v &= \beta_0 + \sum_{n=1}^{\infty} [(\beta_n r^n + \beta_{-n} r^{-n}) \cos n\theta + (\alpha_n r^n - \alpha_{-n} r^{-n}) \sin n\theta] + \theta. \end{aligned} \tag{11.1.19}$$

In the first equation in (11.1.19) we set  $r = r_1$  and  $r = r_2$ . This gives us the Fourier series expansions for the functions  $u_1(\theta)$  and  $u_2(\theta)$ , respectively, where the Fourier coefficients are given by

$$\begin{aligned} a_0^{(1)} &= \alpha_0 + A \log r_1 = \frac{1}{2\pi} \int_{-\pi}^{\pi} u_1(\theta) d\theta, \\ a_0^{(2)} &= \alpha_0 + A \log r_2 = \frac{1}{2\pi} \int_{-\pi}^{\pi} u_2(\theta) d\theta, \\ a_n^{(1)} &= \alpha_n r_1^n + \alpha_{-n} r_1^{-n} = \frac{1}{2\pi} \int_{-\pi}^{\pi} u_1(\theta) \cos n\theta d\theta, \\ a_n^{(2)} &= \alpha_n r_2^n + \alpha_{-n} r_2^{-n} = \frac{1}{2\pi} \int_{-\pi}^{\pi} u_2(\theta) \cos n\theta d\theta, \\ b_n^{(1)} &= \beta_{-n} r_1^{-n} - \beta_n r_1^n = \frac{1}{2\pi} \int_{-\pi}^{\pi} u_1(\theta) \sin n\theta d\theta, \\ b_n^{(2)} &= \beta_{-n} r_2^{-n} - \beta_n r_2^n = \frac{1}{2\pi} \int_{-\pi}^{\pi} u_2(\theta) \sin n\theta d\theta. \end{aligned}$$

Hence

$$\begin{aligned} A &= \frac{a_0^{(2)} - a_0^{(1)}}{\log M}, & \alpha_0 &= \frac{a_0^{(1)} \log r_2 - a_0^{(1)} \log r_1}{\log M}, \\ \alpha_n &= \frac{a_n^{(1)} r_2^{-n} - a_n^{(2)} r_1^{-n}}{r_1^n r_2^{-n} - r_1^{-n} r_2^n}, & \alpha_{-n} &= \frac{a_n^{(1)} r_2^n - a_n^{(2)} r_1^n}{r_2^n r_1^{-n} - r_2^{-n} r_1^n}, \\ \beta_n &= \frac{b_n^{(2)} r_1^{-n} - b_n^{(1)} r_2^{-n}}{r_1^n r_2^{-n} - r_1^{-n} r_2^n}, & \beta_{-n} &= \frac{b_n^{(1)} r_2^n - b_n^{(2)} r_1^n}{r_2^n r_1^{-n} - r_2^{-n} r_1^n}. \end{aligned} \tag{11.1.20}$$

**CASE STUDY 11.1.3** (Neumann problem for the annulus). Let  $F_1(\theta)$  and  $F_2(\theta)$  denote the normal derivatives of the harmonic function  $u(r, \theta)$  on the boundaries  $\Gamma_1 = \{|z| = r_1\}$  and  $\Gamma_0 = \{|z| = r_2\}$  of the annulus  $A(r_1, r_2)$ .

Then the function  $f(z) = u + i v$  has the same representation as in (11.1.18), where separating real and imaginary parts and satisfying the Neumann conditions on the boundaries  $\Gamma_1$  and  $\Gamma_0$ , respectively, we get

$$\begin{aligned} F_1(\theta) &= \sum_{n=1}^{\infty} n [ (\alpha_n r_1^{n-1} - \alpha_{-n} r_1^{n-1}) \cos n\theta \\ &\quad - (\beta_n r_1^{n-1} - \beta_{-n} r_1^{n-1}) \sin n\theta] + \frac{A}{r_1}, \\ F_2(\theta) &= - \sum_{n=1}^{\infty} n [ (\alpha_n r_2^{n-1} - \alpha_{-n} r_2^{n-1}) \cos n\theta \\ &\quad - (\beta_n r_2^{n-1} - \beta_{-n} r_2^{n-1}) \sin n\theta] - \frac{A}{r_2}. \end{aligned} \quad (11.1.21)$$

The coefficient  $A$  is determined in two ways which are equal:

$$A = \frac{r_1}{2\pi} \int_{-\pi}^{\pi} F_1(\theta) d\theta = -\frac{r_2}{2\pi} \int_{-\pi}^{\pi} F_2(\theta) d\theta. \quad (11.2.22)$$

The other coefficients in the Fourier series expansions of  $F_1(\theta)$  and  $F_2(\theta)$  are given by

$$\begin{aligned} a_n^{(1)} &= n (\alpha_n r_1^{n-1} - \alpha_{-n} r_1^{-n-1}) = \frac{1}{\pi} \int_{-\pi}^{\pi} F_1(\theta) \cos n\theta d\theta, \\ a_n^{(2)} &= -n (\alpha_n r_2^{n-1} - \alpha_{-n} r_2^{-n-1}) = \frac{1}{\pi} \int_{-\pi}^{\pi} F_2(\theta) \cos n\theta d\theta, \\ b_n^{(1)} &= -n (\beta_n r_1^{n-1} + \beta_{-n} r_1^{-n-1}) = \frac{1}{\pi} \int_{-\pi}^{\pi} F_1(\theta) \sin n\theta d\theta, \\ b_n^{(2)} &= n (\beta_n r_2^{n-1} + \beta_{-n} r_2^{-n-1}) = \frac{1}{\pi} \int_{-\pi}^{\pi} F_2(\theta) \sin n\theta d\theta. \end{aligned} \quad (11.1.23)$$

Thus, after solving (11.1.23), we find that the coefficients  $\alpha_{\pm n}$  and  $\beta_{\pm n}$  in the series (11.1.21) are given by

$$\begin{aligned} \alpha_n &= \frac{1}{n} \frac{a_n^{(1)} r_1 r_2^{-n} + a_n^{(2)} r_2 r_1^{-n}}{r_1^n r_2^{-n} - r_2^n r_1^{-n}}, & \beta_n &= -\frac{1}{n} \frac{b_n^{(1)} r_1 r_2^{-n} + b_n^{(2)} r_2 r_1^{-n}}{r_1^n r_2^{-n} - r_2^n r_1^{-n}}, \\ \alpha_{-n} &= \frac{1}{n} \frac{a_n^{(1)} r_1 r_2^n + a_n^{(2)} r_2 r_1^n}{r_1^n r_2^{-n} - r_2^n r_1^{-n}}, & \beta_{-n} &= \frac{1}{n} \frac{b_n^{(2)} r_2 r_1^n + b_n^{(1)} r_1 r_2^n}{r_1^n r_2^{-n} - r_2^n r_1^{-n}}. \blacksquare \end{aligned} \quad (11.1.24)$$

## 11.2. Source Density

Let  $w = f_\Omega(z)$  map conformally a finite, doubly connected region  $\Omega$ , bounded by two Jordan contours  $\Gamma_1$  and  $\Gamma_0$ ,  $\Gamma_1 \subset \Gamma_0$ , onto the annulus  $A(\rho, 1)$ , with  $M = 1/\rho$ ,  $\rho < 1$ , where  $\rho$  is initially unknown and is to be determined. Let us assume that the origin lies inside the region  $\text{Int}(\Gamma_1)$ . Then the function  $f_\Omega(z)$ , which is uniquely determined except for a rotation, can be represented in the form (as in §9.1)

$$f_\Omega(z) = e^{\log z + g(z) + i h(z)}, \quad (11.2.1)$$

where  $g$  and  $h$  are conjugate harmonic functions in  $\Omega$  such that

$$\left| f_\Omega(z) \right| = \begin{cases} \rho, & \text{for } z \in \Gamma_1, \\ 1, & \text{for } z \in \Gamma_0. \end{cases} \quad (11.2.2)$$

Thus,

$$f_\Omega(z) = e^{\log |z| + g(x, y) + i [\arg\{z\} + h(x, y)]}, \quad z = x + iy, \quad (11.2.3)$$

where the boundary conditions (11.2.2) become

$$g(x, y) = \begin{cases} \log \rho - \log |z|, & z \in \Gamma_1, \\ -\log |z|, & z \in \Gamma_0. \end{cases} \quad (11.2.4)$$

As in §9.1, we shall represent  $g(x, y)$  as a single-layer logarithmic potential

$$g(x, y) = \int_{\Gamma=\Gamma_1+\Gamma_0} \log |z - \zeta| \mu(\zeta) |d\zeta|, \quad (11.2.5)$$

where  $\mu(\zeta)$  is the source density on  $\Gamma$ . Also,

$$h(x, y) = \int_{\Gamma} \arg\{z - \zeta\} \mu(\zeta) |d\zeta| + q, \quad (11.2.6)$$

where  $q$  is an arbitrary constant corresponding to an arbitrary rotation in the mapping function  $f_\Omega(z)$  defined by (11.2.1). Then the boundary conditions (11.2.4) become

$$\int_{\Gamma} \log |z - \zeta| \mu(\zeta) |d\zeta| = \begin{cases} \log \rho - \log |z|, & z \in \Gamma_1, \\ -\log |z|, & z \in \Gamma_0, \end{cases} \quad (11.2.7)$$

and the condition (9.1.7) on the single-valuedness of  $h$  reduces to

$$\int_{\Gamma_1} \mu(\zeta) |d\zeta| = 0, \quad (11.2.8)$$

as in (9.1.13). Note that Eqs (11.2.7) and (11.2.8), known as Symm's integral equations, are coupled equations for  $\mu(\zeta)$  and  $\rho$  and possess a unique solution (see Jawson, 1963). Once  $\mu(\zeta)$  is determined, the functions  $g$  and  $h$  can be computed from (11.2.5) and (11.2.6), respectively, and hence, the mapping function  $f_\Omega(z)$  from (11.2.1).

The numerical computation of  $\mu(\zeta)$ ,  $g$ ,  $h$ , and  $f_\Omega$  is carried out by the ONP method as in §9.2, i.e., by partitioning the boundary  $\Gamma$  into  $N$  sections  $G_1, \dots, G_N$  and approximating  $\mu(\zeta)$  by  $\mu_j$  which is constant over each  $G_j$ ,  $j = 1, \dots, N$ . Then Eq (11.2.7) is computed at each node  $z_k = x_k + iy_k$ ,  $j = 1, \dots, N$ , together with Eq (11.2.8). This yields a system of  $(N+1)$  linear equations in  $(N+1)$  unknowns  $\mu_1, \dots, \mu_N$  and  $\log \rho$ . The solution of this system leads to the approximate value of  $\rho$ . Then the functions  $g$  and  $h$  are approximated by finite terms corresponding to the integrals in (11.2.5) and (11.2.6), and the mapping function  $f_\Omega(z)$  is finally obtained from (11.2.1). The method follows the same set of steps as in §9.2.

Let  $\hat{f}_\Omega(z)$  and  $\hat{\rho}$  denote the numerical approximations to  $f_\Omega(z)$  and  $\rho$ . Then

$$|\hat{\rho} - \rho| \ll \max_z |\hat{f}_\Omega(z) - f_\Omega(z)|, \quad (11.2.9)$$

and, as Symm (1969) has noted,  $\hat{\rho}$  is more accurate than  $\hat{f}_\Omega(z)$ . In fact, by the maximum modulus theorem,  $|\hat{f}_\Omega(z) - f_\Omega(z)|$  takes its maximum value somewhere on the boundary  $\Gamma = \Gamma_1 \cup \Gamma_0$ , and, as in §9.2, this maximum value rarely exceeds  $2 \max_z |\hat{f}_\Omega(z) - f_\Omega(z)|$ . But since

$$|\hat{f}_\Omega(z) - f_\Omega(z)| = \begin{cases} |\hat{\rho} - \rho|, & \text{at the nodes of } \Gamma_1, \\ 0, & \text{at the nodes of } \Gamma_0, \end{cases}$$

then, in view of (11.2.9), we should compute  $|\hat{f}_\Omega(z)|$  at some point  $z = Z_j$  between the nodes (which may be end points of  $G_j$ ). Thus, the point  $Z_j$  is called the internodal point for  $G_j$ . The error  $E$  in  $|\hat{f}_\Omega(z)|$  then is given by

$$E = \max_{Z_j} \left\{ \max_{z \in \Gamma_1} \left| |\hat{f}_\Omega(z)| - \rho \right|, \max_{z \in \Gamma_0} \left| |\hat{f}_\Omega(z)| - 1 \right| \right\}. \quad (11.2.10)$$

If the doubly connected regions are symmetric about one or both coordinate axes, then the total number of equations to be solved reduces from  $(N + 1)$  to  $(N/2 + 1)$  or  $(N/4 + 1)$ , respectively. We shall denote the approximate values of  $u$ ,  $v$ , and  $w = u + i v$  by  $\hat{u}$ ,  $\hat{v}$ , and  $\hat{w}$ , respectively.

CASE STUDY 11.2.1. Consider a pair of Limaçons

$$\begin{aligned}\Gamma_1 &= \{x = a_1 \cos t + b_1 \cos 2t, y = a_1 \sin t + b_1 \sin 2t, a_1 > 0, b_1 > 0\}, \\ \Gamma_0 &= \{x = a_2 \cos t + b_2 \cos 2t, y = a_2 \sin t + b_2 \sin 2t, a_2 > 0, b_2 > 0\},\end{aligned}$$

(see Fig. 11.2.1 with  $a_1 = 5$ ,  $a_2 = 10$ ,  $b_2 = 3$ , and  $b_1 = b_2/4$ ) where  $t = 0$  ( $2\pi/N$ )  $2\pi$  defines the distribution of nodes on each boundary and  $N = 2(n - 1)$ . The values of  $a_1, a_2, b_1, b_2$  are chosen such that  $b_1/b_2 = (a_1/a_2)^2$  which ensures that the function

$$f_\Omega(z) = \frac{\sqrt{a_2^2 + 4b_2 z} - a_2}{2b_2},$$

which maps  $\Gamma_0$  onto the unit circle (see Muskhelishvili, 1963, §48, who has determined analytic solutions for some doubly connected regions like Pascal's limaçons, epitrochoids, hypotrochoids, and elliptic rings), also maps  $\Gamma_1$  onto a concentric circle of radius  $\rho = a_1/a_2$ , where  $M = 1/\rho$ . Because of symmetry about the  $x$ -axis, we take  $t = 0(\pi/10)\pi$ . The values of  $\hat{u}$  and  $\hat{v}$  are given below in Table 1.

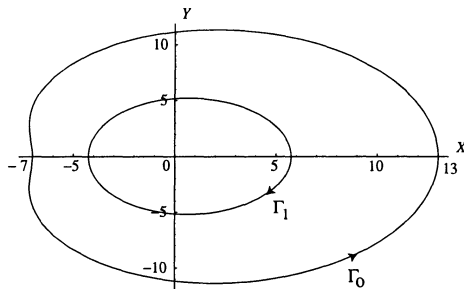


Fig. 11.2.1.

Symm (1969) has taken  $a_1 = 5$ ,  $a_2 = 10$ ,  $b_2 = 3$  and  $b_1 = b_2/4$  and has shown that the error  $E$  increases as  $b_2$  increases and that the boundary  $\Gamma_0$  gradually changes from a circle ( $b_2 = 0$ ) to a cardioid ( $b = 5$ ). In each case  $E$  decreases

as  $N$  increases. However,  $\hat{\rho}$  varies very little, which indicates that even a crude partition of  $\Gamma$  is sufficient for a good approximation of  $\rho$ . ■

Table 1. Values of  $\hat{u}$  and  $\hat{v}$ .

| $x$      | $y$     | $\hat{u}$ | $\hat{v}$ |
|----------|---------|-----------|-----------|
| 13.0     | 0.0     | 1.00000   | -0.00006  |
| 11.9376  | 4.95353 | 0.95106   | 0.30902   |
| 9.01722  | 8.73102 | 0.80902   | 0.58778   |
| 4.95080  | 10.9433 | 0.58779   | 0.80902   |
| 0.66316  | 11.2739 | 0.30902   | 0.95106   |
| -3.0     | 10.0    | 0.00002   | 1.00000   |
| -5.51722 | 7.7472  | -0.30902  | 0.95106   |
| -6.8049  | 5.237   | -0.58779  | 0.80902   |
| -7.16312 | 3.02468 | -0.80912  | 0.58779   |
| -7.08351 | 1.32681 | -0.95106  | 0.30902   |
| -7.0     | 0.0     | -0.99999  | 0.00002   |
| <hr/>    |         |           |           |
| 5.75     | 0.0     | 0.49999   | -0.00001  |
| 5.36205  | 1.98592 | 0.47552   | 0.15451   |
| 4.27685  | 3.65222 | 0.40452   | 0.29389   |
| 2.70716  | 4.75838 | 0.29389   | 0.40542   |
| 0.938322 | 5.19612 | 0.15451   | 0.47553   |
| -0.75    | 5.0     | 0.00002   | 0.49999   |
| -2.15185 | 4.31444 | -0.15452  | 0.47553   |
| -3.17069 | 3.33179 | -0.29389  | 0.40452   |
| -3.81322 | 2.22563 | -0.36698  | 0.42726   |
| -4.14852 | 1.10425 | -0.47554  | 0.15452   |
| -4.25    | 0.0     | -0.49999  | 0.00003   |

### 11.3. Dipole Distribution

It is known that in a simply connected region  $D$  bounded by a Jordan contour  $\Gamma : \{z = \gamma(s)\}$ , where  $s$  denotes the arc length along  $\Gamma$ ,  $0 \leq s \leq L$ , the dipole

distribution density  $\mu(s)$  satisfies the integral equation

$$\mu(s) = \frac{1}{\pi} \left[ g(s) - \int_0^L \mu(t) \frac{\partial}{\partial n_t} \left( \log \frac{1}{r_{tz}} \right) dt \right] \quad (11.3.1)$$

where  $n_t$  is the inward normal at a point  $\zeta = \gamma(t) \in \Gamma$ ,  $0 \leq t \leq L$ ,  $s \neq t$ , and  $r_{tz} = |z - \zeta|$ ,  $z \in D$ , and  $g(s)$  denotes the boundary value of the potential function  $u(z)$  on  $\Gamma$  (see Case Study 7.4.3, and Problem 7.6.4). The following result is useful in numerical evaluation of conformal mapping: If the density  $\mu(t)$  can be determined by solving Eq (11.3.1), then the Dirichlet problem and hence the problem of conformal mapping is reduced to quadratures.

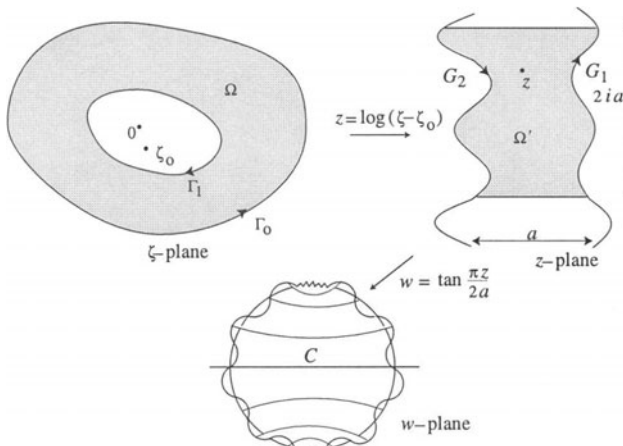


Fig. 11.3.1.

This dipole distribution formulation can be used for a doubly connected region  $\Omega$  in the  $\zeta$ -plane bounded by two Jordan contours  $\Gamma_1$  and  $\Gamma_0$ ,  $\Gamma_1 \subset \Gamma_0$ , and  $0 \in \text{Int}(\Gamma_1)$ , by transforming the region  $\Omega$  into a simply connected region by the function  $z = \log(\zeta - \zeta_0)$  which transforms  $\Omega$  into an irregular strip  $\Omega'$  with period  $2i\pi$ . Then the region  $\Omega'$  is further transformed into an irregular circlelike region  $C$  in the  $w$ -plane by the function  $w = \tan \frac{\pi z}{2a}$ , where  $a$  is the meanwidth of  $\Omega'$ . Note that the region  $C$  may have infinitely many extrema ('humps') in the neighborhood of the two points corresponding to  $\pm\infty$  (Fig. 11.3.1). Thus, the boundary problem for the region  $\Omega$  reduces to a boundary problem for the strip  $\Omega'$ , where the boundary values are  $2i\pi$ -periodic. Without loss of generality, we shall consider the general case of the period  $ib$ , where  $b$  need not be  $2\pi$ . Let the equations of the two boundaries  $G_1$  and  $G_2$  of the

strip  $\Omega'$  be  $G_1 : z = \gamma(s_1)$  and  $G_2 : z = \gamma(s_2)$ , where  $s_1$  and  $s_2$  are the arc lengths on  $G_1$  and  $G_2$ , respectively. If one period covers the arc lengths  $L_1$  and  $L_2$  such that  $\gamma(s_1 + L_1) = \gamma(s_1) + ib$ , and  $\gamma(s_2 + L_2) = \gamma(s_2) + ib$ , then the kernel in Eq (11.3.1) becomes

$$\begin{aligned} \frac{\partial}{\partial n_t} \left( \log \frac{1}{r_{tz}} \right) &= \Re \left\{ \frac{\partial}{\partial n_t} \left( \log \frac{1}{\gamma(s) - \gamma(t)} \right) \right\} \\ &= \Re \left\{ \frac{1}{\gamma(s) - \gamma(t)} \frac{\partial \gamma}{\partial n_t} \right\} = \Re \left\{ \frac{i}{\gamma(s) - \gamma(t)} \frac{\partial \gamma}{\partial t} \right\} \\ &= -\Im \left\{ \frac{1}{\gamma(s) - \gamma(t)} \gamma'(t) \right\}, \end{aligned} \quad (11.3.2)$$

where  $n$  is the inward normal,  $z = \gamma(s) \in \Omega'$ ,  $\gamma(t) \in G_{1,2}$ , and the potential at a point  $z \in \Omega'$  is given by

$$\begin{aligned} u(z) &= \int_{-\infty}^{\infty} \Im \left\{ \frac{1}{\gamma(s) - \gamma_2(t_2)} \gamma'_2(t_2) \right\} \mu_2(t_2) dt_2 \\ &\quad - \int_{-\infty}^{\infty} \Im \left\{ \frac{1}{\gamma(s) - \gamma_1(t_1)} \gamma'_1(t_1) \right\} \mu_1(t_1) dt_1, \end{aligned} \quad (11.3.3)$$

where the parameters  $t_1$  and  $t_2$  run from  $-\infty$  to  $+\infty$  as  $z$  traverses from  $-i\infty$  to  $+i\infty$ . Let us assume that the dipole densities  $\mu_1(t_1)$  and  $\mu_2(t_2)$  are periodic, i.e.,  $\mu_1(t_1 + L_1) = \mu_1(t_1)$ , and  $\mu_2(t_2 + L_2) = \mu_2(t_2)$ . Then the integrals in (11.3.3) can be written as sum of integrals, and we have

$$\begin{aligned} u(z) &= \sum_{n=-\infty}^{\infty} \int_0^{L_2} \Im \left\{ \frac{1}{\gamma(s) - \gamma_2(t_2) - inb} \gamma'_2(t_2) \right\} dt_2 \\ &\quad - \sum_{n=-\infty}^{\infty} \int_0^{L_1} \Im \left\{ \frac{1}{\gamma(s) - \gamma_1(t_1) - inb} \gamma'_1(t_1) \right\} dt_1. \end{aligned} \quad (11.3.4)$$

Note that the two integrals in (11.3.3) and the two sums in (11.3.4) are convergent in the Cauchy sense. Since the series in (11.3.4) are uniformly convergent, we can interchange the integration and summation. Using the formula (1.2.15) we find that

$$\begin{aligned} \sum_{n=-\infty}^{\infty} \frac{1}{\gamma(s) - \gamma(t) - inb} &= \frac{1}{\gamma(s) - \gamma(t)} \\ &\quad + \frac{1}{2ib} \sum_{n=1}^{\infty} \left\{ \frac{1}{\frac{\gamma(s) - \gamma(t)}{ib} - n} + \frac{1}{\frac{\gamma(s) - \gamma(t)}{ib} + n} \right\} \\ &= \frac{\pi}{ib} \cot \left( \pi \frac{\gamma(s) - \gamma(t)}{ib} \right), \end{aligned}$$

and (11.3.4) becomes

$$\begin{aligned} u(z) = & \pi \int_0^{L_2} \Im \left\{ \frac{1}{ib} \cot \left( \pi \frac{\gamma(s) - \gamma_2(t_2)}{ib} \right) \gamma'_2(t_2) \right\} \mu_2(t_2) dt_2 \\ & - \pi \int_0^{L_1} \Im \left\{ \frac{1}{ib} \cot \left( \pi \frac{\gamma(s) - \gamma_1(t_1)}{ib} \right) \gamma'_1(t_1) \right\} \mu_1(t_1) dt_1. \end{aligned} \quad (11.3.5)$$

Let the point  $z \in \Omega'$  approach a point  $z_s$  on the boundary of  $\Omega'$ . Then, in view of Problem 7.6.4, if  $g(s) = u_+(z_s)$  is the prescribed boundary value, then  $\lim_{z \rightarrow z_s} u(z) = u_+(z_s) = u(z_s) + \pi g(s)$ , and the integral equation for  $\mu(s)$  is

$$\begin{aligned} \mu(s) = & \frac{1}{\pi} g(s) + \int_0^{L_1} \Im \left\{ \frac{1}{ib} \cot \left( \pi \frac{\gamma(s) - \gamma_1(t_1)}{ib} \right) \gamma'_1(t_1) \right\} \mu_1(t_1) dt_1 \\ & - \int_0^{L_2} \Im \left\{ \frac{1}{ib} \cot \left( \pi \frac{\gamma(s) - \gamma_2(t_2)}{ib} \right) \gamma'_2(t_2) \right\} \mu_2(t_2) dt_2. \end{aligned} \quad (11.3.6)$$

This integral equation can be solved by an iterative method, e.g., the one in §7.4. Although this method of *reduction of connectivity* seems especially suitable for those doubly connected regions that can be easily transformed into parallel strips, yet no numerical study has been done for it. In some special cases, however, the analysis becomes simpler, and it is presented in the following two case studies.

**CASE STUDY 11.3.1** (Andersen et al., 1962). Consider the symmetric doubly connected region  $\Omega$  which is transformed into the unit disk (or an annulus) by a chain of conformal maps  $f_1, f_2, f_3, f_4, f_5, f_6$  and  $f_7$ , as shown in Fig. 11.3.2.

Note that in the  $z$ -plane  $z_0 \in \Gamma_0$  is chosen as a point on the axis of symmetry. The mapping goes from the  $z$ -plane through the  $z_1$ -plane,  $z_2$ -plane,  $z_3$ -plane,  $z_4$ -plane and finally to the unit disk in the  $w$ -plane. The conformal maps are as follows:

$$\begin{aligned} f_1 : z_1 &= \log(z - z_0); \quad f_2 : z_2 = \tan \frac{\pi z_1}{2a}; \\ f_3 : z_3 &= \frac{(q+1)z_2 - 1 + q}{(q-1)z_2 + 1 + q}; \\ f_4 : z_4 &= \frac{1}{i\sqrt{k}} \frac{z_3 - 1}{z_3 + 1}; \quad f_5 : w = \frac{z_4 - i}{z_4 + i}; \\ f_6 : z_6 &= \int_0^{z_4} \frac{dt}{\sqrt{(1-t^2)(1-k^2t^2)}}; \quad f_7 : z_7 = \exp \left\{ \frac{2\pi z_4}{ia} \right\}. \end{aligned}$$

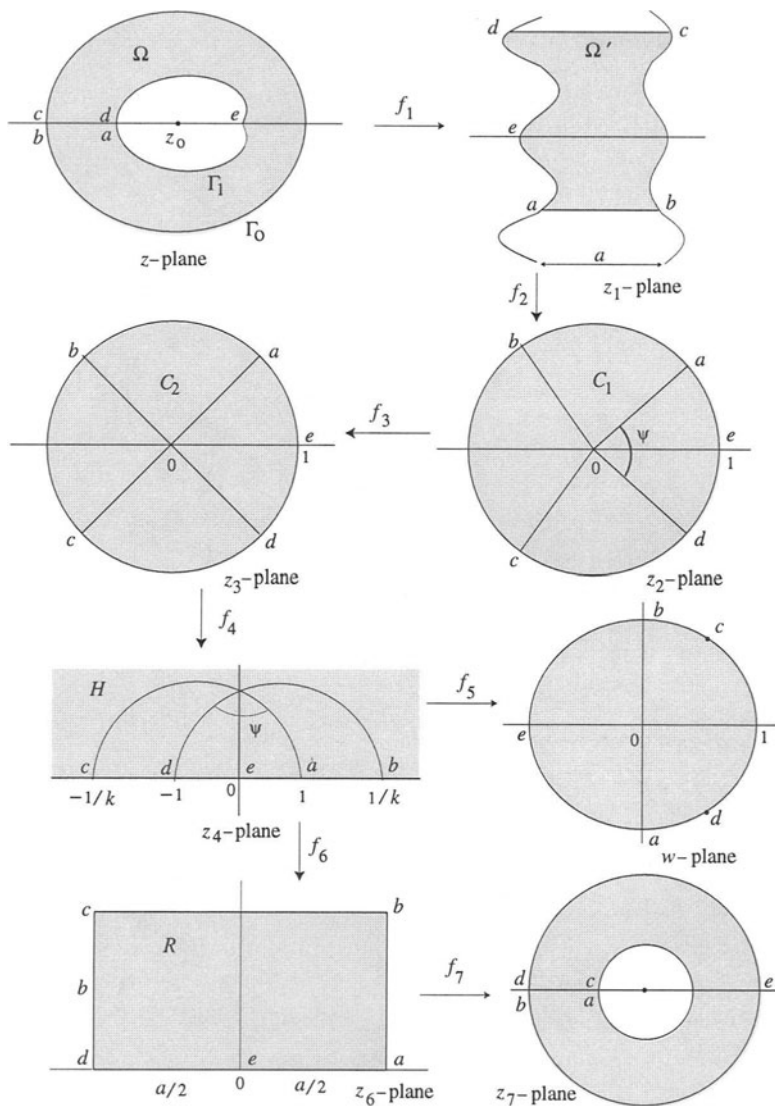


Fig. 11.3.2.

The five points marked as  $a, b, c, d$ , and  $e$  are traced through all of these mappings. The maps  $f_1$  and  $f_2$  are used in Fig. 11.3.1; the map  $f_2$  carries the points  $a$  and  $b$  into the points  $e^{\pm i\alpha}$  and the points  $c$  and  $d$  into the points  $e^{\pm i\beta}$ , respectively, on the unit disk  $C_1$ , which are mapped by  $f_3$  into the end points of

two diameters of the unit disk  $C_2$ , where the angle  $\psi$  between these diameters is given by (11.1.5) and  $k = \frac{\tan(\alpha/2)}{\tan(\beta/2)}$  (see §11.1.1); map  $f_4$  carries the unit disk  $C_2$  into the upper half-plane  $H$ , and finally  $f_5$  maps the upper half-plane  $H$  onto the unit disk in the  $w$ -plane. Note in passing that  $f_6$  maps the upper half-plane  $H$  onto the rectangle  $R$  which is mapped onto an annulus by  $f_7$ . Conversely, by using the maps  $f_7^{-1}$ ,  $f_6^{-1}$ , and  $f_5^l$  in that order, an annulus can be mapped onto the unit disk.

In this example the numerical computations are needed only for the mapping  $f_2 (\Omega' \mapsto C_1)$ ; other mappings are straightforward. The relation between the mapping  $f_2 (\Omega' \mapsto C_1)$  is provided by Gershgorin's integral equation (7.2.6) and the relation between their interior points by the Poisson integral (6.4.6). The mapping  $f_6 (H \mapsto R)$  is defined by the elliptic integral (2.3.13). ■

**CASE STUDY 11.3.2** (Andersen et al., 1962). In the nonsymmetric case the horizontal lines in the  $z$ -plane need not go into straight horizontal lines in the  $w$ -plane, as shown in Fig. 11.3.3. We shall apply the above method of reduction of connectivity (from 2 to 1) to a periodic irregular strip  $\Omega'$  onto a parallel strip  $S$  of width  $\pi/2$ . Then we can use the chain mapping of Case Study 11.3.1 to obtain the conformal mapping of a doubly connected region onto a unit disk or an annulus. This method involves the following steps:

1. Compute Green's function for the parallel strip  $S$ . This Green's function is not the usual Green's function with a logarithmic singularity; besides, it is Green's function with some unspecified period  $iq$ .
2. Use this Green's function to derive the integral equation for the boundary correspondence between the boundaries of the strip  $\Omega'$  and  $S$ .

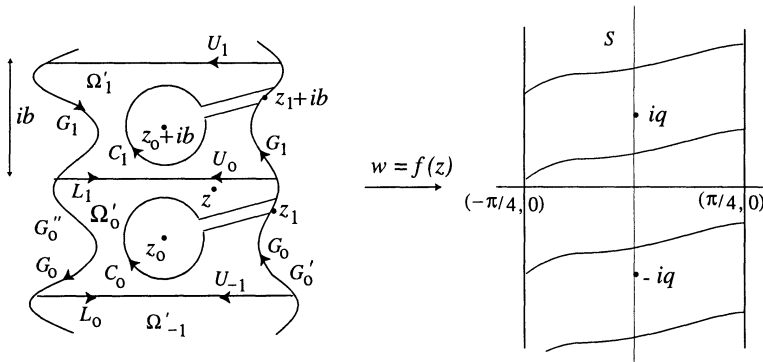


Fig. 11.3.3.

STEP 1. To compute Green's function, note that the function  $w = \tan z$ , where  $z = 0$  goes into  $w = 0$ , maps the parallel strip  $S : \left\{ -\frac{\pi}{4} \leq \Re\{z\} \leq \frac{\pi}{4} \right\}$  onto the unit circle  $|w| \leq 1$ . The usual Green's function for the point  $z = 0$  is  $\mathcal{G}(z, 0) = \log \tan z$ . Then the  $iq$ -periodic Green's function is given by

$$\mathcal{G}(z, q) = \sum_{n=-\infty}^{\infty} \log \tan(z + inq), \quad (11.3.7)$$

where the series is convergent in the Cauchy sense. This periodic Green's function can be represented in terms of elliptic theta functions as

$$\begin{aligned} \mathcal{G}(z, q) &= \log \tan z + \sum_{n=1}^{\infty} \log [\tan(z + inq) \tan(z - inq)] \\ &= \log \tan z - \log \left\{ \prod_{n=1}^{\infty} \tanh(iz - nq) \tanh(iz + nq) \right\} \\ &= \log \left\{ \frac{1}{i} \frac{u - u^{-1}}{u + u^{-1}} \prod_{n=1}^{\infty} \frac{(1 - h^{2n}u^2)(1 - h^{2n}u^{-2})}{(1 + h^{2n}u^2)(1 + h^{2n}u^{-2})} \right\} \\ &= \log \frac{\vartheta_1(z, h)}{\vartheta_2(z, h)}, \end{aligned} \quad (11.3.8)$$

where we have set  $u = e^{iz}$  and  $h = e^{-q}$ , and  $\vartheta_{1,2}$  are elliptic theta functions such that  $\vartheta_1(z + \pi/2, h) = \vartheta_2(z, h)$ . These functions are numerically evaluated by the formulas (Abramowitz and Stegun, 1968)

$$\begin{aligned} \vartheta_1(z, h) &= 2 \sum_{n=1}^{\infty} (-1)^{n-1} h^{(2n-1)^2/4} \sin(2n-1)z, \\ \vartheta_2(z, h) &= 2 \sum_{n=1}^{\infty} h^{(2n-1)^2/4} \cos(2n-1)z, \end{aligned} \quad (11.3.9)$$

where the series are convergent for  $h < 1$ , i.e.,  $q > 0$ . If  $q$  is not too close to unity, the series converge very rapidly, and the computation of  $\vartheta_{1,2}$  is straightforward.

STEP 2. We shall derive Gershgorin's equation for the periodic strip  $\Omega'$  which we assume consists of congruent regions  $\dots, \Omega'_{-1}, \Omega'_0, \Omega'_1, \Omega'_2, \dots$  (Fig. 11.3.3). Let  $C$  denote the contour  $C = L_n \cup U_n \cup \left( \bigcup_{j=-n}^n (C_j \cup G_j) \right)$ ,

where  $G_j$  consists of the boundary curves on both sides of  $\Omega'_j$ ,  $C_j$  is a circle around  $z_0 + jib$  and two lines of the cut connecting this circle and  $z_1 + jib$ ,  $U_j$  is the upper boundary line, and  $L_j$  the lower boundary line of  $\Omega'_j$  (Fig. 11.3.3). The point  $z_0$  corresponds to  $w = 0$ , and  $z_1$  to  $w = \pi/4$ . The variable  $\zeta$  traverses  $C$  in the positive sense. If  $z \in \text{Int}(C)$ , then  $\zeta = z$  is the only simple pole of  $f(z)$ , in which case by Cauchy's formula

$$\mathcal{G}(f(z), q) = \frac{1}{2i\pi} \int_C \frac{\mathcal{G}(f(\zeta), q)}{\zeta - z} d\zeta.$$

Now, let the radii of the circles  $C_j$  tend to zero. Then the above integral along these circles vanishes because  $\mathcal{G}(f(\zeta), q) \approx \log(\zeta - z_0 - jib)$ , and thus

$$\begin{aligned} \mathcal{G}(f(z), q) &= \frac{1}{2i\pi} \int_{C \setminus \{C_j\}} \frac{\mathcal{G}(f(\zeta), q)}{\zeta - z} d\zeta \\ &\quad + \frac{1}{2i\pi} \sum_{j=-n}^n \int_{z_1 + jib}^{z_0 + jib} \frac{\mathcal{G}^+(f(\zeta), q) - \mathcal{G}^-(f(\zeta), q)}{\zeta - z} d\zeta, \end{aligned}$$

where  $\mathcal{G}^+(f(\zeta), q) - \mathcal{G}^-(f(\zeta), q) = 2i\pi$  (for this notation, see §1.4). Therefore,

$$\mathcal{G}(f(z), q) = \frac{1}{2i\pi} \int_{C \setminus \{C_j\}} \frac{\mathcal{G}(f(\zeta), q)}{\zeta - z} d\zeta + \sum_{j=-n}^n \log \frac{z_0 + jib - z}{z_1 + jib - z}.$$

Since  $G_j = G_0 + jib$  and  $\mathcal{G}(f(\zeta + jib), q) = \mathcal{G}(f(\zeta) = iq, q) = \mathcal{G}(f(\zeta), q)$ , we find that

$$\begin{aligned} \mathcal{G}(f(z), q) &= \frac{1}{2i\pi} \int_{U_n \cup L_{-n}} \frac{\mathcal{G}(f(\zeta), q)}{\zeta - z} d\zeta \\ &\quad + \frac{1}{2i\pi} \int_{G_0} \mathcal{G}(f(\zeta), q) \sum_{j=-n}^n \frac{1}{\zeta + jib - z} d\zeta \quad (11.3.10) \\ &\quad + \sum_{j=-n}^n \log \frac{z_0 + jib - z}{z_1 + jib - z} \equiv I_1 + I_2 + I_3. \end{aligned}$$

Let  $n \rightarrow \infty$ . Then  $I_2 \rightarrow 0$ . Using the formula (1.2.15), we have

$$\sum_{j=-n}^n \frac{1}{\zeta + jib - z} = \frac{1}{iL} \sum_{j=-n}^n \frac{1}{\frac{\zeta - z}{iL} + j} \rightarrow \frac{\pi}{iL} \cot \frac{\pi(\zeta - z)}{iL} \quad \text{as } n \rightarrow \infty,$$

and using formula (1.2.14), we find that, as  $n \rightarrow \infty$ ,

$$\prod_{j=-n}^n \frac{z_0 + jib - z}{z_1 + jib - z} = \frac{z_0 - z}{z_1 - z} \prod_{j=1}^n \frac{1 - \left(\frac{z_0 - z}{jib}\right)^2}{1 - \left(\frac{z_1 - z}{jib}\right)^2} \rightarrow \frac{\sin \frac{z_0 - z}{jib}}{\sin \frac{z_1 - z}{jib}}.$$

Hence, as  $n \rightarrow \infty$  in the Cauchy sense, we find from (11.3.1) that

$$\begin{aligned} I_2 + I_3 &= \frac{1}{2i\pi} \int_{G_0} \mathcal{G}(f(\zeta), q) \frac{\pi}{iL} \cot \frac{\pi(\zeta - z)}{iL} d\zeta + \log \frac{\sin \frac{z_0 - z}{jib}}{\sin \frac{z_1 - z}{jib}} \\ &= \mathcal{G}(f(z), q). \end{aligned} \quad (11.3.11)$$

Since  $\mathcal{G}(f(z), q)$  is purely imaginary, let  $\mathcal{G}(f(z), q) = i\Phi(f(z), q)$ , where  $\Phi$  is a real-valued function that defines the boundary correspondence and, by taking the imaginary part of (11.3.11), is defined by

$$\begin{aligned} \Phi(f(z), q) &= \frac{1}{2\pi} \int_{G_0} \Phi(f(\zeta), q) \Im \left\{ \frac{\pi}{iL} \cot \frac{\pi(\zeta - z)}{iL} d\zeta \right\} \\ &\quad + \arg \left\{ \frac{\sin \frac{z_0 - z}{jib}}{\sin \frac{z_1 - z}{jib}} \right\} \equiv J_1 + J_2. \end{aligned} \quad (11.3.12)$$

Now let the point  $z$  approach a point  $z_s$  on the boundary of  $G_0$ . Then

$$J_1 \rightarrow \frac{1}{2\pi} \int_{G_0} \Phi(f(\zeta), q) \Im \left\{ \frac{\pi}{iL} \cot \frac{\pi(\zeta - z)}{iL} d\zeta \right\} + \frac{1}{2} \Phi(f(z_s), q). \quad (11.3.13)$$

Hence, as  $z \rightarrow z_s$ , from (11.3.12) and (11.3.14) we obtain

$$\begin{aligned} \Phi(f(z_s), q) &= \frac{1}{\pi} \int_{G_0} \Phi(f(\zeta), q) \Im \left\{ \frac{\pi}{iL} \cot \frac{\pi(\zeta - z)}{iL} d\zeta \right\} \\ &\quad + 2 \arg \left\{ \frac{\sin \frac{z_0 - z}{jib}}{\sin \frac{z_1 - z}{jib}} \right\}, \end{aligned} \quad (11.3.14)$$

which is Gershgorin's integral equation for the periodic strip  $\Omega'$ .

Eq (11.3.14) can be simplified by taking the parametric equation of the curve  $G_0$  as  $\zeta = \zeta(t)$ , where  $t$  is the arc length on  $G_0$ . Since  $G_0$  has two parts,  $G'_0$  and  $G''_0$ , this parametric equation represents two equations. If we set  $w(t) = f(\zeta(t))$ ,  $z_s = \zeta(s)$ , and  $\Phi(f(\zeta(t)), q) = \phi(t, q)$ , then Eq (11.3.14) becomes

$$\begin{aligned}\phi(s) &= \frac{1}{\pi} \left( \int_{G'_0} + \int_{G''_0} \right) \phi(t, q) \Im \left\{ \frac{\pi}{iL} \cot \frac{\pi(\zeta(t) - \zeta(s))}{iL} \zeta'(t) \right\} d\zeta \\ &+ 2 \arg \left\{ \frac{\sin \frac{z_0 - \zeta(s)}{jib}}{\sin \frac{z_1 - \zeta(s)}{jib}} \right\} = \arg \left\{ \frac{\vartheta_1(w(s), q)}{\vartheta_2(w(s), q)} \right\}. \end{aligned} \quad (11.3.15)$$

Since  $w(s) = \pm \frac{\pi}{4} + i y(s)$  for  $\zeta(s) \in G_0$ , we find from (11.3.9) that

$$\frac{\vartheta_1(w(s), q)}{\vartheta_2(w(s), q)} = \frac{\pm A(y(s)) + i B(y(s))}{A(y(s)) \mp i B(y(s))}, \quad (11.3.16)$$

where the upper and the lower sign is chosen according as  $w(s) = \pm \frac{\pi}{4} + i y(s)$ , and

$$\begin{aligned}A(y) &= \sum_{n=1}^{\infty} \sqrt{2} h^{n(n-1)} \cos \frac{(2n-1)\pi}{4} \cosh(2n-1)y, \\ B(y) &= \sum_{n=1}^{\infty} \sqrt{2} h^{n(n-1)} \sin \frac{(2n-1)\pi}{4} \sinh(2n-1)y = \frac{1}{i} A \left( y + \frac{i\pi}{2} \right).\end{aligned}$$

Hence the simplified form of Eq (11.3.14) is

$$\phi(s, q) = \arg \left\{ \frac{\vartheta_1(w(s), q)}{\vartheta_2(w(s), q)} \right\} = \begin{cases} 2 \arg \{A(y(s)) + i B(y(s))\} & \text{on } G'_0, \\ \pi - 2 \arg \{A(y(s)) + i B(y(s))\} & \text{on } G''_0. \end{cases} \quad (11.3.17)$$

This equation can be numerically computed by an iterative method. ■

## 11.4. Problems

**PROBLEM 11.4.1.** Prove that a doubly connected region  $\Omega$  can be mapped univalently onto an annulus  $A(1, R)$ ,  $R > 1$ , and the mapping is unique if a

point  $z_0$  on the boundary of  $\Omega$  is transformed into a point  $w_0$  on the boundary of  $A(1, R)$ . (Goluzin, 1969, p.208; Wen, 1992, p.97.)

**PROBLEM 11.4.2.** Prove that a necessary and sufficient condition for the existence of a univalent mapping function, which maps the annulus  $A(\rho_1, \rho_2)$  onto the annulus  $A(r_1, r_2)$ , is  $\rho_2/\rho_1 = r_2/r_1$ . (Goluzin, 1969, p.208; Wen, 1992, p.97.)

**PROBLEM 11.4.3.** If a doubly connected region  $\Omega$  contains a doubly connected region  $\Delta$ ,  $\Delta \subset \Omega$ ,  $\Delta \neq \Omega$ , then show that the conformal modulus of  $\Omega$  is greater than that of  $\Delta$ . (Goluzin, 1969, pp.209–210; Wen, 1992, p.133.)

**PROBLEM 11.4.4.** Show that the kernel in Eq (11.3.1) can be evaluated from

$$\begin{aligned}\frac{\partial}{\partial n_s} \left( \log \frac{1}{r_{sz}} \right) &= \frac{\cos(n_s, r_{sz})}{r_{sz}} \\ &= \frac{\xi'(s)[y - \eta(s)] - \eta'(s)[x - \xi(s)]}{[x - \xi(s)]^2 + [y - \eta(s)]^2},\end{aligned}$$

where  $\zeta(s) = \xi(s) + i\eta(s)$ , and  $z = x + iy$ . (See Case Study 7.4.3; also Andersen et al., 1962, p.178.)

**PROBLEM 11.4.5.** Consider coaxial ellipses

$$\Gamma_1 : \frac{x^2}{a_1^2} + \frac{y^2}{b_1^2} = 1, \quad \Gamma_0 : \frac{x^2}{a_2^2} + \frac{y^2}{b_2^2} = 1,$$

which are symmetric about both coordinate axes. Take the distribution  $\alpha = 0$  ( $2\pi/N$ )  $2\pi$  for the partition of the boundaries, and  $N = 4(n - 1)$ . Note that if (i)  $a_1 = 5$ ,  $b_1 = 1$ ,  $a_2 = 7$ ,  $b_2 = 5$ , (ii)  $a_1 = 6$ ,  $b_1 = 2$ ,  $a_2 = 9$ ,  $b_2 = 7$ , or (iii)  $a_1 = 7$ ,  $b_1 = 2$ ,  $a_2 = 9$ ,  $b_2 = 6$ , then the ellipses  $\Gamma_1$  and  $\Gamma_0$  are confocal, i.e.,  $a_1^2 - b_1^2 = a_2^2 - b_2^2$ . In these cases there is an exact mapping function

$$f_\Omega(z) = \frac{z + \sqrt{z^2 - (a_2^2 - b_2^2)}}{a_2 + b_2},$$

with  $\rho = \frac{a_1 + b_1}{a_2 + b_2}$ . By computing  $E$  show that  $E$  decreases as  $N$  increases. (Symm, 1969.)

**PROBLEM 11.4.6.** Show that the curve  $\Gamma_0$  in Case Study 11.4.1 gradually changes from a circle ( $b_2 = 0$ ) to a cardioid for values of  $b_2$  up to 5 and the point where  $\Gamma_0$  crosses the negative  $x$ -axis becomes a singularity in the final case. (Symm, 1969.)

**PROBLEM 11.4.7.** Consider Cassini's ovals

$$\begin{aligned}\Gamma_1 &= \{(x + b_1)^2 + y^2\}[(x - b_1)^2 + y^2] = a_1^4\}, \\ \Gamma_0 &= \{(x + b_2)^2 + y^2\}[(x - b_2)^2 + y^2] = a_2^4\},\end{aligned}$$

(see Fig. 9.2.1), which have symmetry about both coordinates axes. Partition  $\Gamma$  by taking equispaced points on the  $x$ -axis on each boundary with the same number of points on  $\Gamma_1$  and  $\Gamma_0$ , and take  $N = 4(n - 1)$ . Note that if (i)  $a_1 = 2, b_1 = 1, a_2 = \sqrt[4]{2506} \approx 7.07389, b_2 = 7$ , or (ii)  $a_1 = 9, b_1 = 6, a_2 = \sqrt[4]{11116} \approx 10.26803, b_2 = 8$ , then  $\frac{a_1^4 - b_1^4}{a_2^4 - b_2^4} = \frac{b_1^2}{b_2^2}$ , and in this case the exact mapping function is given by

$$f_\Omega(z) = \frac{a_2 z}{\sqrt{a_2^4 - b_2^4 + b_2^2 z^2}},$$

with  $\rho = \frac{a_2 b_1}{a_1 b_2}$ . Show that  $E$  decreases as  $N$  increases. (Symm, 1969.)

**PROBLEM 11.4.8.** Consider a square in a circle, defined by  $\Gamma_1 = \{-b \leq x, y \leq b\}$  and  $\Gamma_0 = \{x^2 + y^2 = a^2\}$ , where  $a > b > 0$ . Because of symmetry about both coordinate axes, partition  $\Gamma_1$  and  $\Gamma_0$  with equi-spaced points in equal number on each boundary, and take  $N = 4(n - 1)$ . Show that  $E$  decreases as  $N$  increases, and that  $E$  decreases rapidly away from  $Z$ . (Symm, 1969.)

**REFERENCES USED:** Abramowitz and Stegun (1968), Andersen et al. (1962), Antonjuk (1958), Gaier (1964), Goluzin (1969), Jawson (1963), Kantorovich and Krylov (1958), Muslhelishvili (1963), Nehari (1952), Symm (1969), Wen (1992).

# Chapter 12

---

## Singularities

---

As Radon (1919) and Carleman (1922) have shown, the method of integral equations can also be used to solve the problem of potential theory when the boundary  $\Gamma$  of a simply connected region  $D$  contains corners. In such cases Carleman separates the kernel into two parts, one of which corresponds to the corner singularities, whereas Radon uses the Stieltjes integral equations to solve this problem. We shall derive the analogues of Gershgorin's integral equation and then obtain Arbenz's integral equation which uses Radon's method to determine conformal maps for boundaries with corners and has a unique solution. The cases of interior and exterior mapping functions  $f(z)$  and  $f_E(z)$  are related to each other through inversion by the relations (7.3.12). We are interested in the behavior of these univalent maps and those of doubly connected regions at singularities on and near the boundary, which are corner-type or pole-type. The nature and location of such singularities are determined.

---

### 12.1. Arbenz's Integral Equation

Let us assume that the boundary  $\Gamma$  of a simply connected region  $D$  consists of two Jordan curves  $\Gamma_1$  and  $\Gamma_2$  ( $\Gamma_1 \cup \Gamma_2 = \Gamma$ ), and suppose that  $\Gamma_1$  and  $\Gamma_2$  meet at a point  $z_0 = \gamma(s_0)$  and form a corner with interior angle  $\alpha\pi$ ,  $0 < \alpha < 2$ . Suppose that  $z_0$  is a regular point of both curves. Let  $f(z) \in \mathcal{K}^0(D)$  denote the function that maps  $D$  univalently onto the unit disk such that  $f(0) = 0$ . Let the parametric equation of the boundary  $\Gamma$  be  $z = \gamma(s)$ ,  $0 \leq s \leq L$ , which is

positively oriented with respect to the region  $D$ . Then  $f(\gamma(s)) = e^{i\phi(s)}$  and  $f_E(\gamma(s)) = e^{i\phi_E(s)}$ , where the boundary correspondence functions  $\phi(s) = \arg \{f(\gamma(s))\}$  and  $\phi_E(s) = \arg \{f_E(\gamma(s))\}$  are continuous principal arguments which play a significant role in integral equation methods. Let the function  $\theta(s) = \arg \{\gamma(s)\}$  be defined for  $0 \leq s \leq L$ , such that it has at most finitely many jump discontinuities of magnitude less than  $\pi$  in the interval  $[0, L]$ . This yields finitely many subintervals of  $[0, L]$ , in each of which  $\theta(s)$  is continuous and has bounded variations. Thus, at a corner point on  $\Gamma$  we have  $|\theta(s^+) - \theta(s^-)| < \pi$ , and the boundary  $\Gamma$  is called a contour with bounded variation. The following result is due to Radon (1919).

**THEOREM 10.1.1.** *If  $\Gamma$  is a contour with bounded variation, then  $\theta_s(t) = \arg \{\gamma(s) - \gamma(t)\}$ , defined in (7.1.1), is of bounded variation for every fixed  $s \in [0, L]$  and is uniformly bounded for all  $s \in [0, L]$ .*

The Stieltjes integral equations that arise in Radon's method have the form  $\int_0^L \phi(t) d_t \theta_s(t) = g(s)$ , where  $\phi(t)$  is continuous in  $[0, L]$ , and the subscript  $t$  denotes the variable of the Stieltjes integration. In fact,

$$\begin{aligned} \lim_{\varepsilon \rightarrow 0} \int_{\tau-\varepsilon}^{\tau+\varepsilon} \phi(t) d_t \theta_s(t) &= \phi(\tau) [\theta_s(\tau^+) - \theta_s(\tau^-)] \\ &= \begin{cases} 0, & \text{if } \tau \neq s, \\ \alpha\pi \phi(s), & \text{if } \tau = s, \end{cases} \end{aligned} \quad (12.1.1)$$

where  $\alpha\pi = \alpha(s)\pi$ ,  $s \in [0, L]$ , denotes the interior angle at the corner point  $\gamma(s)$  on the boundary  $\Gamma$ .

To derive the Stieltjes integral equation associated with Gershgorin's integral equation (7.2.6), let  $z = \gamma(s)$  be a corner point on  $\Gamma$ . Then, in view of (1.2.10), the left side of Eq (7.2.2) becomes  $\alpha \log f(z)$ , and then instead of Eq (7.2.6) we obtain

$$\alpha \phi(s) = \frac{1}{\pi} \int_0^L \phi(t) d_t \theta_s(t) - 2\beta(s), \quad (12.1.2)$$

where the integral takes the Cauchy p.v. at  $t = s$ . Since, by (12.1.1),

$$\begin{aligned}\int_0^L \phi(t) d_t \theta_s(t) &= \frac{1}{\pi} \lim_{\varepsilon \rightarrow 0} \left( \int_0^{s-\varepsilon} + \int_{s-\varepsilon}^{s+\varepsilon} + \int_{s+\varepsilon}^L \right) \phi(t) d_t \theta_s(t) \\ &= \int_0^L \phi(t) d_t \theta_s(t) + \alpha \pi \phi(s),\end{aligned}$$

from (12.1.2) we find that

$$\frac{1}{\pi} \int_0^L \phi(t) d_t \theta_s(t) = 2 \beta(s), \quad s \neq 0. \quad (12.1.3)$$

Since  $\int_0^L d_t \theta_s(t) = 0$ , the solution of Eq (12.1.3) is determined up to an additive constant, and hence, it is not unique. This situation is avoided in Arbenz's integral equation which can be derived from (12.1.3) as follows: For  $s \neq 0$  set

$$\begin{aligned}\hat{\theta}_s(t) &= \begin{cases} \theta_s(t), & t < s, \\ \theta_s(s^-), & t = s, \\ \theta_t(s), & t > s, \end{cases} \\ &= \theta_s(t) + \begin{cases} 0, & t < s, \\ \pi, & t > s. \end{cases}\end{aligned} \quad (12.1.4)$$

Also,  $\theta_s(t) = \hat{\theta}_s(t) - \theta_0(t)$ , where

$$\theta_0(t) = \begin{cases} \theta_0(0^+) & \text{for } t = 0, \\ \theta_0(L) = \theta_0(L^-) & \text{for } t = L. \end{cases} \quad (12.1.5)$$

The angle  $\theta_s(t)$  is shown in Fig. 12.1.1. Then for  $s \neq 0$  we find from (12.1.3) that

$$\begin{aligned}\frac{1}{\pi} \int_0^L \phi(t) d_t \theta_s(t) &= \frac{1}{\pi} \int_0^L \phi(t) d_t \theta_s(t) + \phi(s) - \frac{1}{\pi} \int_0^L \phi(t) d_t \theta_0(t) \\ &= 2 \beta(s) + \phi(s) - \frac{1}{\pi} \int_0^L \phi(t) d_t \theta_0(t).\end{aligned} \quad (12.1.6)$$

To determine the integral in (12.1.6), let  $s \rightarrow 0^+$  in (12.1.3), and use Hally's theorem which states that  $\lim_{s \rightarrow 0^+} \theta_s(0) = \theta_0(0) + \pi$ . Then the limit value of this integral is given by

$$\frac{1}{\pi} \int_0^L \phi(t) d_t \theta_0(t) = \phi(0^+) + 2 \beta(0^+),$$

which yields

$$\frac{1}{\pi} \int_0^L \phi(t) d_t \theta_s(t) = 2\beta(s) + \phi(s) - [\phi(0^+) + 2\beta(0^+)].$$

If we require that the boundary correspondence function be  $\phi(0^+) = -2\beta(0^+)$ , then  $\phi(s)$  is uniquely determined from the integral equation

$$\frac{1}{\pi} \int_0^L \phi(t) d_t \theta_s(t) = \phi(s) + 2\beta(s), \quad s \neq 0, \quad (12.1.7)$$

which is known as Arbenz's integral equation. Note that the integral in (12.1.7) is not evaluated as a Cauchy p.v. as in (12.1.3).

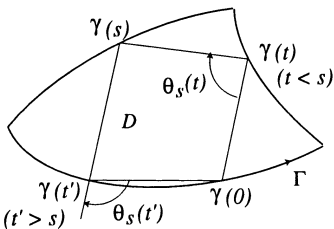


Fig. 12.1.1.

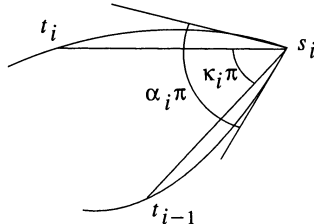


Fig. 12.1.2.

The discretization method should be used when the boundary  $\Gamma$  is represented geometrically rather than analytically. In order to discretize Arbenz's equation (12.1.7), we partition the interval  $[0, L]$  into  $N$  subintervals  $[t_{k-1}, t_k]$  of equal or unequal length with  $s_k$  as an interior point,  $t_{k-1} < s_k < t_k$ ,  $k = 1, 2, \dots, N$ . In practice, it is useful to take a corner point coincident with a partition point and have more subintervals in its neighborhood. Then for  $s = s_i$  Eq (12.1.7) becomes

$$\frac{1}{\pi} \sum_{k \neq i} \int_{t_{k-1}}^{t_k} [\phi(t) - \theta(t)] d_t \theta_{s_i}(t) = \phi(s_i) + 2\beta(s_i). \quad (12.1.8)$$

The solution  $\phi(s)$  is continuous and can be taken as

$$\phi_i = \phi(s_i) = \sum_{k=1}^N a_{ik} \phi_k, \quad (12.1.9)$$

where

$$a_{ik} = \frac{1}{\pi} \int_{t_{k-1}}^{t_k} d_t \theta_{s_i}(t). \quad (12.1.10)$$

For  $i = k$  the integral in (12.1.10) takes the principal value of Stieltjes integration. In fact, if  $s_i$  is a corner point, then the arcs at  $s_i$  subtend the interior angle  $\alpha_i\pi$ . Let  $\kappa_i\pi$  denote the angle between the chords  $(s_i, t_{i-1})$  and  $(s_i, t_i)$  (Fig. 12.1.2). Then

$$\begin{aligned} a_{ik} &= \frac{1}{\pi} \theta_{s_i}(t_{k-1}, t_k), \quad i \neq k, \\ a_{ii} &= \alpha_i \left(1 - \frac{\kappa_i}{\alpha_i}\right), \end{aligned} \quad (12.1.11)$$

and

$$\sum_{k=1}^N a_{ik} = \frac{1}{\pi} \int_0^L d_t \theta_{s_i}(t) = \alpha_i, \quad (12.1.12)$$

where the integral takes the p.v. of Stieltjes integration.

**CASE STUDY 12.1.1** (Gaier, 1964, p.57). For the mapping of the square  $\{-1 < x, y < 1\}$  onto the unit disk  $|w| < 1$ , we have discretized the boundary of the square with  $N = 40$  subintervals, where  $t = 0$  and  $t = L$  at the point  $t_0$ , although in Fig. 12.1.3 only quarter regions of each boundary are presented because of the symmetry of the square with respect to the  $x$  and  $y$  axes and the symmetry of  $\phi(s)$ , i.e.,  $\phi_{20+j} = \pi + \phi_j$  and  $\phi_{10+j} = \pi/2 + \phi_j$ .

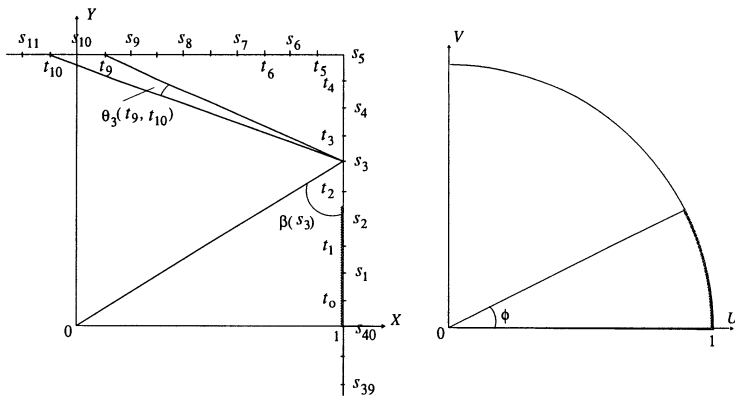


Fig. 12.1.3.

Then

$$\frac{1}{\pi} \sum_{k=1}^{40} [\arg \{\gamma(t_k) - \gamma(s_i)\} - \arg \{\gamma(t_{k-1}) - \gamma(s_i)\}] \phi_k = 2\beta(s_i). \quad (12.1.13)$$

Thus,

$$\frac{1}{\pi} \sum_{k=1}^{40} \theta_i(t_{k-1}, t_k) \phi_k = 2\beta(s_i). \quad (12.1.14)$$

The coefficient for  $\phi_k$  is 0.5 for  $k = i$  when  $i = 5, 15, 25, 35$ , and is equal to 1 otherwise. The following results, obtained after computing Eqs (12.1.3) and (12.1.6), are compared with the exact solutions in the following table:

| $i$ | Eq (12.1.3) | Eq (12.1.6) | Exact    |
|-----|-------------|-------------|----------|
| 1   | 0.256503    | 0.256738    | 0.256319 |
| 2   | 0.480278    | 0.481440    | 0.479890 |
| 3   | 0.648856    | 0.654261    | 0.648240 |
| 4   | 0.751901    | 0.789932    | 0.751028 |
| 5   | 0.785394    | 0.785406    | 0.785398 |
| 6   | 0.818887    | 0.780878    | 0.819768 |
| 7   | 0.921933    | 0.916549    | 0.922556 |
| 8   | 1.090511    | 1.089369    | 1.090906 |
| 9   | 1.314286    | 1.314071    | 1.314477 |

The exact boundary correspondence function is given by

$$\cos \phi = \operatorname{dn}(K y), \quad K = K \left( \frac{1}{\sqrt{2}} \right), \quad (12.1.15)$$

where  $\operatorname{dn}$  is one of the twelve Jacobian elliptic functions which is a meromorphic function with pole at  $i K'(m)$ ,  $K(m) = K'(1 - m)$ , and  $\operatorname{dn}^2 u = 1 - \operatorname{sn}^2 u$  (see Case Study 3.3.2). The inverse mapping is given by

$$z = A \sum_{n=0}^{\infty} \frac{\binom{1/2}{n}}{4n-1} w^{-4n+1}, \quad (12.1.16)$$

where  $A$  is a constant (cf. with Case Study 4.2.2 and 4.5.1, and for the Green's Function and the associated mapping function, see Case Study 12.5.1). ■

## 12.2. Boundary Corner

Symm's integral equations (9.1.6) and (9.1.12)–(9.1.13) for determining the density function  $\mu(s)$  can be written as

$$\int_0^L \mu(s) \log |\gamma(t) - \gamma(s)| ds = k(t), \quad t \neq s, \quad (12.2.1)$$

where

$$k(t) = \begin{cases} -\log |\gamma(t)| & \text{for } z = \gamma(s) \in D = \text{Int}(\Gamma), \\ 1 & \text{for } z = \gamma(s) \in D^* = \text{Ext}(\Gamma). \end{cases} \quad (12.2.2)$$

This equation has a unique solution provided that the capacity  $\text{cap}(\Gamma) \neq 1$  (see §1.3, 1.4). The density function  $\mu(s)$  is related to the boundary correspondence function  $\phi(s)$  by

$$\phi'(s) = \begin{cases} -2\pi\mu(s) & \text{for } z \in \text{Int}(\Gamma), \\ 2\pi\hat{\gamma}\mu(s) & \text{for } z \in \text{Ext}(\Gamma), \end{cases} \quad (12.2.3)$$

where  $\hat{\gamma}$  is Robin's constant ( $\hat{\gamma} = -\log \{\text{cap}(\Gamma)\}$ , see §1.3).

If  $z_0$  is a corner point on a portion of the boundary  $\Gamma$  with interior angle  $\alpha\pi$ , where  $\alpha = p/q$  ( $p$  and  $q$  are relatively prime), then we should analyze the asymptotic behavior of the mapping function in the neighborhood of the point  $z_0 \in \Gamma$ . If  $D$  is a polygonal region, we know from the Schwarz–Christoffel transformation that in the neighborhood of  $z_0$

$$f(z) - f(z_0) = \sum_{k=1}^{\infty} a_k (z - z_0)^{k/\alpha}, \quad (12.2.4)$$

or, if  $f \in \mathcal{K}^0(D)$  (i.e.,  $f(0) = 0$ ), then

$$f(z) = \sum_{k=1}^{\infty} a_k \left[ (z - z_0)^{k/\alpha} - (-z_0)^{k/\alpha} \right], \quad a_1 \neq 0, \quad (12.2.5)$$

(see Copson, 1975, p.170). Thus, if  $1/\alpha$  is not an integer, then  $f(z)$  has a branch point singularity at  $z_0$  (see §2.1). This corresponds to Case 3 in Theorem 12.2.1 given below. Lichtenstein (1911) was the first to show that if a corner point is located at the origin, then  $\frac{df(z)}{dz} = z^{1/\alpha-1} h(z)$ , where  $h(z)$  is a continuous function such that  $h(0) \neq 0$ , and  $\alpha$  is irrational. Warschawski (1932, 1955) proved this result for all  $\alpha$ . In the case when the two arcs at  $z_0$  are straight line segments with  $\alpha = 1$ , Lewy (1950) proved the stronger result that  $f(z)$  has an asymptotic expansion in powers of  $z$  and  $\log z$ . This result was generalized by Lehman (1957) in the development of the mapping function at an analytic corner as  $z \rightarrow z_0$ , as follows:

**THEOREM 12.2.1.** *Let  $z_0 \in \Gamma$  denote a corner point. Then there are three cases of asymptotic expansions for the mapping function  $f(z)$  as  $z \rightarrow z_0$ :*

**CASE 1.** *If  $\alpha$  is rational,  $\alpha = p/q$  where  $p$  and  $q$  are relatively prime, then as  $z \rightarrow z_0$*

$$f(z) = f(z_0) + \sum_{k,l,m} B_{k,l,m} (z - z_0)^{k+l/\alpha} (\log(z - z_0))^m, \quad B_{0,1,0} \neq 0, \quad (12.2.6)$$

where  $k, l$  and  $m$  are integers,  $k \geq 0$ ,  $1 \leq l \leq p$  and  $0 \leq m \leq k/q$ . The terms in (12.2.6) are ordered such that the term containing  $B_{k',l',m'}$  always follows the term containing  $B_{k,l,m}$  if  $k' + l'/\alpha \geq k + l/\alpha$  and  $m' < m$ .

**CASE 2.** *If  $\alpha$  is irrational, then as  $z \rightarrow z_0$*

$$f(z) = f(z_0) + \sum_{k,l} B_{k,l} (z - z_0)^{k+l/\alpha}, \quad B_{0,1} \neq 0, \quad (12.2.7)$$

where  $k$  and  $l$  are integers,  $k \geq 0$  and  $l \geq 1$ .

**CASE 3.** *In the case when the two boundary arcs at  $z_0$  are straight line segments, then the asymptotic expansions (12.2.6) and (12.2.7) simplify to*

$$f(z) = f(z_0) + \sum_{l=1}^{\infty} B_l (z - z_0)^{l/\alpha}, \quad B_1 \neq 0. \quad (12.2.8)$$

Cases 1 and 2 correspond to the situation when  $D$  is not a polygonal region, whereas Case 3 applies when  $D$  is a polygonal region. In this case, to eliminate the effect of a branch point singularity at  $z_0$ , if such a singularity exists, we augment the basis  $\{\phi_j(z)\}_{j=1}^n$  by the functions (Papamichael and Kokkinos, 1981)

$$\phi(z) = \frac{d}{dz} \left\{ (z - z_0)^{k/\alpha} - (-z_0)^{k/\alpha} \right\} - d = \frac{k}{\alpha} (z - z_0)^{k/\alpha-1} - d, \quad (12.2.9)$$

where

$$d = \begin{cases} \frac{k}{\alpha} (-z_0)^{k/\alpha-1} & \text{for RM,} \\ 0 & \text{for BKM.} \end{cases}$$

Note that  $(z - z_0)^{1/\alpha}$  is the dominant term in each of the asymptotic expansions (12.2.6)–(12.2.8). It appears that the mapping  $z \mapsto z^{1/\alpha}$  that transforms an

angle  $\alpha\pi$  at  $z_0 \in \Gamma$  into the angle  $\pi$  at the point  $w_0 = f(z_0)$  (see §2.1) will solve the corner problem. But this does not happen because if  $1/\alpha$  is not an integer, a branch singularity always occurs at the corner  $z_0$ , and when  $\alpha$  is an integer, the existence of the logarithm in (12.2.6) makes the corner  $z_0$  a logarithmic branch point singularity even if  $1/\alpha$  is an integer.

In the RM and BKM (§4.2) the minimum polynomial is constructed by taking the basis set as that of monomials  $z^j$ ,  $j = 0, 1, 2, \dots$ . Then the singular basis function  $\phi(z)$  associated with the corner singularity at  $z_0 \in \Gamma$  in the above three cases of asymptotic expansions (12.2.6)–(12.2.8) has the form

$$\phi(z) = \begin{cases} \frac{d}{dz} \left\{ (z - z_0)^{k+l/\alpha} (\log(z - z_0))^m \right\} & \text{in Case 1,} \\ \frac{d}{dz} \left\{ (z - z_0)^{k+l/\alpha} \right\} & \text{in Case 2,} \\ \frac{d}{dz} \left\{ (z - z_0)^{l/\alpha} \right\} & \text{in Case 3,} \end{cases} \quad (12.2.10)$$

which is used to augment the basis set in RM and BKM when determining the mapping function  $f(z)$  from (4.2.25). It may be noted that the function  $f(z)$ , originally defined on  $D$ , can be extended by analytic continuation through a portion of its boundary into  $\text{Ext}(\Gamma)$ . This procedure is used in §12.4 to investigate the nature and location of poles and pole-type singularities of  $f(z)$  near the boundary  $\Gamma$ . The singularities of the Bergman kernel  $K(z, a)$  in the region  $\text{Ext}(\Gamma)$  also affect the convergence of the polynomial series (4.2.20). These singularities are either poles of  $K(z, a)$  that lie close to the boundary  $\Gamma$  or branch point singularities of the boundary itself. Their effect should always be taken into account when determining the mapping function for the exterior regions (see §12.5).

### 12.3. Singularity Behavior

In the neighborhood of a corner point  $z_0 = \gamma(s_0)$  let the function  $\gamma(s)$  have a Taylor series representation

$$\gamma(s) = \gamma(s_0) + \begin{cases} \sum_{n=1}^{\infty} \frac{(s - s_0)^n}{n!} \gamma^{(n)}(s_0^-), & s < s_0, \\ \sum_{n=1}^{\infty} \frac{(s - s_0)^n}{n!} \gamma^{(n)}(s_0^+), & s > s_0, \end{cases} \quad (12.3.1)$$

where  $\gamma^{(n)}(s_0^\pm) = \lim_{s \rightarrow s_0^\pm} \left\{ \frac{d^n \gamma(s)}{ds^n} \right\}$ . The boundary correspondence function  $\phi(s)$  associated with the mapping function  $f$  is given by

$$\phi'(s) = i \frac{f'(\gamma(s)) \overline{f(\gamma(s))}}{|f(\gamma(s))|^2}. \quad (12.3.2)$$

Then, by (12.2.3), the density function  $\mu(s)$  is related to  $f$  by

$$\mu(s) = -\frac{\Im \left\{ f'(\gamma(s)) \overline{f(\gamma(s))} \right\}}{2\pi \hat{\gamma}}, \quad (12.3.3)$$

where  $|f(\gamma(s))| = 1$ . Note that for the mapping function  $f_E$  this relation is, in view of (12.2.3), given by

$$\mu(s) = -\frac{\Im \left\{ f'_E(\gamma(s)) \overline{f_E(\gamma(s))} \right\}}{2\pi \hat{\gamma}}. \quad (12.3.4)$$

Hence, using (12.2.6)–(12.2.8), (12.3.1), and (12.3.3), a formal asymptotic expansion for  $\mu(s)$  as  $s \rightarrow s_0$  is given by

$$\mu(s) = \begin{cases} \sum_{j=1}^{\infty} a_j^- \psi_j(s - s_0), & s < s_0, \\ \sum_{j=1}^{\infty} a_j^+ \psi_j(s - s_0), & s > s_0, \end{cases} \quad (12.3.5)$$

where the functions  $\psi_j$  depend on the value of  $\alpha$ ,  $0 < \alpha < 2$  (see Problem 12.7.1). Then from (12.3.5) we conclude the following:

- (a) If  $1 < \alpha < 2$ , i.e., if the corner  $z_0$  is re-entrant, then  $\mu(s)$  becomes unbounded at  $s = s_0$ .
- (b) If  $\frac{1}{1+q} < \alpha < 1$ , where  $q \geq 1$  is an integer, then  $\mu(s)$  becomes unbounded at  $s = s_0$ .
- (c) If  $\alpha = \frac{1}{q}$ , where  $q \geq 1$  is an integer, then (12.3.5) does not involve rational powers of  $(s - s_0)$ . Since  $a_1^- \neq a_1^+$ , the function  $\mu^{(q-1)}(s)$  has a jump discontinuity at  $s = s_0$ . Moreover, for some  $j > 1$ , one of the functions  $\psi_j$  in (12.3.5), obtained from the expansion (12.2.6), is a function of the form  $\sigma^{2q-1} \log \sigma$ , where  $\sigma$  stands for  $(s - s_0)$  or  $(s_0 - s)$ . Thus, in general, the left and right  $(2q-1)$ -th derivatives of  $\mu(s)$  at  $s = s_0$  become unbounded.

- (d) In Case 3 of Theorem 12.2.1, without loss of generality, we take  $\gamma(s)$  in the form

$$\gamma(s) = \gamma(s_0) + \begin{cases} (s_0 - s) e^{i\alpha\pi}, & s \leq s_0, \\ s - s_0, & s \geq s_0. \end{cases} \quad (12.3.6)$$

Then,  $\psi_j(\sigma) = \sigma^{-1+j/\alpha}$  for  $j = 1, 2, \dots$ , and  $a_j^+ = (-1)^{j+1} a_j^-$  for  $j = 1, 2, \dots$ . In this case conclusions (a) and (b) remain the same, but (c) changes, viz., if  $\alpha = 1/q$  ( $q \geq 1$  an integer), then

- (d.1) if  $q$  is odd, then  $\mu(s)$  has no singularity at  $s = s_0$ ; and
  - (d.2) if  $q$  is even, then  $\mu^{(q-1)}(s)$ , in general, has a jump discontinuity at  $s = s_0$ .
- 

## 12.4. Pole-Type Singularities

Sometimes the function  $f$  (or  $f_E$ ) has poles or pole-type singularities adjacent to the boundary  $\Gamma$ , which are located in the region  $D^*$  (or  $D$ ). We shall examine the nature and location of such singularities. This analysis, based on the work of Papamichael et al (1986), will be confined to the function  $f$ . Thus, we shall determine the nature and location of poles and pole-type singularities of  $f$  in  $D^*$ , which are obtained by considering an analytic continuation of  $f$  across the boundary  $\Gamma$  into  $D^*$ . The procedure expands the domain of  $f$  as much as possible provided the function  $f$  on the extended domain agrees with the original.

To determine the dominant poles of the mapping function  $w = f(z)$  in  $\text{Ext}(\Gamma)$ , which are actually the poles of the analytic continuation of  $f$  across  $\Gamma$  into  $\text{Ext}(\Gamma)$  that lie close to  $\Gamma$ , we can use the Schwarz reflection principle in the case when the boundary  $\Gamma$  consists of straight line segments and circular arcs. Then  $f$  has simple poles at the (finite) symmetric points of the origin with respect to the straight line segments and the circular arcs (see §1.4). But when the boundary  $\Gamma$  is more analytic than straight line segments and circular arcs, then in many cases the dominant poles of  $f$  can be determined by using a generalized symmetry principle as follows: Let the parametric equation of an analytic arc  $\hat{\Gamma}$  of  $\Gamma$  be given by

$$z = \gamma(s), \quad s_1 < s < s_2. \quad (12.4.1)$$

Let  $G^*$  be a simply connected region in the complex  $\zeta$ -plane,  $\zeta = s + i t$ , that satisfies the following two conditions:

C1. The function  $z = \gamma(s)$  is univalent in  $G^*$ .

C2. The straight line  $L = \{\zeta : \zeta = s + it, s_1 < s < s_2, t = 0\}$  divides the region  $G^*$  into two partitions  $G_1$  and  $G_2$  which are symmetric to each other with respect to  $L$  and  $G^* = G_1 \cup L \cup G_2$ , and the image  $D_1$  of  $G_1$  under the transformation (12.4.1) is contained in  $D$  ( $D_1 \subseteq D$ ).

Obviously,  $G_1$  and  $G_2$ , each subsets of  $G^*$ , are defined by

$$\begin{aligned} G_1 &= \{\zeta : \zeta \in G^* \text{ and } t > 0\}, & G_1 &= \{\zeta : \zeta \in G^* \text{ and } t < 0\}, \\ G_2 &= \{\zeta : \zeta \in G^* \text{ and } t < 0\}, & \text{or} & & G_2 &= \{\zeta : \zeta \in G^* \text{ and } t > 0\}. \end{aligned}$$

Under conditions (i) and (ii) above the function (12.4.1) maps the region  $G^*$  conformally onto a region  $D^* = D_1 \cup \hat{\Gamma} \cup D_2$  such that the regions  $G_1$ ,  $G_2$  and the straight line  $L$  are mapped onto the regions  $D_1$ ,  $D_2$  and the arc  $\hat{\Gamma}$ , respectively. Then the function

$$h(\zeta) = f(\gamma(\zeta)), \quad (12.4.2)$$

where  $f(z)$  maps the region  $D$  onto the disk  $|w| < R$ , is univalent in the region  $G_1 \cup L$ , and  $w = h(\zeta)$  maps the straight line  $L$  onto an arc of the circle  $|w| = R$ . Thus, by the reflection principle the function

$$H(\zeta) = \begin{cases} h(\zeta), & \zeta \in G_1 \cup L, \\ \frac{1}{\overline{h(\zeta)}}, & \zeta \in G_2, \end{cases} \quad (12.4.3)$$

is meromorphic in  $G_2$  and defines an analytic continuation of  $h$  across  $L$  into  $G_2$ . If  $\eta$  denotes the inverse of  $\gamma$ , then the function

$$F(z) = H(\eta(z)) = \begin{cases} f(z), & z \in D_1 \cup \hat{\Gamma}, \\ \frac{1}{\overline{f(\beta(z))}}, & z \in D_2, \end{cases} \quad (12.4.4)$$

where  $\beta(z) = \gamma(\overline{\eta(z)})$  is analytic in  $D_1$  and meromorphic in  $D_2$ , defines an analytic continuation of  $f$  across  $\hat{\Gamma}$  into  $D_2$ , where the points  $z$  and  $\beta(z)$  are symmetric points with respect to the arc  $\hat{\Gamma}$ . Hence, we have the following result (Papamichael and Kokkinos, 1983):

**THEOREM 12.4.1.** *The following cases hold:*

(a) *If  $0 \in D_1$ , then  $\gamma(z)$  has exactly one zero in  $G_1$ , i.e., the function*

$F(z)$  has a simple pole at a point  $z_0 \in D_2$ , where  $z_0 = \gamma(\bar{\zeta}_0) = a(0)$  is the inverse point of the origin with respect to the arc  $\hat{\Gamma}$ .

(b) If  $0 \in \partial D_1 \setminus \hat{\Gamma}$ , then  $\gamma(z)$  has at least one zero  $\zeta_0 \in \partial G_1 \setminus L$ , and the function  $\gamma(z)$  need not be one-to-one in the neighborhood of the points  $\zeta_0$  and  $\bar{\zeta}_0$ .

(c) If  $0 \in D_1 \cup (\partial D_1 \setminus \hat{\Gamma})$ , then  $F$  has no poles in the region  $D_2 \cup (\partial D_2 \setminus \hat{\Gamma})$ .

To determine the behavior of  $F(z)$  at the point  $z_0 = \gamma(\zeta_0) \in \partial D_2 \setminus \hat{\Gamma}$  in part (b) of the above theorem, let us assume that  $\gamma$  is analytic at  $\zeta_0$  and  $\bar{\zeta}_0$ . Then

$$\gamma(\zeta) = (\zeta - \zeta_0)^m \gamma_1(\zeta), \quad (12.4.5)$$

and

$$\gamma(\zeta) - \gamma(\bar{\zeta}_0) = (\zeta - \zeta_0)^n \gamma_2(\zeta), \quad (12.4.6)$$

where  $\gamma_1$  and  $\gamma_2$  are analytic and nonzero at the points  $\zeta_0$  and  $\bar{\zeta}_0$ , respectively. Then the mapping function is  $f(z) = z f_1(z)$ ,  $f_1(0) \neq 0$ . Hence, from (12.4.4), for  $z \in D_2$  the function  $G(z) = \frac{1}{F(z)}$  can be written as

$$G(z) = \overline{\beta(z)} g_1(z), \quad g_1(z_0) \neq 0, \quad (12.4.7)$$

where  $g_1$  is analytic at  $z_0$ . Since

$$\overline{\beta(z)} = (\eta(z) - \eta(z_0))^m a_1(z), \quad a_1(z_0) \neq 0, \quad (12.4.8)$$

we find that

$$\eta(z) - \eta(z_0) = (z - z_0)^{1/n} \eta_1(z), \quad \eta_1(z_0) \neq 0, \quad (12.4.9)$$

where  $a_1$  and  $\eta_1$  are analytic at  $z_0$ . Hence, from (12.4.8) and (12.4.9) we get

$$\overline{\beta(z)} = (z - z_0)^{m/n} (\eta_1(z))^m a_1(z),$$

and thus, from (12.4.7)

$$G(z) = (z - z_0)^{m/n} g_2(z), \quad g_2(z_0) \neq 0, \quad (12.4.10)$$

where  $g_2$  is analytic at  $z_0$ . This leads to the following:

**THEOREM 12.4.2.** *The following cases hold:*

- (b.1) *If  $m = n = 1$ , then  $F$  has a simple pole at  $z_0$ .*
- (b.2) *If  $m = 2, n = 1$ , then  $F$  has a double pole at  $z_0$ .*
- (b.3) *If  $m = 1, n = 2$ , then  $F$  has a branch singularity of the form  $(z - z_0)^{-1/2}$  at the point  $z_0$ .*

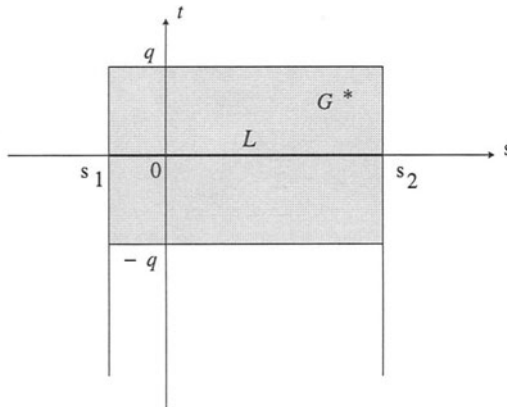


Fig. 12.4.1.

**CASE STUDY 12.4.1.** Let the arc  $\hat{\Gamma}$  be defined by the ellipse  $E$  :  $\frac{(x - x_c)^2}{a^2} + \frac{(y - y_c)^2}{b^2} = 1$ ,  $a > b$ , and let the parametric equation of  $\hat{\Gamma}$  be  $z = \gamma(s) = z_c + a e \cos(s - i q)$ ,  $0 \leq s_1 < s < s_2 < 2\pi$ , where  $z_c = x_c + i y_c$  is the center  $C$ ,  $e = \sqrt{1 - b^2/a^2}$  the eccentricity of the ellipse,  $\cosh q = 1/e$ , and  $s_2 - s_1 < 2\pi$ . Then the function  $z = \gamma(\zeta)$ ,  $\zeta = s + i t$ , is univalent in the strip  $\{\zeta : \zeta + s + i t, s_1 < s < s_2, -\infty < t < q\}$ , and the region  $G^*$  is a symmetric subregion of the rectangle  $\{\zeta : \zeta + s + i t, s_1 < s < s_2, -q < t < q\}$  (see Fig. 12.4.1). Consider the case when  $G^*$  is the entire rectangle. Then the region  $D^* = D_1 \cup \hat{\Gamma} \cup D_2$  can be determined by finding the images of the four sides of this rectangle under the transformation  $z = \gamma(\zeta)$ ,  $\zeta = s + i t$ . Assuming that the regions  $G_1$  and  $G_2$  are defined by (12.4.1), the four typical regions  $D^*$  are presented in Fig. 12.4.2(a)–(d) which correspond to the following four cases, respectively:

- |   |  |
|---|--|
| (a) $s_1 = 0, 0 < s_2 \leq \frac{\pi}{2};$    | (b) $s_1 = 0, \frac{\pi}{2} < s_2 \leq \pi;$ |
| (c) $s_1 = 0, \pi < s_2 \leq \frac{3\pi}{2};$ | (d) $s_1 = 0, \frac{3\pi}{2} < s_2 < 2\pi.$  |

In each Fig. 12.4.2, the equations of the different arcs are

$$\begin{aligned}\hat{\Gamma} &= \text{arc } \widehat{PQ} : \{z = z_c + a e \cos(s - iq), \quad 0 < s < s_2\}, \\ \hat{\Gamma}' &= \text{arc } \widehat{P'Q'} : \{z = \gamma(s - iq), \quad 0 < s < s_2\}, \\ \hat{\Gamma}^* &= \text{arc } \widehat{Q'R} : \{z = \gamma(s_2 + it), \quad -q < t < q\}.\end{aligned}$$

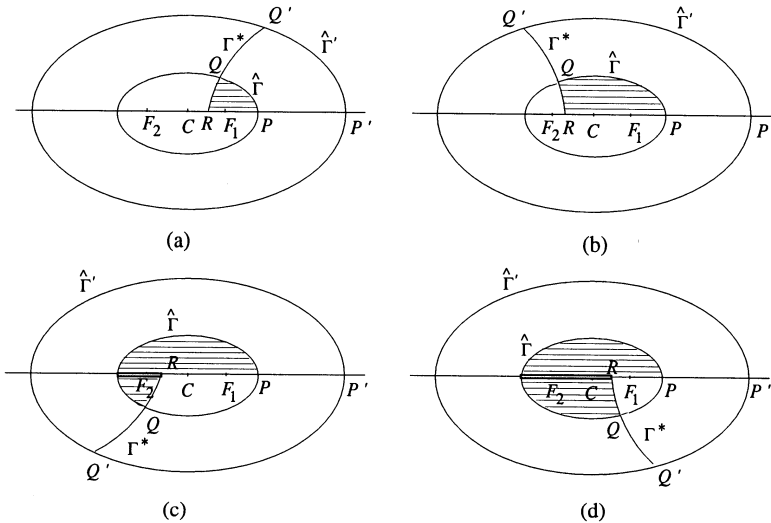


Fig. 12.4.2.

Arc  $\hat{\Gamma}'$  is that of an ellipse  $E'$ , and  $\Gamma^*$  that of a hyperbola orthogonal to both ellipses  $E$  and  $E'$  (the right branch of the hyperbola if  $\cos s_2 > 0$  and the left branch if  $\cos s_2 < 0$ ). In the case when  $s_2 = \pi/2$  or  $3\pi/2$ , the hyperbola degenerates into a vertical straight line through the center  $C$  ( $R$  coincides with  $C$  and  $\hat{\Gamma}$  becomes a part of the minor axis), whereas when  $s = \pi$ , it degenerates into the major axis,  $R$  coincides with the focus  $F_2$ , and  $\hat{\Gamma}$  becomes a part of the major axis. The region  $D_1$  is shaded in each figure, and  $D_2$  is the region bounded by the arcs  $\hat{\Gamma}$ ,  $\hat{\Gamma}'$  and the subarc  $\widehat{Q'Q}$  of  $\Gamma^*$ . Note that in figures (c) and (d) the region  $D_1$  includes a cut on the major axis from  $F_2$  to  $R$  (because in this case the mapping  $z = \gamma(\zeta)$  yields a common image  $z_c - a e \cos s$  of the points  $(\pi \pm s) + iq, s > 0$ ).

The region  $D^*$  associated with any arc  $\hat{\Gamma}$  with  $0 \leq s_1 < s < 2\pi$  can be

obtained from Fig. 12.4.2 (a)–(d). For example, the region  $D^*$  associated with an arc  $\hat{\Gamma}$  for  $0 < s_1 \leq \pi/2$  and  $\pi < s_2 < 3\pi/2$  is obtained by deleting the region of figure (a) from that of figure (c). The region  $D^*$  associated with an arc  $\hat{\Gamma}$ , which includes the two vertices  $z_c \pm a$  of the ellipse  $E$  can also be obtained from these four figures. For example, if  $-\pi/2 < s_1 < 0$  and  $\pi < s_2 < 3\pi/2$ , then the region  $D^*$  is the union of the region of figure (c) with the region obtained by reflecting the region of figure (a) on the major axis.

Now, using the results of Theorems 12.4.1 and 12.4.2, we conclude that  $\gamma(\zeta)$  has exactly one zero in  $G_1$  at the point  $\zeta_0 = \cos^{-1}\left(-\frac{z_c}{ae}\right) + iq$ , which means that the function  $f$  has a simple pole at the point

$$z_0 = \gamma(\bar{\zeta}_0) = z_c - \frac{(a^2 + b^2)\bar{z}_c - 2ia b \sqrt{a^2 - b^2 - \bar{z}_c^2}}{a^2 - b^2} \in D_2, \quad (12.4.11)$$

where the square root is chosen such that  $0 < \arg \left\{ \sqrt{a^2 - b^2 - \bar{z}_c^2} \right\} < \pi$ .

If  $0 \in \partial D_1 \setminus \hat{\Gamma}$ , then the origin lies on the major axis between the foci  $F_1$  and  $F_2$ , i.e.,  $-ae \leq x_c \leq ae$  and  $y_c = 0$ . Then, the following three situations arise:

(i) If the origin lies on a cut in the region  $D_1$  but does not coincide with either focus of  $E$ , then there are two distinct values of  $\cos^{-1}(-x_c/ae)$  in the interval  $(s_1, s_2)$ , and associated with these two values there are two distinct zeros of  $\gamma(\zeta)$  on the side  $t = q$  of  $G_1$ . Hence,  $f$  has two simple poles at the two points

$$z_0 = \frac{-2b^2 x_c \pm 2ia b \sqrt{a^2 - b^2 - x_c^2}}{a^2 - b^2} \in \hat{\Gamma}''. \quad (12.4.12)$$

(ii) If the origin does not lie on a cut of  $D_1$  and does not coincide with either focus of  $E$ , then there is exactly one value of  $\cos^{-1}(-x_c/ae)$  in the interval  $(s_1, s_2)$ , and so  $\gamma(\zeta)$  has a zero on the side  $t = q$  of  $G_1$ . Thus,  $f$  has a simple pole at  $z_0$  given by (12.4.12), where a proper sign is chosen so that  $z_0$  lies on  $\hat{\Gamma}''$ .

(iii) If the origin coincides with either focus of  $E$ , i.e.,  $x_c = \pm ae$ ,  $y_c = 0$ , then  $\gamma(\zeta)$  has a double zero at  $\zeta_0 = iq$  and  $\zeta_0 = \pi + iq$ . Hence,  $f$  has a double pole at one of the vertices of the ellipse  $E'$ , i.e., at one of the points

$$z_0 = \pm \frac{2b^2}{\sqrt{a^2 - b^2}}, \quad (12.4.13)$$

where the  $\pm$  sign is chosen according as the origin is at  $F_1$  or  $F_2$ .

If the origin is not in  $D_1 \cup (\Gamma \setminus \hat{\Gamma})$ , then  $f$  has no poles in  $D_2 \cup \hat{\Gamma}'$ . If the origin lies in  $\partial D_1 \setminus \hat{\Gamma}$ , then  $f$  has a simple pole at the point  $z_0$  given by (12.4.11), except when the origin coincides with one of the vertices of  $E'$ , i.e., when

$$x_c = \pm \frac{a^2 + b^2}{\sqrt{a^2 - b^2}}, \quad \text{and} \quad y_c = 0. \quad (12.4.14)$$

In this case  $f$  has a singularity of the form  $(z - z_0)^{-1/2}$  at one of the foci of  $E$ , i.e., at one of the points  $z_0 = \pm \frac{2b^2}{\sqrt{a^2 - b^2}}$ . ■

CASE STUDY 12.4.2. (a) Let the boundary  $\Gamma$  of the region  $D$  be the union of an elliptic curve  $\Gamma_1$  and the straight line segment  $\Gamma_2$ , defined by

$$\begin{aligned}\Gamma_1 &= \{z : z = 4 \cos s - 2e + i b \sin s, -\pi/2 < s < \pi/2, 0 < b < 4\}, \\ \Gamma_2 &= \{z : z = x + iy, x = -2e, -b < y < b\},\end{aligned}$$

where  $e = \frac{\sqrt{16 - b^2}}{2}$  (see Fig. 12.4.3).

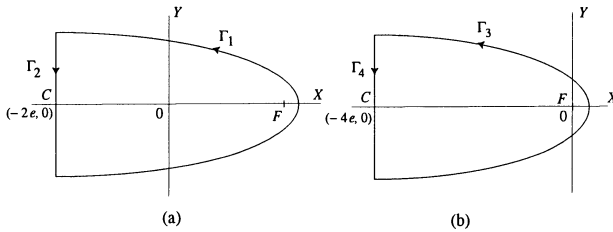


Fig. 12.4.3.

There are two poles of  $f$  with respect to the curve  $\Gamma_1$ , and in view of (12.4.12) they are at

$$z_{1,2} = \frac{b^2 \pm 4\sqrt{3}bi}{\sqrt{16 - b^2}}.$$

There is one pole with respect to the line  $\Gamma_2$  at  $z_3 = -\sqrt{16 - b^2}$ , which is the mirror image of 0 in  $\Gamma_2$ .

(b) If we translate the region  $D$  by  $2e$  in the negative  $x$  direction, then the origin 0 coincides with the focus  $F_1$ , and the new region  $D'$  is bounded by arcs

$$\begin{aligned}\Gamma_3 &= \{z : z = 4(\cos s - e) + i b \sin s, -\pi/2 < s < \pi/2\}, \\ \Gamma_4 &= \{z : z = x + iy, x = -4e, -b < y < b\}.\end{aligned}$$

Then, in view of (12.4.13), the function  $f$  has a double pole with respect to the curve  $\Gamma_3$  at  $z_4 = \frac{2b^2}{\sqrt{16-b^2}}$ , and with respect to the line  $\Gamma_4$  it has a simple pole at  $z_5 = -2\sqrt{16-b^2}$ , which is the mirror image of  $O$  in  $\Gamma_4$ . Note that the boundary of the region  $D'$  is very close to the origin. In view of (6.2.3), in such a situation the mapping function  $f$  is connected to the mapping function  $f_1$  of part (a) by

$$f(z) = \frac{|\alpha|}{\alpha} \frac{f_1(z) - \alpha}{1 - \bar{\alpha} f_1(z)}, \quad \alpha = f_1 \left( \frac{ae}{2} \right). \blacksquare$$

**CASE STUDY 12.4.3** Let the region  $D$  be bounded by the straight line segments

$$\overline{AB} : \{z : z = x + iy, -2 < x < 2, y = -1/3\},$$

$$\overline{BC} : \{z : z = x + iy, x = 2, -1/3 < y < 1\},$$

$$\overline{AE} : \{z : z = x + iy, x = -2, -1/3 < y < 1\},$$

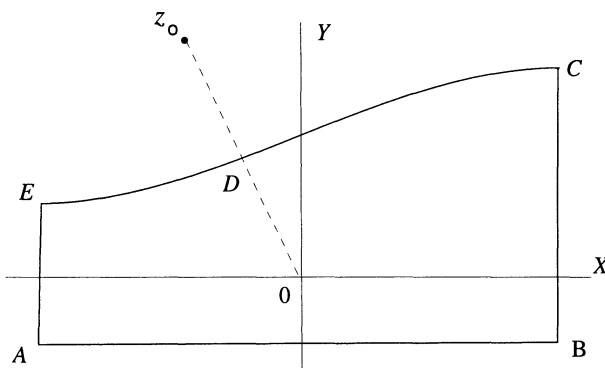


Fig. 12.4.4.

and the cubic arc

$$\widehat{EDC} : \{z : z = \gamma(s), -2 < s < 2\},$$

where  $\gamma(s) = s + i \left( \frac{2}{3} + \frac{1}{4}s - \frac{1}{48}s^3 \right)$  (see Fig. 12.4.4). The arc  $\widehat{CDE}$  has a point of inflection at  $x = 0$ . The function  $\gamma(\zeta)$  has a zero inside the boundary

of the region  $D$  at the point

$$\zeta_0 = -0.160784962923 - 0.626680456065 i.$$

Then

$$z_0 = \gamma(\bar{\zeta}_0) = -0.321569925846 + 1.25336091213 i.$$

Also, since  $c(\zeta_1) - c(\zeta_2) = (\zeta_1 - \zeta_2) R(\zeta_1, \zeta_2)$ , where

$$R(\zeta_1, \zeta_2) = 1 + i \left( \frac{1}{4} - \frac{1}{48} (\zeta_1^2 + \zeta_1 \zeta_2 + \zeta_2^2) \right),$$

and  $R(\zeta_1, \zeta_2) \neq 0$  for all  $\zeta_1$  and  $\zeta_2$  in the rectangle  $G = \{\zeta : \zeta = s + it, -2 < s < 2, -1 < t < 1\}$ , the function  $\gamma(\zeta)$  is one-to-one in  $G$ . Thus, there exists a simply connected region  $G^*$  that contains the points  $\zeta_0$  and  $\bar{\zeta}_0$  and is such that the conditions  $C1$  and  $C2$ , mentioned in the beginning of this section, are satisfied. Hence, in view of Theorem 12.4.1(a), the function  $f$  has a simple pole with respect to the arc  $\widehat{CDE}$  at the point  $z_0$ . ■

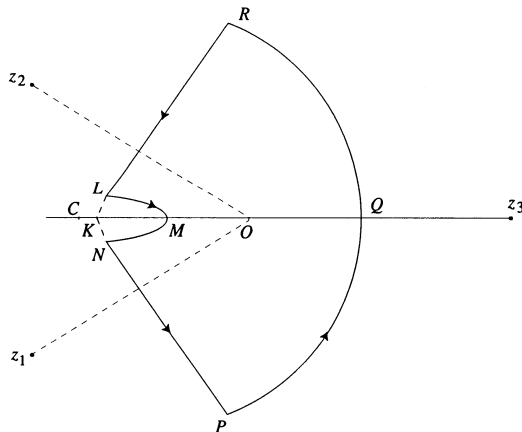


Fig. 12.4.5.

**CASE STUDY 12.4.4.** The region  $D$  bounded by the elliptic arc  $\widehat{LMN}$  which is defined by  $z = 5 \cos s - 17/2 + 3i \sin s$ ,  $-\pi/5 < s < \pi/5$ , the straight lines  $\overline{NP}$  and  $\overline{LR}$ , and the circular arc  $\widehat{PQR}$  whose center is at the point  $K$  and radius is  $KQ$ , where  $Q = (7/2, 0)$  and  $K$  is the point where the normals to the ellipse at  $L$  and  $N$  intersect the  $x$ -axis. The coordinates of the center  $C$  of the ellipse are  $(x_c, 0) = (-17/2, 0)$ , and the focus  $F_1$  is at

$(-9/2, 0)$ . Thus, the origin 0 and the focus  $F_1$  are inverse points with respect to the elliptic arc  $\widehat{LMN}$  (Fig. 12.4.5). Then, in view of (12.4.14), the mapping function  $f$  has (i) a singularity of the type  $(z + 9/2)^{-1/2}$  at  $F_1$ , and (ii) a simple pole at the mirror image  $z_1, z_2$  of the origin with respect to the line segments  $\overline{NP}$  and  $\overline{LR}$ , and at the geometric inverse  $z_3$  of the origin with respect to the circular arc  $\widehat{PQR}$ . ■

## 12.5. Exterior Regions

In §7.3.3 we considered the case of the function  $w = f_E(z)$  which maps the region  $\text{Ext}(D)$  univalently onto the region  $U^* = \{|w| > 1\}$  such that  $f_E(\infty) = 0$  and  $\lim_{z \rightarrow \infty} f'_E(z) > 0$ . In this case, by using the inversion  $z \mapsto z^{-1}$ , we reduced the problem to that of the mapping of interior regions by the function  $f(z)$ .

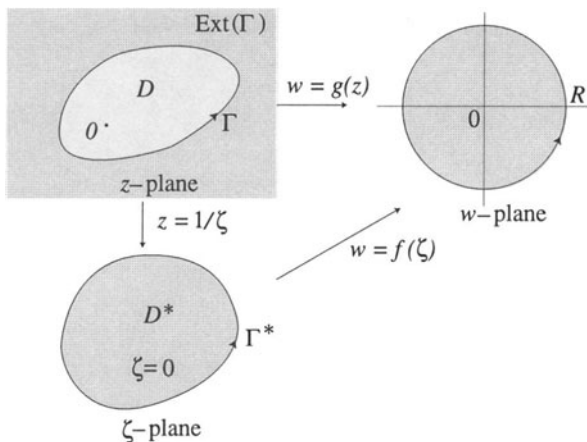


Fig. 12.5.1.

In this section we are concerned with the following mapping problem: Assume that the origin lies inside a simply connected region  $D$  with the Jordan boundary  $\Gamma$ . Let a function  $w = g(z)$  map the region  $\text{Ext}(\Gamma)$  conformally onto the disk  $B(0, R) = \{|w| < R\}$  in the  $w$ -plane. Also, the transformation

$\zeta = 1/z$  maps the boundary  $\Gamma$  onto a Jordan contour  $\Gamma^*$  so that  $z = \infty$  goes into  $\zeta = 0$ . Let  $w = f(\zeta)$ ,  $f(0) = 0$ ,  $f'(0) = 1$ , map the region  $D^*$ , bounded by the contour  $\Gamma^*$ , conformally onto the disk  $B(0, R)$  (Fig. 12.5.1). Thus,  $w = g(z) = f(1/\zeta)$  maps the region  $\text{Ext}(\Gamma)$  conformally onto the disk  $B(0, R)$  such that  $g(\infty) = 0$ . Hence, determining the mapping function  $g$  reduces to determining the interior mapping function  $f$  in such problems of exterior regions, which correspond to Case 2 of §5.4. Also, the function  $w = 1/g(z)$  maps the region  $\text{Ext}(\Gamma)$  conformally onto the exterior of the circle  $|w| = 1/R$ , and the quantity  $d = 1/R$  is the transfinite diameter of the region  $D \cup \Gamma$  (see §1.1).

Note that the function  $g$  is different from the function  $f_E$  studied earlier. We shall use the RM and BKM to approximate the mapping function  $g$ . Since  $f \in \mathcal{K}^1(D^*)$ , the basis in RM is taken as  $\{\phi_j(\zeta)\}$ , as in §4.1, so that  $\phi_1(0) = 1$  and  $\phi_j(0) = 0$  for  $j = 2, 3, \dots$ , which leads to the complex linear system

$$\sum_{j=1}^n \langle \phi_j, \phi_i \rangle c_j = -\langle \phi_1, \phi_i \rangle, \quad i = 2, \dots, n, \quad (12.5.1)$$

which is solved for the unknowns  $c_j$ ,  $j = 2, \dots, n$ . Thus, the  $n$ -th RM approximations for the mapping function  $f(\zeta)$  and the radius  $R$  are given by

$$f_n(\zeta) = \int_0^\zeta \Phi_n(t) dt, \quad R = \sqrt{\pi} \|\Phi_n\|, \quad (12.5.2)$$

where

$$\Phi_n(\zeta) = \phi_1(\zeta) + \sum_{j=2}^n \phi_j(\zeta), \quad (12.5.3)$$

is the  $n$ -th approximation of  $f'(\zeta)$ .

In the RM and BKM (§4.2.2), since the basis set  $\{\phi_j(\zeta)\}$  is a known complete set, first we approximate the Bergman kernel  $K(\zeta, 0)$  of  $D^*$  by a finite Fourier sum. Then

$$f'(\zeta) = \frac{K(\zeta, 0)}{K(0, 0)}, \quad (12.5.4)$$

and  $R = (\pi K(0, 0))^{-1/2}$ , as in (4.2.23) and (4.2.24). The details of the process are the same as in the five steps given in §4.2.2.

The basis set is taken as the set of monomials  $\{\zeta^{j-1}\}$ ,  $j = 1, 2, \dots$ . Depending on the singularities of  $K(\zeta, 0)$ , the boundary singularities, and the

poles of  $f(\zeta)$ , however, this basis is augmented by the functions  $\phi(z)$  defined in (12.2.10).

CASE STUDY 12.5.1. Consider mapping the rectangle

$$\Omega_{ab} = \{(x, y) : |x| < a/2, |y| < b/2\}, \quad a \geq b,$$

onto the unit disk  $U$ . In view of the Case Study 2.3.2, the mapping function  $f(z)$ , known in terms of the elliptic functions, is given by

$$f(z) = \beta \frac{\zeta - \alpha}{\zeta - \bar{\alpha}}, \quad \zeta = \operatorname{sn}(z, k), \quad |\beta| = 1, \quad \Im\{\alpha\} > 0.$$

Alternately, using the Green's function method, it is also known that the mapping function  $f(z)$  is related to Green's function  $\mathcal{G}(z, z_0)$  of the rectangle  $\Omega_{ab}$  with a pole at  $z_0$  by

$$f(z) = \exp\{-2\pi\mathcal{G}(z, z_0) + i\mathcal{H}(z)\}, \quad (12.5.5)$$

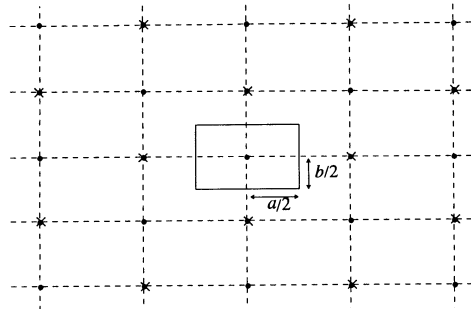


Fig. 12.5.2.

where  $\mathcal{H}(z)$  is the conjugate harmonic function of  $\mathcal{G}(z, z_0)$ . The method of images can be used to express Green's function of  $\Omega_{ab}$  as a double sum of logarithm functions (see Kythe, 1996, p.81). In particular, at  $z_0 = 0$

$$\mathcal{G}(z, z_0) = \frac{1}{2\pi} \sum_{m,n=-\infty}^{\infty} (-1)^{m+n} \log \frac{1}{|z - z_{mn}|}, \quad (12.5.6)$$

where  $z_{mn} = ma + i nb$  (Fig. 12.5.2). Since the conjugate harmonic function of  $\log |z - z_{mn}|$  is  $\arg\{z - z_{mn}\}$ , we find from (12.5.5) and (12.5.6) that the function  $f(z)$  that maps the rectangle  $\Omega_{ab}$  onto  $U$  such that  $f(0) = 0$  is given by

$$f(z) = \exp \left\{ \sum_{m,n=-\infty}^{\infty} (-1)^{m+n} \log (z - z_{mn}) = \frac{\prod_{m+n=\text{even}} (z - z_{mn})}{\prod_{m+n=\text{odd}} (z - z_{mn})} \right\}. \quad (12.5.7)$$

As noted in Case Study 4.2.3, in the present case both  $f$  and the kernel function  $K(z, 0)$  have poles at all ‘negative’ images of the point  $z_0 = 0$  with respect to the four sides of  $\Omega_{ab}$  (these points are identified by an  $\times$  in Fig. 12.5.2). The poles at  $z = \pm a$  and  $z = \pm ib$  affect the convergence of the representation (4.2.10) of  $K(z, 0)$ , even when  $a = b$ . But their effect is more significant the thinner the rectangle becomes, because in such cases ( $b \ll a$ ) the distance of the poles at  $\pm ib$  from the boundary of  $\Omega_{ab}$  gets smaller compared with the dimensions of  $\Omega_{ab}$ . Then the mapping function  $f(z)$  from (12.5.7) is given by

$$f(z) = \frac{z}{(z^2 - a^2)(z^2 + b^2)} g(z), \quad (12.5.8)$$

where  $g(z)$  is analytic in the region  $\{(x, y) : |x/a| + |y/b| < 3\}$ . Also, since from (4.2.25)

$$K(z, 0) = \sqrt{\frac{K(0, 0)}{\pi}} f'(z), \quad f'(0) = 0,$$

the set

$$\left\{ \left( \frac{z}{z-a} \right)', \quad \left( \frac{z}{z+a} \right)', \left( \frac{z}{z-ib} \right)', \left( \frac{z}{z+ib} \right)', z^j, \quad j = 0, 1, \dots, \right\}$$

where the prime denotes differentiation with respect to  $z$ , is best suited as the basis set for both BKM and VM (see the next case study). ■

**CASE STUDY 12.5.2.** Consider the rectangle  $\Omega_{a1} = \{(x, y) : |x| \leq a, |y| \leq 1\}$  (Fig. 12.5.3).

**CASE 1 ( $a \neq 1$ ).** Since the region has fourfold symmetry about 0, the odd powers of  $z$  do not appear in the polynomial representation (4.2.20) of the kernel function  $K(z, 0)$ . Hence we take the basis set as  $\{\phi_j^*(z)\} = \left\{ z^{2(j-1)} \right\}_{j=1}^N$ .

CASE 2 ( $a = 1$ ). Since the region has eightfold symmetry about the origin and the polynomial representation of  $K(z, 0)$  has only powers of  $z$  that are multiples of 4, we take the basis set as  $\{\phi_j^*(z)\} = \left\{z^{4(j-1)}\right\}_{j=1}^N$ .

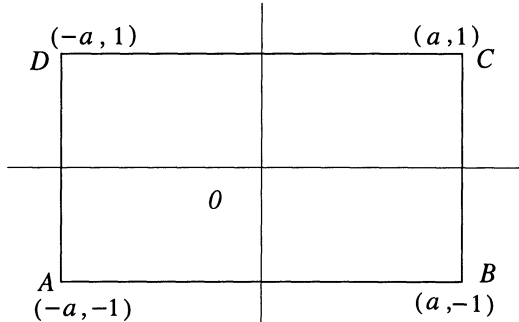


Fig. 12.5.3.

The augmented basis (AB) is obtained by adding to the above orthonormal basis set the four singular functions that correspond to the four poles at  $z = \pm 2a$  and  $z = \pm 2i$ . Because of the symmetry of the region, these four singular functions are combined into two functions  $\left(\frac{z}{z^2 - 4a^2}\right)'$  and  $\left(\frac{z}{z^2 + 4}\right)'$  when  $a \neq 1$ . In the case when  $a = 1$ , these singular functions simplify to a single function  $\left(\frac{z}{z^4 - 16}\right)'$ . Hence the AB is given by

$$\begin{aligned}\phi_1(z) &= \left(\frac{z}{z^2 - 4a^2}\right)', \quad \phi_2(z) = \left(\frac{z}{z^2 + 4}\right)', \\ \phi_{j+3} &= z^{2j}, \quad j = 0, 1, \dots, \quad \text{when } a \neq 1; \\ \phi_1(z) &= \left(\frac{z}{z^4 - 16}\right)', \quad \phi_{j+2} = z^{4j} \quad j = 0, 1, \dots, \quad \text{when } a = 1. \blacksquare\end{aligned}$$

CASE STUDY 12.5.3. Consider the bean-shaped region  $D$  bounded by the contour (Fig. 12.5.4)

$$\begin{aligned}\Gamma : \left\{ z : z = \gamma(s) = \frac{9}{4}[0.2 \cos s + 0.1 \cos 2s - 0.1 \right. \\ \left. + i(0.35 \sin s + 0.1 \sin 2s - 0.02 \sin 4s)] \right\}, \quad -\pi \leq s \leq \pi.\end{aligned}$$

The conformal mapping of this region  $D$  was found by Reichel (1985) who, based on geometric considerations, predicted that the function  $f$  has a simple pole at  $z \approx -0.61$ . Papamichael, Warby and Hough (1986) have shown that in the neighborhood of the  $s$ -axis ( $= \{\zeta : \zeta = s + it, -\pi \leq s \leq \pi, t = 0\}$ ) the function  $f$  has (i) a simple pole at each of the points  $z_1 = -0.650225813375$  and  $z_2 = 1.311282520094$ ; and (ii) a singularity of the form  $\sqrt{z - z_j}$ ,  $j = 3, 4$ , at the points  $z_{3,4} = \pm 0.565672547402 \mp 0.068412683544 i$ . Hence, for BKM with augmented basis (AB), we take

$$\psi(z) = \frac{d}{dz} \left\{ \frac{\sqrt{\sqrt{z - z_4} - \sqrt{z_3 - z_4}}}{z - z_1} \right\},$$

and the AB consists of the functions

$$\begin{aligned}\phi_1(z) &= \left( \frac{z}{z - z_1} \right)', & \phi_2(z) &= \psi(z) + \psi(\bar{z}), \\ \phi_3(z) &= \left( \frac{z}{z - z_2} \right)', & \phi_{4+j}(z) &= z^{j-1}, \quad j = 1, 2, \dots.\end{aligned}$$

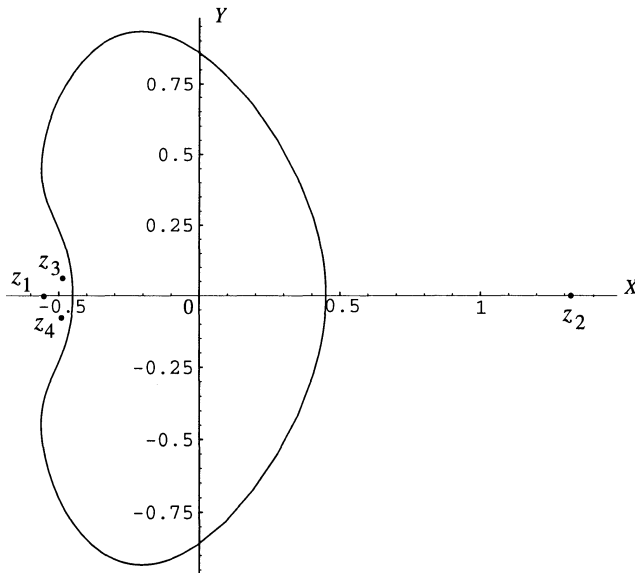


Fig. 12.5.4.

---

## 12.6. Doubly Connected Regions

In Gaier's variational method we first determine the approximate function

$$H(z) = \frac{f'_\Omega(z)}{f_\Omega(z)} - \frac{1}{z} \quad (12.6.1)$$

by taking a finite series representation as

$$H(z) = \sum_{j=1}^n a_j \phi_j(z),$$

where  $\{\phi_j(z)\}$  is the basis set of functions in  $L^2(\Omega)$  which possess single-valued indefinite integrals in  $\Omega$ . This set is augmented by adding appropriate singular functions to account for singularities on the boundary  $\partial\Omega = \Gamma_1 \cup \Gamma_0$  and in  $\text{Int}(\Gamma_1) \cup \text{Ext}(\Gamma_0)$ . In fact, since the variational problem to minimize the integral

$$\|u\|^2 = \iint_{\Omega} |u(z)|^2 dx dy, \quad u \in \mathcal{K}^1(\Omega), \quad (12.6.2)$$

(see §4.2) has a unique solution  $u_0$  such that  $u_0$  is orthogonal to  $\mathcal{K}^0(\Omega)$ , the function  $H$  is related to  $u_0$  by

$$H(z) = \frac{u_0(z)}{\|u_0\|^2}. \quad (12.6.3)$$

Let us denote

$$A(z) = \log f_\Omega(z) - \log z. \quad (12.6.4)$$

Then  $H(z) = A'(z)$ , and for each function  $\phi_j \in L^2(\Omega)$  which is continuous on  $\partial\Omega$ , we have, in view of Green's formula (1.1.29),

$$\langle \phi_j, H \rangle = \frac{1}{2i} \int_{\partial\Omega} \phi_j(z) \overline{A(z)} dz = i \int_{\partial\Omega} \phi_j(z) \log |z| dz. \quad (12.6.5)$$

The modulus  $M = r_2/r_1$  of  $\Omega$  is related to the function  $H$  by

$$\log M = \frac{1}{2\pi} \left\{ \frac{1}{i} \int_{\partial\Omega} \frac{1}{z} \log |z| dz - \|H\|^2 \right\}. \quad (12.6.6)$$

Gaier's variational method (VM) resembles the RM (§4.2) in many ways. Let the basis set  $\{\phi_j(z)\} \in L^2(\Omega)$  be such that  $\phi_1 \in \mathcal{K}^0(\Omega)$ . Let  $\mathcal{K}_n^m$ ,  $m = 0, 1$ , denote the  $n$ -dimensional counterparts of  $\mathcal{K}^m(\Omega)$ , i.e.,

$$\mathcal{K}_n^m(\Omega) = \mathcal{E}_n \cap \mathcal{K}^m(\Omega), \quad m = 0, 1, \quad (12.6.7)$$

where  $\mathcal{E}_n = \text{span } (\phi_1, \phi_2, \dots, \phi_n)$ . The set  $\mathcal{K}_n^m$  is nonempty for  $n = 1, 2, \dots$ , and the  $n$ -dimensional problem corresponding to (12.6.2) is as follows:

**PROBLEM  $I_n^m$ :** In the class  $\mathcal{K}_n^1(\Omega)$  minimize  $\|u\|$ , defined by (12.6.2), over all  $u \in \mathcal{K}_n^1(\Omega)$ .

As in Problem  $I_n$ , the following results hold for the above problem:

- (i) the problem  $I_n^m$  has a unique solution  $u_0$ ;
- (ii) the minimal function  $u_n$  is orthogonal to  $\mathcal{K}_n^0(\Omega)$ ; and
- (iii) the sequence  $\{u_n\} \rightarrow u_0$  uniformly in  $\Omega$ , i.e., in view of (12.6.3),

$$\frac{u_n(z)}{\|u\|^2} \rightarrow H(z), \quad (12.6.8)$$

almost uniformly in  $\Omega$  (i.e., there is mean convergence in every compact subset of  $\Omega$ ). Hence,  $\lim_{n \rightarrow \infty} \|u_n - u_0\| = 0$ . Let

$$h_j = \langle H, \phi_j \rangle, \quad j = 1, 2, \dots. \quad (12.6.9)$$

Note that  $h_j \neq 0$ . Also, since  $\mathcal{K}_n^0(\Omega) = \{u \in \mathcal{E}_n : \langle H, u \rangle = 0\}$ , the set  $\{\bar{h}_1 \phi_j(z) - \bar{h}_j \phi_1(z)\}$ ,  $j = 2, 3, \dots, n$ , is the basis of  $\mathcal{K}^0(\Omega)$ . Thus, if we take

$$u_n(z) = \sum_{j=1}^n c_j \phi_j(z), \quad (12.6.10)$$

then, since  $u_n$  is orthogonal to  $\mathcal{K}^0(\Omega)$  and  $\langle H, u_n \rangle = 1$ , we obtain the linear  $(n \times n)$  system of equations

$$\begin{aligned} \sum_{j=1}^n \{h_1 \langle \phi_j, \phi_i \rangle - h_i \langle \phi_j, \phi_1 \rangle\} c_j &= 0, \quad j = 2, 3, \dots, n, \\ \sum_{j=1}^n \bar{h}_j c_j &= 1, \end{aligned} \quad (12.6.11)$$

which determines the coefficients  $c_j$ . Then, in view of (12.2.8), the formula  $H_n(z) = \frac{u_n(z)}{\|u_0\|^2}$  gives the  $n$ -th approximation of the function  $H(z) = A'(z)$  and the  $n$ -th VM approximation of the mapping function  $f_\Omega(z) \equiv f(z)$

$$f_n(z) = z e^{\int_z^\zeta H_n(t) dt}, \quad \zeta \in \bar{\Omega}. \quad (12.6.12)$$

Also, from (12.6.6)

$$M = \exp \left\{ \frac{1}{2\pi} \left( \frac{1}{i} \int_{\partial\Omega} \frac{1}{z} \log |z| dz - \|H_n\|^2 \right) \right\}, \quad (12.6.13)$$

which gives the  $n$ -th VM approximation of the modulus  $M$  of the region  $\Omega$  ( $M_n$  gives an upper bound to  $M$ ).

Let us assume that the mapping function  $f_\Omega$  is normalized so that the region  $\Omega$  is mapped conformally onto the annulus  $A(\rho, 1)$ . Then the density function  $\mu(s)$  (see §10.2) is related to the boundary correspondence function  $\phi_\Omega(s)$  by

$$\phi'_\Omega(s) = 2\pi \gamma_1 \mu(s), \quad (12.6.14)$$

where  $\gamma_1 = \log M = -\log \rho$ .

Let  $\{\phi_j^*(z)\}$  denote the orthonormal basis of  $L^2(\Omega)$ . Then the function  $H$  has the Fourier series expansion

$$H(z) = \sum_{j=1}^{\infty} \beta_j \phi_j(z), \quad (12.6.15)$$

where the Fourier coefficients are given by  $\beta_n = \langle \phi_n^*, H \rangle$ . Then the VM follows the same five-step procedure explained in §4.2.2, which leads to the  $n$ -th approximation

$$H_n(z) = \sum_{j=1}^n \beta_j \phi_j^*(z), \quad \beta_j = \langle \phi_j^*, H \rangle, \quad j = 1, 2, \dots, n, \quad (12.6.16)$$

which, from (12.6.12), yields the  $n$ -th approximation  $f_n(z)$  of the mapping function  $f_\Omega(z)$ .

The basis set is taken as the set  $\{z^j\}_{j=-\infty}^{\infty}$  which is a complete set in  $L^2(\Omega)$ . But the use of this set results in the same kind of problems as in the RM and

BKM for simply connected regions. Due to the presence of singularities of the function  $H$  in the complement of  $\Omega$  and corner points on the boundary, this basis set is augmented by adding singular functions related to each singular behavior. Thus, in the neighborhood of a branch point singularity at  $z_j \in \partial\Omega$  the asymptotic expansion of the mapping function involves fractional powers of  $(z - z_j)$ , for which Lehman's theorem (§10.2) is used to account for the singularity problem and determine the augmented basis (AB). For a corner point  $z_j \in \partial\Omega$  the asymptotic expansion of  $H$  is given by (10.2.6) which augments the basis by singular functions of the form

$$\phi_j(z) = \begin{cases} \frac{1}{z^2} \left( \frac{1}{z} - \frac{1}{z_j} \right)^{r-1}, & \text{if } z_j \in \Gamma_1, \\ (z - z_j)^{r-1}, & \text{if } z_j \in \Gamma_0, \end{cases} \quad (12.6.17)$$

where  $r = k + l/\alpha$ ,  $\alpha = p/q > 0$ ,  $k = 0, 1, 2, \dots$ , and  $1 \leq l \leq p$ . A branch point singularity occurs if  $p \neq 1$ . If the arcs at a corner point are straight line segments, then the exponent  $k + l/\alpha$  in (12.6.17) is replaced by  $l/\alpha$ ,  $l = 1, 2, \dots$  (see (10.2.8)). Depending on the rational values of  $k + l/\alpha$ , the first few singular functions (12.6.17) are added to the basis set  $\{z^j\}_{j=-\infty}^{\infty}$  to form the AB. Note that the singular functions in (12.6.17) for  $z_j \in \Gamma_0$  are the same type as used for interior mappings and those in (12.6.17) for  $z_j \in \Gamma_1$  are those used for exterior mappings of the simply connected regions discussed in Chapter 10. The function  $f_{\Omega}$  may involve logarithmic terms if the asymptotic expansion (10.2.6) is valid, but these logarithmic singularities can generally be ignored as they produce no serious computational problem.

**CASE STUDY 12.6.1.** Consider the doubly connected region  $\Omega$  bounded by a circle in a square, defined by

$$\Omega : \{(x, y) : |x| < 1, |y| < 1\} \cap \{z : |z| > a, \quad a < 1\}.$$

There are no corner singularities, so no AB is required. The region has eightfold symmetry about the origin, and thus, the basis set is taken as  $z^{(-1)^{j+1}(2j+1)}$ ,  $j = 1, 2, \dots$  ■

**CASE STUDY 12.6.2.** Let  $G_a = \{(x, y) : |x| < a, |y| < a\}$  define a square region. Consider the doubly connected region  $\Omega$  as a square in a square (square frame, Fig. 12.6.2) defined by

$$\Omega = \{G_1 \cap \text{compl}(\bar{G}_a)\}, \quad a < 1.$$

Let  $z_j$  denote the four corners of the inner square. Then the singular functions associated with the branch point singularities at these corners are the functions  $\phi_{rj}(z)$ ,  $j = 1, 2, 3, 4$ , where

$$r = k + \frac{2l}{3}, \quad k = 0, 1, \dots, \text{and } 1 \leq l \leq 3. \quad (12.6.18)$$

Since the region  $\Omega$  has eightfold symmetry about the origin, these four singular functions  $\phi_{rj}(z)$  are combined into a single function

$$\tilde{\phi}_r(z) = \phi_{r1}(z) + \sum_{j=2}^4 e^{i\theta_j} \phi_{rj}(z), \quad (12.6.19)$$

where the arguments  $\theta_j$  are chosen such that

$$e^{i\pi/2} \tilde{\phi}_r \left( e^{i\pi/2} z \right) = \tilde{\phi}_r(z).$$

Since  $\theta_j$  depend on the branches used in defining the functions  $\phi_{rj}(z)$ , care must be taken while constructing the singular functions of the form  $\tilde{\phi}_r(z)$ . The AB is

$$z^{(-1)^{j+1}(2j+1)}, \quad j = 1, 2, \dots; \quad \tilde{\phi}_r(z), \quad r = \frac{2}{3}, \frac{4}{3}, \frac{5}{3}, \frac{7}{3}. \blacksquare$$

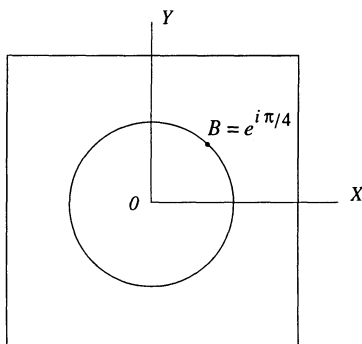


Fig. 12.6.1

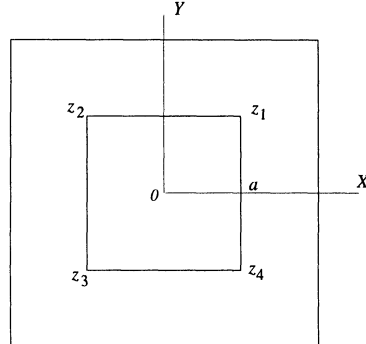


Fig. 12.6.2.

CASE STUDY 12.6.3. Let

$$G_{ab} = \{(x, y) : |x| < a, |y| < b\} \cup \{|x| < b, |y| < a\}, \quad (12.6.20)$$

and

$$G_c = \{(x, y) : |x| < c, |y| < c\}.$$

Then consider the doubly connected region  $\Omega$  which is a cross in a square (Fig. 12.6.3), defined by

$$\Omega = G_c \cap \text{compl}(\bar{G}_{ab}), \quad a < c, b < c.$$

Let the eight corners  $A, B, C, D, E, F, G, H$  of the cross-shaped region  $G_{ab}$  be denoted by  $z_j$ ,  $j = 1, 2, \dots, 8$ , respectively. The singular functions associated with the branch point singularities at  $z_j$ ,  $j = 1, \dots, 8$ , are given by

$$\phi_{rj}(z) = \frac{1}{z^2} \left( \frac{1}{z} - \frac{1}{z_j} \right)^{r-1},$$

as in (12.6.17), and  $r$  is defined by (12.6.18). In view of the symmetry these eight singular functions can be combined into two functions

$$\tilde{\phi}_{rj}(z) = \phi_{rj}(z) + \sum_{k=1}^3 e^{i\theta_{2k+j}} \phi_{r,2k+j}(z), \quad j = 1, 2, \quad (12.6.21)$$

where the arguments  $\theta_{2k+j}$  are chosen such that

$$e^{i\pi/2} \tilde{\phi}_{rj} \left( e^{i\pi/2} z \right) = \tilde{\phi}_{rj}(z), \quad j = 1, 2.$$

as in Case Study 12.6.2. ■

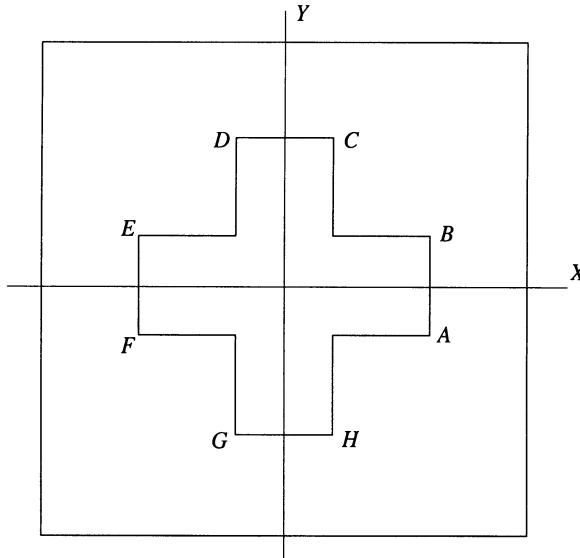


Fig. 12.6.3.

## 12.7. Problems

PROBLEM 12.7.1. Let  $\alpha$  be rational. Use (10.2.6), and show that the first four functions  $\psi_j$  in the formal asymptotic expansion (10.3.5) for the density function  $\mu(s)$  are given by:

$$\begin{aligned}\psi_1(\sigma) &= \sigma^{-1+1/\alpha}, \quad 0 < \alpha < 2, \\ \psi_2(\sigma) &= \begin{cases} \sigma^{1/\alpha}, & 0 < \alpha < 1, \\ \sigma \log \sigma, & \alpha = 1, \\ \sigma^{-1+2/\alpha}, & 1 < \alpha < 2, \end{cases} \\ \psi_3(\sigma) &= \begin{cases} \sigma^{1+1/\alpha}, & 0 < \alpha < 1/2, \\ \sigma^3 \log \sigma, & \alpha = 1/2, \\ \sigma^{-1+2/\alpha}, & 1/2 < \alpha < 1, \\ \sigma^{1/\alpha}, & 1 \leq \alpha < 2, \end{cases} \\ \psi_4(\sigma) &= \begin{cases} \sigma^{2+1/\alpha}, & 0 < \alpha < 1/3, \\ \sigma^5 \log \sigma, & \alpha = 1/3, \\ \sigma^{-1+2/\alpha}, & 1/3 < \alpha \leq 1/2, \\ \sigma^{1+1/\alpha}, & 1/2 < \alpha < 1, \\ \sigma^2 (\log \sigma)^2, & \alpha = 1, \\ \sigma^{-1+3/\alpha}, & 1 < \alpha < 2, \end{cases}\end{aligned}$$

where, in particular,  $a_j^\pm$ ,  $j = 1, 2, 3$ , satisfy the relations

$$\left. \begin{aligned} a_1^- &= \lambda^{1/\alpha} a_1^+, \quad 0 < \alpha < 2, \\ a_2^- &= -\lambda^{2/\alpha} a_2^+, \quad 1 \leq \alpha < 2, \\ a_3^- &= -\lambda^{2/\alpha} a_3^+, \quad 1/2 \leq \alpha < 1 \end{aligned} \right\}, \quad \text{and} \quad \lambda = \left| \frac{\gamma'(s_0^-)}{\gamma'(s_0^+)} \right|.$$

(Papamichael, Warby and Hough, 1986.)

PROBLEM 12.7.2. Discuss the nature of the singularity of the cardioid  $\Gamma_0$  in Case Study 11.2.1 when  $b_2 = 5$  (Fig. 11.2.1).

PROBLEM 12.7.3. Let  $\hat{\Gamma}$  be an arc of the parabola  $(y - y_v)^2 = 4a^2(x - x_v)$ ,  $a > 0$ , where  $z_v = x_v + iy_v$  denotes the vertex, and let the parametric equation of  $\hat{\Gamma}$  be

$$z = \gamma(s) = z_v + a [1 + (s + i)^2], \quad s_1 < s < s_2.$$

Let  $G^*$  be taken as an appropriate subregion of the rectangle  $\{\zeta : \zeta = s + it, s_1 < s < s_2, -1 < t < 1\}$ . Show that the conditions  $C1$  and  $C2$  of §10.4 are satisfied, and  $z = \gamma(\zeta)$  maps  $G^*$  onto the region  $D^* = D_1 \cup \hat{\Gamma} \cup D_2$ . Also, if  $0 \in D_1 \cup (\partial D_1 \setminus \hat{\Gamma})$ , then show that

- (i) if  $z_v$  does not lie on the half-line  $l : \{(x, y) : x < -a, y = 0\}$  and does not coincide with the points  $(-a, 0)$  and  $(3a, 0)$ , then  $f$  has a simple pole at the point  $z_0 = 2iy_v - 4a \left[ 1 - i(-z_v/a - 1)^{1/2} \right]$ , where the square root is chosen such that  $\arg \{(\cdot)^{1/2}\} < \pi$ ;
- (ii) if  $z_v \in l$ , then  $f$  has a simple pole at one or both of the points  $z_0 = -4a \left[ 1 \pm \sqrt{-x_v/a - 1} \right]$ , depending on the values of  $s_1$  and  $s_2$  taken in the equation  $z = \gamma(s)$  of  $\hat{\Gamma}$ ;
- (iii) if the focus of the parabola is at the origin, i.e., if  $z_v = -a$ , then  $f$  has a double pole at the point  $z_0 = -4a$ ;
- (iv) if  $z_v = 3a$ , then  $f$  has a singularity of the type  $(z - z_0)^{-1/2}$  at the point  $z_0 = 4a$  which in this case is the focus of the parabola. (Papamichael, Warby and Hough, 1983.)

PROBLEM 12.7.4. Let  $\hat{\Gamma}$  be the right branch of the hyperbola

$$\frac{(x - x_v)^2}{a^2} - (y - y_v)^2 b^2 = 1,$$

and let the parametric equation of  $\hat{\Gamma}$  be  $z = \gamma(s) = z_v + ae \cosh(s + iq)$ , where  $z_v = x_v + iy_v$  is the center of the hyperbola,  $e = \sqrt{1 + b^2/a^2}$ , and  $\cos q = 1/e$ . Show that the conditions  $C1$  and  $C2$  of §10.4 are satisfied by taking  $G^*$  as a symmetric subregion of the rectangle in Fig. 12.4.1; also, show that

- (i) if  $z_v$  does not lie on the half-line  $l = \{(x, y) : x < -ae, y = 0\}$  and does not coincide with the points  $(-ae, 0)$  and  $\left( \sqrt{\frac{b^2 - a^2}{a^2 + b^2}}, 0 \right)$ , then  $f$  has a simple pole at the point

$$z_0 = z_v + \frac{(a^2 - b^2) \bar{z}_v + 2ia b \sqrt{\bar{z}_v^2 - a^2 - b^2}}{a^2 + b^2};$$

- (ii) if  $z_v \in l$ , then  $f$  has a simple pole at one or both of the points  $z_0 = \frac{2b^2 x_v \pm 2ia b \sqrt{x_v^2 - a^2 - b^2}}{a^2 + b^2}$ , depending on the values of  $s_1$  and  $s_2$  taken in the equation  $z = \gamma(s)$  of  $\hat{\Gamma}$ ;

- (iii) if the focus of the hyperbola under consideration is at the origin, i.e., if  $z_v = -a e$ , then  $f$  has a double pole at the point  $z_0 = -\frac{2b^2}{\sqrt{a^2 + b^2}}$ .
- (iv) If  $z_v = \frac{b^2 - a^2}{\sqrt{a^2 + b^2}}$ , then  $f$  has a singularity of the type  $(z - z_0)^{-1/2}$  at the point  $z_0 = \frac{2b^2}{\sqrt{a^2 + b^2}}$  which in this case is the focus of the hyperbola.  
(Papamichael, Warby and Hough, 1983.)

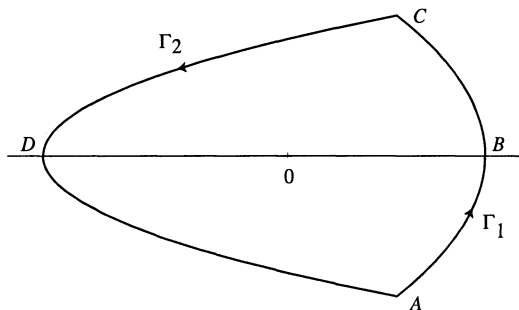


Fig. 12.7.1.

PROBLEM 12.7.5. Consider two parabolic arcs  $\Gamma_1$  and  $\Gamma_2$ , defined by

$$\text{arc } \widehat{ABC} : \{z : z = 0.6 + 0.4\alpha^2 - s^2 + 2is, -1 < s < 1\},$$

$$\text{arc } \widehat{CDA} : \{z : z = -0.4 - 0.6\alpha^2 + s^2 - 2is, -\alpha < s < \alpha, \alpha > 1\},$$

respectively, which intersect orthogonally at the points  $A$  and  $C$  (Fig. 12.7.1). Show that the mapping function  $f$  has (i) two simple poles with respect to the arc  $\widehat{CDA}$  at the points  $z_{1,2} = -4 \pm 4i\sqrt{0.6\alpha^2 - 0.6}$ , and (ii) a simple pole with respect to the arc  $\widehat{ABC}$  at the point  $z_3 = 4\alpha(\alpha - \sqrt{0.6\alpha^2 - 0.6})$ .  
(Papamichael, Warby and Hough, 1983.)

PROBLEM 12.7.6. Consider the region  $D$  bounded by two hyperbolic arcs

$$\Gamma_1 = \text{arc } \widehat{ABC} : \{z : z = x_0 - 2\cosh s + i(y_0 - \sinh s), s_1 < s < s_2\},$$

$$\Gamma_2 = \text{arc } \widehat{CDA} : \{z : z = -x_0 + 2\cosh s + i(-y_0 + \sinh s), s_1 < s < s_2\},$$

where  $x_0 = \cosh s_1 + \cosh s_2$ ,  $y_0 = (\sinh s_1 + \sinh s_2)/2$  are the coordinates of the center  $z_0$  of the arc  $\widehat{ABC}$  (see Fig. 12.7.2). Take  $s_2 = 1$ , and choose

$s_1$  such that  $4 \tanh s_1 \cdot \tanh s_2 + 1 = 0$ . Show that  $f$  has simple poles at the points  $z_{1,2} = \pm z_0 \mp \frac{1}{5} \left( 3\bar{z}_0 + 4i\sqrt{\bar{z}_0^2 - 5} \right)$ . (Papamichael, Warby and Hough, 1983.)

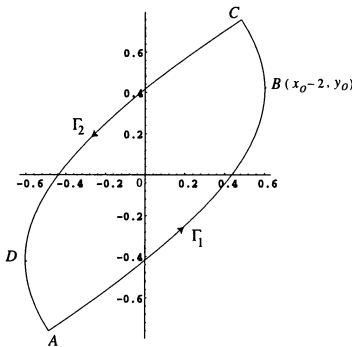


Fig. 12.7.2.

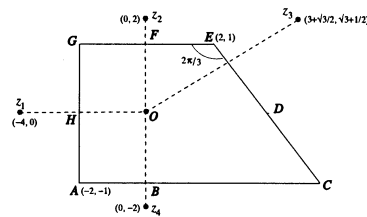


Fig. 12.7.3.

PROBLEM 12.7.7. Consider the quadrilateral in Fig. 12.7.3. Show that the AB is  $\phi_j = \left( \frac{z}{z - z_j} \right)', j = 1, 2, 3, 4; \phi_5 = 1; \phi_6 = \sqrt{z - z_E}; \phi_7 = z; \phi_8 = z^2; \phi_9 = z^3; \phi_{10} = (z - z_E)^{7/2};$  and  $\phi_{10+j} = z^{3+j}, j = 1, 2, \dots,$  where  $z_E = 2 + i$ . Take the parametric equations of the sides as

$$\begin{aligned} AC : z &= \left( 2 + \frac{1}{\sqrt{3}} \right) t + z_A, \quad 0 \leq t \leq 2, \\ CE : z &= -\frac{4}{\sqrt{3}}(t-3)^2 e^{2i\pi/3} + z_E, \quad 2 \leq t \leq 3, \\ EG : z &= -(t-3)^2 + z_E, \quad 3 \leq t \leq 5, \\ GA : z &= -2(t-6)i + z_A, \quad 5 \leq t \leq 6, \end{aligned}$$

and evaluate  $K(z, 0)$ . (Levin, Papamichael and Sideridis, 1978; Papamichael and Kokkinos, 1981.)

PROBLEM 12.7.8. Consider the octagonal region in Fig. 12.7.4. Since this region has fourfold symmetry about the origin, show that the orthonormal basis set is  $\left\{ z^{2(j-1)} \right\}_{j=1}^N$ , and the AB is given by

$$\phi_1 = \left( \frac{z}{z^2 - 100} \right)'; \quad \phi_2 = \left( \frac{z}{z^2 + 100} \right)';$$

$$\phi_{2+j} = (z - z_j)^{-1/3}, \quad j = 1, 2; \quad \phi_5 = 1; \quad \phi_{5+j} = (z - z_j)^{1/3}, \quad j = 1, 2;$$

$$\phi_{7+j} = (z - z_j)^{5/3}, \quad j = 1, 2; \quad \phi_{9+j} = z^{2j}, \quad j = 1, 2, \dots.$$

Take the parametric equations of the sides as

$$LA: z = 2it^3 + z_1, \quad -1 \leq t \leq 0,$$

$$AB: z = 2t^3 + z_1, \quad 0 \leq t \leq 1,$$

$$BD: z = t^3 z_D + (1-t)^3 z_B, \quad 0 \leq t \leq 1,$$

$$DF: z = t^3 z_F + (1-t)^3 z_D, \quad 0 \leq t \leq 1,$$

$$FG: z = -2it^3 + z_2, \quad -1 \leq t \leq 0,$$

$$GH: z = -2t^3 + z_2, \quad 0 \leq t \leq 1,$$

$$HK: z = t^3 z_K + (1-t)^3 z_H, \quad 0 \leq t \leq 1,$$

$$KL: z = t^3 z_L + (1-t)^3 z_K, \quad 0 \leq t \leq 1,$$

and determine  $K(z, 0)$ . (Levin, Papamichael and Sideridis, 1978.)

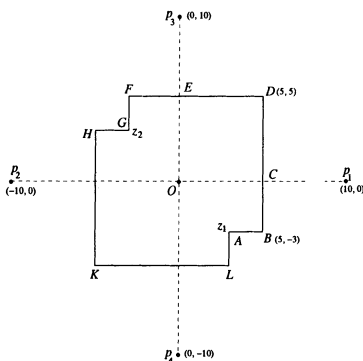


Fig. 12.7.4.

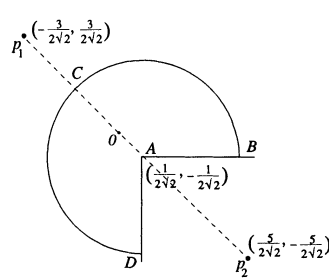


Fig. 12.7.5.

PROBLEM 12.7.9. Consider the circular sector of radius 1 and angle  $3\pi/2$  (Fig. 12.7.5). Show that the AB is given by

$$\phi_j = \left( \frac{z}{z - p_j} \right)', \quad j = 1, 2; \quad \phi_3 = (z - z_A)^{-1/3}; \quad \phi_4 = 1;$$

$$\phi_5 = (z - z_A)^{1/3}; \quad \phi_6 = z; \quad \phi_7 = (z - z_A)^{5/3}; \quad \phi_8 = z^2;$$

$$\begin{aligned}\phi_9 &= (z - z_a)^{7/3}; & \phi_{10} &= z^3; & \phi_{11} &= (z - z_A)^{11/3}; \\ \phi_{11+j} &= z^{3+j}, & j &= 1, 2, \dots.\end{aligned}$$

Compute  $K(z, 0)$  by taking the parametric equation of the arc  $BCD$  as  $z = z_A + e^{it}$ ,  $0 \leq t \leq 3\pi/2$ , and of the sides  $AB$  and  $DA$  as  $z = t^3 + (1 - 3t + 3t^2) z_A$  and  $z = (1 - 3t + 3t^2) z_A - i(1 - t)^3$ ,  $0 \leq t \leq 1$ , respectively. (Levin, Papamichael and Sideridis, 1978.)

**PROBLEM 12.7.10.** Let  $G_{ab} = \{(x, y) : |x| < a < 1, |y| < b < 1\}$  denote a rectangular region. Consider the doubly connected region  $\Omega$  which is a rectangle in a circle (Fig. 12.7.6) and defined by

$$\Omega = \{z : |z| < 1\} \cap \text{compl}(\bar{G}_{ab}).$$

If  $a \neq b$ , the region  $\Omega$  has fourfold symmetry. Show that the four singular functions  $\phi_{rj}(z)$  can be combined into two functions  $\tilde{\phi}_{rj}(z) = \phi_{rj}(z) + e^{i\theta_j}$ ,  $j = 1, 2$ , where  $r$  is defined in (12.6.18), and  $\theta_j$  are chosen such that  $e^{i\pi} \tilde{\phi}_{rj}(e^{i\pi} z) = \tilde{\phi}_{rj}(z)$ . If  $a = b$ , the region  $\Omega$  has eightfold symmetry. Show that for each value of  $r$  the four functions  $\phi_{rj}(z)$ ,  $j = 1, 2, 3, 4$ , can be combined into a single function of the same form as (12.6.19), and in each case the monomial basis set can be taken as  $\{z, z^{\pm(2j+1)}\}$ ,  $j = 1, 2, \dots$  (Papamichael and Kokkinos, 1984.)

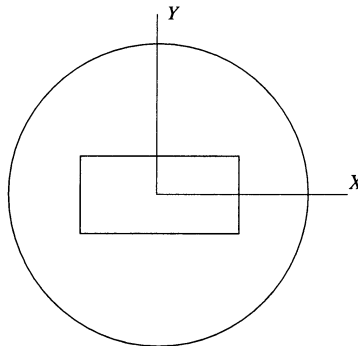


Fig. 12.7.6

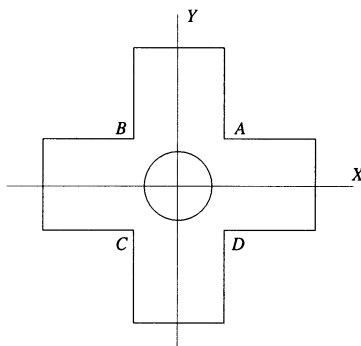


Fig. 12.7.7.

**PROBLEM 12.7.11.** Let  $G_{ab}$  be the cross-shaped region defined by (12.6.20). We shall consider the circle-in-a-cross region  $\Omega$  (Fig. 12.7.7) defined by

$$\Omega = G_{ab} \cap \{z : |z| > c\}.$$

Let  $z_j, j = 1, 2, 3, 4$ , denote the four corners  $A, B, C, D$  of the outer boundary. Show that the singular functions associated with the branch point singularities at these points  $z_j$  are  $\phi_{rj}(z) = (z - z_j)^{r-1}$ , where  $r$  is defined in (12.6.18). Use the symmetry to show that these four functions can be combined into a single function  $\tilde{\phi}_{rj}(z)$  of the form (12.6.21), and that the AB is formed by the monomial basis set  $z^{(-1)^{j+1}(2j+1)}$  plus the functions  $\tilde{\phi}_{rj}(z)$  with  $r = 2/3, 4/3, 8/3, 10/3$ . (Papamichael and Kokkinos, 1984.)

REFERENCES USED: Carleman (1916), Copson (1975), Gaier (1964), Lehman (1957), Hough and Papamichael (1981, 1983), Levin, Papamichael and Sideridis (1978), Lewy (1950), Lichtenstein (1911), Papamichael and Kokkinos (1981, 1982, 1984), Papamichael, Warby and Hough (1983, 1986), Papamichael and Warby (1984), Radon (1919), Reichel (1985), Warschawski (1932, 1955).

# Chapter 13

---

## Multiply Connected Regions

---

We shall discuss some existence and uniqueness theorems for the conformal mappings of multiply connected regions onto canonical regions. The numerical method presented here is based on Mikhlin's integral equation formulation on the boundary, which is a Fredholm integral equation of the second kind and has a unique periodic solution. Then a numerical method, called Mayo's method, that uses a fast Poisson solver for the Laplacian (Mayo 1984) is employed to determine the mapping function in the interior of the region which can be simply, doubly, or multiply connected, with accuracy even near the boundary. This method, in fact, computes the derivatives of the mapping function in the first application and the mapping function itself if applied twice.

As we have seen, most of the methods for conformal mapping compute the boundary correspondence function only. Thus, the problem of finding the mapping function in the interior (or exterior) is reduced to that of evaluating certain integrals in the interior (or exterior) of the region. But these integrals are often difficult to compute directly because of (i) the time consumed in evaluating the kernels at many interior (or exterior) points, and (ii) the difficulty in evaluating the mapping function accurately near the boundary where it is mostly needed since the kernels become unbounded at points near the boundary due to the presence of pole-type singularities (see §10.4, 10.6). Mayo's method presented here overcomes these two difficulties. In fact, this method embeds the multiply connected region to be mapped into a rectangular region, computes the integrals on the boundary of this rectangle, and finally evaluates the mapping function at all points of the region to second order accuracy.

The choice of Mikhlin's integral equation reduces the conformal mapping problem to that of a Dirichlet problem for simply connected regions. For

regions of higher connectivity it reduces the problem to a modified Dirichlet problem which is an elliptic boundary value problem for which the boundary values are prescribed only up to additive constants on all but one of the boundary contours, and the constants are determined by the condition that the problem must be single-valued in the region.

---

### 13.1. Existence and Uniqueness

Let  $\Omega$  denote a multiply connected region of connectivity  $n + 1$ ,  $n = 0, 1, \dots$ , such that a Jordan contour  $\Gamma_0$  contains  $n$  Jordan contours  $\Gamma_j$ ,  $j = 1, 2, \dots, n$ , in its interior and the origin is an interior point of  $\Gamma_1$  (Fig. 13.1.1). The connectivity is taken as  $n + 1$  simply because the value of  $n$  tells the number of ‘holes’ inside  $\Gamma_0$ . The boundary of the multiply connected region shall be

denoted by  $\Gamma = \partial\Omega \left( = \bigcup_{j=0}^n \Gamma_j \right)$ .

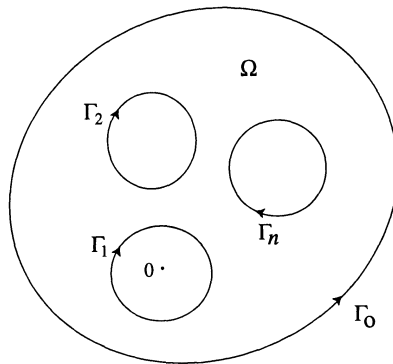


Fig. 13.1.1. An  $(n + 1)$ -connected region.

We shall define some canonical regions, besides the unit disk and the annulus. A region with parallel cuts (slits) is understood to be a region obtained from the extended complex plane  $\mathbb{C}_\infty$  by removing several mutually parallel line segments inclined at an angle  $\theta$  to the positive real axis (we call them parallel finite cuts of inclination  $\theta$ ). By a region with spiral cuts we mean a region which is obtained by removing several logarithmic spirals from  $\mathbb{C}_\infty$ . Let  $\alpha$  and

$c$  be real constants. The equation

$$\Im \{ e^{-i\alpha} \log w \} = c \quad (13.1.1)$$

represents a logarithmic spiral in the  $w$ -plane with the origin as its asymptotic point, where  $\alpha$  is the angle between the logarithmic spiral and a fixed ray emanating from the origin ( $\alpha$  is known as the oblique angle of the spiral cuts). For  $a = 0$  the logarithmic spiral reduces to a ray  $\arg\{w\} = c$  emanating from the origin, and for  $\alpha = \pi/2$  it becomes a circle  $|w| = e^c$  (unit circle for  $c = 0$ ). The following theorem establishes the existence and uniqueness of the conformal mapping from a multiply connected region onto a region with parallel or spiral cuts. A result due to Hilbert is as follows:

**THEOREM 13.1.1.** *Let  $\Omega$  be a multiply connected region in the extended  $z$ -plane  $\mathbb{C}_\infty$  and  $\theta$  a real number. Then there exists a univalent meromorphic function  $w = f_\theta(z)$  in  $\Omega$  such that (i) it maps  $\Omega$  conformally onto a region with parallel finite cuts of inclination  $\theta$  in the extended  $w$ -plane; and (ii) it maps a given point  $z = a$  into  $w = \infty$ , and in a neighborhood of  $z = a$  the function  $f_\theta(z)$  may be represented by a series of the form*

$$f_\theta(z) = \frac{1}{z-a} + a_1(z-a) + \cdots, \quad (13.1.2)$$

or

$$f_\theta(z) = z + \frac{a_1}{z} + \cdots, \quad (13.1.3)$$

according as  $a$  is finite or not. Each of these functions is unique for the region  $\Omega$ .

A similar theorem holds if the image of  $\Omega$  has spiral cuts of oblique angle  $\alpha$  in the  $w$ -plane. The mapping functions are the same as (13.1.2) and (13.1.3) which in this case are denoted by  ${}_a$  instead of  $f_\theta$ . A proof of this theorem can be found in Goluzin (1969, p.213) or Wen (1992, p.118). Two results on the existence and uniqueness of conformal mapping of a multiply connected region  $\Omega$  contained inside the unit disk  $|z| < 1$  onto a region inside the unit disk  $|w| < 1$  with concentric finite circular cuts and inside an annulus  $r < |z| < 1$  are as follows:

**THEOREM 13.1.2.** *Let  $\Omega$  be a multiply connected region of connectivity  $(n+1)$  inside the unit disk  $|z| < 1$  where  $\Gamma = |z| = 1$  is the boundary*

component of  $\Omega$  and  $0 \in \Omega$ . Then there exists a unique, univalent analytic function  $w = f(z)$  in  $\Omega$  such that (i) it maps  $\Omega$  conformally onto a region  $G$  inside the unit disk  $|w| < 1$  which has  $n$  circular cuts centered at  $w = 0$  and (ii) it maps the unit circle  $|z| = 1$  conformally onto the unit circle  $|w| = 1$  with  $f(0) = 0$  and  $f(1) = 1$ .

**THEOREM 13.1.3.** Let  $\Omega$  be a multiply connected region of connectivity  $n + 1$  inside the annulus  $r < |z| < 1$  where  $\Gamma_0 = \{|z| = 1\}$  and  $\Gamma_1 = \{|z| = r\}$  are the two boundary components of  $\Omega$ . Then there exists a unique univalent analytic function  $w = f(z)$  in  $\Omega$  such that (i) it maps  $\Omega$  conformally onto a region  $G$  in the  $w$ -plane formed by removing  $n$  concentric circular arcs centered at  $w = 0$  from the annulus  $\rho < |w| < 1$ , where  $0 < \rho < 1$ , and (ii) it maps the unit circle  $\Gamma_0$  conformally onto the unit circle  $|w| = 1$ , and the circle  $\Gamma_1$  onto the circle  $|w| < \rho$ , with  $f(1) = 1$ .

A region whose boundary consists of a finite union of circles is known as a *circular region*. We shall consider the conformal mapping of a multiply connected region  $\Omega$  onto a circular region  $G$ . This can be accomplished by a chain of two conformal mappings: (i) that of  $\Omega$  onto a region  $G$  with parallel cuts and (ii) that of  $G$  onto a circular region  $\Delta$ . The former mapping is already established in Theorem 13.1.1. We need to discuss only the latter mapping. We shall state the uniqueness theorem for conformal mappings onto circular regions; the existence of this mapping can be proved by the continuity method (see Wen, 1992, p.118).

**LEMMA 13.1.1.** Let  $D$  be an  $(n + 1)$ -connected circular region obtained by removing  $n$  disks from the unit disk  $|z| < 1$ , with  $0 \in D$ , and let  $\Delta$  be an  $(n + 1)$ -connected circular region obtained by removing  $n$  disks from the unit disk  $|w| < 1$ , with  $0 \in \Delta$ . If  $w = f(z)$  maps  $D$  conformally onto  $\Delta$  such that (i)  $f(0) = 0$ ,  $f(1) = 1$ , and (ii)  $f(\zeta_j) = \zeta_j$ ,  $j = 1, 2, 3$ , where  $\zeta_j$  are three distinct points on  $|z| = 1$ , then  $f(z) = z$ .

This lemma establishes the identity mapping; its proof is available in Wen (1992, p.118).

**THEOREM 13.1.4.** Let  $\Omega$  be a multiply connected region in the extended  $z$ -plane. Then there exists at most one univalent meromorphic

function  $w = f(z)$  in  $\Omega$ , which maps  $\Omega$  conformally onto a circular region  $G$  in the  $w$ -plane, such that the point  $z = \infty$  goes into  $w = \infty$ , and in a neighborhood of  $z = \infty$  the function  $f(z)$  has the series expansion (13.1.2).

**PROOF.** Suppose that  $w = f_1(z)$  and  $w = f_2(z)$  are two univalent meromorphic functions in  $\Omega$ , each of which satisfies the hypothesis of the theorem. Then the function  $f_2(f_1^{-1}(w))$ , where  $z = f_1^{-1}(w)$  denotes the inverse of  $w = f_1(z)$ , is univalent and meromorphic in the region  $G$ , maps  $G$  onto another circular region  $G'$  in the  $\zeta$ -plane, maps the point  $w = \infty$  into the point  $\zeta = \infty$ , and in the neighborhood of the point  $w = \infty$  has the series expansion

$$f_2(f_1^{-1}(w)) = w + \frac{b_1}{w} + \dots \quad (13.1.4)$$

Now we must show that if  $\zeta = F(w)$  is the function that maps the region  $G$  conformally onto  $G'$ , such that  $F(\infty) = \infty$ , and has the series representation (13.1.4) in the neighborhood of the point  $w = \infty$ , then  $F(w) = w$ . In fact, by using linear transformations of  $w$  and  $\zeta$ , we can map the regions  $G$  and  $G'$ , respectively, onto circular regions  $D$  and  $\Delta$  of Lemma 13.1.1. The univalent function obtained from these linear transformations satisfies conditions (i) and (ii) of this lemma and thus represents an identity mapping. Hence,  $\zeta = F(w)$  is a linear transformation with  $F(\infty) = \infty$ , and therefore,  $F(w) = aw + b$ . But since  $F(w)$  has an expansion of the form (13.1.4) in the neighborhood of  $w = \infty$ , we require that  $a = 1$  and  $b = 0$ , i.e.,  $F(w) = w$ . It proves that  $f_2(f_1^{-1}(w)) = w$ , and hence,  $f_1(z) \equiv f_2(z)$ . ■

The function  $f_\theta(z)$ , defined by (13.1.2) or (13.1.3), can be evaluated for arbitrary  $\theta$  from the equation

$$f_\theta(z, a) = e^{i\theta} [\cos \theta f_0(z, a) - i \sin \theta f_{\pi/2}(z, a)]. \quad (13.1.5)$$

The difference  $d(z)$  between the two sides of Eq (13.1.5) is regular in the region  $\Omega$ , and  $d(a) = 0$ . Also, all values taken by  $d(z)$  on any contour  $\Gamma_j$  lie on a circle (in the extended sense)  $\Im \{e^{-i\theta} w\} = c$ . The above equation also enables us to compute the function  $f_\theta(z, a)$  for arbitrary  $\theta$  if we know the functions  $f_0(z, a)$  and  $f_{\pi/2}(z, a)$ . To get these relations in a symmetric form, we set

$$P(z, a) = \frac{1}{2} [f_{\pi/2}(z, a) - f_0(z, a)], \quad Q(z, a) = \frac{1}{2} [f_{\pi/2}(z, a) + f_0(z, a)]. \quad (13.1.6)$$

Since  $\Im \{f_0(z, a)\} = \text{const}$ , and  $\Im \{f_{\pi/2}(z, a)\} = \text{const}$  on  $\Gamma_j, j = 0, 1, \dots, n$ , for fixed  $a \in \Omega$ , i.e., since

$$f_0(z, a) = \overline{f_0(z, a)} + \text{const}, \quad f_{\pi/2}(z, a) = -\overline{f_{\pi/2}(z, a)} + \text{const},$$

we have on  $\Gamma_j$ , in view of (13.1.6),

$$P(z, a) = -\overline{Q(z, a)} + \overline{q_j(a)}, \quad (13.1.7)$$

where  $q_j(a)$  are independent of  $z \in \Gamma_j$ . Now, for fixed  $a, b \in \Omega$ , we set

$$\begin{aligned} P(z, a, b) &= \frac{1}{2} [\log f_{\pi/2}(z, a, b) - \log f_0(z, a, b)], \\ Q(z, a, b) &= \frac{1}{2} [\log f_{\pi/2}(z, a, b) + \log f_0(z, a, b)]. \end{aligned} \quad (13.1.8)$$

Then

$$\begin{aligned} P'_z(z, a, b) &= \frac{d}{dz} P(z, a, b) = \overline{P(b, z)} - \overline{P(a, z)}, \\ Q'_z(z, a, b) &= \frac{d}{dz} P(z, a, b) = Q(b, z) - Q(a, z). \end{aligned} \quad (13.1.9)$$

Since  $\Im \{\log f_0(z, a, b)\} = \text{const}$ , and  $\Im \{\log f_{\pi/2}(z, a, b)\} = \text{const}$  on  $\Gamma_j$ , from (13.1.8) we find that

$$P(z, a, b) = -\overline{Q(z, a, b)} + \overline{q_j(a, b)}, \quad (13.1.10)$$

where  $q_j(a, b)$  are independent of  $z \in \Gamma_j$ . We also consider an integral on the entire boundary  $\Gamma$  of the region  $\Omega$  in the positive direction:

$$\begin{aligned} I_1 &= \frac{1}{2i\pi} \int_{\Gamma} P(t, z) P'_t(t, a, b) dt \\ &= \sum_{j=0}^n \frac{1}{2i\pi} \int_{\Gamma_j} P(t, z) dP(t, a, b) \\ &= \sum_{j=0}^n \frac{1}{2i\pi} \int_{\Gamma_j} \left[ -\overline{Q(t, z)} + \overline{q_j(z)} \right] d \left( -\overline{Q(t, a, b)} + \overline{q_j(a, b)} \right) \\ &= \sum_{j=0}^n \frac{1}{2i\pi} \int_{\Gamma_j} \overline{Q(t, z)} d \left( \overline{Q(t, a, b)} \right) \\ &= -\frac{1}{2i\pi} \int_{\Gamma} Q(t, z) Q'_t(t, a, b) dt, \end{aligned}$$

because the function  $Q(t, a, b)$  is single-valued on each contour  $\Gamma_j$ . Since  $Q(t, z)$  and  $Q(t, a, b)$  have simple poles in  $\Omega$  at the point  $z$  and the points  $a$  and  $b$ , respectively, by using the residue theorem, we get  $I_1 = -\overline{Q'_z(z, a, b)} - \overline{Q(a, z)} + \overline{Q(b, z)}$ . But since  $I_1 = 0$ , we obtain the formula

$$Q'_z(z, a, b) = Q(b, z) - Q(a, z). \quad (13.1.11)$$

Similarly, if we consider the integral  $I_2 = \frac{1}{2i\pi} \int_{\Gamma} Q(t, z) P'_t(t, a, b) dt$  and follow the above technique, we obtain the formula

$$P'_z(z, a, b) = \overline{P(b, z)} - \overline{P(a, z)}. \quad (13.1.12)$$

Note that the functions  $P(z, a)$  and  $Q(z, a)$  are themselves not necessarily analytic functions of  $a$ , as shown by taking the region  $\Omega$  as  $|z| > 1$ . Then, in this case

$$P(z, a) = \frac{1}{1 - |a|^2} \frac{z - a}{1 - \bar{a}z}, \quad Q(z, a) = \frac{1}{1 - |a|^2} \frac{1 - \bar{a}z}{z - a}.$$

In the next section we shall use the above formulas to solve the Dirichlet problem and construct Green's function for the multiply connected region  $\Omega$ .

## 13.2. Dirichlet Problem

Let  $\Omega$  be an  $(n+1)$ -connected region in the finite  $z$ -plane, bounded by  $(n+1)$  Jordan contours  $\Gamma_j$ ,  $j = 0, 1, \dots, n$  (Fig. 13.1.1). Let  $u_j(z)$ ,  $j = 0, 1, \dots, n$ , be a set of harmonic functions that have the boundary values  $u_j = \delta_{jk}$  on  $\Gamma_j$ ,  $k = 0, 1, \dots, n$  (i.e., the boundary value is 1 on  $\Gamma_j$  and zero on  $\Gamma_k$ ,  $k \neq j$ ), and satisfy the relation  $\sum_{j=0}^n u_j(z) = 1$  because the sum on the right side is

a harmonic function and it must be 1 everywhere on the boundary  $\Gamma = \partial\Omega$ . The conjugate harmonic function  $v_j(z)$ ,  $j = 0, 1, \dots, n$ , in general, is not single-valued. Let  $[\Delta v_j(z)]_{\Gamma_k}$  denote the increment in the function  $v_j(z)$  as  $z$  traverses the contour  $\Gamma_k$  in the positive sense (marked by arrowheads in Fig. 13.1.1), and suppose that

$$[\Delta v_j(z)]_{\Gamma_k} = 2\pi p_{k,j}, \quad k, j = 0, 1, \dots, n, \quad (3.2.1)$$

where  $p_{k,j}$  are constants. Then the set of analytic functions  $w_j(z) = u_j(z) + i v_j(z)$ ,  $j = 0, 1, \dots, n$ , satisfies the following conditions:

- (i)  $w_j(z) = -\overline{w_j(z)} + c_{k,j}$  on  $\Gamma_k$ , where  $c_{k,j}$  is a constant;
- (ii)  $[\Delta w_j(z)]_{\Gamma_k} = 2i\pi p_{k,j}$ ;
- (iii)  $w'_j(z)$  is regular in  $\bar{\Omega}$ .

Now consider the integrals

$$I_1 = \frac{1}{2i\pi} \int_{\Gamma} P(t, u) w'_j(t) dt, \quad I_2 = \frac{1}{2i\pi} \int_{\Gamma} P(t, u, v) w'_j(t) dt. \quad (13.2.3)$$

In view of Cauchy's theorem, each integral is equal to zero. We shall use the formulas (13.2.2), (13.1.7), and (13.1.10) to obtain

$$\begin{aligned} I_1 &= \frac{1}{2i\pi} \int_{\Gamma} P(t, u) dw_j(t) = - \sum_{j=0}^n \frac{1}{2i\pi} \int_{\Gamma_j} \left( -\overline{Q(t, u)} + \overline{q_j(u)} \right) \overline{dw_j(t)} \\ &= \sum_{j=0}^n \frac{1}{2i\pi} \int_{\Gamma_j} (-Q(t, u) + q_j(u)) dw_j(t) \\ &= - \overline{\frac{1}{2i\pi} \int_{\Gamma} Q(t, u) w'_j(t) dt} + \overline{\sum_{j=0}^n q_j(u) p_{k,j}} \\ &= -\overline{w'_j(u)} + \overline{\sum_{j=0}^n q_j(u) p_{k,j}}, \end{aligned}$$

which gives

$$w'_j(u) = \sum_{j=0}^n q_j(u) p_{k,j}, \quad k = 0, 1, \dots, n. \quad (13.2.4)$$

Similarly, for the integral  $I_2$  by using integration by parts we get

$$\begin{aligned} I_2 &= - \overline{\frac{1}{2i\pi} \int_{\Gamma} Q(t, u, v) w'_j(t) dt} + \overline{\sum_{j=0}^n q_j(u, v) p_{k,j}} \\ &= -\overline{w_j(u) - w_j(v)} + \overline{\sum_{j=0}^n q_j(u, v) p_{k,j}}, \end{aligned}$$

which yields

$$w_j(v) - w_j(u) = \sum_{j=0}^n q_j(u, v) p_{k,j}, \quad k = 0, 1, \dots, n. \quad (13.2.5)$$

Formulas (13.2.4) and (13.2.5) express the solution of the Dirichlet problem for a multiply connected region in terms of the functions  $q_j(u)$  and  $q_j(u, v)$  which define univalent mappings.

To find Green's function  $\mathcal{G}(z, z_0)$  for the region  $\Omega$ , let the corresponding analytic function be denoted by  $F(z, z_0)$  so that  $\mathcal{G}(z, z_0) = \Re\{F(z, z_0)\}$ . The function  $F(z, z_0)$  has a logarithmic singularity at the point  $z = z_0 \in \Omega$  and is not single-valued in  $\Omega$ . The function  $F(z, z_0)$  has the following properties:

- (a)  $F(z, z_0) = -\overline{F(z, z_0)} + \text{const on } \Gamma_j$ ;
- (b)  $[\Delta F(z, z_0)]_{\Gamma_j} = -2i\pi w_j(z_0)$ , where  $w_j$  is defined in (13.2.2);
- (c)  $F'(z, z_0)$  is regular in  $\Omega$  except at a simple pole  $z = z_0$  with residue  $-1$ .

Now, consider the integrals

$$I_3 = \frac{1}{2i\pi} \int_{\Gamma} P(t, u) F'_z(t, z_0) dt,$$

and

$$I_4 = \frac{1}{2i\pi} \int_{\Gamma} P(t, u, v) F'_z(t, z_0) dt,$$

where  $u, v \in \Omega$ . Evaluating these integrals first by using the residue theorem and then using (13.1.7), (13.1.10) and the above mentioned property (b), we obtain

$$\begin{aligned} F'_z(u, z_0) &= Q(z_0, u) + \overline{P(z_0, u)} - \sum_{j=0}^n q_j(u) w_j(z_0), \\ F(v, z_0) - F(u, z_0) &= Q(z_0, u, v) + \overline{P(z_0, u, v)} - \sum_{j=0}^n q_j(u, v) w_j(z_0). \end{aligned} \quad (13.2.6)$$

After separating the real parts in (13.2.6), we find that

$$\mathcal{G}(v, z_0) - \mathcal{G}(u, z_0) = \log \left| f_{\pi/2}(z_0, u, v) \right| - \sum_{j=0}^n \log \rho_j(u, v) \cdot w_j(z_0), \quad (13.2.7)$$

where  $\rho_j(u, v)$  are the radii of the circles on which lie the images of the contours  $\Gamma_j$  for  $j = 0, 1, \dots, n$  under the mapping  $w = f_{\pi/2}(z, u, v)$ . Using the

symmetry property of Green's functions and replacing  $z_0$  by  $z$  in (13.2.7), we also get

$$\mathcal{G}(v, z_0) - \mathcal{G}(u, z_0) = \Re \{ f_{\pi/2}(z_0, u, v) \} - \sum_{j=0}^n \log \rho_j(u, v) \cdot w_j(z_0). \quad (13.2.8)$$

Together the two formulas (13.2.7) and (13.2.8) yield

$$F(z, v) - F(z, u) = \log f_{\pi/2}(z_0, u, v) - \sum_{j=0}^n \log \rho_j(u, v) \cdot w_j(z_0), \quad (13.2.9)$$

which is the analytic representation of functions that are meromorphic in the region  $\Omega$  and real on its boundary  $\Gamma$ . These functions are known as Schottky functions.

### 13.3. Mikhlin's Integral Equation

As we have seen in §9.1, the function  $w = f(z)$  that maps a simply connected region  $D$  with Jordan boundary  $\Gamma$  conformally onto the unit disk  $|w| < 1$ , such that a point  $z_0 \in D$  goes into the point  $w = 0$ , can be written in the form  $f(z) = (z - z_0)g(z)$ , where  $g(z)$  is analytic and nonzero in  $D$ . The function  $F(z) = \log g(z)$  is also analytic in  $D$ . If  $\zeta \in \Gamma$ , then  $|f(\zeta)| = |\zeta - z_0| |g(\zeta)| = 1$ , and hence,  $\Re \{F(\zeta)\} = \log |g(\zeta)| = -\log |\zeta - z_0|$ . The problem of finding the function  $F(z)$  reduces to solving the Laplace equation with the Dirichlet boundary value  $-\log |\zeta - z_0|$ , which determines  $\Re \{F(z)\}$ . This, followed by finding the conjugate harmonic function, leads to determining  $g(z) = e^{F(z)}$  which finally yields the mapping function  $f(z)$ . This formulation is the same as in (9.1.1) in Symm's method.

In the case of a doubly connected region  $\Omega$  in the  $z$ -plane bounded by the Jordan contours  $\Gamma_0$  and  $\Gamma_1$ ,  $\Gamma_1 \subset \Gamma_0$ , such that  $0 \in \Gamma_1$ , let the function  $w = f_\Omega(z)$  map  $\Omega$  conformally onto the annulus  $A(\rho, 1)$ . Since the function  $f_\Omega(z)$  is bounded and nonzero in  $\Omega$ , the function  $\log f_\Omega(z)$  is nonsingular in  $\Omega$ . Let

$$F_\Omega(z) = \log \frac{f_\Omega(z)}{z} = \log f_\Omega(z) - \log z, \quad (13.3.1)$$

where the function  $F_\Omega(z)$  is single-valued and regular in  $\Omega$ . If  $z$  traverses  $\Gamma_0$  and  $\Gamma_1$  in the positive direction, both  $\arg \{f_\Omega(z)\}$  and  $\arg \{z\}$  increase by  $2\pi$ .

Let  $g(z) = \Re\{F_\Omega(z)\}$ . Since the contours  $\Gamma_0$  and  $\Gamma_1$  are mapped onto circles, it is easy to find the boundary values of  $g(z)$ . Since  $|f_\Omega(\zeta)| = \zeta$  for  $\zeta \in \Gamma_1$  and  $|f_\Omega(\zeta)| = 1$  for  $\zeta \in \Gamma_0$ , we find that

$$g(z) = \begin{cases} \log \rho - \log |\zeta|, & \zeta \in \Gamma_1, \\ -\log \zeta, & \zeta \in \Gamma_0, \end{cases} \quad (13.3.2)$$

which is the same as (11.2.4). Thus, the value of  $\rho$  (conformal modulus) is determined under the condition that the function  $h(z)$ , conjugate to  $g(z)$ , must be single-valued, i.e., it must satisfy the condition (11.2.8). The mapping function  $f_\Omega$  is then determined from (11.2.1).

We shall consider the mapping of a multiply connected region  $\Omega$  onto the slit unit disk by the function  $w = w(z)$ . Let the region  $\Omega$  be  $(n+1)$ -connected,  $n \geq 2$ , and bounded by Jordan contours  $\Gamma_j$ ,  $j = 0, 1, \dots, n$ . We shall assume that a point  $z_0 \in \Omega$  is mapped into the point  $w = 0$ . As in the case of a simply connected region, the mapping function can be written as  $w(z) = (z - z_0) g(z)$ , where  $g(z)$  is analytic and nonzero in  $\Omega$ . Thus, if  $W(z) = \log g(z)$ , then  $u(z) = \Re\{W(z)\} = -\log |\zeta - z_0|$ ,  $\zeta \in \Gamma_0$ . Now, suppose that the contours  $\Gamma_k$ ,  $k = 1, \dots, n$ , are mapped onto the circles  $|w| = \rho_k$ , i.e.,  $|w(\zeta)| = \rho_k$  for  $\zeta \in \Gamma_k$ . Then

$$u(z) = \begin{cases} -\log |\zeta - z_0|, & \zeta \in \Gamma_0, \\ \log \rho_k - \log |\zeta - z_0|, & \zeta \in \Gamma_k, k = 1, \dots, n. \end{cases} \quad (13.3.3)$$

The problem of determining  $u(z)$  reduces to solving a Dirichlet problem, and the mapping function  $w(z)$  can be determined from  $w(z) = e^{u(z)+iv(z)}$ , where  $v(z) = \Im\{W(z)\}$  must be single-valued.

As in §11.3, we shall assume that the mapping problem can be solved in terms of the integral of a dipole density function  $\mu(s)$  on the boundary  $\Gamma \equiv \partial\Omega$ , which is the real part of the Cauchy integral with density  $\mu$ , i.e.,

$$\begin{aligned} u(t) &= \Re\left\{\frac{1}{2i\pi} \int_{\Gamma} \frac{\mu(z)}{\zeta - z} dz\right\} \\ &= \frac{1}{2i\pi} \int_{\Gamma} \mu(s) \frac{\partial}{\partial n_s} \log r_{st} ds, \end{aligned} \quad (13.3.4)$$

where  $z = x + iy = \gamma(t)$ ,  $r_{st} = |\zeta - z|$ , and  $\zeta = \gamma(s)$ ,  $0 \leq s, t \leq L$  (as in (11.3.1)). Note that if  $\Omega$  is simply connected, then we have an ordinary Dirichlet

problem with boundary data  $\mu(\zeta) = -\log |\zeta - z_0|$ ,  $\zeta \in \Gamma$  and  $z_0 \in \Omega$ , and the density function  $\mu(s)$  is obtained by solving the integral equation

$$\mu(t) + \frac{1}{\pi} \int_{\Gamma} \mu(s) \frac{\partial}{\partial n_s} \log r_{st} ds = -2 \log |\zeta - z_0|. \quad (13.3.5)$$

But in the case of a multiply connected region a modified Dirichlet problem is solved, where we must determine the density function  $\mu(s)$  as well as the radii  $\rho_k$  which appear in (13.3.3). Let  $\mu(t)$  denote the solution of the integral equation (Mikhlin, 1957)

$$\mu(t) + \frac{1}{\pi} \int_{\Gamma} \left[ \mu(s) \frac{\partial}{\partial n_s} \log r_{st} - \chi(s, t) \right] ds = -2 \log |\zeta - z_0|, \quad (13.3.6)$$

where

$$\chi(s, t) = \begin{cases} 1 & \text{if } s, t \text{ lie on the same contour,} \\ 0 & \text{otherwise.} \end{cases}$$

The radii (conformal moduli)  $\rho_k$  are given by

$$\rho_k = \frac{1}{\pi} \int_{\Gamma} \mu(s) ds. \quad (13.3.7)$$

Eq (13.3.6) is known as *Mikhlin's integral equation*. It is a Fredholm integral equation of the second kind whose kernel is given by

$$M(s, t) = \frac{\partial}{\partial n_s} \log r_{st} \in L^2[0, L],$$

which is bounded, because we have  $M(s, t) = 0.5 \kappa(s)$  for  $s, t \in \Gamma$ , where  $\kappa(s)$  is the curvature of the contour at  $s$ .

The numerical solution of Eq (13.3.6) is obtained by using a Nyström method (quadrature) with the trapezoidal rule (see, Atkinson, 1976; Delves and Mohamed, 1985; Mayo, 1986)

$$\mu_n(t_i) + \frac{1}{\pi} \sum_j \left[ \frac{\partial}{\partial n_{t_j}} \log r_{t_i, t_j} + \chi(t_i, t_j) \right] \mu_n(t_j) h = d(t_i), \quad (13.3.8)$$

where  $h$  is the mesh size,  $d(t_i) = -2 \log |t_i - s_0|$ , and  $s_0 = \gamma(z_0)$ . The mesh points are taken as equispaced points with respect to some boundary parameter, but the points used as nodes to compute the above quadrature are independent of the mesh points which are used for a fast Poisson solver (see next two sections).

Since the trapezoidal rule is highly accurate on periodic regions, the accuracy of the solution of Mikhlin's equation is the same as that of the quadrature formula (13.3.8). This equation can also be solved by the methods developed in chapters 9 and 11, and although the equation, in general, is not symmetric, it has positive real eigenvalues (Kellogg, 1929).

---

### 13.4. Mayo's Method

After the density function  $\mu(s)$  is computed by the quadrature formula (13.3.8), we must still compute the Cauchy integral

$$W(t) = \frac{1}{2\pi} \int \frac{\mu(t)}{z - t} dz$$

at points in the interior of the region  $\Omega$ . For this purpose a fast Poisson solver, developed by Mayo (1984), is used (see details in the next section). This is accomplished in the following two steps:

STEP 1. Compute

$$\Re \{W(t)\} = \frac{1}{2\pi} \int M(s, t) \mu(t) dt. \quad (13.4.1)$$

STEP 2. Compute  $\Im \{W(t)\}$ .

The details of step 1 are as follows: Embed the region  $\Omega$  in a larger region  $R$  which is a rectangle with uniform mesh in both  $x$  and  $y$  directions. There exists a fast Poisson solver for the Laplacian in a rectangle (§13.5). Then the function  $\Re \{W(t)\}$  defines another harmonic function  $\hat{u}$  at points in  $R \setminus \Omega$ . The function  $\hat{u}$  is a discontinuous extension of  $u$  from  $\Omega$  into  $R \setminus \Omega$ . Define a function

$$U(t) = \begin{cases} u(t), & t \in \Omega, \\ \hat{u}(t), & t \in R \setminus \Omega. \end{cases}$$

Then we use the fast Poisson solver to compute an approximate solution of the discrete Laplace equation  $\nabla^2 U = 0$  at all mesh points of  $R$ . Since both  $u$  and  $\hat{u}$  are harmonic, we set the Laplacian zero at those mesh points that have all four of their adjacent mesh points on the same side of the boundary. But to approximate the Laplacian at all remaining (irregular) mesh points, we take the following approach: Since both  $u$  and  $\hat{u}$  are continuous along the normal

direction but have a jump equal in magnitude to the density  $\mu$ , we evaluate the jumps in the derivatives of  $u$  and  $\hat{u}$  along the coordinate directions:

$$u_x - \hat{u}_x = \mu'(s) \frac{x'(s)}{x'(s)^2 + y'(s)^2}, \quad u_y - \hat{u}_y = \mu'(s) \frac{y'(s)}{x'(s)^2 + y'(s)^2}, \quad (13.4.2)$$

where the suffix indicates the variable of partial differentiation, and the prime denotes the derivative with respect to  $s$ . Note that these derivatives contain derivatives of  $\mu$  and those of the boundary contours. Therefore, these jumps are used to approximate the discrete difference operators at irregular mesh points (see §13.5 for details).

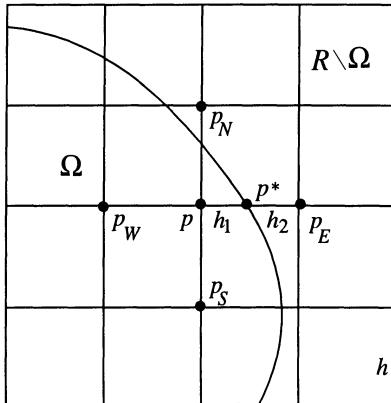


Fig. 13.4.1.

As an example, suppose that a point  $p$  is inside  $\Omega$ , but its adjacent neighbor to the right,  $p_E$ , is not inside  $\Omega$ . Let  $p^*$  denote the point where the grid line between  $p$  and  $p_E$  cuts the boundary, and let  $h_2 = |p^* - p_E|$  (Fig. 13.4.1). Using the Taylor series at  $p$  and  $p_E$ , we find that

$$\begin{aligned} \hat{u}(p_E) - u(p) &= [\hat{u}(p^*) - u(p^*)] + h_2 [\hat{u}_x(p^*) - u_x(p^*)] \\ &\quad + \frac{h_2^2}{2} [\hat{u}_{xx}(p^*) - u_{xx}(p^*)] + h u_x(p) + \frac{h^2}{2} u_{xx}(p) + O(h^3) \\ &= \{\sum(3)\} + h u_x(p) + \frac{h^2}{2} u_{xx}(p) + O(h^3), \end{aligned} \quad (13.4.3)$$

where  $\{\sum(3)\}$  denotes the sum of the first three terms on the right side which are known quantities and can be expressed in terms of the solution of the integral equation and the boundary data, whereas the remaining terms account for the

usual Taylor series. We also obtain the same kind of expression as (13.4.3) for the difference  $U(p) - U(p_E)$  except that there may be no boundary term. Thus, an approximate solution of the discrete Laplacian of  $U$  can be computed as the sum of the four difference operators at all mesh points (details in the next section). The boundary data of  $U$  are obtained by approximating the values of the integral (13.4.1) at mesh points that lie at the edge of  $R$ .

In step 2, the values of  $\Im\{W(t)\} = v(t)$  are easy to compute because, in view of the Cauchy–Riemann equations, we can express the discontinuities of  $v$  in terms of the discontinuities in  $u$ . Thus, the discrete Laplacian of  $v$  can be computed easily.

Once the discrete Laplacians of  $u$  and  $v$  are computed, we apply the fast Poisson solver twice to obtain the values of  $u$  and  $v$  at the mesh points. Thus, the solution of (13.3.8) has second-order accuracy in  $h$ .

**CASE STUDY 13.4.1.** For Cassini's oval (Fig. 9.2.1) where two different paths of the boundary are close to each other, the method described above in step 1 may fail to give very accurate results because the kernel becomes very large there. In this case (and others like it) the kernel is integrated exactly, i.e.,

$$\int_{t_{i-1}}^{t_{i+1}} M(s, t) ds = \int_{t_{i-1}}^{t_{i+1}} \frac{\partial \phi(s, t_j)}{\partial s} ds = \phi(t_{i+1}, t_j) - \phi(t_{i-1}, t_j),$$

where  $\phi = \arg\{W(t)\}$ . Then Eq (13.3.8) yields the system of equations

$$\mu(t_i) + \frac{1}{2\pi} \sum_j \hat{\phi} + h \chi(t_i, t_j) \mu(t-j) = d(t_i), \quad (13.4.4)$$

where  $\hat{\phi} = \tan^{-1} \frac{t_{i+1} - t_j}{t_{i-1} - t_j}$  is the angle between the lines joining the points  $t_{i+1}$  and  $t_{i-1}$  to the point  $t_j$ .

Mayo (1986) has considered the case of Cassini's oval

$$\Gamma = \{ [(x+c)^2 + y^2] [(x-c)^2 + y^2] = a^4 \},$$

whose polar equation is  $r(\theta) = \sqrt{c^2 \cos 2\theta + \sqrt{a^4 - c^2 \sin^2 2\theta}}$ ,  $x(\theta) = r(\theta) \cos(\theta)$ ,  $y(\theta) = r(\theta) \sin(\theta)$ , with  $c = 0.1$  and  $a = 0.43$  (Fig. 13.4.2).

Note that all Cassini's ovals in Fig. 9.2.1 (Case Study 9.2.1) have  $c = 1$ .

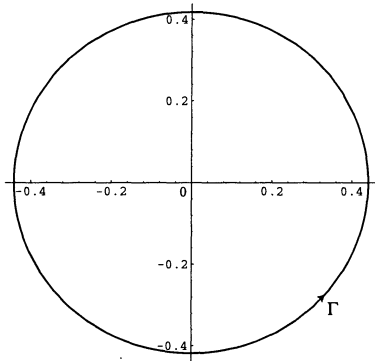


Fig. 13.4.2. Cassini's oval.

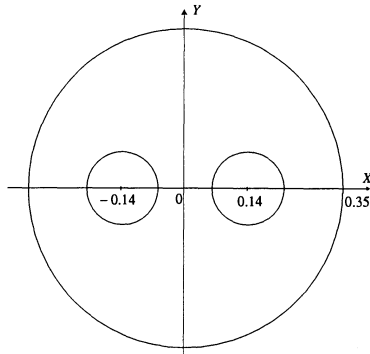


Fig. 13.4.3.

The method described above is used for this contour with 90 mesh points equispaced with respect to  $\theta$ . The exact mapping function is known (Symm, 1966, p.256). The simply connected region  $\text{Int}(\Gamma)$  is embedded in the unit square. The maximum error found was  $0.54 \times 10^{-2}$  with  $h = 1/32$ , and  $0.24 \times 10^{-2}$  with  $h = 1/64$ . ■

**CASE STUDY 13.4.2.** Consider the triply connected region bounded by the three circles  $\Gamma_0 = \{|z| = 0.35\}$ ,  $\Gamma_1 = \{|z - 0.14| = 0.08\}$ ,  $\Gamma_2 = \{|z + 0.14| = 0.08\}$  (Fig. 13.4.3). A total of 180 mesh points on the boundary  $\Gamma$  with mesh size  $h = 1/128$  were taken to solve Eq (13.3.8). The region  $\Omega$  and its image with the images of the grid lines, together with the unit circle and the slits, are given in Mayo (1986). ■

## 13.5. Fast Poisson Solver

Now we shall discuss the details of the fast Poisson solver for the Laplacian. Consider the integral equation (13.3.6) which we write as

$$\mu(t) + \frac{1}{\pi} \int_{\Gamma} M(s, t) \mu(s) ds = 2g(t), \quad t \in \Gamma, \quad (13.5.1)$$

where the kernel  $M(s, t)$  is bounded and represents the normal derivative of

Green's function for the Laplacian in the plane. In the region  $R \setminus \Omega$  we define a harmonic function  $\hat{u}$ , by using the same formula as (13.3.4) in the form

$$\hat{u}(t) = \frac{1}{2\pi} \int_{\Gamma} M(s, t), \mu(s) ds. \quad (13.5.2)$$

The function  $\hat{u}$  is a discontinuous extension of  $u$  in the region  $R \setminus \Omega$ . Let  $(x_i, y_j)$  denote the mesh points of the rectangle  $R$ , and let  $U$  be defined on  $R$  by

$$U_{ij} = \begin{cases} u(x_i, y_j), & \text{if } (x_i, y_j) \in \Omega, \\ \hat{u}(x_i, y_j), & \text{if } (x_i, y_j) \in R \setminus \Omega. \end{cases} \quad (13.5.3)$$

Since  $u$  and  $\hat{u}$  are both harmonic, a five-point discrete Laplacian defined by

$$\nabla_h^2 U_{ij} = \frac{1}{h^2} [U_{i+1,j} + U_{i-1,j} + U_{i,j+1} + U_{i,j-1} - 4U_{ij}]$$

will be zero (up to terms of second order) at those mesh points of  $R$  whose four adjacent neighbors are on the same side of the boundary. Let  $S$  denote the set of irregular mesh points. At these points although the analytic Laplacian of  $u$  and  $\hat{u}$  is each zero, the discrete Laplacian  $\nabla_h^2 U$  is not zero. The central idea for solving the conformal mapping problem is to compute  $\nabla_h^2 U$  at the points in  $S$ , evaluate values of  $\hat{u}$  on  $\partial R$ , and then apply the fast Poisson solver on  $R$ .

Now, it is possible to approximate this discrete Laplacian without explicitly solving for  $u$  or  $\hat{u}$  anywhere because we need only compute the jump discontinuities between  $u$  and  $\hat{u}$  and those in their derivatives at the boundary in terms of the density  $\mu$ . The procedure to compute these jump discontinuities is as follows: Since the discontinuity between the tangential derivatives of  $u$  and  $\hat{u}$  at a point on the boundary is equal to the value of the density at that point, we have  $u_s - \hat{u}_s = \mu'(s)$ . Also, there is no discontinuity between their normal derivatives, i.e.,  $\frac{\partial u}{\partial n_s} = \frac{\partial \hat{u}}{\partial n_s}$ . These two results and the knowledge of the direction of the contour lead to the formula (13.4.2) which computes the discontinuities between  $u_x$  and  $\hat{u}_x$  and between  $u_y$  and  $\hat{u}_y$ . Higher order derivatives of  $u$  and  $\hat{u}$  can be obtained by differentiating (13.4.2).

Since the function  $U$  is the real part of the Cauchy integral with the same density function  $\mu$ , we shall consider

$$W(t) = \frac{1}{2i\pi} \int_{\Gamma} \frac{\mu(\zeta)}{\zeta - z} d\zeta. \quad (13.5.4)$$

Since the kernel in Eq (13.5.1) is the real part of the kernel in (13.5.4), we have

$$\begin{aligned}\Re \left\{ \frac{1}{2i\pi} \frac{d\zeta/ds}{\zeta - z} \right\} &= \frac{1}{2\pi i} \frac{y'(s)[x(s) - x(t)] - x'(s)[y(s) - y(t)]}{[x(s) - x(t)]^2 + [y(s) - y(t)]^2} ds \\ &= \frac{1}{2\pi} M(s, t) ds,\end{aligned}\quad (13.5.5)$$

where  $\zeta = \gamma(s) = x(s) + iy(s)$  and  $z = \gamma(t) = x(t) + iy(t)$ . Thus,  $u(z) = \Re\{W(t)\}$  for  $z \in \Omega$ , and  $\hat{u}(z) = \Re\{W(z)\}$  for  $z \in R \setminus \Omega$ . Then the jump between  $u$  and  $\hat{u}$  can be computed from the jump discontinuities of Cauchy integrals across the boundary contour (recall that Cauchy integrals are analytic functions). Thus, for example,

$$2W(z) = \begin{cases} \mu(z) + \frac{1}{i\pi} \int_{\Gamma} \frac{\mu(\zeta)}{\zeta - z} d\zeta, & \text{if } z \rightarrow \Gamma_-, \\ -\mu(z) + \frac{1}{i\pi} \int_{\Gamma} \frac{\mu(\zeta)}{\zeta - z} d\zeta, & \text{if } z \rightarrow \Gamma_+, \end{cases} \quad (13.5.6)$$

where  $z \rightarrow \Gamma_{\pm}$  stands for whether  $z$  approaches from inside  $\Omega$  or from outside  $\Omega$ . Hence, there exists a discontinuity of magnitude  $\mu(z)$  in  $W$  as  $z$  crosses  $\Gamma$ . Since  $\mu(z)$  is a real function, we find that  $u(z) - \hat{u}(z) = \mu(z)$  if  $z \in \Gamma$ .

The discontinuities in the first and second derivatives of  $W(z)$  can be computed as follows: Since by integration

$$\frac{d}{dz} W(z) = \frac{1}{2i\pi} \int_{\Gamma} \frac{d}{dz} \frac{\mu(\zeta)}{\zeta - z} d\zeta = \frac{1}{2i\pi} \int_{\Gamma} \frac{\mu'(\zeta)}{\zeta - z} d\zeta,$$

we find that the derivative of a Cauchy integral with density  $\mu$  is another Cauchy integral with density  $\mu'$ , and thus,  $W'(z)$  has discontinuity of magnitude  $\mu'(z)$  as  $z$  crosses  $\Gamma$ . Also, since  $W(z)$  is analytic and  $u_x(z) = \Re\{W'(z)\}$ , we have

$$\begin{aligned}u_x(z) - \hat{u}_x(z) &= \Re\{\mu'(z)\} = \Re\left\{\frac{d\mu/ds}{ds/dz}\right\} = \frac{\mu'(s)x'(s)}{x'(s)^2 + y'(s)^2}, \\ u_y(z) - \hat{u}_y(z) &= -\Im\{\mu'(z)\} = \frac{\mu'(s)y'(s)}{x'(s)^2 + y'(s)^2},\end{aligned}\quad (13.5.7)$$

and since  $\Re\{W''(z)\} = u_{xx}(z)$ , we have

$$u_{xx}(z) - \hat{u}_{xx}(z) = \Re\{\mu''(z)\}, \quad u_{yy}(z) - \hat{u}_{yy}(z) = -\Im\{\mu''(z)\}.$$

These discontinuities can be used to approximate the discrete Laplacian at mesh points near the boundary.

An approximation of the discrete Laplacian of  $U$  at points of the set  $S$  can be computed as follows: If we consider a point  $p_E$  to the right of a point  $p \in \Omega$  (Fig. 13.4.1), we find that the difference  $\hat{u}(p_E) - u(p)$  is given by (13.4.3), of which the first three terms  $\{\sum(3)\}$  can be computed in terms of the density function  $\mu$  and the distances of the irregular mesh points from the boundary. Now, if  $p_W$  is the mesh point to the left of  $p \in \Omega$ , then

$$U(p_W) - U(p) = \begin{cases} -h u_x(p) + \frac{h^2}{2} u_{xx}(p) + O(h^3), & \text{if } p_W \in \Omega, \\ \{\sum(3)\} - h u_x(p) + \frac{h^2}{2} u_{xx}(p) + O(h^3), & \text{if } p_W \notin \Omega. \end{cases} \quad (13.5.8)$$

Thus, in either case, from (13.4.3) and (13.5.8) we find that

$$U(p_W) + U(p_E) - 2U(p) = \{\sum(3)\} + h^2 u_{xx}(p) + O(h^3).$$

Similarly, if  $p_N$  and  $p_S$  are points above and below  $p$ , respectively (Fig. 13.4.1), then

$$U(p_N) + U(p_S) - 2U(p) = \{\sum(3)\} + h^2 u_{yy}(p) + O(h^3).$$

Hence,  $\nabla^2 u(p) = u_{xx}(p) + u_{yy}(p) = 0$  yields

$$h^2 \nabla_h^2 U(p) = \{\sum(3)\} + O(h^3). \quad (13.5.9)$$

By an analogous argument, if  $p$  is in  $R \setminus \Omega$ , then  $\nabla^2 \hat{u}(p) = 0$  will also lead to formula (13.5.9). This formula gives second-order accuracy in approximating the discrete Laplacian of  $U$  at points of the set  $S$ . If we want to reach fourth-order accuracy in this approximation at points of  $S$ , we must use the fourth order Taylor series expansion. Then, for example, at the point  $p_E$  we will have

$$\begin{aligned} \hat{u}(p_E) - u(p) &= [\hat{u}(p^*) - u(p^*)] + h_2 [\hat{u}_x(p^*) - u_x(p^*)] \\ &\quad + \frac{h^2}{2} [\hat{u}_{xx}(p^*) - u_{xx}(p^*)] + \frac{h^3}{6} [\hat{u}_{xxx}(p^*) - u_{xxx}(p^*)] \\ &\quad + h u_x(p) + \frac{h^2}{2} u_{xx}(p) + \frac{h^3}{6} u_{xxx}(p) + O(h^4) \\ &= \{\sum(4)\} + h u_x(p) + \frac{h^2}{2} u_{xx}(p) + \frac{h^3}{6} u_{xxx}(p) + O(h^4), \end{aligned}$$

where  $\{\sum(4)\}$  is the sum of the first four terms on the right side in the above expression. Then

$$h^2 \nabla_h^2 U(p) = \{\sum(4)\} + O(h^4). \quad (13.5.10)$$

This shows that if the solution of the integral equation is known almost accurately, we can compute an approximate solution with second order accuracy. Mayo's method solves Mikhlin's integral equation with machine accuracy because of the use of trapezoidal rule in the quadrature formula with smooth boundary data. However, splines can be used to compute more accurate values for the derivatives of the density function. It has been found that in practice second-order accuracy is sufficient to obtain an accurate solution.

The computational algorithm consists of the following steps:

- STEP 1. Embed the region  $\Omega$  in a rectangle  $R$ . This rectangle is chosen at least  $3h$  distance away from  $\Gamma$ .
- STEP 2. Find all irregular mesh points and their distances to the boundary in the  $x$  and  $y$  directions.
- STEP 3. Solve the integral equation by using the quadrature formula (13.3.8), which replaces the integral equation by a sum at a set of boundary points. This yields a dense linear system of equations

$$\mu(t_i) + \sum w_i K(i, j) \mu(t_j) = 2g(t_i), \quad i = 1, \dots, n, \quad (13.5.11)$$

where the points used as nodes are different from the mesh points. These nodes are chosen as equispaced points with respect to the parameter used on the boundary, and the trapezoidal rule is used for quadrature. (in cases where the boundary data is not smooth, or for points near those boundary portions where the curvature is large, a Galerkin method with augmented bases containing singular points is needed (see §12.5). System (13.5.11) is solved by the Gaussian elimination method.

- STEP 4. Interpolate the values of the density with a quintic spline which yields sixth order accuracy for values of the density at intermediate points.
- STEP 5. Compute the discrete Laplacian at irregular points in the set  $S$  by using (13.4.3).
- STEP 6. Compute the values of  $U$  at the edge of the grid.
- STEP 7. Apply the fast Poisson solver.
- STEP 8. Compute the derivatives  $u_x$  and  $u_y$  by (13.5.7).
- STEP 9. Compute the conjugate function  $v(z)$ .

## 13.6. Problems

PROBLEM 13.6.1. Let  $\mathcal{A}$  denote a family of univalent meromorphic func-

tions of the form  $f(z) = z + \frac{a_1}{z} + \dots$  on the exterior region  $|z| > R$ ,  $0 < R < \infty$ . Let  $U(f) = \Re\{e^{-2i\theta} a_1\}$ ,  $f \in \mathcal{A}$ . Show that there exists a unique function  $f_0(z) = z + \frac{r^2 e^{-2i\theta}}{z} \in \mathcal{A}$  such that  $U(f)$  attains the maximum  $U_0(f) = R^2$ , and  $w = f_0(z)$  maps the region  $|z| > R$  conformally onto the slit  $w$ -plane obtained by removing the line segment joining the points  $\pm 2Re^{i\theta}$ . (Wen, 1992, p.102.)

**PROBLEM 13.6.2.** Suppose that the function  $f(z)$  defined by (13.1.3) is univalent and meromorphic in the exterior region  $E = \{|z| > R, 0 < R < \infty\}$ . Show that  $|f(z) - a_0| \leq 2|z|$  on  $E$ . (Wen, 1992, p.103.)

**PROBLEM 13.6.3.** Let  $\mathcal{A}$  denote the family of univalent meromorphic functions of the form  $f(z) = z + \frac{a_1}{z} + \dots$  on the exterior region  $|z| > R$ ,  $0 < R < \infty$ . Let  $U(f) = \Re\{e^{-2i\pi\theta} a_1\}$ ,  $f \in \mathcal{A}$ . Show that there exists a unique function  $f_0(z) = z + \frac{R^2 e^{-2i\pi\theta}}{z} \in \mathcal{A}$  such that  $U(f)$  attains a maximum  $U_0(f) = R^2$  and  $w = f_0(z)$  maps  $|z| > R$  conformally onto a region obtained from the extended  $w$ -plane with a cut along the line segment joining the two points  $\pm 2Re^{i\theta}$ . (Wen, 1992, p.102.)

**PROBLEM 13.6.4.** Show that the analytic function  $F(z, z_0)$  defined on a multiply connected region  $\Omega$  such that  $\Re\{F(z, z_0)\}$  is Green's function for  $\Omega$  is not single-valued in  $\Omega$ . (Goluzin, 1969, p.286.)

**PROBLEM 13.6.5.** Derive (13.4.3) by writing the Taylor series expansions of  $u$  about  $p$  evaluated at  $p^*$ . (Mayo, 1984, pp.289–290.)

**PROBLEM 13.6.6.** Consider the triply connected region  $\Omega$  bounded by  $\Gamma_0 = \{|z| = 0.35\}$ , which is a circle, and  $\Gamma_1$  and  $\Gamma_2$  which are ellipses  $x^2/a^2 + y^2/b^2 = 1$  with  $a = 0.06$ ,  $b = 0.13$  and centered at  $(0.17, 0)$  and  $(-0.17, 0)$ , respectively. By embedding the region in a unit square and using the mesh size  $h = 1/128$  and 180 mesh points on the boundary, plot the images of the grid lines and the image region with the slits. (Mayo, 1986, p.152.)

**REFERENCES USED:** Atkinson (1976), Goluzin (1969), Kellogg (1929), Mayo (1984, 1986), Mikhlin (1957), Symm (1966), Wen(1992).

# Chapter 14

---

## Grid Generation

---

Exact solutions of boundary value problems for simple regions, such as a circle, square or annulus, can be determined with relative ease even in cases where the boundary conditions are rather complicated. Although Greens functions for such simple regions are known, the solution of a boundary value problem for regions with complex structures often becomes more difficult, even for a simple problem, such as the Dirichlet problem. One approach to solving these difficult problems is to conformally transform a given region into the simplest form. This will, however, result in change not only in the region and the associated boundary conditions but also in the governing differential equation. Grid generation methods using conformal mappings are presented for problems dealing with a cascade of blades, and inlet flow configurations.

---

### 14.1. Computational Region

Conformal mapping has been used to generate orthogonal boundary-fitted coordinates in solving various boundary value problems in simply connected regions. A useful work in this area is the book by Thompson, Warsi and Mastin (1985). A grid is an integral part of finite difference or finite element methods. A discrete model becomes more efficient when it is constructed by using natural coordinate systems and maintaining a uniform connectivity pattern between grid nodes. These two requirements are met when the grid is obtained by coordinate transformations using conformal mapping methods so that the boundary of the physical region is represented by constant coordinate

lines. Besides this adaptive feature, the conformal maps can be made to adapt to certain salient features, such as singularities. A grid generation methodology must be able to control the grid spacing effectively, especially near the boundary (see Tamamidis and Assanis, 1991).

Computational methods, like the finite differences or the finite elements, for solving boundary value problems are usually simple if the physical region has regular geometry over which a uniformly distributed grid can be imposed. However, if the region has arbitrary irregular geometry, such a region is first transformed into an associated computational region with regular geometry, like a rectangle or circle. In such cases the difficulty arises not only from the transformation of the governing equation(s) but also from the boundary conditions. The coordinate transformation and conformal boundary maps are generally used to transform an irregular physical region into the corresponding computational region. But such transformations and conformal mappings, in general, are very difficult to construct except in relatively simpler cases.

First, we shall gather some transformation formulas from the physical  $(x, y)$ -region into the computational  $(\xi, \eta)$ -region.

**14.1.1. Coordinate Transformations.** To find the transformation from independent variables  $x, y$  of the physical plane into a set of independent variables  $\xi, \eta$  of the computational plane, let us assume that

$$\xi = \xi(x, y), \quad \eta = \eta(x, y), \quad (14.1.1)$$

or inversely,

$$x = x(\xi, \eta), \quad y = y(\xi, \eta). \quad (14.1.2)$$

The Jacobian  $J$  of the transformation is given by

$$J = \frac{\partial(x, y)}{\partial(\xi, \eta)} = \begin{vmatrix} x_\xi & y_\xi \\ x_\eta & y_\eta \end{vmatrix} = x_\xi y_\eta - x_\eta y_\xi \neq 0, \quad (14.1.3)$$

where the subscripts denote partial differentiation with respect to the indicated variable. If  $u = u(x, y)$ , then

$$\frac{\partial u}{\partial x} = \frac{1}{J} \left( y_\eta \frac{\partial u}{\partial \xi} - y_\xi \frac{\partial u}{\partial \eta} \right), \quad \frac{\partial u}{\partial y} = \frac{1}{J} \left( -x_\eta \frac{\partial u}{\partial \xi} + x_\xi \frac{\partial u}{\partial \eta} \right). \quad (14.1.4)$$

For the gradient, the transformation formulas for the conservative form are

$$u_x = \frac{1}{J} \left[ (y_\eta u)_\xi - (y_\xi u)_\eta \right], \quad u_y = \frac{1}{J} \left[ -(x_\eta u)_\xi + (x_\xi u)_\eta \right], \quad (14.1.5)$$

and for the nonconservative form are

$$u_x = \frac{1}{J} (y_\eta u_\xi - y_\xi u_\eta), \quad u_y = \frac{1}{J} (-x_\eta u_\xi + x_\xi u_\eta). \quad (14.1.6)$$

Let  $\mathbf{u} = u_1 \mathbf{i} + u_2 \mathbf{j}$ . Then for divergence the transformation formulas for the conservative form are

$$\nabla \cdot \mathbf{u} = \frac{1}{J} \left[ (y_\eta u_1 - x_\eta u_2)_\xi + (-y_\xi u_1 + x_\xi u_2)_\eta \right], \quad (14.1.7)$$

and for the nonconservative form are

$$\nabla \cdot \mathbf{u} = \frac{1}{J} \left[ y_\eta (u_1)_\xi - x_\eta (u_2)_\xi - y_\xi (u_1)_\eta + x_\xi (u_2)_\eta \right]. \quad (14.1.8)$$

CASE STUDY 14.1.1. Using formulas (14.1.4), the equation of continuity

$$\frac{\partial u}{\partial x} + \frac{\partial v}{\partial y} = 0, \quad (14.1.9)$$

when transformed from  $(x, y)$ -coordinates of the physical plane into  $(\xi, \eta)$ -coordinates of the computational plane, becomes

$$y_\eta \frac{\partial u}{\partial \xi} - y_\xi \frac{\partial u}{\partial \eta} - x_\eta \frac{\partial v}{\partial \xi} + x_\xi \frac{\partial v}{\partial \eta} = 0. \blacksquare \quad (14.1.10)$$

CASE STUDY 14.1.2. The Laplacian  $\nabla^2 \equiv \frac{\partial^2}{\partial x^2} + \frac{\partial^2}{\partial y^2}$  is transformed into the following forms:

Conservative form:

$$J \nabla^2 u = \left\{ \frac{1}{J} y_\eta \left[ (y_\eta u)_\xi - \frac{1}{J} (y_\xi u)_\eta \right] - x_\eta \left[ -(x_\eta u)_\xi + (x_\xi u)_\eta \right] \right\}_\xi + \left\{ -\frac{1}{J} y_\xi \left[ (y_\eta u)_\xi + (y_\xi u)_\eta \right] + \frac{1}{J} x_\eta \left[ -(x_\eta u)_\xi + (x_\xi u)_\eta \right] \right\}_\eta.$$

Nonconservative form:

$$\begin{aligned} \nabla^2 u = & \frac{1}{J^2} \left[ (x_\eta^2 + y_\eta^2) u_{\xi\xi} - 2(x_\xi x_\eta + y_\xi y_\eta) u_{\xi\eta} + (x_\xi^2 + y_\xi^2) u_{\eta\eta} \right] \\ & + [(\nabla^2 \xi) u_\xi + (\nabla^2 \eta) u_\eta]. \blacksquare \end{aligned}$$

Next, to present the basic concept of numerical grid generation for different boundary value problems, we shall consider a very simple one-dimensional transformation and show how the computational region with uniformly distributed grids is obtained and how the governing equations are changed.

CASE STUDY 14.1.3. Consider a plane steady state boundary layer flow over a flat rectangular plate  $\{0 \leq x \leq a, 0 \leq y \leq b\}$ . If this problem is solved by the finite difference or finite element method, a rectangular grid is constructed over the physical region with more nodes concentrated near the wall ( $x$ -axis) where the gradients are assumed to be larger than elsewhere (see Fig. 14.1.1). This grid is uniform along the  $x$ -axis but nonuniform along the  $y$ -axis.

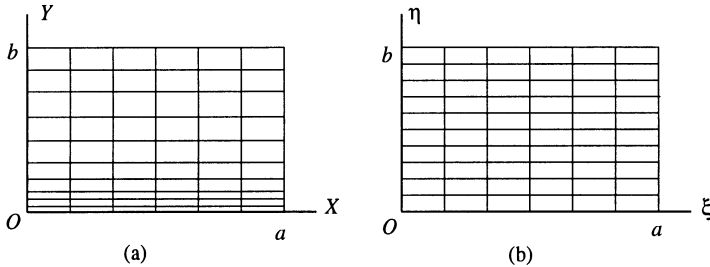


Fig. 14.1.1. (a) Physical region, (b) Computational region.

In order to transform the grid in Fig. 14.1.1(a) into the uniform grid of Fig. 14.1.1(b), we use the coordinate transformation

$$\xi = x, \quad \eta = 1 - \frac{\ln \phi(y)}{\ln A}, \quad (14.1.11)$$

where

$$\phi(y) = \frac{\alpha + \left(1 - \frac{y}{b}\right)}{\alpha - \left(1 - \frac{y}{b}\right)}, \quad A = \frac{\alpha + 1}{\alpha - 1}, \quad 1 < \alpha < \infty. \quad (14.1.12)$$

The inverse transformation is given by

$$x = \xi, \quad y = b \frac{(\alpha + 1) - (\alpha - 1) A^{1-\eta}}{1 + A^{1-\eta}}. \quad (14.1.13)$$

This transformation (Roberts, 1971) makes the grid spacing uniform along the  $y$ -axis. The parameter  $\alpha$  is known as the *stretching parameter*. The grid

concentration as  $\alpha \rightarrow 1$  is presented in Fig. 14.1.2 where values of  $y$  are plotted for different values of  $\alpha$  and  $\eta$  with  $b = 1$ .

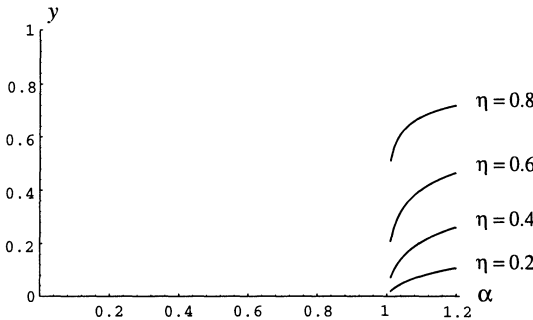


Fig. 14.1.2. Grid concentration as  $\alpha \rightarrow 1$ .

Next, we shall transform the differential equation from the physical region into the computational region by the transformation (14.1.11). For brevity, let us consider the equation of continuity (14.1.9). Since

$$\xi_x = 1, \quad \xi_y = 0, \quad \eta_x = 0, \quad \eta_y = \frac{2\alpha}{b \ln A} \left[ \alpha^1 - \left( 1 - \frac{y}{b} \right)^2 \right]^{-1} \quad (14.1.14)$$

for the geometry of the plate, the continuity equation is transformed into

$$\frac{\partial u}{\partial \xi} + \eta_y \frac{\partial v}{\partial \eta} = 0, \quad (14.1.15)$$

where  $\eta_y$  is defined in (14.1.14). Note that the effect of uniformizing the grid makes the governing equation rather complicated compared to the original form. Moreover, after the problem is solved in the computational region, the solution is transformed back to the physical region by using (14.1.11). ■

**14.1.2. Orthogonal Method.** The use of conformal mappings to generate grids has some important limitations: (i) they are applicable to plane problems, (ii) they have no control over the interior grids, (iii) multiple-valued mapping functions are difficult to implement, (iv) orthogonality is lost in arbitrary distribution of boundary points, (v) a very small change in the shape of the original boundary results in changes in the location of image boundary points,

and (vi) finding a boundary map is in itself a difficult task.

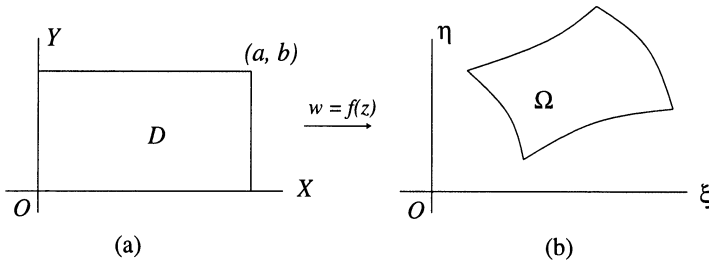


Fig. 14.1.3.

A consequence of the Riemann mapping theorem is that a rectangle  $R = \{0 \leq x \leq 1, 0 \leq y \leq b\}$  cannot be mapped univalently onto an arbitrary region  $D$  with four sides, as shown in Fig. 14.1.3, unless the ratio  $a/b$  is restricted to a particular constant  $m$ , known as the *conformal module*. Then the mapping  $w = f(z)$  can be constructed by solving the partial differential equation

$$m^2 w_{\xi\xi} + w_{\eta\eta} = 0. \quad (14.1.16)$$

This yields a *quasiconformal* map (see Lehto and Virtaanen (1973)). Since  $m$  is domain-dependent and not known *a priori*, this approach is not feasible for grid generation. On the other hand, orthogonal transformations in the plane can be regarded as quasi-conformal mapping with a real dilation (Knupp and Steinberg, 1993).

## 14.2. Inlet Configurations

We shall develop the orthogonal grid generation method by using conformal mapping. In this method the physical region is mapped onto the computational method by one- or two-step conformal maps. First, we shall consider the grid generation for a case study involving inlet configuration in flow problems and determine the basic mappings by using both one-step and two-step methods.

**CASE STUDY 14.2.1 (One-step method).** Consider the physical region in the  $z$ -plane in Fig. 14.2.1(a). The boundary of this region, defined by

$y = y_1(x)$  and  $y = y_2(x)$ , is given by two sets of data:

$$\begin{aligned} z_1^{(n)} &= x_1^{(n)} + i y_1^{(n)}, \quad 2 \leq n \leq n_1 - 1, \\ z_2^{(n)} &= x_2^{(n)} + i y_2^{(n)}, \quad 2 \leq n \leq n_2 - 1, \end{aligned} \quad (14.2.1)$$

where  $x_2$  takes the minimum value  $x_2^{n_3}$  at  $n = n_3$ , i.e., at the point  $E$ . This region is mapped onto the computational region in the  $\zeta = (\xi, \eta)$ -plane, which is a rectangular strip  $0 \leq \eta \leq 1$  (Fig. 14.2.1).

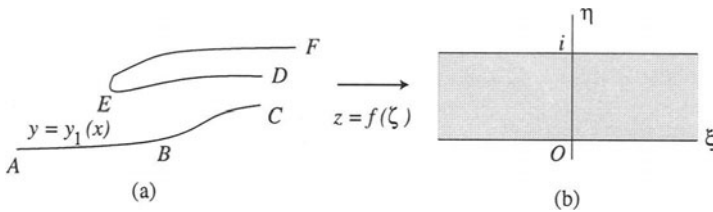


Fig. 14.2.1. (a) Physical plane ( $z$ -plane);  
(b) Computational plane ( $\zeta$ -plane).

The mapping function is given by

$$\begin{aligned} z &= h \left[ \zeta - \frac{1}{\pi} (1 + e^{-\pi\zeta}) \right] + A_1 + i B_1 \\ &+ \sum_{j=2}^{\kappa} \left[ A_j \sin \frac{(j-1)\pi(\zeta - \xi_0)}{L} + i B_j \cos \frac{(j-1)\pi(\zeta - \xi_0)}{L} \right], \end{aligned} \quad (14.2.2)$$

where  $h$ ,  $A_j$ ,  $B_j$  ( $j = 1, 2, \dots, \kappa$ ),  $\xi_0$  and  $L$  are yet unknown real constants to be determined. A particular case from (14.2.2) for  $A_j = B_j = 0$ ,  $j = 1, 2, \dots, \kappa$ , is given by

$$z = h \left[ \zeta - \frac{1}{\pi} (1 + e^{-\pi\zeta}) \right], \quad (14.2.3)$$

which maps the upper half-plane  $y \geq 0$  with a cut at  $y = h$ ,  $x \geq 0$ , onto the rectilinear strip  $0 \leq \eta \leq i$  in the  $\zeta$ -plane (Fig. 14.2.1). If we rewrite (14.2.2) as

$$\begin{aligned} x + i y &= h \left[ (\xi + i \eta) - \frac{1}{\pi} (1 + e^{-\pi(\xi + i \eta)}) \right] + A_1 + i B_1 \\ &+ \sum_{j=2}^{\kappa} \left[ A_j \sin \frac{(j-1)\pi(\xi + i \eta - \xi_0)}{L} + i B_j \cos \frac{(j-1)\pi(\xi + i \eta - \xi_0)}{L} \right], \end{aligned} \quad (14.2.4)$$

set  $\eta = 0$ , and equate real and imaginary parts, we get

$$\begin{aligned} x = x_1(\xi) &= h \left[ \xi - \frac{1}{\pi} (1 + e^{-\pi\xi}) \right] + A_1 \\ &+ \sum_{j=2}^{\kappa} A_j \sin \frac{(j-1)\pi(\xi - \xi_0)}{L}, \end{aligned} \quad (14.2.5)$$

and

$$y = y_1 = B_1 + \sum_{j=2}^{\kappa} B_j \cos \frac{(j-1)\pi(\xi + i\eta - \xi_0)}{L}. \quad (14.2.6)$$

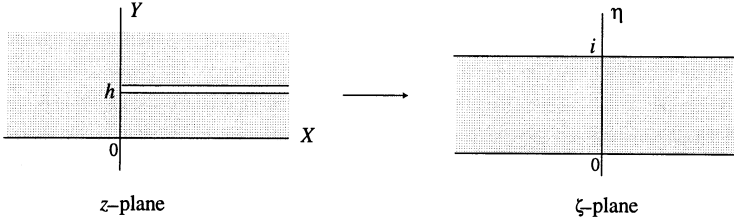


Fig. 14.2.2. The map  $z = h \left[ \zeta - \frac{1}{\pi} (1 + e^{-\pi\zeta}) \right]$ .

Again, if we set  $\eta = 1$  in (14.2.4) and equate real and imaginary parts, we obtain

$$\begin{aligned} x + x_2(\xi) &= h \left[ \xi - \frac{1}{\pi} (1 + e^{-\pi\xi}) \right] + A_1 \\ &+ \sum_{j=2}^{\kappa} \left[ A_j \cosh \frac{(j-1)\pi}{L} + B_j \sinh \frac{(j-1)\pi}{L} \right] \sin \frac{(j-1)\pi(\xi - \xi_0)}{L}, \end{aligned} \quad (14.2.7)$$

and

$$\begin{aligned} y = y_2 &= h + B_1 \\ &+ \sum_{j=2}^{\kappa} \left[ A_j \sinh \frac{(j-1)\pi}{L} + B_j \cosh \frac{(j-1)\pi}{L} \right] \cos \frac{(j-1)\pi(\xi - \xi_0)}{L}. \end{aligned} \quad (14.2.8)$$

Note that (14.2.6) and (14.2.8) imply that  $y_1$  and  $y_2$  are even,  $2L$ -periodic functions of  $\xi - \xi_0 \equiv t$ . The unknown constants are determined by the iterative

method as follows: Assume that the  $n$ -th approximations for  $h$ ,  $A_j$ ,  $B_j$ ,  $\xi_0$ , and  $L$  are known. Let us denote them by  $h^{(n)}$ ,  $A_j^{(n)}$ ,  $B_j^{(n)}$ ,  $\xi_0^{(n)}$ , and  $L^{(n)}$ . Then proceed as follows:

1. Substitute  $h^{(n)}$ ,  $A_j^{(n)}$ ,  $B_j^{(n)}$ ,  $\xi_0^{(n)}$ , and  $L^{(n)}$  into (14.2.5) and (14.2.7) and obtain the  $(n+1)$ -st approximations for  $x_1$  and  $x_2$ .
2. Find  $\xi = \xi_{n_3}$ , which makes  $x_2(\xi)$  minimum, and determine  $A_1$  so that  $x_2(\xi_{n_3}) = x_2^{(n_3)}$ .
3. Obtain the solutions of  $x_1(\xi) = x_1^{(2)}$  and  $x_2(\xi) = x_2^{(2)}$  and take the smaller value as  $\xi_1$ .
4. Obtain the solutions of  $x_1(\xi) = x_2^{(n_1-1)}$  and  $x_2(\xi) = x_2^{(n_2-1)}$ , and take the smaller value as  $\xi_2$ .
5. Determine  $z_1(\xi_1) = z_1^{(1)}$ ,  $z_2(\xi_1) = z_2^{(1)}$ ,  $z_1(\xi_2) = z_1^{(n_1)}$  and  $z_2(\xi_2) = z_2^{(n_2)}$  by extrapolation.

Steps 1 through 5 determine  $x_1(\xi)$  and  $x_2(\xi)$  for the interval

$$\xi_1 \leq \xi \leq \xi_2 = \xi_1 + L. \quad (14.2.9)$$

6. Set  $L = \xi_2 - \xi_1$  and  $\xi_0 = \xi_1$ .
7. Now the left sides of (14.2.6) and (14.2.8) for  $y_1$  and  $y_2$  are determined as functions of  $\xi$  on the interval (14.2.9) through the functions  $x_1(\xi)$  and  $x_2(\xi)$ .
8. The constants  $h$ ,  $A_j$  (for  $j = 2, 3, \dots, \kappa$ ) and  $B_j$  (for  $j = 1, 2, \dots, \kappa$ ) are determined by Fourier analysis. Thus,

$$\begin{aligned} B_1 &= \frac{1}{L} \int_0^L y_1(t) dt, \\ B_j &= \frac{2}{L} \int_0^L y_1(t) \cos \frac{(j-1)\pi t}{L} dt, \quad 1 \leq j \leq \kappa, \\ h &= \frac{1}{L} \int_0^L y_2(t) dt - B_1, \\ A_j &= \operatorname{csch} \frac{(j-1)\pi}{L} \left[ \frac{2}{L} \int_0^L y_2(t) \cos \frac{(j-1)\pi t}{L} dt - B_j \cosh \frac{(j-1)\pi}{L} \right], \end{aligned} \quad (14.2.10)$$

for  $2 \leq j \leq \kappa$ , where  $t = \xi - \xi_0$ .

9. All  $(n+1)$ -st approximations, denoted generically by  $\phi^{(n+1)}$ , thus obtained are replaced by  $(1-r)\phi^{(n)} + r\phi^{(n+1)}$ , where  $r$  is a relaxation constant, usually 0.5. This assures the convergence of the successive approximations.
10. Repeat steps 1 through 9 until the desired convergence is achieved.

Note that the first approximation is given by  $h = y_2^{(n_3)}$ ,  $A_j = B_j = 0$

$(1 \leq j \leq \kappa)$ ,  $\xi_1 = 0$ , and  $L = x_1^{(n_1-1)} - x_1^{(2)}$ . Since the hyperbolic functions are involved, double precision should be used in all computations. ■

CASE STUDY 14.2.2 (Two-step method). Consider the same flow problem as in Case Study 14.2.1. The mapping is carried out as follows: First, map the region  $ABC'DEF$  in the  $z$ -plane onto the rectilinear strip  $0 \leq \eta \leq 1$  in the  $\zeta$ -plane (see Fig. 14.2.3) by

$$z = h \left[ \zeta - \frac{1}{\pi} \left( 1 + e^{-/p i \zeta} \right) \right] + A_1 + \sum_{k=2}^{\kappa_1} \kappa_1 A_k \sin \frac{(k-1)\pi(\zeta - \xi_0)}{L_1}, \quad (14.2.11)$$

where the constants  $h, A_k, \xi_0$  and  $L_1$  are computed by an iterative method similar to that in Case Study 14.2.1. Note that the mapping (14.2.11), which is the mapping function for the inlet without center bodies, is obtained by taking  $B_k = 0$  ( $k \geq 1$ ) in (14.2.2). The image of the arc  $BC$  in the  $\zeta$ -plane is denoted by

$$\eta = \eta_1(\xi), \quad \xi_3 \leq \xi \leq \xi_4. \quad (14.2.12)$$

Next, map the region  $ABCDEF$  in the  $\zeta$ -plane onto the semi-infinite strip  $u \geq 0, 0 \leq v \leq 1$ , in the  $w$ -plane ( $w = u + i v$ ) by

$$\zeta = \frac{2}{\pi} \log \cosh \frac{\pi w}{2} + B_0 + \sum_{k=1}^{\kappa_2} B_k \cos \frac{(2k-1)\pi(w-i)}{2L_2}, \quad (14.2.13)$$

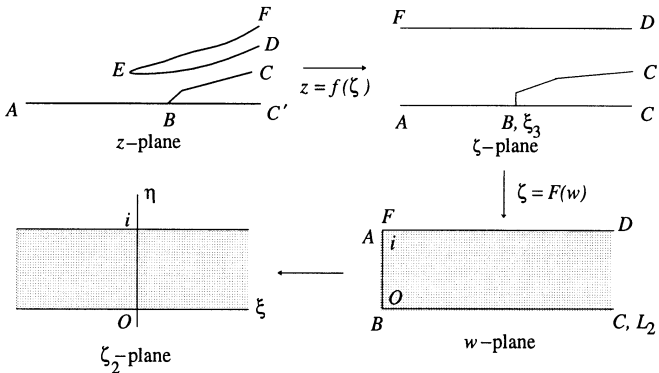


Fig. 14.2.3.

such that the points  $B$  ( $\zeta = \xi_3$ ) and  $C$  ( $\zeta = \xi_4 + i \eta_4$ ) go into the points  $w = 0$  and  $w = L_2$ , respectively. The unknown constants  $B_k$  ( $0 \leq k \leq \kappa_2$ ) and  $L_2$

are determined as in §14.2.1. Thus,

$$\begin{aligned} \xi + i\eta &= \frac{2}{\pi} \log \cosh \frac{\pi(u + iv)}{2} \\ &+ B_0 \sum_{k=1}^{\kappa_2} B_k \cos \frac{(2k-1)(u - i(1-v))}{2L_2} \\ &= \frac{2}{\pi} \log \cosh \frac{\pi(u + iv)}{2} \\ &+ B_0 \sum_{k=1}^{\kappa_2} B_k \left[ \cos \frac{(2k-1)\pi u}{2L_2} \cosh \frac{(2k-1)\pi(1-v)}{2L_2} \right. \\ &\quad \left. + i \sin \frac{(2k-1)\pi u}{2L_2} \sinh \frac{(2k-1)\pi(1-v)}{2L_2} \right], \end{aligned} \quad (14.2.14)$$

which for  $v = 0$  gives, after separating the real and imaginary parts,

$$\xi = \frac{1}{\pi} \log \cosh^2 \frac{\pi u}{2} + B_0 + \sum_{k=1}^{\kappa_2} B_k \cosh \frac{(2k-1)\pi}{2L_2} \cos \frac{(2k-1)\pi u}{2L_2}, \quad (14.2.15)$$

$$\eta = \eta_1(\xi) = \sum_{k=1}^{\kappa_2} B_k \sinh \frac{(2k-1)\pi}{2L_2} \sin \frac{(2k-1)\pi u}{2L_2}. \quad (14.2.16)$$

Hence,

$$B_k = \frac{2}{L_2} \operatorname{csch} \frac{(2k-1)\pi}{2L_2} \int_0^{L_2} \eta_1 \sin \frac{(2k-1)\pi u}{2L_2} du, \quad 1 \leq k \leq \kappa_2. \quad (14.2.17)$$

Also, at the point  $B$  ( $w = 0$ ) we have from (14.2.13)

$$\xi_3 = B_0 + \sum_{k=1}^{\kappa_2} B_k \cosh \frac{(2k-1)\pi}{2L_2}.$$

Thus,

$$B_0 = \xi_3 - \sum_{k=1}^{\kappa_2} B_k \cosh \frac{(2k-1)\pi}{2L_2}. \quad (14.2.18)$$

It is obvious from (14.2.16) that  $\eta_1(u)$  is an odd,  $4L_2$ -periodic function symmetric about the line  $u = L_2$ .

The semi-infinite strip  $CBAFED$  in the  $w$ -plane is mapped onto the infinite strip  $0 \leq \eta_2 \leq 1$  on the  $\zeta_2$ -plane ( $\zeta_2 = \xi_2 + i\eta_2$ ) by

$$w = \frac{2}{\pi} \cosh^{-1} \left( e^{\pi\xi_2/2} \right). \quad (14.2.19)$$

The lines  $\xi_2 = \text{const}$  or  $\eta_2 = \text{const}$  produce the grid lines on the  $z$ -plane. ■

### 14.3. Cascade Configurations

The Ives–Liutermozza method (Ives and Liutermozza, 1977) deals with the mapping problem that transforms the region exterior to a cascade of blades first onto a region exterior to a near circle. Then the second mapping transforms the interior of the near circle onto the unit disk. The success of the first mapping depends on the solidity of cascades; if it is low, the mapping yields an acceptable near circle, but if it increases, the image boundary degenerates into a peanut-shaped contour, in which case the second mapping will not work at all, and the Ives–Liutermozza method fails. To overcome this difficulty for the mapping problem of the cascade of blades, we shall first determine the function that maps the region directly onto a rectangle for two periods of the cascade of blades, which can then be mapped onto the unit disk (see Fig. 11.1.2 and 11.3.2). We shall consider three cases described in the following case studies.

**CASE STUDY 14.3.1.** First we shall study the ordinary type of grids. Let two periods of the cascade of blades make a row in the  $y$  direction in the  $z$ -plane (physical plane  $z = x + iy$ , Fig. 14.3.1(a)). The contour of one of the blades is defined by a set of data  $z_n = x_n + iy_n$ ,  $n = 1, \dots, N$ ,  $z_N = z_1$ , which are ordered clockwise, with  $|x_n| \leq 1$ . Let  $h$  denote the pitch of the blades in the  $y$ -direction. The function that maps them onto an infinite strip in the  $\zeta$ -plane (computational plane, Fig. 14.3.1(b)) has the form

$$z = A_0 \left[ \frac{h}{\pi} \log \operatorname{sn}(\zeta, k) - 1 + \sum_{j=1}^M MC_j \cos \frac{(j-1)\pi\zeta}{K'} \right], \quad (14.3.1)$$

where  $A_0$  is a real parameter that finally approaches unity in an iterative scheme (see Step 3 of the algorithm given below),  $C_j = A_j + iB_j$  and  $k$ ,  $0 < k < 1$ , are constants to be determined,  $K$  and  $K'$  are complete elliptic integrals of the first kind with moduli  $k$  and  $k' = \sqrt{1-k^2}$ , respectively, and  $\operatorname{sn}$  is one of the Jacobian elliptic functions (see §2.3). In particular when  $A_0 = 1$ ,  $k = e^{-2\pi/h}$ ,  $A_j = 0 = B_j$  for  $j \geq 1$ , the function (14.3.1) represents the mapping of a cascade of flat plates of chord 2, pitch  $h$ , and zero stagger. If we set  $\zeta = K + i\eta$  in (14.3.1) and separate the real and imaginary parts, we get

$$\begin{aligned} x = A_0 \left[ \frac{h}{\pi} \log \operatorname{dn}(\eta, k') - 1 + A_1 + \sum_{j=2}^M \left\{ A_j \cosh \frac{(j-1)\pi K}{K'} \cos \frac{(j-1)\pi\eta}{K'} \right. \right. \\ \left. \left. - B_j \sinh \frac{(j-1)\pi K}{K'} \sin \frac{(j-1)\pi\eta}{K'} \right\} \right], \end{aligned} \quad (14.3.2)$$

$$y = A_0 \left[ B_1 + \sum_{j=2}^M \left\{ A_j \sinh \frac{(j-1)\pi K}{K'} \sin \frac{(j-1)\pi \eta}{K'} + B_j \cosh \frac{(j-1)\pi K}{K'} \cos \frac{(j-1)\pi \eta}{K'} \right\} \right], \quad (14.3.3)$$

where dn is another Jacobian elliptic function.

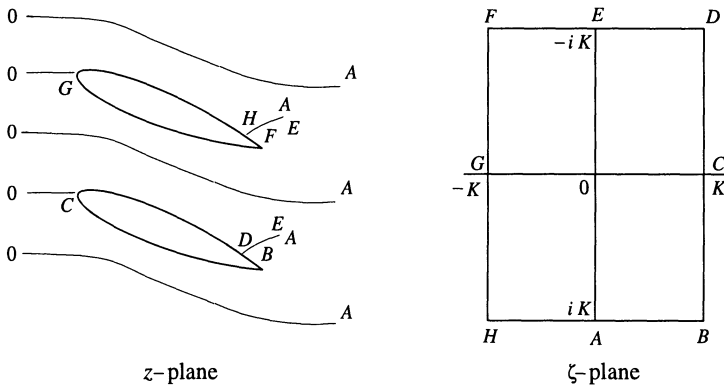


Fig. 14.3.1. (a) Physical region, (b) Computational region.

The following algorithm for the iterative method which starts with the data for the initial guess as that of the flat cascade assumes that the  $n$ -th approximations  $A_j^{(n)}$ ,  $B_j^{(n)}$  and  $k^{(n)}$  are known. Then proceed as follows:

STEP 1. Substitute the known values of  $A_j^{(n)}$ ,  $B_j^{(n)}$  and  $k^{(n)}$  into (14.3.2) and compute the values of  $A_1^{(n+1)}$  such that  $x_{\max} + x_{\min} = 0$ . Then compute the constant  $A_0^{(n+1)}$  such that  $x_{\max} - x_{\min} = 2$ . use this data on the left side of (14.3.2) to yield the relation

$$\eta = \eta^{(n+1)}(x). \quad (14.3.4)$$

STEP 2. Choose a relaxation constant  $\varepsilon_0 (= 0.5)$ , and replace  $A_0^{(n+1)}$  by  $(1 - \varepsilon_0) A_0^{(n)} + \varepsilon_0 A_0^{(n+1)}$ , to yield a new value of  $A_0^{(n+1)}$ .

STEP 3. Use this value of  $A_0^{(n+1)}$  to obtain  $k^{(n+1)}$  from

$$\log k^{(n+1)} = A_0^{(n+1)} \log k^{(n)}. \quad (14.3.5)$$

In this process  $A_0 \rightarrow 1$  as  $n$  increases.

STEP 4. Use (14.3.4) to write the profile of the blade in the form  $y = y^{(n+1)}(\eta)$ .

Substitute this  $y$  on the left side of (14.3.3), and use Fourier series analysis on it to obtain

$$\begin{aligned} A_j^{(n+1)} &= \left[ K' A + 0 \sinh \frac{(j-1)\pi K}{K'} \right]^{-1} \int_{-K'}^{K'} y \sin \frac{(j-1)\pi\eta}{K'} d\eta, \quad j \geq 2, \\ B_j^{(n+1)} &= \left[ K' A + 0 \sinh \frac{(j-1)\pi K}{K'} \right]^{-1} \int_{-K'}^{K'} y \cos \frac{(j-1)\pi\eta}{K'} d\eta, \quad j \geq 1, \end{aligned} \quad (14.3.6)$$

STEP 5. Chooses a relaxation constant  $\varepsilon_1 (= 0.1)$ , and replace  $A_j^{(n+1)}$  and  $B_j^{(n+1)}$  by  $(1-\varepsilon_1) A_j^{(n)} + \varepsilon_1 A_j^{(n+1)}$  and  $(1-\varepsilon_1) B_j^{(n)} + \varepsilon_1 B_j^{(n+1)}$ , respectively.

STEP 6. Repeat steps 1 through 5 until the required convergence is achieved. Note that Steps 3 and 5 guarantee the convergence of successive approximations in this scheme. The grids drawn with solidity 1.58,  $N = 42$ ,  $M = 20$ ,  $k = 4.1 \times 10^{-5}$ ,  $K = 1.57$ , and  $K' = 11.5$  can be found in Inoue (1983), where the lines  $\xi = \text{const}$  surround the blades, and the lines  $\eta = \text{const}$  continue across the periodic boundaries  $OA$  and  $OE$ . The constant  $k$  and the ratio  $K/K'$  both decrease as the solidity of the blade increases. It has been observed that this method remains successful for solidity up to 0.29. ■

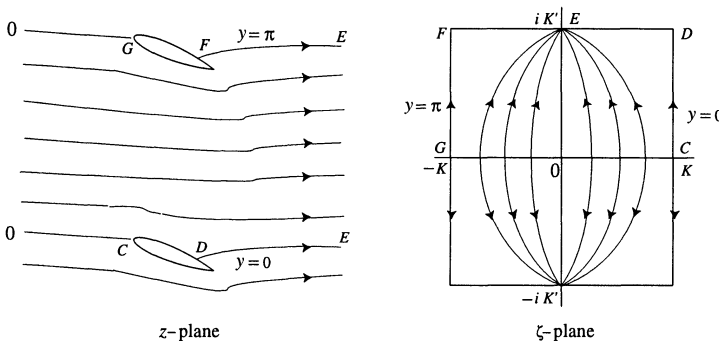


Fig. 14.3.2. (a) Physical region, (b) Computational region.

CASE STUDY 14.3.2. Another kind of grid is generated when the streamlines flow parallel to the  $x$ -axis in a special situation induced by the presence of sources and sinks in the physical plane. We shall consider the problem of a cascade of two periodic blades. Let the streamlines of the flow through the cascade from left to right, as shown in Fig. 14.3.2(a), represent a family of grid lines in the  $z$ -plane. Let  $Z = X + i Y$  denote the complex velocity potential of the flow induced by the following distribution of sources and sinks in the

$\zeta$ -plane (Fig. 14.3.2(b)):

unit sinks at  $\zeta = 2mK + 2niK'$ ; and

unit sources at  $\zeta = 2mK + (2n - 1)iK'$ , where  $m, n$  are integers.

(14.3.7)

Since the through-flow grid is based on  $(X, Y)$  coordinates, the flow induced by sources and sinks(4.106) is defined by (see (2.3.13))

$$Z = \log \operatorname{sn}(\zeta, k), \quad (14.3.8)$$

or

$$\zeta = \int_0^{e^Z} [(1-t^2)(1-k^2t^2)]^{-1/2} dt. \quad (14.3.9)$$

Also, we have  $Z(K) = 0$  and  $Z(K + iK') = -\log k$ , where  $\zeta = K$  and  $\zeta = K + iK'$  are the stagnation points of the flow. The through-flow grids for the cascade of Fig. 14.3.2 can be drawn with the same data as above.

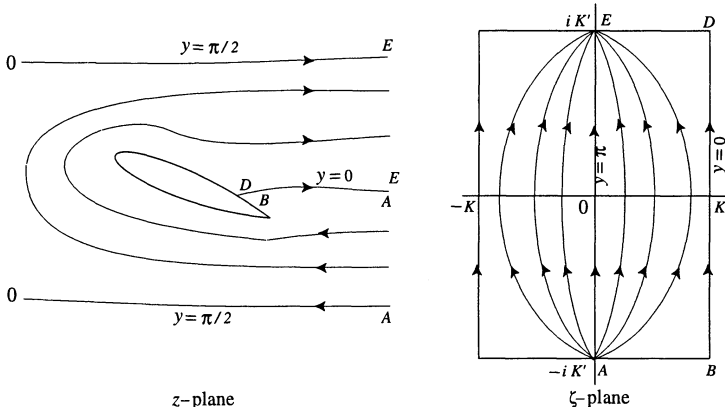


Fig. 14.3.3. (a) Physical region, (b) Computational region.

CASE STUDY 14.3.3. A different type of grid arises in the case when the streamlines of the flow that starts from infinity on the right encircles the cascade and returns to infinity to the right (Fig. 14.3.3(a)). These streamlines represent the grid as a family of coordinate lines. The flow is induced by the distribution of sources and sinks in the  $\zeta$ -plane which are as follows (Fig. 14.3.3(b)):

unit sinks at  $\zeta = 2mK + (4n + 1)iK'$ ; and

unit sources at  $\zeta = 2mK + (4n - 1)iK'$ , where  $m, n$  are integers.

(14.3.10)

The complex velocity potential of this flow is defined by

$$Z = X + i Y = \log \operatorname{sn} \left( \frac{K'}{K} (\zeta + i K'), k_1 \right), \quad (14.3.11)$$

where  $K_1$  and  $K'_1$  are the complete elliptic functions of the first kind with moduli  $k_1$  and  $k'_1 = \sqrt{1 - k_1^2}$ , respectively, such that  $\frac{K'_1}{K_1} = \frac{2K'}{K}$  and  $k_1 = \frac{1 - k'}{1 + k'}$  (see Landen transformation, §2.3). The inverse mapping of (14.3.11) is given by

$$\zeta = \frac{K}{K'} \int_0^{e^Z} \frac{dt}{\sqrt{(1 - t^2)(1 - k_1^2 t^2)}} - i K'. \quad (14.3.12)$$

Note that  $Z(K - i K') = 0$  and  $Z(K + i K') = -\log k_1$ , where  $K \pm i K'$  are the stagnation points of the flow. The grid lines generated by this method for the above cascade can be drawn for the same data as in Case Study 14.4.1.

**CASE STUDY 14.3.4.** The design of an airfoil and wing becomes significant in the transonic flow problem. The basic equations of fully developed flow potential  $\phi$  around the configuration of an axisymmetric inlet of arbitrary geometry, shown in Fig. 14.3.4, is given by

$$(a^2 - \phi_x^2) \phi_{xx} - 2 \phi_x \phi_r \phi_{xr} + (a^2 - \phi_r^2) \phi_{rr} + \frac{a^2}{r} \phi_r = 0, \quad (14.3.13)$$

where  $(x, r)$  denote the coordinates along and normal to the centerline, respectively, and  $a$  is the velocity of sound. We shall use the subscripts int and ext to denote the interior and exterior inlets, respectively.

The mapping of the physical region ( $z$ -plane) is carried out by functions with scale factors that depend only on the mapping modulus. The basic idea in the construction of a composite conformal map is to transform the physical boundary (inlet contour) into a Jordan contour and then into the unit circle using Fourier series. Finally the circle is mapped onto a rectangle, as in §11.1 and 11.3, supplemented by a coordinate stretching of type (14.1.11) to obtain the computational plane. The chain of conformal mappings  $f_1, \dots, f_8$ , presented in Fig. 14.3.5, is described as follows:

MAPPING  $f_1$  from the  $z$ -plane onto the  $z_1$ -plane is given by

$$z_1 = \frac{2 r_*}{z_* - z},$$

where  $z_* = x_* + i r_*$  is the inversion point of the stagnation point  $z = x + i r$ .

MAPPING  $f_2$  from the  $z_1$ -plane onto the  $z_2$ -plane is

$$z_2 = i \sqrt{i(z_1 + i)} + 1.$$

This separates the interior and exterior points at infinity and thus opens up the closed centerline in the  $z_1$ -plane. The square root of  $z_1 + i$  is used with a cut starting at the branch point  $z_1 = -i$ .

MAPPING  $f_3$  from the  $z_2$ -plane onto the  $z_3$ -plane is given by

$$z_3 = \frac{i z_2}{z_2 - 2}.$$

This bilinear transformation takes the point  $z_2 = 2$  into  $\infty$  and the centerline into the positive real axis in the  $z_3$ -plane. While approaching the interior infinity the inside inlet in the  $z_3$ -plane tends to a line with a constant imaginary part for increasing positive values of the real part. This leads to a situation where the flow field in the  $z_3$ -plane ‘opens up’ as in the  $z_4$ -plane.

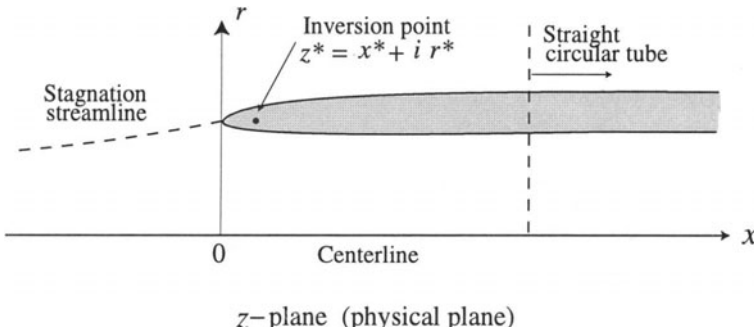


Fig. 14.3.4.

MAPPING  $f_4$  from the  $z_3$ -plane to the  $z_4$ -plane is given by

$$z_4 = e^{c_3 z_3},$$

where the constant  $c_3$  is chosen such that  $\Im \left\{ \lim_{z_3 \rightarrow \infty} c_3 z_3 \right\} = \pi$  on the inlet interior side of the contour; thus  $c_3 = \frac{\pi r_*}{2 r_{\text{int}}}$ , where  $r_{\text{int}}$  denotes the interior radius for downstream in the inlet (see Fig 14.3.5 where the flow field contour is transformed into a Jordan contour without corners).

MAPPING  $f_5$  from the  $z_4$ -plane onto the  $z_5$ -plane is given by

$$z_5 = -\frac{z_4 + (1 + i b_4)}{z_4 - (1 - i b_4)},$$

where the constant  $b_4$  takes some suitable value between 0.1 and 1. Although the contour in the  $z_5$ -plane has a continuously varying tangent, it has curvature singularities at the two points at infinity.

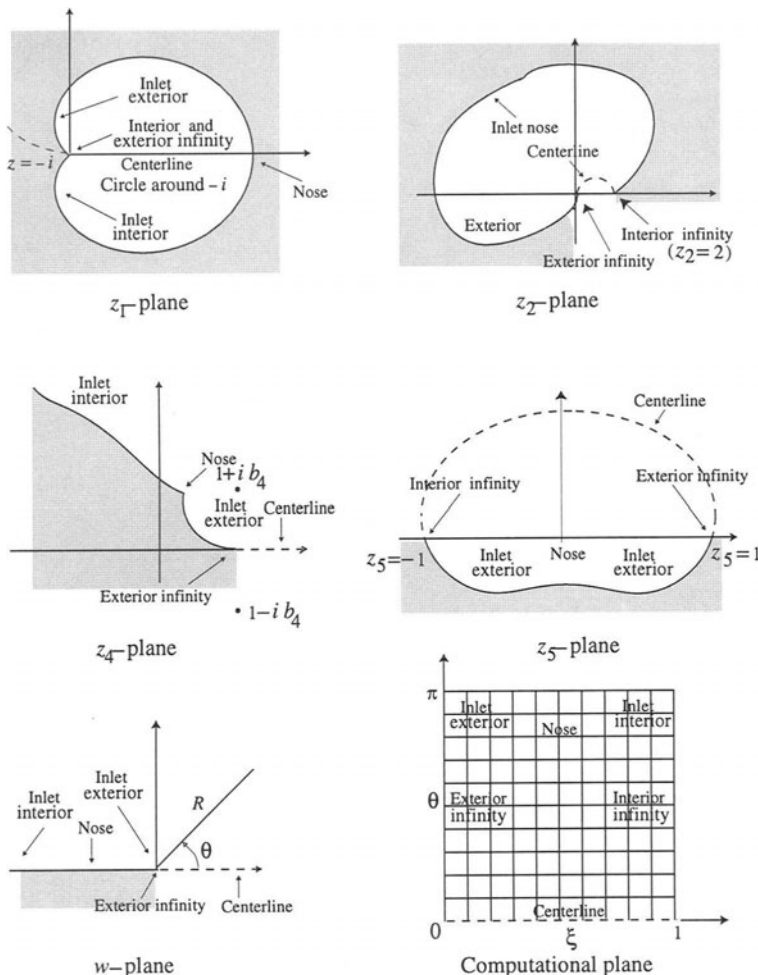


Fig. 14.3.5.

At this point we would like to use the Fourier series to transform the boundary into the unit circle. Since the exponential function is used in the mapping  $f_4$ , the far downstream region in the inlet interior is very dense around the interior infinity. Thus, the Fourier series mapping of the region in the  $z_5$ -plane will not be highly accurate in the neighborhood of the interior infinity which is at  $z_5 = -1$ . To avoid this, we use a Taylor series expansion of the mapping function  $f_5$  about this point. Since the leading terms of this series do not contain the curvature at the interior infinity, the curvature singularity becomes negligible and can be neglected. We shall further discuss the case of interior infinity at  $z_5 = -1$  hereafter. At the exterior infinity, which is mapped into  $z_5 = 1$  the curvature has a finite discontinuity, where, to compute the behavior of  $z$  near the exterior infinity, we use the transformation  $f_7$ , defined below, which removes the curvature singularity at  $z_5 = 1$  before the boundary is mapped onto the unit circle.

A transformation of the type

$$z_5 \sim z_6 \left[ 1 + c_6 (z_6 - 1)^2 \log(z_6 - 1) \right],$$

where

$$c_6 = -\frac{2i b_4 r_{\text{int}} r_{\text{ext}}}{\pi^2 r_*^2},$$

and  $r_{\text{int}}$  and  $r_{\text{ext}}$  denote the interior and exterior radius of the downstream constant geometric part of the inlet. Thus,

MAPPING  $f_6$  from the  $z_5$ -plane onto the  $z_6$ -plane is given by

$$z_5 = \left[ 1 + c_6 \frac{(z_6 - 1)^2 [\log(c_6 - 1) - i\pi/2]}{1 - i a_6 c_6 (z_6 - 1)} \right],$$

where the constant  $a_6$  has the value of about 5. This mapping is single-valued.

MAPPING  $f_7$  from the  $z_6$ -plane onto the  $z_7$ -plane is given by

$$z_6 - z_6^* = z_7 \exp \left[ \sum_{n=0}^M (\alpha_n + i\beta_n) z_7^n \right],$$

where the point  $z_6^*$  is located near or at  $z_6 = 0$ . This function maps the boundary in the  $z_6$ -plane onto the unit circle in the  $z_7$ -plane such that the exterior infinity goes into the point  $z_7 = 1$  and the interior infinity into some point  $z_7 = e^{i\theta_7}$ .

MAPPING  $f_8$  from  $z_7$ -plane to the  $w$ -plane is given by

$$w = -e^{i\theta_7/2} \frac{z_7 - 1}{z_7 - e^{i\theta_7}}.$$

This bilinear transformation maps the flow field from the unit disk onto the upper half-plane  $\Im\{w\} > 0$ .

The problem at the interior infinity at  $z_5 = -1$  can be remedied by taking, instead of  $f_4$ , the mapping  $f'_4$ , defined by

$$z'_3 = z_3 - \frac{a_3}{z_3 + b_3},$$

where  $a_3$  and  $b_3$  are properly chosen. Then the new  $z_5$ -contour will be much ‘fuller’ below the point  $z_5 = -1$  instead of  $z_5 = -1$ . This will affect the subsequent mappings  $f_5$  and  $f_6$ , which will then be defined by

$$f'_5 : z_5 = -\frac{z_4 - (a_4 + i b_4)}{z_4 - (a_4 - i b_4)},$$

with

$$c_6 = -\frac{2 i b_4 r_{\text{int}} r_{\text{ext}}}{\pi^2 r_*^2 a_4 (1 + a_3/b_3^2)},$$

where, in practice, we take  $1 < a_3 < 2.5$ , and  $b_3 \approx 2$ .

The Fourier coefficients in the mapping  $f_6$  are computed from

$$\frac{dz_6}{dz_7} = \exp \left[ \sum_{n=0}^M (\gamma_n + i \delta_n) z_7^n \right].$$

This increases the numerical accuracy over that obtained from differentiating the function  $f_6$ .

As a result of this chain of mappings the governing equation (14.3.13) is transformed into

$$(a^2 - q_1^2) \phi_{RR} - 2q_1 q_2 \frac{1}{R} \phi_{R\theta} + (a^2 - q_2^2) \frac{1}{R^2} \phi_{\theta\theta} + a^2 B \left( q_1 \frac{r_R}{r} + \frac{q_2}{R} \frac{r_\theta}{r} + B (a^2 + q_2^2) \frac{q_1}{R} + (q_1^2 + q_2^2) \left( q_1 B_R + \frac{q_2}{R} B_\theta \right) \right) = 0, \quad (14.3.14)$$

where  $q_1$  and  $q_2$  are the velocity components in the  $R$  and  $\theta$  direction, respectively, i.e.,

$$q_1 = \frac{1}{B} \phi_R, \quad q_2 = \frac{1}{RB} \phi_\theta.$$

Arlinger (1975) solved this problem by the finite difference method on the rectangle shown in Fig. 14.3.5 (the computational plane). ■

A Fortran code (TOMCAT) for a method of automatic numerical generation of curvilinear coordinate system with grid lines coinciding with all boundaries of a multiply connected region is available (Thompson, Thames and Mastin, 1977). The computer code is independent of the boundary shapes and numbers, which are input data. The program has the following features: (i) automatic convergence controls activated by input parameters, if needed; (ii) a choice of several different types of initial guesses for the iterative process; (iii) gradual addition of coordinate system control; and (iv) general movement of the outer boundary out to its final position. Another program is available in Thompson et al (1976) for computing the scale factors from the coordinates for use in solving partial differential equations on a coordinate system.

An adaptive grid scheme to solve the Poisson grid generation equations by methods related to Green's function, where the source terms are only position-dependent, uses the boundary element method and is given by Munipalli and Andersen (1996). All of these schemes and programs solve the types of problems discussed in the above case studies.

## 14.4. Problems

**PROBLEM 14.4.1.** Show that under the mapping of a region  $D$  in the  $z$ -plane onto a region  $G$  in the  $w$ -plane by the function  $w = f(z) = u(x, y) + i v(x, y)$ , the Laplace equation for the function  $u(x, y)$  is transformed into the Laplace equation for the function  $U(\xi, \eta) = u(x(\xi, \eta), y(\xi, \eta))$ , i.e., the Laplacian  $\nabla^2$  satisfies the relation

$$\nabla_{xy}^2 = |f'(z)|^2 \nabla_{\xi\eta}^2 = \frac{1}{|F'(w)|^2} \nabla_{\xi\eta}^2,$$

where  $z = F(w)$  denotes the inverse mapping function. (Sveshnikov and Tikhonov, 1978, p.194.)

PROBLEM 14.4.2. Derive the condition (14.3.5) by using the conditions that the pitch of the cascade remains  $h$  if  $A_0 = 1$  and  $A_0 \log \operatorname{dn}(\eta, k'^{(n)}) = \log \operatorname{dn}(\eta, k'^{(n+1)})$ . [Hint: Use  $\operatorname{sn}(\eta, k') \approx \tanh \eta$ ,  $\operatorname{sn}(\eta, k') \approx 1$ , and  $\operatorname{dn}(\eta, k') = \sqrt{1 - k'^2 \operatorname{sn}^2(\eta, k')}$ ] (Inoue, 1983, p.133.)

PROBLEM 14.4.3. Generate graphical representations of the grid lines in the Case Studies in §14.2 and §14.3.

REFERENCES USED: Arlinger (1975), Inoue (1983, 1985), Ives and Liutermoza (1977), Knupp and Steinberg (1993), Lehto and Virtaanen (1973), Munipalli and Andersen (1996), Özisik (1994), Roberts (1971), Sveshnikov and Tikhonov (1978), Thompson et al. (1977, 1985).

# Appendix A

---

## Cauchy's P. V. Integrals

---

### A.1. Numerical Evaluation

We shall derive approximate formulas to compute Cauchy principal value integrals. In practical problems it is often necessary to evaluate Cauchy p.v. integrals which arise in boundary value problems or in singular integral equations. We shall consider the Cauchy p.v. integral

$$F(t_0) = \frac{1}{i\pi} \int_{\Gamma} \frac{f(t)}{t - t_0} dt, \quad t_0 \in \Gamma, \quad (\text{A.1.1})$$

where  $\Gamma$  is a smooth, open arc or a Jordan contour and  $f \in H^1(\Gamma)$ , i.e.,  $f$  satisfies the Hölder condition on  $\Gamma$  with  $\alpha = 1$  (see §1.1). We can rewrite (A.1.1) as

$$\begin{aligned} F(t_0) &= \frac{1}{i\pi} \int_{\Gamma} \frac{f(t) - f(t_0)}{t - t_0} dt + \frac{f(t_0)}{i\pi} \int_{\Gamma} \frac{dt}{t - t_0} \\ &= F_1(t_0) + F_2(t_0). \end{aligned} \quad (\text{A.1.2})$$

The integral  $F_1(t_0)$  is an improper integral whereas  $F_2(t_0)$  may be evaluated directly. Therefore, the problem reduces to evaluating the improper integral

$$F_1(t_0) = \frac{1}{i\pi} \int_{\Gamma} f_1(t) dt, \quad (\text{A.1.3})$$

where

$$f_1(t) = \frac{f(t) - f(t_0)}{t - t_0}.$$

**A.1.1. Method of Separation of Singularities.** If the independent variable  $t$  in (A.1.3) is changed to the arc length parameter of  $\Gamma$  or a real parameter in the parametric equation of  $\Gamma$ , then certain classical results can be applied to the improper integral (A.1.3). In fact, if  $f(t) \in H^1$ , then  $f_1(t)$  is bounded, and (A.1.3) becomes a proper integral. In particular, if  $\Gamma$  is a straight line segment on the real axis, then the variable  $t$  is real. If  $\Gamma$  is a circle or a circular arc with a fixed radius  $r$ , then the substitution  $t = r e^{i\theta}$  also transforms (3.2.3) into an integral of the real variable  $\theta$ . The method of separation of singularities is very easy to use when  $\Gamma$  is a straight line segment  $[a, b]$  of the real axis. The following result can be proved by induction.

**THEOREM A.1.1.** *Let*

$$G(t) = \begin{cases} \frac{g(t) - g(t_0)}{t - t_0}, & \text{if } t \neq t_0, \\ g'(t_0), & \text{if } t = t_0, \end{cases}$$

where  $g(t) \in C^{n+1}[a, b]$ ,  $n \geq 0$ , and  $a \leq t_0 \leq b$ . Then

$$G^{(k)}(t) = \begin{cases} \frac{g^{(k+1)}(\tau_k)}{k+1}, & \text{if } t \neq t_0, \\ \frac{g^{(k+1)}(t_0)}{k+1}, & \text{if } t = t_0, \end{cases} \quad (\text{A.1.4})$$

where  $t_0 < \tau_k < t$ .

In the case when

$$F(t_0) = \frac{1}{i\pi} \int_{\Gamma} \frac{f(t)}{t - t_0} w(t) dt, \quad t_0 \in \Gamma, \quad (\text{A.1.5})$$

where  $w(t) \geq 0$  is a weight function which may have integrable singularities at certain points, e.g., at the end points, then the above theorem can be used, provided (A.1.5) is written as

$$F(t_0) = \frac{1}{i\pi} \int_{\Gamma} f_1(t) w(t) dt + \frac{f(t_0)}{i\pi} \int_{\Gamma} \frac{w(t)}{t - t_0} w(t) dt, \quad t_0 \in \Gamma, \quad (\text{A.1.6})$$

in which the second integral may be evaluated exactly. The above results are due to Ivanov (1968) and Pukhteev (1980).

**A.1.2. Gauss–Chebyshev Type Quadrature.** As an application of above result we shall find an approximate value of the Cauchy p.v. integral

$$I(x) = \frac{1}{\pi} \int_{-1}^1 \frac{g(t)}{t-x} \frac{dt}{\sqrt{1-t^2}}, \quad -1 < x < 1, \quad (\text{A.1.7})$$

with weight function  $w(t) = \frac{1}{\sqrt{1-t^2}}$ , where  $g(x)$  is sufficiently smooth.

First, note that if  $g(t) \equiv 1$ , the value of the integral (A.1.7) is zero. In fact, it can be proved by the contour integration method that

$$\frac{1}{\pi} \int_{-1}^1 \frac{dt}{(t-x)\sqrt{1-t^2}} = 0, \quad -1 < x < 1, \quad (\text{A.1.8})$$

by taking a closed contour  $\Gamma^-$  containing the line segment  $-1 \leq x \leq 1$ , and using the residue theorem to obtain

$$\frac{1}{2i\pi} \int_{\Gamma^-} \frac{d\zeta}{\zeta-z} \frac{d\zeta}{\sqrt{1-\zeta^2}} = \frac{1}{\sqrt{1-z^2}},$$

where  $\Gamma^-$  is clockwise and  $\sqrt{1-\zeta^2}$  is the analytic continuation of the positive real-valued function  $\sqrt{1-x^2}$  along the upper side of  $-1 < x < 1$ . As  $\Gamma$  shrinks to  $-1 \leq x \leq 1$ , we get

$$\frac{1}{i\pi} \int_{-1}^1 \frac{dt}{(t-z)\sqrt{1-t^2}} = \frac{1}{\sqrt{1-z^2}}, \quad z \notin [-1, 1].$$

Then (A.1.7) follows as  $z \rightarrow x$  from the upper (or lower side) and using Plemelji formula (1.2.13). Thus, we can rewrite (A.1.7) as

$$I(x) = \frac{1}{\pi} \int_{-1}^1 \frac{g(t)-g(x)}{t-x} \frac{dt}{\sqrt{1-t^2}}, \quad -1 < x < 1. \quad (\text{A.1.9})$$

Now, if  $f \in C^{2n}[-1, 1]$ , then we have the following Gauss–Chebyshev quadrature formula (see Abramowitz and Stegun, 1964)

$$I \equiv I[f] = \frac{1}{\pi} \int_{-1}^1 \frac{f(t)}{\sqrt{1-t^2}} dt \approx \frac{1}{n} \sum_{k=1}^n f(t_k), \quad (\text{A.1.10})$$

where  $t_k$ ,  $k = 1, 2, \dots, n$ , are the zeros of the Chebyshev polynomial  $T_n(x) = \cos(n \cos^{-1} x)$  of the first kind and degree  $n$ , i.e.,  $t_k = \cos \frac{(2k-1)\pi}{2n}$ ,  $k = 1, 2, \dots, n$ , with the remainder  $R_n$  after  $n$  terms

$$R_n = \frac{1}{(2n)! 2^{2n-1}} f^{2n}(\tau), \quad -1 < \tau < 1. \quad (\text{A.1.11})$$

If we set  $f(t) = \frac{g(t) - g(x)}{t - x}$  in (A.1.10), we obtain the quadrature formula

$$I(x) \approx \frac{1}{n} \sum_{k=1}^n \frac{g(t_k)}{t_k - x} + \frac{g(x)}{n} \sum_{k=1}^n \frac{1}{x - t_k}, \quad -1 < x < 1, \quad x \neq t_k. \quad (\text{A.1.12})$$

However, since  $\sum_{k=1}^n \frac{1}{x - t_k} = \frac{T'_n(x)}{T_n(x)}$  and  $T'_n(x) = n U_{n-1}(x)$ , where

$$U_{n-1}(x) = \frac{\sin(n \cos^{-1} x)}{\sqrt{1 - x^2}}$$

is the Chebyshev polynomial of the second kind and degree  $n - 1$ , we find that

$$\sum_{k=1}^n \frac{1}{x - t_k} = \frac{n U_{n-1}(x)}{T_n(x)},$$

and formula (A.1.12) becomes

$$I(x) \approx \frac{1}{n} \sum_{k=1}^n \frac{g(t_k)}{t_k - x} + g(x) \frac{U_{n-1}(x)}{T_n(x)}, \quad -1 < x < 1, \quad x \neq t_k, \quad (\text{A.1.13})$$

which is a Gauss–Chebyshev type quadrature formula. In particular, if  $x = x_j$  is taken as a zero of  $U_{n-1}(x)$ , i.e., if  $x_j = \cos \frac{j\pi}{n}$ ,  $j = 1, 2, \dots, n - 1$ , then formula (A.1.13) simplifies to

$$I(x_j) \approx \frac{1}{n} \sum_{k=1}^n \frac{g(t_k)}{t_k - x_j}, \quad j = 1, 2, \dots, n - 1. \quad (\text{A.1.14})$$

This quadrature formula is useful in solving the following integral equation of the first kind:

$$\frac{1}{\pi} \int_{-1}^1 \frac{\phi(t)}{t - x} dt + \int_{-1}^1 k(x, t) \phi(t) dt = f(x), \quad -1 < x < 1, \quad (\text{A.1.15})$$

where  $k(x) \in H^0([-1, 1] \times [-1, 1])$ .

**A.1.3. Approximation by arcwise linear functions.** The arc length parameter  $s$  can be used for approximating (A.1.1) in the case of simple contours (of integration). If the contour is complicated, we shall first approximate the function  $f(t)$  by an arcwise linear function and estimate error.

Let  $AB$  denote an open, smooth arc, and let  $f(t) \in H^\alpha$ ,  $0 < \alpha \leq 1$  be defined on  $AB$ . We partition  $AB$  by  $A = t_1, \dots, t_n = B$  and let  $\Gamma_j$  denote a partition  $(t_j, t_{j+1})$ . Let  $y_j = f(t_j)$ ,  $\Delta y_j = y_{j+1} - y_j$ , and  $D_j = \Delta y_j / \Delta t_j$ . We shall define arcwise linear functions  $L_j(t)$  on  $AB$  such that  $L_j(t) = y_j + D_j(t - t_j)$  for  $t \in \Gamma_j$ ,  $j = 1, \dots, N$ . Then, if the error is denoted by  $e_j(t)$ , we have

$$\begin{aligned} |e_j(t)| &= |f(t) - L_j(t)| \leq |f(t) - y_j| + |D_j| |t - t_j| \\ &\leq C |t - t_j|^\alpha + \frac{C}{|\Delta(t_j)|^{1-\alpha}} |t - t_j| \leq C \delta^\alpha, \end{aligned} \quad (\text{A.1.16})$$

where  $C$  is a constant and  $\delta = \max_j |\Delta y_j|$ . This inequality implies that the error  $e_j(t)$  becomes very small if  $\{t_j\}$  is very dense, i.e., if  $\delta$  is very small.

For example, let us consider the error when the integral in (A.1.1) is replaced by  $\int_\Gamma \frac{L_j(t)}{t - \tau} dt$ . Then

$$\int_\Gamma \frac{e_j(t)}{t - \tau} dt = \int_\Gamma \frac{e_j(t) - e_j(\tau)}{t - \tau} dt + e_j(\tau) \int_\Gamma \frac{dt}{t - \tau} = I_1(\tau) + I_2(\tau),$$

and, in view of (A.1.16),

$$|I_2(\tau)| \leq C |e_j(\tau)| \leq C \delta^\alpha. \quad (\text{A.1.17})$$

Now, if  $t$  and  $\tau$  are in the same  $\Gamma_j$ , we have

$$|e_j(t) - e_j(\tau)| \leq C |t - \tau|^\alpha \leq C \delta^{\alpha-\varepsilon} |t - \tau|^\varepsilon, \quad (\text{A.1.18})$$

where  $\varepsilon$ ,  $0 < \varepsilon < \alpha$ , is very small. If  $\tau \in \Gamma_{j-1}$  and  $t \in \Gamma_k$ ,  $j \leq k$ , then, since  $e_j(\tau_j) = e_j(\tau_k) = 0$ , we find that

$$\begin{aligned} |e_j(t) - e_j(\tau)| &\leq |e_j(t)| + |e_j(\tau)| \leq |e_j(t) - e_j(\tau_k)| + |e_j(\tau) - e_j(\tau_j)| \\ &\leq C (|t - \tau_k|^\alpha + |t - \tau_j|^\alpha) \\ &\leq C \delta^{\alpha-\varepsilon} (|t - \tau_k|^\varepsilon + |t - \tau_j|^\varepsilon) \\ &\leq C \delta^{\alpha-\varepsilon} (|\tau_k t|^\varepsilon + |\tau_j t|^\varepsilon) \\ &\leq C \delta^{\alpha-\varepsilon} (|\tau t|^\varepsilon) \leq C \delta^{\alpha-\varepsilon} (|t - \tau|^\varepsilon). \end{aligned}$$

Thus, (A.1.18) always holds for some constant  $C$ , and

$$|I_1(t)| \leq C \delta^{\alpha-\varepsilon} \int_\Gamma |t - \tau|^{-1+\varepsilon} |dt| \leq C \delta^{\alpha-\varepsilon} \int_\Gamma s^{-1+\varepsilon} ds \leq C_\varepsilon \delta^{\alpha-\varepsilon}, \quad (\text{A.1.19})$$

where  $C_\varepsilon$  is a constant that depends on  $\varepsilon$ . In general,  $C_\varepsilon \rightarrow +\infty$  as  $\varepsilon \rightarrow 0$ . Hence, the inequalities (A.1.18) and (A.1.19) yield

$$\left| \int_{\Gamma} \frac{f(t)}{t - \tau} dt - \frac{L_j(t)}{t - \tau} dt \right| \leq C_\varepsilon \delta^{\alpha-\varepsilon}, \quad 0 < \varepsilon < \alpha. \quad (\text{A.1.20})$$

Since  $\varepsilon$  is arbitrary, we find that for very small  $\delta$  the left side of (A.1.20) becomes arbitrarily small. Thus,  $\sum_{j=1}^N L_j(t)$  approximates the kernel  $f(t)$  in Cauchy's p.v. integral (A.1.1), and

$$\int_{\Gamma} \frac{f(t)}{t - \tau} dt \approx \sum_{j=1}^N \int_{\Gamma_j} \frac{L_j(t)}{t - \tau} dt, \quad (\text{A.1.21})$$

which can be easily computed. For more on this topic, see the references cited below.

REFERENCES USED: Ivanov (1968), Lu (1984, 1994), Pukhteev (1980).

# Appendix B

---

## Green's Identities

---

### B.1. Green's Identities

Let  $\Omega$  be a finite domain in  $R^n$  bounded by a piecewise smooth, orientable surface  $\partial\Omega$ , and let  $w$  and  $F$  be scalar functions and  $\mathbf{G}$  a vector function in the class  $C^0(\Omega)$ . Then

$$\text{Gradient theorem: } \int_{\Omega} \nabla F \, d\Omega = \oint_{\partial\Omega} \mathbf{n} F \, dS,$$

$$\text{Divergence theorem: } \int_{\Omega} \nabla \cdot \mathbf{G} \, d\Omega = \oint_{\partial\Omega} \mathbf{n} \cdot \mathbf{G} \, dS,$$

$$\text{Stokes's theorem: } \int_{\Omega} \nabla \times \mathbf{G} \, d\Omega = \oint_{\partial\Omega} \mathbf{G} \cdot \mathbf{t} \, dS,$$

where  $\mathbf{n}$  is the outward normal to the surface  $\partial\Omega$ ,  $\mathbf{t}$  is the tangent vector at a point on  $\partial\Omega$ ,  $\oint$  denotes the surface or line integral, and  $dS$  (or  $ds$ ) denotes the surface (or line) element depending on the dimension of  $\Omega$ . The divergence theorem in the above form is also known as the Gauss theorem. Stokes's theorem in  $\mathbb{R}^2$  is a generalization of *Green's theorem* which states that if  $\mathbf{G} = (G_1, G_2)$  is a continuously differentiable vector field defined on a region containing  $\Omega \cup \partial\Omega \subset \mathbb{R}^2$  such that  $\partial\Omega$  is a Jordan contour, then

$$\int_{\Omega} \left( \frac{\partial G_2}{\partial x_1} - \frac{\partial G_1}{\partial x_2} \right) dx_1 dx_2 = \oint_{\partial\Omega} G_1 dx_1 + G_2 dx_2. \quad (\text{B.1})$$

Let the functions  $M(x, y)$  and  $N(x, y)$ , where  $(x, y) \in \Omega$ , be the components of the vector  $\mathbf{G}$ . Then, by the divergence theorem

$$\begin{aligned} \int_{\Omega} \left( \frac{\partial M}{\partial x} + \frac{\partial N}{\partial y} \right) dx dy &= \oint_{\Gamma} [M \cos(\mathbf{n}, x) + N \cos(\mathbf{n}, y)] ds, \\ &= \oint_{\Gamma} M dx + N dy, \end{aligned} \quad (\text{B.2})$$

with the direction cosines  $\cos(\mathbf{n}, x)$  and  $\cos(\mathbf{n}, y)$ , where  $\Gamma = \partial\Omega$ . If we take  $M = f g_x$  and  $N = f g_y$ , then (B.2) yields

$$\int_{\Omega} \left( \frac{\partial f}{\partial x} \frac{\partial g}{\partial x} + \frac{\partial f}{\partial y} \frac{\partial g}{\partial y} \right) dx dy = \int_{\Gamma} f \frac{\partial g}{\partial n} ds - \int_{\Omega} f \nabla^2 g dx dy, \quad (\text{B.3})$$

which is known as *Green's first identity*. Moreover, if we interchange  $f$  and  $g$  in (B.2), we get

$$\int_{\Omega} \left( \frac{\partial f}{\partial x} \frac{\partial g}{\partial x} + \frac{\partial f}{\partial y} \frac{\partial g}{\partial y} \right) dx dy = \int_{\Gamma} g \frac{\partial f}{\partial n} ds - \int_{\Omega} g \nabla^2 f dx dy. \quad (\text{B.4})$$

If we subtract (B.3) from (B.4), we obtain *Green's second identity*:

$$\int_{\Omega} (f \nabla^2 g - g \nabla^2 f) dx dy = \int_{\Gamma} \left( f \frac{\partial g}{\partial n} - g \frac{\partial f}{\partial n} \right) ds, \quad (\text{B.5})$$

which is also known as *Green's reciprocity theorem*. Note that Green's identities are valid even if the domain  $\Omega$  is bounded by finitely many closed curves. In that case, however, the line integrals must be evaluated over all paths that make the boundary of  $\Omega$ . If  $f$  and  $g$  are real and harmonic in  $\Omega \subset \mathbb{R}$ , then from (B.5)

$$\int_{\Gamma} \left( f \frac{\partial g}{\partial n} - g \frac{\partial f}{\partial n} \right) ds = 0. \quad (\text{B.6})$$

Let  $D$  be a simply connected region in the complex plane  $\mathbb{C}$  with boundary  $\Gamma$ . Let  $z_0$  be any point inside  $D$ , and let  $\Omega$  be the region obtained by indenting a disk  $B(z_0, \varepsilon)$  from  $D$ , where  $\varepsilon > 0$  is small (Fig. B.1 (a)). Then  $\partial D$  consists of the contour  $\Gamma$  together with the contour  $\partial B(z_0, \varepsilon) = \Gamma_\varepsilon$ .

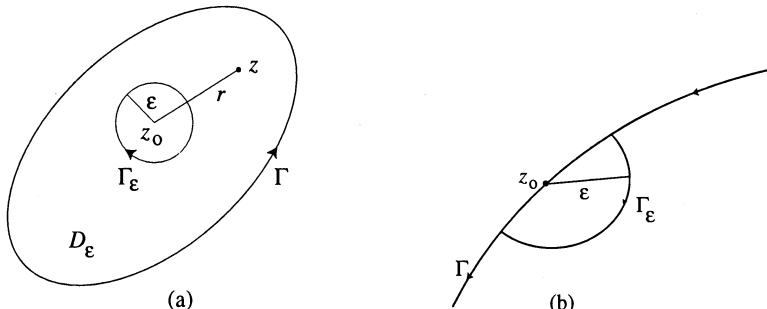


Fig. B.1.

If we set  $f = u$  and  $g = \log r$  in (B.6), where  $z \in D$  and  $r = |z - z_0|$ , then, since  $\frac{\partial}{\partial n} = -\frac{\partial}{\partial r}$  on  $\Gamma_\varepsilon$ , we get

$$\int_{\Gamma} \left( u \frac{\partial}{\partial n} (\log r) - (\log r) \frac{\partial u}{\partial n} \right) ds - \int_{\Gamma_\varepsilon} \left( \frac{u}{r} - (\log r) \frac{\partial u}{\partial r} \right) ds = 0. \quad (\text{B.7})$$

Now, let  $\varepsilon \rightarrow 0$  in (B.7). Then, since

$$\begin{aligned} \lim_{\varepsilon \rightarrow 0} \int_{\Gamma_\varepsilon} \frac{u}{r} ds &= \lim_{\varepsilon \rightarrow 0} \int_0^{2\pi} u(z_0 + \varepsilon\theta) \frac{1}{\varepsilon} \varepsilon d\theta = 0, \\ \lim_{\varepsilon \rightarrow 0} \int_{\Gamma_\varepsilon} \log r \frac{\partial u}{\partial r} ds &= \lim_{\varepsilon \rightarrow 0} \int_0^{2\pi} \log \varepsilon \frac{\partial u}{\partial \varepsilon} \varepsilon d\theta = 0, \end{aligned}$$

we obtain

$$2\pi u(z_0) = \int_{\Gamma} \left[ u \frac{\partial}{\partial n} (\log r) - (\log r) \frac{\partial u}{\partial n} \right] ds, \quad (\text{B.8})$$

which is known as *Green's third identity*. Note that Eq (B.8) gives the value of a harmonic function  $u$  at an interior point in terms of the boundary values of  $u$  and  $\frac{\partial u}{\partial n}$ . If the contour  $\Gamma$  has no corners and if the point  $z_0$  is on the boundary  $\Gamma$ , then instead of the whole disk  $B(z_0, \varepsilon)$  we consider a half disk at the point  $z_0$  deleted from  $D$  (Fig. B.1(b)), and Green's third identity becomes

$$\pi u(z_0) = \text{p.v.} \int_{\Gamma} \left[ u \frac{\partial}{\partial n} (\log r) - (\log r) \frac{\partial u}{\partial n} \right] ds, \quad (\text{B.9})$$

where p.v. denotes the principal value of the integral, i.e., it is the limit, as  $r \rightarrow 0$ , of the integral over the contour  $\Gamma$  obtained by deleting that part of  $\Gamma$  which lies within the circle of radius  $\varepsilon$  and center  $z_0$ .

REFERENCES USED: Carrier, Krook and Pearson (1966), Kythe (1996), Kythe, Puri and Schäferkotter (1997).

# Appendix C

---

## Riemann–Hilbert Problem

---

We shall also consider two boundary value problems of the theory of analytic functions. They are the Hilbert and the Riemann problems. A close relationship exists between the Hilbert problem and the theory of singular integral equations. Although the latter may be developed to a large extent without the former, it is this relationship that makes the latter simple and clear. For example, the iterative method for solving Theodorsen's integral equation, as outlined in Chapter 8, is based on a certain Riemann–Hilbert problem. In fact, Theodorsen's problem is a linearized version of a singular integral equation of the second kind.

---

### C.1. Homogeneous Hilbert Problem

Consider the  $n$ -tuply connected region of Fig. C.1.1, with the boundary  $\Gamma = \cup_{k=1}^n \Gamma_k$ . The *homogeneous Hilbert problem* states: Find a sectionally analytic function  $\Phi(z)$  of finite degree at infinity such that

$$\Phi^+(t) = G(t) \Phi^-(t) \quad \text{on } \Gamma, \quad (\text{C.1.1})$$

where  $\Phi^+(t)$  and  $\Phi^-(t)$  are limiting values from the right and the left at a point  $t \in \Gamma$  (if  $t$  is an end point, then  $\Phi^+(t) = \Phi^-(t) = \Phi(t)$ ), and  $G(t)$ , defined on  $\Gamma$ , satisfies the Hölder condition and  $G(t) \neq 0$  at the point  $t \in \Gamma$ . If we take the logarithm on both sides of (C.1.1), we get

$$[\log \Phi(t)]^+ - [\log \Phi(t)]^- = \log G(t). \quad (\text{C.1.2})$$

As  $t$  moves along the contours  $\Gamma_k$  in the positive sense, i.e., counterclockwise for  $k = 0$  and clockwise for  $k = 1, \dots, n$  (Fig. C.1.1),  $\log G(t)$  increases by integral multiples of  $2i\pi$ . Thus,

$$\frac{1}{2i\pi} [\log \Phi(t)]_{\Gamma_k} = \frac{1}{2\pi} [\arg\{G(t)\}]_{\Gamma_k} = \lambda_k, \quad k = 0, 1, \dots, n, \quad (\text{C.1.3})$$

where  $\lambda_k$  are integers (positive, negative, or zero), and  $[\arg\{G(t)\}]_{\Gamma_k}$  denotes the increment of  $\arg\{G(t)\}$  as it goes around the contour  $\Gamma_k$ . The sum

$$\kappa = \sum_{k=0}^n \lambda_k = \frac{1}{2i\pi} [\log \Phi(t)]_{\Gamma} = \frac{1}{2\pi} [\arg\{G(t)\}]_{\Gamma} = \lambda_k \quad (\text{C.1.4})$$

is known as the *index* of the Hilbert problem and also as the *index* of the function  $G(t)$  given on  $\Gamma$ . The index  $\kappa$  is an integer.

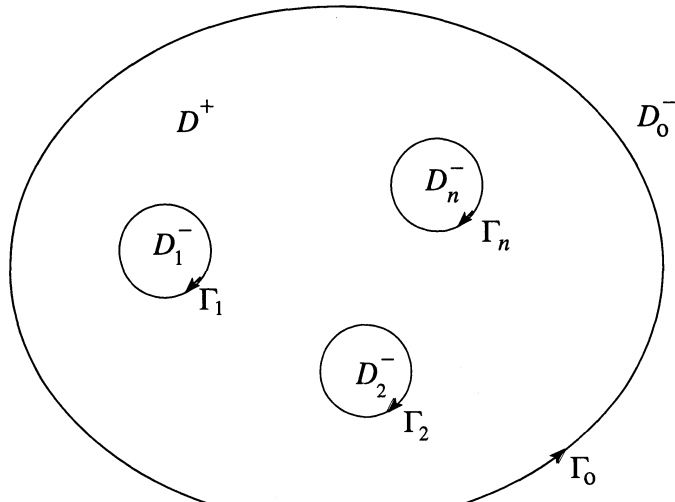


Fig. C.1.1.

Let  $a_1, \dots, a_n$  be arbitrary fixed points in the regions  $D_1^-, \dots, D_n^-$ , and let the origin of the coordinates be in the region  $D^+$ . Let

$$p(z) = \begin{cases} (z - a_1)^{-\alpha_1} \cdots (z - a_n)^{-\alpha_n} & \text{if } \Gamma = \cup_{k=1}^n \Gamma_k, \\ 1 & \text{if } \Gamma = \Gamma_0. \end{cases} \quad (\text{C.1.5})$$

Let

$$G_0(t) = t^{-\kappa} p(t) G(t). \quad (\text{C.1.6})$$

Then, after traversing the contours  $\Gamma_0, \Gamma_1, \dots, \Gamma_n$ , the function  $\arg \{G_0(t)\}$  returns to its initial value, and therefore  $\log G_0(t)$  is a well-defined single-valued and continuous function on  $\Gamma$  and satisfies the Hölder condition there with an arbitrarily fixed branch on each contour  $\Gamma_k$ .

To determine the solution  $\Phi(z)$  of the homogeneous Hilbert problem (C.1.1), we introduce a new unknown function

$$\Psi(z) = \begin{cases} p(z) \Phi(z) & \text{in } D^+ \\ z^k \Phi(z) & \text{in } D^-, \end{cases} \quad (\text{C.1.7})$$

which is regular except possibly at  $z = \infty$ . Then the condition (C.1.1) can be written as

$$\Psi^+(t) = G_0(t) \Psi^-(t). \quad (\text{C.1.8})$$

First we shall find the *fundamental solution* for the homogeneous Hilbert problem. By taking the logarithm on both sides of (C.1.8), we formally get

$$\log \Psi^+(t) - \log \Psi^-(t) = \log G_0(t). \quad (\text{C.1.9})$$

If we assume that  $\log \Psi(z)$  is single-valued, sectionally regular on  $\Gamma$ , and zero at  $z = \infty$ , then

$$\log \Psi(z) = \frac{1}{2i\pi} \int_{\Gamma} \frac{\log G_0(t)}{t - z} dt,$$

thus, by using the Plemelj formulas (1.2.13) we find that

$$\Psi(z) = e^{g(z)}, \quad (\text{C.1.10})$$

where

$$g(z) = \frac{1}{2i\pi} \int_{\Gamma} \frac{\log G_0(t)}{t - z} dt. \quad (\text{C.1.11})$$

Obviously,  $\Psi(z)$  is sectionally regular on  $\Gamma$ ,  $\Psi(z) \neq 0$  for all finite  $z$ , and  $\Psi(\infty) = 1$ . It is also a particular solution of problem (C.1.8), since, in view of (C.1.11),  $g^+(t_0) - g^-(t_0) = \log G_0(t_0)$  for an arbitrary point  $t_0 \in \Gamma$ . Thus,

$$\frac{\Psi^+(t_0)}{\Psi^-(t_0)} = e^{\log G_0(t_0)} = G_0(t_0),$$

which is the same as (C.1.9). Hence, from this particular solution we obtain a particular solution of the homogeneous Hilbert problem (C.1.1) which we represent as

$$Z(z) = \begin{cases} \frac{1}{p(z)} & \text{for } z \in D^+ \\ z^{-\kappa} e^{g(z)} & \text{for } z \in D^-, \end{cases} \quad (\text{C.1.12})$$

where  $g(z)$  is defined by (C.1.10). This particular solution  $Z(z)$  is called a *fundamental solution* of the homogeneous Hilbert problem (C.1.1) because it vanishes nowhere in any finite part of the  $z$ -plane if  $\kappa > 0$  and  $Z(\infty) = 0$ . This also holds for the boundary values  $Z^+(t)$  and  $Z^-(t)$ . Note that  $Z(z)$  is of degree  $(-\kappa)$  at  $z = \infty$ . By using the Plemelj formulas (1.2.13), we get

$$\begin{aligned} g^+(t_0) &= \frac{1}{2} \log G_0(t_0) + g(t_0), \\ g^-(t_0) &= -\frac{1}{2} \log G_0(t_0) + g(t_0), \end{aligned}$$

and then, in view of (C.1.12), the boundary values  $Z^+(t)$  and  $Z^-(t)$  are given by

$$\begin{aligned} Z^+(t_0) &= \frac{e^{g(t_0)} \sqrt{G_0(t_0)}}{p(t_0)} = \frac{e^{g(t_0)} \sqrt{G(t_0)}}{t_0^{\kappa/2} \sqrt{p(t_0)}}, \\ Z^-(t_0) &= \frac{e^{g(t_0)}}{t_0^\kappa \sqrt{G_0(t_0)}} = \frac{e^{g(t_0)}}{t_0^{\kappa/2} \sqrt{p(t_0)G_0(t_0)}}, \end{aligned} \quad (\text{C.1.13})$$

where we have used (C.1.6) which also gives

$$\frac{\sqrt{G(t)}}{t^{\kappa/2} \sqrt{p(t)}} = \frac{\sqrt{G_0(t)}}{p(t)}. \quad (\text{C.1.14})$$

**THEOREM C.1.1.** *All solutions of the homogeneous Hilbert problem (C.1.1) which have finite degree at infinity are given by*

$$\Phi(z) = Z(z) P(z), \quad (\text{C.1.15})$$

where  $P(z)$  is an arbitrary polynomial.

**PROOF.** Let  $\Phi(z)$  be any solution. Then by (C.1.1)

$$\Phi^+(t) = G(t) \Phi^-(t), \quad \text{and} \quad Z^+(t) = G(t) Z^-(t).$$

Since  $Z^+(t) \neq 0$  and  $Z^-(t) \neq 0$ , we find that

$$\frac{F^+(t)}{Z^+(t)} = \frac{F^-(t)}{Z^-(t)} = G(t),$$

which implies that the function  $\frac{\Phi(z)}{Z(z)}$  is regular in the entire  $z$ -plane, and has finite degree at  $z = \infty$ . Thus, it is a polynomial, which proves the theorem. ■

Some of the consequences of this theorem are as follows:

(i) The limiting values  $\Phi^+(t)$  and  $\Phi^-(t)$  of any solution  $\Phi(z)$  of the homogeneous Hilbert problem satisfy the Hölder condition because the function  $G(t)$  does so.

(ii) If the polynomial  $P(z)$  is of degree  $n$ , then the degree of the solution  $\Phi(z)$ , given by (C.1.15), at  $z = \infty$  is  $(n - \kappa)$ , i.e., the degree of this solution is not less than the degree  $(-\kappa)$  of  $Z(z)$ . The degree of  $\Phi(z)$  and  $Z(z)$  at  $z = \infty$  are the same only if  $n = 0$ , i.e., if  $P(z) \equiv \text{const} \neq 0$ . Hence, the index  $(-\kappa)$  is the lowest possible degree of a solution of the homogeneous Hilbert problem.

(iii) The fundamental solution  $Z(z)$  has the following properties:

- (a)  $Z(z)$  does not vanish in any finite part of the  $z$ -plane;
- (b)  $Z(z)$  has the lowest possible degree  $(-\kappa)$  at  $z = \infty$ ; and
- (c)  $Z(z)$  is a factor of every solution of the problem (C.1.1).

(iv) An application of the solution (C.1.1) produces the following result: If  $\kappa \leq 0$ , the homogeneous Hilbert problem has no solution vanishing at  $z = \infty$ , except the trivial solution  $\Phi(z) \equiv 0$ . If  $\kappa > 0$ , it has exactly  $\kappa$  linearly independent solutions  $\Phi(z), z\Phi(z), \dots, z^{\kappa-1}\Phi(z)$ , each of which vanishes at  $z = \infty$ . In fact, since the polynomial  $P(z)$  in (C.1.15) is of degree at most  $(\kappa - 1)$ , all solutions of (C.1.1) that vanish at  $z = \infty$  must have the form  $\Phi(z) = Z(z)p_{\kappa-1}(z)$ , where

$$p_{\kappa-1}(z) = c_0 + c_1z + \dots + c_{\kappa-1}z^{\kappa-1},$$

and  $c_0, c_1, \dots, c_{\kappa-1}$  are arbitrary constants.

(v) If the contour  $\Gamma_0$  is at infinity, then the solution (C.1.15) holds only for  $\lambda_k = 0$ , i.e., for  $\kappa = 0$ .

(vi) The homogeneous Hilbert problems that correspond to the conditions

$$\Phi^+(t) = G(t)\Phi^-(t) \quad \text{and} \quad \Psi^+(t) = [G(t)]^{-1}\Psi^-(t), \quad (\text{C.1.16})$$

are known as adjoint problems of one another. Hence, if the former problem has index  $\kappa$  and fundamental solution  $Z(z)$ , then the latter has index  $(-\kappa)$  and fundamental solution  $[Z(z)]^{-1}$ .

## C.2. Nonhomogeneous Hilbert Problem

A generalization of the homogeneous Hilbert problem is the nonhomogeneous problem which states: Find a sectionally analytic function  $\Phi(z)$  of finite degree at infinity such that

$$\Phi^+(t) = G(t) \Phi^-(t) + g(t) \quad \text{on } \Gamma, \quad (\text{C.2.1})$$

where  $G(t)$  and  $g(t)$ , defined on  $\Gamma$  ( $t \in \Gamma$ ), satisfy the Hölder condition on  $\Gamma$  and  $G(t) \neq 0$  on  $\Gamma$ .

The nonhomogeneous Hilbert problem can easily be solved by using the results of the previous section. Let  $Z(z)$  be the fundamental solution for the homogeneous problem, defined by (C.1.12). Then this is also the fundamental solution for (C.2.1) with  $g(t) \equiv 0$ , in which case Eq (C.2.1) yields

$$G(t) = \frac{Z^+(t)}{Z^-(t)}, \quad (\text{C.2.2})$$

which when substituted in (C.2.1) gives

$$\frac{\Phi^+(t)}{Z^+(t)} - \frac{\Phi^-(t)}{Z^-(t)} = \frac{g(t)}{Z^+(t)}. \quad (\text{C.2.3})$$

Since the function  $\frac{\Phi(z)}{Z(z)}$  has finite degree at infinity, we get

$$\frac{\Phi(z)}{Z(z)} = \frac{1}{2i\pi} \int_{\Gamma} \frac{g(t)}{Z^+(t)} \frac{dt}{t-z} + P(z), \quad (\text{C.2.4})$$

where  $P(z)$  is an arbitrary polynomial. Hence, the general solution of the nonhomogeneous Hilbert problem (C.2.1) is given by

$$\Phi(z) = \frac{Z(z)}{2i\pi} \int_{\Gamma} \frac{g(t)}{Z^+(t)} \frac{dt}{t-z} + Z(z)P(z). \quad (\text{C.2.5})$$

The function  $Z(z)$  which is the fundamental solution for the corresponding homogeneous problem is called the *fundamental function* for the nonhomogeneous Hilbert problem. The index of this problem is also  $\kappa$ .

We shall examine the solution (C.2.5) when  $\Phi(\infty) = 0$ . Then the degree of  $Z(z)$  at infinity is  $(-\kappa)$ , and the solution (C.2.5) will vanish at infinity for  $\kappa \geq 0$  iff the degree of  $P(z)$  is  $\leq (\kappa - 1)$ . Hence, for  $\kappa = 0$  it suffices to take  $P(z) \equiv 0$ . For  $\kappa < 0$ , obviously  $P(z) \equiv 0$ , and the coefficients of  $z^{-1}, z^{-2}, \dots, z^{-\kappa}$  must be zero in the expansion

$$\frac{1}{2i\pi} \int_{\Gamma} \frac{g(t)}{Z^+(t)(t-z)} dt = - \sum_{j=0}^{\infty} \frac{z^{-(j+1)}}{2i\pi} \int_{\Gamma} \frac{t^j g(t)}{Z^+(t)} dt,$$

i.e.,

$$\frac{1}{2i\pi} \int_{\Gamma} \frac{t^j g(t)}{Z^+(t)} dt = 0, \quad \text{for } j = 0, 1, \dots, -\kappa - 1, \quad (\text{C.2.6})$$

which is a necessary and sufficient condition for the solution to vanish at infinity for  $\kappa < 0$ . Hence, we have proved the following:

**THEOREM C.2.1.** *If  $\kappa \geq 0$ , the general solution of the nonhomogeneous Hilbert problem (C.2.1) that vanishes at infinity is given by*

$$\Phi(z) = \frac{Z(z)}{2i\pi} \int_{\Gamma} \frac{g(t)}{Z^+(t)} \frac{dt}{t-z} + Z(z) P_{\kappa-1}(z), \quad (\text{C.2.7})$$

where  $P_{\kappa-1}(z)$  are arbitrary polynomials of degree  $\leq (\kappa-1)$  and  $P_{\kappa-1}(z) = 0$  for  $\kappa = 0$ . If  $\kappa < 0$ , then the solution is given by

$$\Phi(z) = \frac{Z(z)}{2i\pi} \int_{\Gamma} \frac{g(t)}{Z^+(t)} \frac{dt}{t-z}, \quad (\text{C.2.8})$$

provided conditions (C.2.7) are satisfied.

Note that for  $\kappa = 0$  there is a unique solution that vanishes at infinity. For  $\kappa < 0$  there is a unique solution vanishing at infinity, if such a solution exists, but for  $\kappa > 0$  there is an unlimited number of solutions, and the general solution (C.2.5) contains  $\kappa$  arbitrary constants.

In view of the Schwarz reflection and symmetry principles the Hilbert problems can be applied to the upper half-plane  $D^+$  or the unit disk by using the results obtained in §1.4 and §2.2. The general theory of Riemann–Hilbert problem is presented in the next section. The Riemann–Hilbert problem studied in §8.8 is a linearized form of a singular integral equation of the second kind.

### C.3. Riemann–Hilbert Problem

A generalization of the Hilbert boundary problem is the Riemann–Hilbert problem. This problem deals with determining a function  $\Phi(z) = u + iv$  which is regular in  $D^+$ , continuous on  $D^+ \cup \Gamma$ , and satisfies the boundary condition

$$\Re\{a + ib\} \Phi^+ \equiv a u - b v = c \quad \text{on } \Gamma, \quad (\text{C.3.1})$$

where  $a(t), b(t), c(t)$  are real continuous functions defined for  $t \in \Gamma$ , satisfy the Hölder condition, and are such that  $a^2 + b^2 \neq 0$  everywhere on  $\Gamma$ . Before we solve this problem, note that if

$$\Phi_k(z) = u_k + iv_k, \quad k = 1, \dots, n, \quad (\text{C.3.2})$$

is any particular solution of the homogeneous problem

$$a u - b v = 0 \quad \text{on } \Gamma, \quad (\text{C.3.3})$$

then any linear combination

$$\Phi(z) = \sum_{k=1}^n C_k \Phi_k(z) \quad (\text{C.3.4})$$

is also a solution of the homogeneous problem, where  $C_k, k = 1, \dots, n$ , are real constants, and the functions  $\Phi_k(z)$  are linearly independent. Now we shall determine the solution of problem (C.3.1) for the circle.

**RIEMANN–HILBERT PROBLEM FOR THE UNIT DISK:** Let  $U^+$  denote the unit disk with boundary  $\Gamma$  ( $|z| = 1$ ). Then boundary condition (C.3.1) becomes

$$2 \Re\{a + ib\} \Phi^+(t) = (a + ib) \Phi^+(t) + (a - ib) \overline{\Phi^+(t)} = 2c \quad \text{on } \Gamma. \quad (\text{C.3.5})$$

Let the solution  $\Phi(z)$  be a sectionally analytic function on  $\Gamma$  such that it can be extended in  $U^+$  by the function  $\Phi^*(z)$ , defined by (2.2.12), i.e.,

$$\Phi^*(z) = \bar{\Phi}\left(\frac{1}{z}\right) = \Phi(z) \quad \text{for } |z| \neq 1. \quad (\text{C.3.6})$$

The function  $\Phi^*(z)$  is bounded at  $z = \infty$ . Boundary condition (C.3.5) becomes

$$(a + ib)\Phi^+(t) + (a - ib)\Phi^-(t) = 2c, \quad (\text{C.3.7})$$

or,

$$\Phi^+(t) = G(t)\Phi^-(t) + g(t), \quad (\text{C.3.8})$$

where

$$G(t) = -\frac{a - ib}{a + ib}, \quad g(t) = \frac{2c}{a + ib}. \quad (\text{C.3.9})$$

Thus, the Riemann–Hilbert problem (C.3.5) reduces to a solution of the Hilbert problem (C.3.7). However, if  $\Phi(z)$  is any solution of the Hilbert problem (C.3.7), it may not be the solution of the original Riemann–Hilbert problem (C.3.1) because it may fail to satisfy condition (C.3.6). But we can always construct a solution of problem (C.3.5) by using the function  $\Phi(z)$ . Note that if  $\Phi^-(t) = \bar{\Phi}^-(1/t)$ , (see (2.2.12)), we get

$$(a - ib)\Phi^{*-}(t) + (a + ib)\Phi^{*+}(t) = 2c,$$

which shows that  $\Phi(z)$  is also the solution of the Hilbert problem (C.3.7). Let

$$\Omega(z) = \frac{1}{2} [\Phi(z) + \Phi^*(z)]. \quad (\text{C.3.10})$$

Then  $\Omega(z)$  is the solution of the Riemann–Hilbert problem (C.3.5), because  $\Phi(z) = \bar{\Phi}^*(z) = \frac{1}{2} [\Phi(z) + \Phi^*(z)]$ .

We shall determine the complete set of solutions of the Riemann–Hilbert problem (C.3.5). First, we shall consider homogeneous problem (C.3.5) for  $c([\Phi(z) + \Phi^*(z)]) \equiv 0$ . Let  $\kappa$  be the index of the function  $G([\Phi(z) + \Phi^*(z)])$ , i.e.,

$$\begin{aligned} \kappa &= \frac{1}{2i\pi} [\log G(t)]_\Gamma = \frac{1}{2i\pi} \left[ \log \frac{a - ib}{a + ib} \right]_\Gamma \\ &= \frac{1}{2\pi} [\arg\{a - ib\} - \arg\{a + ib\}]_\Gamma \\ &= \frac{1}{\pi} [\arg\{a - ib\}]_\Gamma. \end{aligned} \quad (\text{C.3.11})$$

Thus,  $\kappa$  is an even integer since  $a(t)$  and  $b(t)$  are continuous functions. The number  $\kappa$  is the index of the Riemann–Hilbert problem (C.3.5).

Let  $Z(z)$  be the fundamental solution of the homogeneous Hilbert problem (C.3.8), i.e.,

$$Z(z) = \begin{cases} C e^{g(z)} & \text{for } |z| < 1, \\ C z^{-\kappa} e^{g(z)} & \text{for } |z| > 1, \end{cases} \quad (\text{C.3.12})$$

where  $C \neq 0$  is an arbitrary constant and

$$g(z) = \frac{1}{2i\pi} \int_{\Gamma} \frac{\log [t^{-\kappa} G(t)]}{t - z} dt = \frac{1}{2\pi} \int_{\Gamma} \frac{h(t)}{t - z} dt, \quad (\text{C.3.13})$$

where

$$h(t) = \arg \left\{ -t^{-\kappa} \frac{a - ib}{a + ib} \right\} \quad (\text{C.3.14})$$

is a real-valued continuous function defined on  $\Gamma$ . Using (2.2.12) we get

$$g^*(z) = \frac{1}{2\pi} \int_{\Gamma} \frac{h(t)}{t - z} dt - i\alpha = g(z) - ia, \quad (\text{C.3.15})$$

where  $\alpha$  is a real constant defined by

$$\alpha = \frac{1}{2i\pi} \int_{\Gamma} \frac{h(t)}{t} dt = \frac{1}{2\pi} \int_0^{2\pi} h(t) d\theta, \quad t = e^{i\theta}. \quad (\text{C.3.16})$$

Hence,

$$Z^*(z) = \begin{cases} \bar{C} e^{g^*(z)} = \bar{C} e^{g(z)-i\alpha} & \text{for } |z| > 1, \\ \bar{C} z^{\kappa} e^{g(z)-i\alpha} & \text{for } |z| < 1, \end{cases}$$

or, for all  $z \notin \Gamma$ ,

$$Z^*(z) = \frac{\bar{C}}{C} z^{\kappa} e^{-i\alpha} Z(z),$$

or, taking  $\bar{C}/C = e^{i\alpha}$ , we get

$$Z^*(z) = z^{\kappa} Z(z). \quad (\text{C.3.17})$$

Now we shall discuss two cases:

CASE 1.  $\kappa \geq 0$ : The homogeneous Hilbert problem (C.3.7) for  $c(t) \equiv 0$  has a nonzero solution bounded at infinity and is given by

$$\Phi(z) = P(z) Z(z), \quad (\text{C.3.18})$$

where

$$P(z) = C_0 z^{\kappa} + C_1 z^{\kappa-1} + \cdots + C_{\kappa} \quad (\text{C.3.19})$$

is an arbitrary polynomial of degree  $\leq \kappa - 1$ . Thus (C.3.18) is a solution of the Riemann–Hilbert problem (C.3.5) iff  $\Phi^*(z) = \Phi(z)$ , i.e.,  $P^*(z)Z^*(z) = P(z)Z(z)$ , where  $P^*(z) = \bar{P}(1/z)$  and  $Z^*(z) = z^\kappa Z(z)$ . Since

$$\begin{aligned} z^\kappa \bar{P}\left(\frac{1}{z}\right) &= \bar{C}_0 + \bar{C}_1 z + \cdots + \bar{C}_\kappa z^\kappa \\ &= C_0 z^\kappa + C_1 z^{\kappa-1} + \cdots + C_\kappa = P(z), \end{aligned} \quad (\text{C.3.20})$$

i.e.,  $C_\kappa = \bar{C}_{\kappa-n}$ ,  $n=0, 1, \dots, \kappa$ , we can set  $C_n = A_n + iB_n$ ,  $n = 0, 1, \dots, \kappa/2$ , where  $A_n, B_n$  are real numbers with  $B_{\kappa/2} = 0$ . Then  $C_m = A_{\kappa-m} - iB_{\kappa-m}$  for  $m = \kappa/2 + 1, \dots, \kappa$ . Thus, there are in all  $(\kappa + 1)$  arbitrary real constants. We shall denote them by  $D_0, D_1, \dots, D_\kappa$ . Then the formal general solution of the homogeneous Riemann–Hilbert problem (C.3.5) is given by

$$\Phi(z) = \sum_{k=0}^{\kappa} D_k \Phi_k(z), \quad (\text{C.3.21})$$

where  $\Phi_k$  ( $k = 0, 1, \dots, \kappa$ ) are linearly independent solutions of the same problem.

**CASE 2.**  $\kappa \leq -2$ : The homogeneous Hilbert problem (C.3.7) has no nonzero solution bounded at infinity. Hence, there is only the trivial (zero) solution of the homogeneous Riemann–Hilbert problem (C.3.7).

**THEOREM C.3.1.** *For  $\kappa \geq 0$  the homogeneous Riemann–Hilbert problem (C.3.7) has exactly  $(\kappa+1)$  linearly independent solutions. Its general solution is given by (C.3.18), where  $Z(z)$  is the fundamental solution of the Hilbert problem (C.3.7) subject to condition (C.3.17). For  $\kappa \leq -2$ , the homogeneous Riemann–Hilbert problem (C.3.5) has only the trivial solution  $\Phi(z) = 0$ .*

Now we shall consider the nonhomogeneous Riemann–Hilbert problem (C.3.5). We can construct its general solution, provided that we find only one particular solution. Then the general solution is the sum of this particular solution and the general solution of the homogeneous problem. However, the problem of finding a particular solution of the Riemann–Hilbert problem (C.3.7) is equivalent to finding any particular solution of the Hilbert problem (C.3.7) that is bounded at  $z = \infty$ , because, in view of (C.3.10), it shall provide us with a particular solution of the Riemann–Hilbert problem (C.3.5). Hence,

**THEOREM C.3.2.** *For  $\kappa \geq 0$  there always exists a solution for the nonhomogeneous Riemann–Hilbert problem (C.3.5). For  $\kappa \leq -2$  this problem has a solution iff the following conditions are satisfied:*

$$\int_0^{2\pi} e^{i(n+\kappa)/2} \Omega(\theta) c(\theta) d\theta = 0, \quad n = 1, 2, \dots, -\kappa - 1, \quad (\text{C.3.22})$$

where

$$\Omega(\theta) = \frac{1}{\sqrt{a^2(\theta) + b^2(\theta)}} \exp \left\{ -\frac{1}{4\pi} \int_0^{2\pi} h(\psi) \cot \frac{\psi - \theta}{2} d\psi \right\}. \quad (\text{C.3.23})$$

Note that conditions (C.3.22) are equivalent to the  $(-\kappa - 1)$  conditions

$$\begin{aligned} \int_0^{2\pi} \Omega(\theta) c(\theta) \cos n\theta d\theta &= 0, \quad n = 0, 1, \dots, -\frac{\kappa}{2} - 1, \\ \int_0^{2\pi} \Omega(\theta) c(\theta) \sin n\theta d\theta &= 0, \quad n = 1, \dots, -\frac{\kappa}{2} - 1. \end{aligned} \quad (\text{C.3.24})$$

The solutions of the Hilbert problem (C.3.7) do not vanish at infinity, although they are bounded there. Thus, conditions (C.3.22) become

$$\int_{\Gamma} \frac{t^n g(t)}{Z^+(t)} dt = 0, \quad n = 0, 1, \dots, -\kappa - 1,$$

or

$$\int_{\Gamma} \frac{t^n c(t)}{[a(t) + ib(t)] Z^+(t)} dt = 0, \quad n = 0, 1, \dots, -\kappa - 2. \quad (\text{C.3.25})$$

Since, in view of (C.3.13),

$$g^+(t_0) = \frac{i}{2} h(t_0) + \frac{1}{2\pi} \int_{\Gamma} \frac{h(t)}{t - t_0} dt,$$

we set  $t = e^{i\theta}$ ,  $t_0 = e^{i\theta_0}$ . Then

$$g^+(t_0) = \frac{i}{2} h(t_0) + \frac{1}{4\pi} \int_0^{2\pi} h(t) \cot \frac{\theta - \theta_0}{2} d\theta + \frac{i}{4\pi} \int_0^{2\pi} h(t) d\theta.$$

In view of (C.3.20) the last term in the above expression is equal to  $i\alpha/2$ . Hence,  $Z(z) = e^{g(z)-i\alpha/2}$  for  $|z| < 1$ , and

$$e^{ih(t_0)} = -t_0^{\kappa} \frac{a(t_0) - ib(t_0)}{a(t_0) + ib(t_0)},$$

which yields

$$Z^+(t_0) = \pm t^{\kappa/2} \sqrt{-\frac{a(t_0) - ib(t_0)}{a(t_0) + ib(t_0)}} \exp \left\{ \frac{1}{4\pi} \int_0^{2\pi} h(t) \cot \frac{\theta - \theta_0}{2} d\theta \right\}.$$

This proves the theorem. ■

Some particular cases of Theorem C.3.2 are as follows:

1. If  $\kappa \leq -2$  and (C.3.25) is satisfied, then the Hilbert problem (C.3.7) has a unique solution which, in view of (C.2.8) and (C.3.9), is given by

$$\Phi(z) = \frac{Z(z)}{i\pi} \int_{\Gamma} \frac{c}{(a + ib) Z^+(t) (t - z)} dt. \quad (\text{C.3.26})$$

Since this solution is unique, it is also the solution of problem (C.3.5).

2. For  $\kappa \geq 0$ , the formula

$$Q(z) = \frac{Z(z)}{i\pi} \int_{\Gamma} \frac{c}{(a + ib) Z^+(t) (t - z)} dt, \quad (\text{C.3.27})$$

gives a particular solution of the problem (C.3.7). Then a particular solution of problem (C.3.5), as in (C.3.10), is given by

$$\Phi(z) = \frac{1}{2} [Q^+(z) + Q^*(z)], \quad (\text{C.3.28})$$

where the function  $Q^*(z)$  is defined as follows: Since, in view of (38.18),  $Z^*(z) = z^\kappa Z(z)$ ,  $\overline{Z^+(t)} = Z^{*-}(t) = t^\kappa Z^-(t)$ , and  $(a - ib) Z^-(t) = -(a + ib) Z^-(t)$ , we have

$$\begin{aligned} Q^*(z) &= Z^*(z) \left\{ -\frac{1}{i\pi} \int_{\Gamma} \frac{c}{(a + ib) \overline{Z^+(t)} (t - z)} dt \right. \\ &\quad \left. + \frac{1}{i\pi} \int_{\Gamma} \frac{c}{(a - ib) \overline{Z^+(t)}} dt \right\} \\ &= z^\kappa Z(z) \left\{ \frac{1}{i\pi} \int_{\Gamma} \frac{ct^\kappa}{(a + ib) Z^+(t) (t - z)} dt \right. \\ &\quad \left. - \frac{1}{i\pi} \int_{\Gamma} \frac{ct^\kappa}{(a + ib) t Z^+(t)} dt \right\}. \end{aligned}$$

Substituting this in (C.3.28), we get a particular solution for the Hilbert problem (C.3.7) for  $\kappa \geq 0$  as

$$\begin{aligned}\Phi(z) = & \frac{Z(z)}{2i\pi} \left\{ \int_{\Gamma} \frac{c dt}{(a+ib) Z^+(t)(t-z)} + z^\kappa \int_{\Gamma} \frac{ct^{-\kappa} dt}{(a+ib) Z^+(t)(t-z)} \right\} \\ & - \frac{z^\kappa Z(z)}{2i\pi} \int_{\Gamma} \frac{ct^{-\kappa} dt}{(a+ib)t Z^+(t)}. \end{aligned}\quad (\text{C.3.29})$$

3. For  $\kappa = 0$ , solution (C.3.29) simplifies to

$$\Phi(z) = \frac{Z(z)}{i\pi} \int_{\Gamma} \frac{c dt}{(a+ib) Z^+(t)(t-z)} - \frac{Z(z)}{2i\pi} \int_{\Gamma} \frac{c dt}{(a+ib)t Z^+(t)}. \quad (\text{C.3.30})$$

CASE STUDY C.3.1: DIRICHLET PROBLEM FOR THE UNIT DISK. We shall discuss this problem for the unit disk  $U^+$ , i.e., we shall find a function  $u$  which is harmonic in  $U^+$ , continuous on  $U^+ \cup \Gamma$ , and satisfies the boundary condition

$$u = f(t), \quad t \in \Gamma, \quad (\text{C.3.31})$$

where  $f(t)$  is a real-valued continuous function given on  $\Gamma$ . This problem is a special case of the Riemann–Hilbert problem with  $a = 1$ ,  $b = 0$ ,  $c = f(t)$ . Then the corresponding Hilbert problem (C.3.7) for  $c \equiv 0$  reduces to

$$\Phi^+(t) + \Phi^-(t) = 0. \quad (\text{C.3.32})$$

This corresponds to case 1 of §C.3.1 with index  $\kappa = 0$ . Then the fundamental solution for the problem (C.3.32) is given by

$$Z(z) = \begin{cases} A & \text{for } z \in U^+, \\ -A & \text{for } z \in U^-, \end{cases} \quad (\text{C.3.33})$$

where  $A$  is an arbitrary constant. To satisfy the condition (C.3.17) we require that  $Z^*(z) = Z(z)$ , and thus it suffices to take  $A = i$ , which yields

$$Z(z) = \begin{cases} i & \text{for } z \in U^+, \\ -i & \text{for } z \in U^-, \end{cases} \quad (\text{C.3.34})$$

Hence, from Theorem C.3.1 the general solution of the corresponding Riemann–Hilbert problem is given by  $\Phi(z) = C i$ , where  $C$  is an arbitrary real constant.

Then from (C.3.30) the general solution of the nonhomogeneous Cauchy problem is given by

$$\begin{aligned}\Phi(z) &= \frac{1}{i\pi} \int_{\Gamma} \frac{f(t)}{t-z} dt - \frac{1}{2i\pi} \int_{\Gamma} \frac{f(t)}{t} dt - iC \\ &= \frac{1}{2i\pi} \int_{\Gamma} \frac{f(t)}{t} \frac{t+z}{t-z} dt + iC.\end{aligned}\tag{C.3.35}$$

This solution is known as the Schwarz formula (see (6.4.12)). Note that this solution has been obtained by applying the results of §C.3.1, which assume that the function  $f(t)$  satisfies the Hölder condition. But the solution (C.3.35) is also valid if instead of this condition only continuity of the function  $f(t)$  is assumed. ■

The Riemann–Hilbert problem for the half–plane can be reduced to that for the unit disk by using the results and the notation of §1.4 and the fact that conformal mapping of a half–plane onto the unit disk leads to an inversion.

REFERENCES USED: Kantorovich and Krylov (1958), Kythe (1996), Kythe, Puri and Schäferkotter (1997), Muskhelishvili (1992), Sveshnikov and Tikhonov (1974), Wegmann (1986).

# Appendix D

---

## Successive Approximations

---

### D.1. Tables

The successive approximations computed for some Case Studies in Chapter 5 are presented in tabular form. The desired level of approximation is obtained by first choosing an initial guess (in all of these tables it is taken as zero for all coefficients). Then substituting these values into the right side of the respective equations, the first approximation is determined. Then the values of the first approximation are substituted into the right side of the same equations, and the second approximation is obtained. This process is continued successively until the desired approximation is attained.

TABLE 1

| Coefficient   | $\alpha_3$                               | $\alpha_5$               | $\alpha_7$                   | $\alpha_9$  | $\alpha_{11}$  |
|---------------|--|--------------------------|------------------------------|-------------|----------------|
| Initial Guess | 0  | 0                        | 0                            | 0           | 0              |
| 1st Approx.   | $-\lambda^2$                             | 0                        | 0                            | 0           | 0              |
| 2nd Approx.   | $-\lambda^2$                             | $\lambda^4$              | 0                            | 0           | 0              |
| 3rd Approx.   | $-\lambda^2 - \lambda^6$                 | $\lambda^4$              | $-\lambda^6$                 | 0           | 0              |
| 4th Approx.   | $-\lambda^2 - \lambda^6$                 | $\lambda^4 + 3\lambda^8$ | $-\lambda^6$                 | $\lambda^8$ | 0              |
| 5th Approx.   | $-\lambda^2 - \lambda^6 - 4\lambda^{10}$ | $\lambda^4 + 3\lambda^8$ | $-\lambda^6 - 5\lambda^{10}$ | $\lambda^8$ | $\lambda^{10}$ |

## APPENDIX D. SUCCESSIVE APPROXIMATIONS

TABLE 2

| Coefficient   | $A_1$                                       | $A_2$   | $A_3$  | $A_4$                  | $A_5$                     |
|---------------|---|---|--|------------------------|---------------------------|
| Initial Guess | $0$   | $0$   | $0$  | $0$                    | $0$                       |
| 1st Approx.   | $-\frac{\lambda}{2}$                        | $0$   | $0$  | $0$                    | $0$                       |
| 2nd Approx.   | $-\frac{\lambda}{2}$                        | $\frac{\lambda^2}{2}$                                 | $0$  | $0$                    | $0$                       |
| 3rd Approx.   | $-\frac{\lambda}{2} + \frac{\lambda^3}{4}$  | $\frac{\lambda^2}{2} - \frac{9\lambda^4}{16}$         | $-\frac{8}{5\lambda^3}$                        | $0$                    | $0$                       |
| 4th Approx.   | $-\frac{\lambda}{2} + \frac{4}{9}\lambda^4$ | $\frac{2}{\lambda^2} - \frac{9\lambda^4}{9\lambda^4}$ | $-\frac{8}{5\lambda^3}$                        | $\frac{7\lambda^4}{8}$ | $0$                       |
| 5th Approx.   | $-\frac{\lambda}{2} + \frac{3}{4}\lambda^5$ | $\frac{1}{2} - \frac{16}{16}$                         | $-\frac{5\lambda^3}{8} + \frac{9\lambda^5}{8}$ | $\frac{7\lambda^4}{8}$ | $-\frac{21\lambda^5}{16}$ |

TABLE 3

| Coefficient   | $a_1$   | $a_5$   | $a_9$                                 | $a_{13}$              |
|---------------|---|---|---------------------------------------|-----------------------|
| Initial Guess | $1$   | $0$   | $0$                                   | $0$                   |
| 1st Approx.   | $1 + \frac{k}{16}$  | $-\frac{k}{16}$   | $0$                                   | $0$                   |
| 2nd Approx.   | $1 + \frac{k}{16} + \frac{3k^2}{256}$                     | $-\frac{k}{16} - \frac{7k^2}{256}$                      | $\frac{k^2}{64}$                      | $0$                   |
| 3rd Approx.   | $1 + \frac{k}{16} + \frac{3k^2}{256} + \frac{3k^3}{1024}$ | $-\frac{k}{16} - \frac{7k^2}{256} - \frac{11k^3}{1024}$ | $\frac{k^2}{64} + \frac{27k^3}{2048}$ | $-\frac{11k^3}{2048}$ |

TABLE 4

| Coefficient   | $a_3$                   | $a_5$                     | $a_7$        | $a_9$       |
|---------------|-------------------------|---------------------------|--------------|-------------|
| Initial Guess | 0                       | 0                         | 0            | 0           |
| 1st Approx.   | $-\lambda$              | 0                         | 0            | 0           |
| 2nd Approx.   | $-\lambda$              | $\lambda^2$               | 0            | 0           |
| 3rd Approx.   | $-\lambda + 5\lambda^3$ | $\lambda^2$               | $-\lambda^3$ | 0           |
| 4th Approx.   | $-\lambda + 5\lambda^3$ | $\lambda^2 - 11\lambda^3$ | $-\lambda^3$ | $\lambda^4$ |

TABLE 5

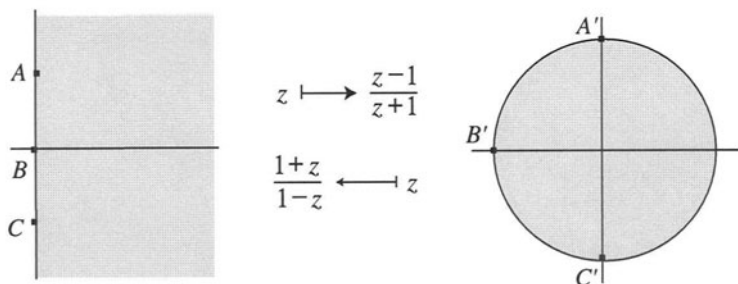
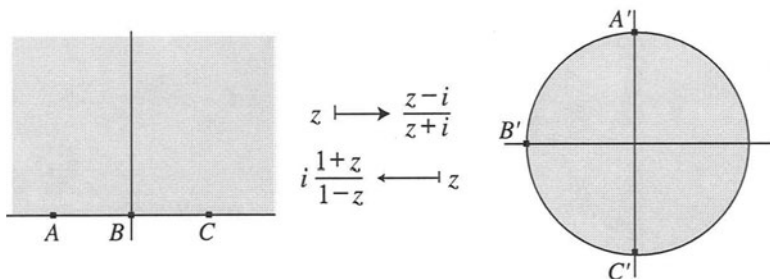
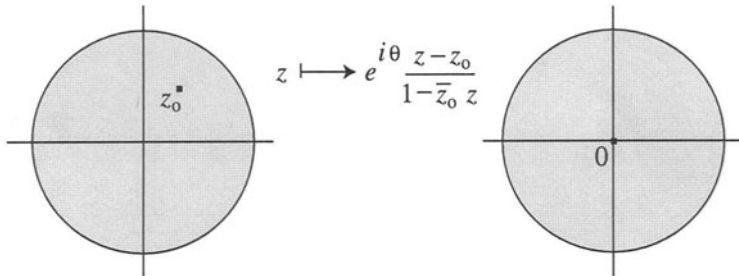
| Coefficient   | $a_1$   | $a_5$   | $a_9$                    |
|---------------|---|---|--------------------------|
| Initial Guess | 1   | 0   | 0                        |
| 1st Approx.   | $1 + \frac{\lambda}{16}$  | $-\frac{-\lambda}{16}$  | 0                        |
| 2nd Approx.   | $1 + \frac{\lambda}{16} + \frac{7\lambda^2}{256}$                           | $-\frac{\lambda}{16} - \frac{7\lambda^2}{256}$                            | 0                        |
| 3rd Approx.   | $1 + \frac{\lambda}{16} + \frac{7\lambda^2}{256} + \frac{9\lambda^3}{1024}$ | $-\frac{\lambda}{16} - \frac{7\lambda^2}{256} - \frac{19\lambda^3}{2048}$ | $\frac{\lambda^3}{2048}$ |

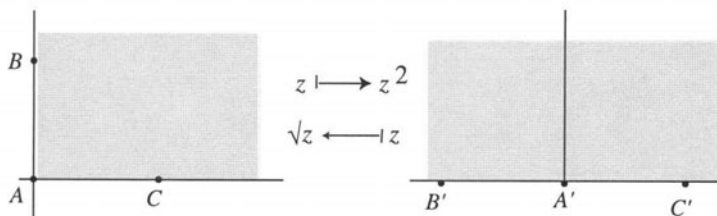
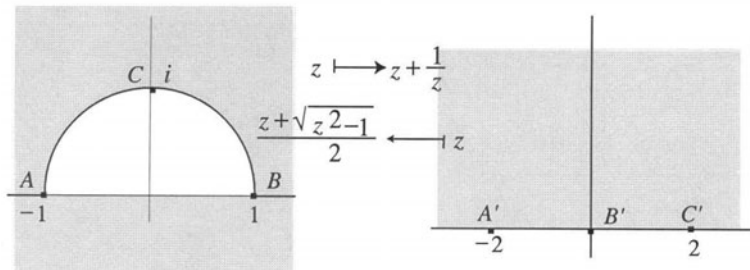
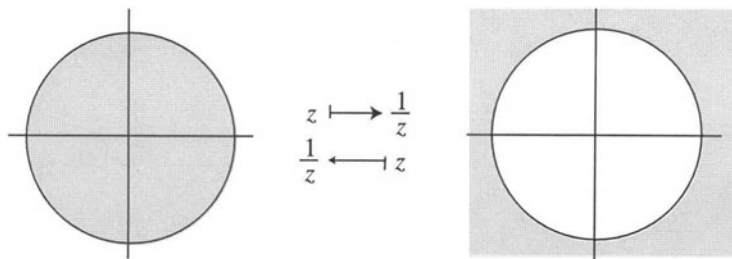
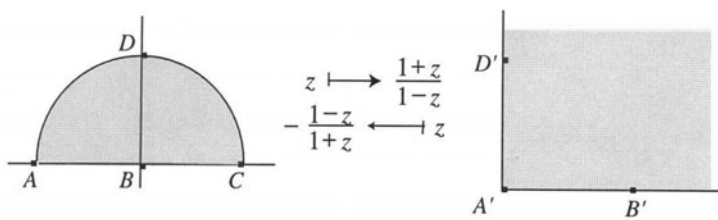
# Appendix E

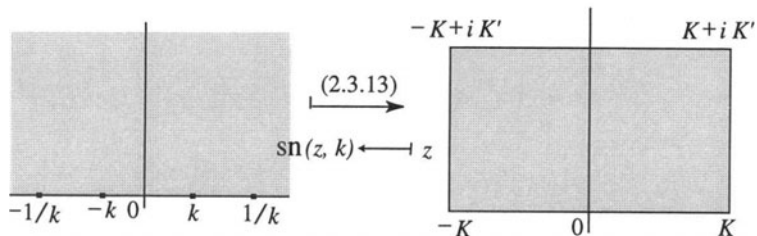
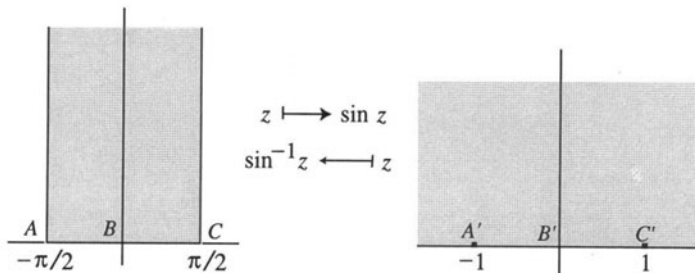
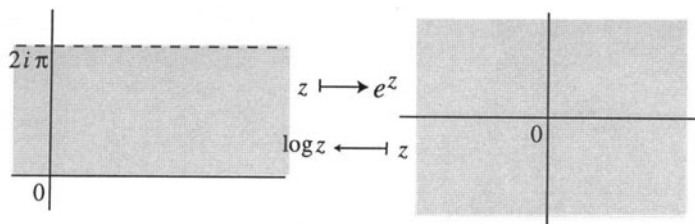
---

## Catalog of Conformal Mappings

---







---

## Bibliography

---

- F. ABRAMOVICI, *The accurate calculation of Fourier integrals by the fast Fourier transform technique*, J. Comp. Phys. **11** (1973), 28–37.
- M. ABRAMOWITZ and I. A. STEGUN (eds.), *Handbook of Mathematical Functions*, Dover, New York, 1968.
- E. N. AHLBERG and J. WALSH, *The Theory of Splines and Their Applications*, Academic Press, New York, 1967.
- L. V. AHLFORS, *Untersuchungen zur Theorie der konformen Abbildung und der gransen Funktionen*, Act Soc. Sci. Fenn. A **1** (1930), 1–40.  
*Remarks on the Neumann–Poincaré integral equation*, Pacific J. Math. **2** (1952), 271–280.  
*Complex Analysis*, McGraw–Hill, New York, 1966.
- JU. E. ALENICYN (Ю. Е. Аленисын), *Conformal mapping of a multiply connected domain onto many-sheeted canonical surfaces*, Izv. Akad. Nauk SSSR Ser. Mat. **28** (1964), 607–644. (Russian)  
*Conformal mapping of multiply connected domains onto surfaces of several sheets with rectilinear cuts*, Izv. Akad. Nauk SSSR Ser. Mat. **29** (1965), 887–902. (Russian)
- CHR. ANDERSEN, S. E. CHRISTIANSEN, O. MØLLER and H. TORNEHAVE, *Conformal Mapping*, Chap. 3 in *Selected Numerical Methods* (C. Gram, ed.), Regnecentralen, Copenhagen, 1962.
- G. K. ANTONJUK (Г. К. Антонюк), *On the covering of areas for functions regular in an annulus*, Vestnik Leningrad Univ. **13**, 45–65. (Russian)
- K. ARBENZ, *Integralgleichungen für einige Randwertprobleme für Gebiete mit Ecken*, Dissertation, ETH Zurich (1958).
- B. G. ARLINGER, *Calculation of transonic flow around axisymmetric inlets*, AIAA J. **13** (1975), 1614–1621.
- K. E. ATKINSON, *A Survey of Numerical Methods for the Solution of Fredholm Integral Equations of the Second Kind*, SIAM, Philadelphia, 1976.
- BALTRUKONIS, M. CHI and P. A. A. LAURA, *Axial shear vibrations of star shaped bars — Kohn–Kato bounds*, Eighth Midwestern Mech. Conf., Developments in Mech. **4** (1965), 449–467.
- A. M. BANIN (А. М. Банин), *Approximate conformal transformation applied to a plane parallel flow past an arbitrary shape*, PMM (Прикладная Математика и Механика), Акад. Наук СССР, Отделение Теч. Наук, Инст. Механики **7** (1943), 131–140. (Russian)

- R. W. BARNARD and K. PEARCE, *Rounding corners of gearlike domains and the omitted area problem*, J. Comput. Appl. Math. **14** (1986), 217–226; also in *Numerical Conformal Mapping* (L. N. Trefethen, ed.), North-Holland, Amsterdam, 1986, pp. 217–226.
- I. S. BEREZIN and N. P. ZHIDKOV (И. С. Березин и Н. П. Жидков), *Computing Methods*, vol. 2, Addison-Wesley, Reading, MA, and Pergamon Press, Oxford, UK, 1965; translation of Методы вычислений, Физматгиз, Москва (Russian).
- S. BERGMAN, *Über die Entwicklung der harmonischen Funktionen der Ebene und des Raumes nach Orthogonalfunktionen*, Math. Annalen **86** (1922), 237–271; Thesis, Berlin 1921.  
*Über Bestimmung der Verzweigungspunkte eines hyperelliptischen Integrals aus seinen Periodizitätsmoduln mit Anwendungen auf die Theorie des Transformators*, Math. Zeit. **19** (1923–24), 8–25.
- Über die Berechnung des magnetischen Feldes in einem Einphasen-Transformatoren*, ZAMM **5** (1925), 319–331.
- Punch-card machine methods applied to the solution of the torsion problem*, Quart. Appl. Math. **5** (1947), 69–81.
- The kernel function and conformal mapping*, AMS Math. Surveys **5** (1970).  
and M. SCHIFFER, *Kernel functions in the theory of partial differential equations of elliptic type*, Duke Math. J. **15** (1948), 535–566.  
and M. SCHIFFER, *Kernel functions and conformal mapping*, I, II, Bull. Am. Math. Soc. **55** (1949), 515–.  
and M. SCHIFFER, *Kernel functions and conformal mapping*, Compositio Math. **8** (1951), 205–249.
- H. BERGSTRÖM, *An approximation of the analytic function mapping a given domain inside or outside the unit circle*, Mém. Publ. Soc. Sci. Arts Lettr. Hainaut, Volume hors Série (1958), 193–198.
- J.-P. BERRUT, *Numerische Lösung der Symmschen Integralgleichung durch Fourier-Methoden*, Master's Thesis, ETH, Zurich, 1976.  
*Über Integralgleichungen und Fourier-Methoden zur numerischen konformen Abbildung*, Doctoral Thesis, ETH, Zurich, 1985.  
*A Fredholm integral equation of the second kind for conformal mapping*, J. Comput. Appl. Math. **14** (1986), 99–110; also in *Numerical Conformal Mapping* (L. N. Trefethen, ed.), North-Holland, Amsterdam, 1986, pp. 99–110.
- A. BETZ, *Konforme Abbildung*, Springer-Verlag, Berlin, 1964.
- W. C. BICKLEY, *Two-dimensional potential problem for the space outside a rectangle*, Proc. Lond. Math. Soc., Ser. 2, **37** (1932), 82–105.
- L. BIEBERBACH, *Zur Theorie und Praxis der konformen Abbildung*, Rend. del Circolo mat. Palermo **38** (1914), 98–112.  
*Über die konforme Kreisabbildung nahezu kreisförmig Bereiche*, Sitzungsberichte der Preuss. Akad. Wissen. (1924), 181–188.
- G. BIRKOFF and D. YOUNG, *Numerical quadrature of analytic and harmonic functions*, J. Math. Phys. **29** (1950), 217–221.  
D. YOUNG and E. H. ZARANTONELLO, *Numerical methods in conformal mapping*, Am. Math. Soc., Proc. Fourth Symposium Appl. Math. (1951), McGraw-Hill, New York, 1953, 117–140.  
and E. H. ZARANTONELLO, *Jets, Waves and Cavities*, Academic Press, New York, 1957.  
D. M. YOUNG and E. H. ZARANTONELLO, *Effective conformal transformation of smooth simply connected domains*, Proc. Nat. Acad. Sci. USA **37** (1951), 411–414.

- D. R. BLASKETT and H. SCHWERDTFEGER, *A formula for the solution of an arbitrary analytic function*, Quart. Appl. Math. **3** (1945–46), 266–268.
- R. P. BOAS, *Invitation to Complex Analysis*, Random House, New York, 1987.
- W. BURNSIDE, *On functions determined from their discontinuities, and a certain form of boundary condition*, Proc. Royal Soc. London, Ser. A **22** (1891), 346–358.
- C. CARATHÉODORY, *Elementarer Beweis für den Fundamentalsatz der konformen Abbildung*, Schwarz–Festschrift, J. Springer, Berlin (1914), 19–41.  
*Über das Neumann–Poincarésche Problem für ein Gebiet mit Ecken*, Dissertation, Uppsala, 1916.  
*Conformal Representation*, Cambridge Tracts in Math. and Math. Phys., No. 28, London; Cambridge University Press, Cambridge, 1969.
- T. CARLEMAN, *Sur la résolution de certaines équations intégrales*, Archiv für mathematik astronomi och fysik **16** (1922).
- G. F. CARRIER, *On a conformal mapping technique*, Quart. Appl. Math. **5** (1947), 101–104.
- M. KROOK and C. E. PEARSON, *Functions of a Complex Variable: Theory and Technique*, McGraw–Hill, New York, 1966.
- M. J. CASARELLA, P. A. A. LAURA and M. CHI, *On the approximate solution of flow and heat transfer through non-circular conduits with uniform wall temperature*, Brit. J. Appl. Phys. **18** (1966), 1327–1335.  
and N. FERRAGUT, *On the approximate solution of flow and heat transfer through non-circular conduits with uniform wall temperature and heat generation*, Nucl. Engg. Design **16** (1971), 387–398.
- S. CHAKRAVARTHY and D. ANDERSON, *Numerical conformal mapping*, Math. Comp. **33** (1979), 953–969.
- N. V. CHALLIS and D. M. BURLEY, *A numerical method for conformal mapping*, IMA J. Numer. Anal. **2** (1982), 169–181.
- S. A. CHAPLYGIN (C. A. Чаплыгин), *A theory of grid wing* (1914), in *Collected Papers*, vol. 2, Gostekhizdat, Moscow, 1933. (Russian)
- E. B. CHRISTOFFEL, *Sul problema della temperatura stazionaria e la rappresentazione di una data superficie*, Annali di Matematica (2) **1** (1867–1868), 89–104.
- J. W. COOLEY and J. W. TUKEY, *An algorithm for the machine calculation of complex Fourier series*, Math. Comp. **19** (1965), 297–301.
- P. A. W. LEWIS and P. D. WELCH, *The fast Fourier transform algorithm: Programming considerations in the calculation of sine, cosine, and Laplace transforms*, J. Sound Vibration **12** (1970), 315–337.
- E. T. COPSON, *Partial Differential Equations*, Cambridge University Press, London, 1975.
- L. DE BRANGES, *A proof of the Bieberbach conjecture*, Acta Math. **154** (1985), 137–152.
- L. M. DELVES, *A fast method for the solution of Fredholm integral equation*, J. Inst. Math. Appl. **20** (1977), 173–182.  
and J. WALSH (eds.), *Numerical Solution of Integral Equations*, Clarendon Press, Oxford, 1974.
- and J. L. MOHAMED, *Computational Methods for Integral Equations*, Cambridge University Press, Cambridge, 1985.
- H. DERESIEWICZ, *Thermal stress in a plate due to disturbance of uniform heat flow in a hole of general shape*, J. Appl. Mech., Trans. ASME **28** (1961), 147–149.
- J. DOUGLAS, *Solution of the problem of Plateau*, Trans. Am. Math. Soc. **33** (1931),

- 263–321.
- A. R. ELCRAT, *Separated flow past a plate with spoiler*, SIAM J. Math. Anal. **13** (1982), 632–639.  
 and L. N. TREFETHEN, *Classical free-streamline flow over a polygonal obstacle*, J. Comput. Appl. Math. **14** (1986), 251–265; also in *Numerical Conformal Mapping* (L. N. Trefethen, ed.), North-Holland, Amsterdam, 1986, pp. 251–265.
- B. EPSTEIN, *A method for the solution of the Dirichlet problem for certain types of domains*, Quart. Appl. Math. **6** (1948), 301–317.
- A. L. FLORENCE and J. N. GOODIER, *Thermal stress due to disturbance of uniform heat flow by an insulated ovaloid hole*, J. Appl. Mech., Trans. ASME **27** (1960), 635–639.
- J. M. FLORYAN, *Conformal-mapping-based coordinate generation method for channel flows*, J. Comput. Phys. **58** (1985), 229–245.  
 and C. ZEMACH, *Schwarz-Christoffel mappings: A general approach*, J. Comput. Phys. **72** (1987), 347–371.
- V. FOCK, *Über die konforme Abbildung eines Kreisvierecks mit verschwindenden Winkeln*, J. Reine angew. Math. **161** (1929), 137–151.
- B. FORNBERG, *A numerical method for conformal mapping*, SIAM J. Sci. Comput. **1** (1980), 386–400.  
*A numerical method for conformal mapping of doubly connected regions*, SIAM J. Sci. Stat. Comp. **5** (1984), 771–783.
- P. FRANKLIN, *Methods of Advanced Calculus*, McGraw-Hill, New York, 1944.
- M. S. FREIBERG, *A new method for the effective determination of conformal maps*, Ph. D. Thesis, Univ. of Minnesota, 1951.
- D. GAIER, *Konstruktive Methoden der konformen Abbildung*, Springer Tracts in Natural Philosophy, vol. 3, Springer-Verlag, Berlin, 1964.  
*Integralgleichung erster Art und konforme Abbildung*, Math. Zeit. **147** (1976), 113–129.  
*Numerical aspects in conformal mapping*, in *Computational Aspects of Complex Analysis*, Reidel, Dordrecht, Boston, 1983, pp. 51–78.  
*Vorlesungen über Approximation in Komplexen*, Birkhäuser Verlag, Basel, 1980.  
 and O. HÜBNER, *Schnelle Auswertung von Ax bei Matrizen A zyklischer Bauart, Toeplitz- und Hankel-Matrizen*, Mitt. Math. Sem. Giessen **121** (1976), 27–38.
- F. D. ГАХОВ (Ф. Д. Гахов), *On the Riemann boundary problem*, Matem. Sbornik **2(44)** (1937), 165–170.
- R. W. G. GANDY and R. V. SOUTHWELL, *Relaxation methods applied to engineering problems. V. Conformal transformation of a region in plane space*, Phil. Trans. Royal Soc. (London), Ser. A **238** (1940), 453–475.
- I. E. GARRICK, *Potential flow about arbitrary biplane wing sections*, Report 542, NACA (1936.).  
*Conformal mapping in aerodynamics, with emphasis on the method of successive conjugates*, Symposium on the Construction and Applications of Conformal Maps, National Bureau of Standards, Appl. Math. Ser. **18** (1949), 137–147.
- C. F. GAUSS, *Allgemeine Auflösung der Aufgabe die Thiele einer gegebenen Fläche so abzubilden, daß die Abbildung dem abgebildeten in den kleinsten Thielen ähnlich wird*, Werke **IV** (1822), 189–216.
- W. GAUTSCHI, *The condition of orthogonal polynomials*, Math. Comp. **26** (1977), 923–924.  
*Questions of numerical condition related to polynomials*, Recent Advances

- in Numerical Analysis (C. de Boor and G. Golub, eds.), Academic Press, New York, 1978.
- Condition of polynomials in power form*, Math. Comp. **33** (1979), 343–352.
- P. R. GERABEDIAN and M. M. SCHIFFER, *Identities in the theory of conformal mapping*, Trans. Am. Math. Soc. **65** (1949), 187–238.
- S. I. GERSHGORIN (С. И. Гершгорин), *On the conformal mapping of a simply connected region onto a disc*, Matem. Sbornik **40** (1933), 48–58. (Russian)
- D. GILBARG, *A generalization of the Schwarz–Christoffel transformation*, Proc. Nat. Acad. Sci. **35** (1949), 609–611.
- Jets and Cavities*, in *Handbuch der Physik*, 9, Springer–Verlag, Berlin, 1960, pp. 311–445.
- H. GLAUERT, *The Elements of Aerofoil and Airscrew Theory*, Cambridge University Press, London, 1948.
- G. M. GOLUZIN (Г. М. Голузин), *The solution of fundamental plane problems of mathematical physics in the case of Laplace's equation and multiply connected regions bounded by circles*, Matem. Sbornik **41** (1934), 246–276. (Russian)  
*Iterationsprozesse für konforme Abbildungen mehrfach zusammenhängender Bereiche*, Matem. Sbornik, New Series **6** (41) (1939), 377–382. (Russian)  
*On conformal mapping of doubly connected regions bounded by rectilinear and circular polygons*, in *Conformal Mapping of Simply and Doubly Connected Regions*, ONTI, Moscow, 1937, pp. 90–97. (Russian)  
*Conformal mapping of multiply connected regions on a slit plane by a method of functional equations*, in *Conformal Mapping of Simply and Doubly Connected Regions*, ONTI, Moscow, 1937, pp. 98–110. (Russian)  
*Geometrische Funktionentheorie*, Deutscher Verlag der Wissenschaften, Berlin, 1957; translation of Геометрическая Теория Функций Комплексного Переменного, Москва–Ленинград, 1952. (Russian)  
*Geometric Theory of Functions of a Complex Variable*, Transl. Math. Monographs vol. 26, American Mathematical Society, Providence, RI, 1969; translation of Геометрическая Теория Функций Комплексного Переменного, Наука, Москва, 1966. (Russian)
- C. Gram (ed.), *Selected Numerical Methods*, Regnecentralen, Copenhagen, 1962.
- T. H. GRONWALL, *Some remarks on conformal representation*, Ann. Math. **16** (1914/15), 72–76.
- H. GRÖTZSCH, *Zur konformen Abbildung mehrfach zusammenhängender, schlichter Bereiche (Iterationsverfahren)*, Berichte Verhand. Sächsischen Akad. Wissen. zu Leipzig, Math.–Phys. Klasse **83** (1931), 67–76.
- H. GRUNSKY, *Neue Abschätzungen zur konformen Abbildung ein- und mehrfach zusammenhängender Bereiche*, Schr. Math. Seminars Inst. Angew. Math. Univ. Berlin **1** (1932), 93–140.
- M. I. GUREVICH (М. И. Гуревич), *Theory of Jets in Ideal Fluids*, Academic Press, New York, 1965; translation of Теория Струи Идал'ное Жидкости, Государственное Издательство Физ.–Мат. Лит., Москва, 1961 (Russian)
- M. H. GUTKNECHT, *Existence of a solution to the discrete Theodorsen equation for conformal mapping*, Math. Comp. **31** (1977), 478–480.  
*Fast algorithms for the conjugate periodic function*, Computing **22** (1979), 79–91.  
*Solving Theodorsen's integral equation for conformal maps with the fast Fourier transform and various nonlinear iterative methods*, Num. Math. **36** (1981), 405–429.  
*On the computation of the conjugate trigonometric rational function and*

- on a related splitting problem*, SIAM J. Numer. Anal. **20** (1983), 1198–1205.
- Numerical experiments on solving Theodorsen's integral equation for conformal maps with the fast Fourier transform and various nonlinear iterative methods*, SIAM J. Sci. Stat. Comput. **4** (1983), 1–30.
- Numerical conformal mapping methods based on function conjugation*, J. Comput. Appl. Math. **14** (1986), 31–77; also in *Numerical Conformal Mapping* (L. N. Trefethen, ed.), North-Holland, Amsterdam, 1986, pp. 31–77.
- J. HADAMARD, *Mémoire sur le problème d'analyse relatif à l'équilibre des plaques élastiques encastrées*, Mémoires Acad. Sci. **33**, No. 4 (1908).
- N. D. HALSEY, *Potential flow analysis of multi-element airfoils using conformal mapping*, AIAA J. **17** (1979), 1281–1288.
- Comparison of the convergence characteristics of two conformal mapping methods*, AIAA J. **20** (1982), 724–726.
- M. HARTMANN and G. OPFER, *Uniform approximation as a numerical tool for constructing conformal maps*, J. Comput. Appl. Math. **14** (1986), 193–206; also in *Numerical Conformal Mapping* (L. N. Trefethen, ed.), North-Holland, Amsterdam, 1986, pp. 193–206.
- J. K. HAYES, D. K. KAHANER and R. G. KELLNER, *An improved method for numerical conformal mapping*, Math. Comput. **26** (1972), 327–334.
- A numerical comparison of integral equations of the first and second kind for conformal mapping*, Math. Comp. **29** (1975), 512–521.
- J. HEINHOLD, *Zur Praxis der konformen Abbildung*, Berichte Math. Tagung, Tübingen (1947), 75–77.
- P. HENRICI, *Einige Anwendungen der schnellen Fouriertransformation*, in *Moderne Methoden der Numerischen Mathematik* (J. Albrecht and L. Collatz, eds.), Birkhäuser, Basel, 1976, pp. 111–124.
- Fast Fourier methods in computational complex analysis*, SIAM Rev. **21** (1979), 481–527.
- Barycentric formulas for trigonometric interpolation*, Numer. Math. **33** (1979), 225–234.
- Applied and Computational Complex Analysis*, vol. III, Wiley, New York, 1986.
- D. HILBERT, *Grundzüge einer allgemeinen Theorie der linearen Integralgleichungen*, 2nd ed., Leipzig–Berlin, 1924, pp. 83–94.
- Das Dirichletsche Prinzip* (1901), in *Gesammelte Abhandlungen*, Bd. 3, Springer–Verlag, Berlin, 1935.
- Zur Theorie der konformen Abbildung* (1909), in *Gesammelte Abhandlungen*, Bd. 3, Springer–Verlag, Berlin, 1935.
- J. HODGKINSON, *Conformal representation by means of Lamé functions*, J. London Math. Soc. **5** (1930), 296–306.
- and E. POOLE, *The conformal representation of the area of a plane bounded by two straight or circular slits*, Proc. London Math. Soc. **23** (1924), 396–422.
- F. HÖHNDORF, *Verfahren zur Berechnung des Auftriebes gegebener Tragflächenprofile*, ZAMM **6** (1926), 265–283.
- R. HOCKNEY, *The potential calculation and some applications*, Methods in Comput. Phys. **9** (1970), 135–211.
- H.-P. HOIDN, *Osculation methods for the conformal mapping of doubly connected regions*, ZAMP **33** (1982), 640–652.
- , *A reparameterisation method to determine conformal maps*, J. Comput. Appl. Math. **14** (1986), 155–161; also in *Numerical Conformal Mapping* (L. N. Trefethen, ed.), North-Holland, Amsterdam, 1986, pp. 155–161.

- D. M. HOUGH and N. PAPAMICHAEL, *The use of splines and singular functions in an integral equation method for conformal mapping*, Numer. Math. **37** (1981), 133–147.  
*An integral equation method for the numerical conformal mapping of interior, exterior and doubly-connected domains*, Numer. Math. **41** (1983), 287–307.
- G. C. HSIAO, P. KOPP and W. L. WENDLAND, *A Galerkin collocation method for some integral equations of the first kind*, Computing **25** (1980), 89–130.
- O. HÜBNER, *Zur Numerik der Theodorsenschen Integralgleichung in der konformen Abbildung*, Mitt. Math. Sem. Giessen **140** (1979), 1–32.  
*Über die Anzahl der Lösungen der diskreten Theodorsen-Gleichung*, Numer. Math. **39** (1982), 195–204.  
*The Newton method for solving the Theodorsen integral equation*, J. Comput. Appl. Math. **14** (1986), 19–30; also in *Numerical Conformal Mapping* (L. N. Trefethen, ed.), North-Holland, Amsterdam, 1986, pp. 19–30.
- K. INOUE, *Grid generation for cascades using conformal mapping*, J. Comput. Phys. **52** (1983), 130–140.  
*Grid generation for inlet configurations using conformal mapping*, J. Comput. Phys. **58** (1985), 146–154.
- V. I. IVANOV and M. K. TRUBETSKOV, *Handbook of Conformal Mapping with Computer-Aided Visualization*, CRC Press, Boca Raton, 1995.
- V. V. Ivanov (B. B. Иванов), *Theory of Approximate Methods and Applications to Numerical Solution of Singular Integral Equations*, Kiev, 1968.
- D. C. IVES, *A modern look at conformal mapping including multiply connected regions*, AIAA J. **14** (1976), 1006–1011.  
and J. F. LIUTERMOZA, *Analysis of transonic cascade flow conformal mapping and relaxation techniques*, AIAA J. **15** (1977), 647–652.
- R. M. JAMES, *A new look at two-dimensional incompressible airfoil theory*, Report Jo918/01, Douglas Aircraft Co., Long Beach, CA (May 1971).
- M. A. JAWSON, *Integral equation methods in potential theory. I.*, Proc. Roy. Soc. A **275** (1963), 23–32.  
and G. T. SYMM, *Integral Equation Methods in Potential Theory and Elastostatics*, Academic Press, London, 1977.
- A. JEFFREY, *Complex Analysis and Applications*, CRC Press, Boca Raton, FL, 1992.
- H. JEFFREYS and B. S. JEFFREYS, *Methods of Mathematical Physics*, Cambridge University Press, Cambridge, 1946.
- N. E. JOUKOWSKI (H. E. Жуковский), *Modification of Kirchhoff's method for determination of fluid motion in two dimensions with constant velocity* (1890), in *Collected Papers*, vol. 2, Gostekhizdat, Moscow, 1950. (Russian)  
Über die Konturen des Tragflächen der Drachenflieger (1910–1912), in *Collected Papers*, vol. 5, Gl. red. av. lit., Moscow, 1937. (Russian)  
*Theoretical foundation of aeronautics* (1911), in *Collected Papers*, vol. 6, Gostekhizdat, Moscow, 1950. (Russian)
- Vorticity theory of the propeller (1915), in *Collected Papers*, vol. 4, Gostekhizdat, Moscow, 1950. (Russian)
- G. JULIA, *Sur le représentation conforme des aires simplement convexes*, Comptes Rendus Acad. Sci. Paris. **182** (1926), 1314–1316.  
*Sur une série de polynômes liée à la le représentation conforme des aires simplement convexes*, Comptes Rendus Acad. Sci. Paris. **183** (1927), 10–12.  
*Développement en série de polynômes ou de fonctions rationnelles de la fonc-*

- tion qui fournit la représentation conforme d'une aire simplement convexe sur un cercle*, Annales de l'École normale Sup. **44** (1927), 289–316.
- L. V. KANTOROVICH (Л. В. Канторович), *Sur quelques méthodes de la détermination de la fonction qui effectue une représentation conforme*, Bull. Acad. Sci. URSS **7** (1933), 229–235.  
*Sur la représentation conforme*, Matem. Sbornik **40** (1933), 294–325.  
*Quelques rectifications à mon mémoire "Sur la représentation conforme"*, Matem. Sbornik **41** (1934), 179–182.  
*On the approximate computation of some types of definite integrals and other applications of the method of removing singularities*, Matem. Sb. (2) **41** (1934), 235–245. (Russian)
- Sur la représentation conforme des domaines multiconvexes*, Comptes Rendus Acad. Sci. URSS **2** (1934), 441–445.  
*Conformal mapping of a circle on a simply connected region*, in *Conformal Mapping of Simply and Doubly Connected Regions*, Gostekhizdat, Leningrad–Moscow, 1937. (Russian)
- and V. I. KRYLOV (В. И. Крылов), *Methods for the Approximate Solution of Partial Differential Equations*, Gostekhizdat, Leningrad–Moscow, 1936. (Russian)  
and V. I. KRYLOV, *Approximate Methods for Higher Analysis*, Interscience, New York, 1958.
- V. A. KASIN and V. V. MERKULOV, *Determination of the eigenvalues for waveguide with complex cross section*, Soviet Phys.: Acoustics **11** (1966), 285–287.
- A. J. KASSAB, R. T. BAILEY and C. K. HSIEH, *CVBEM in simply- and multiply-connected domains for the solution of heat conduction problems*, in *Advances in Boundary Element Methods* (M. H. Aliabadi and C. A. Brebbia, eds.), Computational Mechanics Publications, Southampton, and Elsevier Applied Science, London, 1993.
- M. V. KELDYŠ (М. В. Келдыш), *Conformal mappings of multiply connected domains on canonical domains*, Uspekhi Matem. Nauk **6** (1939), 90–119 translation of Конформные отображения много связных областей на канонические области, Успехи мат. наук, **6** (1939), 90–119. (Russian)
- O. D. Kellogg, *Foundations of Potential Theory*, Springer–Verlag, Berlin, 1929; Dover, New York, 1953.
- N. KERZMAN and E. M. STEIN, *The Cauchy kernel, the Szegö kernel, and the Riemann mapping function*, Math. Ann. **236** (1978), 85–93.  
and M. R. TRUMMER, *Numerical conformal mapping via the Szegö kernel*, J. Comput. Appl. Math. **14** (1986), 111–123; also in *Numerical Conformal Mapping* (L. N. Trefethen, ed.), North–Holland, Amsterdam, 1986, pp. 111–123.
- G. KHAJALIA (Г. Хаялия), *Sur la théorie de la représentation conforme des domaines doublement convexes*, Matem. Sbornik, New Series **8** (1940), 97–106.
- B. V. KHVEDELIDZE (Б. В. Хведелидзе), *On the Poincaré boundary value problem of the theory of logarithmic potential for multiply connected regions*, Soobshcheniya AN Gruz. SSR (Сообщения АН Груз. ССР) **2** (1941), 571–578, 865–872. (Russian)
- G. R. KIRCHHOFF, *Zur Theorie freier Flüssigkeitsstrahlen*, J. Reine Angew. Math. **70** (1869), 289–298.
- P. KNUPP and S. STEINBERG, *Fundamentals of Grid Generation*, CRC Press, Boca Raton, FL, 1993.
- H. KOBER, *Dictionary of Conformal Representations*, Admiralty Computing Ser-

- vice, Dept. of Scientific Research and Experiment, Admiralty, London, Parts 1–5, 1945–1948.
- Dictionary of Conformal Representations*, Dover, New York, 1952; 2nd ed., Dover, New York, 1957.
- P. KOEBE, *Abhandlungen zur Theorie der konformen Abbildung. I. Die Kreisabbildung des allgemeisten einfach und zweifach zusammenhängenden schlichten Bereichs und die Ränderzuordnung bei konformer Abbildung*, J. Reine Angew. Math. **145** (1915), 177–223.
- Abhandlungen zur Theorie der konformen Abbildung. IV. Abbildung mehrfach zusammenhängender schlichter Bereiche auf Schlichtbereiche*, Acta Math. **41** (1918), 304–344.
- W. VON KOPPENFELS, *Das hypergeometrische Integral als Periode der Vierecksabbildung*, Sitzungsberichte Akad. Wissen. Wien **146** (1937), 11–22.
- Konforme Abbildung besonderer Kreisbogenvierecke*, J. Reine Angew. Math. **181** (1939), 83–124.
- and F. STALLMANN, *Praxis der konformen Abbildung*, Springer–Verlag, Berlin, 1959.
- V. I. KRYLOV (В. И. Крылов), *Concerning a method of constructing a function which maps a region conformally on a circle*, in *Conformal Mapping of Simply and Doubly Connected Regions*, Gostekhizdat, Leningrad–Moscow, 1937. (Russian)
- Integral equations of the conformal map of a region on a slit plane*, in *Conformal Mapping of Simply and Doubly Connected Regions*, Leningrad–Moscow, 1937. (Russian)
- Integral equations of the conformal map of doubly connected regions on a ring*, in *Conformal Mapping of Simply and Doubly Connected Regions*, Gostekhizdat, Leningrad–Moscow, 1937. (Russian)
- An application of integral equations to the proof of certain theorems for conformal mapping*, Matem. Sbornik **4** (1938), 9–30. (Russian)
- and N. BOGOLYUBOV, *Sur la solution approchée du problème de Dirichlet*, Comptes Rendus Acad. Sci. URSS (1929), 283–288.
- P. P. KUFAREV (П. П. Куфарев), *Über das zweifachzusammenhängende Minimalgebiet*, Bull. de l'Institut de Math. et Mécan. Univ. Kouybycheff de Tomsk **1** (1935–1937), 228–236.
- On a method of numerical determination of the parameters in the Schwarz–Christoffel integral*, Doklady Akad. Nauk SSSR (new Series) **57** (1947), 535–537. (Russian)
- On conformal mapping of complementary regions*, Doklady Akad. Nauk SSSR **73** (1950), 881–884.
- U. KULISCH, *Ein Iterationsverfahren zur konformen Abbildung des Einheitskreises auf ein Stern*, ZAMM **43** (1963), 403–410.
- P. K. KULSHRESTHA, *Distortion of spiral-like mappings*, Proc. Royal Irish Acad. **73**, Sec. A (1973), 1–5.
- Generalized convexity in conformal mappings*, J. Math. Anal. Appl. **43** (1973), 441–449.
- Coefficients for alpha-convex univalent functions*, Bull. Amer. Math. Soc. **80** (1974), 341–342.
- Coefficient problem for alpha-convex univalent functions*, Archive Ratnl. Mech. Anal. **54** (1974), 204–211.
- Coefficient problem for a class of Močanu–Bazilevič functions*, Annales Polon. Math. **31** (1976), 291–299.

- Bounded Robertson functions*, Rendi. di Matem. **9**, Ser. VI (1976), 137–150.
- Convex combinations of some regular locally univalent functions*, Bull. Inst. Math., Acad. Sinica **12** (1984), 37–50.
- P. K. KYTHE, *An Introduction to Boundary Element Methods*, CRC Press, Boca Raton, FL, 1995.
- Fundamental Solutions for Differential Operators and Applications*, Birkhäuser, Boston, 1996.
- P. PURI and M. R. SCHÄFERKOTTER, *Partial Differential Equations and Mathematica*, CRC Press, Boca Raton, FL, 1997.
- E. LANDAU, *Einige Bemerkungen über schlichte Abbildung*, Jahresbericht Deut. Math.-Vereinigung **34** (1926), 239–243.
- P. A. A. LAURA, *Calculations of eigenvalues for uniform fluid waveguide with complicated cross section*, J. Acoust. Soc. Am. **42** (1967), 21–26.
- A survey of modern applications of the method of conformal mapping*, Revista de la Unión Matematica Argentina **27** (1975), 167–179.
- and M. CHI, *Approximate method for the study of heat conduction in bars of arbitrary cross section*, J. Heat Transfer, Trans. ASME **86**, Ser. C (1964), 466–467.
- and M. CHI, *An application of conformal mapping to a three-dimensional unsteady heat conduction problem*, Aeronaut. Quart. **16** (1965), 221–230.
- and A. J. FAULSTICH, *Unsteady heat conduction in plates of polygonal shape*, Int. J. Heat Mass Transfer **11** (1968), 297–303.
- and P. A. SHAHDY, *Longitudinal vibrations of a solid propellant rocket motor*, Proc. Third Southeastern Conf. on Theor. Appl. Mech. (1966), Pergamon Press, New York, 623–633.
- E. ROMANELLI and M. J. MAURIZI, *On the analysis of waveguides of doubly-connected cross section by the method of conformal mapping*, J. Sound Vibration **20** (1972), 27–38.
- M. A. LAVRENT'EV (М. А. Лаврентьев), К Теории Конформных Отображений, Труды физ.-мат. и-та им. Б. А. Стеклова, 1934. (Russian)
- Boundary problems in the theory of univalent functions*, Amer. Math. Soc. Transl. (2) **32** (1963), 1–35; translation of М. А. Лаврентьев, О некоторых граничных задачах в теории однолистных функций, Мат. Сб., 1 (43), 1936, 815–844 (Russian)
- Conformal Mappings with Applications to Some Problems of Mechanics*, Gostekhizdat, Moscow–Leningrad, 1947 translation of Конформные отображения и приложения к некоторым вопросам механики, Гостехиздат, Москва–Ленинград, 1947. (Russian)
- On the theory of conformal mappings*, Amer. Math. Soc. Transl. (2) **122** (1984), 1–69; translation of М. А. Лаврентьев, К теории конформных отображений, Труды Физ.–Мат. Инст. Стеклова, 5 (1934), 159–245 (Russian)
- M. A. LAVRENT'EV and B. W. SCHABAT (М. А. Лаврентьев и Б. В. Шабат), *Methoden der komplexen Funktiontheorie*, VEB Deutscher Verlag der Wissenschaften, Berlin, 1967; translation of Методы теории функций комплексного переменного, Издат. «Наука», Москва, 1965. (Russian)
- N. N. LEBEDEV (Н. Н. Лебедев), *On the theory of conformal mappings of a circle onto nonoverlapping regions*, Doklady Akad. Nauk SSSR **103** (1955), 553–555. (Russian)
- R. S. LEHMAN, *Development of the mapping function at an analytic corner*, Pacific J. Math. **7** (1957), 1437–1449.

- O. LEHTO and K. I. VIRTAAEN, *Quasiconformal Mappings in the Plane*, Springer-Verlag, Berlin, 1973.
- F. LEJA, *Une méthode de construction de la fonction de Green appartenant à un domaine plan quelconque*, Comptes Rendus Acad. Sci. Paris **198** (1934), 231–234.  
*Construction de la fonction analytique effectuant la représentation conforme d'un domaine plan quelconque sur le cercle*, Math. Ann. **111** (1935), 501–504.  
 Sur une suite de polynômes et la représentation conforme d'un domaine plan quelconque sur le cercle, Annales Soc. Polonaise Math. **14** (1936), 116–134.
- A. F. LEONT'EV (А. Ф. Леонтиев), *Representation of functions in convex domains by generalized exponential series*, Amer. Math. Soc. Transl. (2) **140** (1988), 121–130; translation of Представление функций в выпуклых областях обобщенными рядами экспонент, Acta Sc. Math. **45** (1983), 305–315.
- D. LEVIN, N. PAPAMICHAEL and A. SIDERIDIS, *The Bergman kernel method for an improved conformal mapping of simply-connected domains*, J. Inst. Math. Appl. **22** (1978), 171–187.
- H. LEWY, *Developments at the confluence of analytic boundary conditions*, Univ. Calif. Publ. Math. **1** (1950), 247–280.
- L. LICHTENSTEIN, *Über die konforme Abbildung ebener analytischer Gebiete mit Ecken*, J. Reine Angew. Math. **140** (1911), 100–119.  
*Zur konformen Abbildung einfach zusammenhängender schlichter Gebiete*, Archiv Math. Phys. **25** (1917), 179–180.
- H. LIEBMANN, *Die angenäherte Ermittlung harmonischer Funktionen und konformer Abbildungen (nach Ideen von Boltzmann und Jacobi)*, Sitzungsberichte math.-phys. Klasse Akad. Wissen. München (1918), 385–416.
- K. LÖWNER, *Untersuchungen über schlichte konforme Abbildungen des Einheitskreises, I.*, Math. Ann. **89** (1923), 103–121.
- A. J. LURYE (А. И. Лурье), *Zur Schwarz–Christoffelschen Formel*, Annales Inst. Polytech. Nom M. I. Kalinin, Leningrad **30** (1927), 113–120. (Russian)
- J. LU, *A class of quadrature formulas of Chebyshev type for singular integrals*, J. Math. Anal. Appl. (2) **100** (1984), 416–435.  
*Boundary value problems for analytic functions and integral equations with transformations*, in *Complex Analysis and Its Applications* (C. C. Yang, G. C. Wen, K. Y. Li and Y. M. Chiang, eds.), Pitman Res. Notes in Math. Series # 305, Longman Scientific and Technical, Essex, UK, 1994, pp. 318–323.
- L. A. LYUSTERNIK (Л. А. Люстерник), *Über einige Anwendungen der direkten Methoden in der Variationsrechnung*, Matem. Sbornik **33** (1926), 173–201. (Russian)  
*Remarks on the numerical solution of boundary problems for Laplace's equation and the calculation of characteristic values by the method of networks*, Trudy Mathem. Inst. V. A. Steklova **20** (1947), 49–64. (Russian)
- R. E. MADER, *Programming in Mathematica*, 2nd ed., Addison–Wesley, Redwood City, CA, 1991.
- M. MAITI, *A note on the integral equation methods in potential theory*, Quart. Appl. Math. **25** (1968), 480–484.
- P. B. MALENTIEV (П. Б. Малентьев), *Approximate conformal mapping*, in *Conformal Mapping of Simply and Doubly Connected Regions*, Gostekhizdat, Leningrad–Moscow, 1937. (Russian)
- A. I. MARKUSHEVICH (А. И. Маркушевич), *Teoriya analiticheskikh funktsii*, Gos-texizdat, Москва–Ленинград, 1950. (Russian)

- J. E. MARSDEN and M. J. HOFFMAN, *Basic Complex Analysis*, 2nd ed., W. H. Freeman and Company, New York, 1987.
- A. MAYO, *The fast solution of Poisson's and the biharmonic equations on irregular regions*, SIAM J. Numer. Anal. **21** (1984), 285–299.  
*Rapid methods for the conformal mapping of multiply connected regions*, J. Comput. Appl. Math. **14** (1986), 143–153; also in *Numerical Conformal Mapping* (L. N. Trefethen, ed.), North-Holland, Amsterdam, 1986, pp. 143–153.
- D. I. MEIRON, S. A. ORSZAG and M. ISRAELI, *Applications of numerical conformal mapping*, J. Comp. Phys. **40** (1981), 345–360.
- P. V. MELENT'EV (П. В. Мелентьев), Несколько новых методов и приёмов приближенных вычислений (*Several New Methods and Devices for Approximate Computations*), ОНТИ, Ленинград–Москва, 1937. (Russian)
- R. MENIKOFF and C. ZEMACH, *Methods for numerical conformal mapping*, J. Comp. Phys. **36** (1980), 366–410.  
*Rayleigh–Taylor instability and the use of conformal maps for ideal fluid flow*, J. Comput. Phys. **51** (1983), 28–64.
- S. G. MIKHLIN (С. Г. Михлин), *Integral Equations and Their Applications*, Pergamon, London, 1957.
- V. N. MONAKOV, *Boundary–Value Problems with Free Boundaries for Elliptic Systems of Equations*, Amererican Mathematical Society, Providence, RI, 1983.
- M. MÜLLER, *Zur konforme Abbildung angenähert kreisförmiger Gebiete*, Math. Zeit. **43** (1938), 628–636.
- R. MUNIPALLI and D. A. ANDERSEN, *An adaptive grid scheme using the boundary element method*, J. Comput. Phys. **127** (1996), 452–463.
- M. I. MURATOV (М. И. Муратов), *Conformal mapping of a half-plane on a region close to it*, in *Conformal Mapping of Simply and Doubly Connected Regions*, Gostekhizdat, Leningrad–Moscow, 1937. (Russian)
- W. MURRAY, *Failure, the Causes and Cures*, Chap. 7 in *Numerical Methods for Unconstrained Optimization* (W. Murray, ed.), Academic Press, London, 1972, p. 118.
- N. I. MUSKHELISHVILI (Н. И. Мусхелишвили), *Some Basic Problems of the Mathematical Theory of Elasticity*, Noordhoff, Groningen, 1963.  
*Singular Integral Equations*, Noordhoff, Leiden, 1953; 2nd ed., Dover, New York, 1992; translation of Сингулярные Интегральные Уравнения, Москва, 1946. (Russian)
- P. S. NAIDU and K. O. WESTPHAL, *Some theoretical considerations of ion optics of the mass spectrometer ion source — I*, Brit. J. Appl. Phys. **17** (1966), 645–651.  
*Some theoretical considerations of ion optics of the mass spectrometer ion source — II*, Brit. J. Appl. Phys. **17** (1966), 653–656.
- Z. NEHARI, *The Schwarzian derivative and schlicht functions*, Bull. Am. Math. Soc. **55** (1949), 545–551.  
*The kernel function and canonical conformal maps*, Duke Math. J. **16** (1949), 165–178.  
*Conformal Mapping*, Dover Publications, New York, 1952.
- C. NEUMANN, *Untersuchungen über das logarithmische und Newtonsche Potential*, Leipzig, 1877.
- R. NEVANLINNA, *Über das alternierende Verfahren von Schwarz*, J. Reine Angew. Math. **180** (1939), 121–128.
- and V. PAATERO, *Introduction to Complex Analysis*, Addison–Wesley Publishing Co., Reading, MA, 1969 *Einführung in die Funktionentheorie* Birkhäuser,

- Basel, 1964.
- F. NOETHER, *Über eine Klasse singulärer Integralgleichungen*, Math. Ann. **82** (1921), 42–63.
- E. J. NYSTRÖM, *Über die praktische Auflösung von Integralgleichungen mit Anwendungen auf Randwertaufgaben*, Acta Math. **54** (1930), 185–204.
- G. OPFER, *New extremal properties for constructing conformal mappings*, Numer. Math. **32** (1979), 423–429.  
*Conformal mappings onto prescribed regions via optimization techniques*, Numer. Math. **35** (1980), 189–200.  
*Solving complex approximation problems by semiinfinite-finite optimization techniques: A study on convergence*, Numer. Math. **39** (1982), 411–420.
- A. OSTROWSKI, *Mathematische Miszellen XV. Zur konformen Abbildung einfachzusammenhängender Gebiete*, Jahresbericht Deut. Math.–Vereinigung **38** (1929), 168–182.  
*Über konforme Abbildungen annähernd kreisförmiger Gebiete*, Jahresbericht Deut. Math.–Vereinigung **39** (1930), 78–81.  
*On a discontinuous analogue of Theodorsen's and Garrick's model, Symposium on the construction and application of conformal maps*, National Bureau of Standards Appl. Math. Ser. **18** (1952), 165–174.
- A. M. OSTROWSKI, *On the convergence of Theodorsen's and Garrick's method of conformal mapping*, National Bureau of Standards, Appl. Math. Ser. **18** (1952), 149–164.  
*Conformal mapping of a special ellipse on the unit circle*, Appl. Math. Ser., National Bureau of Standards **42** (1955).
- M. N. ÖZİSİK, *Finite Difference Methods in Heat Transfer*, CRC Press, Boca Raton, FL, 1994.
- N. PAPAMICHAEL and J. WHITMAN, *A cubic spline technique for the one-dimensional heat conduction equation*, J. Inst. Math. Appl. **11** (1973), 111–113.  
 and C. A. KOKKINOS, *Two numerical methods for the conformal mapping of simply-connected domains*, Comput. Meth. Appl. Mech. Engg. **28** (1981), 285–307.  
 and C. A. KOKKINOS, *Numerical conformal mapping of exterior domains*, Comput. Meth. Appl. Mech. Engg. **31** (1982), 189–203.  
 and C. A. KOKKINOS, *The use of singular functions for the approximate conformal mapping of doubly-connected domains*, SIAM J. Sci. Stat. Comput. **5** (1984), 93–106.  
 and M. K. WARBY, *Pole-type singularities and the numerical conformal mapping of doubly-connected domains*, J. Comput. Appl. Math. **10** (1984), 93–106.  
 M. K. WARBY and D. M. HOUGH, *The determination of the poles of the mapping function and their use in numerical conformal mapping*, J. Comput. Appl. Math. **9** (1983), 155–166.  
 M. K. WARBY and D. M. HOUGH, *The treatment of corner and pole-type singularities in numerical conformal mapping techniques*, J. Comput. Appl. Math. **14** (1986), 163–191; in *Numerical Conformal Mapping* (L. N. Trefethen, ed.), North-Holland, Amsterdam, 1986, pp. 163–191.
- L. L. PENNISI, L. I. GORDON and S. LASHER, *Elements of Complex Variables*, Holt, Rinehart and Winston, New York, 1963.
- E. G. PHILLIPS, *Functions of a Complex Variable with Applications*, Interscience, New York, 1943.  
*Some Topics in Complex Analysis*, Pergamon Press, Oxford, 1966.

- H. B. PHILLIPS and N. WIENER, *Nets and the Dirichlet problem*, J. Math. Phys., MIT **2** (1923), 105–124.
- H. T. H. PIAGGIO and M. N. STRAIN, *The conformal transformation  $Z = (lz^2 + 2mz + n)/(pz^2 + 2qz + r)$* , J. London Math. Soc. **22** (1947), 165–167.
- É. PICARD, *Leçons aux quelques types simples d'équations aux dérivées partielles*, Paris, 1927.
- J. PLEMELJ, *Ein Ergänzungssatz zur Cauchyschen Integraldarstellung analytischer Funktionen*, Monatshefte für Math. Phys. **19** (1908), 205–210.
- G. PÓLYA and G. SZEGÖ, *Isoperimetric Inequalities in Mathematical Physics*, Princeton University, 1951.
- I. PRIVALOFF, *Sur les fonctions conjuguées*, Bull. Soc. Math. France **44** (1916), 100–103.
- I. I. PRIVALOV (И. И. Привалов), *On the boundary problem in the theory of analytic functions*, Matem. Sbornik, N. S. **41** (1934), 519–526.  
*Randeigenschaften Analytischer Funktionen*, 2nd ed., Deutscher Verlag der Wissenschaften, Berlin, 1956. (Russian)
- G. N. PUKHTEEV (Г. Н. Пухтеев), *Exact Methods for Calculation of Cauchy-type Integrals*, Nauka, Novosibirsk, 1980.
- P. RABINOWITZ, *Numerical experiments in conformal mapping by the method of orthogonal polynomials*, J. Assoc. Comp. Mach. **13** (1966), 296–303.
- J. RADON, *Über die Randwertaufgaben beim logarithmischen Potential*, Sitz.–Ber. Wien. Akad. Wiss., Abt. IIa **128** (1919), 1123–1167.
- E. REICH and S. E. WARSCHAWSKI, *On canonical conformal maps of regions of arbitrary connectivity*, Pacific J. Math. **10** (1960), 965–989.
- L. REICHEL On polynomial approximation in the complex plane with application to conformal mapping, Math. Comp. **44** (1985), 425–433.  
*A fast method for solving certain integral equations of the first kind with application to conformal mapping*, J. Comput. Appl. Math. **14** (1986), 125–142; also in *Numerical Conformal Mapping* (L. N. Trefethen, ed.), North-Holland, Amsterdam, 1986, pp. 125–142.
- M. K. RICHARDSON, *A numerical method for the conformal mapping of finite doubly connected regions with application to the torsion problem for hollow bars*, Ph. D. Thesis, University of Alabama, 1965.
- B. RIEMANN, *Grundlagen für eine allgemeine Theorie der Funktionen einer veränderlichen komplexen Grösse* (1851), in *Collected Works*, Dover, New York, 1953.
- F. and M. RIESZ, *Über die Randwerte einer analytischen Funktion*, Comptes Rendus du Quatrième Congrès des Mathématiciens Scandinaves à Stockholm (1916), 27–44; Math. Zeitschrift **18** (1923), 95.
- G. O. ROBERTS, *Computational meshes for boundary layer problems*, Lecture Notes in Physics, vol. 8, Springer–Verlag, New York, 1971, pp. 117–177.
- J. A. ROBERTSON, *Hydrodynamics in Theory and Application*, Prentice–Hall, Englewood Cliffs, NJ, 1965.
- A. ROSENBLATT, *Sur la représentation conforme de domaines plans*, Comptes Rendus Acad. Sci. Paris **202** (1936), 1398–1400.  
*Sur la représentation conforme de domaines bornés par des courbes générales*, Comptes Rendus Acad. Sci. Paris **202** (1936), 1832–1834.  
*On Mr. L. Kantorović's method in the theory of conformal mapping and on the application of that method to aerodynamics*, Actas de la Academia Nacional de Ciencias Exactas, Fisicas y Naturales de Lima **6** (1943), 199–219.
- and S. TURSKI, *Sur la représentation conforme de domaines plans*, Comptes Rendus Acad. Sci. Paris **202** (1936), 899–901.

- H. ROTHE, *Über das Grundtheorem und die Obertheoreme der automorphen Funktionen im Falle der Hermite-Laméschen Gleichung mit vier singulären Punkten*, Monatshefte Math. Phys. **19** (1908), 258–288.
- E. B. SAFF and A. D. SNIDER, *Fundamentals of Complex Analysis for Mathematics, Science and Engineering*, Prentice-Hall, Englewood Cliffs, NJ, 1976.
- P. G. SAFFMAN, *The structure and decay of trailing vortices*, Arch. Mech. (Archivum Mechaniki Stosowanej) **26** (1974), 423–439.
- G. SANSONE and J. GERRETSEN, *Lectures on the Theory of a Complex Variable*, Noordhoff, Groningen, 1960.  
*Lectures on the Theory of a Complex Variable, II*, Wolters-Noordhoff, Groningen, 1969.
- A. L. SCHAGINYAN (А. Л. Шагинян), *Sur les polynômes extrémaux qui présentent l'approximation d'une fonction réalisant la représentation conforme d'un domaine sur un cercle*, Comptes Rendus (Doklady) de l'Académie des Sciences de l'URSS, New Series **45** (1944), 50–52.
- M. SCHIFFER, *The kernel function of an orthonormal system*, Duke Math. J. **13** (1946), 529–540.  
Hadamard's formula and variation of domain functions, Am. J. Math. **68** (1946), 417–448.  
*An application of orthonormal functions in the theory of conformal mapping*, Am. J. Math. **70** (1948), 147–156.
- H. A. SCHWARZ, *Über einige Abbildungsaufgaben*, J. Reine Angew. Math. **70** (1869), 105–120; also in *Gesammelte Mathematische Abhandlung*, II (1890), Springer-Verlag, Berlin, 65–83.  
*Notizia sulla rappresentazione conforme di un'area ellittica sopra un'area circolare* (1869,); in *Gesammelte Mathematische Abhandlung*, II (1890), Springer-Verlag, Berlin, 102.  
*Über die Integration der partiellen Gleichung  $\frac{\partial^2 u}{\partial x^2} + \frac{\partial^2 u}{\partial y^2}$  unter vorgeschriebenen Bedingungen*, M. B. Preußische Akademie (1980), 767–795; Werke **2**, 144–171.  
*Über diejenigen Fälle, in welchen die Gaussische hypergeometrische Reihe eine algebraische Funktion ihres vierten Elementes darstellt* (1872,); in *Gesammelte Mathematische Abhandlung*, II (1890), Springer-Verlag, Berlin, 211.  
*Formeln und Lehrsätze zum Gebrauch der elliptischen Funktionen*, Springer-Verlag, Berlin, 1893.
- W. SEIDEL, *Über die Ränderzuordnung bei konformen Abbildungen*, Math. Ann. **104** (1931), 182–243.  
*Bibliography of numerical methods in conformal mapping*, National Bureau of Standards Appl. Math. Ser. **8** (1952), 269–280.
- M. SHIFFMAN, *The Plateau problem for non-relative minima*, Annals of Math. **40** (1939), 834–854.
- R. SIEGEL, M. E. GOLDSTEIN and J. M. SAVINO, *Conformal mapping procedure for transient and steady state two-dimensional solidification*, Heat Transfer, Elsevier, Amsterdam, 1970, 1970.
- R. A. SILVERMAN, *Introductory Complex Analysis*, Prentice-Hall, Englewood Cliffs, NJ, 1967.
- V. SMIRNOV (Б. Смирнов), *Sur la théorie des polynomes orthogonaux à une variable complexe*, J. Soc. Phys.-math. Léningrade **2** (1928), 155–179.  
*Über die Ränderzuordnung bei konformen Abbildungen*, Math. Ann. **107** (1932), 313–323.

- R. V. SOUTHWELL, *Relaxation Methods in Theoretical Physics*, Oxford University Press, Oxford, 1946.
- E. M. SPARROW and A. HAJI-SHEIKH, *Flow and heat transfer in ducts of arbitrary shape with arbitrary thermal boundary conditions*, J. Heat Transfer, Trans. ASME **88** (1966), 351–356.
- N. P. STEIN (Н. П. Штейн), *The determination of parameters in the Schwarz-Christoffel formula*, in *Conformal Mapping of Simply and Doubly Connected Regions*, Gostechizdat, Leningrad-Moscow, 1937. (Russian)
- E. STIEFEL, *On solving Fredholm integral equations. Applications to conformal mapping and variational problems of potential theory*, J. Soc. Indust. Appl. Math. **4** (1956), 63–85.
- A. G. SVESHNIKOV and A. N. TIKHONOV (А. Г. Свешников и А. Н. Тихонов), *The Theory of Functions of a Complex Variable*, Mir Publishers, Moscow, 1978; translation of Теория Функций Комплексной Переменной, Наука, Москва, 1974. (Russian)
- G. T. SYMM, *Integral equation methods in potential theory. II.*, Proc. Roy. Soc. A **275** (1963), 33–46.  
*An integral equation method in conformal mapping*, Numer. Math. **9** (1966), 250–258.  
*Numerical mapping of exterior domains*, Numer. Math. **10** (1967), 437–445.  
*Conformal mapping of doubly-connected domains*, Numer. Math. **13** (1969), 448–457.  
*The Robin problem for Laplace's equation*, in *New Developments in Boundary Element Methods* (C. A. Brebbia, ed.), CML Publications, Southampton, 1980.
- G. SZEGÖ, *Über orthogonale Polynome, die zu einer gegebenen Kurve der komplexen Ebene gehören*, Math. Zeit. **9** (1921), 218–270.  
*Orthogonal Polynomials*, AMS Colloquium Publications 23, American Mathematical Society, New York, 1939.  
*Conformal mapping of the interior of an ellipse onto a circle*, Amer. Math. Monthly **57** (1950), 474–478.
- O. TEICHMÜLLER, *Untersuchungen über konforme und quasikonforme abbildung*, Deutsche Math. **3** (1938), 621–678.
- T. THEODORSEN, *Theory of wing sections of arbitrary shape*, National Advisory Committe on Aeronautics, Tech. Rep. 411 (1931).  
and I. E. GARRICK, *General potential theory of arbitrary wing sections*, National Advisory Committe on Aeronautics, Tech. Rep. 452 (1933).
- J. F. THOMPSON, *Numerical Grid Generation*, North-Holland, Amsterdam, 1982.  
*Elliptic Grid Generation*, Elsevier Publishing Co., Inc., New York, 1982.  
F. C. THAMES and C. W. MASTIN, *Boundary-fitted coordinate system for solution of partial differential equations on fields containing any number of arbitrary two-dimensional bodies*, NASA, CR-2729 (1976).
- F. C. THAMES and C. W. MASTIN, *TOMCAT — A code for numerical generation of boundary-fitted curvilinear coordinate system on fields containing any number of arbitrary two-dimensional bodies*, J. Comput. Phys. **24** (1977), 274–302.
- Z. U. A. WARSI and C. W. MASTIN, *Boundary-fitted coordinate systems for numerical solution of partial differential equations — A Review*, J. Comput. Phys. **47** (1982), 1–108.
- Z. A. WARSI and C. W. MASTIN, *Numerical Grid Generation: Foundations*

- and Applications*, North-Holland, New York 1985.
- R. TIMMAN, *The direct and the inverse problem of airfoil theory. A method to obtain numerical solutions*, Nat. Luchtv. Labor. Amsterdam, Report F.16 (1951).
- J. TODD (ed.), *Experiments in the Computation of Conformal Maps*, U.S. National Bureau of Standards, Appl. Math. Ser. 42, U.S. Govt. Printing Office, 1955.  
and S. E. WARSCHAWSKI, *On the solution of the Lichtenstein-Gershgorin integral equation in conformal mapping, II, Computation experiments*, National Bureau Standards Appl. Math. Series **42** (1955), 31-44.
- L. N. TREFETHEN, *Numerical computation of the Schwarz-Christoffel transformation*, SIAM J. Sci. Stat. Comput. **1** (1980), 82-102.  
*SCPACK Version 2 User's Guide, Internal Report 24*, Institute for Computer Applications in Science and Engineering, NASA Langley Research Center, 1983.  
*Analysis and design of polygonal resistors by conformal mapping*, ZAMP **35** (1984), 692-704.
- (ed.), *Numerical Conformal Mapping*, North-Holland, Amsterdam, 1986.  
and R. J. WILLIAMS, *Conformal mapping solution of Laplace's equation on a polygon with oblique derivative boundary conditions*, J. Comput. Appl. Math. **14** (1986), 227-249; also in *Numerical Conformal Mapping* (L. N. Trefethen, ed.), North-Holland, Amsterdam, 1986, pp. 227-249.
- M. R. TRUMMER, *An efficient implementation of a conformal mapping method based on the Szegő kernel*, SIAM J. Numer. Anal. **23** (1986), 853-872.
- B. A. VERTGEIM (B. A. Вертгейм), *Approximate construction of some conformal mappings*, Doklady Akad. Nauk SSSR **119** (1958), 12-14. (Russian)
- S. VLADIMIRSKY, *Sur la représentation conforme des domaines limités intérieurement par des segments rectilignes et arcs circulaires*, Comptes Rendus Acad. Sci. Paris **212** (1941), 379-382.
- T. VON KARMAN and E. TREFFFTZ, *Potential-stromung um gegebene Tragflächenquerschnitte*, Zeitschrift für Flugtechnische Motorluftsch **9** (1918), 111-116.
- J. L. WALSH, *Interpolation and Approximation by Rational Functions in the Complex Domain*, 5th ed., American Mathematical Society, Providence, RI, 1969.
- S. E. WARSCHAWSKI, *Über das Randverhalten der Ableitung der Abbildungsfunktion bei konformer Abbildung*, Math. Zeit. **35** (1932), 321-456.  
*Über einen Satz von O. D. Kellogg*, Nachr. Akad. Wiss. Göttingen, Math. Phys. Kl. (1932), 73-86.  
*On the higher derivatives at the boundary in conformal mapping*, Trans. Am. Math. Soc. **38** (1935), 326.  
*On Theodorsen's method of conformal mapping of nearly circular regions*, Quart. Appl. Math. **3** (1945), 12-28.  
*On conformal mapping of nearly circular regions*, Proc. Amer. Math. Soc. **1** (1950), 562-574.  
*On the solution of the Lichtenstein-Gershgorin integral equation in conformal mapping, I, Theory*, National Bureau Standards Appl. Math. Series **42** (1955), 7-30.  
*Recent results in numerical methods of conformal mapping*, in *Proc. Symp. Appl. Math.*, vol. 6, McGraw-Hill, New York, 1956, pp. 219-250.  
*On differentiability at the boundary in conformal mapping*, Proc. Am. Math. Soc. **12** (1961), 614-620.  
*On conformal mapping of certain classes of Jordan domains*, Arch. Ratnl. Mech. Anal. **22** (1966), 201-209.  
and G. E. SCHOBER, *On conformal mapping of certain classes of Jordan*

- domains*, Arch. Ratnl. Mech. Anal. **22** (1966), 201–209.
- H. WAYLAND, *Complex Variables Applied in Science and Engineering*, Van Nostrand Reinhold, New York, 1970.
- R. WEGMANN, *Ein Iterationsverfahren zur konformen Abbildung*, Numer. Math. **30** (1978), 453–466.  
*Ein Iterationsverfahren zur konformen Abbildung*, ZAMM **59** (1979), T85–86.  
*Convergence proofs and error estimates for an iterative method for conformal mapping*, Numer. Math. **44** (1984), 435–461.  
*An iterative method for conformal mapping*, J. Comput. Appl. Math. **14** (1986), 7–18; also in *Numerical Conformal Mapping* (L. N. Trefethen, ed.), North-Holland, Amsterdam, 1986, pp. 7–18.  
*An iterative method for the conformal mapping of doubly connected regions*, J. Comput. Appl. Math. **14** (1986), 79–98; also in *Numerical Conformal Mapping* (L. N. Trefethen, ed.), North-Holland, Amsterdam, 1986, pp. 79–98.
- G.-C. WEN, *Conformal Mappings and Boundary Value Problems*, Translations of Mathematical Monographs, Vol. 106, American Mathematical Society, Providence, RI, 1992.
- E. T. WHITTAKER and G. N. WATSON, *A Course of Modern Analysis*, 4th ed., Cambridge University Press, Cambridge, UK, 1927.
- H. B. WILSON, *A method of conformal mapping and the determination of stresses in solid propellant rocket grains.*, Rep. S-38 (1963), Rohm and Haas Co., Huntsville, AL.
- W. WIRTINGER, *Über die konforme Abbildung der Halbebene auf ein Kreisbogen-dreieck*, Atti Pontif. Accad. Sci. Nuovi Lincei **80** (1927), 291–309.
- H. WITTICH, *Konforme Abbildung einfach zusammenhängender Gebiete*, ZAMM **25/27** (1947), 131–132.
- L. von WOLFERDORF, *Zur Unität der Lösung der Theodorsenschen Integralgleichung der konformen Abbildung*, Z. Anal. Anwendungen **3** (1984), 523–526.
- S. WOLFRAM, *The Mathematica Book*, 2nd and 3rd eds., Wolfram Media, Champaign, IL, 1991, 1996.
- K. ZARANKIEWICZ, *Sur la représentation conforme d'un domaine doublement convexe sur un anneau circulaire*, Comptes Rendus Acad. Sci. Paris **198** (1934), 1347–1349.  
*Über ein numerisches Verfahren zur konformen Abbildung zweifach zusammenhängender Gebiete*, ZAMM **14** (1934), 97–104.
- C. ZEMACH, *A conformal map formula for difficult cases*, J. Comput. Appl. Math. **14** (1986), 207–215; also in *Numerical Conformal Mapping* (L. N. Trefethen, ed.), North-Holland, Amsterdam, 1986, pp. 207–215.
- V. A. ZMOROVICH (B. A. Зморович), *Deux problèmes du domaine des représentations conformes*, J. de l'Institut Math. de l'Académie des Sciences de l'Ukraine **3/4** (1935), 215–222.
- A. ZYGMUND, *Trigonometric Series*, Monografie Matematyczne, Warsaw, 1935; also Cambridge University Press, London, 1959.

---

## Notation

---

(The number within parentheses represents the page number where the notation is first introduced.)

|                       |  |
|-----------------------|--|
| $\bar{A}$             | closure of a set $A$ (15)  |
| $A \setminus B$       | complement of a set $B$ with respect to a set $A$ (15)   |
| $A \times B$          | product of sets $A$ and $B$ (15)   |
| $A(z, a)$             | Kerzman–Stein kernel (200)   |
| $A(\rho_1, \rho_2)$   | annulus $\{\rho_1 <  w  < \rho_2\}$ (296)  |
| $\text{Area}(G)$      | area of a region $G$ (38)  |
| $B(a, r)$             | open disk $\{ z - a  < r\}$ (16)   |
| $\bar{B}(a, r)$       | closed disk $\{ z - a  \leq r\}$ (16)  |
| $B(0, 1)$             | open unit disk $\{ z  < 1\}$ (16)  |
| $B(m, n)$             | beta function (55)   |
| $\text{cap}(D)$       | capacity of a region $D$ (30)  |
| $\text{comp}(B)$      | complement of a set $B$  |
| $\text{cond}(M_n)$    | condition of the map $M_n$ (252)   |
| $C^0(D)$              | class of functions continuous on a region $D$ (15)   |
| $C^k(D)$              | class of continuous functions with $k$ -th continuous derivative<br>on a region $D$ , $0 \leq k < \infty$ (15) |
| $C^\infty(D)$         | class of continuous functions infinitely differentiable on<br>a region $D$ (15)                                |
| $C$ -function         | same as a $C^0$ -function (15)   |
| $\mathbb{C}$          | complex plane (16)   |
| $\mathbb{C}_\infty$   | extended complex plane (16)  |
| $\text{diam}(E)$      | transfinite diameter of a set $E$ (18)   |
| $d(\{s_i\}, \{t_i\})$ | Fréchet metric (21)  |
| $\text{dn}$           | a Jacobian elliptic function (325)   |
| $D$                   | region (16)  |

|                             |   |
|-----------------------------|---|
| $\bar{D}$                   | closure of $D$ (16)   |
| $D^*$                       | complement of a set $D$ (29);<br>= $\text{Ext}(\Gamma)$ region exterior to $\Gamma$ (239)                       |
| $\text{Ext}(\Gamma)$        | region exterior to $\Gamma$ (18)  |
| $f$                         | analytic function (19);<br>mapping of $D = \text{Int}(\Gamma)$ onto $U = \{ w  < 1\}$ , $f(0) = 0$ (237)        |
| $f_E$                       | mapping of $D^* = \text{Ext}(\Gamma)$ onto $U^* = \{ w  > 1\}$ , $f_E(0) = 1$ ,<br>$f_E(\infty) = \infty$ (239) |
| $f_\Omega$                  | mapping of a doubly connected region $\Omega$ onto the annulus<br>$A(\rho_1, \rho_2)$ (296)                     |
| $\langle f, g \rangle$      | inner product (22)  |
| $\ f\ _\infty$              | norm of $f \in L^\infty$ (23)   |
| $\ f\ _{2,\Gamma}^2$        | (line)-norm of $f$ (22)   |
| $\ f\ _{2,D}^2$             | (surface)-norm of $f$ (22)  |
| $F^+, F^-$                  | limit values of $F$ from right and left of $\Gamma$ (27)  |
| $\mathcal{F}$               | operator (235)  |
| $\mathcal{F}'$              | $F$ -derivative of $\mathcal{F}$ (235)  |
| $\bar{g}$                   | complex conjugate of an analytic function $g$ (22)  |
| $gd$                        | Gudermannian (40)   |
| $G$                         | region (31)   |
| $\mathcal{G}(\cdot, \cdot)$ | Green's function (29)   |
| $H^1$                       | Lipschitz condition (20)  |
| $H^\alpha$                  | Hölder condition of order $\alpha$ (20)   |
| $H(z, z_0)$                 | Cauchy kernel (25)  |
| $\text{Int}(\Gamma)$        | region interior of $\Gamma$ (18)  |
| $I(\Gamma, z_0)$            | index of a contour $\Gamma$ (winding number) (18)   |
| $\Im\{\cdot\}$              | imaginary part of a complex quantity (17)   |
| $K(k)$                      | elliptic integral (57)  |
| $K(z, a)$                   | Bergman kernel (94)   |
| $\mathcal{K}$               | conjugation operator (234)  |
| $\mathcal{K}^0(D)$          | class of functions $f \in L^2(D)$ , $f(a) = 0$ , $a \in D$ (92)   |
| $\mathcal{K}^1(D)$          | class of functions $f \in L^2(D)$ , $f(a) = 1$ , $a \in D$ (92)   |
| $l^p$                       | a vector space (21)   |
| $l_k(z)$                    | Lagrange's interpolation functions (254)  |
| $L^2$                       | Hilbert space of square-integrable functions (21)   |
| $L^\infty$                  | Hilbert space of $2\pi$ -periodic and bounded functions (23)  |
| $L^2(D)$                    | class of square-integrable functions defined on<br>a region $D$ (21)  |

|                             |   |
|-----------------------------|---|
| $\mathcal{L}^1(\Gamma)$     | class of functions $f \in L^2(\Gamma)$ , $f(a) = 1$ , $a \in D$ (104)   |
| $M = \rho_2/\rho_1$         | conformal modulus of a doubly connected region $\Omega$ (296)   |
| $N(s, t)$                   | Neumann kernel (169)  |
| $\mathcal{N}(\cdot, \cdot)$ | Neumann function (160)  |
| $P_n(z)$                    | complex polynomials (41)  |
| $\mathcal{P}$               | partition of an interval $[a, b]$ (19)  |
| $Q_n(z)$                    | orthonormal polynomials (117)   |
| $\Re\{\cdot\}$              | real part of a complex quantity (17)  |
| $\mathbb{R}^n$              | Euclidean $n$ -space (16)   |
| $\mathbb{R}^+$              | set of nonnegative real numbers (16)  |
| $\text{sn}$                 | a Jacobian elliptic function (57)   |
| $S(z, a)$                   | Szegő kernel (105)  |
| $T_n(z)$                    | Chebyshev polynomials of the first kind (185)   |
| $U$                         | open unit disk (16)   |
| $U^*$                       | region exterior of the unit circle (239)  |
| $U_n(z)$                    | Chebyshev polynomials of the second kind (119)  |
| $V(z_1, \dots, z_n)$        | Vandermonde determinant (17)  |
| $w$                         | $= f(z) = u + i v = \rho e^{i\phi}$ , image of $z$ under $f$ (16)   |
| $\{w, z\}$                  | Schwarzian derivative (65)  |
| $W$                         | Sobolev space of $2\pi$ -periodic and absolutely continuous functions $f$ with $f' \in L^2[0, 2\pi]$ (23)                                   |
| $(W, \ \cdot\ )$            | Banach space (23)   |
| $z$                         | $= x + i y = r e^{i\theta}$ , complex variable (16)   |
| $z^*$                       | point symmetric to $z$ (47)   |
| $(z_1, z_2, z_3, z_4)$      | cross-ratio (46)  |
| $\{z_k\}_1^\infty$          | a set of distinct points in $D$ (29)  |
| $Z(z)$                      | fundamental solution (414)  |
| $\gamma$                    | path, contour (18); Robin's constant (30)   |
| $\gamma(s)$                 | a point $z$ on $\Gamma$ for a given $s \in [a, b]$ (18, 169)  |
| $\tilde{\gamma}$            | reparametrization of $\gamma$ (19)  |
| $\Gamma = \partial D$       | boundary of a region $D$ (a simple closed curve or a Jordan contour) (18)   |
| $\partial, \bar{\partial}$  | partial differential operators $\partial f = \frac{\partial f}{\partial z}$ , $\bar{\partial} f = \frac{\partial f}{\partial \bar{z}}$ (16) |
| $\partial B(a, r)$          | circle $ z - a  = r$ (16)   |
| $\partial_\infty D$         | boundary of $D$ in $\mathbb{C}_\infty$ (16)   |
| $\kappa$                    | Neumann constant (181);   |
|                             | index of a Hilbert problem (411)  |
| $\mu(\zeta)$                | density function (238)  |

|                                      |  |
|--------------------------------------|--|
| $\pi_n(z)$                           | Bieberbach polynomial (100)  |
| $\Pi_n(z)$                           | orthogonal polynomials (116)   |
| $\sigma_k$                           | arcs (18)  |
| $\sigma_n(z)$                        | Szegö polynomials (111)  |
| $\phi_n(z)$                          | minimal polynomials (96)   |
| $\Omega$                             | doubly connected region (295);<br>multiply connected region (359)  |
| $\nabla$                             | gradient vector = $\mathbf{i} \frac{\partial}{\partial x} + \mathbf{j} \frac{\partial}{\partial y}$ (17) |
| $\langle \nabla u, \nabla v \rangle$ | inner (scalar) product (17)  |

---

# Index

---

## A

- Ahlfors estimate 185
- airfoil(s) 174, 207, 269ff, 394
  - Joukowski 275, 293
  - main 287ff
    - multi-element 8, 284, 291ff
    - secondary 287ff
    - single-element 8, 279ff, 284ff
    - symmetric Joukowski 276ff
    - two-element 279, 288ff
- analytic continuation 15, 34, 327, 331, 403
- annulus 296ff, 299, 317, 347, 360ff, 367, 379
- approximation(s), Chebyshev 11
  - nearly circular 277ff
  - polynomial 92ff, 115, 251
  - Ritz 11
  - spline 237, 258ff, 337
  - successive 3, 123ff, 138, 144ff, 425
  - VM 347
- argument principle 185

## B

- Banach space 23, 235
- basis 259, 340, 345, 346ff
  - augmented (AB) 281, 327ff, 342ff, 347ff, 354ff, 357
  - monomial 252
  - orthonormal 347, 354
  - well-conditioned 251ff
- bean-shaped curve 165, 344
- bilinear transformation 45ff, 65ff, 293, 398
- binomial expansion 131

## boundary corner 325ff

- boundary correspondence function 187ff, 192, 202, 208, 212, 255, 259, 296, 316, 321, 323, 325ff, 329, 347, 358

## C

- capacity 29ff, 33
- cardioid 48, 307, 318, 351
- cascade of blades 379, 390ff
  - pitch 400
- Cassini's oval(s) 157, 165, 203, 243ff, 250, 267, 319, 372ff
- Cauchy-Goursat theorems 24
- Cauchy formula 9, 109, 233, 315
  - principal value 7, 10, 26, 170, 205, 209, 234, 321, 323
  - p.v. integrals 206, 234, 321, 401, 406ff
- Cauchy's inequality 25
  - integral(s) 26, 111, 132, 367, 370, 374ff
  - integral formula 24, 148, 164, 315
  - kernel 11, 15, 25, 198ff
  - theorem 15, 23, 365
- Cauchy-Riemann equations 16ff, 27, 239, 273, 371
- Cauchy-Schwarz inequality 21
- centerline 396ff
- chain property 33ff
- Chebyshev approximation 11
  - polynomials 118, 185, 252
- circle(s) 16, 83, 191, 379
  - eccentric 190
  - in a cross 356ff

- in a square 348ff
  - circular cuts 359ff
    - cylinder 294
    - region 361ff
    - tube 395
  - circulation 273
  - closure 15
  - collocation points 263
  - complement 15
  - complete set 95, 102
    - orthonormal set 101, 118
  - conformal mapping(s) 30ff, 41ff
    - equivalence 38, 296
    - invariants 296ff
    - module 384
    - modulus 295ff, 299ff, 318, 345, 368ff
    - radius 33
  - conjugation operator 234
  - convergence factor 184
  - convergence of iterations 179, 387, 392
  - continued fraction 67
  - corner 235, 260, 321, 325ff, 328, 348
    - re-entrant 259, 329
    - singularities 246, 265, 282, 320, 328, 348
  - Cramer's rule 193
  - cross in a square 350
  - cross-ratio 46
  - curve, nonrectifiable 19
    - rectifiable 18, 255
  - curve-fit coefficients 281ff
  - cusp 275, 277
- D**
- de Branges estimate 40
  - dilatation 41
  - diameter 16
    - transfinite 17, 33, 245ff
  - difference operator(s) 371
  - dipole density 309ff, 371
    - distribution 190, 205, 308ff
    - strength 190, 205
  - Dirichlet problem 1ff, 6, 10, 31, 147ff,
- 190, 309, 358ff, 364ff, 368, 379, 423ff
  - for the annulus 302ff
  - for the unit disk 423
  - modified 359, 369
  - discontinuity 259, 329, 375, 397
  - disk(s) 16, 361
  - divergence 381
  - domain 16
- E**
- electromagnetics 12
  - ellipse 119, 123ff, 131, 134, 141, 145ff, 155, 203, 242, 246, 251ff, 257, 266ff, 333ff, 378
  - cambered 282
  - coaxial 318
  - confocal 270
  - inverted 203, 234
  - nondegenerate 254
  - elliptic arc 338
    - rings 307
  - epitrochoid 203, 307
  - equation(s), Bernoulli's 83
    - Cauchy-Riemann 16ff, 27, 239, 273, 371
    - collocation 260ff
    - continuity 262, 381ff
    - Laplace 4ff, 12, 370, 399
  - error estimate 194, 242ff, 245ff, 250, 257, 263, 265ff, 306
  - expansions, asymptotic 327ff, 351
    - Laurent series 126
    - small parameter 121ff
  - exterior maps 177ff
  - $\epsilon$ -condition 235
- F**
- fast Fourier transform (see FFT)
  - fast Poisson solver 11, 358, 369ff, 373ff, 377
  - Fatou's lemma 20
  - F-derivative 235
  - Fejér points 254ff
  - FFT, 1, 10, 235, 269, 285ff

- flow(s), aerodynamic 8  
 fluid 12, 272  
 boundary layer 382
- formula(s), Cauchy 9, 1109, 233, 315  
 Cauchy's integral 24, 148, 164, 315  
 Chaplygin's 273  
 Green's 23, 101, 345  
 Hadamard 5  
 interpolation 202  
 modified Schwarz-Christoffel 86  
 Plemelj 26, 403, 412  
 quadrature 369ff, 376, 403ff  
 Schwarz 158ff, 208, 423  
 Schwarz-Christoffel 5, 12, 51, 64, 68, 259
- force flux 204
- Fourier analysis 387  
 coefficients 108, 134, 163, 229, 303, 347, 398  
 series 99, 110, 133, 146, 194, 229, 303ff, 347, 392, 397  
 sum 340  
 transform, discrete 232, 286
- Fréchet metric 21
- function(s), arc-wise linear 404ff  
 Bergman kernel 6, 11, 94ff, 119, 328, 340ff  
 beta 55  
 biharmonic 3  
 boundary correspondence 187ff, 192, 202, 208, 212, 255, 259, 296, 316, 321, 323, 325ff, 329, 347, 358  
 collocation 261  
 complete elliptic 297, 394  
 density 238, 294, 329, 351, 368ff, 374, 376ff  
 dipole density 309ff, 368  
 elliptic 6, 267, 340  
 elliptic sine 57, 257  
 elliptic theta 314ff  
 exponential 397  
 Green's 4, 29ff, 33, 147ff, 160, 237, 267, 313, 325, 341, 366ff, 373, 378ff, 399  
 harmonic 3, 15, 27, 31, 147ff, 228, 239, 267, 280ff, 283, 302, 342, 364, 367, 370, 373
- hyperbolic 387
- hypergeometric 301
- implicit 132
- incomplete beta 82
- Jacobian elliptic 57, 116, 187, 325, 391
- Joukowski 269ff, 277
- kernel 6, 162, 319, 341ff, 406
- Koebe 40
- Lagrange's interpolation 254ff, 257ff
- meromorphic 361, 367, 377
- minimal 93
- minimizing 5
- Neumann 160ff
- periodic Green's 314
- potential 204, 309
- rational 41
- Riemann mapping 11, 119ff
- Schottky 367
- sectionally analytic 418
- singular 344, 347ff, 356ff
- source density 238, 240, 260
- spline 11, 259, 264
- Szegö kernel 105ff
- trigonometric 141
- univalent 32, 39, 318, 330, 333, 377
- weight 402
- fundamental solution 412ff, 418, 423
- fundamental theorem of line integrals 19
- G**
- Gauss quadrature 102, 264
- Gauss-Chebyshev type quadrature 403ff
- Gautschi criterion 251
- Glaubert's mapping 276  
 modification 275ff
- gradient 380

- theorem 407
- Gram-Schmidt process 101, 117
- Green's formula 23, 101, 345
  - identities 407ff
  - theorem 407
  - reciprocity theorem 408
- grid concentration 379, 383, 390ff
  - adaptive scheme 399
  - generation 12, 13, 379ff, 382
  - lines 371ff, 378, 389ff, 399
  - orthogonal 384
  - uniformization 383
- Gudermannian 40
  
- H**
- half-line 352
- Harnack theorem 29
- hermitian 98, 170
  - quadratic forms 110
- Hilbert problem, homogeneous 7, 410ff, 419
  - nonhomogeneous 7ff, 415ff
- Hilbert space 21, 99, 106, 170
- Hölder condition 7, 20, 27, 168, 222ff, 401, 410ff, 417, 424
  - inequality 21
- Hölder-continuous 20, 209, 232
- horizontal strip 60
- hyperbola 334, 351ff
- hyperbolic arcs 165, 353
- hypertrochoids 307
  
- I**
- identity, Green's first 408
  - Green's second 149, 408
  - Green's third 150, 409
  - mapping 361ff
  - theorem 29
- inclination 359ff
- index of a curve 24
  - of Hilbert problem 411, 415, 418, 423
- inequality, Cauchy's 25
  - Cauchy-Schwarz 21
- Hölder 21
  
- Minkowsky's 21, 217, 219, 221, 225
- Schwarz 179, 181, 213, 221
- triangle 19
- infinity, exterior 396ff
  - interior 396ff
- initial guess 70, 79, 183
- inlet 395
  - configuration(s) 379, 384ff
  - exterior 396
  - interior 396ff
  - nose 396ff
- inner product 22
- integral(s), Bernoulli 237
  - Cauchy 7, 10, 26, 111, 132, 267, 360, 374ff
  - Cauchy p.v. 206, 234, 401ff, 406
  - complete elliptic 267
  - elliptic, of first kind 57, 311
  - hyperelliptic 6
  - improper 401ff
  - of Cauchy type 25
  - Poisson 158, 214, 313
  - Schwarz-Christoffel 52, 64, 68ff, 79, 86
  - Stieltjes 320ff
- integral equation(s), Arbenz's 320ff
  - Banin's 176
  - Carrier's 173
  - coupled 240
  - Fredholm 7, 10, 12, 193, 358, 368
  - Gershgorin's 172, 188, 313, 314, 316, 320ff
  - Lichtenstein's 171ff
  - Mikhlin's 259, 358, 367ff, 377
  - modified Symm's 255ff
  - singular 231
  - Stieltjes 321ff
  - Symm's 1, 10ff, 237ff, 261, 267, 295, 306, 325ff
  - Symm's, for interior regions 238ff
  - Symm's, modified 255ff

- Theodorsen's 1, 3, 8, 10, 207ff,  
234ff, 237, 410
- Warschawski-Stiefel's 177
- integral representation 222ff
- interior maps 177ff
- interpolation error 257  
formula 202  
Lagrange 237, 251ff, 257ff  
polynomials 233  
trigonometric 194, 228ff
- inverse points 395
- inversion 45, 177, 339, 424
- J**
- Jacobian 380ff
- Jordan contour 17, 181
- Joukowski airfoil 275, 293  
function 269ff, 277  
generalized mapping 274ff  
theorem 274
- jump discontinuity 259, 329, 374ff
- K**
- kernel 6, 162, 318, 341ff, 369ff, 373,  
375, 406  
Bergman 11, 94ff, 118, 328,  
340ff, 406  
Cauchy 11, 15, 25, 198ff  
conjugate 178  
degenerate 192ff  
iterated 178  
Kerzman-Stein 200ff  
Neumann 168ff, 180ff, 192ff  
Szegő 11, 92, 105ff, 113, 198ff,  
201
- Kirchhoff flow problem 13, 83ff
- knots 261
- Kronecker delta 110
- L**
- Lagrange functions 254ff, 257ff  
interpolation 237, 251ff, 257ff  
polynomials 5, 254
- Lamé differential equation 6
- Landen transformation 58ff, 394
- Laplace equation 4ff, 12, 370, 399
- Laplacian 11, 358, 370, 372ff, 381ff  
399
- analytic 374
- discrete 372ff, 375ff, 399
- limacon 165, 265, 307  
Pascal's 307
- linear programming 11
- Lipschitz condition 20
- Lipschitz-continuous 20, 236
- Liouville theorem 25, 163
- logarithmic singularity 265, 313, 366  
spiral(s) 359ff
- log-hodograph plane 83  
variable 85
- M**
- magnification 41
- matrix, hermitian 98, 170  
skew-hermitian 202
- maximum modulus theorem 25ff, 28,  
242, 246, 306  
principle 28ff
- mean-value property 25  
theorem 28, 147ff
- mesh points 370ff, 376ff  
size 373, 378
- metric spaces 20ff
- method, Bergman kernel (BKM) 95,  
101ff, 280, 327, 340ff  
Bieberbach 3  
Carleman's 7  
classical hodograph 85ff  
classical iterative 207ff  
collocation 261  
conjugate gradient 206  
contour integration 403  
discretization 323ff  
Elcrat-Trefethen 86ff  
fast Fourier transform (FFT) 1,  
10, 235, 269, 285ff
- finite difference 379ff, 399
- finite element 379ff
- fixed-point iteration 10
- Fourier 10

- Fourier-Galerkin 11  
 Fredholm 3  
 Gaier's variational (VM) 4ff,  
     92, 341, 346  
 Gakhov's 7  
 Galerkin 377  
 Garrick's, of conjugate functions 8, 13, 269, 288ff  
 Gaussian elimination 377  
 generalized conjugate gradient (GCM) 202, 206  
 Green's function 5  
 Hadamard variational 4  
 integral equation 9, 168ff  
 iteration 1, 230, 390, 399  
 iterative 178ff, 202, 207, 233,  
     269, 285ff, 311, 317, 387ff,  
     391  
 Ives-Liutermoza 390  
 James's 8, 269, 279ff, 281ff,  
     294  
 Kantorovich 71ff  
 Lagrange's interpolation 237,  
     251ff  
 Mayo's 358, 370ff, 377  
 modified ONP 247ff  
 modified Symm's 255  
 modified Theodorsen's 284  
 Newton's 1, 10, 60, 68, 70,  
     72ff, 77, 207, 231, 234ff  
 Newton-like 207  
 Newton-Raphson iteration 292  
 Nyström 202, 369ff  
 of images 341ff  
 of infinite systems 125ff, 132,  
     141, 207  
 of networks 6  
 of reduction of connectivity  
     311  
 of separation of singularities  
     402ff  
 of successive approximations  
     123, 137, 139, 144ff  
 of successive conjugates 280ff  
 one-step 384ff  
 orthogonal 383ff  
 orthonormal polynomial (ONP)  
     240ff, 265ff, 280, 306  
 Picard's 7  
 polynomial approximation 1  
 quadratic convergence 229  
 Radon's 320ff  
 relaxation 6  
 Ritz (RM) 95ff, 280, 327, 340ff  
 small parameters 7  
 Symm's 367  
 Theodorsen's iterative 209ff,  
     269, 279ff, 294  
 two-step 388ff  
 variational (VM) 4ff, 92, 341,  
     346  
 Wegmann's 207, 229ff, 236  
 Minkowsky's inequality 21  
 Mercator's projection 1, 40  
 Möbius transformation 45ff, 69, 257,  
     288ff
- N**
- near circle 210ff, 213, 229, 288, 290,  
     390  
 nearly circular approximations 277ff  
 boundary 133  
 contour 208, 267, 284  
 region 2ff, 120ff, 145, 181,  
     209, 277  
 nearly convex 182  
 Neumann conditions 304  
     constant 181  
     function 160ff  
     kernel 168ff, 180ff, 192ff  
     lemma 181  
     problem 3ff, 7, 159ff  
     problem for the annulus 303  
     series 178  
*n*-gon 51, 83  
 nodes 240ff, 245, 246, 307, 369
- O**
- oblique angle 360  
 octagonal curve 165

**P**

- parabola 351ff  
 parabolic arcs 351, 353  
 parallel cuts 359, 361  
     strip 296, 313  
 perturbations 251  
 plane, computational 381ff  
     physical 83, 381ff  
 Plemelj formula 26  
 point of inflection 337  
 Poisson grid generation 399  
     integral 158, 214, 313  
 pole(s) 63, 235, 330ff, 335ff, 342ff  
 polygon 69  
 polygonal obstacles 83ff  
 polynomial(s), Bieberbach 100, 107  
     Bochner-Bergman type 4  
     Chebyshev 118, 185, 252,  
       403ff  
     complex 41  
     Fourier 228  
     harmonic 153  
     interpolation 233  
     Lagrange 5, 254  
     minimal 96, 98, 100, 106  
     orthogonal 109ff, 116ff  
     orthonormal 111, 117, 237, 295  
     Szegö 4, 110ff  
 potential 190, 204  
     complex 272ff  
     complex velocity 84, 394  
     flow 174, 269, 279  
     function 204, 309  
     logarithmic 2  
     single-layer 2  
     single-layer logarithmic 305  
 principle, argument 185  
     Bieberbach minimizing 92  
     maximum 28, 30  
     maximum modulus 210  
     minimum 4  
     Schwarz reflection 15, 35ff,  
       330ff  
     symmetry 49ff, 417  
 problem, Dirichlet 1ff, 6, 10, 31,  
     147ff, 190, 309, 358ff, 364ff,  
       368, 379, 423ff  
 Dirichlet, for the unit disk 423  
 Hilbert 7, 410ff, 419  
     homogeneous Hilbert 7, 410ff,  
       417  
 Kirchhoff flow 13, 84ff, 90  
 minimum area 92ff  
 minimum boundary 103ff  
 modified Dirichlet 359, 369  
 Neumann 3ff, 7, 159ff  
     nonhomogeneous Hilbert 7ff,  
       415ff  
 parameter 76ff  
 Plateau 5  
 Riemann-Hilbert 8, 10, 147,  
   207, 235, 410ff, 417ff  
 Schwarz-Christoffel 87  
 transonic flow 394  
 variational 345  
 projection, Mercator's 1, 39  
 orthogonal 199  
     stereographic 1, 30  
 property, mean-value, 25

**Q**

- quadrature 309, 369ff, 377, 404  
     formula 370  
     Gaussian 102, 264  
 quadric functional 170  
     Gauss-Chebyschev type 403ff  
 quadrilaterl 60ff, 72, 165, 354  
 quasiconformal map 384

**R**

- rectangle(s) 56, 242, 251, 264, 267,  
   297, 333, 337, 341ff, 352,  
   370, 384  
     in a circle 356  
 rectifiable curve 18  
 reflection 46  
     principle 331  
 region 16  
     bean-shaped 343ff  
     canonical 5, 359ff

- circular 361ff
  - computational 379ff
  - cross-shaped 350, 356
  - doubly connected 295ff, 345ff, 367
  - exterior 140ff, 174ff, 226ff, 239ff, 245ff, 339ff
  - interior 171ff, 237ff, 240ff
  - lens-shaped 66
  - multiply connected 358ff, 368
  - nearly circular 2ff, 121ff, 146, 181, 209, 277
  - nearly convex 181
  - nose 284, 289
  - octagonal 354
  - physical 379ff
  - rectangular 356
  - starlike 207, 214, 224ff
  - triply connected 373, 378
- relaxation constant 391ff
- reparametrization 19
- resolvent 194ff
- Riemann-Hilbert problem 8, 10, 147, 207, 235, 410ff, 417ff
  - for the unit disk 417ff
  - homogeneous 410
- Riemann mapping theorem 2, 4, 9, 15, 31ff, 70, 93, 208, 384
- Riemann surface(s) 2, 16, 230, 270, 299
- Ritz approximations 11
- Robin's constant 29ff, 33, 240, 326
- rotation 41, 298
  
- S**
- S-condition 107, 108, 118
- scaling factor 252
- Schwarz formula 158ff, 208
  - differential operator 65
  - inequality 179, 181, 213, 221
  - lemma 39, 187
  - reflection principle 15, 35ff, 330ff, 416
  - symmetry principle 417
- Schwarz-Christoffel formula 5, 12, 51, 64, 68, 259
  - integral(s) 52, 64, 68ff, 86
  - modified formula 87
  - problem 87
  - transformation 1, 13, 51ff, 66, 83, 86, 90, 116, 326
- Schwarzian derivative 65
- semi-infinite strip 62, 66, 389
- series, Fourier 99, 110, 132, 145, 194, 230, 290, 303ff, 350, 392, 397
- Laurent 125, 302
- Neumann 178
- Taylor 70ff, 132, 163, 194, 201, 371ff, 376, 378, 397
- trigonometric 121, 123, 138, 141, 288
- Simpson's rule 72, 241
- single-valuedness condition 239, 306
- singularity behavior 328ff
  - problem 11
- singularities 257, 320ff, 336, 340, 345, 348ff
  - branch point 326ff, 333ff, 348
  - corner 246, 265, 282, 320, 328, 348
  - curvature 397
  - logarithmic 265, 313, 366
  - pole-type 330ff, 358
  - removal of 81ff
- slit(s) 378
- small parameter expansions 120ff
- Smirnov class 107
- Sobolev space 23, 235
- solidification 12
- solidity 390
- source strength 205
  - density function 238, 260, 305ff
- sources and sinks 205, 392ff
- spiral cut(s) 359ff
- spline, approximations 237, 259ff, 337
  - augmented 264
  - augmented cubic 264
  - B- 264

- cubic 285ff
- function 11, 264
- periodic cubic 285, 288, 291
- quintic 377
- square(s) 89, 100, 136, 143ff, 154, 242, 324, 348, 379
  - family of 137
  - in a circle 319
  - with round corners 165, 258
- stadium 203
- stagnation point 84, 393ff
  - streamline 395
- star of a region 299ff
- stereographic projection 1, 30
- Stieltjes integral 320ff
  - integration 321, 324
- streamlines 84, 392ff
- stretching parameter 382
- Symm's integral equation 1, 10ff, 237ff, 261, 267, 295, 306, 325ff
  - for interior regions 238ff
  - modified 255ff
- symmetric points 36, 46ff, 289, 331
- symmetry principle 49ff, 417
  - property 367
- Szegö kernel 11, 92, 105ff, 113, 198ff, 201
  - polynomials 4, 110ff
- T**
- Taylor series 70ff, 132, 163, 194, 201, 371ff, 376, 378, 397
- Theodorsen's integral equation 1, 3, 8, 10, 207ff, 234ff, 237, 410
  - uniqueness 222ff
- theorem, area 2, 38, 298
  - Cauchy-Goursat 24
  - Cauchy's 15, 23, 365
  - conformal mapping 30
  - divergence 407ff
  - gradient 407ff
  - Green's 407
  - Green's reciprocity 408
  - Hally's 322
- Harnack 29
- identity 29
- Joukowski 274
- Lehman's 350
- Liouville 25, 163
- maximum modulus 25ff, 28, 242, 246, 306
- mean value 28, 147ff
- of F. and M. Riesz 214
- Osgood-Carathéodory 4
- residue 364, 366, 403
- Riemann mapping 2, 4, 9, 15, 31ff, 70, 93, 208, 384
- Stokes' 407ff
- three-element loop 283
- tolerance 184
- torsion problem 5
- trailing edge 285ff, 288ff
- trapezoid 78
- trapezoidal rule 11, 202, 369ff, 377
- transfinite diameter 17, 33, 245ff
- transformation, bilinear 45ff, 65ff, 293, 398
  - coordinate 380ff
  - Landen 58ff, 394
  - linear 69, 362
  - linear-fractional 45ff
  - Möbius 45ff, 69, 257, 288ff
  - Schwarz-Christoffel 1, 13, 51ff, 66, 83, 85, 90, 116, 326
- Theodorsen-Garrick 285
- von Karman-Trefftz 8, 269, 283ff, 288, 291
- translation 41, 71, 284
- triangle 54ff, 62, 89,
  - isosceles 250ff
  - inequality 19
- trigonometric interpolation 228ff, 231
- U**
- unit disk 16, 51, 80, 115, 119, 132, 134, 145, 214, 279
  - slit 368
  - square 203, 378
- univalent function 32, 39, 318, 330,

- 333, 377  
mapping 32, 244, 366  
upper half-plane 51ff, 56, 60, 63, 66,  
69, 72, 78, 83, 89, 165
- V**  
Vandermonde determinant 16  
velocity, complex 83  
von Karman-Trefftz transformation 8,  
269, 283ff, 288, 291
- W**  
Wallis criterion 67  
Warschawski's sufficient condition  
283, 289  
Weddle's rule 190  
Wing profile, elliptic 294, 394  
tear-drop 294
- Z**  
zeros 63